

Development of a Recyclable Molybdenum Dearomatization Agent

Jeffery Todd Myers
Rock Hill, South Carolina

B. S., Winthrop University, 2012

A Dissertation presented to the Graduate Faculty
of the University of Virginia in Candidacy for the Degree of
Doctor of Philosophy

Department of Chemistry

University of Virginia
May 2017







Copyright Information

Chapters 2 and 3 are compilations of two published works and have been reproduced in accordance with Section II.1 of American Chemical Society Journal Publishing Agreement. Proper citations for Chapters 2 and 3 are given. Chapter 5 is an outline for an upcoming publication.

Chapter 2: Jeffery T. Myers, Philip J. Shivokevich, Jared A. Pienkos, Michal Sabat, William H. Myers, and W. Dean Harman, *Organometallics*, **2015**, 34 (14), pp 3648–3657.

Chapter 3: Jeffery T. Myers, Steven J. Dakermanji, Timothy R. Chastanet, Philip J. Shivokevich, Laura J. Strausberg, Michal Sabat, William H. Myers, and W. Dean Harman, DOI: 10.1021/acs.organomet.6b00780.

Chapter 5: Jeffery T. Myers, Jacob A. Smith, Steven J. Dakermanji, Katy B. Wilson, Philip J. Shivokevich, W. Dean Harman.

Acknowledgments/ A Reflection on the Past 10 Years

There are a lot of people that I would like to acknowledge for their help and guidance as I have explored chemistry. This section cannot come close to conveying how indebted I feel to all of you. Whether you have helped me understand a concept, encouraged me not to give up, or simply helped me relax by enjoying a beer with me, I am truly grateful for your aid. Thank you.

When I was in high school I had no desire to go to college: I wanted to be a firefighter. In my senior year of high school I was learning how to connect SCBAs and clear rooms when I took my first class in chemistry. I started to think that this might be a fun thing to study further, but college felt so out of reach because I didn't have a financial plan. One night after work I called my grandparents and asked if there was any help they could give me. They told me that if I got into college, then they would pay for my books. This was the spark that I needed. I had to take the SATs three times to qualify for South Carolina's LIFE scholarship, but I did it, got accepted into Winthrop University, and began my journey in chemistry.

I would like to thank all of the professors in the chemistry department at Winthrop. There are two key events during my time at Winthrop that specifically altered my life. The first occurred in my general chemistry class, taught by Dr. Patrick Owens. Dr. Owens commanded respect when he entered a room. He is a man who demanded your focus and accepted nothing but your best. I would not have a career in chemistry without him. His class was comprised of two tests and a final exam. I failed his first test. I went to his office after receiving my grade and tried to explain.

“I tried hard. I studied a lot and just didn’t get it, but—”

“No you didn’t.” said Dr. Owens. “You didn’t study hard enough. You failed, Jeff. However, unlike other people who got a good grade and now think they don’t have to study as hard, you know differently. You are going to work harder, study longer, and you are going to pass.”

I did. I studied harder than I ever had before and I passed. If he hadn’t said that, then I would not have even met the next person to change my life: my advisor, Dr. James Hanna. Dr. Hanna saw that I had done well in Dr. Owens’ class and offered me a research opportunity. I had no lab experience and a pyromaniac mindset. Not the best combination for an organic chemistry lab. Before I got my hands on these Molotov cocktail mixers, Dr. Hanna asked me to write a literature review on “Palladium-Catalyzed Cross Coupling Reactions.” I had to look up the definition of every word, but once I finished this assignment and began hands-on research, I knew chemistry was my passion. I stayed in Dr. Hanna’s lab for three and a half years and loved every second of it. Without this experience, I probably would not have stuck with chemistry. I learned that although I am not the smartest person, I am a good researcher.

During my time at Winthrop, my graduating class grew as a family. We studied together, got coffee together, and complained about classes together. We stayed in this love-hate relationship because we knew how rewarding chemistry was to us. One of these late nights of studying led me to look outside the window and admire the trees outside. With the building stress of the impending organic exam, all I could think to say was, “I’d like to be a tree.” Then, without skipping a beat, Paisley said, “Yeah.” I was hooked. This beautiful girl that could outperform me in any chemistry class had my full attention. She

had caught my attention in our first chemistry class. Sitting behind me, I grew jealous as she talked to the guy sitting beside her, Zayed. Admittedly, she may have been partly to blame for my failing Dr. Owens' first chemistry test. Paisley, Amber and I would study all hours of the night in Wofford Hall. We would make competitions out of studying; *Who Can Write the Electron Configuration the Fastest* was a game I always lost. But this, this understanding of wanting to be a tree, confirmed that she would be the one.

Senior year at Winthrop I began planning my next step: I wanted to be a nuclear engineer for the Navy. Around the time that I began interviews I decided to make my move on Paisley. After numerous rejections, she eventually agreed. I will not bore you with the details of how we accidentally wedding crashed or how we got lost in the middle of nowhere, but needless to say it was perfect. Again, I was hooked but there was a problem. Paisley wanted to go to grad school and the boomers that I would be stationed on would make a relationship with Paisley difficult. So, again I changed my direction and set my eyes on grad school. We applied to the same schools, with a few different ones, and hoped for the best. I really wanted to go to Wake Forest to work with Dr. Mark Welker on some cool Diels-Alder reactions. Of course, Paisley's impressive academic record won her a fellowship at Wake, but I got rejected. Out of the 7 or 8 schools that we applied to, the University of Virginia was the only one we both got in to. Paisley was ecstatic because she wanted to work for Dr. Don Hunt, but I had no clue who I wanted to work for.

During graduate prospective weekend at UVa I met Dr. Dean Harman. Dean's explanation of chemistry was like a child's obsession with his toys. He wanted me to understand how every little part worked. "The metal donates electron density into the π^*

orbital of the aromatic and this disruption of aromaticity allows us to activate the aromatic for chemical transformations...For example, we can take a pyrrole and through a cycloaddition create this epibatidine derivative. Have you ever heard of epibatidine?” Little did Dean know, I had just given a presentation on a total synthesis of epibatidine at Winthrop. This was the sign.

After joining Dean’s lab I was asked if I wanted to work on the inorganic or the organic side. I decided the inorganic side because I wanted to broaden my horizons; this answer led me to be trained by Laura Straussberg. Laura was a great teacher. She taught me how to use a glovebox for the first time, how to interpret 2D NMR spectra, and how to keep my glovebox clean. With Laura’s training, I soon became proficient at setting up small-scale reactions and the in-and-outs of the lab. I always think of Laura when I fold a sheet of paper in half to write on it. I am very grateful for Laura’s patience with me. I may have been too anxious for independence and as such I was a little...annoying. Soon after I started, Laura went off to write her dissertation and Phil Shivokevich joined the Harman Lab. This changed everything.

From this point on, Jared Pienkos trained the two of us. Phil and I joined forces and began working on a single project that Dean set out for us. I still have the first sheet of paper that Dean handed us, which listed our project goals. It was titled *The Road to Molybdenum Dearomatization*. In essence, our project was to get “molly” off the ground. Our first of many goals was to synthesize $\text{TpMo}(\text{NO})(\text{L})(\text{Br})$ on a “usable” scale. So, Phil, Jared and I tackled this one step at a time. Every step in this procedure had some issue that we fixed together. Phil and I had weekly meetings with Dean to discuss our progress (more often our lack of progress), but these meetings always digressed into a

discussion on general chemistry. In these meetings Dean showed us that the success of a reaction was not whether the reaction yielded the desired product, rather the success of a reaction is setting it up correctly. Did we consider our previous observations? Did we attempt a logical way to address these observations? Did we consider the error in our assumptions? These fundamental questions were instilled in us during our meetings with Dean.

A very important lesson Dean taught us was how to respect one another. I never felt afraid to ask for an explanation no matter how basic of a concept it would seem. Dean encouraged us to understand that in grad school everyone has a different background and to be sensitive towards someone's lack of knowledge. This was very important to me because I felt (and still feel) less knowledgeable than my colleagues. There were times when I was literally red in the face with embarrassment. One particular example of this was when I couldn't define the difference between diastereomers and enantiomers during group meeting. Dean did not let this lack of knowledge degrade his respect for me. What I did to earn this respect I do not know, but I am very grateful that he gave me a chance. Furthermore, I am honored that Dean has offered me a position in his lab as a post-doc. I know that there is still much for me to learn from Dean and I am excited that I will have another couple of years to do so. Thank you.

Another respectful man in the Harman Lab was Dr. Bill Myers. Bill was a post-doc for Dean that, thankfully, never left. After moving to Richmond to teach, Bill stayed on as our lab manager during the summer. Lab manager doesn't do justice to Bill's title. He was our teacher of all things (chemistry and more), counselor, spectra interpreter, but most importantly he was our friend. On my first day in lab, I walked into the conference

room to find this gentle giant sitting at his desk. “You look like someone who has had a rough go,” Bill said. I was baffled. What do you say to that?! Our time with Bill would be riddled with interesting events like this. From discussions of beautiful women in convertibles to *The Terror of Tiny Town*, Bill was always a fierce friend and avid teacher.

In the Harman Lab we always know that we can call on Dean whenever we need help, but more often we call on one another for help. The respect that Dean taught us to have for one another allows us to enjoy meetings and discussions unencumbered by a fear of being singled out for not knowing something. Furthermore, during our time in lab we have enjoyed a melting pot of music. From the Green Day fanatics to the *Les Miserables* enthusiasts, we have an unspoken respect for individuals’ choices in music. A fun game Phil and I would play is *Who Put that Song On*, where we would identify the individual in lab that started a particular song. From this we have developed a few key identifying songs that I would like to share.

“Wake Me Up” by Avicii

What can I say about Dr. Jared Pienkos? You are a great friend first and foremost. You saved my life after I stabbed myself with an NMR tube, but were too good to wash my dishes for me. Jared had an incredible knack for scaling up the molly preps. He perfected the dimethylfuran synthesis (with MeIm as the ligand) while using me as an iodo complex monkey. He was the first person I showed Paisley’s engagement ring to and, after she amazingly said yes, was the best man at our wedding. One of my favorite of many moments with Jared was when he (dressed up as a sandwich) got into a fight

with a person (Tom Dawson maybe?) that was dressed up as a hot dog during a Halloween party. Jared did it for the sheer corniness of saying he was in a food fight.

“The Middle” by Jimmy Eat World

Dr. Ben Liebov is by far the most honest man I know. Ben would never miss an opportunity to help someone. Nor would Ben ever miss an opportunity to learn. With his Trader O’s and sushi grade tuna, Ben always stuck to his principles and passions. Whether he was reminding us to wash the white caps or to keep the waste closed, Ben kept our lab in line. Two more songs that I cannot help but relate to him are “It Wasn’t Me” by Shaggy and “Sugar” by Maroon 5. Whenever Shaggy came on, I knew that he was annoyed with Bri and I couldn’t help but laugh. Whenever “Sugar” came on I would (and still do) curse Ben’s name for ruining the music video’s magic by explaining that it was not real. Lastly, I miss going to brunch at *Beer Run* with him and Nicole. Mimosas on Sunday mornings just aren’t the same without you, Ben.

“Shake it Off” by Taylor Swift

Dr. Bri MacLeod drove me to be a better chemist. With Bri in lab I was driven to obtain the cleanest spectra and highest yields possible. Imperfections in my NMRs during group meeting would not go unnoticed by Bri’s eagle eye. I believe she obtained an eagle eye enhancement during her “eye bubble” doctor’s visits second year. Bri had me questioning the validity of my research quite a bit, which, although annoying at times, encouraged me to define what I found to be important with my own work. Phil will probably read that and say, “Meh.” Bri was an overbearing mother at times, but was also

a fun person to vent with. Sharing our failures with one another in hopes of making the other feel better became a small tradition between us. Bri was a strong proponent of our weekly outings, and as such our Thursday night trips to Three Notch'd (TKT!) have significantly decreased since she left, which is disheartening.

“Whiskey Lullaby” by Brad Paisley

There is not enough room to say all that I want to about Philip Shivokevich. Phil and I have spent the past 5 years figuring out everything to do with molybdenum dearomatization. Phil has a wealth of knowledge and every desire to share it with whoever wants to learn. Furthermore, Phil has been our local handyman when it comes to all things rotovap and more. Anywhere Phil goes he will be an asset. I will greatly miss our conversations about the future of the lab. Like Ben, I cannot help but relate another song to Phil, “The Gummy Bear Song” by Gummibär. We would play Señor Gummibär’s song on a loop until someone would turn it off.

During our time as boxmates we would often argue about the stupidest things. For instance, whether lions sleep in the jungle or not, if our gloves are purple or blue, if high school is over or not... Phil always won those arguments, but never could win a beer bet with me. Speaking of not winning, I will be surprised if the North will defeat the South before you graduate, bet a 6-pack?

“I hate u, I love u” by Gnash

Katy “Jumbo Zinc” Wilson came into our lab shortly after Phil and I passed candidacy. At first Katy came off as quiet and shy. How wrong was that first

impression?! What I mistook for bashfulness turned out to be Katy listening intently and learning everything she could. She has a vast knowledge of organic chemistry with tungsten. Katy has kindly put up with my continued badgering for her to try experiments, even when they don't align with Dean's desired reactions. She never misses a chance to hear about my "cool" observations or whacky thoughts. Even during my ludicrous discussion about an electrophile that can sometimes be a nucleophile, Katy listened; for that I am grateful. One of these days she is going to try Chicken Salad Chick. Like all of my suggestions, after a year of my suggesting it she will realize that I am right.

"Hooked on a Feeling" by Blue Suede

Tim Chastanet was the first person I trained as a graduate student. Tim taught me how to teach. His first project was to optimize the allyl preps in Chapter 3, so big shout out to him for that. Tim never missed an opportunity to talk about food. His gourmet tastes and my fast food tendencies often clashed, but he nonetheless was always excited to talk about his most recent culinary adventure. Tim never feared trying a new reaction. He perfected a methanol quenching of the acenaphthene reduction that would revolutionize the dimethylfuran prep (with DMAP as the ligand). Furthermore, without this "methanol workup" I doubt that the TFT prep in Chapter 5 would have become so successful. I owe you a great debt of gratitude, Tim.

"Amish Paradise" by "Weird" Al Yankovich

Steven Dakermanji optimized the $\text{TpMo}(\text{NO})(\text{DMAP})(\eta^2\text{-dimethylfuran})$ prep discussed in Chapter 3. This is the first of many advances Steven has contributed to the

molly system. Steven's love for the lab is evident in his desire to help change tanks, do stockroom runs, and volunteer for random lab maintenance. This motivation is a rare quality and I am grateful to have him help keep the lab running. Furthermore, Steven's persistence in keeping Jared's/Ben's/my tradition alive by playing "Friday" by Rebecca Black on Fridays is much appreciated.

"Closer" by The Chainsmokers (ft. Halsey)

Alex Heyer has a drive for research that is unstoppable. Even to the point where he focuses on his own research while others are giving group meeting. He continues to push forward with a meticulous scientific approach, even if day after day he gets "black death". Furthermore, Alex encourages a community among the lab with weekly hypothetical/would you rather/personal questions on his board. For the official "Fun Friday" record, I won the whole pizza challenge, which will be added to my CV.

"Arrival" by Jóhann Jóhannsson

Jacob Smith is a titan of all things fluorine. All of the kinetic data, the newly bound fluorinated aromatics, and the benzene complex in Chapter 5 were all accomplished by Jacob. Let me repeat that, just in case someone didn't catch it. THE MOLLY BENZENE COMPLEX! Wow! When Jacob joined our lab it instantly felt like he had been there all along. One of the first challenges we tackled together was optimizing the TFT prep. This beast of an optimization was only accomplished by careful collaboration between the two of us. Sadly, we could not find a good enough reason to incorporate sand, whether white or brown, into this prep. Sorry, Dean. Once the

optimization was completed, Jacob took off like a baby bird kicked out of the nest. Wranglin'!

Although he has not played any songs in lab I imagine Kevin's song to be something along the lines of the following: 80's song...by 80's artist...

Dr. Kevin Welch has been a tutor to me for the past four months. I've only known him for this short period of time and have noticed a few key qualities about him. He is difficult to piss off, fun to argue with, and talentedly sarcastic. Most memorable to me was his comment in Chapter 5, "Technically naphthalene is a substituted benzene..." After reading this comment I promptly shouted "@#\$% you!" at my laptop. Thank you for your time and advice, Kevin.

For the rest of the members in lab, I cannot pick out a specific song that I associate with you, my apologies. Ben "Bento Box" Cavannaugh is a mystery to me. His shy temperament yet happy personality are calming and intriguing. I think of Mr. Box as a Bruce Wayne of sorts. I would like to thank Hannah Nedz "Baller" for giving Katy an adversary worthy of her competitiveness. I also thank Hannah for being a whistler and enjoyer of Eric Hutchinson. Justin Wilde has an uncanny knowledge of organic chemistry. I give full credit to him for the pyridine-borane, pyridinium, and MVK-pyridine complexes in Chapter 6. I have no doubt that molly dearomatization of ANHs will soon take off with Justin at the helm. Spenser Simpson has recently joined our lab. He has the spunk of a new kid, which will go far in our lab. Furthermore, he enjoys the outreach group, LEAD, and has a real talent with teaching kids science. I hope to pass on

some of my experiences with LEAD in the hopes that he will continue with this important group.

Now to come back to the person who this dissertation is dedicated to: my wife, Dr. Paisley Myers. I don't know why you eventually said yes to my repeated attempts to ask you out, but you did, and I am so happy for that. It was in Dr. Owens' general chemistry class that our relationship began, and it was there that our relationship took its next step. You have a kind, caring, passionate heart and an incredible intelligence. Over the past five years you have made the tough times easier and the easy times joyful. You are my best friend and most cherished confidant. Thank you.

Aside from Kevin and Dean, our dog, Riley, was probably the most helpful in writing this dissertation. When I was stressed from writing at home, I knew I could come out to the living room and find him relaxed on the couch without a care in the world. The relaxing walks we'd take or belly rubs I'd give him during those times were a blessing that I treasure. Thank you.

My family has been a great supporter of my studying in Virginia. Specifically I want to thank my mom and sister. I am very thankful to have a mom who has sacrificed so much for us. Your example of perseverance and determination has driven me to do all that I have done. Jessica, I am so proud of the wonderful family you have created. I hope Paisley and I are as great of parents as you and Josh. To Dad and Carolyn, thank you for your support and guidance. I continue to live by the motto "adapt and overcome" that you taught me. To the rest of my family, I cannot thank you all personally, but I want each individual to know that I am very thankful for your continued support and encouragement. Thank you.

Abstract

Chapter 1 includes a review on the past 30 years of electron-rich dearomatization agents. Specifically, the binding of aromatics to $\{\text{Os}(\text{NH}_3)_5\}^{2+}$, $\{\text{TpRe}(\text{CO})(\text{L})\}$, $\{\text{TpW}(\text{NO})(\text{PMe}_3)\}$, and $\{\text{TpMo}(\text{NO})(\text{MeIm})\}$ fragments is investigated. A primary focus of this review is to identify advantages and disadvantages discovered with each metal fragment. With this knowledge, ideal expectations of a more universally applicable dearomatization agent are stated, and the ensuing Chapters address instances where these expectations are met.

In Chapter 2 we demonstrate the ability of the $\{\text{TpMo}(\text{NO})(\text{MeIm})\}$ fragment to activate naphthalene and anthracene towards organic transformations. After isolating these organically transformed complexes, the oxidative decomplexation of the new organics is achieved by stirring overnight in the presence of air. Next, we show that by using a halogen as an oxidant (iodine) we can improve the yield of the isolated organic, while also recovering a reusable metal center, $\text{TpMo}(\text{NO})(\text{MeIm})(\text{I})$.

Chapter 3 addresses a common disadvantage found in the comparison of molybdenum to its third-row congeners. Eta-2 bound aromatic complexes of $\{\text{TpMo}(\text{NO})(\text{MeIm})\}$ are more susceptible to oxidation in the presence of electrophiles. By adjusting the ligand set, specifically replacing MeIm with DMAP, molybdenum becomes more resistant towards oxidation by electrophiles. A testament to this resistance is shown by the isolation of arenium complexes of naphthalene and anthracene bound to $\{\text{TpMo}(\text{NO})(\text{DMAP})\}$. Furthermore, molybdenum's resistance towards electrophilic oxidation is investigated with the addition of carbon-based electrophiles.

Chapter 4 continues the investigation of carbon-based electrophilic additions to $\text{TpMo(NO)(DMAP)(}\eta^2\text{-naphthalene)}$. Specifically, we explore the ability to perform MIMIRC additions on η^2 bound naphthalene. This reaction is shown to be successful with various Michael acceptors and is used in the isolation of a fused ring system with a steroidal core.

In Chapters 5 and 6 we identify two new classes of aromatics that can bind to $\{\text{TpMo(NO)(DMAP)}\}$ in an η^2 fashion, fluorinated aromatics and pyridines. We then explore initial reactions that these complexes are capable of.

List of Abbreviations

Cp	Cyclopentadienyl (Cyclopentadienide Anion)
Cp*	Pentamethylcyclopentadienyl (Pentamethylcyclopentadienide Anion)
DMA	N,N-dimethylacetamide
DMAP	4-N,N-Dimethylaminopyridine
DME	1,2-Dimethoxyethane
DMF	N,N-Dimethylformamide
EA	Elemental analysis
ESI	Electrospray ionization
EVK	Ethyl vinyl ketone
HATR	Horizontal attenuated total reflectance
IR	Infrared
KTp	Potassium hydridotris(pyrazolyl)borate
MeIm	1-Methylimidazole
MS	Mass spectrometry
MTDA	Methyl trimethylsilyl dimethylketene acetal
MVK	Methyl vinyl ketone
NHE	Normal hydrogen electrode
NMR	Nuclear magnetic resonance
NOE	Nuclear Overhauser effect
ORTEP	Oak Ridge Thermal Ellipsoid Program
OTf	Trifluoromethanesulfonate (Triflate) anion
Pz	A pyrazole group in hydridotris(pyrazolyl)borate
TBAH	Tetrabutylammonium hexafluorophosphate
TBDMSOTf	Tert-butyl-dimethylsilyl triflate

THF	Tetrahydrofuran
TIPSOTf	Tri-isopropylsilyl triflate
TLC	Thin layer chromatography
TP	Hydridotris(pyrazolyl)borate anion

Table of Contents

Copyright Information	ii
Acknowledgments/ A Reflection on the Past 10 Years	iii
List of Abbreviations	xvii
List of Figures	xxi
List of Schemes	xxiii
Chapter 1: Introduction	
1.1 Introduction	2
1.2 $\{\text{Os}(\text{NH}_3)_5\}^{2+}$ Dearomatization	3
1.3 $\{\text{TpRe}(\text{CO})(\text{L})\}$ Dearomatization	6
1.4 $\{\text{TpMo}(\text{NO})(\text{MeIm})\}$ Dearomatization	15
1.5 $\{\text{TpW}(\text{NO})(\text{PMe}_3)\}$ Dearomatization	18
1.6 Developing the $\{\text{TpMo}(\text{NO})(\text{L})\}$ Dearomatization Agent	23
1.7 References	24
Chapter Two: Synthesis of 2-Substituted 1,2-Dihydronaphthalenes and 1,2-Dihydroanthracenes Using a Recyclable Molybdenum Dearomatization Agent	
2.1 Introduction	29
2.2 Results	30
2.2.1 Improved Synthesis of $\text{TpMo}(\text{NO})(\text{MeIm})(\text{L}\pi)$ ($\text{L}\pi = \text{naphthalene or anthracene}$)	30
2.2.2 Oxidation of $\text{TpMo}(\text{NO})(\text{MeIm})(\eta^2\text{-naphthalene})$ with Iodine	33
2.2.3 Spectroscopic Profile of $\text{TpMo}(\text{NO})(\text{MeIm})(\eta^2\text{-1,2-dihydroarene})$	36
2.2.4 Isolation of 1,2-Dihydroarenes Through Air Oxidation	39
2.2.5 Recyclable Oxidation of $\text{TpMo}(\text{NO})(\text{MeIm})(\eta^2\text{-1,2-dihydroarenes})$	41
2.2.6 Chemical Elaboration of Isolated 1,2-Dihydroarenes	44
2.3 Discussion	44
2.4 Conclusion	55
2.5 Experimental	57
2.6 References	83
Chapter 3: 4-(Dimethylamino)pyridine (DMAP) as an Acid-Modulated Donor Ligand for PAH Dearomatization	
3.1 Introduction	86
3.2 Results	87
3.2.1. Synthesis of $\text{TpMo}(\text{NO})(\text{DMAP})(\text{L}\pi)$	87
3.2.2. Synthesis of $\text{TpMo}(\text{NO})(\text{DMAP})(\eta^2\text{-arenium})$ complexes	90
3.2.3. Protonation and nucleophilic addition to 24 and 25	93
3.2.4. Nucleophilic additions to 27 and 28	97

3.2.5 <i>Varying the electrophiles added to 24 and 25</i>	98
3.3 Discussion	101
3.4 Conclusion	113
3.5 Experimental	114
3.6 References	163
Chapter 4: Michael-Michael Ring Closures on TpMo(NO)(DMAP)(η^2-naphthalene)	
4.1. Introduction	165
4.2 Results and Discussion	168
4.3 Conclusion	191
4.4 Experimental	192
4.5 References	206
Chapter 5: Binding and Activation of α,α,α-Trifluorotoluene with {TpMo(NO)(DMAP)}	
5.1 Introduction	209
5.2 Results	210
5.3 Discussion	221
5.4 Conclusion	225
5.5 Experimental	226
5.6 References	235
Chapter 6: Activation of Pyridines Using {TpMo(NO)(DMAP)}	
6.1 Introduction	238
6.2 Results and Discussion	240
6.3 Conclusion	257
6.4 Experimental	258
6.5 References	270
Concluding Remarks	273
Appendix	277

List of Figures

Figure 1.1. Tandem electrophilic-nucleophilic addition to [Os]-benzene complex.	4
Figure 1.2. Regioselectivity obtained through greater retention of aromaticity.	5
Figure 1.3. Coordination diastereomers of $\text{TpRe}(\text{CO})(\text{L})(\eta^2\text{-naphthalene})$.	11
Figure 2.1. NOESY correlations for 6p and the proposed assignment of 6d as its coordination diastereomer, rather than a constitutional isomer resulting from a 1,4-addition. $J_{\text{H1b-H2}} < 1$ Hz.	37
Figure 2.2. Crystal structure of dihydronaphthalene complex 6 .	38
Figure 2.3. Cyclic voltammogram of the reaction mixture following oxidation of 6 and air (top), CAN (middle), or iodine (bottom).	42
Figure 2.4. Naphthafuranones pygmaeocin A and arthrinin A, and the anthrafurane olivinolide.	47
Figure 2.5. Analysis using NOE (red arrows).	58
Figure 3.1. Solid-state structures of two dihydronaphthalene complexes 30 , using Melm (Left) ¹¹ and DMAP (Right).	95
Figure 3.2. NOESY correlations for 30p .	96
Figure 3.4. Analysis of NOE interactions.	115
Figure 4.1. Selected proton assignments for 61 .	172
Figure 4.2. Crystal structure of 87 .	178
Figure 4.3. Numbering scheme of 87 .	179
Figure 4.4. Analysis of possible steric interaction among different geometries of 61 .	180
Figure 4.6. <i>Cis</i> and <i>trans</i> orientations of H13 in 92 .	186
Figure 4.7. Examples of steroidal cores found in the literature.	188
Figure 5.1. ¹ H NMR spectra of $\text{TpMo}(\text{NO})(\text{DMAP})(\eta^2\text{-TFT})$ (100) in	

d ⁶ -acetone at various temperatures.	212
Figure 5.2. Coordination diastereomers of 100 and their relative free energies as predicted from DFT calculations.	213
Figure 5.3. Intrafacial isomerization between 100-A and 100-B .	215
Figure 5.4. Pharmaceuticals containing CF ₃ groups.	221
Figure 5.5. Newly bound fluorinated aromatic complexes of {TpMo(NO)(DMAP)}.	224
Figure 6.1. Resonance structures showing the delocalization of electron density on 2-methoxypyridine via coordinating at the C3-C4 double bond.	244
Figure 6.2. Crystal structure of 124A . The triflate anion is omitted for clarity.	247
Figure 6.3. ¹ H NMR of 125 (d ⁶ -Acetone, 25 °C).	251
Figure 6.4. ¹ H NMR spectra of 124 at various temperatures in CD ₃ CN.	253

List of Schemes

Scheme 1.1. Examples of hydrogenation, electrophilic addition, and cycloaddition mediated by $\{\text{Os}(\text{NH}_3)_5\}^{+2}$.	6
Scheme 1.2. Organic products isolated as a racemic mixture from a diastereomeric mixture of a stereogenic metal center.	9
Scheme 1.3. Diastereoselective control of electrophilic-nucleophilic additions to $\text{TpRe}(\text{CO})(\text{L})(\eta^2\text{-naphthalene})$.	12
Scheme 1.4. Enantioenrichment of $\text{TpRe}(\text{CO})(\text{L})(\eta^2\text{-benzene})$.	14
Scheme 1.5. Enantioselective organic modifications using $\{\text{TpRe}(\text{CO})(\text{MeIm})\}$.	14
Scheme 1.6. Synthesis of $\text{TpMo}(\text{NO})(\text{MeIm})(\eta^2\text{-L}\pi)$.	16
Scheme 1.7. Diels-Alder synthesis of cycloadducts promoted by $\{\text{TpMo}(\text{NO})(\text{MeIm})\}$.	17
Scheme 1.8. In situ protonation during the exchange of $\text{TpW}(\text{NO})(\text{PMe}_3)(\eta^2\text{-benzene})$ 19 with aniline, indoline, or quinoline.	19
Scheme 1.9. Organic modification of $\text{TpW}(\text{NO})(\text{PMe}_3)(\eta^2\text{-indolinium})$.	20
Scheme 1.10. Isolation of enantioenriched $\text{TpW}(\text{NO})(\text{PMe}_3)(\eta^2\text{-benzene})$ complex.	21
Scheme 1.11. Synthesis of the $\eta\text{-}2$ bound pyrrolium complex and subsequent synthesis of an indolizidine core.	22
Scheme 2.1. Synthesis of dihapto-coordinated naphthalene and anthracene complexes of molybdenum.	32
Scheme 2.2. Proposed formal catalytic cycle for the dearomatization of naphthalene with $\{\text{TpMo}(\text{NO})(\text{MeIm})\}$.	34
Scheme 2.3. Oxidation of 4 with iodine.	35
Scheme 2.4. Iodolactonization of 12 and 13 .	44
Scheme 2.5. Dearomatization of naphthalene using $\{\text{Cr}(\text{CO})_3\}$.	45
Scheme 2.6. Organic additions to anthracene.	45

Scheme 2.7. Tandem electrophilic-nucleophilic addition reactions to 4 or 5 .	48
Scheme 2.8. Potential pathways from the addition of an electrophile to 4 or 5 .	50
Scheme 2.9. Exchange of 2,5-dimethylfuran with CH ₃ CN to form TpMo(NO)(MeIm) (η^2 -acetonitrile), and the resulting complex observed through CV.	52
Scheme 2.10. Potential pathways after adding a nucleophile to an allylic species of 4 or 5 .	53
Scheme 3.1. Arene protonation versus metal oxidation.	87
Scheme 3.2. Synthesis of η^2 -coordinated naphthalene, anthracene, and 2,5-dimethylfuran complexes.	89
Scheme 3.3. Protonation and isolation of allylic naphthalene and anthracene complexes.	91
Scheme 3.4. Formal catalytic cycle for the generation of dihydronaphthalenes and dihydroanthracenes.	93
Scheme 3.5. Tandem addition of dimethoxypropane, and LiDMM, to 24 and 25 .	99
Scheme 3.6. Possible pathways after the addition of electrophile (E ⁺) to 24 or 25 .	104
Scheme 3.7. Oxidative decomposition of C by excess electrophile, H ⁺ in this case.	105
Scheme 3.8. Addition of dimethoxypropane and LiDMM to 24 using HOTf.	107
Scheme 3.9. Comparison of regiochemistry between 1,2 and 1,4-additions on 25 .	109
Scheme 3.10. Addition of dimethoxycyclohexane as an electrophile to 25 , followed by a nucleophilic addition with either NaCNBH ₃ (bottom) or LiDMM (top).	111
Scheme 3.11. Formation of the propanylidine dihydroanthracene complex 60 .	112
Scheme 3.12. Electrophilic addition of HOTf and LiDMM to form 14 and the product of a Michael-Michael ring closure, 61 .	113
Scheme 4.1. Tandem Michael-Michael-ring closure to yield (\pm)-9,11-Dehydroestrone.	165

Scheme 4.2. MIMIRC reactions on $\{\text{Os}(\text{NH}_3)_5(\eta^2\text{-2-methylfuran})\}^{2+}$ and $\text{TpRe}(\text{CO})(\text{MeIm})(\eta^2\text{-2-methoxynaphthalene})$.	167
Scheme 4.3. Attempted tandem electrophilic-nucleophilic addition of EVK and LiDMM to 24 .	168
Scheme 4.4. Analysis of mixture resulting from the attempted tandem electrophilic nucleophilic addition of EVK and LiDMM to 24 .	170
Scheme 4.5. Proposed mechanism for the synthesis of 61 .	173
Scheme 4.6. Synthesis of 61 from 24 as well as common side-products (e.g., 85 , 86 , and free naphthalene)	175
Scheme 4.7. Synthesis of 87 and 88 and their subsequent oxidations to yield 61 and 89 .	181
Scheme 4.8. [A+B] MIMIRC additions to 24 .	184
Scheme 4.8. Samarium diiodide-induced cyclization of naphthyl-substituted ketone (95).	189
Scheme 4.9. Competitive pathways encountered during the synthesis of 87 .	190
Scheme 5.1. Exchange of 26 with TFT to yield 100 .	211
Scheme 5.2. Reduction of 23 to 100 .	217
Scheme 5.3. Tandem addition reaction sequence with $\text{TpRe}(\text{CO})(\text{MeIm})(\eta^2\text{-toluene})$ (101).	218
Scheme 5.4. Tandem electrophilic-nucleophilic additions to $\text{TpMo}(\text{NO})(\text{DMAP})(\eta^2\text{-TFT})$ (100) complex.	219
Scheme 5.5. Future reactivity for chemical elaboration from 100 .	222
Scheme 6.1. Traditional synthetic methods for the reduction of pyridines.	238
Scheme 6.2. Coordination and reactivity of pyridines dearomatized through coordination to $\{\text{TpW}(\text{NO})(\text{PMe}_3)\}$.	239
Scheme 6.3. Exchange of 2,5-dimethylfuran with 2-methoxy- and 2,6-dimethoxypyridine to form $\text{TpMo}(\text{NO})(\text{DMAP})(\eta^2\text{-2-methoxypyridine})$ and $\text{TpMo}(\text{NO})(\text{DMAP})(\eta^2\text{-2,6-dimethoxypyridine})$ complexes 121 and 122 , respectively.	242

Scheme 6.4. Electrophilic addition to 121 .	245
Scheme 6.5. Attempted electrophilic-nucleophilic additions to 123 and 124 .	248
Scheme 6.6. Reduction of 124 to yield 125 .	248
Scheme 6.7. Oxonium demethylation of 124 .	249
Scheme 6.8. Attempted tandem electrophilic-nucleophilic additions to 123 and 124 .	250
Scheme 6.9. Protonation of 122 .	254
Scheme 6.10. Exchange of TFT ligand for pyridine-borane and subsequent reactivity.	255

Chapter 1

Introduction

1.1 Introduction

Molecular libraries are largely made up of unsaturated, “flat” molecules.¹ These planar, achiral molecules do not provide the complexity that medicinal chemists need to fully investigate the importance of molecular topology in the design and development of successful drug candidates. For this reason, functionalized alicyclic molecules are inherently more advantageous than their planar analogues because they contain potential stereocenters. Arenes represent a wealth of opportunities as synthons for functionalized alicyclic molecules because of their abundance in nature, their stability, and the diversity of substituents present. Being unsaturated, aromatic molecules offer numerous locations for addition and thus the functionalization and creation of stereocenters can, in theory, easily be achieved. Traditional methods for creating alicyclic molecules from aromatics include the Birch reduction,^{2,3} photocycloaddition,⁴ and enzymatic oxidation.⁵ However, perhaps the greatest potential lies in the ability to complete these transformations using transition metals.

Transition metal fragments such as $\{\text{Cr}(\text{CO})_3\}^{6-8}$, $\{\text{Mn}(\text{CO})_3\}^{+9-11}$, and $\{\text{FeCp}\}^{+12,13}$ can activate aromatics through an electron-withdrawing, η^6 -coordination that makes the arene susceptible to nucleophilic attack. Although this method can yield alicyclic molecules, it more commonly results in the creation of substituted aromatics. A complementary strategy to this use of these electron-poor transition metals lies in the activation of aromatic molecules through η^2 -coordination to an electron-rich metal complex.^{14,15} This coordination is controlled by the donation from a $d\pi$ orbital of the metal into a π^* orbital of the aromatic ligand. This donation results in a disruption of the aromaticity (e.g., dearomatization) making the ligand susceptible to tandem electrophilic-

nucleophilic additions. Utilizing this dearomatization method, the stepwise, controlled synthesis of functionalized alicyclic compounds directly from aromatic molecules can be achieved. The use of electron-rich transition metals in the disruption of aromaticity has been investigated over the past three decades with the following metals: osmium (II),¹⁴ rhenium (I),¹⁴ tungsten (0),¹⁵ and molybdenum (0).^{16, 17}

1.2 {Os(NH₃)₅}²⁺ Dearomatization

The ability to form a thermally stable, η^2 -bound arene complex was first demonstrated in the coordination of {Os(NH₃)₅}²⁺ ([Os]) to benzene.¹⁸ The coordination of the metal occurs through the electron donation from a metal $d\pi$ orbital into a π^* orbital of the aromatic as well as a σ -donation from the aromatic to the metal (Figure 1.1). A key difference in comparison to other η^2 -bound aromatic complexes (i.e., Cu(I),¹⁹ Ag(I),¹⁹ Pt(0),²⁰ Ni(0),²¹ etc.) is that the resulting [Os]-arene complex shows enhanced reactivity of the arene with electrophiles (*vide infra*). In contrast to the other η^2 -bound aromatic complexes mentioned above, [Os] complexes are coordinatively saturated which prevents disfavored electrophilic attack at the metal center when attempting electrophilic additions to the aromatic ligand (Figure 1.1).

The coordination of benzene to [Os] accomplishes two key changes to the reactivity of the arene. First, the double bond bound to the metal is generally protected from further reactivity. In the case of benzene, the resulting dearomatization imparted by the metal yields an organic ligand resembling a diene. Second, the unbound portion of the ring exhibits a greater localization of electron density. The donation of electron density into the ring makes the uncoordinated organic more nucleophilic and promotes the

addition of an electrophile. After the addition of the electrophile, the resulting positively charged allyl complex is stabilized through electron donation from the metal and, in some cases, this cationic complex can be isolated (Figure 1.1).²²

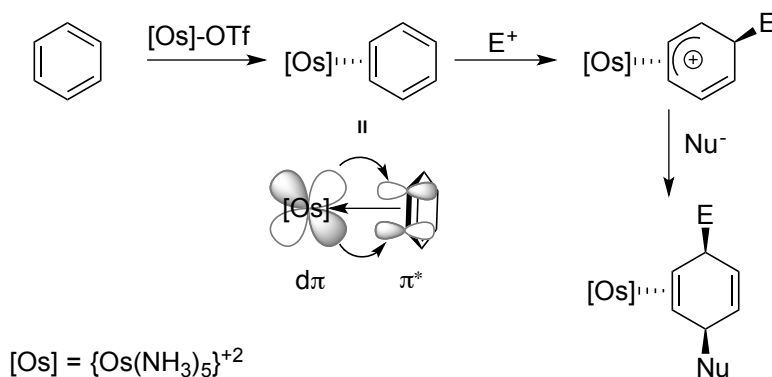


Figure 1.1. Tandem electrophilic-nucleophilic addition to [Os]-benzene complex.

These allyl complexes can then be subjected to nucleophilic attack yielding a net tandem electrophilic-nucleophilic addition product: an [Os]-(η^2 -1,4-cyclohexadiene) complex. Upon oxidation of the metal complex, donation into the π^* orbital is reduced and the functionalized organic ligand is released. Using this method while varying the electrophile (i.e., HOTf, acetals, ketals, Michael acceptors, etc.) and nucleophile (i.e., silyl ketene acetals, enolates, pyrroles, etc.), a variety of functionalized alicyclic molecules were synthesized.²²⁻²⁶

Further expanding upon this approach, [Os] has been shown to bind substituted benzenes, naphthalenes,²⁷ pyrroles,²⁸ pyridines,²⁹ thiophenes,³⁰ and furans.³¹ The regiochemistry of the coordination is dictated by the electronic preference of the aromatic. Binding occurs where aromaticity is least disrupted or linear conjugation is best retained.¹⁴ For instance, [Os] binds naphthalene across the C(1) and C(2) rather than the C(2) and C(3) bond. Binding across the C(1) and C(2) bond retains the aromatic nature of

one of the benzene rings, whereas coordination across the C(2) and C(3) bond disrupts the aromaticity of both rings (Figure 1.2). Once bound, these ligands can undergo simple organic transformations (i.e., Michael additions, Michael-Michael ring closure, Diels-Alder, hydrogenation, etc.) to yield novel small molecules (Scheme 1.1).^{24, 32-34}

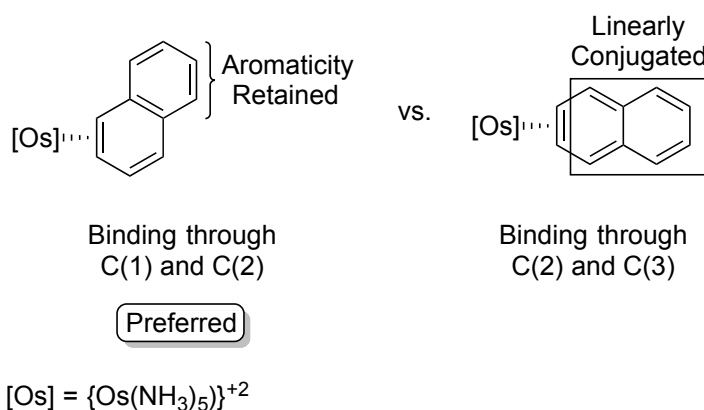
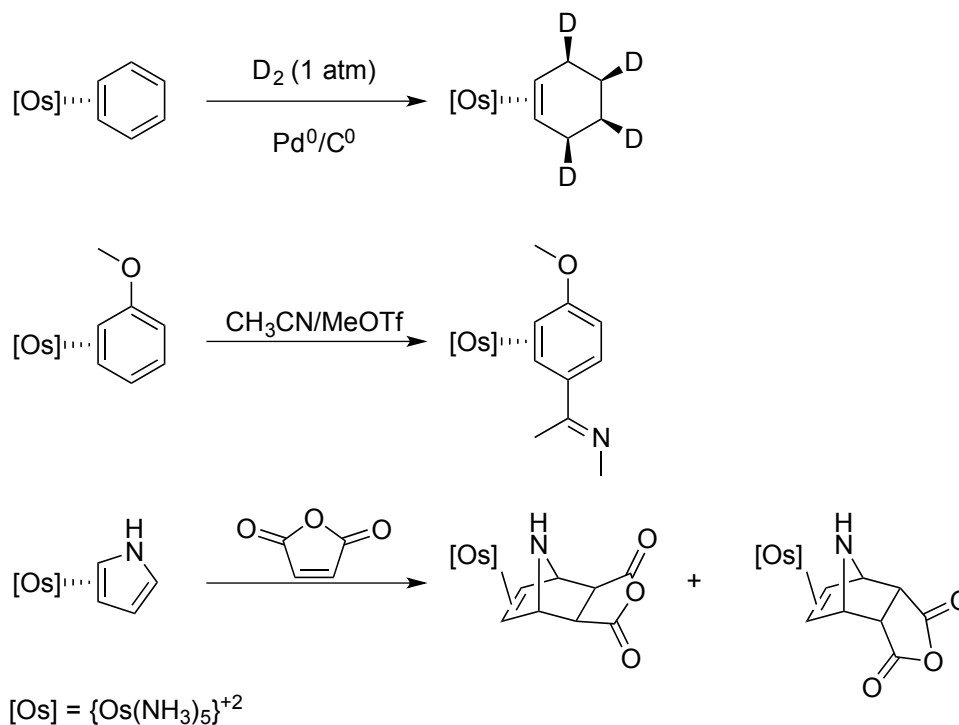


Figure 1.2. Regioselectivity obtained through greater retention of aromaticity.

$[\text{Os}]$, being achiral, cannot differentiate the two entiofaces of prochiral, aromatic ligands being coordinated. Thus racemic mixtures of the $[\text{Os}]$ -aromatic complexes are isolated. Due to the large steric bulk of the metal complex, additions to the coordinated organics occur stereoselectively *anti* to the metal center. However, because the $[\text{Os}]$ -arene complex is racemic, the product of these additions generates enantiomers of the liberated organic products. Aromatics containing chiral substituents have been used to impact the preference in binding orientation; however, this limits the variability in products that can be synthesized using $[\text{Os}]$.³⁵ Incorporating chiral amines into the osmium (II) ligand set impacted the sterics and electronics of the metal center, thus preventing coordination of aromatics.^{36, 37}

Scheme 1.1. Examples of hydrogenation, electrophilic addition, and cycloaddition mediated by $\{\text{Os}(\text{NH}_3)_5\}^{+2}$.



Although $[\text{Os}]$ has proven useful for the synthesis of novel organics from aromatic molecules, its utility was limited due to the high cost and lack of chirality. With the expectation of fixing these issues, the development of dearomatization agents using other transition metals was explored.

1.3 $\{\text{TpRe}(\text{CO})(\text{L})\}$ Dearomatization

Initial attempts to form a new dearomatization agent were focused on retaining several key features that differentiate $[\text{Os}]$ from the unstable or unreactive η^2 -aromatic complexes reported in the literature. To maintain the high electron density needed to overcome aromatic stability, a low-valent d^6 metal with primarily σ -donating ligands is needed. Also desired was a metal center that is coordinatively saturated upon

coordination of the aromatic ligand. As seen by [Os], a coordinatively saturated metal center offers greater compatibility with electrophiles as it disfavors oxidation at the metal center. With these stringent requirements, sufficient electron donation to overcome aromatic stability can be achieved, while oxidation during organic modification is hindered.

Among the literature, reports showed rhenium (I) to have potential in forming thermally stable η^2 bound aromatic complexes.³⁸⁻⁴⁰ The significantly lower cost ($\sim 1/12$ the cost per gram) to use rhenium (I) in place of osmium (II) fixed one of the greatest disadvantages of [Os]. This cost difference can be seen by a comparison of the starting material used for rhenium (I) and osmium (II), perrhenic acid and osmium tetroxide respectively. Although the benefit of cost reduction was promising, the electron-donating ability of rhenium (I) needed to be investigated to determine its ability to backbond and stabilize η^2 bound aromatics. To compare rhenium (I) and osmium (II), dinitrogen-ligand stretching frequencies were used to probe the electron density of potential new dearomatization agents.¹⁴ This analysis showed that the initial rhenium (I) complexes investigated (e.g., $\{cis-[Re(en)_2(PPh_3)]\}^{+1}$, $\{cis-[Re(ampy)_2(PPh_3)]\}^{+1}$, and $\{cis-[Re(ampy)(tbpy)(PPh_3)]\}^{+1}$) (where en = ethylenediamine, ampy = 2-amino-6-methylpyridine, and tbpy = tris(bipyridine)) are too electron rich.⁴¹ To reduce the electron density on rhenium (I), a single π -acidic ligand (e.g., CO) was added to the metal center.

Incorporation of a CO into the ligand set provided enough stability so that a *fac*-[Re(dien)(PPh₃)(CO)(η^2 -furan)](OTf) could be isolated.⁴¹ The isolation of this complex demonstrated the ability of a rhenium (I) complex to coordinate an aromatic molecule;

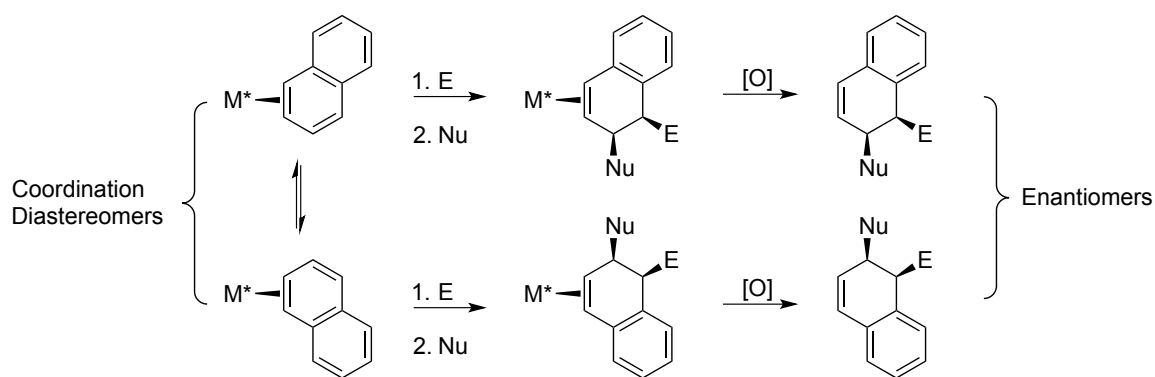
however, no other η^2 bound complexes of this fragment could be isolated. This limitation was believed to be a consequence of the greater steric bulk of the ligand set, mainly the large PPh_3 ligand; and so, a complex with similar electronics, but decreased steric hindrance was sought after. In this vein, studies had shown that a $\text{Cp}^*\text{Re}(\text{CO})_2(\eta^2\text{-benzene})$ complex ($\text{Cp}^* = \text{pentamethylcyclopentadiene}$) was believed to be the intermediate to a bridged binuclear complex, $\text{Cp}^*-(\text{CO})_2\text{Re}(\mu\text{-}1,2\text{-}\eta^2\text{-}3,4\text{-}\eta^2\text{-C}_6\text{H}_6)\text{Re}(\text{CO})_2\text{Cp}^*$.⁴² Although similar in their electronic donations, Tp ($\text{Tp} = \text{hydridotris(pyrazolyl)borate}$) shows a greater ability than Cp^* to stabilize a 6-coordinate octahedral geometry.⁴³⁻⁴⁶ This enforced geometry is believed to reduce the likelihood of potential $\text{TpRe}(\text{L})_2(\eta^2\text{-aromatic})$ complexes to undergo aromatic C-H oxidative addition. Using this information, the synthesis of $\text{TpRe}(\text{CO})_2(\eta^2\text{-aromatic})$ complexes was investigated. However, the $\{\text{TpRe}(\text{CO})_2\}$ fragment proved too electron poor to stabilize η^2 binding of aromatics.¹⁴

To provide more electron density within the rhenium (I) metal center, one of the CO ligands of $\{\text{TpRe}(\text{CO})_2\}$ was replaced with a more σ -donating ligand (L). The donating abilities of the $\{\text{TpRe}(\text{CO})(\text{L})\}$ fragment vary based on the differing degree of σ -donation from L. Subsequent success was found with complexes of the form $\text{TpRe}(\text{CO})(\text{PMe}_3)(\text{L}\pi)$ (where $\text{L}\pi = \text{naphthalene, thiophene, and furan}$). Thus a new generation of dearomatization agents was born of the form $\{\text{TpM}(\pi\text{-acid})(\text{L})\}$ (where $\text{M} = \text{Re, Mo, or W}$; $\pi\text{-acid} = \text{CO or NO}$; and $\text{L} = \text{1-methylimidazole (MeIm), 1-butylimidazole (BuIm), trimethylphosphine (PMe}_3\text{), triphenylphosphine (PPh}_3\text{), trimethylphosphite (POMe}_3\text{), tert-butylnitrile (}^t\text{BuCN), pyridine, NH}_3\text{, or 4-dimethylaminopyridine (DMAP)}$).⁴⁷⁻⁴⁹ In the case of $\{\text{TpRe}(\text{CO})(\text{L})\}$, using MeIm as an

ancillary ligand creates a complex able to bind the largest variety of aromatics.¹⁵ These include substituted pyrroles, benzenes, and pyridines, which can be coordinated directly during the reduction of the $\text{TpRe}(\text{CO})(\text{Br})_2$ precursor in the presence of MeIm. It was found that other ligands could replace benzene in the complex $\text{TpRe}(\text{CO})(\text{MeIm})(\eta^2\text{-benzene})$ as a result of the lability of the coordinated benzene ligand.⁴⁸ Through this exchange the binding of lutidine, which is sensitive to the reduction conditions (i.e., Na^0) mentioned above, occurred to yield the $\text{TpRe}(\text{CO})(\text{MeIm})(\eta^2\text{-lutidine})$ complex.⁴⁸

Complexes of the form $\text{TpM}(\pi\text{-acid})(\text{L})(\text{L}\pi)$ are chiral. Assuming one could start with a single enantiomer, stereoselective organic transformations on the aromatic ligand would theoretically yield enantio-enriched products. However, coordination of prochiral, unsaturated molecules yields a diastereomeric mixture differing in either the position or enantioface that the metal binds to (Scheme 1.2).

Scheme 1.2. Organic products isolated as a racemic mixture from a diastereomeric mixture of a stereogenic metal center.



Where M^* is a chiral metal center

Theoretically, if these coordination diastereomers were isolated as a 1:1 ratio, then organic transformations on said mixture would yield the organic as a racemic mixture. Thus, an in-depth analysis on how to selectively obtain or react one coordination diastereomer over the other is required.

In complexes of the form $\text{TpM}(\pi\text{-acid})(\text{L})(\text{L}\pi)$ the coordinated ligand ($\text{L}\pi$) will orient itself so that the π -bond is parallel to the M-L bond. This preference is due to the double-faced π -acid (e.g., CO or NO) that lowers the energy of two $d\pi$ orbitals, leaving the remaining filled $d\pi$ orbital (the HOMO) unaffected. This metal-centered HOMO overlaps with the antibonding orbital of the ligand, favoring the ligand to orient orthogonal to the M- π -acid bond.⁵⁰ In addition to this electronic impact on ligand orientation, the electronic preference to orient partial positive charges distal to the ancillary ligand (L) as well as potential π -stacking with L (i.e., where L contains a π -system) can determine the preferred orientation of the coordinated ligand ($\text{L}\pi$). Furthermore, the prevention of steric hindrance can cause a preference for different coordination diastereomers.⁴⁹ By observing the preferred coordination diastereomers formed by coordination of various ligands to $\{\text{TpRe}(\text{CO})(\text{MeIm})\}$, the steric repulsion in each quadrant formed by the ligands *cis* to the $\text{L}\pi$ ligand was found to increase in the order of $d < a < b < c$ (Figure 1.3).⁵¹ Following this trend, coordination diastereomers of $\text{TpRe}(\text{CO})(\text{MeIm})(\eta^2\text{-aromatic})$ favor placing the bulk of the unbound portion of the ring in the least hindered quadrant d. This can be seen in Figure 1.3 where coordination diastereomer **A** positions the naphthalene ring “up” or proximal to the ancillary ligand where $\text{L} = \text{MeIm}$ or Py . For rhenium (I), replacing L with a bulkier ancillary ligand increases the steric hindrance in quadrant d. For instance, $\text{TpRe}(\text{CO})(\text{PMe}_3)(\eta^2\text{-$

naphthalene) has a greater steric hindrance in quadrant d thus favoring the “down” coordination diastereomer (**B**).⁵²

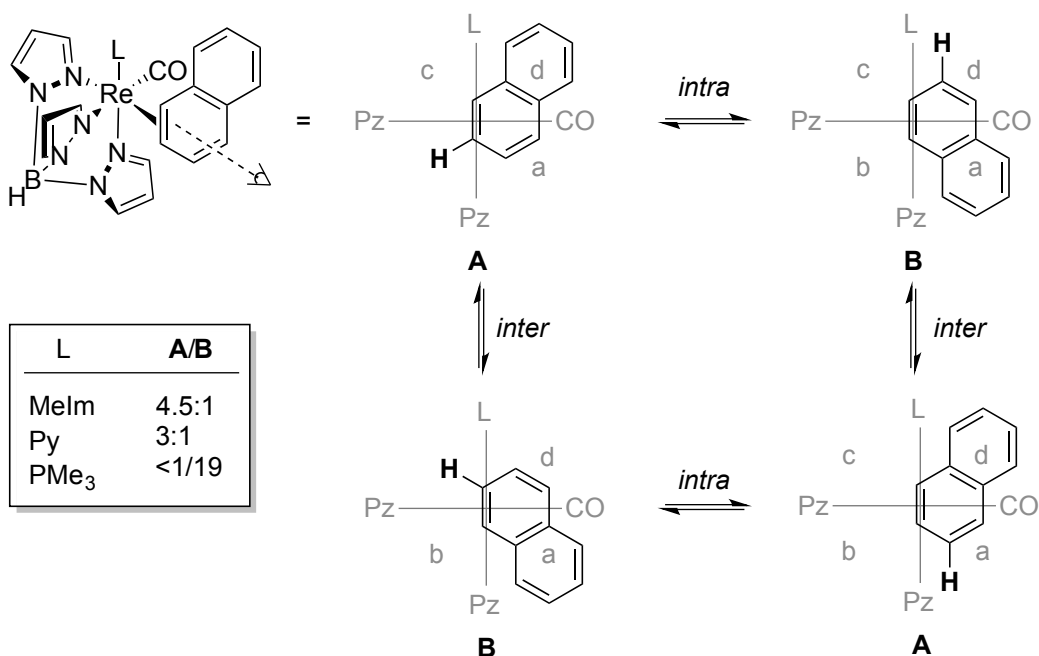
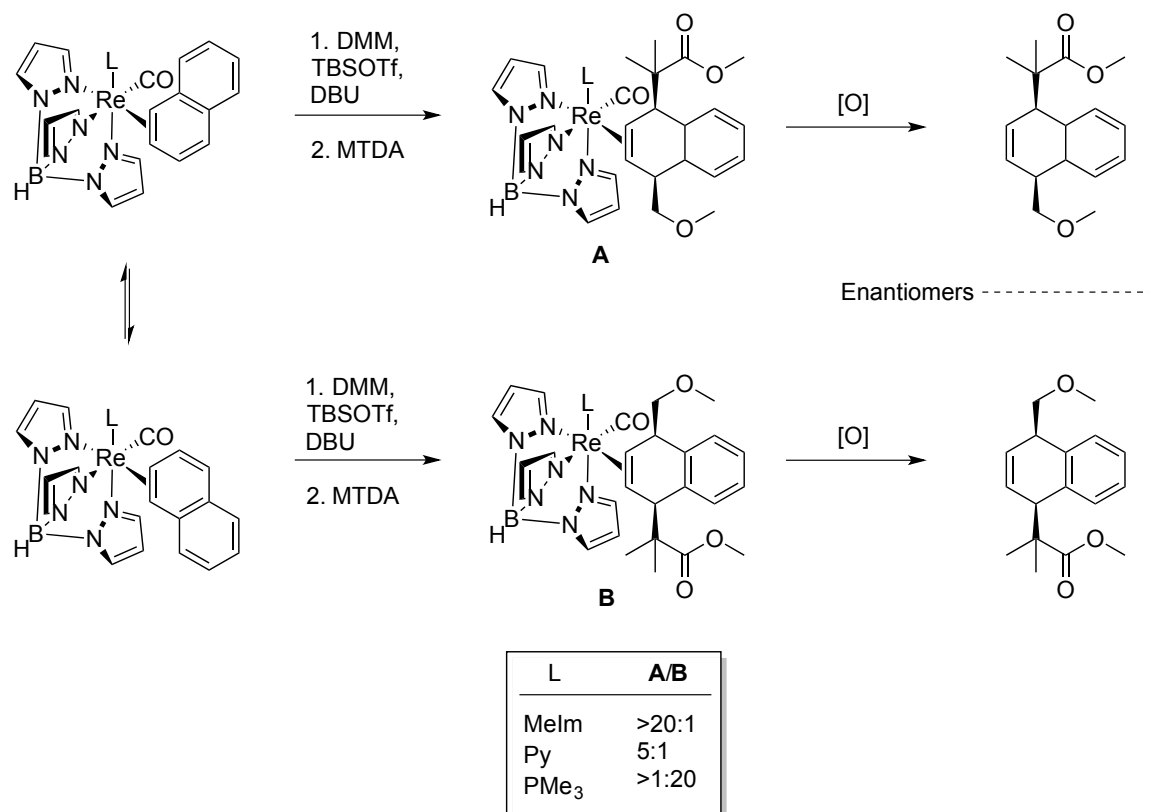


Figure 1.3. Coordination diastereomers of $\text{TpRe}(\text{CO})(\text{L})(\eta^2\text{-naphthalene})$.

Although the coordination diastereomers can be controlled by sterics, as described above, these diastereomers maintain isomerization equilibrium. The mechanism of this isomerization has been determined to occur through two non-dissociative pathways, interfacial (face-flip) and intrafacial (ring walk) isomerization. By studying spin-saturation experiments of $\text{TpRe}(\text{CO})(\text{L})(\text{L}\pi)$, it was found that both face-flip and ring walk mechanisms are operative and preference of either mechanism depends on the aromatic being bound as well as the ability to backbond from the metal. In the case of naphthalene, spin-saturation experiments, depicted by the bold hydrogens in Figure 1.3, support a preference for intrafacial isomerization during the conversion between **A** and **B**.⁵¹

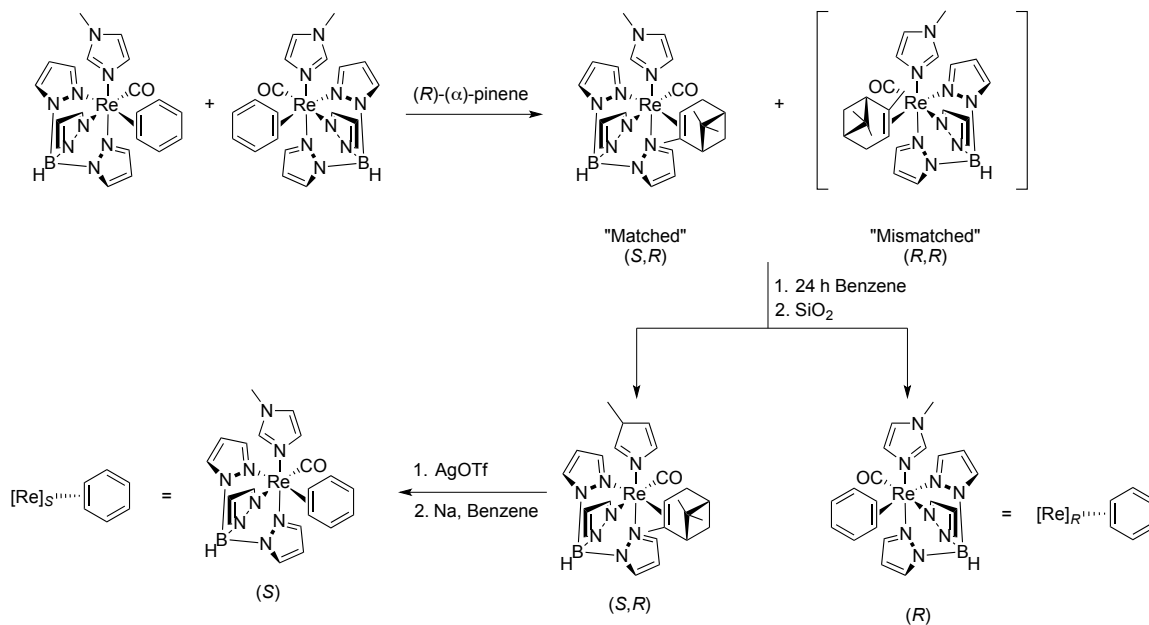
Scheme 1.3. Diastereoselective control of electrophilic-nucleophilic additions to $\text{TpRe}(\text{CO})(\text{L})(\eta^2\text{-naphthalene})$.



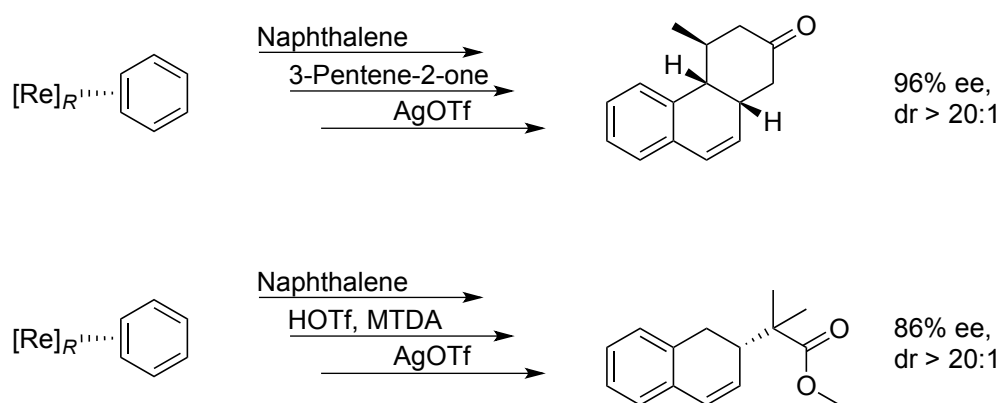
With this steric control of coordination diastereomers, the desired enantiomer of an organic can be selectively synthesized, provided that the metal stereocenter is of a single configuration (R/S). For instance, $\text{TpRe}(\text{CO})(\text{L})(\eta^2\text{-naphthalene})$ undergoes a tandem electrophilic-nucleophilic addition to form a specific enantiomer of a 1,4-dihydronaphthalene depending on the ancillary ligand (L) used (Scheme 1.3).⁵² In addition to the stereoselective control, $\text{TpRe}(\text{CO})(\text{L})(\eta^2\text{-naphthalene})$ has demonstrated regioselective control by isolating a 1,2- or 1,4-dihydronaphthalene based on which ancillary ligand is used.⁵³ Although controlling the diastereomeric ratio allows for the selective synthesis of enantiomers, because complexes of the form $\text{TpRe}(\text{CO})(\text{L})(\eta^2\text{-$

aromatic) are synthesized as a racemic mixture of the two enantiomers of the metal, the organic products isolated directly from these complexes will also be racemic mixtures.

Utilizing the steric profile described above, it was found that enantioenrichment of rhenium (I) could be induced using the coordination of the chiral and bulky α -pinene.⁵⁴ Stirring the $\text{TpRe}(\text{CO})(\text{MeIm})(\eta^2\text{-benzene})$ complex with (*R*)- α -pinene yields two diastereomers of the metal alkene complex. To minimize steric repulsion in these diastereomers, the metal coordinates to the face of the alkene opposite to the geminal methyls. A more stable, “matched” diastereomer (*S* hand of the metal) is isolated where the olefinic methyl is placed into quadrant b with no substituents in quadrant c. The less stable, “mismatched” diastereomer (*R* hand of the metal) is suspected to form by placing the olefinic methyl in quadrant c, creating great steric repulsion. Stirring a mixture of the matched and mismatched complexes in benzene allows for the steric repulsion in the mismatched isomer to be relieved by exchanging with benzene. The resulting *R*- $\text{TpRe}(\text{CO})(\text{MeIm})(\eta^2\text{-benzene})$ complex can then be separated from the matched α -pinene complex through chromatography. The remaining matched α -pinene complex can then be oxidized and reduced in the presence of benzene to isolate the *S*- $\text{TpRe}(\text{CO})(\text{MeIm})(\eta^2\text{-benzene})$ complex (Scheme 1.4), effectively resolving the two hands of the chiral metal complex.

Scheme 1.4. Enantioenrichment of $\text{TpRe}(\text{CO})(\text{L})(\eta^2\text{-benzene})$.

The benzene ligands of these enantioenriched complexes can then be exchanged for other aromatic ligands, while retaining the chiral enrichment of the metal center. The resulting enantioenriched complexes can undergo organic transformations to yield organics with high levels of enantiopurity (Scheme 1.5).^{52, 55, 56}

Scheme 1.5. Enantioselective organic modifications using $\{\text{TpRe}(\text{CO})(\text{MeIm})\}$.

$\{\text{TpRe}(\text{CO})(\text{L})\}$ demonstrated a wide breadth of reactivity and adjustability in the ligand set. However, in addition to the high cost associated with its stoichiometric use, another disadvantage was the inability to consistently synthesize the $\text{TpRe}(\text{CO})(\text{MeIm})(\eta^2\text{-benzene})$ on a multigram scale. Some reports even indicate that upwards of 30 days are needed for the completion on a 5 g scale.⁵⁷ Over the course of 15 years, the development of $\{\text{TpRe}(\text{CO})(\text{L})\}$ provided well-learned lessons that were subsequently applied to other transition metals.

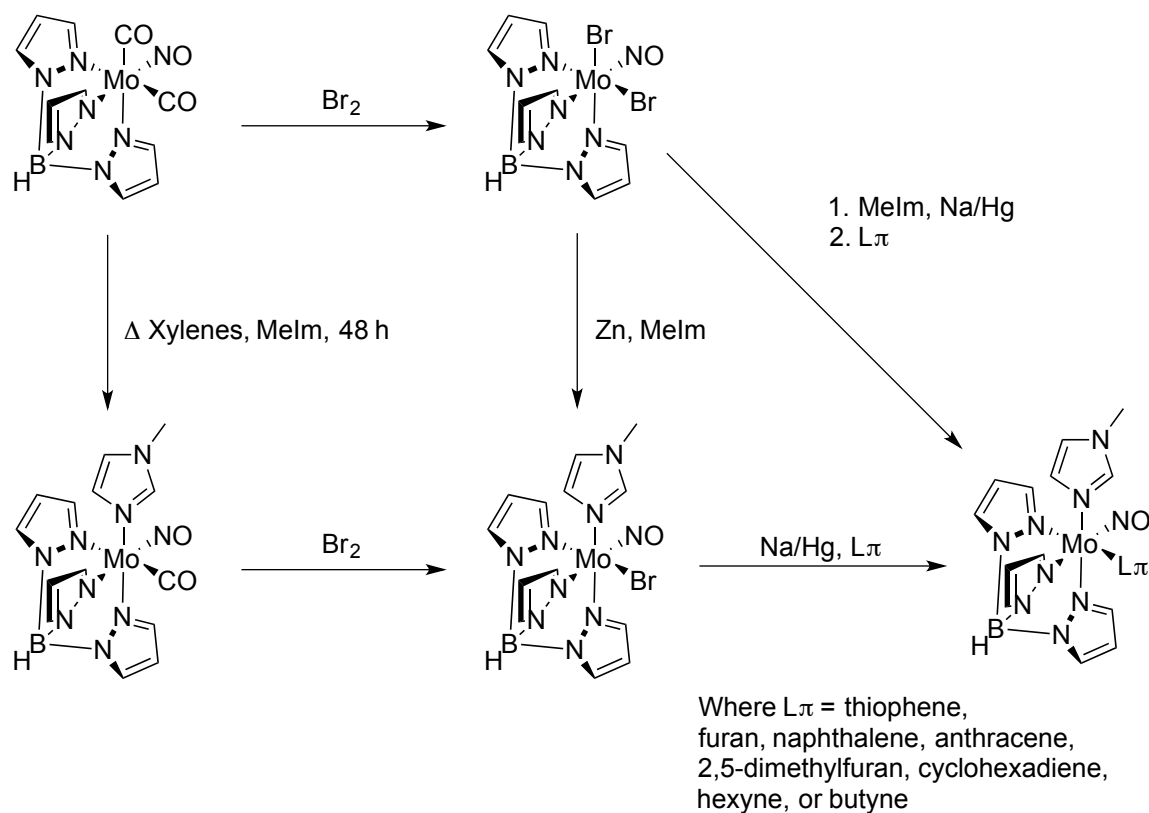
1.4 $\{\text{TpMo}(\text{NO})(\text{MeIm})\}$ Dearomatization

Molybdenum offers an attractive candidate for the center of these metal scaffolds as it is a nontoxic, second row metal that is commercially available at a fraction of the cost of osmium (II) or rhenium (I). Comparing the reduction potentials of $[\text{Re}(\text{CO})_2(\text{dmpe})_2]^+1$ (1.66 V) and $\text{Mo}(\text{CO})_2(\text{dmpe})_2$ (0.22 V) suggests that molybdenum, being more electron rich, requires a stronger π -acid than CO. Through a comparison of $[\text{TpMo}(\text{CO})_3]^{-1}$ and $\text{TpMo}(\text{CO})_2(\text{NO})$ it was found that replacement of CO with NO^+ raises the reduction potential of molybdenum by approximately 1 V.¹⁷ This increase in reduction potential provides the correct electronics needed to stabilize an eta-2 coordinated aromatic. The addition of NO^+ also balances the charge from the Tp ligand, which provides a neutral complex and allows for a greater compatibility with purification through chromatography. Thus the development of $\text{TpMo}(\text{NO})(\text{L})(\text{L}\pi)$ was pursued.

Utilizing reports by McCleverty, $\text{TpMo}(\text{NO})(\text{Br})_2$ was made and subsequent reductions were attempted.⁵⁸ By reducing $\text{TpMo}(\text{NO})(\text{Br})_2$ in the presence of the desired MeIm and an excess of $\text{L}\pi$ (where $\text{L}\pi$ = thiophene, furan, naphthalene), the desired

TpMo(NO)(MeIm)(L π) can be isolated in fair yields (~40% average).¹⁷ In addition to this method, a stepwise synthesis was developed wherein TpMo(NO)(MeIm)(Br) is isolated, thereby preventing potential decomposition pathways in the aforementioned one-pot synthesis.¹⁶

Scheme 1.6. Synthesis of TpMo(NO)(MeIm)(η^2 -L π).

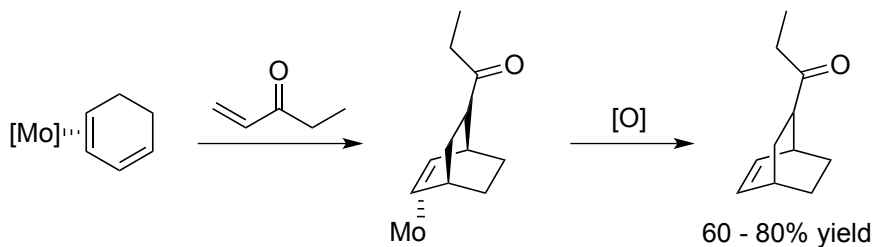


The isolation of TpMo(NO)(MeIm)(Br) is accomplished through a reduction of TpMo(NO)(Br)₂ with Zn⁰ in the presence of MeIm. Alternatively, by refluxing a xylenes solution of TpMo(CO)₂(NO) and MeIm, TpMo(CO)(NO)(MeIm) can be isolated and subsequently oxidized to yield TpMo(NO)(MeIm)(Br) (Scheme 1.6). In addition to isolating the TpMo(NO)(MeIm)(L π) described above in the one-step process from TpMo(NO)(Br)₂, the reduction of TpMo(NO)(MeIm)(Br) in presence of the desired

ligand yielded $\text{TpMo(NO)(MeIm)(L}\pi\text{)}$ ($\text{L}\pi$ = anthracene, 2,5-dimethylfuran, cyclohexadiene, hexyne, and butyne) in comparable yields (Scheme 1.6).

Organic modifications with complexes of the form $\text{TpMo(NO)(MeIm)(L}\pi\text{)}$ were demonstrated for complexes where $\text{L}\pi$ = naphthalene or cyclohexadiene. $\text{TpMo(NO)(MeIm)(}\eta^2\text{-naphthalene)}$ was found to undergo a tandem electrophilic-nucleophilic addition via protonation and subsequent addition of methyl trimethylsilyl dimethylketene acetal (MTDA) to yield a 1,2-dihydronaphthalene. For the complex $\text{TpMo(NO)(MeIm)(}\eta^2\text{-cyclohexadiene)}$, the electron donation from the metal fragment is able to activate the conjugated diene towards Diels-Alder transformations, resulting in the formation of cycloadducts not directly accessible from the uncoordinated diene (Scheme 1.7).⁵⁹ However, further elaboration of the organic modification of arenes using the $\{\text{TpMo(NO)(MeIm)}\}$ was prevented due to a greater sensitivity of $\{\text{TpMo(NO)(MeIm)}\}$ towards oxidation in comparison to its osmium (II) and rhenium (I) analogues. For instance, relative to $\text{TpRe(CO)(MeIm)(}\eta^2\text{-naphthalene)}$ ($E_{1/2}$ = 0 V), $\text{TpMo(NO)(MeIm)(}\eta^2\text{-naphthalene)}$, with a more negative anodic wave ($E_{\text{p,a}}$ of -0.26 V), is more prone to oxidation by electrophilic reagents.

Scheme 1.7. Diels-Alder synthesis of cycloadducts promoted by $\{\text{TpMo(NO)(MeIm)}\}$.



In addition to the difficulties with transforming aromatics through organic modifications, $\{\text{TpMo}(\text{NO})(\text{MeIm})\}$ also failed to form stable complexes with benzene, pyrrole, pyridine, and their derivatives. These limitations led to a discontinuation of the pursuit of molybdenum metal complexes as dearomatization agents; however, a promising tungsten moiety proved successful.

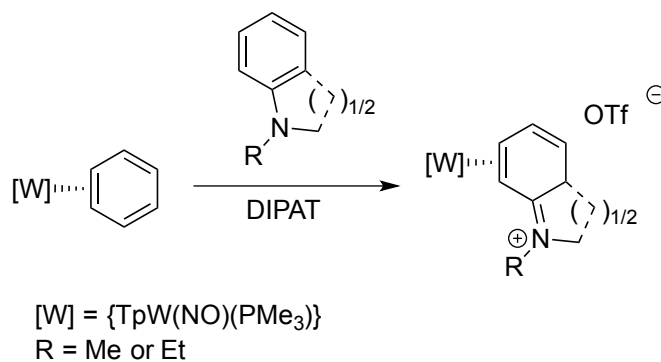
1.5 $\{\text{TpW}(\text{NO})(\text{PMe}_3)\}$ Dearomatization

It was hypothesized that $\{\text{TpMo}(\text{NO})(\text{MeIm})\}$ lacks the sufficient backbonding capabilities that the third-row transition metal fragments $\{\text{Os}(\text{NH}_3)_5\}^{2+}$ and $\{\text{TpRe}(\text{CO})(\text{MeIm})\}$ provide to support η^2 binding with benzene. For this reason, the development of $\{\text{TpW}(\text{NO})(\text{L})\}$ was targeted as a more capable group VI congener for dearomatization. Comparing the reduction potentials of $\text{TpRe}(\text{CO})_3$ and $\text{TpW}(\text{NO})(\text{CO})_2$, it is seen that the latter is approximately 300 mV more reducing.⁶⁰ Analyzing the various σ -donating capabilities of ancillary ligands used with $\{\text{TpRe}(\text{CO})(\text{L})\}$ ⁴⁹, it was hypothesized that PMe_3 would properly balance the increased reducing power of $\{\text{TpW}(\text{NO})(\text{CO})\}$ to generate a complex capable of coordinating aromatic molecules in an η^2 fashion. $\text{TpW}(\text{NO})(\text{Br})_2$ is synthesized following a similar method used to make $\text{TpMo}(\text{NO})(\text{Br})_2$. By subjecting $\text{TpW}(\text{NO})(\text{Br})_2$ to reductive conditions in the presence of PMe_3 , the precursor $\text{TpW}(\text{NO})(\text{PMe}_3)(\text{Br})$ is made and can subsequently be reduced in the presence of benzene to isolate $\text{TpW}(\text{NO})(\text{PMe}_3)(\eta^2\text{-benzene})$.⁶¹

Similar to the previous dearomatization agents mentioned above, the $\{\text{TpW}(\text{NO})(\text{PMe}_3)\}$ ($[\text{W}]$) fragment is able to bind a broad array of aromatic molecules (i.e., substituted benzenes, pyridines, furans, thiophenes, pyrroles, etc.).⁶² In contrast to

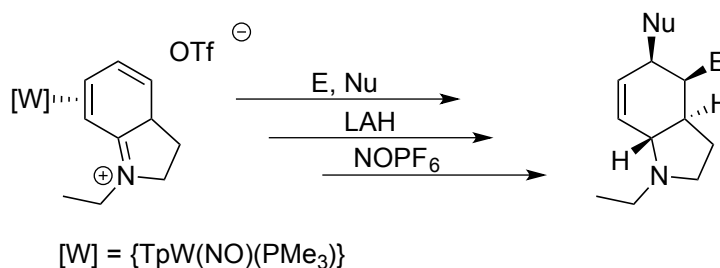
small scales and long reaction times in the synthesis of $\text{TpRe}(\text{CO})(\text{MeIm})(\eta^2\text{-benzene})$, $\text{TpW}(\text{NO})(\text{PMe}_3)(\eta^2\text{-benzene})$ can be isolated on a multigram scale (upwards of 12 g) requiring only 24 h for reaction completion.⁶³ Attempts to coordinate more electron-rich aromatic molecules, such as N-alkylated anilines, indolines, and quinolines, through a direct ligand exchange from the benzene complex result in the formation of intractable mixtures. However, purported η^2 -coordinated complexes of these aromatics have been observed during these exchanges using cyclic voltammetry (CV). These unstable complexes can be trapped by in situ protonation during the ligand exchange reaction through the addition of weak anilinium acids (Scheme 1.8).^{64, 65}

Scheme 1.8. In situ protonation during the exchange of $\text{TpW}(\text{NO})(\text{PMe}_3)(\eta^2\text{-benzene})$ with aniline, indoline, or quinoline.



Following a similar method for organic modification, the indolinium species has shown a great utility in organic modification utilizing tandem electrophilic-nucleophilic additions. The resulting functionalized tetrahydroindolines contain upwards of four additional stereocenters controlled by the metal (Scheme 1.9).⁶⁶

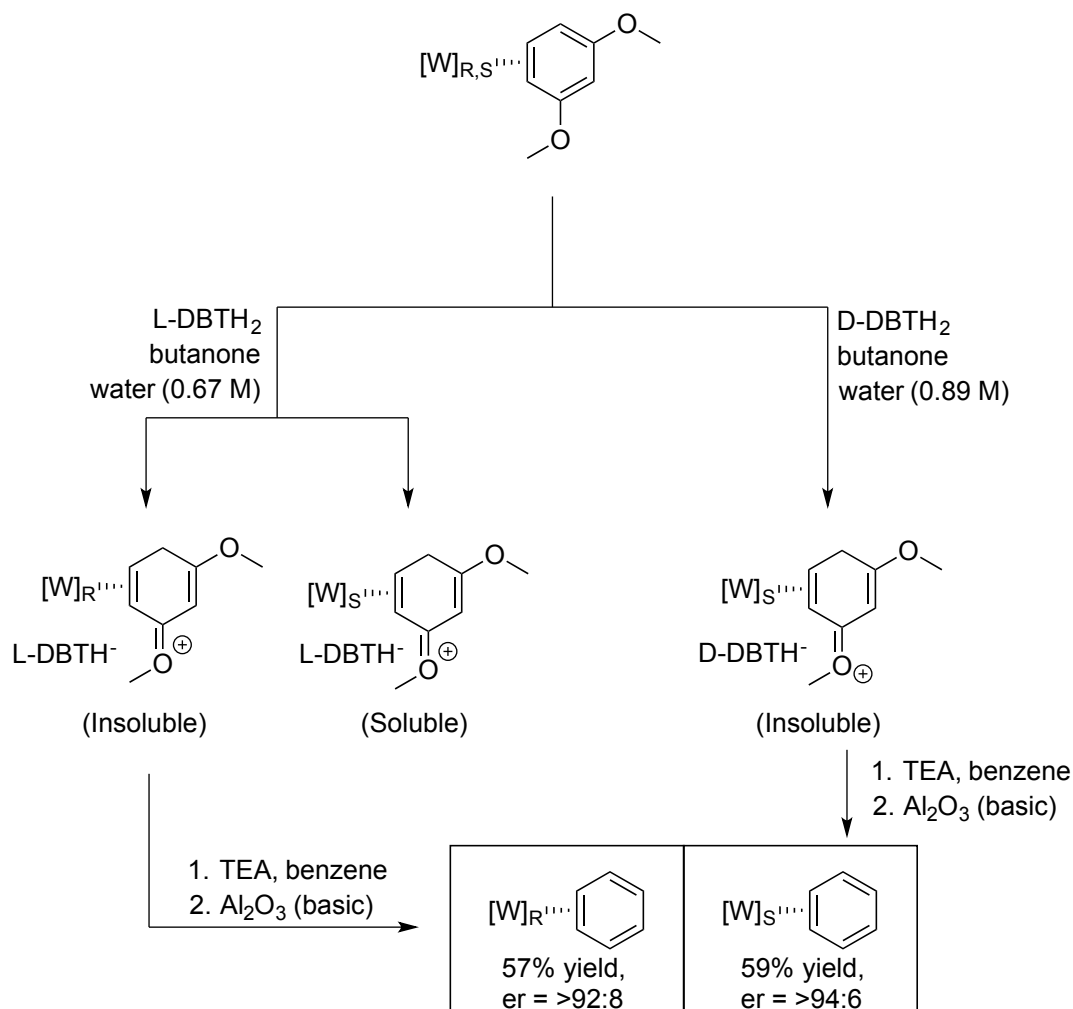
Scheme 1.9. Organic modification of $\text{TpW}(\text{NO})(\text{PMe}_3)(\eta^2\text{-indolinium})$.



Similar to $\{\text{TpRe}(\text{CO})(\text{MeIm})\}$, the chiral $[\text{W}]$ fragment can be resolved to generate enantioenriched complexes of aromatic molecules. Although attempts to follow the same enrichment method as $\{\text{TpRe}(\text{CO})(\text{MeIm})\}$ (e.g., α -pinene exchange) showed limited effectiveness,⁶⁷ the use of chiral tartrate salts proved much more successful. Protonation of $\text{TpW}(\text{NO})(\text{PMe}_3)(\eta^2\text{-1,3-dimethoxybenzene})$ with *L*-dibenzoyltartaric acid results in the formation of thermally stable oxonium complexes. The diastereomeric salts of these complexes can be separated by the differences in their solubility. Once separated, the salts can be deprotonated and the resulting resolved dimethoxybenzene complex can undergo exchange with benzene, yielding the primary precursor for dearomatization complexes formed using $[\text{W}]$ (Scheme 1.10).⁶⁸ Current methods to utilize this enantioenriched complex for organic modifications are underway.

Although the $\{\text{TpW}(\text{NO})(\text{PMe}_3)\}$ fragment has shown a great versatility in organic synthesis and scale, a few disadvantages remain. The use of PMe_3 as an ancillary ligand provides a useful handle for monitoring reactions through ^{31}P NMR; however, the high cost of this ligand limits the practicality of the widespread use of this complex. Unlike $\{\text{TpRe}(\text{CO})(\text{L})\}$, the ancillary ligand of $[\text{W}]$ cannot be altered without sacrificing the ability to bind a broad array of aromatics.

Scheme 1.10. Isolation of enantioenriched $\text{TpW}(\text{NO})(\text{PMe}_3)(\eta^2\text{-benzene})$ complex.



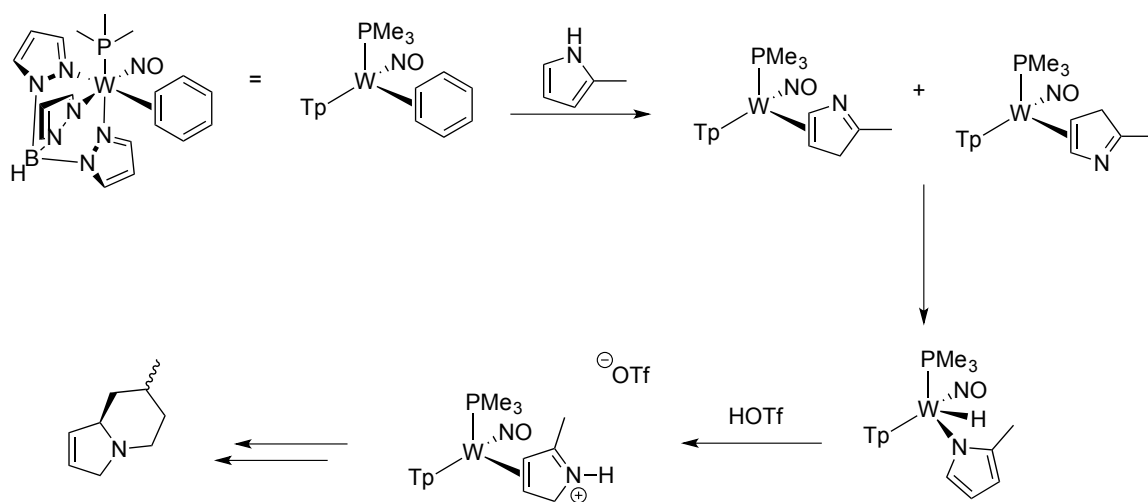
Coordination of a limited number of aromatic molecules has been shown using $\text{P}(\text{OMe})_3$ as the ancillary ligand on the tungsten complex,⁶² but broad applicability is only seen with tungsten for the PMe_3 complex. The high cost of this one ligand of the complex is a severe limitation to the adoption of this dearomatization methodology for synthetic applications, due to the stoichiometric nature of this chemistry.

In comparison to $\{\text{Os}(\text{NH}_3)_5\}^{+2}$ and $\text{TpRe}(\text{CO})(\text{L})$, $[\text{W}]$ has shown a greater propensity to undergo oxidative addition into C-H and N-H bonds. As such, multiple 7-coordinate hydride complexes have been reported during the binding of various ligands

(i.e., benzene,⁶³ α,α,α -trifluorotoluene (TFT),⁶³ and substituted pyrroles⁶⁹) to $\{\text{TpW}(\text{NO})(\text{PMe}_3)\}$. For instance, in the binding of 2-methylpyrrole, a 7-coordinate hydride complex is made by oxidative addition into the N-H bond. This hydride complex can be converted to an eta-2 bound, pyrrolium complex via protonation and then subjected to a Michael addition and ring closure to form an indolizidine core (Scheme 1.11).

In addition to the greater propensity for oxidative additions into C-H and N-H bonds, [W] has also demonstrated an ability to oxidatively add C-F bonds of fluorinated aromatics.⁷⁰ Unlike the hydride complexes described above, the product of an oxidative addition into C-F bonds cannot be converted to an eta-2 bound complex via protonation. For this reason, tungsten is limited in the dearomatization of fluorinated aromatics where the fluorine is bound directly to the arene.

Scheme 1.11. Synthesis of the eta-2 bound pyrrolium complex and subsequent synthesis of an indolizidine core.



Furthermore, to isolate the modified organics via oxidative decomplexation, harsh oxidants (i.e., ceric ammonium nitrate (CAN) and 2,3-Dichloro-5,6-dicyano-1,4-benzoquinone (DDQ)) are often required, which can create unwanted side reactions. To address this issue, further development of complexes of the form $\{\text{TpMo}(\text{NO})(\text{L})\}$ has been explored and will be discussed herein.

1.6 Developing the $\{\text{TpMo}(\text{NO})(\text{L})\}$ Dearomatization Agent

The project presented in this dissertation seeks to develop a dearomatization agent that contains all of the advantages of the previous three decades worth of exploration in one metal scaffold. Mainly, we are looking to incorporate the following characteristics: recyclability, scalability, adjustability in the ligand set, and the ability to enantioenrich the metal center. As mentioned previously, $\text{TpRe}(\text{CO})(\text{MeIm})(\alpha\text{-pinene})$ can be oxidized and subsequently reduced to yield $\text{TpRe}_{(\text{S})}(\text{CO})(\text{MeIm})(\eta^2\text{-benzene})$. With a great stability in its plus one oxidation state, we believe $\{\text{TpMo}(\text{NO})(\text{L})\}$ has the potential to follow a similar method for recyclability. With the demonstrated ability to consistently isolate [W]-aromatic complexes on multigram scales, we wish to develop a molybdenum analogue that can form isolable η^2 bound complexes on the same or greater scale as [W]. Furthermore, we aim to develop a metal center where electronic and steric factors can be tuned by the use of various ancillary ligands (L) to allow for the binding of a broad array of aromatic ligands and their subsequent organic transformation. The ability to enantioenrich the metal center is beyond the scope of this project; however, progress on the project described above is reported herein.

1.7 References

1. Lovering, F.; Bikker, J.; Humblet, C. *J. Med. Chem.* **2009**, 52, (21), 6752.
2. Mander, L. N.; Hook, J. M. *Nat. Prod. Reports* **1986**, 37.
3. Birch, A. J.; Hinde, A. L.; Radom, L. *J. Am. Chem. Soc.* **1981**, 103, 284.
4. Schreiber, S. L. *Science* **1985**, 227, 857.
5. Hudlicky, T. *Pure & Appl. Chem.* **1994**, 66, 2067.
6. Amurrio, D.; Kahn, K.; Kündig, E. P. *J. Org. Chem.* **1996**, 61, 2258.
7. Barluenga, J.; Trabanco, A. A.; Flórez, J.; García-Granda, S.; Martín, E. *J. Am. Chem. Soc.* **1996**, 118, 13099.
8. Davies, S. G.; Coote, S. J.; Goodfellow, C. L., *Synthetic Applications of Chromium Tricarbonyl Stabilized Benzylic Carbanions*. JAI Press, Ltd.: London, 1991; Vol. 2, p 2.
9. Blagg, J. *Contemporary Organic Synthesis* **1995**, 2, (1), 43.
10. Davies, S. G.; McCarthy, T. D., *Comprehensive Organometallic Chemistry II*. Abel, E. W., Ed. Pergamon Press: Oxford, 1995; Vol. 12, Chapter 9.3.
11. Thompson, R. L.; Lee, S.; Rheingold, A. L.; Cooper, N. J. *Organometallics* **1991**, 10, 1657.
12. Astruc, D. *Tetrahedron* **1983**, 39, (24), 4027
13. Bakhtiar, R.; Jacobson, D. B. *J. Am. Soc. Mass Spectrom.* **1996**, 7, 938.
14. Brooks, B. C.; Gunnoe, T. B.; Harman, W. D. *Coord. Chem. Rev.* **2000**, (206-207), 3.
15. Keane, J. M.; Harman, W. D. *Organometallics* **2005**, 24, 1786.
16. Mocella, C. J.; Delafuente, D. A.; Keane, J. M.; Warner, G. R.; Friedman, L. A.; Sabat, M.; Harman, W. D. *Organometallics* **2004**, 23, (16), 3772.
17. Meiere, S. H.; Keane, J. M.; Gunnoe, T. B.; Sabat, M.; Harman, W. D. *J. Am. Chem. Soc.* **2003**, 125, (8), 2024.
18. Harman, W. D.; Taube, H. *J. Am. Chem. Soc.* **1987**, 109, 1883.
19. Silverthorn, W. E. *Adv. Organomet. Chem.* **1975**, 13, 48.

20. Browning, J.; Green, M.; Spencer, J. L.; Stone, F. G. *J. Chem. Soc., Dalton Trans.* **1974**, 97.
21. Boese, R.; Stanger, A.; Stellberg, P.; Shazar, A. *Angew. Chem. Int. Ed. Engl.* **1993**, 32, 1475.
22. Harman, W. D.; Hasegawa, T.; Taube, H. *Inorg. Chem.* **1991**, 113, 453.
23. Chordia, M. D.; Harman, W. D. *J. Am. Chem. Soc.* **2000**, 122, (12), 2725.
24. Harman, W. D.; Taube, H. *J. Am. Chem. Soc.* **1988**, 110, 7906.
25. Kopach, M. E.; Harman, W. D. *J. Am. Chem. Soc.* **1994**, 116, 6581.
26. Kopach, M. E.; Harman, W. D.; Hipple, W. G. *J. Am. Chem. Soc.* **1992**, 114, 1737.
27. Winemiller, M. D.; Harman, W. D. *J. Org. Chem.* **2000**, 65, 1249.
28. Gonzalez, J.; Koontz, J. I.; Myers, W. H.; Hodges, L. M.; Sabat, M.; Nilsson, K. R.; Neely, L. K.; Harman, W. D. *J. Am. Chem. Soc.* **1995**, 117, 3405.
29. Cordone, R.; Taube, H. *J. Am. Chem. Soc.* **1987**, 109, 8101.
30. Spera, M. L.; Harman, W. D. *Organometallics* **1995**, 14, 1559.
31. Chen, H.; Hodges, L. M.; Liu, R.; Stevens, W. C.; Sabat, M.; Harman, W. D. *J. Am. Chem. Soc.* **1994**, 116, 5499.
32. Harman, W. D.; Sekine, M.; Taube, H. *J. Am. Chem. Soc.* **1988**, 110, 5725.
33. Kopach, M. E.; Gonzalez, J.; Harman, W. D. *J. Am. Chem. Soc.* **1991**, 113, 8972.
34. Cordone, R.; Harman, W. D.; Taube, H. *J. Am. Chem. Soc.* **1989**, 111, 5969.
35. Chordia, M. D.; Harman, W. D. *J. Am. Chem. Soc.* **1998**, 120, 5637.
36. Barrera, J.; Orth, S. D.; Harman, W. D. *J. Am. Chem. Soc.* **1992**, 114, 7316.
37. Orth, S. D.; Barrera, J.; Rowe, S. M.; Helberg, L. E.; Harman, W. D. *Inorg. Chim. Acta* **1998**, 270, 337.
38. Sweet, J. R.; Graham, W. A. G. *Organometallics* **1983**, 2, (1), 135.
39. Sweet, J. R.; Graham, W. A. G. *J. Am. Chem. Soc.* **1983**, 105, 305.
40. v.d.Heijden, H.; Orpen, A. G.; Pasman, P. *J. Chem. Soc. Chem. Commun.* **1985**, 1576.

41. Brooks, B. C.; Chin, R. M.; Harman, W. D. *Organometallics* **1998**, 17, 4716.
42. Heijden, H. v. d.; Orpen, A. G.; Pasman, P. J. *Chem. Soc., Chem. Commun.* **1985**, 1576.
43. Curtis, M. D.; Shiu, K.-B.; Butler, W. M. *J. Am. Chem. Soc.* **1986**, 108, 1550.
44. Curtis, M. D.; Shiu, K. *Inorg. Chem.* **1985**, 24, 1213.
45. Gelabert, R.; Moreno, M.; Lluch, J. M.; Lledos, A. *Organometallics* **1997**, 16, 3805.
46. Oldham, J., W. J.; Hinkle, A. S.; Heinekey, D. M. *J. Am. Chem. Soc.* **1997**, 119, 11028.
47. Gunnoe, T. B.; Sabat, M.; Harman, W. D. *J. Am. Chem. Soc.* **1999**, 121, 6499.
48. Meiere, S. H.; Brooks, B. C.; Gunnoe, T. B.; Sabat, M.; Harman, W. D. *Organometallics* **2001**, 20, 1038.
49. Meiere, S. H.; Brooks, B. C.; Gunnoe, T. B.; Carrig, E. H.; Sabat, M.; Harman, W. D. *Organometallics* **2001**, 20, (17), 3661.
50. Harrison, D. P.; Nichols-Nieler, A. C.; Zottig, V. E.; Strausberg, L.; Salomon, R. J.; Trindle, C. O.; Sabat, M.; Gunnoe, T. B.; Iovan, D. A.; Myers, W. H.; Harman, W. D. *Organometallics* **2011**, 30, (9), 2587.
51. Brooks, B. C.; Meiere, S. H.; Friedman, L. A.; Gunnoe, T. B.; Harman, W. D. *J. Am. Chem. Soc.* **2001**, 123, 3541.
52. Ding, F.; Valahovic, M. T.; Keane, J. M.; Anstey, M. R.; Sabat, M.; Trindle, C. O.; Harman, W. D. *J. Org. Chem.* **2004**, 69, (7), 2257.
53. Valahovic, M. T.; Gunnoe, T. B.; Sabat, M.; Harman, W. D. *J. Am. Chem. Soc.* **2002**, 124, 3309.
54. Meiere, S. H.; Valahovic, M. T.; Harman, W. D. *J. Am. Chem. Soc.* **2002**, 124, (50), 15099.
55. Friedman, L. A.; You, F.; Sabat, M.; Harman, W. D. *J. Am. Chem. Soc.* **2003**, 125, 14980.
56. Keane, J. M.; Ding, F.; Sabat, M.; Harman, W. D. *J. Am. Chem. Soc.* **2004**, 126, 785.
57. Keane, J. M. Synthesis and Nucleophilic Activity of Eta-2 Arene Complexes. Ph. D. Dissertation, University of Virginia, 2003.

58. McCleverty, J. A.; Seddon, D.; Bailey, N. A.; Joe' Walker, N. W. *Journal of the Chemical Society, Dalton Transactions* **1976**, (10), 898.
59. Liu, W.; You, F.; Mocella, C. J.; Harman, W. D. *J. Am. Chem. Soc.* **2006**, 128, (5), 1426.
60. Trofimenko, S. *Inorganic Chemistry* **1969**, 8, (12), 2675.
61. Graham, P.; Meiere, S. H.; Sabat, M.; Harman, W. D. *Organometallics* **2003**, 22, 4364.
62. Ha, Y.; Dilsky, S.; Graham, P. M.; Liu, W.; Reichart, T.; Sabat, M.; Kenae, J. M.; Harman, W. D. *Organometallics* **2006**, 25, 5184.
63. Welch, K. D.; Harrison, D. P.; Lis, E. C.; Liu, W.; Salomon, R. J.; Harman, W. D.; Myers, W. H. *Organometallics* **2007**, 26, (10), 2791.
64. Salomon, R. J.; Todd, M. A.; Sabat, M.; Myers, W. H.; Harman, W. D. *Organometallics* **2010**, 29, (4), 707.
65. MacLeod, B. L.; Pienkos, J. A.; Myers, J. T.; Sabat, M.; Myers, W. H.; Harman, W. D. *Organometallics* **2014**, 33, (22), 6286.
66. MacLeod, B. L.; Pienkos, J. A.; Wilson, K. B.; Sabat, M.; Myers, W. H.; Harman, W. D. *Organometallics* **2016**, 35, (3), 370.
67. Graham, P. M.; Delafuente, D. A.; Liu, W.; Myers, W. H.; Sabat, M.; Harman, W. D. *J. Am. Chem. Soc.* **2005**, 127, (30), 10568.
68. Lankenau, A. W.; Iovan, D. A.; Pienkos, J. A.; Salomon, R. J.; Wang, S.; Harrison, D. P.; Myers, W. H.; Harman, W. D. *J. Am. Chem. Soc.* **2015**, 137, (10), 3649.
69. Welch, K. D.; Harrison, D. P.; Sabat, M.; Hejazi, E. Z.; Parr, B. T.; Fanelli, M. G.; Gianfrancesco, N. A.; Nagra, D. S.; Myers, W. H.; Harman, W. D. *Organometallics* **2009**, 28, (20), 5960.
70. Liu, W.; Welch, K.; Trindle, C. O.; Sabat, M.; Myers, W. H.; Harman, W. D. *Organometallics* **2007**, 26, (10), 2589.

Chapter Two

Synthesis of 2-Substituted 1,2-Dihydronaphthalenes and 1,2-Dihydroanthracenes Using a Recyclable Molybdenum Dearomatization Agent

2.1 Introduction

The dearomatization of polycyclic aromatic hydrocarbons (PAHs), such as naphthalene or anthracene, has been explored via organometallic methods, but far less so than for benzenes.¹⁻⁷ In η^6 complexes such as $\text{Cr}(\text{CO})_3(\eta^6\text{-L})$, metal-arene bonds are weaker for PAH ligands (L) than for benzenes, whereas for the corresponding η^2 -coordinated complexes, the opposite is true. For example, naphthalene has been reported to form stable dihapto-coordinated complexes with a wide range of metals, including Ni,⁸ Ru,⁹ Mo,¹⁰ W,¹¹ Re,⁵ and Os,¹ with much greater kinetic stability toward arene substitution than their benzene counterparts.¹² Furthermore, in the case of the third row transition metal systems $\{\text{Os}^{\text{II}}(\text{NH}_3)_5\}^{2+}$,¹⁻³ $\{\text{TpRe}^{\text{I}}(\text{MeIm})(\text{CO})\}$,^{4, 5, 13} and $\{\text{TpW}(\text{PMe}_3)(\text{NO})\}$,¹⁴ tandem electrophilic-nucleophilic additions have been demonstrated, via an arenium intermediate. Such a synthetic approach has led to novel *cis*-1,2- or *cis*-1,4-disubstituted dihydronaphthalenes.

Previous reports¹⁵ have suggested that the complex $\text{TpMo}(\text{NO})(\text{MeIm})(\eta^2\text{-naphthalene})$, **4**, prepared from $\text{Mo}(\text{CO})_6$ in four steps (Scheme 2.1), may exhibit similar chemical reactivity to the known tungsten complex $\text{TpW}(\text{NO})(\text{PMe}_3)(\eta^2\text{-naphthalene})$.¹⁴ Furthermore, $\text{TpMo}(\text{NO})(\text{MeIm})(\text{X})$, the expected product of $\text{TpMo}(\text{NO})(\text{MeIm})(\text{L}\pi)$ reacting with a halogen oxidant ($\text{X}_2 = \text{Br}_2$ or I_2), exhibits a broader range of electrochemical stability for the Mo^{I} oxidation state (e.g., $\sim +0.6$ V to -1.5 V), compared to its W^{I} analogue, ($\sim +0.3$ V to -1.4 V for $\text{TpW}(\text{NO})(\text{PMe}_3)(\text{Br})$).¹⁶ For the tungsten system, the potential required to oxidize, and thereby remove the final organic product (typically $> +0.5$ V), is greater than that required to further oxidize $\text{TpW}(\text{NO})(\text{PMe}_3)(\text{solvent})$ to W^{II} ($0.1 - 0.3$ V for most common solvents). However, the

greater stability of the Mo^{I} analogues toward oxidation suggested that a decomplexation procedure could be developed that would return an intact Mo^{I} complex, which in turn could serve as the direct precursor to the naphthalene complex **4**. This process is similar to that previously reported for rhenium analogues, which uses AgOTf as the oxidant.¹⁷ Herein, we describe a promising new approach for the dearomatization of PAHs on a practical scale (up to ~800 mg of organic product) with highly efficient recovery of the dearomatization agent.

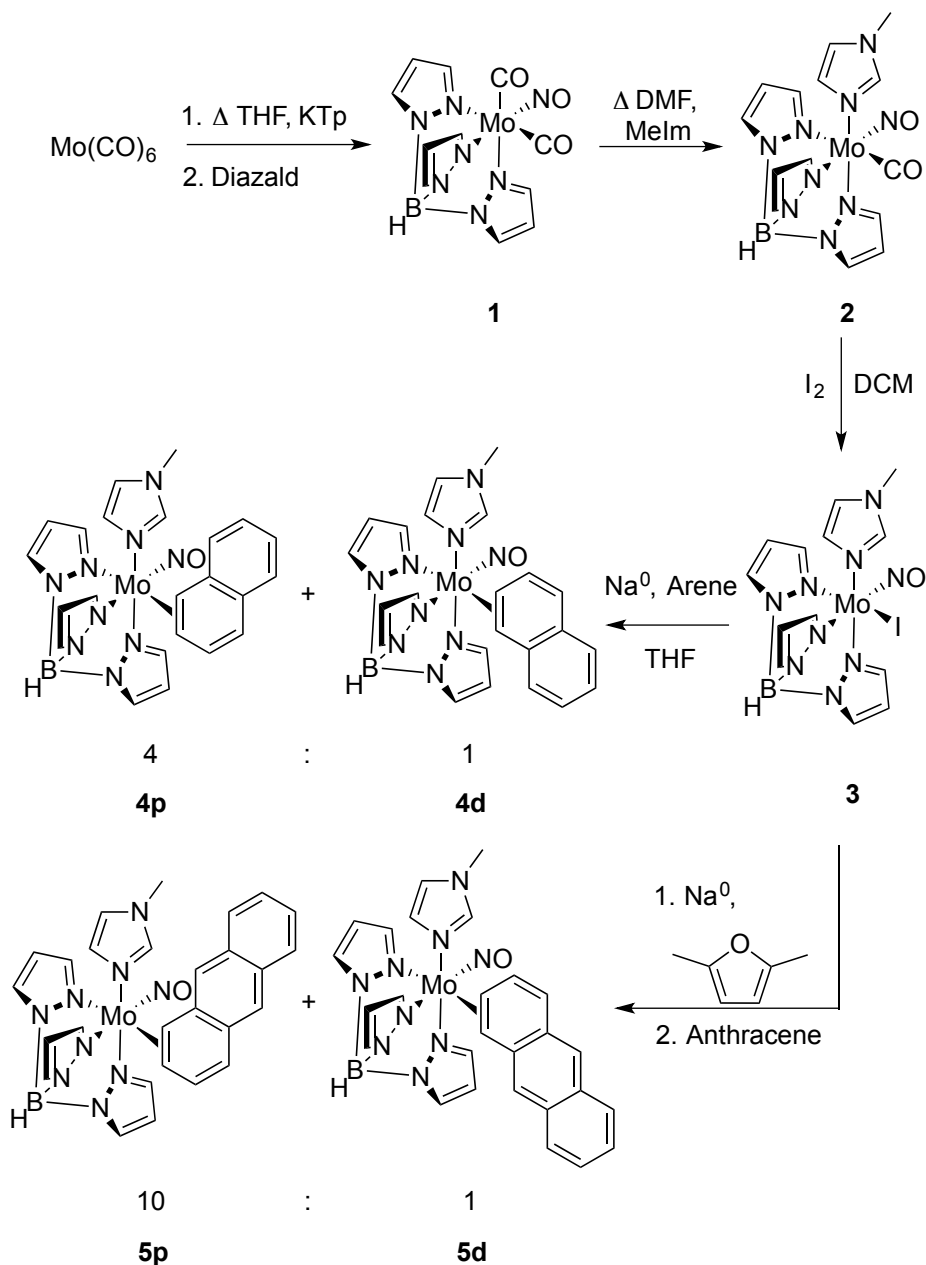
2.2 Results

2.2.1 Improved Synthesis of $\text{TpMo}(\text{NO})(\text{MeIm})(L\pi)$ ($L\pi$ = naphthalene or anthracene)

Although the syntheses of **4** and $\text{TpMo}(\text{NO})(\text{MeIm})(\eta^2\text{-anthracene})$ (**5**) have been previously reported, several steps in the synthetic sequence have been optimized in order for the envisioned method to be practical (Scheme 2.1). The reflux time for the synthesis of $\text{TpMo}(\text{NO})(\text{CO})(\text{MeIm})$ (**2**) from the dicarbonyl (**1**) was reduced from 48 to 1 hour by using dimethylformamide (DMF) as the solvent in place of xylenes. Replacing xylenes with DMF achieves a higher temperature for reflux (154 °C), which increases the rate of the reaction. Also improved was the isolation of **2**, which can now be accomplished through a precipitation in water rather than the previously reported chromatographic workup. Notably, the syntheses of **2** and $\text{TpMo}(\text{NO})(\text{MeIm})(\text{I})$ (**3**) were found to be successful in air with no noticeable degradation to yield or purity of the isolated products. Overall, the precursor (**3**) for the dearomatization products (**4** and **5**) could be isolated on a multigram scale (>100 g) with an overall yield of 68% from $\text{Mo}(\text{CO})_6$. In comparison, the previously reported $\text{TpMo}(\text{NO})(\text{MeIm})(\text{Br})$ was made on a 21 gram scale with an overall 47% yield from $\text{Mo}(\text{CO})_6$ with **2** and **3** being made under a nitrogen atmosphere.

To improve the reductive formation of the arene complexes **4** and **5**, we sought to move away from the use of mercury in these reactions by replacing the sodium-mercury amalgam with sodium dispersion. By using hexanes to dissolve the wax from the sodium dispersion in paraffin, elemental sodium flakes could be obtained. With the use of these flakes, the reduction of **3** to make **4** was found to be uncontrollably fast. This is believed to be due to the in situ reduction of naphthalene to sodium naphthalenide, which provides a homogeneous, rather than heterogeneous, reducing agent. Sodium naphthalenide then reduces **3** at an uncontrolled rate, yielding reaction completion in less than 5 minutes, followed by decomposition due to over-reductive conditions. This over-reduction was previously not an issue as a sodium mercury amalgam was used. The amalgam is believed to have slowly integrated sodium into the reaction mixture. In a similar manner we found that adding sodium dispersion in paraffin wax directly to the reaction solution delivers the reducing agent at a slower, more controlled rate as the wax dissolves. Using this method, sodium-mercury amalgam was replaced by sodium dispersion and the scale was increased to 5 g yielding **4** at 34% yield from **3**. The synthesis of the anthracene analogue, **5**, was also accomplished under mercury-free conditions.

Scheme 2.1. Synthesis of dihapto-coordinated naphthalene and anthracene complexes of molybdenum.



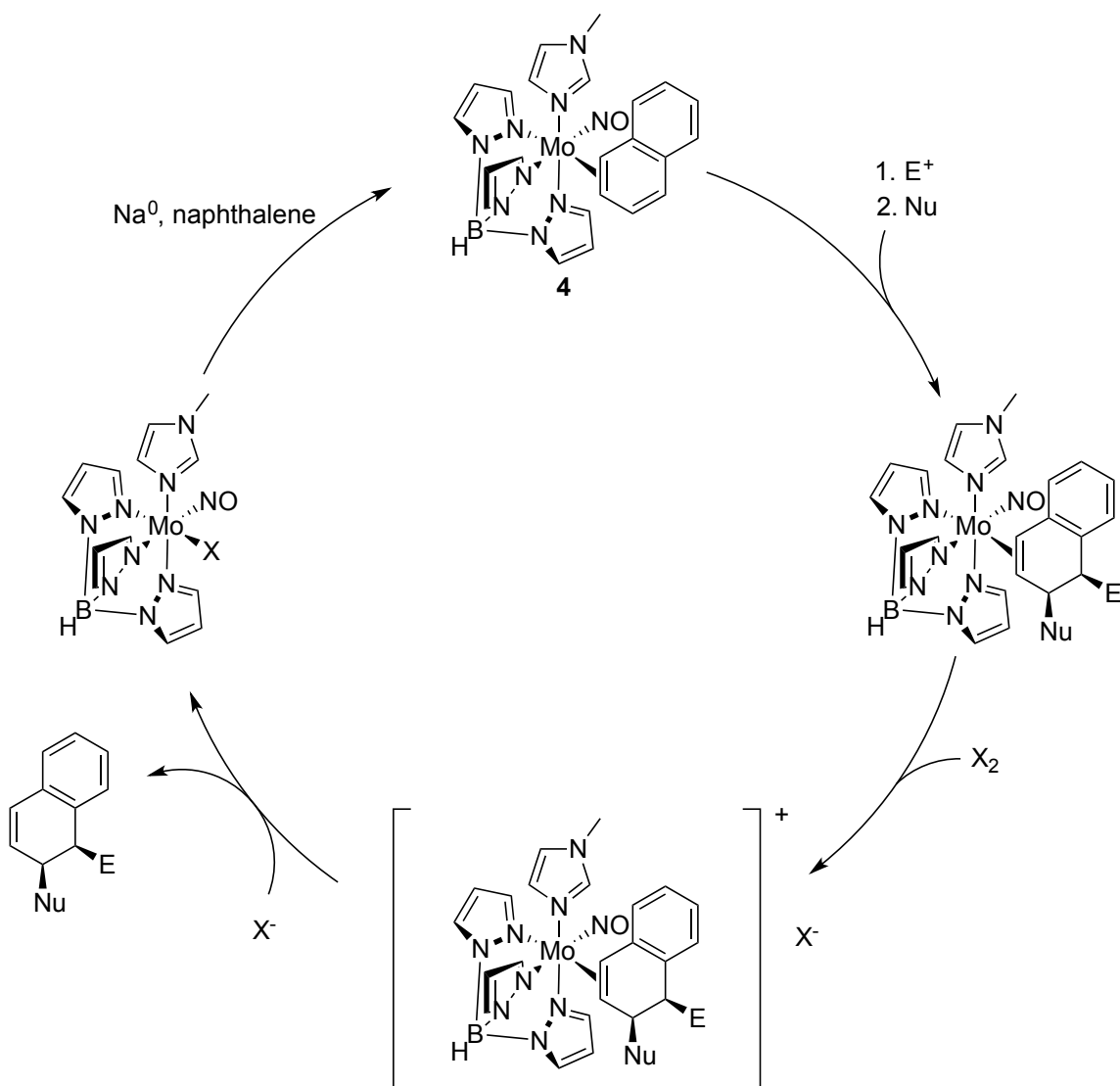
Adding the sodium dispersion in paraffin wax directly into THF increased the reaction time from 5 min with the sodium flakes to 24 h, but provided **5** in serviceable yield (19%). However, the product was contaminated (~20%) by another material, thought to be the binuclear complex $[(\text{TpMo}(\text{MeIm})(\text{NO}))_2(\eta^2:\eta^2\text{-}\mu\text{-anthracene})]$ based

on the ^1H NMR spectrum containing resonances at 3.95 and 3.14 ppm with coupling identical to the desired product's proton resonances. This byproduct could be avoided by synthesizing $\text{TpMo}(\text{NO})(\text{MeIm})(\eta^2\text{-2,5-dimethylfuran})$ in situ, removing the sodium, and subsequently stirring in the presence of anthracene. Thus, the anthracene derivative **5** was cleanly produced on a multigram scale in yields over 50% from **3**.

2.2.2 Oxidation of $\text{TpMo}(\text{NO})(\text{MeIm})(\eta^2\text{-naphthalene})$ with Iodine

After improving the synthesis of **4**, the possibility of recycling the dearomatization agent was investigated. Following a tandem electrophilic-nucleophilic addition reaction on **4**, it was theorized that an electron could be removed from the metal center in the presence of an oxidant (i.e., a halogen (X_2)). After oxidation, the ability for Mo^{I} to backbond into this dihydronaphthalene dramatically decreases, as the metal center is substantially less electron-rich, significantly destabilizing the metal ligand bond. Thus the modified organic would be released and a halide could subsequently coordinate to the metal center. This coordination would produce $\text{TpMo}(\text{NO})(\text{MeIm})(\text{X})$, which could then be reduced in the presence of naphthalene to regenerate **4**. Although the incompatibility of the reagents used in this sequence prevent a one-pot catalytic cycle, the stepwise isolation of each complex would result in a formal catalytic cycle for the organic modification of aromatics using a molybdenum dearomatization agent (Scheme 2.2).

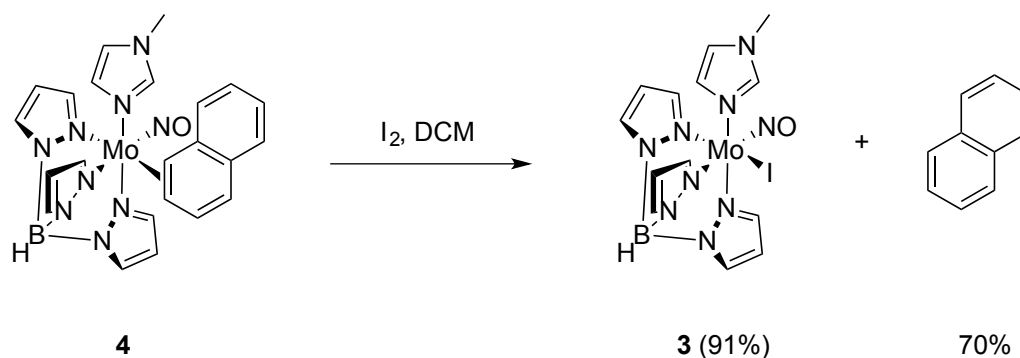
Scheme 2.2. Proposed formal catalytic cycle for the dearomatization of naphthalene with $\{\text{TpMo}(\text{NO})(\text{MeIm})\}$.



To test the feasibility of this proposed recycling scheme, **4** was subjected to oxidation with iodine in dichloromethane (DCM). In addition to having a mild, but sufficiently strong reduction potential, iodine offers an ease of use, as it is less volatile and toxic than the alternative halogen oxidants. A notable color change from yellow to green was observed upon addition of iodine to a DCM solution of **4** that is in agreement

with the formation of the emerald green product, **3**. This solution was added to hexanes to yield a precipitate that was then isolated on a fritted disc. This solid was confirmed through cyclic voltammetry to be **3** (91%). The filtrate from this precipitation was evaporated *in vacuo* and analyzed by ^1H NMR to confirm that it contained pure naphthalene (70%) (Scheme 2.3).

Scheme 2.3. Oxidation of **4** with iodine.



Although the ability to recover **3** and free naphthalene from the oxidation of **4** in good yields was promising, the applicability of this method needed to be proven on modified organics (e.g., dihydroarenes). Given that there had been only one example of the organic modification of a molybdenum η^2 -arene complex (*vide infra*), the expansion of organic transformations of PAHs bound in an η^2 fashion to molybdenum was pursued.

2.2.3 Spectroscopic Profile of $\text{TpMo}(\text{NO})(\text{MeIm})(\eta^2\text{-1,2-dihydroarene})$

For the purposes of this study, we focused on three addition reactions, thought to represent a broader reactivity pattern for the PAH ligands of **4** and **5** with carbon nucleophiles. The only previous report of ligand-centered reactivity for a molybdenum η^2 -arene complex is the protonation of **4**, followed by the addition of the ketene acetal MTDA (1-methoxy-2-methyl-1-trimethylsiloxy-propene). In addition to optimizing this reaction, the addition of an enolate salt (lithium dimethylmalonate; LiDMM), and an aromatic heterocycle (*N*-methylpyrrole) were explored as nucleophiles.

While the protonation and addition of MTDA were previously reported for **4**,¹⁵ the product complex **6** was never characterized. The NO stretching frequency (1565 cm^{-1}) of **6** is modestly lower than its precursor **4** (*cf.* $\nu_{\text{NO}} = 1576\text{ cm}^{-1}$), an observation that suggests that the dihydronaphthalene ligand is a weaker π -acid than naphthalene itself. However, the electrochemical analysis of $\text{TpMo}(\text{NO})(\text{MeIm})(\eta^2\text{-1,2-dihydronaphthalene})$ reveals an anodic wave with $E_{\text{p,a}} = +0.12\text{ V}$ (100 mV/s) indicating its diminished susceptibility to oxidation, relative to **4** (*cf.* $E_{\text{p,a}} = -0.26\text{ V}$). While at first glance, the electrochemical and infrared data seem at odds, the more negative anodic peak for **4** is likely a consequence of the decreased *kinetic* stability of $[\text{TpMo}^{\text{I}}(\text{NO})(\text{MeIm})(\eta^2\text{-naphthalene})]^+$,¹⁸ which is expected to undergo rapid dissociation of the arene ligand. For this type of chemically coupled electrochemical process (E_{rC_i}), a larger rate constant for the chemical step (i.e., arene dissociation) results in a negative shift for $E_{\text{p,a}}$. This explanation is more likely than a true shift in the formal d^5/d^6 reduction potential in the comparison of **6** and **4**.

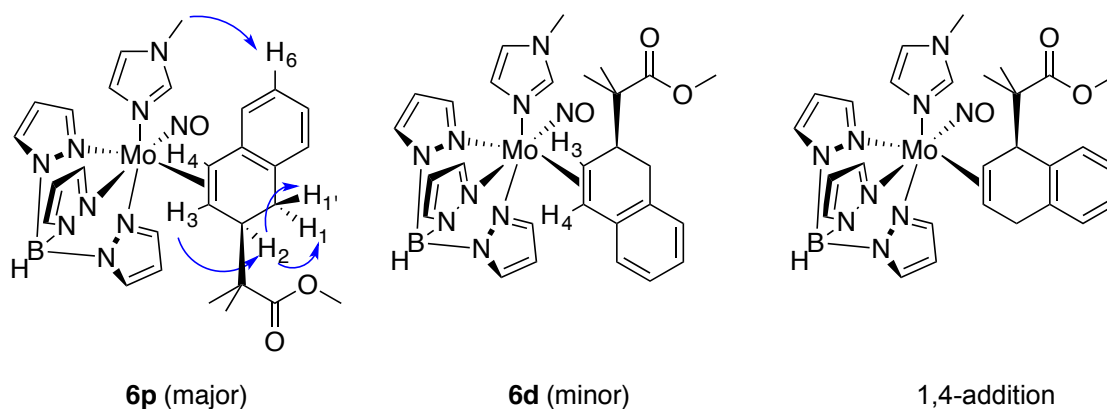


Figure 2.1. NOESY correlations for **6p** and the proposed assignment of **6d** as its coordination diastereomer, rather than a constitutional isomer resulting from a 1,4-addition. $J_{\text{H1b-H2}} < 1$ Hz.

In addition to resonances for the nine Tp and three MeIm protons, ^1H NMR data reveal a diastereotopic methylene group, H1' (doublet of doublets at 3.52 ppm) and H1 (doublet at 2.55 ppm), identified by its large coupling constant (17.2 Hz), and confirmed by HSQC data. Proton H2 (doublet at 3.23 ppm) was identified through NOESY and COSY correlations with H1 and H1'. Proton H3 was identified through its NOESY and COSY correlations to H2, as well as a COSY correlation to H1. A distinctive doublet of triplets is seen at 2.05 ppm due to H3 coupling to H4 (a doublet at 3.13 ppm), H1', and H2. These data, along with a strong NOESY correlation between Pz3A and H2, confirm that the MTDA addition occurs *anti* to the metal. This stereochemistry was confirmed by the X-ray crystal structure analysis of **6** (Figure 2.2).

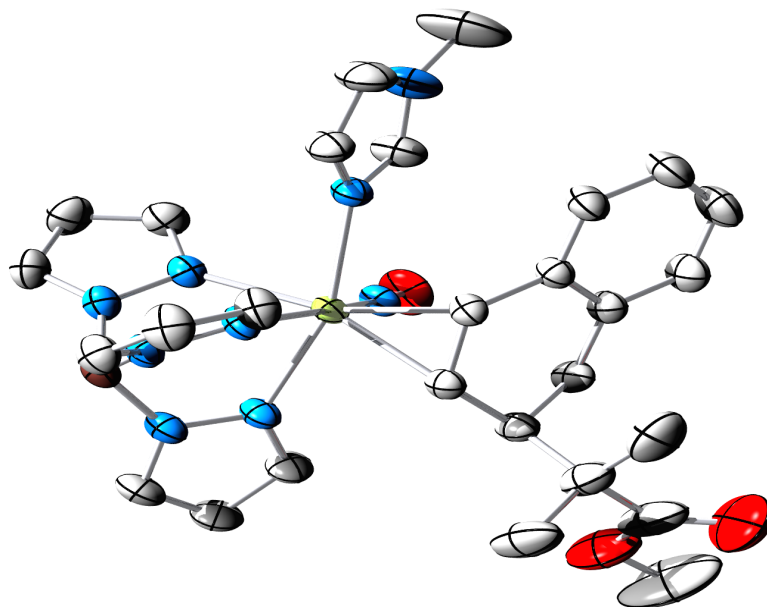


Figure 2.2. Crystal structure of dihydronaphthalene complex **6**. Bond lengths (Å): Mo—C(4) 2.232(2); Mo—C(3) 2.242(2); Mo—C(4) 2.32(2); Mo—N(MeIm) 2.2103(17); Mo—N(NO) 1.7544(17).

The axial positioning observed for the C2 substituent of the dihydronaphthalene ligand is also present in solution according to COSY and H/H coupling data, which indicate an H1-C1-C2-H2 dihedral angle approaching 90°. Identification of the major coordination diastereomer, in which the remaining aromatic portion of the ring is positioned proximal to the MeIm ligand, was determined in solution by the observation of an NOE interaction between H6 and the methyl of the MeIm ligand.

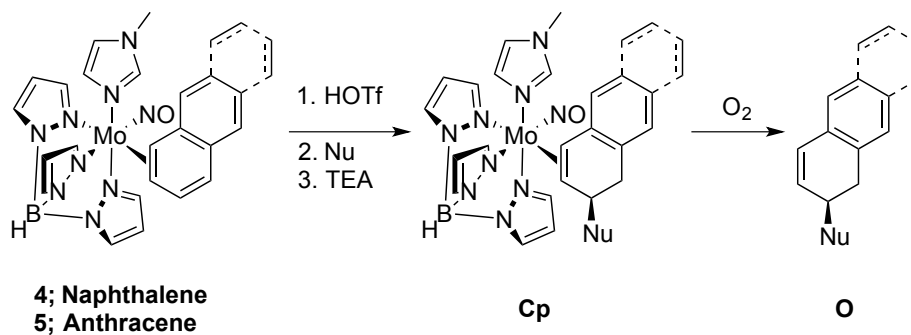
Signals for an additional complex (**6d**) are observed in the ^1H NMR spectrum of **6** at a 25:1 ratio of **6p**:**6d**, showing signals and splitting patterns very similar to those of the major species (**6p**). Most notably, a doublet-of-triplets at 1.84 ppm has the same coupling constants as H3 of the major isomer. This minor product is thought to be a coordination diastereomer of **6p** in which the unbound aromatic ring is oriented distal to the imidazole (Figure 2.1). While overlapping signals in the NMR spectrum prevent the conclusive

assignment of the minor species, the oxidation of a sample of **6** upon exposure to air generates a single new dihydronaphthalene product, consistent with **6p** and **6d** being coordination diastereomers (see Figure 2.1). Were **6p** and **6d** constitutional isomers (e.g., 1,2- vs 1,4-addition), then oxidation of **6** would have yielded constitutional isomers of **12** upon oxidative decomplexation.

2.2.4 Isolation of 1,2-Dihydroarenes Through Air Oxidation

Similar 1,2-addition reactions for the naphthalene ligand of **4** are accomplished through the protonation and subsequent addition of either *N*-methylpyrrole or LiDMM. Further, all three nucleophiles are successfully added to the anthracene ligand of **5** (Table 2.1). Of note, addition products (**C**) are isolated as racemic mixtures of both enantiomers of the chiral metal center thus yielding the organics (**O**) as racemic mixtures as well.

Complexes of type **C** (Table 2.1) are all capable of being oxidized via exposure to air. Although these organics are obtained in poor yield (average 28%), their synthesis demonstrates the ability to remove the metal using a mild oxidant that does not react with the sensitive organic products. Of note, when *N*-methylpyrrole is used as the nucleophile, isolation of the organic product reveals two isomers for both naphthalene and anthracene. Using COSY correlations, it was determined that *N*-methylpyrrole adds primarily at the alpha position of the pyrrole, but a small amount (~10%) of the beta-substituted analogue is also formed. For the alpha isomer, the ¹H NMR spectrum shows triplets at 6.60 and 6.07 ppm as well as a doublet-of-doublets at 5.98 ppm. For the beta form, triplets at 6.52 and 6.43 as well as a triplet at 6.04 are observed. The protons on the isolated alkene bond of the naphthalene ring retain their splitting as would be expected if both products were the result of 1,2-additions. The beta addition apparently occurs during the initial addition

Table 2.1. Tandem electrophilic-nucleophilic addition to **4** and **5**.

Arene Complex		C (% yield)	dr (Cp:O)	O (% yield)
4		6; 61 (5 g scale)	10:1	12; 24
5		7; 43	25:1	13; 22
4		8; 66	8:1 ^a	14; 24
5		9; 48	15:1 ^a	15; 44
4		10; 53	5:1	16; 14
5		11; 27	8:1	17; 39

^a The values reported in this table are more accurate than those published

process, as NMR spectra for both pyrrole derivatives **10** and **11** show ~10% of an additional molybdenum complex, besides the minor coordination diastereomer (**10d**, **11d**).

2.2.5 Recyclable Oxidation of $\text{TpMo(NO)(MeIm)}(\eta^2\text{-1,2-dihydroarenes})$

As discussed above, decomplexation of the organic product for the ester derivative **6** can be accomplished using air to oxidize the molybdenum. However, as is the case with $\{\text{TpW(NO)(PMe}_3\text{)}(\text{alkene})\}$ complexes, a M^{I} co-product could not be recovered.¹⁹ This is illustrated by cyclic voltammetric data, which shows that, upon exposure to air, no electrochemically active molybdenum products are observed over a range of +1.0 to -1.7 V (Figure 2.3). A similar result was observed using ceric ammonium nitrate (CAN) as the oxidant (Figure 2.3). However, the ease of oxidation for the metal complexes **6** - **11** ($\sim +0.2$ V) suggests that milder oxidants can be used, including iodine.

The $\text{I}_2/2\text{I}^-$ standard reduction potential, +0.53 V, is sufficiently large that it can oxidize the dihydronaphthalene and dihydroanthracene product complexes *but is not powerful enough to over-oxidize the metal* (the oxidation of Mo^{I} to Mo^{II} for $[\text{TpMo(NO)(MeIm)(I)}]$ occurs with an $E_{\text{p,a}} = +0.65$ V at 100 mV/s). In contrast to that observed when air or CAN is used to oxidize ester complex **6** (Figure 2.3), a cyclic voltammogram of the reaction mixture resulting from iodine oxidation of **6** contains a pseudo-reversible couple near -1.4 V and $E_{\text{p,a}} \sim +0.65$ V. This feature is consistent with TpMo(NO)(MeIm)(I) being generated as the major inorganic product.

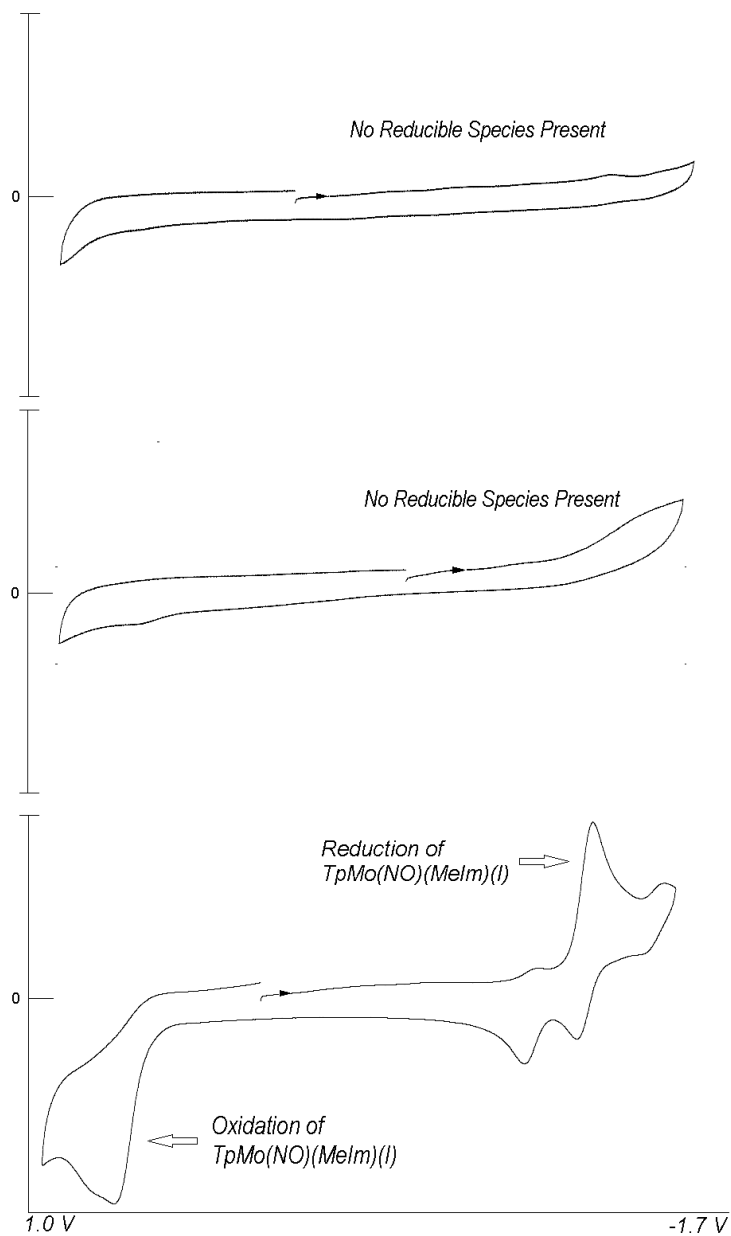
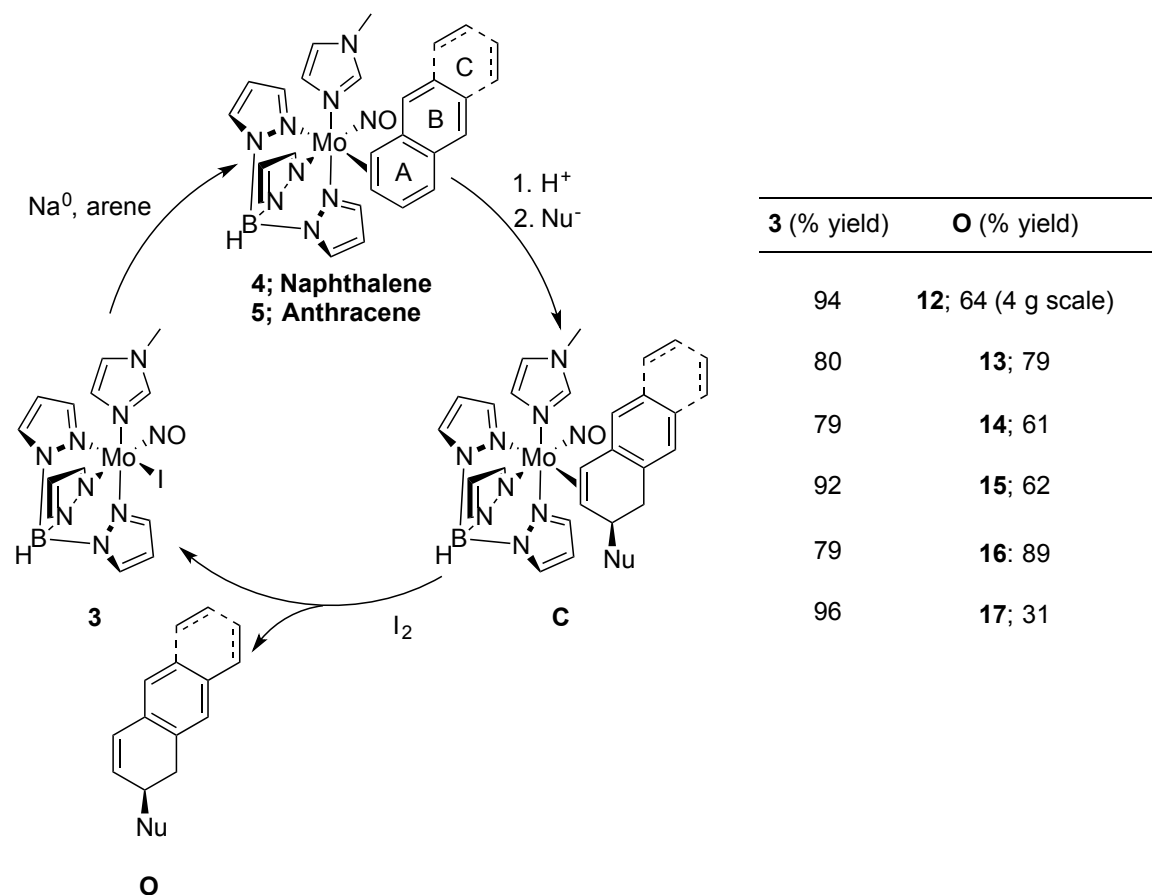


Figure 2.3. Cyclic voltammogram of the reaction mixture following oxidation of **6** and air (top), CAN (middle), or iodine (bottom).

Inspired by the electrochemical data in Figure 2.3, we set out to develop conditions to liberate the organic compounds from complexes **6** - **11** using I_2 and then recover **3** by precipitation from DCM:hexanes. Isolated yields for both organic products and **3** are reported in Table 2.2. The average recovery of **3** is 84% (recovering up to 3 g

of **3**) and the use of iodine significantly improves yields of the isolated organic products (average 64%). Of note, ~800 mg of **12** was isolated from the oxidation of **6** with iodine on a 4 g scale, truly representing the great scale at which {TpMo(NO)(MeIm)} can yield modified organics. With the recovery of **3**, a formal catalytic cycle is completed for the PAH dearomatization, although incompatibilities of the chemical reagents defeat any possibility of a practical 'one-pot' process.

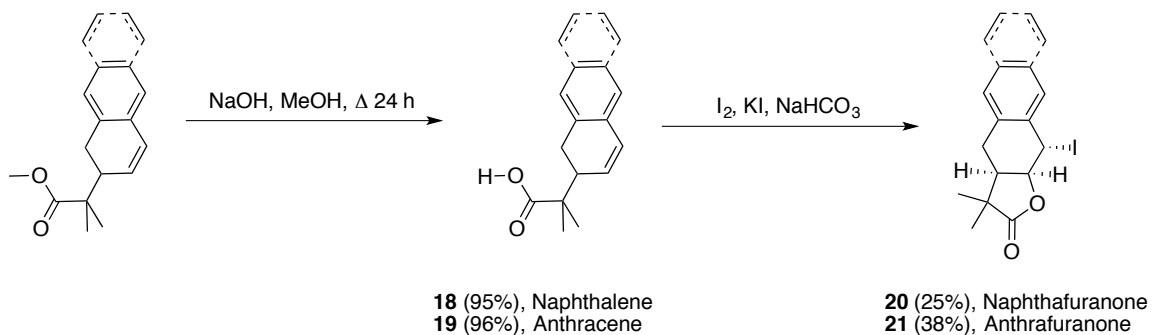
Table 2.2. Formal catalytic cycle for the generation of dihydronaphthalenes and dihydroanthracenes.



2.2.6 Chemical Elaboration of Isolated 1,2-Dihydroarenes

The organic products **12** - **17** are themselves susceptible to oxidative dehydrogenation,²⁰ especially in the presence of base, but can be stabilized by addition across the isolated alkene bond. To stabilize the products and illustrate the synthetic potential of this dearomatization method, we elected to apply an iodolactonization process to isolated esters **12** and **13**. Hence, these esters were first hydrolyzed to their carboxylic acids (**18** and **19**) then cyclized in the presence of iodine to form **20** and **21** (Scheme 2.4). Through full 2D analysis, the stereochemistry of **20** and **21** was determined. In particular, the proposed *cis* ring juncture was confirmed by a strong NOE interaction of the bridgehead protons, a feature that would not be expected in the *trans* isomer.

Scheme 2.4. Iodolactonization of **12** and **13**.

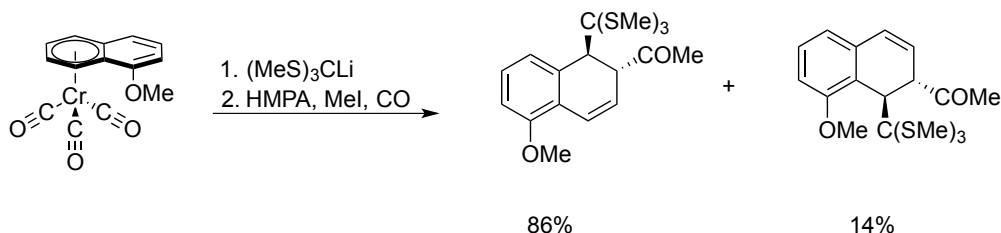


2.3. Discussion

Naphthalenes are typically derivatized through Friedel-Crafts acylation²¹ and alkylation^{22, 23} to yield *substituted* naphthalene products. In one report, $\{\text{Cr}(\text{CO})_3\}$ was used to promote the nucleophilic addition of various sulfur-stabilized carbanions to 1-methoxynaphthalene.²⁴ While subsequent addition of methyl iodide can produce

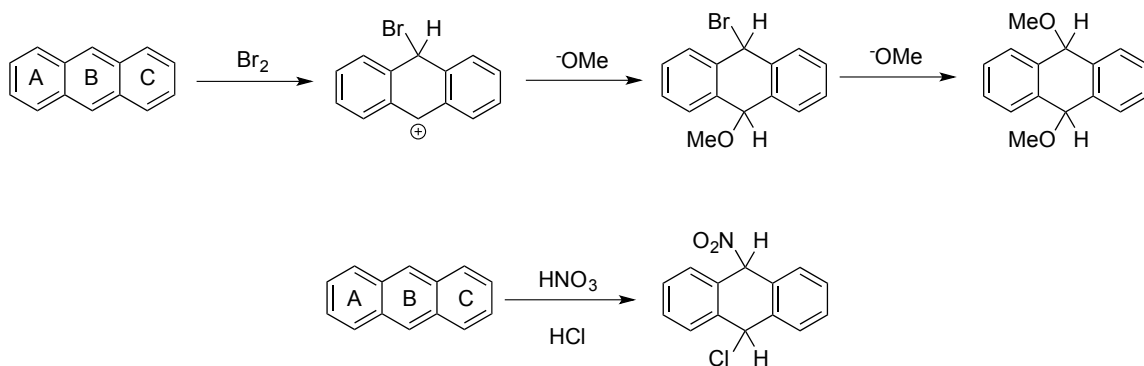
acetylated dihydronaphthalenes, the regioselectivity for these reactions is typically poor (Scheme 2.5).

Scheme 2.5. Dearomatization of naphthalene using $\{\text{Cr}(\text{CO})_3\}$.



Anthracenes are inherently more reactive at the internal (B) ring than the terminal (A or C) rings due to a greater thermodynamic stability yielded from the retention of two benzene rings (Scheme 2.6).²⁵ This trend in reactivity can be seen in the formation of 9,10-dihydro-9,10-dimethoxyanthracenes as well as in the reductive nitration of anthracene in the presence of hydrochloric acid to form 9,10-dihydroanthracenes. As a result of the relative lack of reactivity at the terminal rings, methods for the preparation of 1,2-dihydroanthracenes directly from anthracene are practically unknown. Aside from minor amounts of cycloaddition and dihydroxylation products formed as part of complex reaction mixtures, reports of addition reactions that involve the terminal rings of anthracene are unknown.

Scheme 2.6. Organic additions to anthracene.



$\{\text{TpMo}(\text{NO})(\text{MeIm})\}$ can be used to regioselectively control tandem electrophilic-nucleophilic additions to naphthalene and anthracene in fair yields, subsequently regenerating the dearomatization precursor **3** through an oxidation with iodine. Furthermore, these 1,2-dihydroarenes have been shown to undergo iodolactonization to yield organics with three new stereogenic centers when compared to their aromatic precursors. This methodology offers a complementary approach to the above-mentioned methods found in the literature for the derivatization of PAHs. These derivatized PAHs represent important classes of compounds of biological interest. For instance, dialin cores are found in many naturally occurring products (i.e., cannabisin C, negundin B, (+)-Phyltetralin, etc.) and pharmaceuticals (i.e., sertraline, tametraline, lometraline, etc.). Lactone **20** contains the same naphthafuranone core as pygmaeocin A,²⁶ used to treat inflammation and malaria, and several arthrinins,²⁷ a well-known class of natural products. Furthermore, the anthrafuranone core of **21** is present in olivinolide, a derivative of the aglycone for the anticancer drug olivomycin.²⁸ A similar 1,2,3,4-tetrahydroanthracene core is found in toyomycin (chromomycin) (Figure 2.4).²⁹ For this reason, compounds **12** – **17**, **20**, and **21** have been submitted to Eli Lilly and Company for screening.

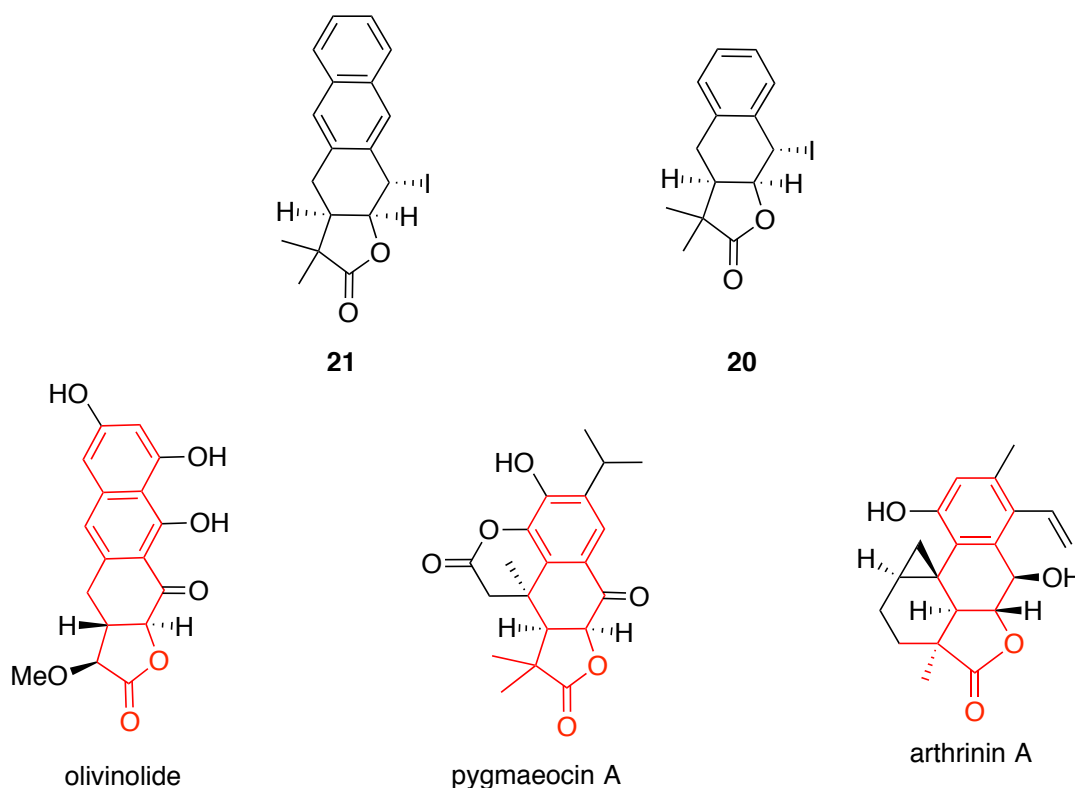
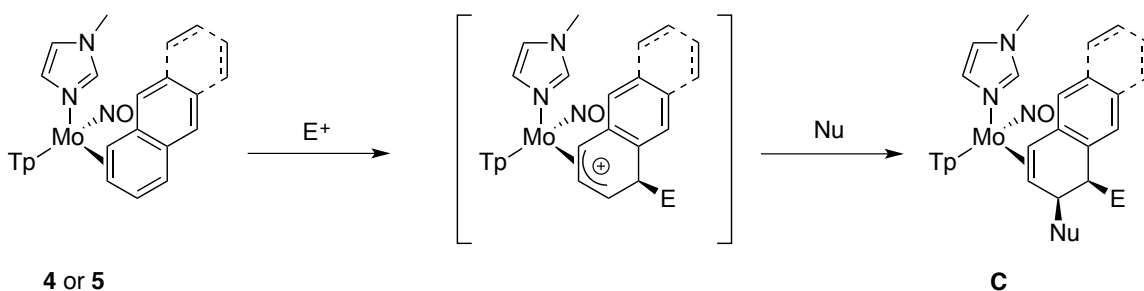


Figure 2.4. Naphthafuranones pygmaeocin A and arthrinin A, and the anthrafuranone olivinolide.

Complexes of the form **C** (Scheme 2.7) represent the first isolation of a complex from the organic modification of aromatics using $\{\text{TpMo}(\text{NO})(\text{MeIm})\}$. For this reason, explanation of how these reactions are monitored is discussed here to aid future work on these and related systems. The general reaction scheme for the tandem electrophilic-nucleophilic addition reactions to form complexes of the form **C** is given in Scheme 2.7. First, a heterogeneous mixture of **4** or **5** suspended in CH_3CN is cooled at $-30\text{ }^\circ\text{C}$ for 15 min. Next, a $-30\text{ }^\circ\text{C}$ solution of between 3 and 4 equivalents of the electrophile in CH_3CN is added to the reaction mixture and the resulting solution is left at $-30\text{ }^\circ\text{C}$ for 15 min. Between 7 to 8 equivalents of the nucleophile is then added to the reaction mixture and

this solution is left at $-30\text{ }^{\circ}\text{C}$. At this point, the reaction is quenched by the addition of a base and the product (**C**) can be isolated by chromatography.

Scheme 2.7. Tandem electrophilic-nucleophilic addition reactions to **4** or **5**.



Whereas the $\{\text{TpW}(\text{NO})(\text{PMe}_3)\}$ fragment has a phosphine ligand, the $\{\text{TpMo}(\text{NO})(\text{MeIm})\}$ fragment lacks a convenient handle for the monitoring of the reaction mixture by NMR spectroscopy. Also of difficulty is the sensitivity of the reactant, intermediate, and product complexes, to air and high temperatures ($> -20\text{ }^{\circ}\text{C}$) under the oxidative conditions of the reaction. This sensitivity adds more difficulty to ^1H NMR monitoring, in addition to the potentially overwhelming signals yielded from electrophiles or nucleophiles used.

We have found that a useful technique for monitoring the reactions to yield complexes of type **C** is cyclic voltammetry (CV). CV allows for the analysis of only the electrochemically active species present in a solution. In this manner we can distinguish metal complexes, utilizing knowledge of the measured potentials of the $\text{Mo}^0/\text{Mo}^{1+}$ oxidation obtained from their isolated products, with minimal interference from the organic reagents and solvents also present in the reaction mixture. To monitor these reactions by CV the following protocol is followed after the addition of both the electrophile and nucleophile at $-30\text{ }^{\circ}\text{C}$: an aliquot of the reaction mixture is removed,

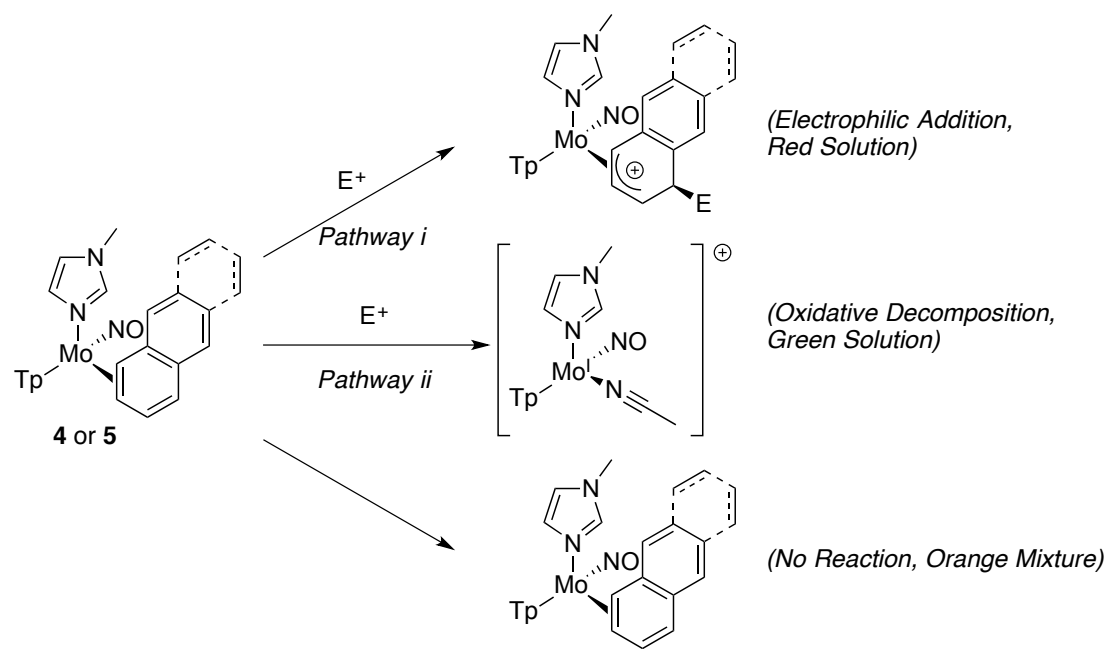
added to base (e.g., TEA), and the resulting solution is added to a CV cell containing room temperature DMA and electrolyte.

The base is added to the aliquot before CV analysis to quench any unreacted electrophile present in the reaction mixture that could potentially react with the starting material or product of this reaction at the higher temperatures of the CV experiment. It should be noted that the allylic species from an electrophilic addition to **4** or **5** is very unstable at temperatures above -20 °C (*vide infra*) and therefore is not observed in this CV monitoring. Were the allylic species still present in the reaction mixture, it is believed to revert back to starting material via deprotonation (*vide infra*). Reaction progress in these reactions is indicated by a decrease in the signal for the oxidation of the starting material ($E_{p,a} \approx -0.26$ V) and an increase in a signal at $\sim +0.2$ V, which corresponds to the oxidation of the 1,2-dihydroarene complexes (**C**). For example, when complex **6** is reacted with HOTf and MTDA, by monitoring the reaction through the disappearance of the $E_{p,a}$ at -0.26 V and the appearance of an $E_{p,a} \sim +0.12$ V, the reaction was determined to be complete 15 minutes after the addition of MTDA to the reaction mixture.

Other key features observed during these addition reactions were color change and homogeneity of the reaction mixture. The reaction starts as a vibrant orange heterogeneous mixture and, upon the addition of acid, changes to a blood red homogeneous solution, indicating the formation of an allyl intermediate (Scheme 2.8, Pathway i). The enhanced basicity of naphthalene when bound to {TpMo(NO)(MeIm)} was compared to its {TpRe(CO)(RIm)} and [Os] analogues in a previous investigation.³⁰ It was found that when **4** was added to a solution containing TpRe(CO)(BuIm)(2,3,4- η^3 -(1*H*-naphthalenium))](OTf) no observable proton transfer occurred over 0.5 h at -20 °C.

However, in contrast to the [Os]-naphthalene complex, **4** is capable of being protonated by diphenylammonium triflate (DPHAT) ($pK_a \sim 6$ in CH_3CN). These experiments show that naphthalene is more basic when bound to $\{TpMo(NO)(MeIm)\}$ than when it's bound to [Os]; however, naphthalene is less basic when bound to $\{TpMo(NO)(MeIm)\}$ than when it is bound to $\{TpRe(CO)(BuIm)\}$. Having a greater basicity, $TpMo(NO)(L)(L\pi)$ complexes are predicted to have the ability to react with weaker electrophiles than those used with the [Os] fragment.

Scheme 2.8. Potential pathways from the addition of an electrophile to **4** or **5**.

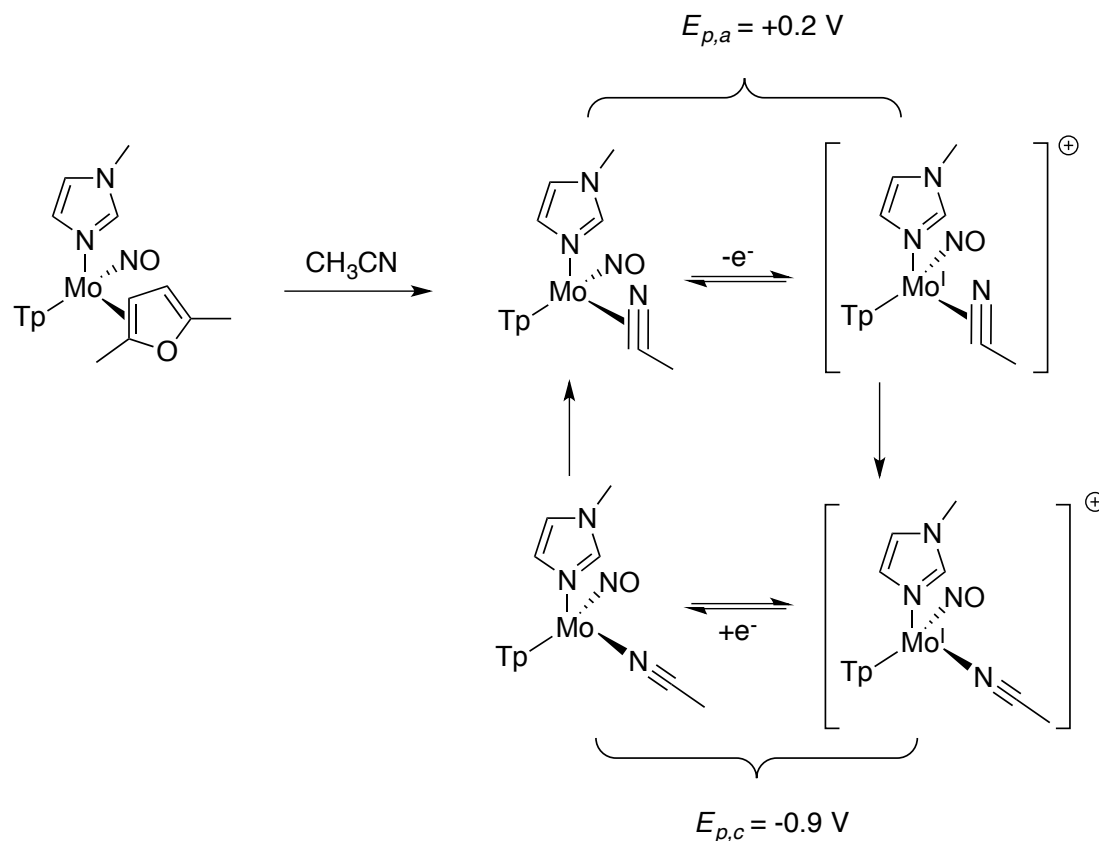


Electrophiles, other than a strong acid ($pK_a < 1$), were attempted (i.e., iminiums, NCS, NBS, selectfluor, acetals, Michael acceptors, etc.); however, either an orange mixture containing a reductive species corresponding to the respective starting material (e.g., **4** or **5**) or a green solution containing a strong $E_{p,c} \sim -0.9$ V were observed. The observation of starting material indicated **4** and **5**'s lack of nucleophilicity under these

conditions (i.e., -30 °C), but raising the temperature appeared to favor the formation of the green solution mentioned above. This green solution contains the cationic acetonitrile complex, $[\text{TpMo}^{\text{I}}(\text{NO})(\text{MeIm})(\kappa^1\text{-acetonitrile})]^{1+}$ complex (Scheme 2.8, Pathway ii) resulting from oxidation of the metal complex.

Previous reports have described the ability to exchange furan with acetonitrile to make $\text{TpMo}(\text{NO})(\text{MeIm})(\eta^2\text{-acetonitrile})$ complex in situ.³¹ Although this complex could not be isolated, the addition of benzylbromide yielded a benzonitrilium complex. Similarly, by stirring $\text{TpMo}(\text{NO})(\text{MeIm})(\eta^2\text{-2,5-dimethylfuran})$ complex in acetonitrile, the 2,5-dimethylfuran can be exchanged with CH_3CN and the purported $\text{TpMo}(\text{NO})(\text{MeIm})(\eta^2\text{-acetonitrile})$ complex is observed in situ with an anodic peak around +0.2 V. Of note, after the electrochemical oxidation of this complex, a cathodic peak appears at -0.9 V that is absent when the oxidation does not occur. This signal is believed to be due to the reduction of the $[\text{TpMo}^{\text{I}}(\text{NO})(\text{MeIm})(\kappa^1\text{-acetonitrile})]^{1+}$ cation, formed by a linkage isomerization of the $\eta^2\text{-acetonitrile}$ complex upon oxidation (Scheme 2.9). Under oxidative conditions it is believed that **4** and **5** can be oxidized to release their η^2 bound aromatic, thereby allowing solvent coordination (e.g., CH_3CN). This represents a chemical, rather than electrochemical, process to access the $\text{TpMo}^{\text{I}}(\text{NO})(\text{MeIm})(\kappa^1\text{-acetonitrile})$ complex and explains the observation of the complex in the monitoring of tandem electrophilic-nucleophilic addition reactions to **4** and **5**.

Scheme 2.9. Exchange of 2,5-dimethylfuran with CH₃CN to form TpMo(NO)(MeIm)(η^2 -acetonitrile), and the resulting complex observed through CV.

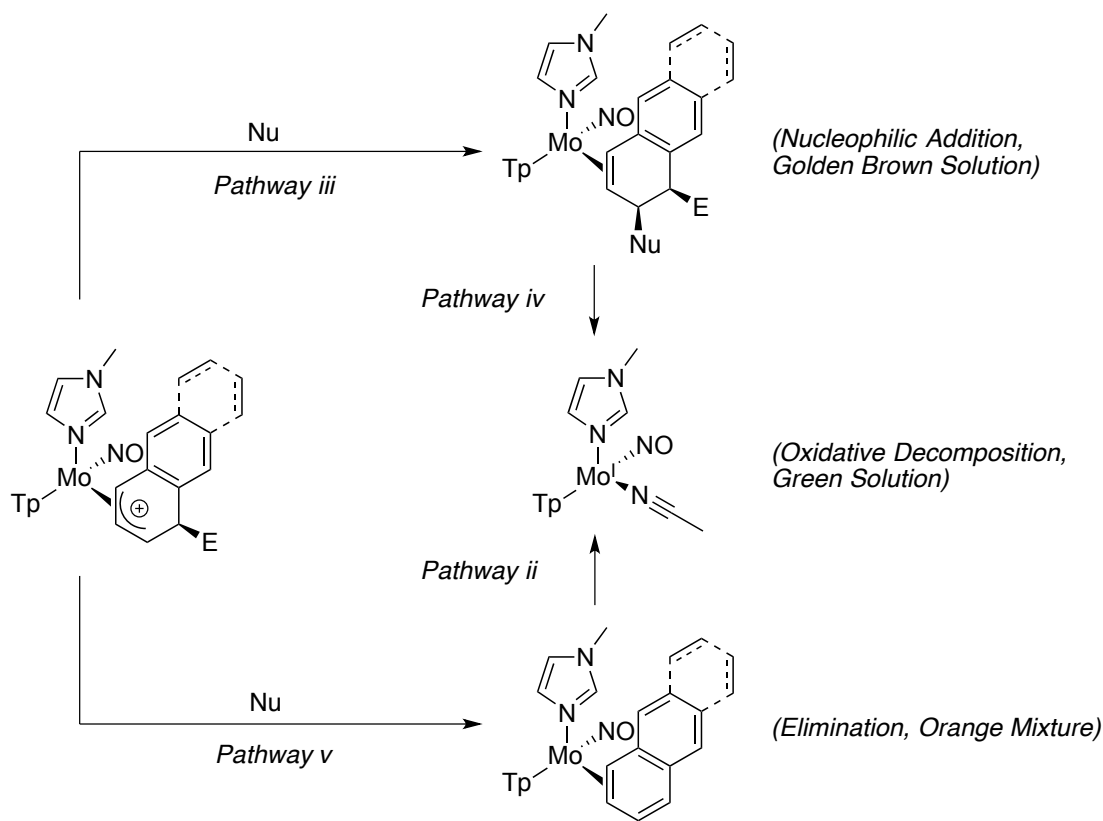


Previous reports also show [TpMo(NO)(MeIm)(η^3 -naphthalenium)](OTf), with a $t_{1/2}$ of several hours at -20°C , to be significantly more unstable than rhenium (I) and osmium (II) analogues.³⁰ Evidence to support this instability can be seen in a more downfield shift of the allylic carbons on [TpMo(NO)(MeIm)(2,3,4- η^3 -naphthalenium)](OTf) (143.4, 101.7, and 88.1 ppm) compared to the allylic carbons of [TpRe(CO)(MeIm)(2,3,4- η^3 -naphthalenium)](OTf) (99.6, 79.0, and 73.0 ppm), a trend suggesting weaker π -donation from molybdenum (0). This weaker donation results in a more electrophilic allyl ligand and allows for the addition of weaker nucleophiles (i.e.,

aromatic heterocycles) in comparison to $\{\text{TpRe}(\text{CO})(\text{L})\}$. However, this also implies a greater acidity of the conjugate acid from the protonation of **4** and **5**, relative to the [Os] analogue.

If electrophilic addition to the arene complex is successful (Scheme 2.8, Pathway i), then several possible outcomes can occur upon addition of the nucleophile to the reaction mixture (Scheme 2.10).

Scheme 2.10. Potential pathways after adding a nucleophile to an allylic species of **4** or **5**.



The addition of a nucleophile to this allylic species could yield a 1,2-dihydroarene complex (Scheme 2.10, Pathway iii). Successful formation of 1,2-dihydroarene complexes results in a color change from the blood red of the allyl, to a golden brown

solution. However, it is also possible that after the successful addition of the nucleophile, the newly formed 1,2-dihydroarene complex is oxidized by the remaining excess of electrophilic reagent in the reaction mixture, generating the κ^1 -acetonitrile complex (Scheme 2.10, Pathway iv). Another possibility upon addition of the nucleophilic reagent is that the allylic species formed could revert back to the original arene complex (**4** or **5**) through deprotonation (Scheme 2.10, Pathway v). After deprotonation, oxidative decomposition of **4** or **5** can occur through Pathway ii described above.

The observation of a single anodic peak around +0.2 V with no starting material or Mo^{I} -acetonitrile complex, gives promise for the success of isolating a clean tandem addition products after workup. Through this method the nucleophiles MTDA, LiDMM, and *N*-methylpyrrole were found to be compatible with HOTf as an electrophile. Additional nucleophiles (i.e., primary amines, thiol salts, triethylsilane as a hydride donor, etc.) were attempted using HOTf as the electrophile; however, none of these produced the desired dihydroarenes under the conditions described here. The above possible pathways make the full analysis of the success or failure of attempted reactions on **4** and **5** difficult. Therefore, although the addition of only one electrophile and three nucleophiles seems limited, it is believed that, given the right conditions, a great breadth of chemical reactivity can be discovered using $\{\text{TpMo}(\text{NO})(\text{MeIm})\}$.

It is also worth addressing the influence of the metal on the stereochemistry of these tandem addition reactions. After protonation of $\text{TpMo}(\text{NO})(\text{MeIm})(\eta^2\text{-PAH})$, the nucleophiles add to the arenium stereoselectively *anti* to the metal center. This, in tandem with the stereogenic metal center, gives the potential for forming enantioenriched organic products using this methodology. As of this writing, two issues prevent the further

development of this chemistry. First, strategies for enantioenrichment or chiral resolution of the $\{\text{TpMo}(\text{NO})(\text{L})\}$ fragment are still being investigated. Therefore, all complexes and all organic compounds are synthesized as racemic mixtures. Second, the relatively low diastereocontrol of the metal-arene coordination (i.e., cdr of **10** = 5:1) limits the effectiveness of the stereoselectivity imparted by the metal on the tandem addition chemistry. In contrast to our current understanding of the $\{\text{TpMo}(\text{NO})(\text{L})\}$ system, $\{\text{TpRe}(\text{CO})(\text{L})\}$ and $\{\text{TpW}(\text{NO})(\text{PMe}_3)\}$ demonstrate potential pathways for controlling these ratios (i.e., sterics or solid state kinetic preference (SICKUS)), and it is our hope that similar strategies may be found for this chemistry. In spite of these limitations, we believe that the $\{\text{TpMo}(\text{NO})(\text{MeIm})\}$ system provides several advantages over these other systems in cost, reactivity, and, most excitingly, recyclability, and it is worth exploring the reactivity of this system. One significant limitation exposed by these tandem addition reactions is the limited scope of the electrophilic additions tolerated by the metal complex. In order to broaden the utility of the $\{\text{TpMo}(\text{NO})(\text{L})\}$ fragment as a dearomatization agent, greater stability under electrophilic conditions is needed. This issue is addressed in the following chapter.

2.4 Conclusion

Naphthalene and anthracene form thermally stable η^2 -bound complexes with the molybdenum system $\{\text{TpMo}(\text{NO})(\text{MeIm})\}$. Complexation leads to an enhanced reactivity toward protonation to form an arenium cation. This electrophilic species reacts with several common carbon nucleophiles to generate 1,2-dihydronaphthalene and 1,2-dihydroanthracene complexes, with the nucleophile adding *anti* to the metal. Through the use of iodine, a clean oxidative decomplexation is effected, providing the free organic,

efficiently returning the Mo^{I} precursor used to prepare the initial η^2 -aromatic complex. Thus, a formal catalytic cycle for the dearomatization of arenes has been demonstrated that is based on a dihapto-coordinated arene complex that does not involve a heavy metal. For the cases where naphthalene and anthracene are converted to tetrahydro- analogues, three new stereogenic centers are created from carbons that were part of the original aromatic rings.

2.5 Experimental

General Methods. NMR spectra were obtained on a 600 or 800 MHz spectrometer. All chemical shifts are reported in ppm, and proton and carbon shifts are referenced to tetramethylsilane (TMS) utilizing residual ^1H or ^{13}C signals of the deuterated solvents as an internal standard. Coupling constants (J) are reported in hertz (Hz). Infrared spectra (IR) were recorded as a glaze on a spectrometer fitted with a horizontal attenuated total reflectance (HATR) accessory or on a diamond anvil ATR assembly. Electrochemical experiments were performed under a dinitrogen atmosphere. Cyclic voltammetry data were taken at ambient temperature ($\sim 25^\circ\text{C}$) at 100 mV/s in a standard three-electrode cell with a glassy carbon working electrode, *N,N*-dimethylacetamide (DMA) or acetonitrile (CH_3CN) solvent (unless otherwise specified), and tetrabutylammonium hexafluorophosphate (TBAH) electrolyte (approximately 0.5 M). All potentials are reported versus NHE (normal hydrogen electrode) using cobaltocenium hexafluorophosphate ($E_{1/2} = -0.78\text{ V}$), ferrocene ($E_{1/2} = +0.55\text{ V}$), or decamethylferrocene ($E_{1/2} = +0.04\text{ V}$) as an internal standard. The peak-to-peak separation was less than 100 mV for all reversible couples. High-resolution mass spectra were acquired in ESI mode, from samples dissolved in a 3:1 acetonitrile/water solution containing sodium trifluoroacetate (NaTFA). Mass spectra are reported as M^+ for monocationic complexes or as $[\text{M} + \text{H}^+]$ or $[\text{M} + \text{Na}^+]$ for neutral complexes, using $[\text{Na}(\text{NaTFA})_x]^+$ clusters as an internal standard. In all cases, observed isotopic envelopes were consistent with the molecular composition reported. For organic products, the monoisotopic ion is reported; for complexes, the major peaks in the isotopic envelope are reported. Unless otherwise noted, all synthetic reactions were performed in a glovebox

under a dry nitrogen atmosphere. Deuterated solvents were used as received. Pyrazole (Pz) protons of the (trispyrazolyl) borate (Tp) ligand were uniquely assigned (e.g., “Pz3B”) using a combination of two-dimensional NMR data and methylimidazole–proton NOE interactions (see Figure 2.5 below). When unambiguous assignments were not possible, Tp protons were labeled as “Pz3/5 or Pz4”. All J values for Pz protons are 2 (± 0.2) Hz. Due to their sensitivity to air, elemental analysis attempts for complexes **6** – **12** were unsuccessful. Column chromatography was employed as the main method of purification for the isolation of complexes **6** – **12**; however, basic extraction was found to provide equally pure complexes along with comparable yields; this was especially useful in smaller scale (< 300 mg) reactions. Compounds **1**, **4**, and **5** were previously reported; however, an alternate synthesis avoiding the use of Na/Hg amalgam for **4** and **5** is reported below.¹⁵

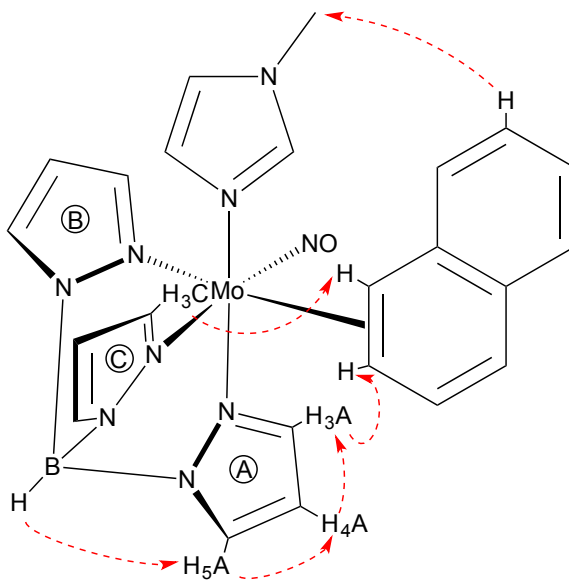
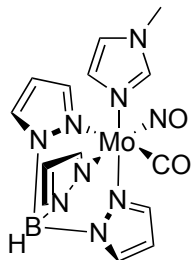


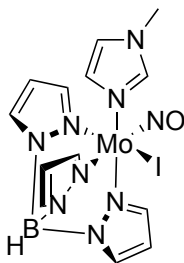
Figure 2.5. Analysis using NOE (red arrows).

Synthesis of TpMo(NO)(CO)(MeIm) (2).



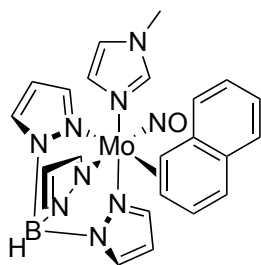
Under an air atmosphere, **1** (80 g, 0.203 mol), *N,N*-dimethylformamide (400 mL), and MeIm (60 mL, 0.73 mol) were added to a 3 neck 3 L round bottom flask charged with a stir egg, reflux condenser, thermometer and septum. The resulting orange mixture was heated at reflux (~154 °C) for 1 h then cooled to RT for 15 min. The reaction mixture was then added to stirring H₂O (1 L) and the resulting green mixture was stirred at RT. After 18 h, the blue precipitate was isolated on a 350 mL medium porosity fritted disc, washed with H₂O (250 mL), 20% MeOH:Et₂O (2 x 250 mL), and Et₂O (3 x 250 mL), and desiccated overnight to yield **2** (68.2 g, 75%). CV (DMAc) $E_{p,a} = +0.22$ V (NHE). IR: $\nu(\text{BH}) = 2480 \text{ cm}^{-1}$, $\nu(\text{CO}) = 1867 \text{ cm}^{-1}$, $\nu(\text{NO}) = 1577 \text{ cm}^{-1}$. ¹H NMR (CDCl₃, δ): 7.73 (d, Pz3/5), 7.72 (1H, d, Pz3/5), 7.67 (2H, m, Pz3/5), 7.56 (1H, s, MeIm), 7.42 (1H, d, Pz3/5), 7.31 (1H, d, Pz3/5), 6.80 (1H, t, $J = 1.4$, MeIm), 6.64 (1H, t, $J = 1.4$, MeIm), 6.19 (2H, m, Pz4), 6.11 (1H, t, Pz4), 3.68 (3H, s, MeIm).

Synthesis of TpMo(NO)(MeIm)(I) (3).



Under an air atmosphere, **2** (67 g, 0.122 mol) and DCM (250 mL) were added to a 2 L Erlenmeyer flask charged with a stir bar and the resulting mixture was stirred at RT until homogeneous. To a 500 mL Erlenmeyer flask charged with a stir bar were added I₂ (18.83 g, 0.074 mol) and Et₂O (200 mL), and the mixture was stirred 15 min at RT until homogeneous. (CAUTION: Evolution of CO) With the hood sash down, the I₂ solution was slowly added to the solution of **2** and the resulting green solution was left stirring at RT. After 15 min, Et₂O (1.5 L) was added to the reaction mixture creating a green precipitation. The precipitate was isolated on a 600 mL fine porosity fritted disc, washed with Et₂O (4 x 500 mL), and desiccated overnight to yield **3** (78.1 g, 95%). CV (DMAc) $E_{p,a} = +0.65$ V (NHE), $E_{1/2} = -1.47$ V (NHE). IR: $\nu(\text{BH}) = 2477$ cm⁻¹, $\nu(\text{NO}) = 1602$ cm⁻¹.

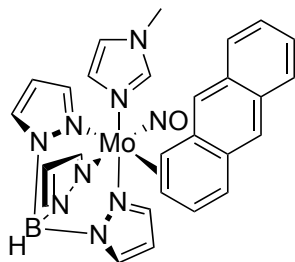
Synthesis of TpMo(MeIm)(NO)(3,4- η^2 -naphthalene) (**4**).¹⁵



To a 500 mL round bottom flask with stir bar was added **3** (12.0 g, 23.9 mmol), naphthalene (40.0 g, 312 mmol), THF (240 mL) and sodium dispersion (5.00 g, 75.0 mmol). This was stirred at room temperature for 18 h at which point the mixture was filtered through a 150 mL fine porosity fritted disc with 2 cm of celite. Et₂O (600 mL) was added to the filtrate that was then filtered through a 600 mL fine porosity fritted disc with 4 cm SiO₂ and an orange band was collected with 2:1 Et₂O:THF (700 mL). The orange solution was then evaporated *in vacuo* to 100 mL, pentane was added (900 mL)

and a yellow precipitate formed. This yellow precipitate was collected on a 60 mL fine porosity fritted disc, washed with pentane (3 x 50 mL), and desiccated 1 h to yield **4** (4.42 g, 34 %).

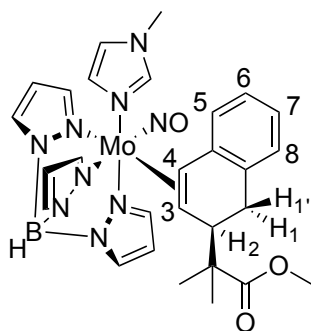
Synthesis of TpMo(MeIm)(NO)(3,4- η^2 -anthracene) (5**).¹⁵**



In a 50 mL round bottom flask with stir bar was added sodium dispersion (1.00 g, 15.0 mmol) and hexanes (50 mL). This was stirred at room temperature for 30 min. The organic layer was decanted, hexanes (50 mL) was added to the flask, and the mixture was stirred at room temperature 1 h. The organic layer was decanted, THF (50 mL) was added and the organic layer was decanted off. THF (10 mL) was added to the flask and the mixture was transferred to a 100 mL round bottom flask charged with stir bar, **3** (1.00 g, 2.00 mmol), THF (12 mL), and 2,5-dimethylfuran (2.00 mL, 18.5 mmol). This mixture was stirred at room temperature for 2 h and then filtered through a 15 mL medium porosity fritted disc with 2 cm celite and washed with THF (2 x 4 mL). This solution was then transferred to a 100 mL round bottom flask charged with stir bar and anthracene (3.56 g, 20.0 mmol). This brown mixture was stirred at room temperature 48 h yielding a red mixture. Et₂O (15 mL) was added to the flask and filtered through a 30 mL medium porosity fritted disc with 2 cm SiO₂. A red filtrate was eluted with 1:1 Et₂O:THF (25 mL) and Et₂O (10 mL). This was evaporated to dryness *in vacuo*. The red solid was then

washed with CH₃CN (20 mL) and the free anthracene was removed on a 30 mL fine porosity fritted disc. This red solution was then evaporated *in vacuo*, dissolved in DCM (6 mL), and precipitated in hexanes (50 mL). The red solid was then collected on a 30 mL fine porosity fritted disc, washed with hexanes (2 x 10 mL) and desiccated 1 h to yield **5** (520 mg, 44 %)

TpMo(MeIm)(NO)(3,4-η²-(methyl-2-(1,2-dihydronaphthalen-2-yl)-2-methylpropanoate)) (6).



To a 250 mL round bottom flask was added **4** (5.00 g, 9.12 mmol) and 100 mL CH₃CN. This orange mixture was cooled while stirring for 30 min at -35 °C. To this orange mixture was added 1M HOTf/CH₃CN (35 mL, 35.0 mmol) cooled to -35 °C. This red solution was left stirring 30 min at -35 °C. This red mixture was stirred at room temperature 15 min yielding a red solution that was then cooled to -35 °C. A -35 °C solution of MTDA (10 mL, 49.2 mmol) was added and the yellow solution was left standing at -35 °C for 15 min. Next, a -35 °C solution of triethylamine (10 mL, 71.7 mmol) was added and the golden solution was warmed to room temperature. The solution was then evaporated *in vacuo* to dryness, picked up in 1:1 Et₂O:benzene (50 mL) and chromatographed through a 300 mL medium porosity fritted disc with 4 cm of silica. The

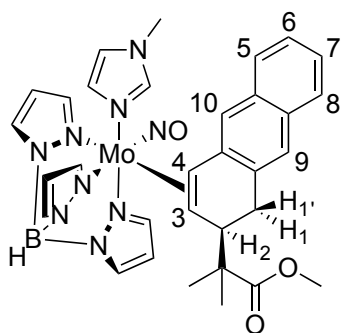
product was eluted with 1:1 Et₂O:benzene (1 L). The yellow filtrate was then evaporated *in vacuo*, dissolved in DCM (25 mL) and precipitated in stirring pentane (250 mL). The precipitate was then collected on a 150 mL fine porosity fritted disc, washed with pentane (3 x 100 mL), and dried for 1 h yielding the yellow precipitate **6** (3.62 g, 61 %).

Basic Extraction Workup of **6**

To a test tube was added **4** (300 mg, 0.546 mmol) and 6 mL CH₃CN. This orange mixture was cooled while stirring for 15 min at -35 °C. To this orange mixture was added 1M HOTf/CH₃CN (2.1 mL, 2.10 mmol) cooled to -35 °C. This red solution was left stirring 15 min at -35 °C. A -35 °C solution of MTDA (0.6 mL, 2.95 mmol) was added and the yellow solution was left stirring at -35 °C for 20 min. Next, a -35 °C solution of triethylamine (0.6 mL, 4.32 mmol) was added and the golden solution was warmed to room temperature. The solution was then evaporated *in vacuo* to dryness, picked up in CHCl₃ (10 mL), and washed with sat. aq. NaHCO₃ (3 x 10 mL). The organic layer was then dried over MgSO₄ and the drying agent was filtered off. The yellow filtrate was then evaporated *in vacuo*, dissolved in DCM (1 mL) and precipitated in stirring pentane (50 mL). The precipitate was then collected on a 15 mL fine porosity fritted disc, washed with pentane (3 x 30 mL), and dried yielding the yellow precipitate **6** (218 mg, 62 %). CV (DMAc) $E_{p,a} = +0.16$ V (NHE). ¹H NMR (d⁶-Acetone, δ): 8.00 (1H, d, Pz5B), 7.93 (1H, d, Pz5C), 7.92 (1H, d, Pz5A), 7.82 (1H, d, Pz3C), 7.74 (1H, d, Pz3A), 7.16 (1H, d, Pz3B), 7.14 (1H, t, $J = 1.7$, MeIm), 6.98 (1H, bt, $J = 1.5$, MeIm), 6.92 (1H, d, $J = 7.3$, H8), 6.78 (1H, tt, $J = 7.3$, 1.0, H6), 6.40 (1H, t, $J = 1.4$, MeIm), 6.39 (1H, t, Pz4A), 6.36 (1H, t, Pz4C), 6.08 (1H, t, Pz4B), 5.88 (1H, dd, $J = 7.3$, 1.3, H5), 3.74 (3H, s, MeIm),

3.52 (1H, dd, $J = 16.7, 8.9$, H1'), 3.32 (3H, s, OMe), 3.23 (1H, d, $J = 8.1$, H2), 3.13 (1H, d, $J = 9.5$, H4), 2.55 (1H, d, $J = 16.7$, H1), 2.06 (1H, dt, $J = 9.5, 1.8$, H3), 1.11 (3H, s, Me), 0.95 (3H, s, Me). ^{13}C NMR (d^6 -Acetone, δ): 178.9 (CO), 144.7, 142.7 (Pz5B), 141.8 (Pz3B), 141.7 (Pz3C), 139.1 (MeIm), 137.2 (Pz5C), 137.0 (Pz5A), 135.4 (Pz3A), 133.8, 129.0, 125.5 (C5), 124.1 (C6), 123.1 (C7), 122.1 (MeIm), 106.5 (Pz4), 106.3 (Pz4), 106.0 (Pz4), 69.0 (C4), 51.2 (C3), 51.0 (OMe), 43.9 (C2), 34.3 (NMe), 30.1 (C1), 23.4 (Me), 23.0 (Me). HRMS: $\text{C}_{28}\text{H}_{34}\text{N}_9\text{O}_3\text{BMo}+\text{Na}^+$ obsd (%), calcd (%), ppm: 670.1867 (46), 670.1843 (52), 3.6; 672.1854 (48), 672.1840 (49), 2.0; 673.1843 (77), 673.1839 (81), 0.5; 674.1854 (83), 674.1835 (87), 2.8; 675.1850 (77), 675.1847 (76), 0.4; 676.1849 (100), 676.1834 (100), 2.2; 677.1870 (36), 677.1862 (38), 1.2; 678.1883 (32), 678.1854 (39), 4.3. **Minor Isomer:** ^1H NMR (d^6 -Acetone, δ): 8.20 (1H, d, Pz3/5), 7.88 (1H, d, Pz3/5), 7.86 (1H, d, Pz3/5), 6.75 (2H, m, naphthalene), 6.30 (1H, t, Pz4), 3.57 (1H, dd, $J = 18.8, 8.6$, H1a), 2.51 (1H, d, $J = 18.8$, H1b), 1.86 (1H, dt, $J = 9.8, 1.8$, H3).

TpMo(MeIm)(NO)(3,4- η^2 -(methyl-(*R*)-2-(1,2-dihydroanthracen-2-yl)-2-methylpropanoate)) (7).

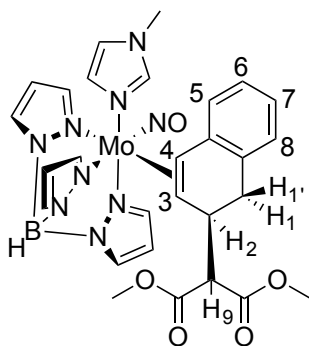


To a test tube was added **5** (200 mg, 0.333 mmol) and 4 mL CH_3CN . This red solution was cooled for 15 min at -35°C . To this solution was added 1M HOTf/ CH_3CN (1.4 mL,

1.40 mmol) cooled to $-35\text{ }^{\circ}\text{C}$. This dark red solution was left standing at $-35\text{ }^{\circ}\text{C}$ for 15 min at which point a $-35\text{ }^{\circ}\text{C}$ solution of MTDA (0.4 mL, 1.96 mmol) was added and left standing at $-35\text{ }^{\circ}\text{C}$ for 2 h. Next, a $-35\text{ }^{\circ}\text{C}$ solution of triethylamine (0.4 mL, 2.87 mmol) was added and the orange solution was warmed to room temperature. The solution was then evaporated *in vacuo* to dryness, picked up in 1:1 benzene:THF (2 mL), and chromatographed through a 15 mL medium porosity fritted disc with 2 cm silica. The product was eluted with 1:1 Et₂O:benzene (20 mL). The orange filtrate was then evaporated *in vacuo*, dissolved in DCM (1 mL) and precipitated in stirring pentane (25 mL). The precipitate was then collected on a 15 mL fine porosity fritted disc and dried for 15 min yielding the yellow precipitate **7** (89 mg, 41%). CV (DMAc) $E_{p,a} = +0.18\text{ V}$ (NHE). IR: $\nu(\text{BH}) = 2480\text{ cm}^{-1}$, $\nu(\text{CO}) = 1720\text{ cm}^{-1}$, $\nu(\text{NO}) = 1562\text{ cm}^{-1}$. ¹H NMR (CDCl₃, δ): 8.07 (1H, d, Pz3C), 7.77 (1H, d, Pz5C), 7.71 (1H, d, Pz5A), 7.69 (1H, d, $J = 8.0$, H8), 7.67 (1H, d, Pz3A), 7.58 (1H, d, Pz3/5B), 7.51 (1H, s, H9), 7.38 (1H, d, $J = 8.2$, H5), 7.23 (1H, m, H6), 7.19 (1H, m, H7), 7.06 (1H, d, Pz3/5B), 6.79 (1H, t, $J = 1.5$, MeIm), 6.63 (1H, s, H10), 6.34 (1H, buried s, MeIm), 6.33 (1H, t, Pz4C), 6.29 (1H, t, Pz4A), 6.18 (1H, s, MeIm), 6.01 (1H, t, Pz4B), 3.70 (1H, dd, $J = 17.4, 7.9$, H1'), 3.35 (3H, s, OMe), 3.34 (3H, s, MeIm), 3.31 (1H, d, $J = 7.1$, H2), 3.26 (1H, d, $J = 9.3$, H4), 2.89 (1H, d, $J = 17.4$, H1), 2.25 (1H, dt, $J = 9.6, 1.7$, H3), 1.18 (3H, s, Me), 1.03 (3H, s, Me). ¹³C NMR (CDCl₃, δ): 179.3 (CO), 142.9, 142.5, 141.3, 140.8, 138.3, 136.3, 136.1, 134.4, 143.3, 132.0, 128.8, 127.4, 125.7, 125.4, 124.2, 123.2, 120.6, 120.5, 105.8, 105.6, 105.4, 100.2, 69.6, 66.0, 65.1, 51.3, 50.2, 43.2, 34.4, 22.8. HRMS: $[\text{M}+\text{Na}^+] = [\text{C}_{32}\text{H}_{36}\text{N}_9\text{O}_3\text{BMo}+\text{Na}^+]$ obsd (%), calcd (%), ppm: 720.2013 (47), 720.2000 (51), 1.8; 722.1990 (40), 722.1998 (48), -1.1; 723.2007 (73), 723.1997 (80), 1.4; 724.1985 (83),

724.1993 (87), -1.1; 725.1990 (77), 725.2005 (77), -2.0; 726.1980 (100), 726.1992 (100), -1.7; 727.1992 (36), 727.2019 (41), -3.8; 728.2007 (34), 728.2012 (40), -0.7. **Minor Isomer:** ^1H NMR (CDCl_3 , δ): 8.28 (1H, d, Pz3/5), 7.79 (1H, d, Pz3/5), 7.78 (1H, d, Pz3/5), 6.11 (1H, t, Pz4), 6.03 (2H, t, Pz4), 2.03 (1H, dt, $J = 10.0, 1.7$, H3).

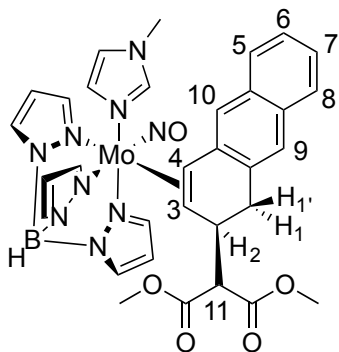
TpMo(MeIm)(NO)(3,4- η^2 -2-(1,2-dihydronaphthalen-2-yl)-dimethylmalonate) (8).



To a 4 dram vial was added **4** (200 mg, 0.364 mmol) and 4 mL CH_3CN . This orange mixture was cooled with stirring for 15 min at -35°C . To this orange mixture was added a 1 mL (1 mmol) of a 1M HOTf/ CH_3CN cooled to -35°C . This red solution was left standing 15 min at -35°C . Lithium dimethylmalonate (270 mg, 1.94 mmol) was added and the yellow solution was left standing at -35°C for 1 h. Next, a -35°C solution of triethylamine (0.4 mL, 2.86 mmol) was added and the golden solution was warmed to room temperature. The solution was then evaporated *in vacuo* to dryness, picked up in benzene (2 mL) and chromatographed through a 15 mL medium porosity fritted disc with 2 cm silica. The product was eluted with 1:1 Et_2O :benzene (40 mL). The yellow filtrate was then evaporated *in vacuo*, dissolved in DCM (2 mL) and precipitated in stirring pentane (40 mL). The precipitate was then collected on a 15 mL medium porosity fritted disc, washed with pentane (3 x 10 mL), and dried for 15 min yielding the yellow

precipitate **8** (165 mg, 66 %). CV (DMAc) $E_{p,a} = +0.23$ V (NHE). IR: $\nu(\text{BH}) = 2484 \text{ cm}^{-1}$, $\nu(\text{CO}) = 1751$ & 1732 cm^{-1} , $\nu(\text{NO}) = 1574 \text{ cm}^{-1}$. ^1H NMR (d^6 -Acetone, δ): 7.93 (2H, d, Pz3A & C), 7.92 (1H, d, Pz5C), 7.90 (1H, d, Pz5A), 7.76 (1H, d, Pz3B), 7.72 (1H, d, Pz5B), 7.16 (1H, t, $J = 1.7$, MeIm), 7.04 (1H, bt, $J = 1.8$, MeIm), 6.92 (1H, d, $J = 7.6$, H8), 6.87 (1H, tt, $J = 7.5$, 1.2, H6), 6.78 (1H, td, $J = 7.4$, 1.3, H7), 6.42 (1H, t, $J = 1.3$, MeIm), 6.40 (1H, t, Pz4A), 6.35 (1H, t, Pz4C), 6.09 (1H, t, Pz4B), 5.97 (1H, dd, $J = 7.4$, 1.4, H5), 3.79 (3H, s, MeIm), 3.61 (3H, s, DMM), 3.56 (1H, dd, $J = 16.3$, 6.0, H1'), 3.46 (1H, m, H2), 3.42 (1H, s, H9), 3.36 (3H, s, DMM), 3.05 (1H, d, $J = 9.5$, H4), 2.50 (1H, d, $J = 16.3$, H1), 2.10 (1H, dt, $J = 9.5$, 2.3, H3). ^{13}C NMR (CDCl_3 , δ): 170.1 (CO), 170.0 (CO), 144.1, 143.3 (Pz5C), 141.9 (MeIm), 141.4 (Pz5B), 139.1 (MeIm), 137.4 (Pz3A & Pz3C), 136.9 (Pz5A), 135.4 (Pz3B), 131.4, 129.4 (C8), 129.0 (MeIm), 125.8 (C5), 124.9 (C6), 123.2 (C7), 122.2 (MeIm), 106.5 (Pz4A & Pz4C), 106.1 (Pz4B), 67.3 (2C's C4 and C3), 59.8 (C9), 52.1 (OMe), 51.8 (OMe), 38.2 (C9), 34.8 (NMe), 34.2, 32.8 (C1). HRMS: $[\text{M}^+] = [\text{C}_{28}\text{H}_{32}\text{N}_9\text{O}_5\text{BMo}^+]$ obsd (%), calcd (%), ppm: 677.1682 (48), 677.1687 (52), -0.8; 679.1673 (44), 679.1685 (49), -1.7; 680.1685 (77), 680.1684 (80), 0.2; 681.1668 (86), 681.1679 (87), -1.6; 682.1681 (79), 682.1691 (76), -1.5; 683.1668 (100), 683.1679 (100), -1.6; 684.1691 (38), 684.1706 (38), -2.3; 685.1672 (41), 685.1698 (40), -3.9. **Minor Isomer** ^1H NMR (d^6 -Acetone, δ): 8.13 (1H, d, Pz3/5), 7.85 (1H, d, Pz3/5), 7.62 (1H, d, Pz3/5), 6.30 (1H, t, Pz4), 6.06 (1H, t, Pz4), 1.84 (1H, dt, $J = 9.7$, 1.6, H3).

TpMo(MeIm)(NO)(3,4- η^2 -(R)-dimethyl-2-(1,2-dihydroanthracen-2-yl)malonate) (9).

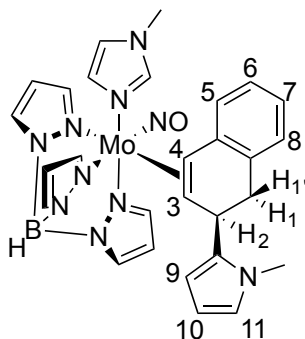


To a test tube was added **5** (200 mg, 0.333 mmol) and 4 mL CH₃CN. This red solution was cooled for 15 min at -35 °C. To this solution was added 1M HOTf/CH₃CN (1.4 mL, 1.40 mmol) cooled to -35 °C. This dark red solution was left standing at -35 °C for 15 min at which point LiDMM (270 mg, 1.97 mmol) was added and left standing at -35 °C for 15 min. Next, a -35 °C solution of triethylamine (0.4 mL, 2.87 mmol) was added and the orange solution was warmed to room temperature. The solution was then evaporated *in vacuo* to dryness and the resulting oil was dissolved in CHCl₃. This solution was then washed with NaHCO₃ (sat. aq., 10 mL), dried over MgSO₄, and filtered through a 15 mL medium porosity fritted disc. The filtrate was then evaporated *in vacuo* and the resulting oil was dissolved in DCM (1 mL). This solution was added to stirred pentane (50 mL) yielding a yellow precipitate that was then isolated on a 15 mL fine porosity fritted disc. This precipitate was then added to acetone (2 mL) and the resulting mixture was stirred for 15 min. This precipitate was then isolated on a 15 mL fine porosity fritted disc, washed with acetone (2 x 2 mL), and desiccated for 15 min to yield the yellow solid **9** (104 mg, 48%). CV (DMAc) $E_{p,a} = +0.25$ V (NHE). IR: $\nu(\text{BH}) = 2453$ cm⁻¹, $\nu(\text{CO}) = 1739$ cm⁻¹, 1720 cm⁻¹ $\nu(\text{NO}) = 1562$ cm⁻¹. ¹H NMR (CDCl₃, δ): 7.99 (1H, d, Pz3A), 7.75 (1H, d, Pz5C), 7.73 (1H, d, Pz5A), 7.69 (1H, d, $J = 8.1$, H8), 7.58 (1H, d, Pz5B), 7.57

(1H, d, Pz3C), 7.52 (1H, s, H9), 7.43 (1H, d, $J = 8.3$, H5), 7.27 (1H, t, $J = 7.4$, H6), 7.22 (1H, t, $J = 7.4$, H7), 7.06 (1H, t, Pz3B), 6.34 (1H, t, Pz4A), 6.27 (1H, s, H10), 6.25 (1H, t, Pz4C), 6.02 (1H, t, Pz4B), 3.75 (1H, m, H1), 3.61 (3H, s, DMM), 3.58 (1H, m, H2), 3.56 (1H, d, $J = 9.7$, H11), 3.45 (3H, s, DMM), 3.41 (3H, s, MeIm), 3.18 (1H, d, $J = 9.4$, H4), 2.85 (1H, d, $J = 16.6$, H1'), 2.31 (1H, dt, $J = 9.4$, 2.0, H3). ^{13}C NMR (CDCl_3 , δ): 179.3, 143.3, 142.9, 142.5, 141.3 (Pz3), 140.8, 138.3 (Pz5C), 136.3 (Pz5A), 136.1, 134.4 (Pz5B), 132.0, 128.8 (C8), 127.4 (C9), 125.7 (C5), 125.4 (C7), 124.2, 123.2 (C10), 120.6, 120.5, 105.8 (Pz4), 105.6 (Pz4), 105.4 (Pz4), 100.2, 69.6 (C4), 66.0 (C3), 65.1, 51.3 (OMe), 50.2 (OMe), 43.2 (C2), 34.4 (NMe), 22.8 (C1). HRMS: $[\text{M}^+] = [\text{C}_{32}\text{H}_{34}\text{N}_9\text{O}_5\text{BMo}^+]$ obsd (%), calcd (%), ppm: 727.1868 (50), 727.1844 (51), 3.3; 729.1831 (43), 729.1843 (48), -1.6; 730.1827 (75), 730.1841 (80), -1.9; 731.1848 (86), 731.1837 (87), 1.5; 732.1832 (75), 732.1849 (77), -2.3; 733.1844 (100), 733.1837 (100), 1.0; 734.1862 (35), 734.1864 (41), -0.2; 735.1854 (27), 735.1857 (40), -0.4. **Minor Isomer:** ^1H NMR (d^6 -Acetone, δ): 8.24 (1H, d, Pz3/5), 6.33 (1H, d, Pz4), 6.01 (1H, t, Pz4).

TpMo(MeIm)(NO)(3,4- η^2 -2-(1,2-dihydronaphthalen-2-yl)-1-methyl-1H-pyrrole)

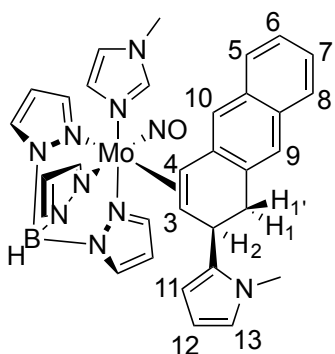
(10).



To a 50 mL round bottom charged with stir bar was added **4** (1.00 g, 1.82 mmol) and 20 mL CH₃CN. This orange mixture was cooled with stirring for 15 min at -35 °C. To this orange mixture was added 1M HOTf/CH₃CN (9.2 mL, 9.20 mmol) cooled to -35 °C. This orange mixture was stirred at room temperature 5 min yielding a red solution that was then cooled to -35 °C. After 15 min standing at -35 °C, *N*-methylpyrrole (16 mL, 179 mmol) was added and left standing at -35 °C for 18 h. Next, a -35 °C solution of triethylamine (2 mL, 14.3 mmol) was added and the golden solution was warmed to room temperature. The solution was then evaporated *in vacuo* to half volume (~10 mL) and chromatographed through a 150 mL coarse porosity fritted disc filled 3 cm with silica. The product was eluted with 1:1 Et₂O:benzene (175 mL). The yellow filtrate was then evaporated *in vacuo*, dissolved in DCM (7 mL) and precipitated in stirring pentane (125 mL). The precipitate was then collected on a 30 mL fine porosity fritted disc and dried for 15 min yielding the yellow precipitate **10** (600 mg, 53 %). CV (DMAc) $E_{p,a} = +0.14$ V (NHE). IR: $\nu(\text{BH}) = 2480 \text{ cm}^{-1}$, $\nu(\text{NO}) = 1562 \text{ cm}^{-1}$. ¹H NMR (d⁶-Acetone, δ): 8.13 (1H, d, Pz3A), 7.93 (1H, d, Pz5A), 7.91 (1H, d, Pz5B), 7.78 (1H, d, Pz3B), 7.77 (1H, d, Pz5C), 7.19 (1H, d, Pz3C), 7.17 (1H, t, $J = 1.5$, MeIm), 7.12 (1H, s, MeIm), 6.93 (1H, d, $J = 7.5$, H8), 6.84 (1H, t, $J = 7.5$, H6), 6.73 (1H, dt, $J = 7.5$, 1.3, H7), 6.47 (1H, t, $J = 1.4$, MeIm), 6.40 (1H, t, Pz4A), 6.33 (1H, t, Pz4B), 6.32 (1H, t, $J = 2.2$, H11), 6.10 (1H, t, Pz4C), 5.98 (1H, d, $J = 7.2$, H5), 5.68 (1H, dd, $J = 3.4$, 1.9, H10), 5.64 (1H, t, $J = 2.9$, H9), 4.02 (1H, d, $J = 7.4$, H2), 3.78 (3H, s, MeIm), 3.75 (1H, dd, $J = 15.7$, 7.0, H1'), 3.4 (3H, s, NMP), 3.11 (1H, d, $J = 9.0$, H4), 2.74 (1H, d, $J = 15.7$, H1) 2.34 (1H, dt, $J = 9.0$, 1.9, H3). ¹³C NMR (d⁶-Acetone, δ): 144.5, 143.1, 141.9, 141.8, 141.7, 139.2, 137.1, 137.0, 135.5, 132.8, 129.1, 128.8, 125.9, 124.4, 123.0, 122.2, 120.4, 106.6, 106.5, 106.5,

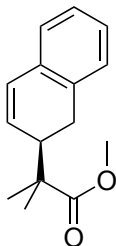
106.2, 106.1, 70.3, 66.9, 34.4, 34.3, 33.7, 33.5. HRMS: $[M+Na^+] = [C_{28}H_{31}N_{10}OBMo+Na^+]$ obsd (%), calcd (%), ppm: 649.1767 (50), 649.1741 (52), 4.1; 651.1740 (47), 651.1738 (48), 0.3; 652.1746 (77), 652.1737 (81), 1.4; 653.1745 (87), 653.1732 (87), 2.0; 654.1745 (75), 654.1744 (76), 0.1; 655.1742 (100), 655.1732 (100), 1.6; 656.1780 (36), 656.1759 (38), 3.2; 657.1766 (37), 657.1751 (39), 2.2. **Minor Isomer:** 1H NMR (d^6 -Acetone, δ): 8.01 (1H, d, Pz3/5), 7.90 (1H, d, Pz3/5), 7.75 (1H, d, Pz3/5), 6.90 (1H, d, naphthalene), 6.38 (1H, t, MeIm), 6.26 (1H, t, Pz4), 6.25 (1H, t, Pz4), 6.08 (1H, t, Pz4), 3.83 (d, $J = 7.2$, H4), 2.46 (1H, dt, $J = 9.4$, 2.2, H3)

TpMo(MeIm)(NO)(3,4- η^2 -2-(1,2-dihydroanthracen-2-yl)-1-methyl-1H-pyrrole) (11).

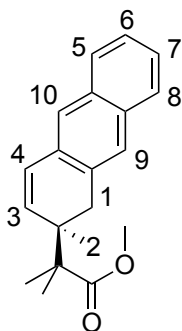


To a test tube was added **5** (300 mg, 0.501 mmol) and 6 mL CH_3CN . This red solution was cooled for 15 min at $-35^\circ C$. To this solution was added 1M HOTf/MeOH (2.1 mL, 2.10 mmol) cooled to $-35^\circ C$. This dark red solution was left standing at $-35^\circ C$ for 15 min at which point *N*-methylpyrrole (4.8 mL, 53.7 mmol) was added and left standing at $-35^\circ C$ for 18 h. Next, a $-35^\circ C$ solution of triethylamine (0.6 mL, 4.30 mmol) was added and the orange solution was warmed to room temperature. The solution was then evaporated *in vacuo* to dryness, dissolved in THF (2 mL), and chromatographed through a 60 mL medium porosity fritted disc 2 cm full with silica. The product was eluted with

1:1 Et₂O:benzene (50 mL). The orange filtrate was then evaporated *in vacuo*, dissolved in DCM (1 mL) and precipitated in stirring pentane (100 mL). The precipitate was then collected on a 15 mL fine porosity fritted disc and dried for 15 min yielding the yellow precipitate **11** (85 mg, 27%). CV (DMAc) $E_{p,a} = +0.15$ V (NHE). IR: $\nu(\text{BH}) = 2476$ cm⁻¹, $\nu(\text{NO}) = 1554$ cm⁻¹. ¹H NMR (d⁶-Acetone, δ): 8.15 (1H, d, Pz3A), 7.94 (2H, m, Pz5A & C), 7.85 (1H, d, Pz3C), 7.76 (1H, d, Pz3/5B), 7.55 (1H, d, $J = 8.3$, H8), 7.49 (1H, d, $J = 8.1$, H5), 7.43 (1H, s, H9), 7.25 (1H, t, $J = 7.5$, H6), 7.21 (1H, t, $J = 1.5$, MeIm), 7.19 (1H, m, H7), 7.19 (1H, buried d, Pz3/5B), 7.05 (1H, bt, MeIm), 6.51 (1H, t, $J = 1.3$, MeIm), 6.42 (1H, t, Pz4A), 6.35 (1H, t, Pz4C), 6.32 (1H, buried s, H10), 6.33 (1H, buried multiplet, H13), 6.09 (1H, t, Pz4B), 5.70 (1H, dd, $J = 3.7, 1.8$, H12), 5.61 (1H, m, H11), 4.09 (1H, d, $J = 6.9$, H2), 3.92 (1H, ddd, $J = 15.7, 7, 1.3$, H1'), 3.64 (3H, s, MeIm), 3.47 (3H, s, NMP), 3.33 (1H, d, $J = 9.6$, H4), 3.00 (1H, d, $J = 15.7$, H1), 2.47 (1H, dt, $J = 9.6, 2.0$, H3). ¹³C NMR (d⁶-Acetone, δ): 143.9, 143.3, 142.0 (Pz3/5), 141.7 (Pz3C), 139.0, 137.2 (Pz5A & Pz5C), 137.1, 135.6 (Pz3/5), 134.1, 133.3, 132.1, 129.1, 127.6 (C8), 126.7 (C5), 126.5 (C9), 124.9 (C6), 123.6 (C7), 122.2 (C10), 121.6, 120.6, 106.6, 106.6, 106.6, 106.3, 106.1, 70.8 (C3), 67.4 (C4), 34.8 (C1), 34.5 (NMe), 33.7 (C2), 33.5 (NMe). HRMS: $[\text{M}+\text{Na}^+] = [\text{C}_{32}\text{H}_{33}\text{N}_{10}\text{OBMo}+\text{Na}^+]$ obsd (%), calcd (%), ppm: 699.1895 (52), 699.1898 (51), -0.4; 701.1902 (38), 701.1896 (48), 0.9; 702.1914 (79), 702.1894 (80), 2.8; 703.1904 (88), 703.1890 (88), 2.0; 704.1865 (76), 704.1902 (77), -5.2; 705.1867 (100), 705.1890 (100), -3.2; 706.1896 (36), 706.1916 (41), -2.9; 707.1875 (39), 707.1910 (39), -4.9.

Methyl-2-(1,2-dihydronaphthalen-2-yl)-2-methylpropanoate (12).

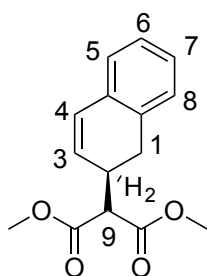
To a 500 mL Erlenmeyer flask charged with stir bar was added **6** (4.00 g, 6.14 mmol) and DCM (100 mL). Next, iodine (756 mg, 3.00 mmol) dissolved in Et₂O (~25 mL) was added to the stirring yellow solution changing instantly to green. This solution was stirred for 5 min and was then add to 300 mL stirring pentane. The green precipitate **3** was then isolated on a 60 mL fine porosity fritted disc and washed with pentane (3 x 60 mL) and Et₂O (3 x 60 mL). The colorless filtrate was then removed from the glovebox and evaporated *in vacuo*. This oil was then filtered through a 30 mL medium porosity fritted disc 2 cm full with silica along with 200 mL DCM. The filtrate was then evaporated *in vacuo*, loaded (6 x 0.6 mL DCM) onto a silica preparatory plate, and was eluted with 10% EtOAc:hexanes (HPLC grade, 200 mL). A KMnO₄ positive band at R_f 0.50-1.00 was isolated and sonicated in HPLC grade EtOAc (100 mL) for 20 min. The silica was then filtered off on a 30 mL fine porosity fritted disc and was washed with DCM (3 x 20 mL). The filtrate was then evaporated *in vacuo* and dried 1 h yielding the colorless oil **12** (836 mg, 64%). This sample matched previous reports.²³

Methyl-2-(1,2-dihydroanthracen-2-yl)-2-methylpropanoate (13).

To a 25 mL filter flask charged with stir bar was added **7** (600 mg, 0.855 mmol) and DCM (5 mL). Next, 0.06 M I₂/Et₂O (7.83 mL, 0.469 mmol) was added to the stirring yellow solution changing instantly to green. This solution was stirred for 5 min and was then evaporated *in vacuo* to 1 mL and added to stirring hexanes (40 mL). The green precipitate **3** was then isolated on a 15 mL medium porosity fritted disc and washed with hexanes (3 x 10 mL) and Et₂O (10 mL). The colorless filtrate was then removed from the glovebox and evaporated *in vacuo*. This oil was then loaded (3 x 0.3 mL DCM) onto a silica preparatory plate and was eluted with 10% EtOAc:hexanes (HPLC grade, 200 mL). A KMnO₄ positive band at R_f 0.56-0.68 was scraped off and sonicated in EtOAc (HPLC grade, 25 mL) for 10 min. The silica gel was then filtered off on a 30 mL fine porosity fritted disc and was washed with DCM (4 x 15 mL). The filtrate was then evaporated *in vacuo* and dried 1 h yielding the colorless oil **13** (162 mg, 79%). IR: $\nu(\text{C-H sp}^2) = 3051 \text{ cm}^{-1}$, $\nu(\text{CO}) = 1732 \text{ cm}^{-1}$. ¹H NMR (CDCl₃, δ): 7.74 (1H, m, H5/8), 7.71 (1H, m, H5/8), 7.51 (1H, s, H9), 7.45 (1H, s, H10), 7.39 (2H, m, H6 & H9), 6.71 (1H, dd, $J = 9.8, 1.6$, H4), 5.95 (1H, dd, $J = 9.8, 3.7$, H3), 3.70 (3H, s, O-CH₃), 2.97 (1H, dd, $J = 13.3, 5.8$, H1'), 2.92 (1H, m, H2), 2.91 (1H, m, H1), 1.24 (3H, s, MMTP), 1.20 (3H, s, MMTP). ¹³C NMR (CDCl₃, δ): 178.0 (CO), 133.9, 133.3, 133.0, 132.2, 130.1 (C3), 129.4 (C4), 127.8

(C5/C8), 127.3 (C5/C8), 125.8, 125.5, 124.3, 52.0 (OMe), 45.9, 41.8 (C2), 30.2 (C1), 22.7 (Me), 22.1 (Me). LRMS: $[M^+] = 280$.

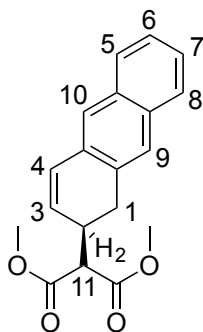
Dimethyl-2-(1,2-dihydronaphthalen-2-yl)malonate (14).



To a 25 mL filter flask charged with stir bar was added **8** (100 mg, 0.146 mmol) and DCM (5 mL). Next, 0.06 M I_2/Et_2O (1.16 mL, 0.07 mmol) was added to the stirring yellow solution changing instantly to green. This solution was stirred for 5 min and was then evaporated *in vacuo* to 1 mL and added to stirring pentane (20 mL). The green precipitate **3** was isolated on a 15 mL fine porosity fritted disc, washed with pentane (3 x 10 mL). The colorless filtrate was then removed from the glovebox and evaporated *in vacuo*. This oil was then loaded (3 x 0.3 mL DCM) onto a silica preparatory plate and was eluted with 10% EtOAc:hexanes (HPLC grade, 200 mL). A $KMnO_4$ positive band at R_f 0.30-0.40 was scraped off and sonicated in 10% EtOAc:hexanes (HPLC grade, 25 mL) for 10 min. The silica was then filtered off on a 30 mL fine porosity fritted disc and was washed with HPLC grade hexanes (3 x 20 mL). The filtrate was evaporated *in vacuo* and dried 1 h yielding the colorless oil **14** (22 mg, 61%). IR: (CO) = 1736 cm^{-1} . 1H NMR ($CDCl_3$, δ): 7.16 (2H, m, H6 & H7), 7.09 (1H, d, $J = 7.2$, H8), 7.05 (1H, d, $J = 7.2$, H5), 6.53 (1H, dd, $J = 9.9, 1.6$, H4), 5.95 (1H, dd, $J = 9.9, 4.6$, H3), 3.73 (3H, s, DMM), 3.71 (3H, s, DMM), 3.41 (1H, d, $J = 9.5$, H9), 3.22 (1H, m, H2), 2.97 (1H, dd, $J = 15.8, 6.9$,

H1'), 2.73 (1H, dd, $J = 15.8, 8.1$, H1). ^{13}C NMR (CDCl_3 , δ): 168.8 (CO), 168.7 (CO), 133.4, 133.2, 129.3 (C4), 128.6 (C3), 128.2, 127.7, 127.0, 126.3, 54.6 (C9), 52.7 (OMe), 52.6 (OMe), 33.7 (C2), 31.7 (C1). HRMS: $[\text{C}_{15}\text{H}_{16}\text{O}_4 + \text{Na}^+]$ obsd (%), calcd (%), ppm: 283.0933 (100), 283.0941 (100), -2.8.

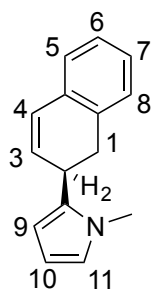
Dimethyl-2-(1,2-dihydroanthracen-2-yl)malonate (15).



To a 25 mL filter flask charged with stir bar was added **9** (100 mg, 0.137 mmol) and DCM (5 mL). Next, 0.06 M $\text{I}_2/\text{Et}_2\text{O}$ (1.2 mL, 0.070 mmol) was added to the stirring yellow solution changing instantly to green. This solution was stirred for 5 min and was then evaporated *in vacuo* to 1 mL and added to stirring hexanes (25 mL). The green precipitate **3** was then isolated on a 15 mL fine porosity fritted disc and washed with Et_2O (3 x 10 mL). The colorless filtrate was then removed from the glovebox and evaporated *in vacuo*. This oil was then loaded (3 x 0.3 mL DCM) onto a silica preparatory plate and was eluted with 10% EtOAc :hexanes (HPLC grade, 200 mL). A KMnO_4 positive band at R_f 0-0.4 was scraped off and sonicated in EtOAc (HPLC grade, 25 mL) for 10 min. The SiO_2 gel was then filtered off on a 30 mL fine porosity fritted disc and was washed with DCM (3 x 15 mL). The filtrate was then evaporated *in vacuo* and dried 1 h yielding the colorless oil **15** (23 mg, 62%). IR: $\nu(\text{C-H sp}^2) = 3047 \text{ cm}^{-1}$, $\nu(\text{CO}) = 1736 \text{ cm}^{-1}$. ^1H NMR

(CDCl₃, δ): 7.75 (1H, m, H8), 7.72 (1H, m, H5), 7.49 (1H, s, H9), 7.40 (2H, m, H6 & H7), 6.7 (1H, d, J = 9.2, H4), 6.06 (1H, dd, J = 9.2, 4.5, H3), 3.75 (3H, s, DMM), 3.71 (3H, s, DMM), 3.42 (1H, d, J = 9.1, H11), 3.30 (1H, m, H4), 3.13 (1H, dd, J = 15.8, 6.0, H1'), 2.91 (1H, dd, J = 15.8, 6.9, H1). ¹³C NMR (CDCl₃, δ): 168.9 (CO), 168.8 (CO), 133.5, 133.2, 132.2, 131.8, 130.0 (C3), 129.7 (C4), 128.0 (C8), 127.5 (C5), 126.7 (C10), 126.2 (C6), 125.9 (C7), 124.9 (C9), 55.0 (C11), 52.9 (OMe), 34.3 (C2), 32.5 (C1). HRMS: [C₁₉H₁₈O₄+Na⁺] obsd (%), calcd (%), ppm: 333.1092 (100), 333.1097 (100), -1.6.

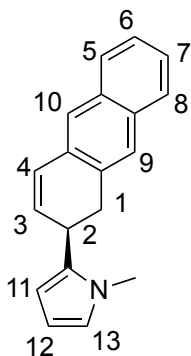
2-(1,2-Dihydronaphthalen-2-yl)-1-methyl-1H-pyrrole (16).



To a 25 mL filter flask charged with stir bar was added **10** (100 mg, 0.158 mmol) and DCM (5 mL). Next, 0.06 M I₂/Et₂O (1.33 mL, 0.08 mmol) was added to the stirring yellow solution changing instantly to green. This solution was stirred for 5 min and was then evaporated *in vacuo* to 1 mL and added to stirring hexanes (25 mL). The green precipitate **3** was then isolated on a 15 mL fine porosity fritted disc and was washed with hexanes (3 x 10 mL). The colorless filtrate was then removed from the box and evaporated *in vacuo*. This oil was then loaded (3 x 0.3 mL DCM) onto a silica preparatory plate and was eluted with 10% EtOAc:hexanes (HPLC grade, 200 mL). A KMnO₄ positive band at R_f 0.5-0.7 was scraped off and sonicated in 10% EtOAc:hexanes (HPLC grade, 25 mL) for 10 min. The silica was then filtered off on a 30 mL fine

porosity fritted disc and was washed with 10% EtOAc:hexanes (3 x 15 mL). The filtrate was then evaporated *in vacuo* and dried 1 h yielding the colorless oil **16** (29 mg, 89%). IR: 2935, 1724, 1489 cm^{-1} . ^1H NMR (CDCl_3 , δ): 7.21 (4H, m, H11, H6, H7 & H8), 6.58 (1H, dd, $J = 4.9, 2.2$, H4), 6.57 (1H, t, $J = 2.3$, H11), 6.03 (1H, dd, $J = 9.7$, H3), 5.87 (1H, t, $J = 3.3$, H10), 5.79 (1H, ddd, $J = 3.6, 1.9, 0.5$, H9), 3.80 (1H, m, H2), 3.64 (3H, s, NMe), 3.05 (1H, dd, $J = 15.4, 6.8$, H1'), 2.91 (1H, dd, $J = 15.4, 10.9$, H1). ^{13}C NMR (CDCl_3 , δ): 135.2, 134.8, 133.8, 131.3, 128.3, 128.0, 127.6, 127.1, 126.4, 122.2, 107.1, 106.0, 35.1, 34.2, 32.7. LRMS: $[\text{M}^+] = 209$.

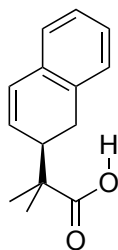
2-(1,2-Dihydroanthracen-2-yl)-1-methyl-1H-pyrrole (17).



To a 25 mL filter flask charged with stir bar was added **11** (75 mg, 0.109 mmol) and DCM (5 mL). Next, 0.06 M $\text{I}_2/\text{Et}_2\text{O}$ (0.83 mL, 0.05 mmol) was added to the stirring yellow solution changing instantly to green. This solution was stirred for 5 min and was then evaporated *in vacuo* to 1 mL and added to stirring hexanes (25 mL). The green precipitate **3** was then isolated on a 15 mL fine porosity fritted disc and was washed with hexanes (3 x 10 mL). The colorless filtrate was then removed from the box and evaporated *in vacuo*. This oil was then loaded (3 x 0.3 mL DCM) onto a silica preparatory plate and was eluted with 10% EtOAc:hexanes (HPLC grade, 200 mL). A band from R_f : 0.5 - 1.0 was scraped off and sonicated in EtOAc (25 mL) for 10 min. The

silica was then filtered off on a 30 mL fine porosity fritted disc and was washed with EtOAc (HPLC grade, 3 x 15 mL). The filtrate was then evaporated *in vacuo* and dried 1 h yielding the colorless oil **17** (11 mg, 31%). IR: bands at 2924, 3379, and 1697 cm^{-1} . ^1H NMR (CDCl_3 , δ): 7.77 (1H, m, H5/H8), 7.72 (1H, m, H5/8), 7.53 (1H, s, H9), 7.52 (1H, s, H10), 7.40 (2H, m, H6 & H7), 6.77 (1H, dd, $J = 9.6, 2.4$, H4), 6.59 (1H, t, $J = 2.3$, H13), 6.15 (1H, dd, $J = 9.6, 3.8$, H3), 6.05 (1H, t, $J = 3.3$, H12), 5.96 (1H, m, H11), 3.87 (1H, m, H2), 3.65 (3H, s, NMP), 3.24 (1H, dd, $J = 15.1, 6.4$, H1), 3.15 (1H, ddd, $J = 15.1, 9.9, 1.0$, H1). ^{13}C NMR (CDCl_3 , δ): 135.1, 133.4, 133.3, 132.4, 132.3, 128.5, 128.1, 127.56, 126.2, 126.1, 125.8, 127.7, 122.3, 107.2, 106.2, 35.7, 34.2, 32.3. LRMS: $[\text{M}^+] = 259$.

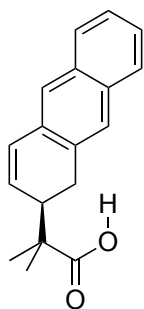
2-(1,2-dihydronaphthalen-2-yl)-2-methylpropanoic acid (**18**)



A solution of **12** (100 mg, 0.43 mmol), MeOH (5 mL), and aqueous NaOH (1M, 4.3 mL, 4.3 mmol), was added to a 25 mL round bottom flask charged with a stir pea and reflux condenser. This solution was stirred at reflux for 24 h at which point the reaction mixture was cooled to room temperature and neutralized (pH \sim 7) with glacial acetic acid (\sim 1 mL). The organic layer was then extracted from this solution with CHCl_3 (15 mL), washed with H_2O (30 mL) and brine (sat. aq. NaCl, 30 mL), and dried over MgSO_4 . The drying agent was filtered off on a 15 mL medium porosity fritted disc, washed with CHCl_3 (3 x 5 mL) and the filtrate was evaporated *in vacuo* yielding the colorless oil **18**.

(89 mg, 96 %). ^1H NMR (CDCl_3 , δ): 12.36 (1H, bs), 7.16 (3H, m), 7.06 (1H, dd, $J = 6.5$, 1.8), 6.59 (1H, dd, $J = 9.9$, 2.3), 5.96 (1H, dd, $J = 9.7$, 3.4), 2.96 (1H, m), 2.91 (1H, dd, $J = 15.7$, 6.9), 2.87 (1H, dd, $J = 15.7$, 11.6), 1.31 (3H, s), 1.27 (3H, s). ^{13}C NMR (CDCl_3 , δ): 184.3, 134.8, 133.5, 129.2, 128.4, 127.7, 127.3, 126.6, 125.9, 45.5, 41.2, 29.5, 22.4, 21.8.

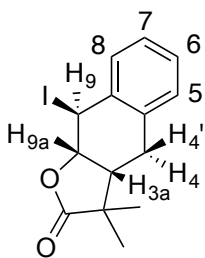
2-(1,2-dihydroanthracen-2-yl)-2-methylpropanoic acid (19**)**



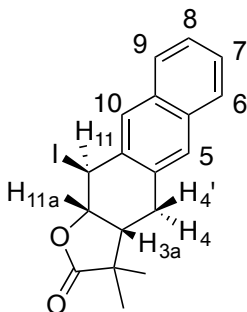
A solution of **13** (144 mg, 0.51 mmol), MeOH (5 mL), and aqueous NaOH (1M, 4.3 mL, 4.3 mmol), was added to a 25 mL round bottom flask charged with a stir pea and reflux condenser. This solution was stirred at reflux for 24 h at which point the reaction mixture was cooled to room temperature and neutralized (pH \sim 7) with glacial acetic acid (\sim 1 mL). The organic layer was then extracted from this solution with DCM (20 mL), washed with H_2O (30 mL) and brine (sat. aq. NaCl, 30 mL), and dried over MgSO_4 . The drying agent was filtered off on a 15 mL medium porosity fritted disc, washed with DCM (3 x 5 mL) and the filtrate was evaporated *in vacuo* yielding the colorless oil **19** (130 mg, 95 %). ^1H NMR (CDCl_3 , δ): 11.21 (1H, bs), 7.75 (1H, m), 7.71 (1H, m), 7.53 (1H, s), 7.46 (1H, s), 7.39 (2H, m), 6.74 (1H, dd, $J = 10.1$, 1.6), 6.01 (1H, dd, $J = 10.1$, 3.3), 3.06 (1H, m), 2.96 (2H, m), 1.26 (3H, s), 1.22 (3H, s). ^{13}C NMR (CDCl_3 , δ): 183.4, 133.7, 133.3,

132.9, 132.1, 129.7, 129.6, 127.8, 127.3, 125.8 (2C), 125.5, 124.4, 45.9, 41.5, 30.2, 22.6, 21.8.

9-Iodo-3,3-dimethyl-3a,4,9,9a-tetrahydronaphtho[2,3-*b*]furan-2(3*H*)-one (20).



To a 4 dram vial was added **18** (90 mg, 0.416 mmol), water (4 mL), saturated NaHCO₃ aq. (1 mL), KI (112 mg, 0.675 mmol), I₂ (79 mg, 0.313 mmol). This was stirred at room temperature for 6 days at which point 30 mL of DCM were added and the organic layer was evaporated *in vacuo*. This was loaded (3 x 0.3 mL DCM) onto a silica preparatory plate and was eluted with 1:4 EtOAc:hexanes (HPLC grade, 200 mL). Scraped off a KMNO₄ band at R_f : 0.25 – 0.5 and sonicated in EtOAc (HPLC grade, 25 mL) for 10 min. Filtered off silica on a 15 mL fine porosity fritted disc, washed with DCM (3 x 5 mL), and evaporated *in vacuo* to isolate the product **20** (35 mg, 25%). IR: $\nu(\text{CO}) = 1766 \text{ cm}^{-1}$. ¹H NMR (CDCl₃, δ): 7.29 (1H, d, $J = 7.5$, H8), 7.25 (1H, t, $J = 7.5$, H6), 7.21 (1H, t, $J = 7.5$, H7), 7.13 (1H, d, $J = 7.5$, H5), 5.55 (1H, d, $J = 2.9$, H9), 5.36 (1H, dd, $J = 7.6$, 2.9, H9a), 3.06 (1H, dd, $J = 16.5$, 8.5, H4'), 2.89 (1H, t, $J = 7.8$, H3a), 2.83 (1H, d, $J = 16.5$, H4), 1.36 (3H, s, Me), 1.22 (3H, s, Me). ¹³C NMR (CDCl₃, δ): 180.8 (CO), 135.7, 134.2, 129.7 (C5), 128.8, 128.7, 128.6 (C7), 79.8 (C9a), 43.2 (C3a), 43.1, 28.7 (Me), 27.2 (C4), 24.1 (C9), 20.6 (Me). MP: 102.8-104.3. Anal. Calc'd for C₁₄H₁₅IO₂: C, 49.14; H, 4.42. Found: C, 49.15; H, 4.27.

11-Iodo-3,3-dimethyl-3a,4,11,11a-tetrahydroanthra[2,3-*b*]furan-2(3*H*)-one (21).

To a 4 dram vial was added **19** (120 mg, 0.451 mmol), water (5 mL), saturated NaHCO₃ aq. (2 mL), KI (150 mg, 0.903 mmol), I₂ (100 mg, 0.397 mmol). This was stirred at room temperature for 2 days at which point 30 mL of DCM were added and the organic layer was evaporated *in vacuo*. Dissolved in DCM (15 mL) and Et₂O (15 mL), reduced to half volume and cooled in an ice bath for 30 min. Isolated white precipitate on a 2 mL medium porosity frit, washed with Et₂O (3 x 2 mL) and desiccated to yield product **21** (79 mg, 38%). IR: $\nu(\text{CO}) = 1759 \text{ cm}^{-1}$. ¹H NMR (CDCl₃, δ): 7.83 (1H, s, H10), 7.78 (1H, d, $J = 8.3$, H6), 7.73 (1H, d, $J = 8.3$, H9), 7.59 (1H, s, H5), 7.48 (1H, t, $J = 6.8$, H7), 7.44 (1H, t, $J = 7.6$, H8), 5.76 (1H, d, $J = 3.1$, H11) 5.40 (1H, dd, $J = 7.5$ & 3.1, H11a), 3.36 (1H, ddd, $J = 15.6, 8.4, 1.7$, H4'), 3.02 (1H, d, $J = 15.6$, H4), 2.95 (1H, t, $J = 7.5$, H3a), 1.38 (3H, s, Me), 1.27 (3H, s, Me). ¹³C NMR (CDCl₃, δ): 180.7 (CO), 134.0, 132.8, 132.6, 132.2, 128.2, 128.1, 127.4, 127.3, 127.0, 126.3, 79.6 (H11a), 43.3 (H3a), 43.2, 28.7 (Me), 27.3 (H4), 24.5 (H11), 20.5 (Me). MP: 118.5-121.5.

2.6 References

1. Winemiller, M. D.; Kelsch, B. A.; Sabat, M.; Harman, W. D. *Organometallics* **1997**, 16, (16), 3672.
2. Winemiller, M. D.; Harman, W. D. *J. Am. Chem. Soc.* **1998**, 120, (31), 7835.
3. Winemiller, M. D.; Harman, W. D. *J. Org. Chem.* **2000**, 65, (5), 1249.
4. Valahovic, M. T.; Gunnoe, T. B.; Sabat, M.; Harman, W. D. *J. Am. Chem. Soc.* **2002**, 124, (13), 3309.
5. Ding, F.; Valahovic, M. T.; Keane, J. M.; Anstey, M. R.; Sabat, M.; Trindle, C. O.; Harman, W. D. *J. Org. Chem.* **2004**, 69, (7), 2257.
6. Ding, F.; Valahovic, M. T.; Keane, J. M.; Anstey, M. R.; Sabat, M.; Trindle, C. O.; Harman, W. D. *J. Org. Chem.* **2004**, 69, (7), 2257.
7. Valahovic, M. T.; Gunnoe, T. B.; Sabat, M.; Harman, W. D. *J. Am. Chem. Soc.* **2002**, 124, 3309.
8. Benn, R.; Mynott, R.; Topalovic, I.; Scott, F. *Organometallics* **1989**, 8, 2299.
9. Tagge, C. D.; Bergman, R. G. *J. Am. Chem. Soc.* **1996**, 118, 6908.
10. Mocella, C. J.; Delafuente, D. A.; Keane, J. M.; Warner, G. R.; Friedman, L. A.; Sabat, M.; Harman, W. D. *Organometallics* **2004**, 23, (16), 3772.
11. Pienkos, J. A.; Zottig, V. E.; Iovan, D. A.; Li, M.; Harrison, D. P.; Sabat, M.; Salomon, R. J.; Strausberg, L.; Teran, V. A.; Myers, W. H.; Harman, W. D. *Organometallics* **2013**, 32, (2), 691.
12. Graham, P.; Meiere, S. H.; Sabat, M.; Harman, W. D. *Organometallics* **2003**, 22, 4364.
13. Chordia, M. D.; Smith, P. L.; Meiere, S. H.; Sabat, M.; Harman, W. D. *J. Am. Chem. Soc.* **2001**, 123, (43), 10756.
14. Pienkos, J. A.; Knisely, A. T.; Liebov, B. K.; Teran, V.; Zottig, V. E.; Sabat, M.; Myers, W. H.; Harman, W. D. *Organometallics* **2013**, 33, (1), 267.
15. Meiere, S. H.; Keane, J. M.; Gunnoe, T. B.; Sabat, M.; Harman, W. D. *J. Am. Chem. Soc.* **2003**, 125, (8), 2024.
16. Cyclic voltammogram taken in DMA at 100 mV/s, the positive value represents Epa and the negative value represents a reversible couple from a I/II Epa

17. Meiere, S. H.; Valahovic, M. T.; Harman, W. D. *J. Am. Chem. Soc.* **2002**, 124, (50), 15099.
18. Bard, A. J.; Faulkner, L. R., *Electrochemical Methods Fundamentals and Applications*. John Wiley & Sons: New York, 1980.
19. Electrochemical analysis reveals that
20. Pines, H., *Base-Catalyzed Reactions of Hydrocarbons and Related Compounds*. Academic Press; Elsevier: New York, 1977.
21. Dowdy, D.; Gore, P. H.; Waters, D. N. *J. Chem. Soc., Perkins Trans. 2* **1991**, (8), 1149.
22. Subrahmanyam, C.; Viswanathan, B.; Varadarajan, T. K. *Journal of Molecular Catalysis A: Chemical* **2005**, 226, (2), 155.
23. Price, C. C.; Ciskowski, J. M. *J. Am. Chem. Soc.* **1938**, 60, (10), 2499.
24. Kuendig, E. P.; Inage, M.; Bernardinelli, G. *Organometallics* **1991**, 10, (8), 2921.
25. Atherton, J. C. C.; Jones, S. *Tetrahedron* **2003**, 59, (46), 9039.
26. Zhou, J.; Xie, G.; Yan, X., *Encyclopedia of Traditional Chinese Medicines - Molecular Structures, Pharmacological Activities, Natural Sources and Applications: Vol. 4: Isolated Compounds N-S*. Springer Science and Business Media: 2011; Vol. 4, p 636.
27. Ebada, S. S.; Schulz, B.; Wray, V.; Totzke, F.; Kubbutat, M. H. G.; Müller, W. E. G.; Hamacher, A.; Kassack, M. U.; Lin, W.; Proksch, P. *Bioorganic & Medicinal Chemistry* **2011**, 19, (15), 4644.
28. Bakhaeva, G. P.; Berlin, Y. A.; Chuprunova, O. A.; Kolosov, M. N.; Peck, G. Y.; Piotrovich, L. A.; Shemyakin, M. M.; Vasina, I. V. *Chemical Communications (London)* **1967**, (1), 10.
29. Faulkner, D. J. *Natural Product Reports* **1991**, 8, (2), 97.
30. Keane, J. M. Synthesis and Nucleophilic Activity of Eta-2 Arene Complexes. Ph. D. Dissertation, University of Virginia, 2003.
31. Lis, E. C.; Delafuente, D. A.; Lin, Y.; Mocella, C. J.; Todd, M. A.; Liu, W.; Sabat, M.; Myers, W. H.; Harman, W. D., *Organometallics* **2006**, 25 (21), 5051.

Chapter 3

4-(Dimethylamino)pyridine (DMAP) as an Acid- Modulated Donor Ligand for PAH Dearomatization

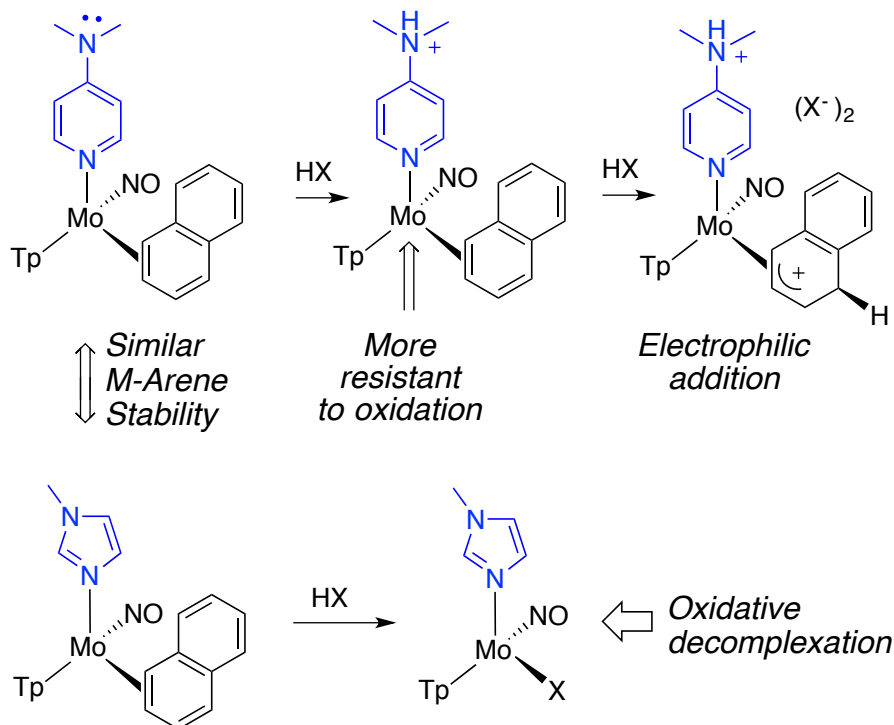
3.1 Introduction

In the previous chapter the ability to perform 1,2-addition reactions to naphthalene and anthracene using the $\{\text{TpMo}(\text{NO})(\text{MeIm})\}$ (Tp = hydridotris(pyrazolyl)borate; MeIm = 1-methylimidazole) system was demonstrated.^{1, 2} This molybdenum dearomatization agent offers the advantages of facile liberation of organic products and recyclability of the $\{\text{TpMo}(\text{NO})(\text{MeIm})\}$ moiety, as well as a substantially lower cost than its heavy metal congeners (e.g., $\{\text{Os}(\text{NH}_3)_5\}^{2+}$, $\{\text{TpRe}(\text{CO})(\text{L})\}$, $\{\text{TpW}(\text{NO})(\text{PMe}_3)\}$). However, the $\{\text{TpMo}(\text{NO})(\text{MeIm})\}$ fragment is more vulnerable to oxidation by electrophilic reagents such as triflic acid (Scheme 3.1), compared to its Os, Re, and W analogues.¹ Previous research with rhenium has shown the ability to significantly influence the reduction potential of the metal by altering the ancillary ligand. We hoped to find an alternative to the MeIm complex that can still bind and activate polycyclic aromatic hydrocarbons (PAHs), but is less susceptible to metal oxidation by electrophilic reagents.

Herein, we report that by the simple replacement of MeIm with 4-(dimethylamino)pyridine (DMAP), a significantly greater scope of addition reactions is accessed for both naphthalene and anthracene, while the economic and environmental benefits of the imidazole system are still maintained. The key to this success lies in the ability of the DMAP ligand to accept a proton at the dimethylamino group, and thereby reduce the donation of electron density to the metal from the pyridine ring.³ Consequently, the d^5/d^6 reduction potential of the metal is temporarily raised, rendering it less susceptible to unintended oxidation by electrophilic reagents (Scheme 3.1). While the protonation of a DMAP ligand has been used previously as a “switch” to modulate

the chemistry of a transition metal,⁴ the acid normally effects the *removal* of the DMAP, opening a coordination site on the metal, rather than influencing the redox properties of the metal via the *coordinated* DMAP.

Scheme 3.1. Arene protonation versus metal oxidation.



3.2 Results

3.2.1. Synthesis of $\text{TpMo}(\text{NO})(\text{DMAP})(\text{L}\pi)$

Similar to the synthesis of $\text{TpMo}(\text{NO})(\text{MeIm})(\text{I})$, $\text{TpMo}(\text{NO})(\text{DMAP})(\text{I})$ (**23**) can be synthesized from $\text{Mo}(\text{CO})_6$ *in air and without chromatography* in an overall yield of 66% on a 170 g scale (> 80% per step; Scheme 3.2). Of note, the Mo(I) complex (**23**) was found to be stable in air for over three months, showing no signs of decomposition. This

is in dramatic contrast to its tungsten counterpart, $\text{TpW}(\text{NO})(\text{PMe}_3)(\text{Br})$, which decomposes rapidly upon exposure to air.⁵

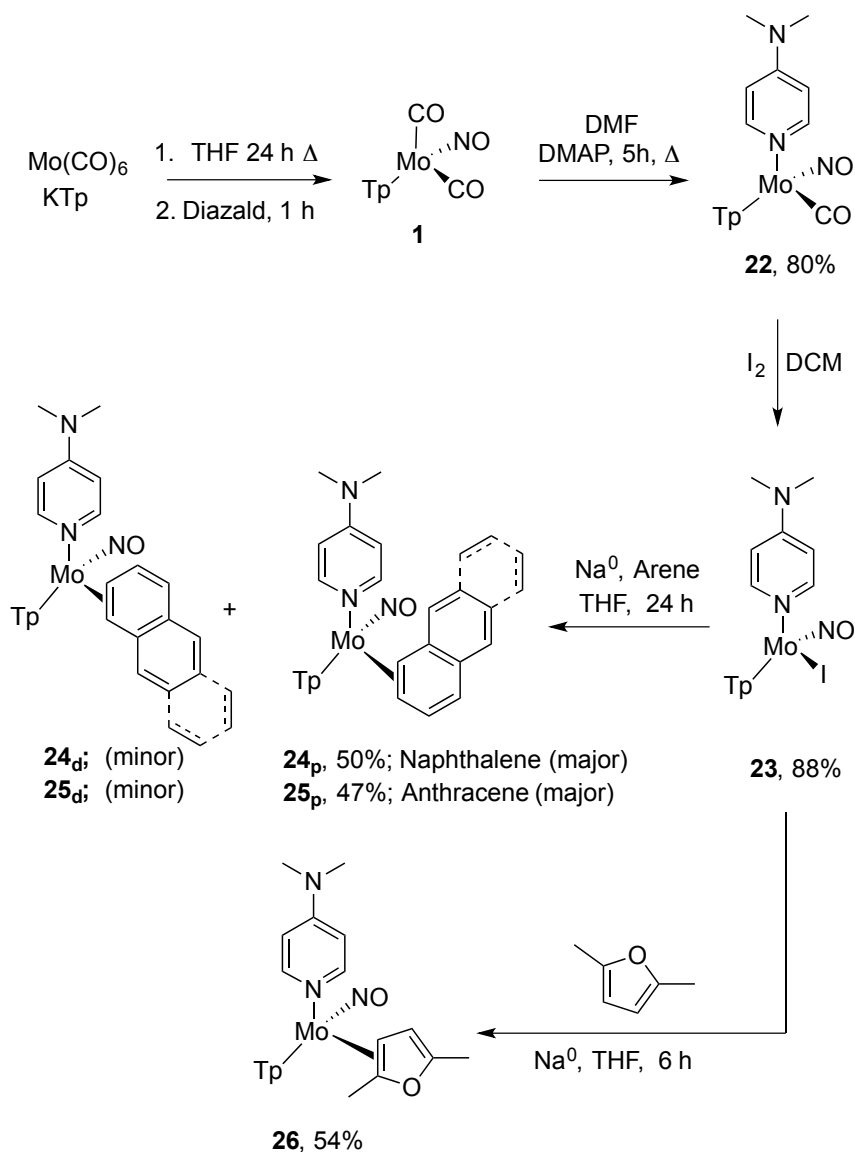
The precursor to **23**, $\text{TpMo}(\text{NO})(\text{CO})(\text{DMAP})$ (**22**), was found to be only slightly less electron-rich in comparison to its MeIm analogue, as judged from an increase in the nitrosyl (from 1577 to 1589 cm^{-1}) and carbonyl (from 1867 to 1871 cm^{-1}) stretch frequencies as well as a more positive potential for the $\text{Mo}^0/\text{Mo}^{\text{I}}$ oxidation observed in a voltammogram (from $E_{\text{p,a}} = +0.22$ to 0.27 V; NHE, 100 mV/s, DMAc).¹

In order to compare the ability of $\{\text{TpMo}(\text{NO})(\text{DMAP})\}$ to bind aromatic molecules with its predecessor, $\{\text{TpMo}(\text{NO})(\text{MeIm})\}$, three ligands were investigated: naphthalene (**24**), anthracene (**25**) and 2,5-dimethylfuran (**26**). The naphthalene and anthracene complexes were prepared on 13-gram scales (~50% yield) via the reduction of **23** in the presence of an excess of the arene. The 2,5-dimethylfuran complex **26** was chosen because of its anticipated role as a precursor to other $\{\text{TpMo}(\text{NO})(\text{DMAP})\}$ complexes, similar to that found for the furan and 2,5-dimethylfuran complexes of $\{\text{TpMo}(\text{NO})(\text{MeIm})\}$.^{6, 7} Reducing **23** with elemental sodium in the presence of 2,5-dimethylfuran generates **26**, which can be isolated in pure form from MeOH (CAUTION: exothermic production of hydrogen) in 54% yield (13 g scale), without the need for chromatography.

The dimethylfuran complex **26** undergoes substitution in acetone forming the complex $\text{TpMo}(\text{NO})(\text{DMAP})(\eta^2\text{-acetone})$, with a k_{obs} of $8.8 \times 10^{-5} \text{ s}^{-1}$ at $22 \pm 1^\circ \text{C}$. This is similar to that observed for the MeIm analogue, where $k_{\text{obs}} = 8.2 \times 10^{-3} \text{ s}^{-1}$ ($22 \pm 1^\circ \text{C}$). This represents a free energy of activation of 23.0 and $22.9 \pm 0.1 \text{ kcal/mol}$ for these complexes, respectively, values well below that observed for naphthalene (26.6 ± 0.1

kcal/mol at 100 °C; L = MeIm).⁷ Utilization of this low barrier for substitution of 2,5-dimethylfuran is demonstrated by its exchange with α,α,α -trifluorotoluene and 2-methoxypyridine in Chapters 5 and 6, respectively.

Scheme 3.2. Synthesis of η^2 -coordinated naphthalene, anthracene, and 2,5-dimethylfuran complexes.



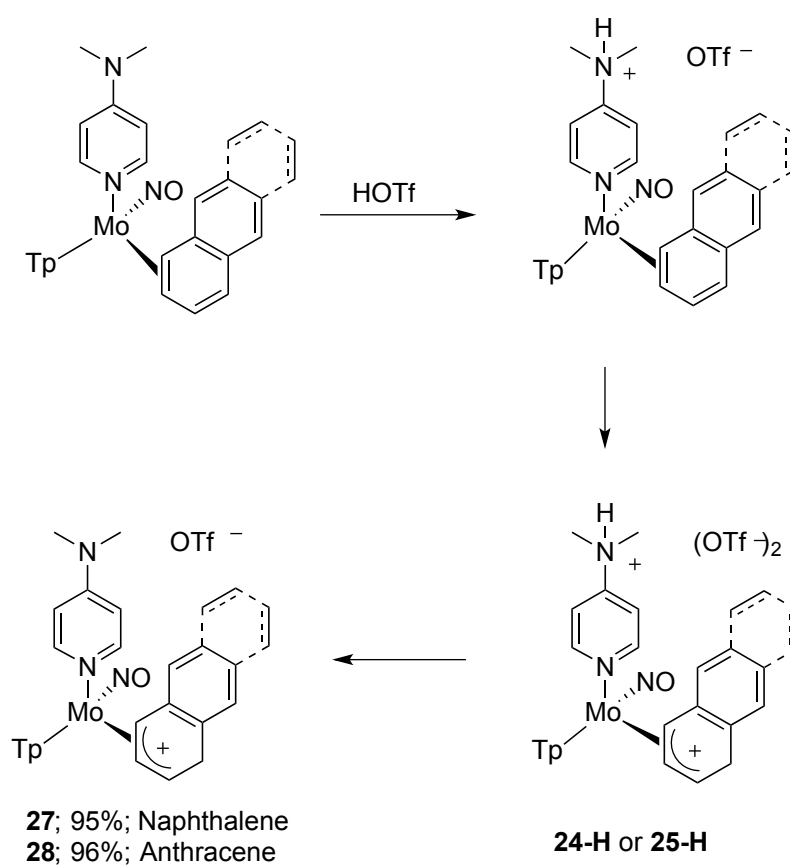
3.2.2. Synthesis of $TpMo(NO)(DMAP)(\eta^2\text{-arenium})$ complexes

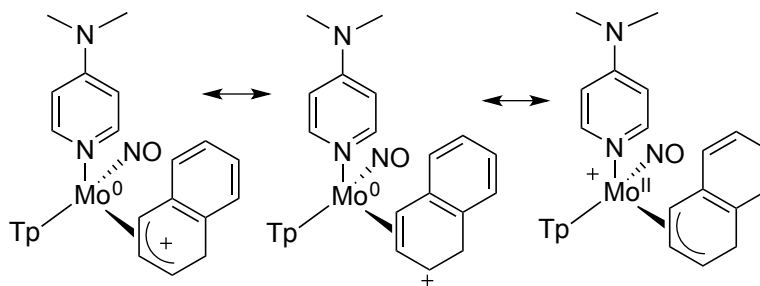
In order to test our central hypothesis that DMAP could be protonated and thereby better prevent metal oxidation than its MeIm forbearer, the naphthalene complex **24** was subjected to HOTf (in CD_3CN ; $-30\text{ }^\circ\text{C}$) and was monitored over time by ^1H NMR ($25\text{ }^\circ\text{C}$). In contrast to that observed for the MeIm complex, with DMAP the formation of a stable allyl complex (**24-H**) was observed. Key spectroscopic features include diastereotopic methylene protons at 4.78 and 4.75 ppm, both doublets with $J = 27.6\text{ Hz}$. This large coupling constant is consistent with a strong π -acceptor adjacent to the geminal protons.⁸ Another spectroscopic feature for **24-H** is a broad singlet at 9.97 ppm that has correlations in COSY and NOESY spectra to two distinct methyl signals near 3.26 ppm (both d with $J = 5.0\text{ Hz}$). These data support the hypothesis that *both* the dimethylamino group and the naphthalene in **24-H** are protonated (Scheme 3.3). Although attempts to isolate this dicationic species were unsuccessful, it was found that a triflate salt could be precipitated from the reaction mixture with Et_2O , and the intact allyl complex (**27**) could be isolated (95%), observed at room temperature (^1H NMR), and stored indefinitely at $-30\text{ }^\circ\text{C}$. Of note, the amino group in **27** no longer appears to be protonated, but allylic protons at 7.12, 5.72 and 5.22 ppm and a diastereotopic methylene group (4.77 and 4.74 ppm) indicate that the allyl-like naphthalenium ligand is intact. In contrast, an allyl complex analogous to **27** could not be isolated or fully characterized in solution for the MeIm system.¹

In a similar fashion, the allyl complex of anthracene (**28**) was isolated, via the formation of the purported dicationic intermediate **25-H**. The thermal stability of **28** is similar to that observed for its naphthalene derivative, **27**. In both **27** and **28**, two of the

three allylic carbon resonances are well upfield of the third (129.1 (C2), 102.1 (C3) and 88.3 (C4) ppm), indicating that the allyl is asymmetrically bound to the metal center. This feature has been observed previously for naphthalenium complexes of W and Re,⁹ as well as a cyclopentadiene-derived allyl complex of TpMo(NO)(MeIm).⁷ Where available, structural data indicate that this downfield allylic carbon is $\sim 0.2\text{-}0.3$ Å farther from the metal than the other allylic carbons and is cationic in nature.⁹ We therefore portray allyl complexes as η^2 -coordinated allyl cations (Eq 3.1).

Scheme 3.3. Protonation and isolation of allylic naphthalene and anthracene complexes.





Eq 3.1.

To estimate the impact on the metal from protonating the amino group of DMAP, the model compound $\text{TpMo}(\text{NO})(\text{pyridine})(\eta^2\text{-naphthalene})$ (**29**) was synthesized.¹⁰ Importantly, there is a minor decrease in the electron density on molybdenum for $\text{TpMo}(\text{NO})(\text{py})(\eta^2\text{-naphthalene})$, as compared to its DMAP analogue, (**24**), as judged by an increase in nitrosyl stretching frequency (1585 cm^{-1} vs. 1580 cm^{-1}) and position of the oxidation wave ($E_{\text{p,a}} = -0.07\text{ V}$ vs. -0.16 V ; 100 mV/s). Furthermore, the ligand exchange in acetone ($t_{1/2} = 29\text{ h}$ at $22\text{ }^{\circ}\text{C} \pm 1\text{ }^{\circ}\text{C}$) leads to a ΔG^{\ddagger} for **29** of $24.5 \pm 0.1\text{ kcal/mol}$, significantly lower than that of **24** ($26.0 \pm 0.1\text{ kcal/mol}$; $T = 22 \pm 1\text{ }^{\circ}\text{C}$). This difference indicates weaker backbonding into the arene π -system due to less electron density donated from the ancillary ligand (py *cf.* DMAP). Similar to **24**, the pyridine complex **29** can be protonated to form an allyl species analogous to **27** at $-30\text{ }^{\circ}\text{C}$; however, upon warming to $25\text{ }^{\circ}\text{C}$ the complex decomposes. This observation demonstrates the potential dual role that the amino group of DMAP plays in supporting the formation and stability of an allyl complex: in its protonated form it protects the metal from oxidation *while* the allyl is being formed. Once formed, however, the amino group can be deprotonated to provide more electron density and stabilize the highly electrophilic arenlenium cation (see Scheme 3.3).

3.2.3. Protonation and nucleophilic addition to **24** and **25**

Next, we endeavored to determine if the replacement of DMAP for MeIm impacted the ability of the metal to activate the arene toward addition reactions. Previously,¹ we reported that protonation could be accomplished at C1 followed by the addition of a carbon nucleophile at C2, and that the final dihydroarene product (**O**) could be removed by action of iodine (Scheme 3.4).

Scheme 3.4. Formal catalytic cycle for the generation of dihydronaphthalenes and dihydroanthracenes.

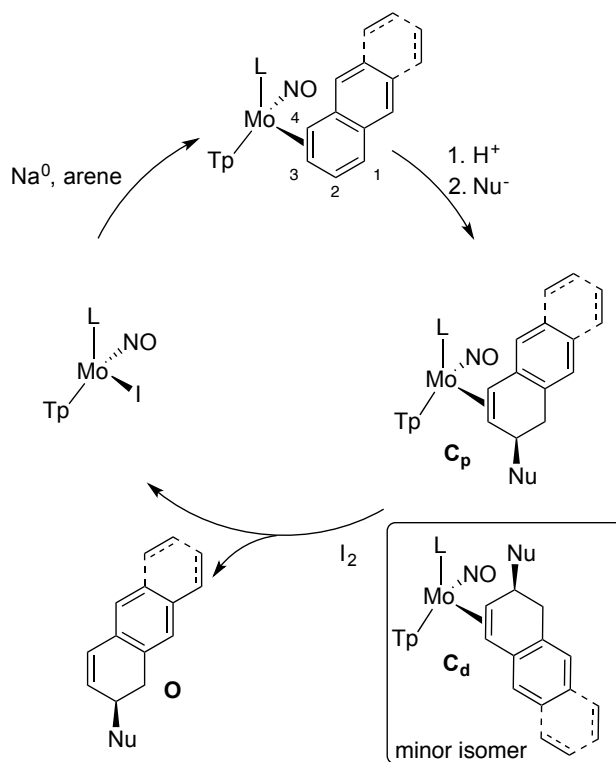


Table 3.1 presents summarized results for conjugate additions to naphthalene (**24**) and anthracene (**25**) complexes using triflic acid as the electrophile and three types of carbon nucleophiles – a pyrrole, a silylated ester enolate, and a lithiated enolate – for both

MeIm and DMAP systems. We found that when MeIm is replaced by DMAP, the yield for isolation of **C** (ranging from 41-95%) improved by an average of 34% compared to those yields obtained with the MeIm system (ranging from 27-66%). Although the yield for organic isolation **O** generally decreased directly from **C**, the improved yield of **C** led to an average 30% increase in *overall* yield of **O** when starting from **24** or **25**.

Table 3.1. Isolated Dihydroarenes (**O**) from Iodine Oxidation of **C**.

Arene Complex	Reagent (source of Nu)	Complex (C)			Product (O)			Metal Recovery 23 (% yield)
		#	% yield	dr (p:d)	#	% yield: step overall		
24		30	95; 61	6:1		12 54; 64	51; 39	70
25		31	52; 43	5:1		13 74; 79	38; 34	77
24		32	82; 66	7:1		14 72; 61	59; 40	88
25		33	41; 48	6:1		15 30; 62	12; 42	94
24		34	68; 53	7:1		16 78; 89	53; 47	94
25		35	51; 27	6:1		17 44; 31	22; 8	96
		(DMAP;MeIm)				(DMAP;MeIm)		

Of note, the product complexes were isolated as a mixture of two coordination diastereomers, differing by which face of the ring is coordinated. These are represented as **C_p** (proximal to L) and **C_d** (distal to L) (Scheme 3.4). In all cases observed, the

dominant isomer (C_p) featured the uncoordinated ring(s) oriented proximal to the DMAP. The allyl intermediates (**27** and **28**) were observed in solution as a 6:1 ratio of diastereomers causing a decrease in the stereoselectivity of $C_p : C_d$ from 25:1 to ~5:1 compared to the MeIm system.¹ Even with the clear preference in both DMAP and MeIm systems for the C_p isomer to dominate, a crystal grown from a solution of the ester product **30** was found to contain the minor *distal* stereoisomer (C_d). In Figure 3.2, this solid-state structure (**30_d**) is compared to the proximal isomer of the MeIm analogue, where the reader will note the enantiomeric relationship of the dihydronaphthalene ligands, despite similar metal configurations.

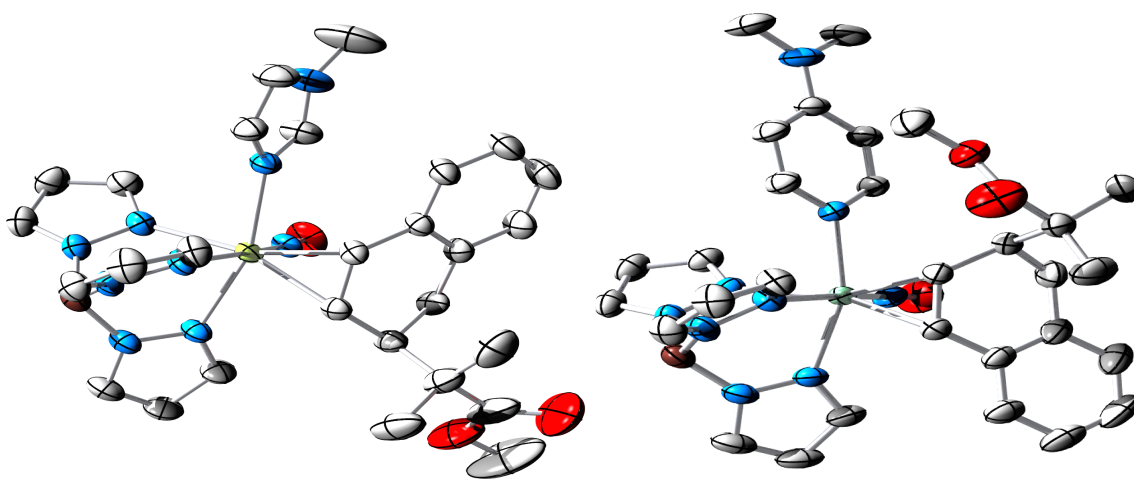


Figure 3.1. Solid-state structures of two dihydronaphthalene complexes **30**, using MeIm (Left)¹¹ and DMAP (Right). Bond lengths of **30** (Å): Mo—C(4) 2.2492(19); Mo—C(3) 2.2157(19); Mo—N(DMAP) 2.2228(16); Mo—N(NO) 1.7549(17).

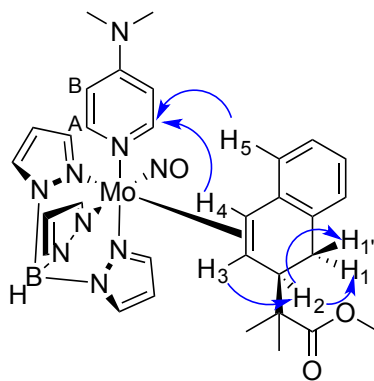


Figure 3.2. NOESY correlations for **30p**.

In addition to the nine protons of the Tp ligand observed in the ^1H NMR spectra of these complexes, the DMAP ancillary ligand offers the following three sets of protons: a broad singlet integrating for 2 protons around 7.40 ppm (DMAP-A), a multiplet integrating for 2 protons around 6.50 ppm (DMAP-B), and a singlet integrating for 6 protons around 3.00 ppm (N-Me's). Identically to the MeIm analogue, **30p** has a diastereotopic methylene group (H1 and H1') that was confirmed by its large coupling constant (16.6 Hz) and HSQC. Similarly, H2 (3.19 ppm) was identified through COSY and NOESY correlations, leading to the identification of H3, which is a doublet of triplets at 2.13 ppm identical to that found for the MeIm system. Through COSY correlation, H4 was found to be a doublet at 3.24 ppm. Using NOESY, H4 was found to correlate through space with a doublet in the aromatic region (H5) as well as with DMAP-A, confirming the major isomer in the solution phase to orient the bulk of the organic ligand proximal, rather than distal, to the DMAP ligand. This is a different coordination isomer to the one seen in the crystal structure for this complex (*vide infra*). To further confirm this, H5 was found to strongly correlate via NOE with DMAP-A (Figure 3.2).

3.2.4. Nucleophilic additions to **27** and **28****Table 3.2.** Synthesis of nitromethyl- and pyrazolyl- substituted dihydroarenes.

Reagent	Product (O) (#, % yield)		Reagent	Product (O) (#, % yield)	
CH ₃ NO ₂		37 ; 39 (recovery of 23 : 90%)		39 ; 19	
CH ₃ NO ₂		38 ; 33		40 ; 20	

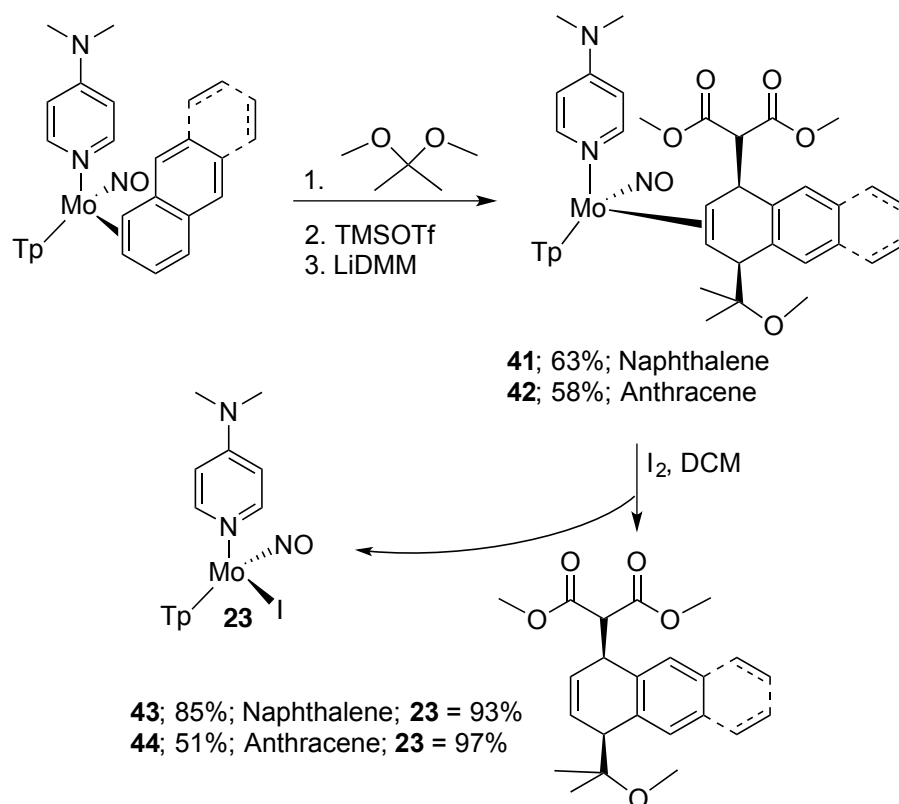
The ability to isolate allyl complexes **27** and **28** away from the strong acid required for their preparation presents the opportunity to explore other classes of nucleophiles that would otherwise be compromised by Brønsted acids. Gratifyingly, we found that both nitromethane (Henry reaction) and pyrazole could be added to C2 of either **27** or **28**. In general, the corresponding complexes proved difficult to isolate, but when the reaction mixture was subjected to air, the desired organic products were obtained in moderate yield. In the case of the nitromethane addition to **27**, the complex (**36**) could be cleanly isolated (63%). When **36** was subsequently treated with iodine the

precursor **23** was recovered in 90% yield. Of the four organic products formed in Table 3.2, only compound **40** could be obtained from the {TpMo(NO)(MeIm)} system (12%).

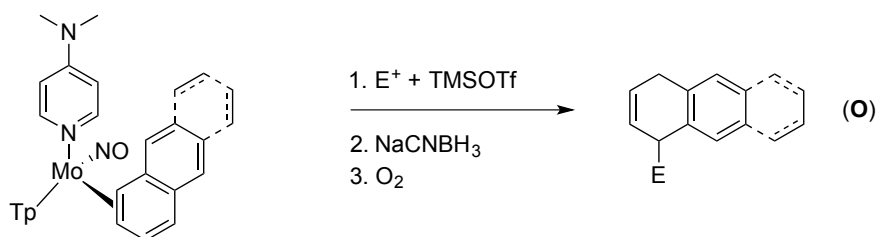
3.2.5 Varying the electrophiles added to **24** and **25**

The enhanced ability of the DMAP system to resist oxidation by acid also provides the opportunity to expand the range of electrophiles that add to C1. Attempts were made to add a single equivalent of acid, be it Brønsted or Lewis, to the dimethylamino group to achieve a greater reductive potential at the metal center and subsequently add a greater variety of electrophiles; however, this process was unsuccessful. Reagents explored include halogens, epoxidation agents, and nitrilium salts, all of which led to oxidation of the metal complex. However, when treated with trifluoromethylsilyl triflate (TMSOTf) at -60 °C, the acetal 2,2-dimethoxypropane reacts with **24** or **25** to give an allyl which can be trapped with lithium dimethylmalonate (LiDMM) to form complexes **41** and **42**, respectively (Scheme 3.5).

Unlike the other arene reactions in this account, the products **41** and **42** are the result of 1,4-addition reactions (Scheme 3.5). While the yields are moderate (~60%), these complexes are formed with good stereocontrol (dr > 8:1 for **Cp:Cd**), with both additions occurring *anti* to the metal. Upon treatment with iodine, organics **43** and **44** were obtained in moderate yield and with good recovery of the precursor **23** (Scheme 3.5). A compound similar to dihydronaphthalene **43** has been previously obtained on a 40 mg scale from naphthalene, lithium dimethylmalonate, and dimethoxymethane using osmium(II) or rhenium(I) dearomatization agents,^{11, 12} but these expensive heavy metals were not recovered.

Scheme 3.5. Tandem addition of dimethoxypropane, and LiDMM, to **24** and **25**.

Other 1,4-tandem additions were achieved by using various carbon electrophiles paired with sodium cyanoborohydride ($NaCNBH_3$) as the nucleophilic partner (Table 3.3). In addition to acetals (1,1-dimethoxycyclohexane as well as the previously mentioned dimethoxypropane), Michael acceptors were found to successfully add to C1 of the PAH, as demonstrated by the use of 3-penten-2-one and cyclopentenone (entries **49-52**).

Table 3.3. Addition of various electrophiles to **24** and **25**.

Arene Complex	Reagent (source of E)	Product (O)	(#)	(% yield)	1,4:1,2
24			45	51	>20:1
25			46	25	>20:1
24			47	27	>20:1
25			48	28	4:1
24			49	61	>20:1 dr= 2:1
25			50	38	2:1 dr= 2:1 and 3.5:1
24			51	27	>20:1 dr= 10:1
25			52	27	>20:1 dr= >20:1

In general, the addition of enones to the PAH complexes resulted in the formation of 1,4-addition products, isolated as a mixture of two diastereomers that presumably are epimers at the benzylic position. This presumption is based on the ^1H NMR observation of identical splitting patterns with small differences in chemical shifts. In one case (**50**) the dihydroanthracene product is believed to be a mixture of four isomers, as supported by the observation of four individual singlets at 2.15, 2.05, 2.01, and 1.97 ppm as well as doublets at 1.03, 0.90, 0.88 and 0.73 ppm. These isomers are believed to be a mixture of 1,4 and 1,2-addition products, as well as the epimers of these 1,4 and 1,2-addition products. Corresponding alkene peaks for the 4 isomers are overlapping, preventing their unambiguous assignment. Due to the complex mixture, **50** was not fully characterized; however, combustion analysis revealed this isomeric mixture to be a match for the desired product when solvent was taken into account. To further test the enhanced stability of DMAP in comparison to MeIm, **45** was also prepared using $\text{TpMoNO}(\text{MeIm})(\eta^2\text{-naphthalene})$ with a significant 26% decrease in yield in comparison to **24**.

3.3 Discussion

Unlike the $\{\text{TpW}(\text{NO})(\text{PMe}_3)\}$ fragment, the ancillary ligand (L) of the $\{\text{TpMo}(\text{NO})(\text{L})\}$ fragment can be changed while still retaining the metal center's ability to bind a wide variety of aromatics. In this way, greater control of the metal center's electron donating abilities is obtained. Isolation of the allyls **27** and **28** represents a unique ability of DMAP to have a sequential dual role. In its protonated state, DMAP

protects the metal center from oxidation by reducing electron donation into the metal. In its deprotonated state, DMAP donates electron density into the metal to help stabilize the allylic species. The allylic species **27** and **28** can be isolated and observed at room temperature via ^1H NMR. As seen in Figure 3.3, the degradation of **27** (noted by the increased formation of free naphthalene) is $\sim 50\%$ after 30 min; however, after 1.5 h at room temperature, significant decomposition has occurred. This is noteworthy when considering that with MeIm as the ancillary ligand, observation of $[\text{TpMo}(\text{NO})(\text{MeIm})(2,3,4\text{-}\eta^3\text{-naphthalenium})](\text{OTf})$ at room temperature has not been achieved.

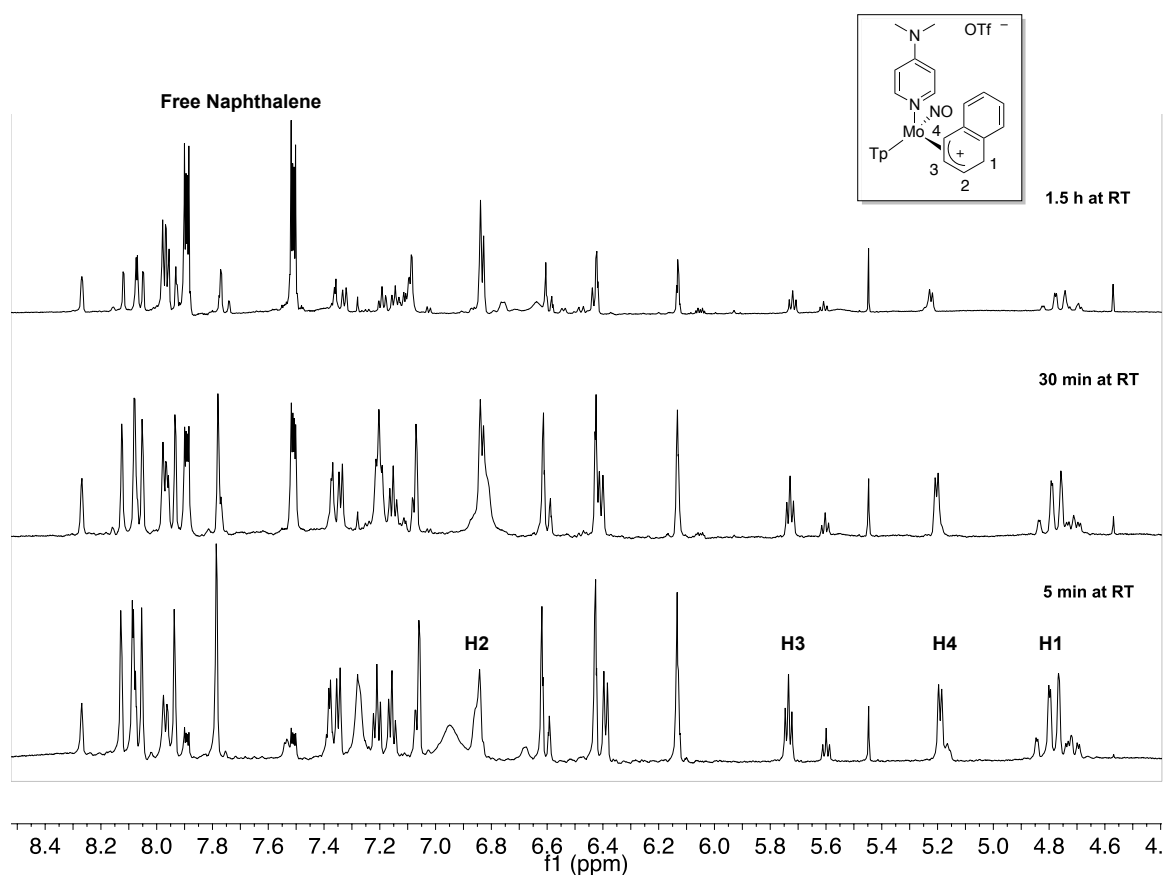
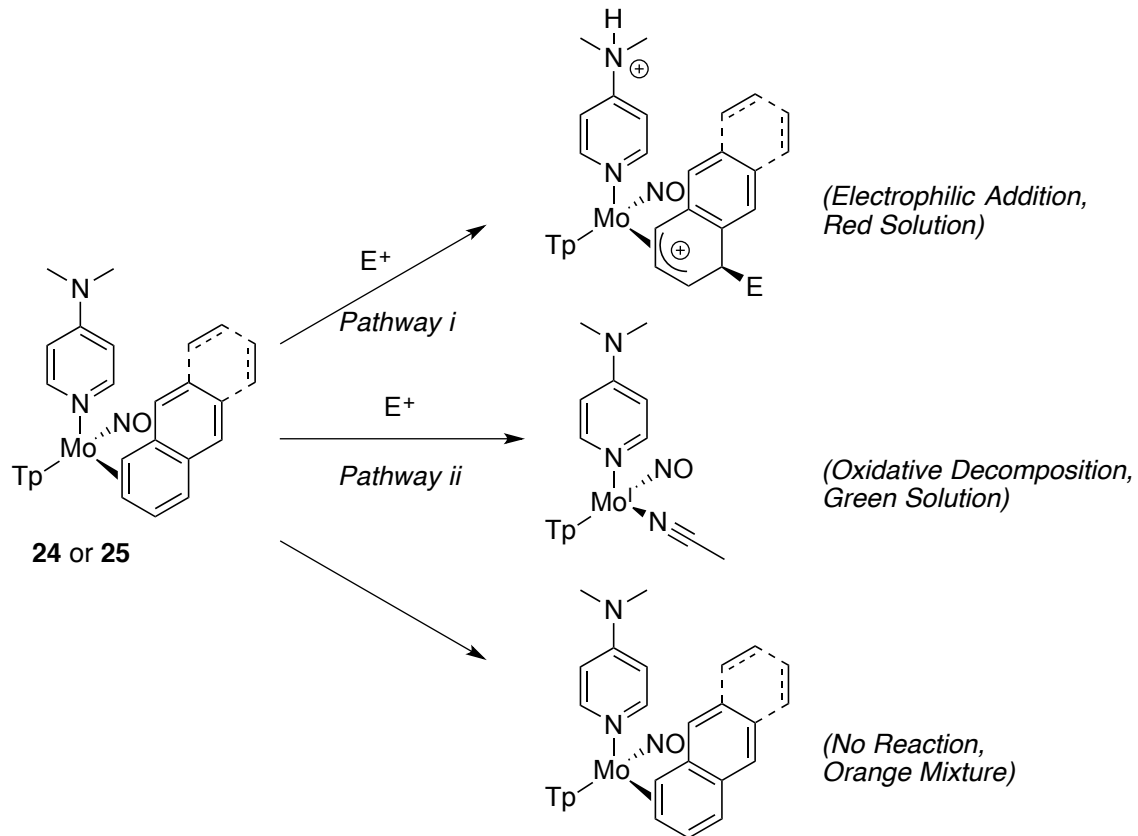


Figure 3.3. Monitoring the decomposition of **27** by ^1H NMR over 1.5 h at RT in CD_3CN .

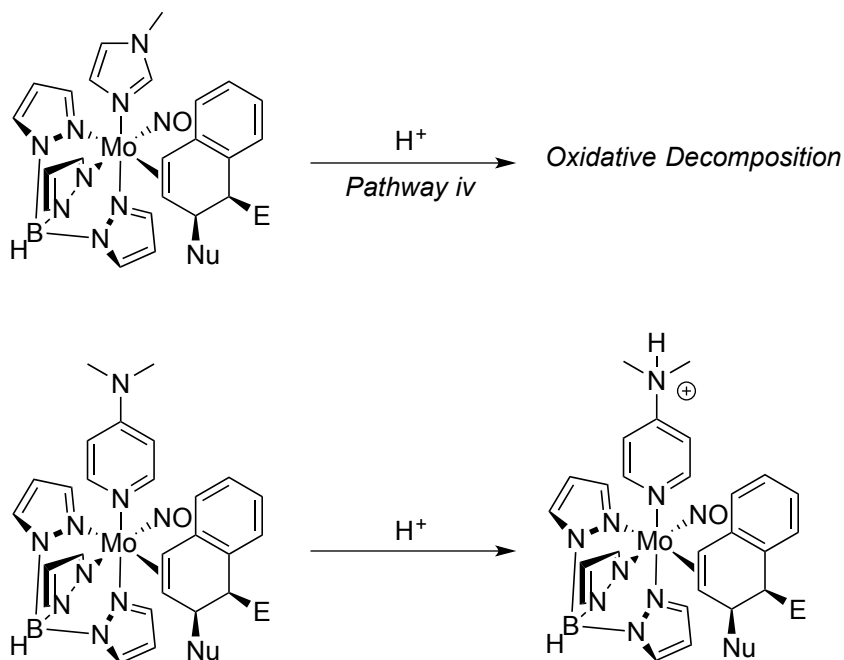
The cationic allyl of **27** significantly withdraws the electron density from the metal center as seen by an increase in the nitrosyl stretching frequency compared to the starting material **24** (from 1580 cm^{-1} to 1620 cm^{-1}). These allylic complexes are asymmetric in their orientation of binding unlike typical complexes binding in an η^3 fashion. In agreement with this asymmetry, the chemical shifts for the carbons associated with the allyl (**27**) are as follows: 129.1 (C2), 102.1 (C3) and 88.3 (C4). Of note, C2 is significantly more upfield in **27** than in the MeIm analogue where C2 is at 143.4 ppm.

As proposed in Chapter 2, a greater stability under oxidative conditions has indeed proven to enhance the breadth of chemical reactivity available for $\{\text{TpMo}(\text{NO})(\text{L})\}$. A few points should be made referring back to the potential pathways of the stepwise electrophilic-nucleophilic additions discussed in Chapter 2. The same qualitative observations are seen with the DMAP analogue as with the MeIm analogue (e.g., initially orange mixture, changes to a red or green solution upon the presence of an electrophile, and then changes to a golden brown or green solution upon presence of a nucleophile). As discussed in Chapter 2, the oxidation of starting material can be accomplished by the presence of an electrophile (Scheme 3.6, Pathway ii). For the DMAP analogue (where the electrophile is a Brønsted acid), oxidation is less likely due to a more positive reduction potential upon protonation of the amino group of DMAP.

Scheme 3.6. Possible pathways after the addition of electrophile (E^+) to **24** or **25**.

Once the allyl is formed, the DMAP ancillary ligand is believed to offer greater stability in two regards. First, the allyl itself is more stable as can be seen by the ability to isolate **27** and **28**. This greater stability is believed to be due to a greater donating ability of the DMAP through resonance donation from the amino group. Secondly, the final product of a nucleophilic addition (**C**) is also more stable to oxidation by excess electrophile present in the reaction mixture, as proposed with MeIm as the ancillary ligand (Scheme 3.7, Pathway iv).

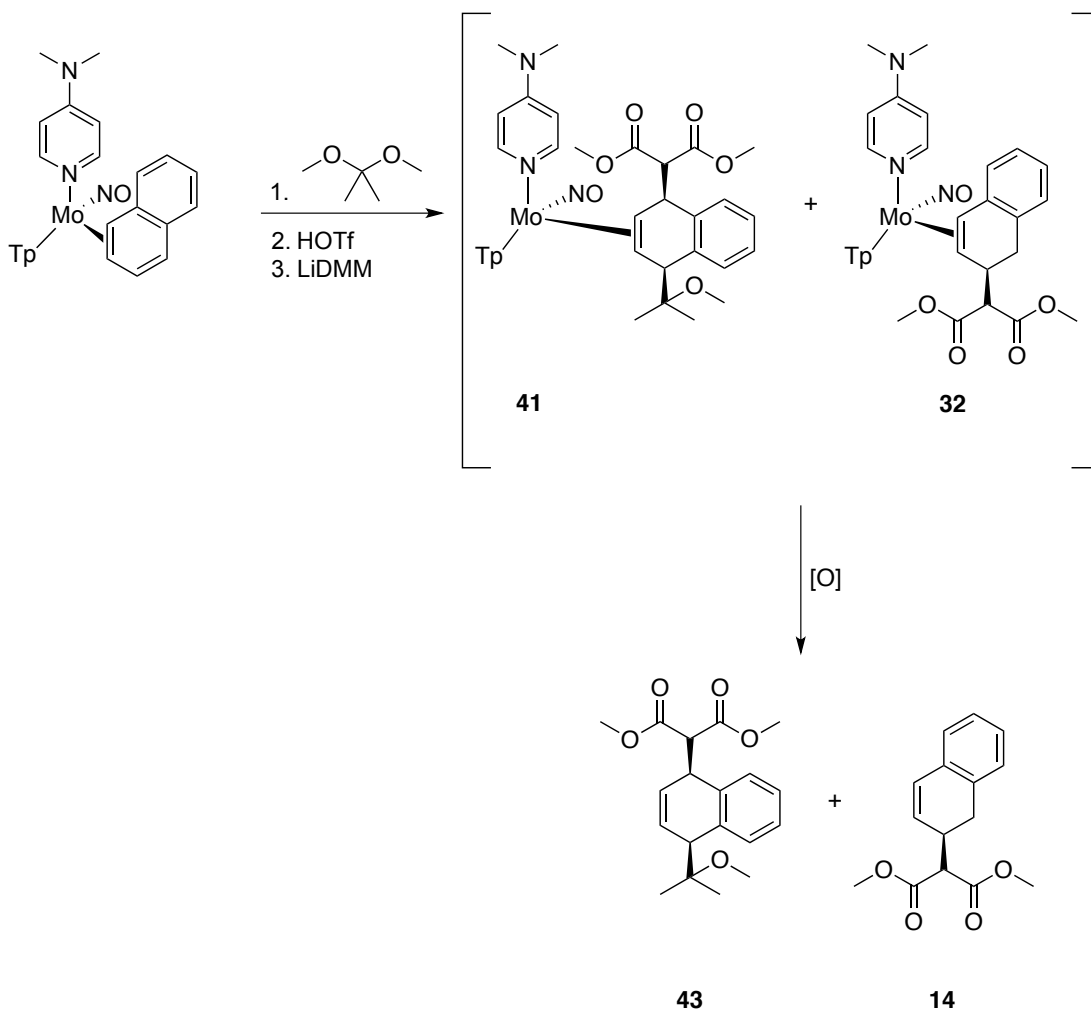
Scheme 3.7. Oxidative decomposition of **C** by excess electrophile, H^+ in this case.



In the case of the DMAP complex, excess acid is believed to preferentially react with the amino group of the DMAP ligand rather than oxidize the metal center. After replicating the previously reported nucleophilic additions observed with the MeIm complex, we hoped to show greater scope in reactivity for the DMAP complex by using a variety of electrophiles.

Initial investigations of electrophile scope began by attempting to add one equivalent of acid (theoretically protonating the amino group) to make the metal center resistant towards oxidation; these attempts proved unsuccessful. However, success has been demonstrated using electrophiles that can be activated with either Brønsted or Lewis acids. For instance, acetals can readily form a more electrophilic, oxonium species in the presence of acid. Similarly, Michael acceptors are enolizable in the presence of an acid, increasing the electrophilicity of the beta position.

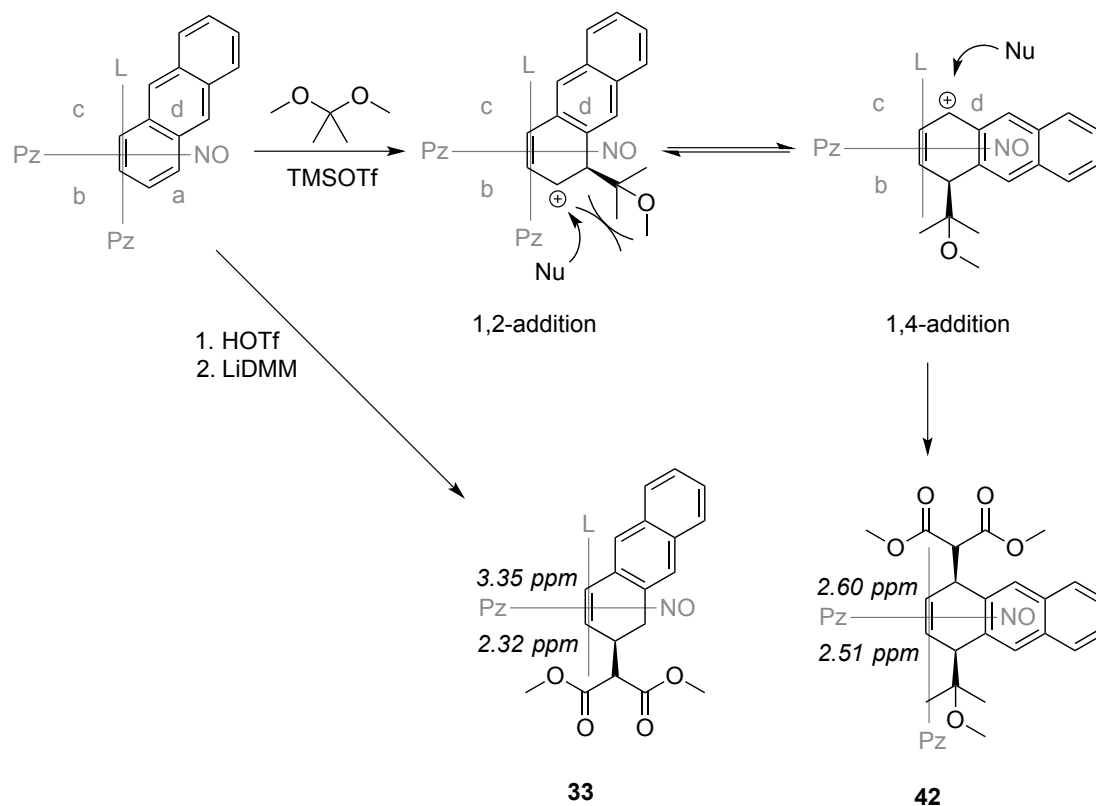
That arene complexes of osmium (II) and rhenium (I) have shown success in using both acetals and Michael acceptors for electrophilic-nucleophilic addition reactions, encouraged the use of these electrophiles for the molybdenum system. It was found that by activating acetals and Michael acceptors with HOTf, **24** and **25** could undergo carbon-carbon bond formation (Scheme 3.8) at -60 °C using propionitrile ($\text{CH}_3\text{CH}_2\text{CN}$) as the solvent in order to achieve the desired temperature. For these electrophilic additions, the starting complex **24** or **25** is dissolved in $\text{CH}_3\text{CH}_2\text{CN}$ containing the inactivated electrophile (either an acetal or Michael acceptor). Once the reaction mixture is cooled to -60 °C, the addition of a -60 °C solution of HOTf in $\text{CH}_3\text{CH}_2\text{CN}$ yields a dark red solution from the previously orange solution. After 15 min, the nucleophile is added (LiDMM or NaCNBH_3). After monitoring these reactions by CV (for more detail on this refer to Chapter 2), the reaction was determined to be complete after 18 hours, as evidenced by the presence of an $E_{\text{p,a}} \sim +0.2$ V. This reaction mixture was then stirred open to air overnight and the organic product yielded from the oxidation of the metal complex was isolated through chromatography. This method yielded the desired organic products, but the organics were only recovered in low yields (< 5%) due, in part, to the formation of unwanted side products. One side product of these reactions was identified as the product formed from initial protonation, followed by a nucleophilic addition (Scheme 3.8). It should be noted that this yields the organic products **14** and **15** (where the nucleophile = LiDMM), as well as 1,2-dihydronaphthalene and 1,2-dihydroanthracene (where the nucleophile = NaCNBH_3).

Scheme 3.8. Addition of dimethoxypropane and LiDMM to **24** using HOTf.

To avoid the undesired protonation side product, TMSOTf was used in place of HOTf to activate the carbon electrophiles. Using the same reaction conditions described above, but replacing HOTf with TMSOTf, complexes **41** and **42** were isolated with minimal signs of complexes **32** or **33** (< 5%). Furthermore, in the CV the 1,4-dihydroarene complexes (**41** and **42**) were found to have a smaller positive shift in $\text{Mo}^0/\text{Mo}^{\text{I}}$ potential from their aromatic precursors (~ 250 mV more positive) in comparison to **32** and **33**, which are shifted ~ 350 mV more positive. This less positive

shift in the anodic wave is in agreement with a decrease in π -acidity of the resulting dihydroarene of a 1,4-addition. The decrease in π -acidity is due to the disruption in conjugation with the remaining π -system.

The preference for regioselectivity in the 1,4-tandem addition reactions is due to the steric interaction between the carbon electrophile added and the incoming nucleophile. To avoid the disfavorable steric repulsion of 1,2-addition of two bulky reagents, the allylic complex can rearrange to provide an electrophilic center without significant steric repulsion (Scheme 3.9). In addition to the difference in their reductive potentials discussed above, the ^1H NMR of these 1,4-addition reactions only varies significantly for the “upbound” and “downbound” protons (the protons on the bound alkene proximal and distal to the DMAP ligand, respectively). For **33**, the downbound proton (H3) is more upfield (2.32 ppm) than the upbound proton (H4, 3.35 ppm). These alkene protons are more upfield than typically seen for a free alkene, which can be attributed to the large electron density localized on this bond from the metal. Furthermore, anisotropic ring currents from the Tp pyrazole rings gives a greater shielding of protons located between two of the rings of that ligand (Scheme 3.9, quadrant b). The ~ 1 ppm difference in chemical shift can also be attributed to a stronger withdrawal of electron density on the H4 carbon. This was determined by a comparison of **33** with **42**, where in **42** the downbound (H2, 2.51 ppm) and the upbound (H3, 2.60 ppm) are much closer in chemical shift.

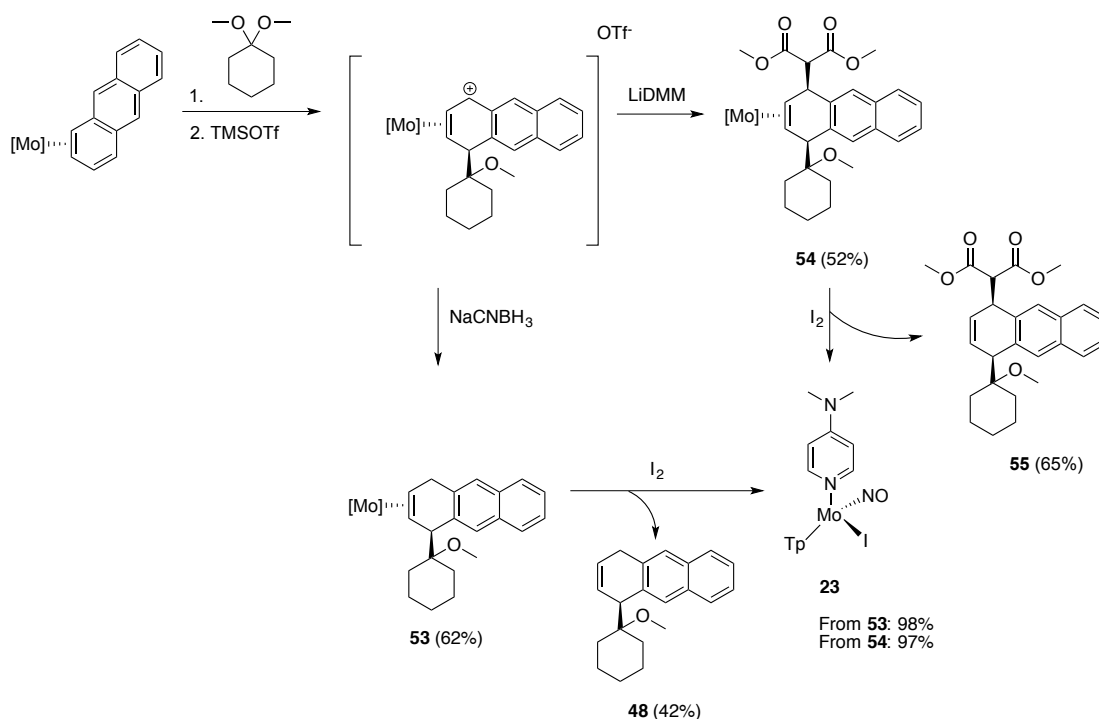
Scheme 3.9. Comparison of regiochemistry between 1,2 and 1,4-additions on **25**.

Other attempts to add electrophiles activated by TMSOTf with NaCNBH₃ as the nucleophile are shown in Table 3.1. These reaction mixtures were analyzed using CV, paying close attention to the subtle difference (< 100 mV) between a 1,2 and 1,4-addition. After determining the success of these reactions through CV, the reaction mixtures were stirred open to air overnight and the organic products were isolated through chromatography. The products of these 1,2 and 1,4-addition reactions have similar ¹H NMR spectra; however, a significant difference is seen in the isolated alkene resonances. In a 1,2-addition reaction, the alkene resonances of the isolated product are typically ~ 1 ppm apart and occur between 7.0 and 5.5 ppm. For a 1,4-addition reaction,

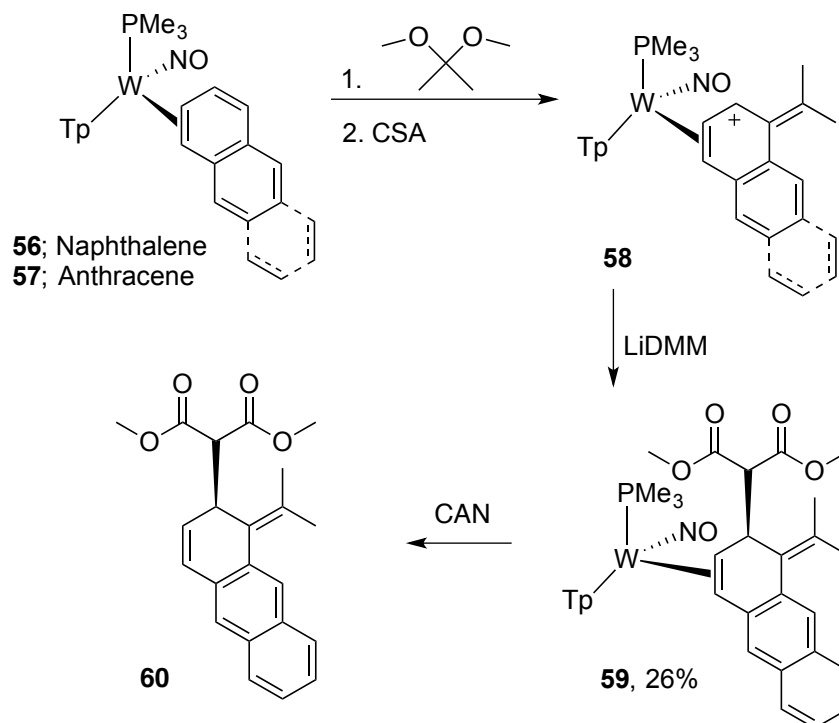
the alkene resonances of the isolated product are typically ~ 0.2 ppm apart and occur between 6.0 and 5.5 ppm. Using this information, the ratio of isomers in a mixture of products yielded from an oxidative decomplexation, can be determined through the integration of the corresponding alkene resonances.

Although oxidation via air does not provide a recyclable metal complex, 1,4-dihydroarenes can be isolated as their metal complexes and subjected to iodine oxidation as seen with **41** and **42**. To further demonstrate the recovery of the metal complex precursor in this system, **53** (the metal-bound complex of the organic **48**) was isolated via extraction before exposure to air (62%). Oxidation of this complex with iodine generated **48** (42%) and the precursor (**23**, 98%) (Scheme 3.10). Encouragingly, the overall yield of **48**, via iodine oxidation of **53**, from **25** was 26%, which is comparable to the yield through in situ formation and air oxidation reported in Table 3.3 (28%). Furthermore, the allyl formed from the addition of dimethoxycyclohexane to **25** (used to make **48**) was trapped with LiDMM to form the 1,4-tandem addition product **54**. This complex was then oxidized with iodine to yield the 1,4-dihydroanthracene **55** in good yield (65%) with 97% recovery of **23** (Scheme 3.10). These observations give the following important implications for future reactions: first, the organics isolated in Table 3.3 can be cleanly isolated as their metal complexes; second, the allyls formed from these new electrophiles can be trapped with a hydride or LiDMM; third, the metal complexes formed from these new electrophilic-nucleophilic additions can be subjected to oxidative decomplexation via iodine, regenerating the metal precursor for these complexes for reuse.

Scheme 3.10. Addition of dimethoxycyclohexane as an electrophile to **25**, followed by a nucleophilic addition with either NaCNBH₃ (bottom) or LiDMM (top).



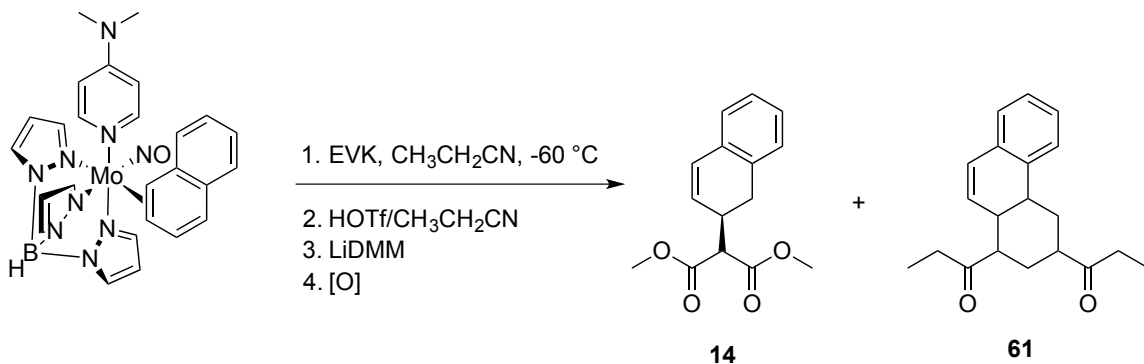
Previous attempts have been made to isolate **43** and **44** using {TpW(NO)(PMe₃)}.¹³ In both cases, the elimination of methanol occurs to yield a transiently stable ylidenium species (Scheme 3.11). For naphthalene, subjecting this intermediate to LiDMM resulted in products that were too unstable to isolate. In the case of anthracene, the ylidenium **58** reacts with LiDMM at C2 to form the stable ylidene complex, **59**. Treatment of **59** with ceric ammonium nitrate (CAN) yields trace amounts of an organic compound thought to be the intact ylidine **60**. The full characterization of this compound was not pursued as this ylidine lacks the additional stereocenter found in **43** and **44**, again representing a benefit of using molybdenum.

Scheme 3.11. Formation of the propenylidene dihydroanthracene complex **60**.

During the initial attempts to vary the electrophile added to **24**, a particularly difficult mixture of products was isolated from the addition of ethyl vinyl ketone (EVK) to **24** using HOTf as the promoter and subsequently trapping the resulting allyl with LiDMM. Subjecting this reaction mixture to an oxidative decomplexation in air and then isolating the resulting products through chromatography gave a mixture initially believed to contain the 1,2 and 1,4-addition products; however, further analysis proved otherwise. Through spectroscopic analysis, the two products of this reaction were identified as the 1,2-tandem addition product, **14**, and, surprisingly, the tricyclic hexahydro-phenanthrene, **61**, which is the product of a Michael-Michael ring closure (MIMIRC) sequence (Scheme

3.12). Full analysis and progress on the ongoing investigation of this reaction can be found in Chapter 4.

Scheme 3.12. Electrophilic addition of HOTf and LiDMM to form **14** and the product of a Michael-Michael ring closure, **61**.



3.4 Conclusion

Herein we have described the large-scale synthesis and properties of TpMo(NO)(DMAP)(I) (**23**), an air-stable precursor for the dearomatization of naphthalene and anthracene. Reduction of **23** in the presence of the PAH results in a stable Mo(0) complex in which the arene is dihapto-coordinated and highly activated toward the sequential addition of an electrophile (H⁺ or acetal) and nucleophile (enolates, pyrazole, pyrrole). We find that compared to the previously reported {TpMo(NO)(MeIm)} system, the DMAP analog offers significant practical advantages and a wider scope of chemical reactivity. The critical advantage of the DMAP ligand lies in its ability to accept a proton, which renders the metal more resistant to acid oxidation.

3.5 Experimental

General Methods

NMR spectra were obtained on a 600 or 800 MHz spectrometer. All chemical shifts are reported in ppm, and proton and carbon shifts are referenced to tetramethylsilane (TMS) utilizing residual ^1H or ^{13}C signals of the deuterated solvents as an internal standard. Coupling constants (J) are reported in hertz (Hz). Infrared spectra (IR) were recorded as a glaze on a spectrometer fitted with a horizontal attenuated total reflectance (HATR) accessory or on a diamond anvil ATR assembly. Electrochemical experiments were performed under a dinitrogen atmosphere. Cyclic voltammetry data were taken at ambient temperature ($\sim 25^\circ\text{C}$) at 100 mV/s in a standard three electrode cell with a glassy-carbon working electrode, *N,N*-dimethylacetamide (DMAc) or acetonitrile (CH_3CN) solvent (unless otherwise specified), and tetrabutylammonium hexafluorophosphate (TBAH) electrolyte (approximately 0.5 M). All potentials are reported versus NHE (normal hydrogen electrode) using cobaltocenium hexafluorophosphate ($E_{1/2} = -0.78\text{ V}$), ferrocene ($E_{1/2} = +0.55\text{ V}$), or decamethylferrocene ($E_{1/2} = +0.04\text{ V}$) as an internal standard. The peak-to-peak separation was less than 100 mV for all reversible couples. High-resolution mass spectra were acquired in ESI mode, from samples dissolved in a 6:1 acetonitrile:water solution containing sodium trifluoroacetate (NaTFA). Mass spectra are reported as M^+ for monocationic complexes or as M^+ , $[\text{M} + \text{H}^+]$, or $[\text{M} + \text{Na}^+]$ for neutral complexes, using $[\text{Na}(\text{NaTFA})_x]^+$ clusters as an internal standard. In all cases, observed isotopic envelopes were consistent with the molecular composition reported. For organic products, the monoisotopic ion is reported; for complexes, the major peaks in the isotopic envelope are

reported. Unless otherwise noted, all synthetic reactions were performed in a glovebox under a dry nitrogen atmosphere. Deuterated solvents were used as received. Pyrazole (Pz) protons of the hydridotris(pyrazolyl)borate (Tp) ligand were uniquely assigned (e.g., “Pz3B”) using a combination of two-dimensional NMR data and 4-(dimethylamino)pyridine–proton NOE interactions (see Figure 3.4 below). When unambiguous assignments were not possible, Tp protons were labeled as “Pz3/5 or Pz4”. BH peaks (around 4–5 ppm) are not identified due to their quadrupole broadening; IR data are used to confirm the presence of a BH group (around 2500 cm^{-1}). All J values for Pz protons are $2 (\pm 0.2)$ Hz. Due to the sensitivity of complexes **25–35**, **36**, **41** and **42** to air, elemental analysis attempts were unsuccessful. Elemental analysis of oils **43**, **44**, **46–50** and **52** show residual solvent (DCM) from sample preparation, even after extended time under vacuum. Compounds **1**, **24** and **12–17** were previously reported; however, an alternate synthesis of **24** from **23** rather than $\text{TpMo}(\text{NO})(\text{Br})_2$ is given.^{1, 10}

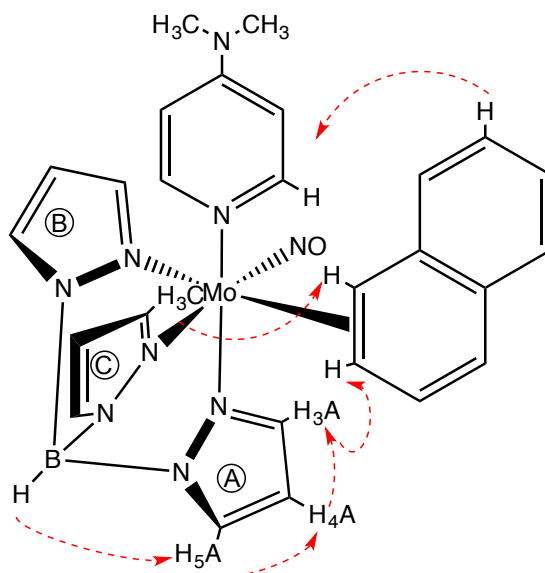
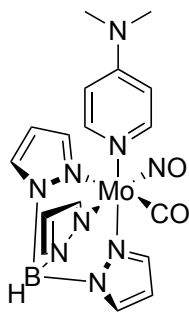


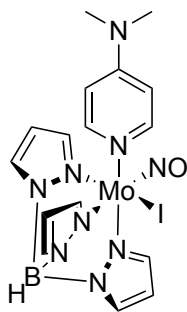
Figure 3.4. Analysis of NOE interactions.

Synthesis of $\text{TpMo}(\text{NO})(\text{CO})(\text{DMAP})$ (**22**).



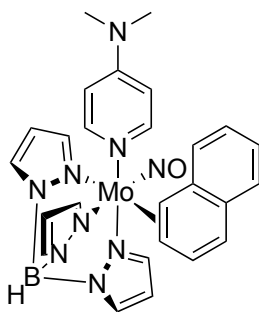
Under an air atmosphere, **1** (166 g, 0.421 mol), *N,N*-dimethylformamide (1.8 L), and DMAP (165 g, 1.35 mol) were added to a 3 neck 3 L round bottom flask charged with a stir egg, reflux condenser, thermometer and septum. The resulting orange mixture was heated to reflux ($\sim 154^\circ\text{C}$) for 5 h then cooled to RT for 15 min. The reaction mixture was then added to stirring H_2O (4 L) and the resulting green mixture was stirred at RT. After 18 h, the green precipitate was isolated on a 3 L coarse porosity fritted disc, washed with H_2O (2 x 1 L), 20% MeOH:Et₂O (2 x 1 L), and Et₂O (4 x 1 L), and desiccated overnight to yield **22** (164.9 g, 80%). CV (DMAc) $E_{\text{p,a}} = +0.27$ V (NHE). IR: $\nu(\text{BH}) = 2484\text{ cm}^{-1}$, $\nu(\text{CO}) = 1871\text{ cm}^{-1}$, $\nu(\text{NO}) = 1589\text{ cm}^{-1}$. ^1H NMR (CDCl_3 , δ): 7.80 (2H, m, DMAP-A), 7.73 (1H, d, Pz3/5), 7.72 (1H, d, Pz3/5), 7.69 (1H, d, Pz3/5), 7.68 (1H, d, Pz3/5), 7.36 (1H, d, Pz3/5), 7.34 (1H, d, Pz3/5), 6.32 (2H, m, DMAP-B), 6.18 (1H, t, Pz4), 6.17 (1H, t, Pz4), 6.14 (1H, t, Pz4), 2.98 (6H, s, NMe). ^{13}C NMR (d^6 -Acetone, δ): 155.1, 152.7, 144.8, 143.1, 142.5, 136.7, 136.5, 136.4, 107.8, 106.5, 106.4, 106.3, 39.1.

Synthesis of TpMo(NO)(DMAP)(I) (**23**).



Under an air atmosphere, **22** (161 g, 0.328 mol) and DCM (750 mL) were added to a 6 L Erlenmeyer flask charged with a stir bar and the resulting mixture was stirred at RT until homogeneous. To a 1 L Erlenmeyer flask charged with a stir bar were added I₂ (41.45 g, 0.164 mol) and Et₂O (1 L), and the mixture was stirred 15 min at RT until homogeneous. (CAUTION: Evolution of CO) With the hood sash down, the I₂ solution was slowly added to the solution of **22** and the resulting green solution was left stirring at RT. After 15 min, Et₂O (4 L) was added to the reaction mixture creating a green precipitation. The precipitate was isolated on a 3 L coarse porosity fritted disc, washed with Et₂O (4 x 1 L), and desiccated overnight to yield **23** (170 g, 88%). CV (DMAc) $E_{p,a} = +0.65$ V (NHE), $E_{1/2} = -1.43$ V (NHE). IR: $\nu(\text{BH}) = 2477 \text{ cm}^{-1}$, $\nu(\text{NO}) = 1607 \text{ cm}^{-1}$.

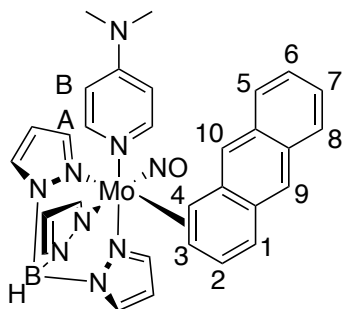
Synthesis of TpMo(NO)(DMAP)(3,4- η^2 -naphthalene) (**24**).



(CAUTION: Pyrophoric!) **23** (24 g, 0.040 mol), THF (500 mL), naphthalene (67 g, 0.508

mol), and sodium dispersion in wax (30-35% by weight, 6.8 g, 88.6 mmol) were added to a 1 L round bottom flask charged with a stir egg and this mixture was stirred at RT. After 24 h, Et₂O (500 mL) was added and the reaction mixture was subsequently loaded onto a 600 mL medium porosity fritted disc ³/₄ full with silica gel. The product was eluted as a yellow band with 1:1 THF:Et₂O (400 mL), collected as an orange solution, and then evaporated *in vacuo* to ~50 mL. This orange solution was added to stirring pentane (900 mL) forming an orange precipitate. This precipitate was isolated on a 350 mL fine porosity fritted disc, washed with pentane (3 x 200 mL), and desiccated to yield **24** (11.91 g, 50% yield).

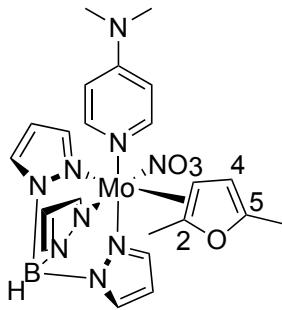
Synthesis of TpMo(NO)(DMAP)(3,4-η²-anthracene) (25).



(CAUTION: Pyrophoric!) **23** (24 g, 0.040 mol), THF (500 mL), anthracene (28 g, 0.157 mol), and sodium dispersion in wax (30-35% by weight, 6.8 g, 88.6 mmol) were added to a 1 L round bottom flask charged with a stir egg and this mixture was stirred at RT. After 24 h, Et₂O (250 mL) was added and the reaction mixture was subsequently loaded onto a 600 mL medium porosity fritted disc ³/₄ full with silica gel. The product was eluted as a red band with 3:1 THF:Et₂O (1 L), collected as a red solution, and then evaporated *in vacuo*. The red solid formed was then suspended in CH₃CN (150 mL) and this red mixture was filtered through a 350 mL fine porosity fritted disc. The orange solid isolated

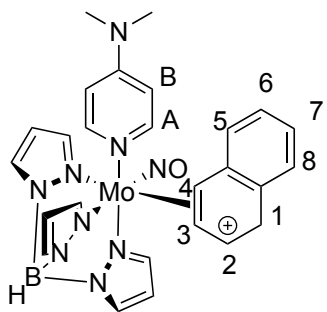
was washed with CH₃CN (2 x 150 mL) and the red filtrate was evaporated *in vacuo* to an oil. This oil was then dissolved in THF (50 mL) and the product was precipitated in stirring pentane (800 mL), isolated on a 350 mL fine porosity fritted disc, washed with pentane (3 x 200 mL), and desiccated to yield **25** (11.89 g, 47% yield). This compound was observed as a 3:1 ratio of diastereomers, the major having the unbound naphthalene ring directed toward the DMAP ligand and the minor having the unbound naphthalene ring directed away from the DMAP ligand. CV (DMAc) $E_{p,a} = -0.04$ V (NHE). IR: $\nu(\text{C-H } sp^2) = 2925 \text{ cm}^{-1}$, $\nu(\text{BH}) = 2477 \text{ cm}^{-1}$, $\nu(\text{NO}) = 1585 \text{ cm}^{-1}$. ¹H NMR (d⁶-Acetone, δ): 8.13 (1H, d, Pz3A), 8.04 (1H, d, Pz5C), 8.00 (2H, bs, DMAP-A), 7.93 (1H, d, Pz5A), 7.84 (1H, d, Pz5B), 7.81 (1H, d, Pz3C), 7.76 (1H, bd, $J = 7.3$, H8), 7.63 (1H, s, H9), 7.28 (1H, d, $J = 7.4$, H5), 7.24 (2H, m, H6 & H7), 7.09 (1H, dd, $J = 9.1$ & 5.6 , H2), 6.93 (1H, d, Pz3B), 6.70 (2H, m, DMAP-B), 6.65 (1H, d, $J = 9.0$, H1), 6.43 (1H, t, Pz4C), 6.37 (1H, t, Pz4A), 6.28 (1H, s, H10), 6.07 (1H, t, Pz4B), 3.79 (1H, d, $J = 8.0$, H4), 3.15 (1H, dd, $J = 7.8$ & 5.6 , H3), 3.06 (6H, s, NMe). ¹³C NMR (d⁶-Acetone, δ): 154.9 (DMAP-C), 150.8 (DMAP-A), 143.6 (Pz3A), 142.6 (Pz3B), 141.8 (Pz3C), 137.6 (Pz5C), 136.8 (Pz5A), 135.9 (Pz5B), 135.7 (C2), 133.0, 132.7, 132.5, 132.1, 127.8 (C8), 126.8 (C5), 124.6 (C6/7), 123.9 (C6/7), 123.2 (C9), 122.9 (C10), 118.7 (C1), 108.4 (DMAP-B), 106.9 (Pz4), 106.3 (Pz4), 106.27 (Pz4), 75.1, 68.9, 39.2 (NMe). HRMS: C₃₀H₃₀N₉O₂Mo⁺Na⁺ obsd (%), calcd (%), ppm: 658.1641 (43), 658.1632 (52), 1.4; 660.1636 (40), 660.1630 (48), 1.0; 661.1614 (78), 661.1628 (81), -2.2; 662.1637 (84), 662.1624 (87), 1.9; 663.1644 (69), 663.1636 (77), 1.2; 664.1643 (100), 664.1624 (100), 2.9; 665.1627 (26), 665.1651 (39), -3.6; 666.1670 (30), 666.1643 (39), 4.0.

Synthesis of TpMo(NO)(DMAP)(2,3- η^2 -2,5-dimethylfuran) (**26**).



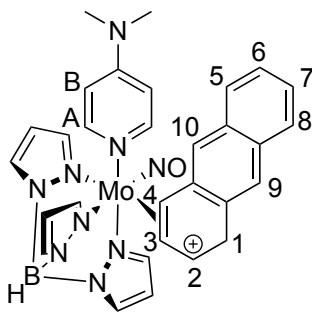
To a 500 mL round bottom flask charged with a stir egg were added sodium dispersion (30-35% by weight, 24 g dispersion, 0.365 mol) and hexanes (250 mL). The grey mixture formed was stirred for 18 h at which point the hexanes was decanted off and THF (250 mL), 2,5-dimethylfuran (24 mL, 0.281 mol) and **23** (24 g, 0.0408 mol) were added to the remaining solid. The resulting green reaction mixture was stirred for 6 h, transferred to a 1 L filter flask, and evaporated *in vacuo* to dryness. (CAUTION: Evolution of hydrogen gas) The resulting black solid was then suspended in MeOH (500 mL) forming a dark yellow precipitation. The yellow precipitate was isolated on a 150 mL medium fritted disc, washed with MeOH (3 x 75 mL) and pentane (3 x 75 mL), and desiccated 1 h to yield **26** (13.03 g, 57%). CV (DMAc) $E_{p,a} = -0.35$ V (NHE). IR: $\nu(\text{BH}) = 2494$ cm^{-1} , $\nu(\text{NO}) = 1620$ cm^{-1} . ^1H NMR (d^6 -Acetone, δ): 8.25 (1H, d, Pz5A), 7.95 (1H, d, Pz3C), 7.94 (1H, d, Pz3A), 7.91 (1H, bs, DMAP-A), 7.83 (1H, d, Pz3B), 7.41 (1H, d, Pz5C), 6.95 (1H, d, Pz5B), 6.65 (2H, d, $J = 7.1$, DMAP-B), 6.38 (1H, t, Pz4A), 6.30 (1H, t, Pz4C), 6.12 (1H, t, Pz4B), 5.67 (1H, bs, H4), 3.08 (7H, s, H3 & NMe), 2.13 (3H, s, H5), 0.93 (3H, s, H2). ^{13}C NMR (d^6 -Acetone, δ): 155.1, 151.2, 147.7, 142.9, 142.6, 142.5, 137.1, 136.3, 135.6, 119.8, 108.4, 107.9, 106.3, 106.3, 106.2, 69.1, 39.2, 29.8, 21.6, 12.9.

Synthesis of TpMo(NO)(DMAP)(3,4- η^2 -naphthalenium)(OTf) (27**).**



24 (1.0 g, 1.70 mmol) and CH₃CN (4 mL) were added to a 4-dram vial and the mixture was cooled at -30 °C for 15 min. A -30 °C, 1M solution of HOTf in CH₃CN (4.0 mL, 4.0 mmol) was added to the reaction mixture and the resulting red solution was left at -30 °C for 15 min. The reaction mixture was evaporated *in vacuo* to an oil that was redissolved in DCM (6 mL). The resulting red solution was added to stirring Et₂O (400 mL) forming an orange precipitation. The precipitate was isolated on a 30 mL fine porosity fritted disc, washed with Et₂O (3 x 30 mL) and desiccated to yield **27** (1.18 g, 95% yield). CV (DMAc) $E_{p,a} = -0.18$ V (NHE). IR: $\nu(\text{BH}) = 2500\text{ cm}^{-1}$, $\nu(\text{NO}) = 1621\text{ cm}^{-1}$. ¹H NMR (CD₃CN, δ): 8.13 (1H, d, Pz5C), 8.09 (1H, d, Pz3C), 8.05 (1H, d, Pz3A), 7.94 (1H, d, Pz5A), 7.79 (1H, d, Pz3/5B), 7.33 (1H, d, $J = 7.6$, H8), 7.27 (2H, bs, DMAP-A), 7.20 (1H, t, $J = 7.6$, H7), 7.14 (1H, t, $J = 7.3$, H6), 7.04 (1H, d, Pz3/5B), 6.96 (2H, bs, DMAP-B), 6.88 (1H, bd, $J = 6.7$, H2), 6.62 (1H, t, Pz4C), 6.42 (1H, t, Pz4A), 6.36 (1H, d, $J = 7.6$, H5), 6.12 (1H, t, Pz4B), 5.72 (1H, t, $J = 7.3$, H3), 5.16 (1H, d, $J = 6.3$, H4), 4.78 (1H, dd, $J = 27.6$ & 3.0, H1), 4.77 (1H, d, $J = 27.6$, H1), 3.12 (6H, s, NMe). ¹³C NMR (CD₃CN, δ): 147.5 (DMAP-C), 143.8 (Pz5C), 143.3 (Pz3C), 140.2, 139.4 (Pz5A), 139.2 (C2), 138.2, 137.2, 136.1 (Pz3/5B), 130.8 (C5), 129.1, 128.7 (C6), 128.3 (C8), 126.9, 122.4, 120.8, 110.3, 108.7 (Pz4C), 107.9 (Pz4A), 107.9 (Pz4B), 102.4, 99.6 (C4), 40.9 (NMe), 33.6 (C1).

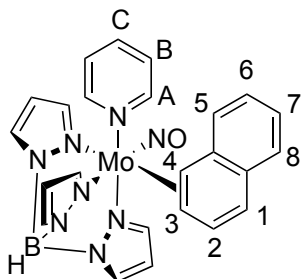
Synthesis of TpMo(NO)(DMAP)(3,4- η^2 -anthracenium)(OTf) (28**).**



25 (1.0 g, 1.56 mmol) and CH₃CN (4 mL) were added to a 4-dram vial and the mixture was cooled at -30 °C for 15 min. A -30 °C, 1M solution of HOTf in CH₃CN (4.0 mL, 4.0 mmol) was added to the reaction mixture, and the resulting dark red solution was left at -30 °C for 15 min. The reaction mixture was then evaporated *in vacuo* to a red oil that was redissolved in DCM (6 mL) forming a red solution. This solution was added to stirring Et₂O (400 mL) forming an orange precipitation. The precipitate was isolated on a 30 mL fine porosity fritted disc, washed with Et₂O (3 x 30 mL) and desiccated to yield **28** (1.14 g, 93% yield). CV (DMAc) $E_{p,a} = -0.40$ V (NHE). IR: $\nu(\text{C-H sp}^2) = 3125 \text{ cm}^{-1}$, $\nu(\text{BH}) = 2515 \text{ cm}^{-1}$, $\nu(\text{NO}) = 1624 \text{ cm}^{-1}$. ¹H NMR (CD₃CN, δ): 8.26 (1H, d, $J = 2.2$, DMAP-A), 8.16 (1H, d, Pz3C), 8.08 (1H, d, Pz3A), 8.08 (1H, s, H10), 8.05 (1H, d, Pz5C), 7.99 (1H, d, $J = 2.0$, DMAP-A), 7.94 (1H, d, Pz5A), 7.82 (1H, d, $J = 8.0$, H5), 7.77 (1H, d, Pz3/5B), 7.76 (1H, s, H9), 7.61 (1H, d, $J = 8.1$, H8), 7.48 (1H, t, $J = 6.8$, H6), 7.44 (1H, t, $J = 7.4$, H7), 7.07 (1H, d, Pz3/5B), 6.82 (2H, bs, DMAP-B), 6.65 (1H, m, H2), 6.62 (1H, t, Pz4C), 6.42 (1H, t, Pz4A), 6.10 (1H, t, Pz4B), 5.78 (1H, t, $J = 7.1$, H3), 5.35 (1H, d, $J = 6.6$, H4), 4.80 (2H, 2d overlapping, $J = 26.5$, H1), 3.17 (6H, s, NMe). ¹³C NMR (CD₃CN, δ): 147.1 (DMAP-C), 143.2, 142.9, 139.0, 138.8, 136.6 (C2), 134.1, 133.2, 131.9, 131.7, 128.9, 128.6, 127.9, 127.5, 127.1, 126.9, 126.7, 126.6, 126.5, 126.1, 122.3, 120.2, 118.3,

108.3 (DMAP-B), 107.5 (Pz4), 107.3 (Pz4), 107.2 (Pz4), 102.6 (C3), 88.8 (C4), 32.9 (C1).

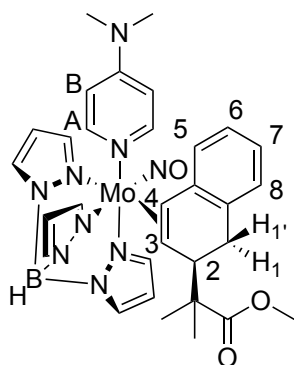
Synthesis of TpMo(NO)(pyridine)(η^2 -naphthalene) (29**).**



TpMo(NO)(Br)₂ (6.01 g, 12.0 mmol) and THF (125 mL) were added to a 250 mL round bottom flask charged with a stir bar. Zn dust (1.63 g, 24.9 mmol) was added to the stirring reaction mixture and was left stirring. After 10 min, pyridine (1.21 mL, 15.0 mmol) was added dropwise to the reaction mixture. After stirring for 30 min the solution darkened to a cranberry color, and then changed to dark green after 60 min. Na dispersion (30 – 35 %, 5.10 g, 58.7 mmol) was washed with hexanes (3 x 30 mL), then THF (25 mL) to produce Na⁰ flakes, which were added to the reaction mixture, followed by naphthalene (16.46 g, 128 mmol). The reaction mixture was stirred for 8 d. The dark reaction mixture was loaded onto a 350 mL medium porosity fritted disc ³/₄ full with silica gel and a bright red band was eluted with Et₂O (400 mL). The filtrate was evaporated *in vacuo*, dissolved in DCM (8 mL), and the product was precipitated in stirring pentane (200 mL). The precipitate was collected on a 30 mL fine porosity fritted disc, washed with pentane (30 mL), and then desiccated yielding **29** (1.60 g, 24%). CV (DMAc) $E_{p,a}$ = -0.69 V (NHE). IR: $\nu(\text{C-H sp}^2)$ = 2994 cm⁻¹, $\nu(\text{BH})$ = 2485 cm⁻¹, $\nu(\text{NO})$ = 1585 cm⁻¹. ¹H-NMR (d⁶-Acetone, δ): 8.13 (1H, d, Pz3A), 8.12 (1H, bs, py-A), 8.06 (1H, d, Pz5C), 7.95 (1H, d, Pz5A), 7.86 (1H, d, Pz3/5B), 7.79 (1H, d, Pz3C), 7.68 (1H, bs, py-

A), 7.32 (3H, m, py-B & H8), 7.10 (1H, dd, $J = 8.9$ & 5.6 , H2), 7.07 (1H, m, py-C), 7.01 (1H, t, $J = 7.4$, H7), 6.84 (1H, t, $J = 7.3$, H6), 6.79 (1H, d, Pz3/5B), 6.62 (1H, d, $J = 8.9$, H1), 6.44 (1H, t, Pz4C), 6.37 (1H, t, Pz4A), 6.07 (2H, bd & t, H5 & Pz4B), 3.88 (1H, d, $J = 8.4$, H4), 3.36 (1H, dd, $J = 8.4$ & 5.6 , H3). ^{13}C -NMR (d^6 -Acetone, δ): 143.3 (Pz3/5), 142.3 (Pz3/5), 141.9 (Pz3/5), 137.7 (Pz3/5), 136.9 (Pz5A), 136.2 (Pz3/5), 134.5, 133.8, 132.7, 132.2, 126.6, 125.7 (PyB & C8), 124.1 (PyC), 123.8 (C6), 119.3 (C1), 107.1 (Pz4C), 106.4 (Pz4A & Pz4B), 78.1 (C4), 71.7 (C3).

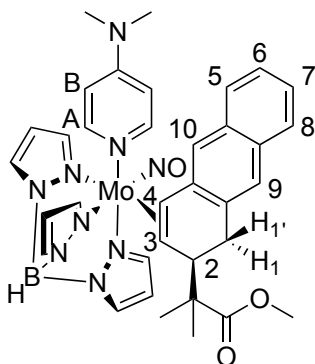
Synthesis of $\text{TpMo}(\text{NO})(\text{DMAP})(3,4\text{-}\eta^2\text{-(2-(2'-(2-carbomethoxy)propyl-1,2-dihydronaphthalene) (30))}$



24 (300 mg, 0.509 mmol) and CH_3CN (6 mL) were added to a 4-dram vial and the orange solution was cooled at $-30\text{ }^\circ\text{C}$ for 15 min. A $-30\text{ }^\circ\text{C}$, 1M solution of HOTf in CH_3CN (2.1 mL, 2.1 mmol) was added to the reaction mixture and the resulting red solution was left at $-30\text{ }^\circ\text{C}$. After 15 min, MTDA (1.0 mL, 4.92 mmol) was added to this red solution and the resulting mixture was left at $-30\text{ }^\circ\text{C}$. After 18 h, TEA (0.6 mL, 4.3 mmol) was added and the resulting brown solution was evaporated *in vacuo* to a brown oil. This oil was redissolved in DCM (10 mL), washed with NaHCO_3 (10 mL, sat. aq.), and the resulting brown solution was dried over MgSO_4 . The drying agent was filtered off on a 15 mL

coarse porosity fritted disc, washed with DCM (3 x 5 mL), and the filtrate was evaporated *in vacuo* to an oil. This oil was then dissolved in DCM (2 mL) and the product was precipitated in stirring pentane (50 mL). The precipitate was collected on a 15 mL medium porosity fritted disc, washed with pentane (3 x 15 mL), and desiccated for 15 min, yielding the yellow precipitate **30** (333 mg, 95 %). CV (DMAc) $E_{p,a} = +0.20$ V (NHE). IR: $\nu(\text{BH}) = 2484\text{ cm}^{-1}$, $\nu(\text{CO}) = 1724\text{ cm}^{-1}$, $\nu(\text{NO}) = 1566\text{ cm}^{-1}$. ^1H NMR (d^6 -Acetone, δ): 7.98 (1H, d, Pz3A), 7.95 (1H, d, Pz5C), 7.93 (1H, d, Pz5A), 7.81 (1H, d, Pz3C), 7.80 (1H, d, Pz5B), 7.39 (2H, bs, DMAP-A), 6.99 (1H, d, Pz3B), 6.95 (1H, d, $J = 7.3$, H8), 6.78 (1H, t, $J = 7.3$, H7), 6.74 (1H, t, $J = 7.2$, H6), 6.51 (2H, m, DMAP-B), 6.41 (1H, t, Pz4A/C), 6.40 (1H, t, Pz4A/C), 6.10 (1H, t, Pz4B), 6.08 (1H, d, $J = 7.2$, H5), 3.56 (1H, dd, $J = 16.6$ & 8.8 , H1'), 3.31 (3H, s, OMe), 3.24 (1H, d, $J = 7.8$, H4), 3.19 (1H, bs, H2), 3.06 (6H, s, NMe), 2.62 (1H, d, $J = 16.6$, H1), 2.19 (1H, dt, $J = 10.1$ & 1.5 , H3), 1.13 (3H, s, OMe), 0.96 (3H, s, OMe). ^{13}C NMR (d^6 -Acetone, δ): 178.9 (CO), 154.9 (DMAP-C), 150.5 (DMAP-A), 144.1, 142.7 (Pz5), 142.7 (Pz5), 142.0 (Pz3B), 137.2, 137.0, 135.7, 135.6, 133.9, 127.9 (C8), 127.2, 127.1, 126.9 (C5), 126.8, 124.6 (C6), 123.3 (C7), 108.2 (DMAP-B), 108.0, 106.9, 106.7 (Pz4A/C), 106.4 (Pz4A/C), 106.2 (Pz4B), 69.5 (OMe), 65.4 (C3), 43.8 (C4), 39.1 (NMe), 29.9 (C1), 23.3 (Me), 23.0. HRMS: $\text{C}_{31}\text{H}_{38}\text{N}_9\text{O}_3\text{BMo}+\text{Na}^+$ obsd (%), calcd (%), ppm: 710.2128 (42), 710.2156 (51), -4.0; 712.2114 (43), 712.2154 (48), -5.7; 713.2159 (77), 713.2153 (80), 0.8; 714.2120 (82), 714.2149 (87), -4.1; 715.2155 (67), 715.2161 (77), -0.8; 716.2128 (100), 716.2149 (100), -2.9; 717.2150 (34), 717.2176 (41), -3.6; 718.2139 (33), 718.2168 (40), -4.1.

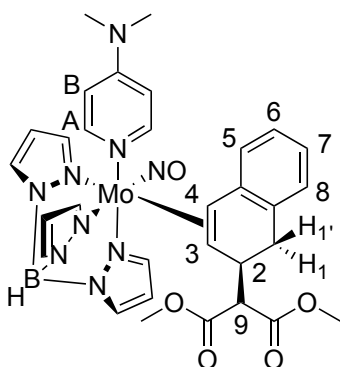
Synthesis of **TpMo(NO)(DMAP)(3,4- η^2 -(2-(2'-(2-carbomethoxy)propyl-1,2-dihydroanthracene) (31).**



25 (200 mg, 0.312 mmol) and CH₃CN (2 mL) were added to a 4-dram vial and this red solution was left for 15 min at -30 °C. A -30 °C, 1M solution of HOTf in CH₃CN (0.7 mL, 0.7 mmol) was added to the reaction mixture and the resulting dark red solution was left at -30 °C. After 15 min, MTDA (0.4 mL, 1.9 mmol) was added and the reaction mixture was left at -30 °C. After 18 h, triethylamine (0.1 mL, 0.717 mmol) was added to the reaction mixture and the resulting orange solution was warmed to RT. This solution was then chromatographed through a 15 mL fine porosity fritted disc $\frac{3}{4}$ full with silica gel. The product was eluted with 1:1 Et₂O:THF (50 mL) as a yellow band, collected as a yellow solution, and evaporated *in vacuo*. The resulting oil was dissolved in DCM (1 mL) and the product was precipitated in stirring hexanes (50 mL). The precipitate was collected on a 15 mL fine porosity fritted disc, washed with hexanes (3 x 10 mL), and dried for 15 min yielding the yellow solid **31** (118 mg, 52%). CV (DMAc) $E_{p,a}$ = +0.16 V (NHE). IR: ν (BH) = 2480 cm⁻¹, ν (CO) = 1720 cm⁻¹, ν (NO) = 1570 cm⁻¹. ¹H-NMR (d⁶-Acetone, δ): 7.99 (1H, d, Pz5A), 7.96 (1H, d, Pz3A), 7.94 (1H, d, Pz5C), 7.87 (1H, d, Pz3C), 7.80 (1H, d, Pz5B), 7.66 (1H, d, J = 7.9, H8), 7.43 (1H, s, H9), 7.35 (2H, bd, J = 6.6, DMAP-A), 7.24 (2H, m, H5 & H6), 7.19 (1H, m, H7), 7.05 (1H, d, Pz3B), 6.42 (1H,

t, Pz4C), 6.41 (2H, bs, DMAP-B), 6.41 (1H, t, Pz4A), 6.17 (1H, s, H10), 6.10 (1H, t, Pz4B), 3.68 (1H, ddd, $J = 17.0, 8.0, \& 2.0$, H1), 3.43 (1H, d, $J = 9.7$, H4), 3.32 (3H, s, OMe), 3.27 (1H, d, $J = 7.7$, H2), 3.04 (6H, s, NMe), 2.80 (1H, d, $J = 17.0$, H1'), 2.27 (1H, dt, $J = 9.5 \& 1.7$, H3), 1.14 (3H, s, Me), 0.96 (3H, s, Me). ^{13}C NMR (d^6 -Acetone, δ): 179.1 (CO), 155.1 (DMAP-C), 143.4, 143.1 (Pz3), 142.4 (Pz3), 141.8 (Pz5C), 137.6 (Pz5A), 137.2, 135.9, 135.3 (Pz5B), 133.2, 132.4, 127.6 (C8), 126.9 (5/6), 125.6 (C9), 124.9 (C5/6), 123.9 (C7), 123.3 (C10), 109.0, 108.2 (DMAP-B), 107.1 (Pz4), 106.6 (Pz4), 106.4 (Pz4), 70.3 (C4), 65.9 (C3), 51.4 (OMe), 47.9, 43.8 (C2), 39.3 (NMe), 30.6 (C1), 23.5 (Me), 23.1 (Me). HRMS: $\text{C}_{35}\text{H}_{40}\text{N}_9\text{O}_3\text{BMo}^+$ obsd (%), calcd (%), ppm: 737.2397 (26), 737.2416 (50), -2.6; 739.2413 (36), 739.2415 (48), -0.2; 740.2448 (55), 740.2413 (80), 4.8; 741.2416 (85), 741.2409 (88), 0.9; 742.2400 (71), 742.2421 (78), -2.8; 743.2437 (100), 743.2409 (100), 3.8; 744.2445 (21), 744.2435 (43), 1.3; 745.2442 (25), 745.2429 (40), 1.7.

Synthesis of $\text{TpMo}(\text{NO})(\text{DMAP})(3,4\text{-}\eta^2\text{-}(1,2\text{-dihydronaphthalen-2-yl)-dimethylmalonate})$ (32).

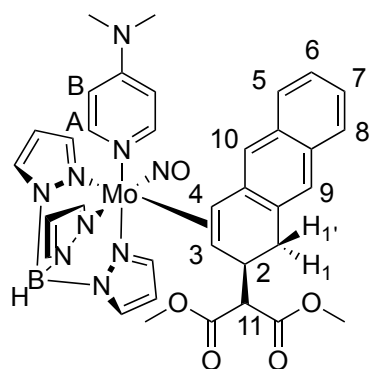


24 (500 mg, 0.849 mmol) and CH_3CN (10 mL) were added to a 4-dram vial and this orange mixture was cooled for 15 min at $-35\text{ }^\circ\text{C}$. A $-35\text{ }^\circ\text{C}$, 1M solution of HOTf in

CH₃CN (3.5 mL, 3.5 mmol) was added to the reaction mixture and the resulting red solution was left standing at -35 °C. After 15 min, LiDMM (700 mg, 5.07 mmol) was added to the reaction mixture and the resulting red solution was left standing at -35 °C. After 18 h, a -35 °C solution of triethylamine (1.0 mL, 7.17 mmol) was added to the reaction mixture and the resulting golden solution was warmed to RT. This solution was evaporated *in vacuo* to 4 mL and chromatographed through a 60 mL medium porosity fritted disc ³/₄ full with silica gel. The product was eluted with 1:1 Et₂O:benzene (75 mL) as a yellow band, collected as a yellow solution, and evaporated *in vacuo*. The resulting yellow oil was then dissolved in DCM (4 mL) and the product was precipitated in stirring hexanes (100 mL). The precipitate was collected on a 15 mL medium porosity fritted disc, washed with hexanes (3 x 50 mL), and desiccated for 15 min yielding the yellow solid **32** (497 mg, 82%). CV (DMAc) $E_{p,a} = +0.22$ V (NHE). IR: $\nu(\text{BH}) = 2484$ cm⁻¹, $\nu(\text{CO}) = 1751$ & 1732 cm⁻¹, $\nu(\text{NO}) = 1574$ cm⁻¹. ¹H NMR (d⁶-Acetone, δ): 7.95 (1H, d, Pz5C), 7.90 (1H, d, Pz5A), 7.88 (1H, d, Pz3A), 7.69 (1H, d, Pz3C), 7.80 (1H, d, Pz3/5B), 7.38 (2H, bs, DMAP-A), 6.99 (1H, d, Pz3/5B), 6.93 (1H, m, H5), 6.81 (2H, m, H6&7), 6.50 (2H, m, DMAP-B), 6.39 (1H, t, Pz4A), 6.38 (1H, t, Pz4C), 6.14 (1H, dd, $J = 6.4$ & 2.8 , H8), 6.09 (1H, t, Pz4B), 3.61 (3H, s, OMe), 3.53 (1H, dd, $J = 16.0$ & 5.9 , H1), 3.45 (1H, m, H2), 3.41 (1H, s, H9), 3.37 (3H, s, OMe), 3.23 (1H, d, $J = 9.6$, H4), 3.04 (6H, s, NMe), 2.51 (1H, d, $J = 16.0$, H1'), 2.16 (1H, dt, $J = 9.5$ & 2.2 , H3). ¹³C NMR (d⁶-Acetone, δ): 170.0 (CO), 169.9 (CO), 154.9 (DMAP-C), 143.5, 142.0, 141.2, 137.5, 136.9, 135.8, 135.6, 131.5, 128.4, 127.5, 127.3, 127.1, 125.2, 123.5, 108.1 (DMAP-B), 106.9 (Pz4), 106.7 (Pz4), 106.5 (Pz4), 106.3, 68.2 (C3), 67.7 (C4), 59.4 (C9), 52.2 (OMe), 52.1 (OMe), 39.1 (NMe), 38.3 (C2), 31.6 (C1). HRMS: C₃₁H₃₆N₉O₅BMo⁺ obsd

(%), calcd (%), ppm: 717.1995 (33), 717.2001 (51), -0.8; 719.1955 (19), 719.1999 (48), -6.1; 720.1998 (82), 720.1997 (80), 0.1; 721.1975 (100), 721.1993 (87), -2.5; 722.2000 (67), 722.2005 (77), -0.7; 723.1968 (83), 723.1993 (100), -3.4; 724.2019 (25), 724.2020 (41), -0.1; 725.2006 (22), 725.2013 (40), -0.9.

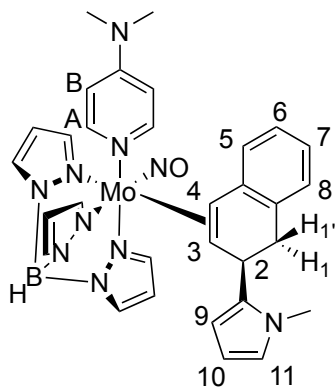
Synthesis of TpMo(NO)(DMAP)(3,4- η^2 -2-(1,2-dihydroanthracen-2-yl)-dimethylmalonate) (33).



25 (100 mg, 0.15 mmol) and CH₃CN (2 mL) were added to a 4-dram vial and the resulting red solution was cooled at -30 °C for 15 min. A -30 °C, 1M solution of HOTf in CH₃CN (0.7 mL, 0.7 mmol) was added to the reaction mixture giving a dark red solution that was left standing at -30 °C for 15 min. LiDMM (138 mg, 1.00 mmol) was added to this solution creating an orange solution that was left standing at -30 °C for 18 h. Triethylamine (0.2 mL, 1.43 mmol) was added to this solution and the reaction mixture was warmed to room temperature. The reaction mixture was extracted with DCM (6 mL) and NaHCO₃ (6 mL, sat. aq.) and the organic layer was dried over MgSO₄. The drying agent was removed on a 15 mL medium porosity fritted disc, washed with DCM (3 x 2 mL), and the filtrate was evaporated *in vacuo*. The oil formed was then dissolved in DCM (1 mL) and the product was precipitated in stirring pentane (25 mL), collected on a

15 mL fine porosity fritted disc, washed with pentane (3 x 10 mL), and desiccated for 15 min yielding the yellow solid **33** (47 mg, 41%). CV (DMAc) $E_{p,a} = +0.28$ V (NHE). IR: $\nu(\text{C-H sp}^2) = 2949 \text{ cm}^{-1}$, $\nu(\text{BH}) = 2485 \text{ cm}^{-1}$, $\nu(\text{CO}) = 1731, 1620 \text{ cm}^{-1}$, $\nu(\text{NO}) = 1567 \text{ cm}^{-1}$. ^1H NMR (d^6 -Acetone, δ): 7.99 (1H, d, Pz5A/C), 7.92 (1H, d, Pz3A), 7.90 (1H, d, Pz5A/C), 7.82 (1H, d, Pz3/5B), 7.77 (1H, d, Pz3C), 7.70 (1H, d, $J = 8.5$, H8), 7.46 (1H, s, H9), 7.34 (1H, d, $J = 6.7$, H5), 7.32 (2H, buried bs, DMAP-A), 7.28 (1H, t, $J = 6.6$, H6), 7.22 (1H, t, $J = 7.6$, H7), 7.04 (1H, d, Pz3/5B), 6.41 (4H, m, DMAP-B, Pz4A&C), 6.29 (1H, s, H10), 6.10 (1H, t, Pz4B), 3.76 (1H, dd, $J = 16.6$ & 5.9 , H1), 3.62 (3H, s, OMe), 3.52 (1H, m, H2), 3.44 (1H, d, $J = 10.3$, H11), 3.40 (3H, s, OMe), 3.35 (1H, d, $J = 9.10$, H4), 3.04 (6H, s, NMe), 2.76 (1H, d, $J = 16.6$, H1'), 2.32 (1H, dt, $J = 9.4$, H3). ^{13}C NMR (d^6 -Acetone, δ): 170.0 (CO), 155.0 (DMAP-C), 143.6 (Pz5), 142.5 (Pz3/5), 142.2, 141.4 (Pz3), 137.6 (Pz5), 136.9 (Pz3), 135.8 (Pz3/5), 133.3, 132.5, 132.2, 127.7 (C8), 127.4 (C9), 126.8 (C5), 125.2 (C6), 124.0 (C7), 123.9, 123.6 (H10), 108.1 (DMAP-B), 106.9 (Pz4), 106.7 (Pz4), 106.4 (Pz4), 68.5 (C4), 68.4 (C3), 66.1 (C11), 52.2 (OMe), 51.9 (OMe), 39.3 (NMe), 38.2 (C2), 32.9 (C1). HRMS: $\text{C}_{35}\text{H}_{38}\text{N}_9\text{O}_5\text{BMo}^+$ obsd (%), calcd (%), ppm: 767.2126 (20), 767.2158 (50), -4.1; 769.2081 (10), 769.2157 (48), -9.8; 770.2138 (62), 770.2155 (79), -2.2; 771.2141 (100), 771.2151 (88), -1.3; 772.2177 (72), 772.2163 (78), 1.9; 773.2154 (68), 773.2151 (100), 0.4; 774.2156 (42), 774.2177 (44), -2.7; 775.2039 (5), 775.2171 (40), -17.0.

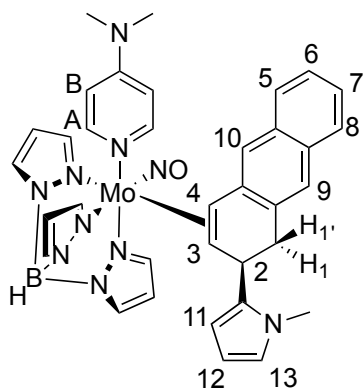
Synthesis of $\text{TpMo}(\text{NO})(\text{DMAP})(3,4\text{-}\eta^2\text{-(1,2-dihydronaphthalen-2-yl)-1-methyl-1H-pyrrole})$ (34**).**



24 (300 mg, 0.509 mmol) and $\text{CH}_3\text{CH}_2\text{CN}$ (5 mL) were added to a test tube charged with a stir pea and this orange mixture was cooled with stirring for 15 min at $-60\text{ }^\circ\text{C}$. A $-60\text{ }^\circ\text{C}$, 1M solution of HOTf in $\text{CH}_3\text{CH}_2\text{CN}$ (2.1 mL, 2.1 mmol) was added to the reaction mixture and the resulting red solution was left stirring for 15 min at $-60\text{ }^\circ\text{C}$. *N*-methylpyrrole (1.0 mL, 11.3 mmol) was added to the reaction mixture and the red solution formed was left stirring at $-60\text{ }^\circ\text{C}$ for 18 h. Next, triethylamine (0.6 mL, 2.1 mmol) was added to the reaction mixture giving a brown solution that was warmed to RT and evaporated *in vacuo*. The oil formed was dissolved in DCM (5 mL) and this solution was chromatographed through a 30 mL medium porosity fritted disc $\frac{3}{4}$ full with silica gel. The product was eluted as a yellow band with 1:1 Et_2O :benzene (100 mL), collected as a yellow solution, and evaporated *in vacuo* to an oil. This oil was dissolved in DCM (1 mL) and the product was precipitated in stirring pentane (50 mL). The precipitate was then collected on a 15 mL fine porosity fritted disc, washed with pentane (3 x 10 mL), and desiccated for 15 min yielding the yellow precipitate **34** (234 mg, 68%). CV (DMAc) $E_{\text{p,a}} = +0.18\text{ V}$ (NHE). IR: $\nu(\text{C-H sp}^2) = 2906\text{ cm}^{-1}$, $\nu(\text{BH}) = 2480\text{ cm}^{-1}$, $\nu(\text{NO}) = 1596\text{ cm}^{-1}$. $^1\text{H-NMR}$ (CDCl_3 , δ): 8.12 (1H, d, Pz3A), 7.99 (1H, d, Pz5C), 7.94 (1H, d, Pz5A), 7.77

(1H, d, Pz3C), 7.81 (1H, d, Pz5B), 7.47 (2H, bs, DMAP-A), 7.01 (1H, d, Pz3B), 6.94 (1H, buried d, H8), 6.77 (2H, m, H6 & H7), 6.51 (2H, m, DMAP-B), 6.40 (1H, t, Pz4A), 6.35 (1H, t, Pz4C), 6.31 (1H, dd, $J = 2.7$ & 1.9 , H11), 6.15 (1H, buried d, H5), 6.10 (1H, t, Pz4B), 5.67 (1H, ddd, $J = 3.4$, 1.9 , & 0.4 , H10), 5.64 (1H, dd, $J = 3.3$ & 2.7 , H9), 4.01 (1H, d, $J = 7.4$, H2), 3.75 (1H, dd, $J = 15.5$ & 6.9 , H1), 3.42 (3H, s, NMe), 3.28 (1H, d, $J = 9.3$, H4), 3.06 (6H, s, NMe), 2.76 (1H, d, $J = 15.5$, H1'), 2.42 (1H, dt, $J = 9.5$ & 2.1 , H3). ^{13}C NMR (CDCl_3 , δ): 153.6 (DMAP-C), 142.3 (Pz3), 142.2, 141.6 (Pz3), 141.4 (Pz5), 140.6 (Pz5), 135.9 (Pz5), 135.8, 134.5 (Pz3), 132.0, 128.4 (C8), 128.3, 126.7 (C5), 124.0, 122.9 (C6 & C7), 119.8 (C11), 107.2 (DMAP-B), 106.3 (Pz4A), 105.7 (Pz4C), 105.6 (Pz4B), 105.4 (C9), 105.1 (C10), 70.6, 66.9 (C4), 39.1 (DMAP-NMe), 33.5 (C2), 33.4 (NMe), 32.9. HRMS: $\text{C}_{31}\text{H}_{35}\text{N}_{10}\text{OBMo}+\text{Na}^+$ obsd (%), calcd (%), ppm: 689.2005 (57), 689.2054 (51), -7.1; 691.2039 (45), 691.2052 (48), -1.9; 692.2043 (87), 692.2051 (80), -1.1; 693.2016 (84), 693.2046 (87), - 4.4; 694.2072 (77), 694.2058 (77), 2.0; 695.2064 (100), 695.2046 (100), 2.6; 696.2089 (27), 696.2073 (41), 2.4; 697.2079 (26), 697.2066 (39), 1.9.

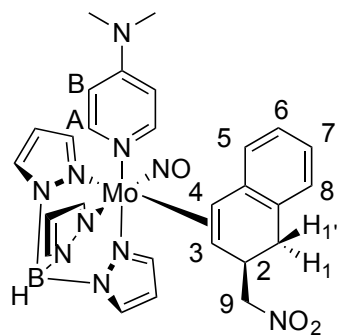
Synthesis of $\text{TpMo}(\text{NO})(\text{DMAP})(3,4\text{-}\eta^2\text{-2-(1,2-dihydroanthracen-2-yl)-1-methyl-1H-pyrrole})$ (35).



25 (300 mg, 0.468 mmol) and CH₃CN (6 mL) were added to a 4-dram vial and the resulting red solution was cooled for 15 min at -30 °C. A -30 °C, 1M solution of HOTf in CH₃CN (2.1 mL, 2.1 mmol) was added to the reaction mixture and the resulting dark red solution was left standing at -30 °C for 15 min. *N*-methylpyrrole (4.0 mL, 45.0 mmol) was added and the reaction mixture was left standing at -30 °C for 18 h. Triethylamine (0.6 mL, 4.30 mmol) was added to the reaction mixture and the resulting orange solution was warmed to RT then evaporated *in vacuo*. The oil formed was then dissolved in THF (1 mL) and the resulting solution was chromatographed through a 30 mL medium porosity fritted disc ³/₄ full with silica gel. The product was eluted as a yellow band with 1:1 Et₂O:benzene (50 mL), collected as a yellow solution, and evaporated *in vacuo* to an oil. This oil was dissolved in DCM (1 mL) and the product was precipitated in stirring pentane (50 mL). The precipitate was collected on a 15 mL fine porosity fritted disc, washed with pentane (3 x 10 mL), and dried for 15 min yielding the yellow precipitate **35** (171 mg, 51%). CV (DMAc) $E_{p,a} = +0.18$ V (NHE). IR: $\nu(\text{C-H } sp^2) = 2916 \text{ cm}^{-1}$, $\nu(\text{BH}) = 2480 \text{ cm}^{-1}$, $\nu(\text{NO}) = 1570 \text{ cm}^{-1}$. ¹H NMR (d⁶-Acetone, δ): 8.12 (1H, d, Pz3A), 7.97 (1H, d, Pz5C), 7.95 (1H, d, Pz5A), 7.83 (1H, d, Pz3C), 7.81 (1H, d, Pz5B), 7.66 (1H, d, $J = 7.4$, H8), 7.45 (2H, bs, DMAP-A), 7.44 (1H, s, H9), 7.30 (1H, d, $J = 8.1$, H5), 7.25 (1H, m, H6), 7.18 (1H, m, H7), 7.06 (1H, d, Pz3B), 6.44 (2H, bs, DMAP-B), 6.42 (1H, t, Pz4A), 6.38 (1H, t, Pz4C), 6.32 (1H, t, $J = 2.2$, H12), 6.31 (1H, s, H10), 6.11 (1H, t, Pz4B), 5.73 (1H, m, H11), 5.61 (1H, m, H13), 4.10 (1H, d, $J = 6.7$, H2), 3.92 (1H, dd, $J = 15.5$ & 6.9, H1), 3.46 (3H, s, NMe), 3.42 (1H, d, $J = 9.4$, H4), 3.06 (6H, s, NMe), 2.99 (1H, d, $J = 15.5$, H1'), 2.57 (1H, dt, $J = 9.7$ & 1.9, H3). ¹³C NMR (d⁶-Acetone, δ): 154.0 (DMAP-C), 143.4 (Pz3/5), 143.2 (Pz3/5), 142.2 (Pz3/5), 141.7 (Pz3/5), 141.6 (Pz3/5),

141.5 (Pz3/5), 137.3, 135.8, 134.1, 132.2, 129.7, 127.6, 126.8, 126.7, 126.6, 124.9, 123.7, 123.5, 120.6, 120.5 (C13), 108.1 (DMAP-B), 108.0 (C11), 106.9 (Pz4), 106.6 (Pz4), 106.6 (Pz4), 106.3 (C12), 68.1, 39.2 (NMe), 34.7, 33.5, 29.8. HRMS: $C_{35}H_{37}N_{10}OBMo^+$ obsd (%), calcd (%), ppm: 716.2271 (16), 716.2314 (50), -5.9; 718.2334 (23), 718.2312 (48), 3.1; 719.2303 (69), 719.2310 (80), -1.0; 720.2297 (100), 720.2307 (88), -1.3; 721.2331 (91), 721.2318 (78), 1.8; 722.2318 (95), 722.2306 (100), 1.6; 723.2349 (48), 723.2332 (43), 2.3; 724.2335 (27), 724.2326 (40), 1.2.

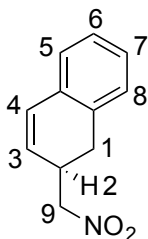
Synthesis of TpMo(NO)(DMAP)(3,4- η^2 -2-(1,2-dihydronaphthalen-2-yl)-nitromethane) (36).



CH_3CH_2CN (2 mL), MeOH (2 mL), LiOMe (30 mg, 0.79 mmol), and nitromethane (300 mg, 4.90 mmol) were added to a test tube charged with a stir pea and this solution was cooled at $-60\text{ }^{\circ}\text{C}$ for 15 min. **27** (250 mg, 0.338 mmol) was added and the resulting brown solution was left stirring at $-60\text{ }^{\circ}\text{C}$ overnight (~ 18 h). This solution was then warmed to RT, extracted with DCM (6 mL) and H_2O (10 mL), and the organic layer was dried over $MgSO_4$ for 15 min. The drying agent was filtered off on a 15 mL medium porosity fritted disc, washed with DCM (2 x 4 mL) and the yellow filtrate was evaporated *in vacuo* to an oil. The oil was dissolved in DCM (1 mL) and the product was precipitated in stirring

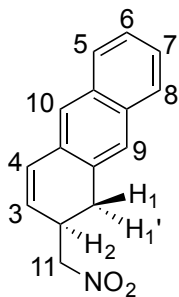
pentane (50 mL). The precipitate was collected on a 15 mL fine porosity fritted disc, washed with pentane (3 x 10 mL), and desiccated for 15 min yielding the yellow solid **36** (150 mg, 63%). CV (DMAc) $E_{p,a} = +0.25$ V (NHE). IR: $\nu(\text{BH}) = 2924 \text{ cm}^{-1}$, $\nu(\text{NO}) = 1574$ & 1543 cm^{-1} . ^1H NMR (d^6 -Acetone, δ): 7.98 (1H, d, Pz5C), 7.93 (1H, d, Pz5A), 7.89 (1H, d, Pz3A), 7.80 (1H, d, Pz5B), 7.73 (1H, d, Pz3C), 7.39 (2H, bs, DMAP-A), 7.01 (2H, m, H6 & H7), 7.00 (1H, d, Pz3B), 6.86 (1H, m, H8), 6.53 (2H, m, DMAP-B), 6.41 (1H, t, Pz4A), 6.39 (1H, t, Pz4C), 6.20 (1H, m, H5), 6.10 (1H, t, Pz4B), 4.40 (1H, dd, $J = 10.2$ & 6.6 , H9), 4.40 (1H, dd, $J = 10.7$ & 8.6 , H9), 3.56 (1H, dd, $J = 16.1$ & 5.9 , H1), 3.45 (1H, m, H2), 3.28 (1H, d, $J = 9.5$, H4), 3.06 (6H, s, NMe), 2.54 (1H, d, $J = 16.1$, H1'), 2.13 (1H, dt, $J = 9.5$ & 2.3 , H3). ^{13}C NMR (d^6 -Acetone, δ): 155.1 (DMAP-C), 150.9 (DMAP-A), 150.7 (Pz5C), 143.2 (Pz3A), 142.1 (Pz3B), 141.5 (Pz3C), 137.1 (Pz5A), 135.8 (Pz5B), 130.6 (C6/7), 129.6 (C6/7), 127.6 (C5), 126.7, 125.5 (C8), 123.7, 108.2 (DMAP-B), 107.0 (Pz4), 106.9 (Pz4), 106.4 (Pz4), 83.1 (C9), 67.0 (C4), 66.5 (C3), 39.1 (NMe), 37.6 (C2), 31.3 (C1). HRMS: $\text{C}_{27}\text{H}_{31}\text{N}_{10}\text{O}_3\text{BMo} + \text{Na}^+$ obsd (%), calcd (%), ppm: 669.1608 (44), 669.1639 (52), -4.6; 671.1629 (41), 671.1636 (49), -1.1; 672.1610 (74), 672.1635 (81), -3.7; 673.1638 (80), 673.1630 (87), 1.1; 674.1628 (79), 674.1643 (76), -2.2; 675.1616 (100), 675.1630 (100), -2.1; 676.1657 (30), 676.1657 (38), -0.1; 677.1651 (29), 677.1650 (39), 0.2.

Synthesis of 2-(nitromethyl)-1,2-dihydronaphthalene (**37**).

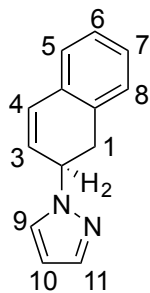


To a 50 mL filter flask charged with a stir pea were added **36** (100 mg, 0.123 mmol), DCM (5 mL), and a 0.06 M solution of I₂/Et₂O (1 mL, 0.06 mmol) resulting in a green solution. The solution was stirred at RT for 5 min and then evaporated *in vacuo* to an oil. The oil was dissolved in DCM (1 mL), giving a solution that was then added to stirring pentane (25 mL), creating a green precipitation. The precipitate was collected on a 15 mL fine porosity fritted disc, washed with pentane (3 x 10 mL), and desiccated to yield **23** (65 mg, 90%). The filtrate was removed from the glovebox and evaporated *in vacuo* to a brown oil. The oil was dissolved in DCM (3 x 0.3 mL) and the resulting solution was dropwise added onto a 250 μ m silica preparatory plate. The product was eluted with 10% EtOAc:hexanes (200 mL), scraped off as a band at R_f: 0.51-0.65 and this silica gel was sonicated in EtOAc (20 mL) for 15 min. The silica was filtered off on a 15 mL medium porosity fritted disc and washed with DCM (3 x 2 mL). The colorless filtrate was then evaporated *in vacuo* and desiccated to yield the colorless oil **37** (9 mg, 39% yield). IR: $\nu(\text{C-H sp}^2) = 3020, 2916, 2850 \text{ cm}^{-1}$, $\nu(\text{NO}) = 1550, 1377 \text{ cm}^{-1}$. ¹H NMR (CDCl₃, δ): 7.20 (2H, m, H6 & H7), 7.14 (1H, d, $J = 7.2$, H5), 7.08 (1H, d, $J = 6.3$, H8), 6.61 (1H, d, $J = 9.5$, H4), 5.88 (1H, dd, $J = 9.5$ & 5.0, H3), 4.35 (1H, dd, $J = 12.2$ & 6.6, H9), 4.31 (1H, dd, $J = 12.2$ & 8.8, H9), 3.29 (1H, m, H2), 3.04 (1H, dd, $J = 16.4$ & 6.6, H1), 2.74 (1H, dd, $J = 16.4$ & 6.9, H1). ¹³C NMR (CDCl₃, δ): 132.7, 132.4, 130.7 (C4), 128.5 (C5), 128.2 (C6/7), 127.4 (C6/7), 126.7 (C8), 125.8 (C3), 77.5 (C9), 32.9 (C2), 30.9 (C1). LRMS: C₁₁H₁₁NO₂, mass found: 189.1, mass required: 189.08.

Synthesis of 2-(nitromethyl)-1,2-dihydroanthracene (**38**).



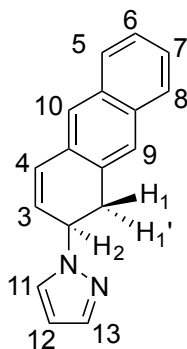
CH₃CN (2 mL), LiOMe (15 mg, 0.39 mmol), MeOH (0.5 mL), and nitromethane (120 mg, 1.97 mmol) were added to a 4-dram vial and this solution was cooled at -30 °C for 15 min. **28** (100 mg, 0.126 mmol) was added to this solution and left at -30 °C for 18 h. The reaction mixture was removed from the glovebox and left open to air overnight (~24 h) resulting in a brown film. The film was dissolved in DCM (3 x 0.3 mL) and the resulting solution was dropwise added onto a 250 µm silica preparatory plate. The product was eluted with 10% EtOAc:hexanes (200 mL), scraped off as a band at R_f: 0.12-0.43 and this silica gel was sonicated in EtOAc (20 mL) for 15 min. The silica was filtered off on a 15 mL fine porosity fritted disc and washed with DCM (3 x 2 mL). The filtrate was evaporated *in vacuo* and desiccated to yield the colorless oil **38** (10 mg, 33%). IR: $\nu(\text{C-H sp}^2) = 2916 \text{ cm}^{-1}$, $\nu(\text{NO}) = 1545 \text{ cm}^{-1}$. ¹H NMR (CDCl₃, δ): 7.78 (1H, m, H5), 7.75 (1H, m, H8), 7.57 (1H, s, H9), 7.53 (1H, s, H10), 7.43 (2H, m, H6 & H7), 6.79 (1H, d, $J = 9.9$, H4), 5.99 (1H, dd, $J = 9.9 \text{ \& } 4.7$, H3), 4.37 (1H, dd, $J = 13.0 \text{ \& } 6.3$, H11), 4.34 (1H, dd, $J = 13.0 \text{ \& } 8.6$, H11), 3.37 (1H, m, H2), 3.19 (1H, dd, $J = 15.5 \text{ \& } 6.1$, H1/H1'), 2.91 (1H, dd, $J = 15.5 \text{ \& } 6.1$, H1/H1'). ¹³C NMR (CDCl₃, δ): 133.4 (C10/9a), 133.1 (C10/9a), 131.0 (C5a/C8a), 130.9 (C4), 130.7 (C5a/C8a), 127.9 (C10), 127.4 (C9), 127.0 (C5), 126.9 (C6/7), 126.4 (C6/7), 126.0 (C3), 125.4 (C8), 77.7 (C11), 33.4 (C2), 31.5 (C1).

1-(1,2-dihydronaphthalen-2-yl)-1*H*-pyrazole (39).

DBU (0.1 mL, 0.068 mmol), CH₃CH₂CN (2 mL) and pyrazole (200 mg, 2.93 mmol) were added to a test tube and this solution was cooled at -60 °C for 15 min. **27** (200 mg, 0.271 mmol) was then added to this solution and left at -60 °C for 18 h. The reaction mixture was then warmed to RT, extracted with DCM (6 mL) and H₂O (10 mL), and the organic layer was dried over MgSO₄. The drying agent was filtered off on a 15 mL medium porosity fritted disc and washed with DCM (3 x 3 mL). The filtrate was evaporated *in vacuo* to an oil, which was then removed from the glovebox. The oil was dissolved in DCM (10 mL) and stirred open to air overnight (18 h) at RT. The brown film formed was dissolved in DCM (3 x 0.3 mL) and the resulting solution was dropwise added onto a 250 μm silica preparatory plate. The product was eluted with 10% EtOAc:hexanes (200 mL), scraped off as a band at R_f: 0.22-0.34 and this silica gel was sonicated in EtOAc (20 mL) for 15 min. The silica was filtered off on a 15 mL fine porosity fritted disc and washed with DCM (3 x 2 mL). The filtrate was evaporated *in vacuo* and desiccated to yield the oil **39** (10 mg, 19%). IR: ν(C-H sp²) = 3018, 2921, 2850 cm⁻¹. ¹H NMR (CDCl₃, δ): 7.52 (1H, d, *J* = 1.8, H11), 7.31 (1H, d, *J* = 2.4, H9), 7.22 (1H, t, *J* = 7.6, H7), 7.19 (1H, td, *J* = 7.6 & 1.5, H6), 7.16 (1H, d, *J* = 7.4, H5), 7.11 (1H, d, *J* = 7.4, H8), 6.76 (1H, dd, *J* = 9.6 & 1.7, H4), 6.17 (1H, t, *J* = 2.1, H10), 6.15 (1H, dd, *J* = 9.6 & 4.4, H3), 5.28 (1H, m, H2), 3.33 (1H, dd, *J* = 16.3 & 7.4, H1/H1'), 3.28 (1H, dd, *J* = 16.3 & 7.3, H1/H1'). ¹³C

NMR (CDCl₃, δ): 139.3 (C11), 132.6, 132.2, 131.1 (2C's) (C4), 128.3 (C8), 128.2 (C9), 127.5, 127.2, 126.8, 125.7, 125.6 (C3), 105.5 (C10), 56.0 (C2), 35.3 (C1).

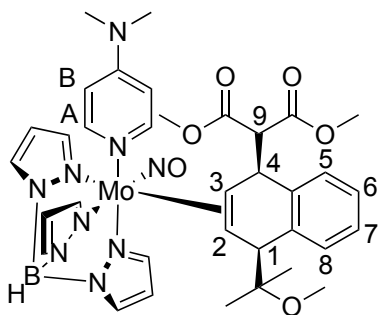
Synthesis of 1-(1,2-dihydroanthracen-2-yl)-1*H*-pyrazole (40).



DBU (0.1 mL, 0.068 mmol), CH₃CH₂CN (2 mL) and pyrazole (200 mg, 2.93 mmol) were added to a test tube and this solution was cooled at -60 °C for 15 min. **28** (100 mg, 0.127 mmol) was added to this solution and left at -60 °C for 18 h. The reaction mixture was warmed to RT, extracted with DCM (6 mL) and H₂O (10 mL), and the organic layer was dried over MgSO₄. The drying agent was filtered off on a 15 mL medium porosity fritted disc and washed with DCM (3 x 4 mL). The filtrate was evaporated *in vacuo* to an oil that was then removed from the glovebox, dissolved in DCM (10 mL) and the resulting brown solution was stirred open to air overnight (18 h). The brown oil formed was dissolved in DCM (3 x 0.3 mL) and the resulting solution was dropwise added onto a 250 μ m silica preparatory plate. The product was eluted with 10% EtOAc:hexanes (200 mL), scraped off as a band at R_f: 0.15-0.28 and this silica gel was sonicated in EtOAc (20 mL) for 15 min. The silica was filtered off on a 15 mL fine porosity fritted disc and washed with DCM (3 x 2 mL). The filtrate was evaporated *in vacuo* and desiccated to yield the oil **40** (6 mg, 20%). IR: $\nu(\text{C-H sp}^2) = 2947 \text{ cm}^{-1}$. ¹H NMR (CDCl₃, δ): 7.79 (1H, m, H5),

7.71 (1H, m, H8), 7.61 (1H, s, H10), 7.53 (1H, s, H9), 7.53 (1H, d, $J = 2.2$, H13), 7.44 (2H, m, H6 & H7), 7.31 (1H, d, $J = 2.2$, H11), 6.96 (1H, d, $J = 9.6$, H4), 6.29 (1H, dd, $J = 9.6$ & 4.4, H3), 6.19 (1H, t, $J = 2.2$, H12), 5.38 (1H, m, H2), 3.50 (1H, dd, $J = 15.9$ & 6.8, H1'), 3.47 (1H, dd, $J = 15.9$ & 6.6, H1). ^{13}C NMR (CDCl_3 , δ): 139.5 (C9), 133.5, 133.0, 131.5 (C4), 130.8, 130.8, 128.0 (C5), 127.6, 127.5 (C11), 127.0 (C8), 126.9 (C3), 126.5 (C9), 126.0 (C6 & C7), 125.8 (C10), 105.6 (C12), 56.4 (C2), 36.0 (C1). LRMS: $\text{C}_{17}\text{H}_{14}\text{N}_2$, mass found $[\text{M}+\text{Na}^+]$: 269, mass required: 246.12.

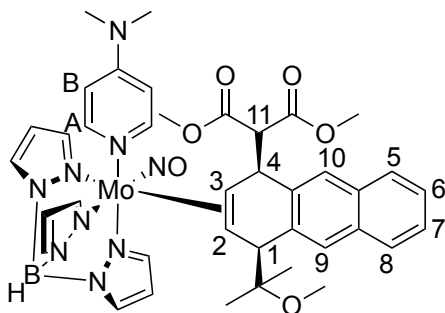
Synthesis of TpMo(NO)(DMAP)(2,3- η^2 -dimethyl 2-(4-(2-methoxypropan-2-yl)-1,4-dihydronaphthalen-1-yl)malonate) (41).



To a test tube charged with a stir pea were added **24** (200 mg, 0.340 mmol), $\text{CH}_3\text{CH}_2\text{CN}$ (6 mL), and dimethoxypropane (0.3 mL, 2.44 mmol). The resulting orange solution was stirred at RT until homogeneous and then cooled at $-60\text{ }^\circ\text{C}$ for 15 min. TMSOTf (0.1 mL, 0.54 mmol) was added to the reaction mixture and the resulting red solution was left stirring at $-60\text{ }^\circ\text{C}$ for 15 min. LiDMM (250 mg, 1.81 mmol) was added to the solution giving a yellow solution that was left stirring at $-60\text{ }^\circ\text{C}$. After 18 h, TEA (0.2 mL, 1.41 mmol) was added and the reaction mixture was warmed to RT, extracted with DCM (6 mL) and H_2O (10 mL), and the organic layer was dried over MgSO_4 . The drying agent was filtered off on a 15 mL medium porosity fritted disc, and washed with DCM (3 x 2

mL), and the filtrate was evaporated *in vacuo*. The resultant oil was dissolved in DCM (1 mL) and the product was precipitated in stirring pentane (50 mL). The beige precipitate was isolated on a 15 mL fine porosity fritted disc, washed with pentane (3 x 10 mL), and desiccated to yield **41** (170 mg, 63% yield). CV (DMAc) $E_{p,a} = +0.17$ V (NHE). IR: $\nu(\text{C-H sp}^2) = 2942 \text{ cm}^{-1}$, $\nu(\text{BH}) = 2477 \text{ cm}^{-1}$, $\nu(\text{CO}) = 1730 \text{ cm}^{-1}$, $\nu(\text{NO}) = 1567 \text{ cm}^{-1}$. ^1H NMR (d^6 -Acetone, δ): 7.94 (1H, d, Pz3A), 7.92 (1H, d, Pz5C), 7.87 (1H, d, Pz5A), 7.80 (2H, bs, DMAP-A), 7.68 (1H, d, Pz5B), 7.58 (1H, d, Pz3C), 7.34 (3H, m, H6, H7, and H8), 7.04 (2H, m, H6 & H7), 7.02 (1H, d, $J = 7.2$, H5), 6.88 (1H, d, Pz3B), 6.66 (2H, m, DMAP-B), 6.35 (1H, t, Pz4C), 6.30 (1H, t, Pz4A), 6.00 (1H, t, Pz4B), 4.49 (1H, d, $J = 10.7$, H9), 4.00 (1H, d, $J = 10.7$, H4), 3.91 (1H, s, H1), 3.57 (3H, s, OMe), 3.43 (3H, s, OMe), 3.89 (6H, s, NMe), 3.03 (3H, s, OMe), 2.52 (1H, d, $J = 10.5$, H3), 2.45 (1H, d, $J = 10.5$, H2), 1.22 (3H, s, Me), 1.21 (3H, s, Me). ^{13}C NMR (d^6 -Acetone, δ): 170.3 (CO), 170.1 (CO), 154.9 (DMAP-C), 151.2 (DMAP-A), 142.9 (Pz3A), 141.6 (Pz3B), 141.6 (Pz3C), 139.1, 138.5, 137.3 (Pz5A), 137.1 (Pz5C), 135.4 (Pz5B), 133.6 (C5), 129.8, 126.1 (C8), 125.9, 108.4 (DMAP-B), 106.7 (Pz4C), 106.2 (Pz4A), 105.9 (Pz4B), 79.6, 69.4 (C3), 63.6 (C9), 61.7 (C2), 53.9 (C1), 52.2 (OMe), 51.7 (OMe), 48.9 (OMe), 44.7 (C4), 39.1 (NMe), 32.3, 25.4 (Me), 24.6 (Me).

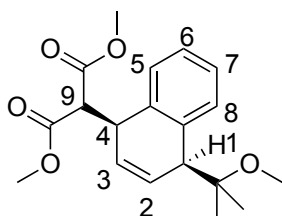
Synthesis of TpMo(NO)(DMAP)(2,3- η^2 -dimethyl 2-(4-(2-methoxypropan-2-yl)-1,4-dihydroanthracen-1-yl)malonate) (42**).**



25 (200 mg, 0.313 mmol), $\text{CH}_3\text{CH}_2\text{CN}$ (6 mL), and dimethoxypropane (0.3 mL, 2.44 mmol) were added to a test tube charged with a stir pea. The reaction mixture was stirred at RT until homogeneous and then cooled at $-60\text{ }^\circ\text{C}$ for 15 min. TMSOTf (0.1 mL, 0.54 mmol) was added to the reaction mixture and the resulting red solution was left stirring at $-60\text{ }^\circ\text{C}$ for 15 min. LiDMM (150 mg, 1.09 mmol) was added to the red solution, giving a brown solution that was left stirring at $-60\text{ }^\circ\text{C}$ for 18 h. TEA (0.2 mL, 1.43 mmol) was added to the brown solution, which was then warmed to RT, extracted with DCM (6 mL) and H_2O (10 mL), and the organic layer was dried over MgSO_4 . The drying agent was filtered off on a 15 mL medium porosity fritted disc, washed with DCM (3 x 2 mL), and the filtrate was evaporated *in vacuo*. The resulting oil was then dissolved in DCM (1 mL) and the product was precipitated in stirring pentane (50 mL). The beige precipitate was isolated on a 15 mL fine porosity fritted disc, washed with pentane (3 x 10 mL), and desiccated to yield **42** (152 mg, 58% yield). CV (DMAc) $E_{\text{p,a}} = +0.07\text{ V}$ (NHE). IR: $\nu(\text{C-H sp}^2) = 2945\text{ cm}^{-1}$, $\nu(\text{BH}) = 2475\text{ cm}^{-1}$, $\nu(\text{CO}) = 1729\text{ cm}^{-1}$, $\nu(\text{NO}) = 1569\text{ cm}^{-1}$. ^1H NMR (d^6 -Acetone, δ): 7.96 (1H, d, Pz3A), 7.93 (1H, d, Pz5C), 7.89 (1H, s, H9), 7.88 (1H, d, Pz5A), 7.84 (2H, bs, DMAP-A), 7.77 (1H, m, H5/H8), 7.73 (1H, m, H5/H8), 7.68 (1H, d, Pz5B), 7.61 (1H, d, Pz3C), 7.59 (1H, s, H10), 7.31 (2H, m, H6 & H7), 6.85 (1H,

d, Pz3B), 6.68 (2H, m, DMAP-B), 6.38 (1H, t, Pz4C), 6.32 (1H, t, Pz4A), 5.97 (1H, t, Pz4B), 4.70 (1H, d, $J = 10.8$, H11), 4.26 (1H, d, $J = 10.9$, H4), 4.10 (1H, s, H1), 3.60 (3H, s, OMe), 3.39 (3H, s, OMe), 3.09 (6H, s, NMe), 3.07 (3H, s, OMe), 2.60 (1H, d, $J = 10.3$, H3), 2.51 (1H, d, $J = 10.3$, H2), 1.30 (3H, s, Me), 1.25 (3H, s, Me). ^{13}C NMR (d^6 -Acetone, δ): 170.4 (CO), 170.1 (CO), 154.9 (DMAP-C), 151.2 (DMAP-A), 142.9, 141.6 (C5/8), 141.5 (Pz3B), 138.1, 137.9, 137.3 (Pz5C), 137.1 (Pz5A), 135.5 (Pz5B), 133.5, 133.4, 131.7 (C9), 128.1, 127.9 (C5/8), 127.7 (C10), 125.1, 125.0, 108.5 (DMAP-B), 106.7 (Pz4C), 106.3 (Pz4A), 105.9 (Pz4B), 79.9, 68.8 (C3), 63.6 (C11), 61.5 (C7), 54.3 (C1), 52.3 (OMe), 51.8 (OMe), 48.9 (OMe), 44.9 (C4), 39.1 (NMe), 29.8, 25.6 (Me), 24.6 (Me).

Synthesis of dimethyl 2-(-4-(2-methoxypropan-2-yl)-1,4-dihydronaphthalen-1-yl)malonate (43).



Via Iodine Oxidation

To a 50 mL filter flask charged with a stir pea were added **41** (100 mg, 0.126 mmol), DCM (5 mL), and a 0.06 M solution of $\text{I}_2/\text{Et}_2\text{O}$ (1 mL, 0.06 mmol), resulting in a green solution. This solution was stirred at RT for 5 min and evaporated *in vacuo*. The resulting green oil was dissolved in DCM (1 mL) forming a green solution. This solution was added to stirring hexanes (50 mL) giving a green precipitation. Collected the green precipitate on a 15 mL fine porosity fritted disc, washed with hexanes (3 x 10 mL), and

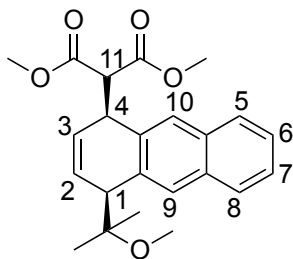
desiccated to yield **23** (69 mg, 93%). The filtrate was removed from the glovebox and evaporated *in vacuo* to an oil. The oil was dissolved in DCM (3 x 0.3 mL) and the resulting solution was dropwise added onto a 250 μ m silica preparatory plate. The product was eluted with 10% EtOAc:hexanes (200 mL), scraped off as a band at R_f : 0.42-0.54 and this silica gel was sonicated in EtOAc (20 mL) for 15 min. The silica was filtered off on a 15 mL medium porosity fritted disc and washed with DCM (3 x 2 mL). The filtrate was evaporated *in vacuo* and desiccated to yield the colorless oil **43** (36 mg, 85% yield).

Via Air Oxidation

24 (200 mg, 0.339 mmol), $\text{CH}_3\text{CH}_2\text{CN}$ (6 mL), and dimethoxypropane (0.3 mL, 2.44 mmol) were added to a test tube charged with a stir pea and the orange solution was stirred at RT for 1 min, then at $-60\text{ }^\circ\text{C}$ for 15 min. TMSOTf (0.1 mL, 0.54 mmol) was added to the reaction mixture and the resulting red solution was stirred at $-60\text{ }^\circ\text{C}$ for 15 min. LiDMM (250 mg, 1.81 mmol) was added to the reaction mixture and the resulting brown solution was left at $-60\text{ }^\circ\text{C}$ for 2 h. The reaction mixture was warmed to RT, extracted with DCM (8 mL) and H_2O (8 mL), and the organic layer was dried over MgSO_4 . The drying agent was filtered off on a 15 mL medium porosity fritted disc, washed with DCM (3 x 5 mL) and the filtrate was evaporated *in vacuo*. The resulting brown oil was dissolved in DCM (1 mL) forming a brown solution. This solution was added to stirring pentane (50 mL) giving a tan precipitation. The tan precipitate was collected on a 15 mL fine porosity fritted disc and washed with pentane (3 x 5 mL). The precipitate was removed from the glovebox, dissolved in DCM (5 mL), and the resulting

solution was left stirring open to air overnight (~18 h). The brown oil formed was dissolved in DCM (3 x 0.3 mL) and the resulting solution was dropwise added onto a 250 μ m silica preparatory plate. The product was eluted with 10% EtOAc:hexanes (200 mL), scraped off as a band at R_f : 0.15-0.48 and this silica gel was sonicated in EtOAc (20 mL) for 15 min. The silica was filtered off on a 15 mL fine porosity fritted disc and washed with DCM (3 x 5 mL). The filtrate was evaporated *in vacuo* and desiccated for 15 min to yield the colorless oil **43** (49 mg, 43% yield). IR: $\nu(\text{C-H } sp^2) = 2974 \text{ \& } 2951 \text{ cm}^{-1}$, $\nu(\text{CO}) = 1791, 1750, \text{ \& } 1734 \text{ cm}^{-1}$. ^1H NMR (CDCl_3 , δ): 7.29 (1H, d, $J = 7.9$, H7), 7.18 (1H, td, $J = 7.3 \text{ \& } 1.8$, H5/H6), 7.14 (1H, td, $J = 7.8 \text{ \& } 1.5$, H5/H6), 7.12 (1H, dd, $J = 7.5 \text{ \& } 1.8$, H9), 6.09 (2H, m, H2 & H3), 4.21 (1H, m, H4), 3.77 (1H, d, $J = 10.0$, H8), 3.76 (3H, s, OMe), 3.64 (3H, s, OMe), 3.55 (1H, m, H1), 3.24 (3H, s, OMe), 1.27 (3H, s, Me), 1.20 (3H, s, Me). ^{13}C NMR (CDCl_3 , δ): 169.4 (CO), 168.6 (CO), 136.5, 131.1 (C7), 136.5, 130.4 (C2 & C3), 128.4, 128.2, 126.2, 126.1, 77.9, 59.7 (C8), 53.1 (OMe), 52.6 (OMe), 49.4 (OMe), 49.3 (C1), 40.2 (C4), 24.2 (Me), 23.6 (Me). EA: Calculated for $\text{C}_{19}\text{H}_{24}\text{O}_5 \cdot 0.08 \text{ CH}_2\text{Cl}_2$: C, 67.52; H, 7.18. Found: C, 67.98; H, 7.18.

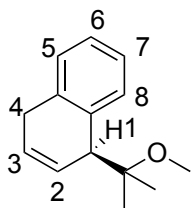
Synthesis of dimethyl 2-(4-(2-methoxypropan-2-yl)-1,4-dihydroanthracen-1-yl)malonate (44).



To a 50 mL filter flask charged with a stir pea were added **42** (100 mg, 0.118 mmol),

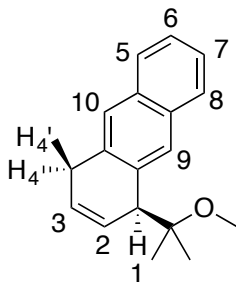
DCM (5 mL), and a 0.06 M solution of I₂/Et₂O (1 mL, 0.06 mmol). The resulting green solution was stirred at RT for 5 min and then evaporated *in vacuo*. The resulting green oil was dissolved in DCM (1 mL) forming a green solution. This solution was added to stirring hexanes (50 mL) creating a green precipitation. The precipitate was collected on a 15 mL fine porosity fritted disc, washed with hexanes (3 x 10 mL), and desiccated to yield **3** (64 mg, 93%). The filtrate was removed from the glovebox and evaporated *in vacuo* to an oil. The oil was dissolved in DCM (3 x 0.3 mL) and the resulting solution was dropwise added onto a 250 μ m silica preparatory plate. The product was eluted with 10% EtOAc:hexanes (200 mL), scraped off as a band at R_f: 0.18-0.42 and this silica gel was sonicated in EtOAc (20 mL) for 15 min. The silica was filtered off on a 15 mL medium porosity fritted disc and washed with DCM (3 x 2 mL). The filtrate was evaporated *in vacuo* and desiccated to yield the colorless oil **44** (22 mg, 49% yield). IR: $\nu(\text{C-H sp}^2) = 3039 \text{ \& } 2947 \text{ cm}^{-1}$, $\nu(\text{CO}) = 1730 \text{ cm}^{-1}$. ¹H NMR (CDCl₃, δ): 7.77 (1H, d, $J = 7.2$, H5/8), 7.75 (1H, s, H9), 7.73 (1H, d, $J = 7.2$, H8), 7.65 (1H, s, H10), 7.41 (2H, m, H6 & H7), 6.19 (2H, m, H2 & H3), 4.41 (1H, m, H4), 3.99 (1H, d, $J = 10.8$, H7), 3.80 (3H, s, OMe), 3.70 (1H, m, H1), 3.61 (3H, s, OMe), 3.24 (3H, s, OMe), 1.35 (3H, s, Me), 1.29 (3H, s, Me). ¹³C NMR (CDCl₃, δ): 169.5 (CO), 168.7 (CO), 135.1, 134.6, 132.0, 131.8, 130.5 (C2/3), 129.5 (C9), 128.4 (C2/3), 127.6 (C5/8), 127.4 (C5/8), 127.1 (C10), 125.6 (C6 & 7), 78.1, 59.8 (C7), 52.7 (OMe), 52.5 (OMe), 49.9 (C1), 49.3 (OMe), 40.2 (C4), 24.2 (Me), 23.6 (Me). EA: Calculated for C₂₃H₂₆O₅: C, 72.23; H, 6.85. Found: C, 72.02; H, 6.87.

Synthesis of 1-(2-methoxypropan-2-yl)-1,4-dihydronaphthalene (45).



24 (200 mg, 0.339 mmol), $\text{CH}_3\text{CH}_2\text{CN}$ (6 mL), and dimethoxypropane (0.3 mL, 2.44 mmol) were added to a test tube charged with a stir pea and this orange solution was stirred at RT for 1 min, then at $-60\text{ }^\circ\text{C}$ for 15 min. TMSOTf (0.1 mL, 0.54 mmol) was added to the reaction mixture yielding a red solution that was stirred at $-60\text{ }^\circ\text{C}$ for 15 min. NaCNBH_3 (226 mg, 3.60 mmol) was added to the red solution and the reaction mixture was left at $-60\text{ }^\circ\text{C}$ for 2 h. The yellow solution formed was removed from the glovebox and stirred open to air overnight ($\sim 18\text{ h}$). Evaporated the resulting brown solution *in vacuo* to an oil. The oil was dissolved in DCM (3 x 0.3 mL) and the resulting solution was dropwise added onto a 250 μm silica preparatory plate. The product was eluted with 10% EtOAc:hexanes (200 mL), scraped off as a band at R_f : 0.53-0.75 and this silica gel was sonicated in EtOAc (20 mL) for 15 min. The silica was filtered off on a 15 mL fine porosity fritted disc and washed with DCM (3 x 5 mL). The filtrate was evaporated *in vacuo* and desiccated for 15 min to yield the colorless oil **45** (35 mg, 51% yield). IR: $\nu(\text{C-H sp}^2) = 2978, 2827\text{ cm}^{-1}$, $\nu(\text{OMe}) = 1362\text{ cm}^{-1}$. $^1\text{H NMR}$ (CDCl_3 , δ): 7.23 (1H, d, $J = 7.5$, H8), 7.17 (2H, m, H6 & H7), 7.13 (1H, d, $J = 7.7$, H5), 6.13 (1H, m, H3), 6.00 (1H, m, H2), 3.64 (1H, m, H1), 3.38 (1H, m, H4), 3.31 (3H, s, OMe), 3.30 (1H, m, H4), 1.12 (3H, s, Me), 1.03 (3H, s, Me). $^{13}\text{C NMR}$ (CDCl_3 , δ): 136.4, 136.1, 130.4, 128.3, 128.0, 127.1 (C2), 126.0 (C3), 125.3, 49.5 (OMe), 47.8 (C1), 31.2 (C4), 22.5 (Me), 22.3 (Me).

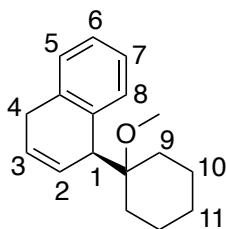
Synthesis of 1-(2-methoxypropan-2-yl)-1,4-dihydroanthracene (46).



25 (200 mg, 0.312 mmol), $\text{CH}_3\text{CH}_2\text{CN}$ (6 mL), and dimethoxypropane (0.3 mL, 2.44 mmol) were added to a test tube charged with a stir pea and this red solution was stirred at RT for 1 min, then at $-60\text{ }^\circ\text{C}$ for 15 min. TMSOTf (0.1 mL, 0.54 mmol) was added to the reaction mixture and the resulting red solution was left at $-60\text{ }^\circ\text{C}$ for 15 min. NaCNBH_3 (226 mg, 3.60 mmol) was added to this solution and the reaction mixture was left at $-60\text{ }^\circ\text{C}$ for 2 h. The reaction mixture was warmed to RT, extracted with DCM (8 mL) and H_2O (8 mL), and the organic layer was dried over MgSO_4 . The drying agent was filtered off on a 15 mL medium porosity fritted disc, washed with DCM (3 x 5 mL), and the filtrate was evaporated *in vacuo*. The brown oil formed was dissolved in DCM (1 mL) creating a brown solution. This solution was added to stirring pentane (50 mL) forming a tan precipitation. The tan precipitate was collected on a 15 mL fine porosity fritted disc and washed with pentane (3 x 5 mL). The precipitate was removed from the glovebox, dissolved in DCM (5 mL), and stirred open to air overnight (~18 h). The resulting brown solution was evaporated *in vacuo* to an oil. The oil was dissolved in DCM (3 x 0.3 mL) and the resulting solution was dropwise added onto a 250 μm silica preparatory plate. The product was eluted with 10% EtOAc:hexanes (200 mL), scraped off as a band at R_f : 0.57-0.72 and this silica gel was sonicated in EtOAc (20 mL) for 15 min. The silica was filtered off on a 15 mL fine porosity fritted disc, washed with DCM (3 x 5 mL). The

filtrate was evaporated *in vacuo* and desiccated for 15 min to yield the colorless oil **46** (20 mg, 25% yield). IR: $\nu(\text{C-H sp}^2) = 2971 \text{ \& 2934 cm}^{-1}$, $\nu(\text{OMe}) = 1074 \text{ cm}^{-1}$. $^1\text{H NMR}$ (CDCl_3 , δ): 7.80 (1H, m, H5), 7.75 (1H, m, H8), 7.71 (1H, s, H9), 7.62 (1H, s, H8), 7.40 (2H, m, H6 & H7), 6.2 (1H, ddd, $J = 9.9, 5.5, \text{ \& } 2.1$, H3), 6.1 (1H, ddd, $J = 9.9, 5.5, \text{ \& } 3.2$, H2), 3.82 (1H, m, H1), 3.58 (1H, dd, $J = 20.6 \text{ \& } 5.4$, H4), 3.50 (1H, d, $J = 20.6$, H4'), 3.34 (3H, s, OMe), 1.14 (3H, s, Me), 1.09 (3H, s, Me). $^{13}\text{C NMR}$ (CDCl_3 , δ): 153.2, 134.8, 132.2, 131.9, 128.8 (C9), 128.4 (C2), 127.8 (C5), 127.3 (C3), 127.0 (C8), 125.9, 125.5 (C6/7), 125.0 (C6/7), 81.0, 49.6 (OMe), 48.5 (C1), 31.3 (C4), 22.6 (Me), 22.3 (Me). EA: Calculated for $\text{C}_{18}\text{H}_{20}\text{O} \cdot 0.5 \text{ CH}_2\text{Cl}_2$: C, 75.37; H, 7.18. Found: C, 75.12; H, 6.78.

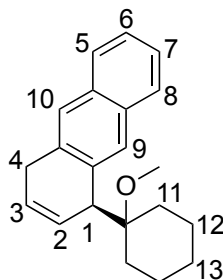
Synthesis of 1-(1-methoxycyclohexyl)-1,4-dihydronaphthalene (47).



24 (200 mg, 0.339 mmol), $\text{CH}_3\text{CH}_2\text{CN}$ (6 mL), and 1,1-dimethoxycyclohexane (0.3 mL, 1.97 mmol) were added to a test tube charged with a stir pea and the orange solution was stirred at RT for 1 min, then at $-60\text{ }^\circ\text{C}$ for 15 min. TMSOTf (0.1 mL, 0.54 mmol) was added to the reaction mixture and the resulting red solution was stirred at $-60\text{ }^\circ\text{C}$ for 15 min. NaCNBH_3 (226 mg, 3.60 mmol) was added to the solution and the reaction mixture was left at $-60\text{ }^\circ\text{C}$ for 5 h. The reaction mixture was removed from the glovebox and stirred open to air overnight (~ 18 h). The resulting brown solution was evaporated *in vacuo*. The oil formed was then dissolved in DCM (1 mL) forming a brown solution.

This solution was added to stirring Et₂O (50 mL) forming a brown precipitation. The precipitate was filtered off on a 15 mL medium porosity fritted disc, washed with Et₂O (3 x 5 mL), and the filtrate was evaporated *in vacuo*. The brown oil formed was dissolved in DCM (3 x 0.3 mL) and the resulting solution was dropwise added onto a 250 μ m silica preparatory plate. The product was eluted with 10% EtOAc:hexanes (200 mL), scraped off as a band at R_f: 0.72-0.93 and this silica gel was sonicated in EtOAc (20 mL) for 15 min. The silica was filtered off on a 15 mL fine porosity fritted disc and washed with DCM (3 x 5 mL). The filtrate was evaporated *in vacuo* and desiccated for 15 min to yield the colorless oil **47** (22 mg, 27% yield). IR: $\nu(\text{C-H sp}^2) = 2925 \text{ \& 2853 cm}^{-1}$, $\nu(\text{OMe}) = 1065 \text{ cm}^{-1}$. ¹H NMR (CDCl₃, δ): 7.17 (2H, m, H6 & H7), 7.13 (2H, m, H5 & H8) 6.15 (1H, ddd, $J = 9.9, 5.4, \text{ \& } 2.1$, H3), 5.95 (1H, ddd, $J = 9.9, 5.7, \text{ \& } 3.3$, H2), 3.71 (1H, m, H1), 3.39 (3H, s, OMe), 3.38 (1H, d, $J = 18.9$, H4), 3.30 (1H, dd, $J = 18.9 \text{ \& } 5.6$, H4), 1.8-0.9 (10H, H9, H10, & H11). ¹³C NMR (CDCl₃, δ): 136.8, 135.9, 129.8 (C5/8), 128.1 (C5/8), 127.8 (C2), 127.3 (C3), 125.9 (C6/7), 125.4 (C6/7), 81.6, 48.5 (OMe), 45.2 (C1), 31.4 (C4), 30.4 (C9), 30.2 (C10), 25.7 (C11), 21.5. EA: Calculated for C₁₇H₂₂O • 0.5 CH₂Cl₂: C, 73.80; H, 8.14. Found: C, 73.95; H, 8.13.

Synthesis of 1-(1-methoxycyclohexyl)-1,4-dihydroanthracene (**48**).



Via Air Oxidation

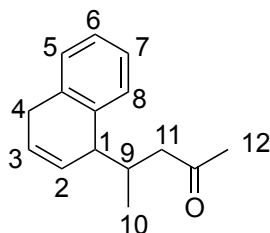
25 (200 mg, 0.312 mmol), CH₃CH₂CN (6 mL), and 1,1-dimethoxycyclohexenone (0.3 mL, 1.97 mmol) were added to a test tube charged with a stir pea and this red solution was stirred at RT for 1 min, then at -60 °C for 15 min. TMSOTf (0.1 mL, 0.54 mmol) was added to the reaction mixture and the resulting red solution was stirred at -60 °C for 15 min. NaCNBH₃ (226 mg, 3.60 mmol) was added to the solution and the reaction mixture was left at -60 °C for 1 h. The reaction mixture was warmed to RT, extracted with DCM (8 mL) and H₂O (8 mL), and the organic layer was dried over MgSO₄. The drying agent was filtered off on a 15 mL medium porosity fritted disc, washed with DCM (3 x 5 mL), and the filtrate was evaporated *in vacuo*. The oil formed was then dissolved in DCM (1 mL) creating a brown solution. This solution was then added to stirring pentane (50 mL) forming a tan precipitation. The tan precipitate was collected on a 15 mL fine porosity fritted disc, washed with pentane (3 x 5 mL), and removed from the glovebox. The precipitate was dissolved in DCM (5 mL), and the resulting solution was stirred open to air overnight (~18 h). The reaction mixture was evaporated *in vacuo* to an oil. This oil was dissolved in DCM (3 x 0.3 mL) and the resulting solution was dropwise added onto a 250 µm silica preparatory plate. The product was eluted with 2.5% EtOAc:hexanes (200 mL), scraped off as a band at R_f: 0.33-0.60 and this silica gel was sonicated in EtOAc (20 mL) for 15 min. The silica was filtered off on a 15 mL fine porosity fritted disc and washed with DCM (3 x 5 mL). The filtrate was evaporated *in vacuo* and desiccated for 15 min to yield the colorless oil **48** (25 mg, 28% yield).

Via Iodine Oxidation

To a 50 mL filter flask charged with a stir pea were added **53** (100 mg, 0.133 mmol), DCM (5 mL), and a 0.06 M solution of I₂/Et₂O (1.1 mL, 0.068 mmol). The resulting green solution was stirred at RT for 5 min and then evaporated *in vacuo*. The resulting green oil was dissolved in DCM (1 mL) forming a green solution. This solution was added to stirring hexanes (50 mL) creating a green precipitation. The precipitate was collected on a 15 mL fine porosity fritted disc, washed with hexanes (3 x 10 mL), and desiccated to yield **23** (77 mg, 98%). The filtrate was removed from the glovebox and evaporated *in vacuo* to an oil. The oil was dissolved in DCM (3 x 0.3 mL) and the resulting solution was dropwise added onto a 250 µm silica preparatory plate. The product was eluted with 10% EtOAc:hexanes (200 mL), scraped off as a band at R_f: 0.22-0.38 and this silica gel was sonicated in EtOAc (20 mL) for 15 min. The silica was filtered off on a 15 mL medium porosity fritted disc and washed with DCM (3 x 2 mL). The filtrate was evaporated *in vacuo* and desiccated to yield the colorless oil **48** (16.5 mg, 42% yield). IR: $\nu(\text{C-H sp}^2) = 2925 \text{ \& } 2853 \text{ cm}^{-1}$, $\nu(\text{OMe}) = 1060 \text{ cm}^{-1}$. ¹H NMR (CDCl₃, δ): 7.79 (1H, m, H5/H8), 7.76 (1H, m, H5/H8), 7.62 (1H, s, H10), 7.60 (1H, s, H9), 7.41 (2H, m, H6 & H7), 6.23 (1H, ddd, $J = 9.9, 5.6, \text{ \& } 1.9$, H3), 6.04 (1H, ddd, $J = 9.9, 5.6, 3.3$, H2), 3.89 (1H, bs, H1), 3.59 (1H, d, $J = 20.4$, H4), 3.48 (1H, dd, $J = 20.4 \text{ \& } 5.6$, H4), 3.44 (3H, s, OMe), 1.85 (1H, d, $J = 14.2$, H11), 1.67 (1H, d, $J = 14.2$, H11), 1.49 (6H, m, H11 & H12), 1.12 (1H, m, H13), 0.92 (1H, m, H13). ¹³C NMR (CDCl₃, δ): 135.5, 134.8, 132.2, 131.8, 128.2 (C10), 127.9 (C2), 127.7 (C5/8), 127.5 (C3), 127.0 (C5/8), 126.0 (C9), 125.5 (C6/7), 125.1 (C6/7), 81.8, 48.6 (OMe), 45.8 (C1), 31.5 (C4), 30.4 (C11), 30.3 (C12), 25.7 (C13), 21.5. EA: Calculated for C₂₁H₂₄O • 0.5 CH₂Cl₂: C, 77.11; H,

7.52. Found: C, 77.27; H, 7.29.

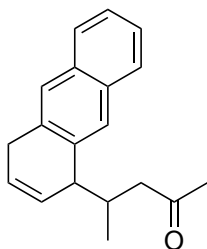
Synthesis of 4-(1,4-dihydronaphthalen-1-yl)pentan-2-one (49).



24 (200 mg, 0.339 mmol), $\text{CH}_3\text{CH}_2\text{CN}$ (6 mL), and 3-penten-2-one (0.2 mL, 2.05 mmol) were added to a test tube charged with a stir pea and this orange solution was stirred at RT for 1 min, then at $-60\text{ }^\circ\text{C}$ for 15 min. TMSOTf (0.1 mL, 0.54 mmol) was added to the reaction mixture and the resulting red solution was stirred at $-60\text{ }^\circ\text{C}$ for 15 min. NaCNBH_3 (226 mg, 3.60 mmol) was added to the solution and the reaction mixture was left at $-60\text{ }^\circ\text{C}$ for 5 h. The reaction mixture was removed from the glovebox and stirred open to air overnight (~ 18 h). The brown solution formed was then evaporated *in vacuo* to an oil. This oil was dissolved in DCM (1 mL) giving a brown solution. This solution was then added to stirring Et_2O (50 mL) forming a brown precipitation. The precipitate was isolated on a 15 mL medium porosity fritted disc, washed with Et_2O (3 x 5 mL), and the filtrate was evaporated *in vacuo*. The oil was dissolved in DCM (3 x 0.3 mL) and the resulting solution was dropwise added onto a 250 μm silica preparatory plate. The product was eluted with 10% EtOAc :hexanes (200 mL), scraped off as a band at R_f : 0.35-0.44 and this silica gel was sonicated in EtOAc (20 mL) for 15 min. The silica was filtered off on a 15 mL fine porosity fritted disc and washed with DCM (3 x 5 mL). The filtrate was evaporated *in vacuo* and desiccated for 15 min to yield the colorless oil **49** (44 mg, 61% yield). IR: $\nu(\text{C-H sp}^2) = 2960\text{ cm}^{-1}$, $\nu(\text{CO}) = 1704\text{ cm}^{-1}$. $^1\text{H NMR}$ (CDCl_3 ,

δ): 7.22-7.15 (3H, m, H6, H7, & H8 major and minor), 7.11 (1H, d, $J = 7.3$, H5 major and minor), 6.09 (1H, m, H2 minor), 6.06 (1H, m, H2 major), 5.91 (1H, m, H3), 5.81 (1H, m, H3), 3.45-3.3 (3H, H1 & H4 major and minor), 2.61 (1H, dd, $J = 16.4$ & 5.7, H11 minor), 2.52 (2H, m, H9 major and minor), 2.30 (1H, dd, $J = 16.4$ & 8.4, H11 minor), 2.16 (3H, s, H12 minor), 2.15 (2H, m, H11 major), 1.96 (3H, s, H12 major), 1.01 (3H, d, $J = 6.9$, H10 major), 0.68 (3H, d, $J = 6.8$, H10 minor). ^{13}C NMR (CDCl_3 , δ): (major) 209.1, 137.2, 135.2, 128.4, 128.3, 126.8, 126.3, 126.2, 126.1, 46.2, 44.6, 37.2, 30.4, 17.9; (minor) 208.6, 137.6, 135.3, 128.4, 127.5, 127.4, 126.2, 126.0, 125.9, 48.5, 43.9, 37.1, 30.7, 30.5, 15.3. EA: Calculated for $\text{C}_{15}\text{H}_{18}\text{O} \cdot 0.3 \text{CH}_2\text{Cl}_2$: C, 76.64; H, 7.82. Found: C, 76.71; H, 7.58.

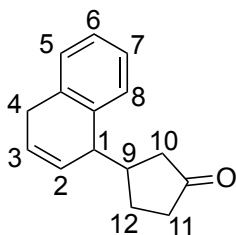
Synthesis of 4-(1,4-dihydroanthracen-1-yl)pentan-2-one (50).



25 (200 mg, 0.312 mmol), $\text{CH}_3\text{CH}_2\text{CN}$ (6 mL), and 3-penten-2-one (0.2 mL, 2.0 mmol) were added to a test tube charged with a stir pea and the red solution was stirred at RT for 1 min, then at -60°C for 15 min. TMSOTf (0.1 mL, 0.54 mmol) was added to the reaction mixture and the resulting red solution was stirred at -60°C for 15 min. NaCNBH_3 (226 mg, 3.60 mmol) was added to the solution and the reaction mixture was left at -60°C for 5 h. The reaction mixture was removed from the glovebox and stirred open to air overnight (~ 18 h). The resulting brown solution was evaporated *in vacuo* to an

oil. This oil was then dissolved in DCM (1 mL) forming a brown solution. This solution was added to stirring Et₂O (50 mL) forming a brown precipitation. The precipitate was collected on a 15 mL medium porosity fritted disc, washed with Et₂O (3 x 5 mL), and evaporated filtrate *in vacuo*. The brown oil formed was dissolved in DCM (3 x 0.3 mL) and the resulting solution was dropwise added onto a 250 μ m silica preparatory plate. The product was eluted with 10% EtOAc:hexanes (200 mL), scraped off as a band at R_f: 0.28-0.56 and this silica gel was sonicated in EtOAc (20 mL) for 15 min. The silica was filtered off on a 15 mL fine porosity fritted disc and washed with DCM (3 x 5 mL). The filtrate was evaporated *in vacuo* and desiccated for 15 min to yield the colorless oil **50** (32 mg, 38% yield). IR: $\nu(\text{C-H } sp^2) = 2959 \text{ \& } 2926 \text{ cm}^{-1}$, $\nu(\text{CO}) = 1703 \text{ cm}^{-1}$. EA: Calculated for C₁₉H₂₀O • 0.5 CH₂Cl₂: C, 76.33; H, 6.90. Found: C, 76.75; H, 6.57.

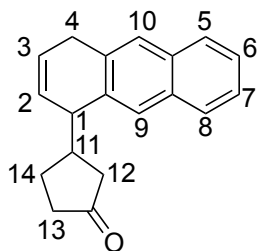
Synthesis of 3-(1,4-dihydronaphthalen-1-yl)cyclopentan-1-one (**51**).



24 (200 mg, 0.339 mmol), CH₃CH₂CN (6 mL), and cyclopenten-2-one (0.3 mL, 3.59 mmol) were added to a test tube charged with a stir pea and the orange solution was stirred at RT for 1 min, then at -60 °C for 15 min. TMSOTf (0.1 mL, 0.54 mmol) was added to the reaction mixture and the resulting red solution was stirred at -60 °C for 15 min. NaCNBH₃ (226 mg, 3.59 mmol) was added to the solution and the reaction mixture was left at -60 °C for 2.5 h. The reaction mixture was removed from the glovebox and stirred open to air overnight (~18 h). The brown solution formed was evaporated *in vacuo*

to an oil. This oil was dissolved in DCM (1 mL), creating a brown solution that was then added to stirring Et₂O (50 mL), forming a brown precipitation. The precipitate was isolated on a 15 mL medium porosity fritted disc, washed with Et₂O (3 x 5 mL), and evaporated filtrate *in vacuo* to an oil. The brown oil was dissolved in DCM (3 x 0.3 mL) and the resulting solution was dropwise loaded onto a 250 μ m silica preparatory plate. The product was eluted with 10% EtOAc:hexanes (200 mL), scraped off as a band at R_f: 0.25-0.43, and the silica gel was sonicated in EtOAc (20 mL) for 15 min. The silica was filtered off on a 15 mL fine porosity fritted disc and washed with DCM (3 x 5 mL). The filtrate was evaporated *in vacuo* and desiccated for 15 min to yield the colorless oil **51** (20 mg, 27% yield). IR: $\nu(\text{C-H sp}^2) = 3026 \text{ \& } 2886 \text{ cm}^{-1}$, $\nu(\text{CO}) = 1737 \text{ cm}^{-1}$. ¹H NMR (CDCl₃, δ): 7.17 (4H, m, H5, H6, H7, & H8), 6.14 (1H, ddd, $J = 10.0, 4.7, \text{ \& } 2.7$, H3), 5.97 (1H, m, H2), 3.51 (1H, m, H1), 3.34 (2H, m, H4), 2.48 (1H, m, H9), 2.28 (1H, m, H10/H11), 2.09 (3H, m, H10/H11), 1.98 (1H, dd, $J = 18.5 \text{ \& } 11.5$, H12), 1.74 (1H, m, H12). ¹³C NMR (CDCl₃, δ): 219.2 (CO), 137.3, 134.9, 128.5, 128.4, 127.8 (C3), 126.9 (C2), 126.3, 126.1, 45.2, 43.2 (C1), 41.7, 38.8, 30.5 (C4), 27.2. LRMS: C₁₅H₁₆O, mass found [M+H⁺] = 213, mass required: 212.2.

Synthesis of 3-(1,4-dihydroanthracen-1-yl)cyclopentan-1-one (**52**).

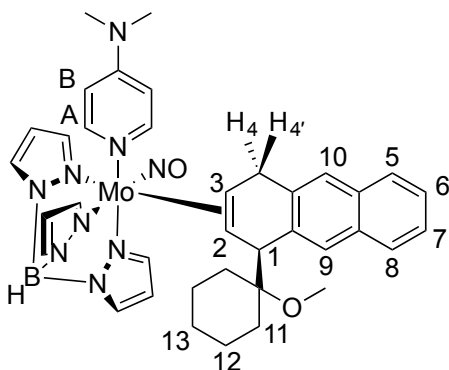


25 (200 mg, 0.312 mmol), CH₃CH₂CN (6 mL), and cyclopentenone (0.3 mL, 3.59 mmol)

were added to a test tube charged with a stir pea and the red solution was stirred at RT for 1 min, then at -60 °C for 15 min. TMSOTf (0.1 mL, 0.54 mmol) was added to the reaction mixture and the resulting red solution was stirred at -60 °C for 15 min. NaCNBH₃ (226 mg, 3.60 mmol) was added to the solution and the resulting brown solution was left at -60 °C for 2 h. The reaction mixture was warmed to RT, extracted with DCM (8 mL) and H₂O (8 mL), and the organic layer was dried over MgSO₄. The drying agent was filtered off on a 15 mL medium porosity fritted disc, washed with DCM (3 x 5 mL), and the filtrate was evaporated *in vacuo*. The resulting oil was dissolved in DCM (1 mL) forming a brown solution. This solution was added to stirring pentane (50 mL) forming a tan precipitation. The tan precipitate was collected on a 15 mL fine porosity fritted disc and washed with pentane (3 x 5 mL). The precipitate was removed from the glovebox, dissolved in DCM (5 mL), and the resulting brown solution was stirred open to air overnight (~18 h). The resulting brown solution was evaporated *in vacuo* to an oil. This oil was dissolved in DCM (3 x 0.3 mL) and the resulting solution was dropwise added onto a 250 µm silica preparatory plate. The product was eluted with 20% EtOAc:hexanes (200 mL), scraped off as a band at R_f: 0.38-0.56 and this silica gel was sonicated in EtOAc (20 mL) for 15 min. The silica was filtered off on a 15 mL fine porosity fritted disc and washed with DCM (3 x 5 mL). The filtrate was evaporated *in vacuo* and desiccated for 15 min to yield the colorless oil **52** (23 mg, 27% yield). IR: $\nu(\text{C-H sp}^2) = 3027 \text{ \& } 2885 \text{ cm}^{-1}$, $\nu(\text{CO}) = 1735 \text{ cm}^{-1}$. ¹H NMR (CDCl₃, δ): 7.77 (2H, m, H5 & H8), 7.65 (1H, s, H10), 7.64 (1H, s, H9), 7.42 (2H, m, H6 & H7), 6.21 (1H, ddd, $J = 9.9, 4.3, \text{ \& } 3.2$, H3), 6.08 (1H, m, H2), 3.68 (1H, m, H1), 3.55 (2H, m, H4), 2.52 (1H, m, H11), 2.28 (1H, m, H12/H13), 2.15 (1H, dd, $J = 18.2 \text{ \& } 7.2$, H12/H13), 2.07 (3H, m,

H12, H13, & H14), 1.76 (1H, m, H14). ^{13}C NMR (CDCl_3 , δ): 219.1 (CO), 136.3, 133.7, 132.3, 132.2, 127.8, 127.6 (C3), 127.4 (C2), 127.2 (C5/8), 126.5 (C10), 125.6 (C6/7), 125.4 (C6/7), 45.4 (C11), 43.9 (C1), 42.1 (C12/13), 38.7 (C12/13), 30.6 (C4), 27.4 (C12/13/14). EA: Calculated for $\text{C}_{19}\text{H}_{18}\text{O} \cdot 0.5 \text{CH}_2\text{Cl}_2$: C, 76.84; H, 6.28. Found: C, 78.11; H, 6.36.

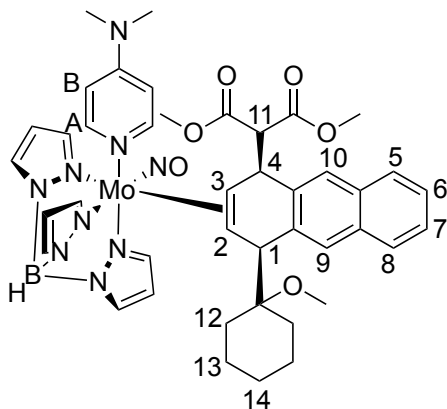
Synthesis of $\text{TpMo}(\text{NO})(\text{DMAP})(2,3\text{-}\eta^2\text{-(S)-1-(1-methoxycyclohexyl)-1,4-dihydroanthracene})$ (53).



25 (200 mg, 0.313 mmol), $\text{CH}_3\text{CH}_2\text{CN}$ (6 mL), and 1,1-dimethoxycyclohexane (0.3 mL, 1.98 mmol) were added to a test tube charged with a stir pea. The reaction mixture was stirred at RT until homogeneous and then cooled at $-60\text{ }^\circ\text{C}$ for 15 min. TMSOTf (0.1 mL, 0.54 mmol) was added to the reaction mixture and the resulting red solution was left stirring at $-60\text{ }^\circ\text{C}$ for 15 min. NaCNBH_3 (226 mg, 3.59 mmol) was added to the red solution, giving a brown solution that was left stirring at $-60\text{ }^\circ\text{C}$ for 2 h. This brown solution was then warmed to RT and washed with H_2O (8 mL). The aqueous layer was back-extracted with DCM (6 mL), combined with the organic layer, and dried over MgSO_4 . The drying agent was filtered off on a 15 mL medium porosity fritted disc, washed with DCM (3 x 2 mL), and the filtrate was evaporated *in vacuo*. The resulting oil

was then dissolved in DCM (1 mL) and the product was precipitated in stirring pentane (50 mL). The beige precipitate was isolated on a 15 mL fine porosity fritted disc, washed with pentane (3 x 10 mL), and desiccated to yield **53** (146 mg, 62% yield). CV (DMAc) $E_{p,a} = -0.07$ V (NHE). IR: $\nu(\text{C-H sp}^2) = 2928 \text{ cm}^{-1}$, $\nu(\text{BH}) = 2471 \text{ cm}^{-1}$, $\nu(\text{NO}) = 1567 \text{ cm}^{-1}$. ^1H NMR (d^6 -Acetone, δ): 7.93 (2H, m, Pz3A & Pz5C), 7.90 (2H, buried s, DMAP-A), 7.87 (1H, d, Pz5A), 7.77 (1H, d, $J = 7.7$, H5/H8), 7.76 (1H, s, H9), 7.72 (2H, d, Pz3C & H5/H8), 6.69 (1H, d, Pz5B), 7.58 (1H, s, H10), 7.29 (2H, m, H6 & H7), 6.88 (1H, d, Pz3B), 6.69 (2H, m, DMAP-B), 6.37 (1H, t, Pz4C), 6.32 (1H, t, Pz4A), 5.98 (1H, t, Pz4B), 4.22 (1H, dd, $J = 17.3$ & 3.6 , H4'), 4.08 (1H, s, H1), 3.40 (1H, d, $J = 17.3$, H4), 3.10 (6H, N-Me), 2.85 (3H, s, OMe), 2.63 (1H, dd, $J = 10.5$ & 3.6 , H3), 2.50 (1H, d, $J = 10.5$, H2), 2.30 (1H, d, $J = 12.8$, H11), 2.03 (1H, buried d, H11), 1.58 – 1.28 (6H, m, H11, H12, & H13), 1.05 (1H, t, $J = 12.8$, H11), 0.81 (1H, m, H13). ^{13}C NMR (d^6 -Acetone, δ): 154.9 (DMAP-C), 151.2 (DMAP-A), 143.6, 141.6, 141.5, 139.2, 138.6, 137.1, 136.9, 135.5, 133.9, 133.3, 129.9 (C9), 128.1 (C5/8), 127.5 (Pz3C), 126.5 (C10), 124.8 (C6/7), 124.5 (C6/7), 108.5 (DMAP-B), 106.6 (Pz4C), 106.2 (Pz4A), 105.9 (Pz4B), 82.5, 66.8 (C3), 61.7 (C2), 49.7 (C1), 47.5 (OMe), 39.2 (NMe), 35.5 (C4), 32.1 (C11), 31.0, 29.8, 26.7, 22.5, 22.3.

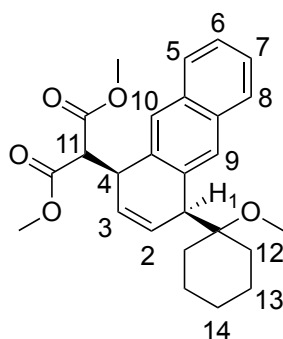
Synthesis of TpMo(NO)(DMAP)(2,3- η^2 -dimethyl 2-((1*S*,4*S*)-4-(1-methoxycyclohexyl)-1,4-dihydroanthracen-1-yl)malonate)) (54).



25 (200 mg, 0.313 mmol), CH₃CH₂CN (6 mL), and 1,1-dimethoxycyclohexane (0.3 mL, 1.98 mmol) were added to a test tube charged with a stir pea. The reaction mixture was stirred at RT until homogeneous and then cooled at -60 °C for 15 min. TMSOTf (0.1 mL, 0.54 mmol) was added to the reaction mixture and the resulting red solution was left stirring at -60 °C for 15 min. LiDMM (250 mg, 1.81 mmol) was added to the red solution, giving a brown solution that was left stirring at -60 °C for 2 h. This brown solution was then warmed to RT and washed with H₂O (8 mL). The aqueous layer was back-extracted with DCM (6 mL), combined with the organic layer, and dried over MgSO₄. The drying agent was filtered off on a 15 mL medium porosity fritted disc, washed with DCM (3 x 2 mL), and the filtrate was evaporated *in vacuo*. The resulting oil was then dissolved in DCM (1 mL) and the product was precipitated in stirring pentane (50 mL). The beige precipitate was isolated on a 15 mL fine porosity fritted disc, washed with pentane (3 x 10 mL), and desiccated to yield **54** (145 mg, 52% yield). CV (DMAc) $E_{p,a} = +0.7$ V (NHE). IR: $\nu(\text{C-H } sp^2) = 2929 \text{ cm}^{-1}$, $\nu(\text{BH}) = 2470 \text{ cm}^{-1}$, $\nu(\text{CO}) = 1730 \text{ cm}^{-1}$, $\nu(\text{NO}) = 1572 \text{ cm}^{-1}$. ¹H NMR (d⁶-Acetone, δ): 7.96 (2H, bs, DMAP-A), 7.94 (1H, d,

Pz5A), 7.89 (1H, d, Pz5C), 7.83 (1H, d, Pz3C), 7.84 (1H, s, H9), 7.78 (1H, m, H5/H8), 7.73 (1H, m, H5/H8), 7.67 (1H, d, Pz5B), 7.63 (1H, s, H10), 7.55 (1H, d, Pz3A), 7.32 (2H, m, H6 & H7), 6.84 (1H, d, Pz3B), 6.73 (2H, m, DMAP-B), 6.39 (1H, t, Pz4A), 6.33 (1H, t, Pz4C), 5.97 (1H, t, Pz4B), 4.46 (1H, d, $J = 11.1$, H4), 4.34 (1H, d, $J = 11.1$, H11), 4.21 (1H, s, H1), 3.56 (3H, s, OMe), 3.44 (3H, s, OMe), 3.12 (6H, s, NMe), 2.76 (3H, s, OMe), 2.46 (1H, d, $J = 10.3$, H3), 2.40 (1H, d, $J = 10.3$, H2), 2.05 (3H, buried multiplet, H12), 1.70 (1H, m, H12), 1.60 (1H, m, H13), 1.50 (2H, m, H13 & H14), 1.35 (2H, m, H13), 1.00 (1H, m, H14). ^{13}C NMR (d^6 -Acetone, δ): 169.9 (CO), 169.5 (CO), 155.0 (DMAP-C), 151.1 (DMAP-A), 143.3, 141.5 (Pz3A), 141.2 (Pz3B), 138.2, 137.4 (Pz5C), 137.3 (Pz5A), 137.1, 135.6 (Pz5B), 133.5, 133.4, 130.8 (Pz3C), 128.6, 128.1 (C5/8), 127.7 (C5/8), 125.3 (C6), 125.2 (C7), 108.6 (DMAP-B), 106.9 (Pz4C), 106.5 (Pz4B), 105.9 (Pz4A), 80.7, 67.1 (C3), 64.2 (C11), 60.8 (C2), 52.5 (OMe), 51.9 (OMe), 47.7 (OMe), 44.9 (C4), 39.2 (NMe), 32.1, 26.6, 22.8.

Synthesis of dimethyl 2-((1*S*,4*S*)-4-(1-methoxycyclohexyl)-1,4-dihydroanthracen-1-yl)malonate (55**).**



To a 50 mL filter flask charged with a stir pea were added **54** (100 mg, 0.113 mmol), DCM (5 mL), and a 0.06 M solution of $\text{I}_2/\text{Et}_2\text{O}$ (1 mL, 0.06 mmol), resulting in a green

solution. This solution was stirred at RT for 5 min and evaporated *in vacuo*. The resulting green oil was dissolved in DCM (1 mL) forming a green solution. This solution was added to stirring hexanes (50 mL) giving a green precipitation. Collected the green precipitate on a 15 mL fine porosity fritted disc, washed with hexanes (3 x 10 mL), and desiccated to yield **23** (65 mg, 97%). The filtrate was removed from the glovebox and evaporated *in vacuo* to an oil. The oil was dissolved in DCM (3 x 0.3 mL) and the resulting solution was dropwise added onto a 250 μ m silica preparatory plate. The product was eluted with 10% EtOAc:hexanes (200 mL), scraped off as a band at R_f : 0.16-0.34 and this silica gel was sonicated in EtOAc (20 mL) for 15 min. The silica was filtered off on a 15 mL medium porosity fritted disc and washed with DCM (3 x 2 mL). The filtrate was evaporated *in vacuo* and desiccated to yield the colorless oil **55** (31 mg, 65% yield). IR: $\nu(\text{C-H sp}^2) = 2936 \text{ cm}^{-1}$ and $\nu(\text{CO}) = 1735 \text{ cm}^{-1}$. ^1H NMR (CDCl_3 , δ): 7.77 (1H, m, H5/H8), 7.72 (1H, m, H5/H8), 7.66 (1H, s, H10), 7.63 (1H, s, H9), 7.41 (2H, m, H6 & H7), 6.18 (1H, ddd, $J = 10.2, 5.2, 1.0$, H3), 6.09 (1H, ddd, $J = 10.2, 5.2, 0.6$, H2), 4.43 (1H, ddd, $J = 10.8, 5.0, 2.2$, H4), 3.94 (1H, m, H1), 3.84 (1H, d, $J = 10.9$, H11), 3.80 (3H, s, OMe), 3.62 (3H, s, OMe), 3.35 (3H, s, OMe), 1.88 (1H, m, H12), 1.73 (1H, m, H12), 1.60 (6H, m, H12, H13, & H14), 1.36 (1H, m, H12), 1H, m, H14). ^{13}C NMR (CDCl_3 , δ): 169.4 (OMe), 168.4 (OMe), 134.8, 134.2, 132.0, 131.9, 130.1 (H2), 129.0 (C10), 127.9 (C3), 127.6 (C5/8), 127.4 (C5/8), 127.3 (C9), 125.8 (C6 & C7), 79.5, 59.8 (C11), 52.7 (OMe), 52.6 (OMe), 48.5 (OMe), 44.8 (C1), 40.0 (C4), 31.9, 31.8, 25.7.

3.6 References

1. Myers, J. T.; Shivokevich, P. J.; Pienkos, J. A.; Sabat, M.; Myers, W. H.; Harman, W. D. *Organometallics* **2015**, 34, (14), 3648.
2. Meiere, S. H.; Keane, J. M.; Gunnoe, T. B.; Sabat, M.; Harman, W. D. *J. Am. Chem. Soc.* **2003**, 125, (8), 2024.
3. Rossi, M. B.; Piro, O. E.; Castellano, E. E.; Alborés, P.; Baraldo, L. M. *Inorg. Chem.* **2008**, 47, (7), 2416.
4. Dunbar, M. A.; Balof, S. L.; Roberts, A. N.; Valente, E. J.; Schanz, H.-J. *Organometallics* **2011**, 30, (2), 199.
5. Graham, P.; Meiere, S. H.; Sabat, M.; Harman, W. D. *Organometallics* **2003**, 22, 4364.
6. Carden, R. G.; Ohane, J. J.; Pike, R. D.; Graham, P. M. *Organometallics* **2013**, 32, (9), 2505.
7. Mocella, C. J.; Delafuente, D. A.; Keane, J. M.; Warner, G. R.; Friedman, L. A.; Sabat, M.; Harman, W. D. *Organometallics* **2004**, 23, (16), 3772.
8. Cahill, R.; Cookson, R. C.; Crabb, T. A. *Tetrahedron* **1969**, 25, (19), 4681.
9. Harrison, D. P.; Nichols-Nieler, A. C.; Zottig, V. E.; Strausberg, L.; Salomon, R. J.; Trindle, C. O.; Sabat, M.; Gunnoe, T. B.; Iovan, D. A.; Myers, W. H.; Harman, W. D. *Organometallics* **2011**, 30, (9), 2587.
10. Ha, Y.; Dilsky, S.; Graham, P. M.; Liu, W.; Reichart, T.; Sabat, M.; Keane, J. M.; Harman, W. D. *Organometallics* **2006**, 25, 5184.
11. Winemiller, M. D.; Harman, W. D. *J. Am. Chem. Soc.* **1998**, 120, (31), 7835.
12. Ding, F.; Valahovic, M. T.; Keane, J. M.; Anstey, M. R.; Sabat, M.; Trindle, C. O.; Harman, W. D. *J. Org. Chem.* **2004**, 69, (7), 2257.
13. Strausberg, L. Reactivity and Functionalization of Naphthalene and Anthracene Complexes of {TpW{NO}(PMe₃)}. Ph. D. Dissertation, University of Virginia, 2008.

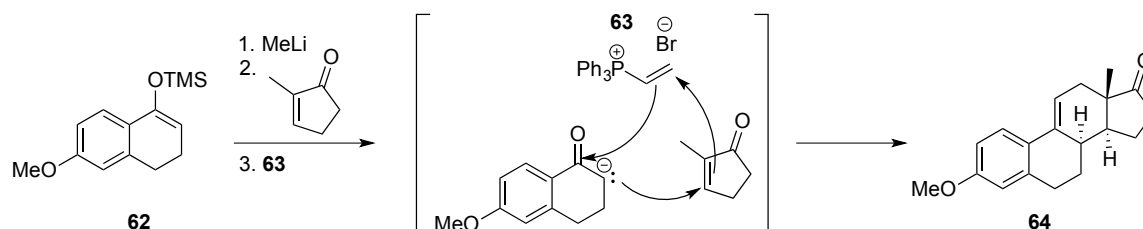
Chapter 4

Michael-Michael Ring Closures on TpMo(NO)(DMAP)(η^2 -Naphthalene)

4.1. Introduction

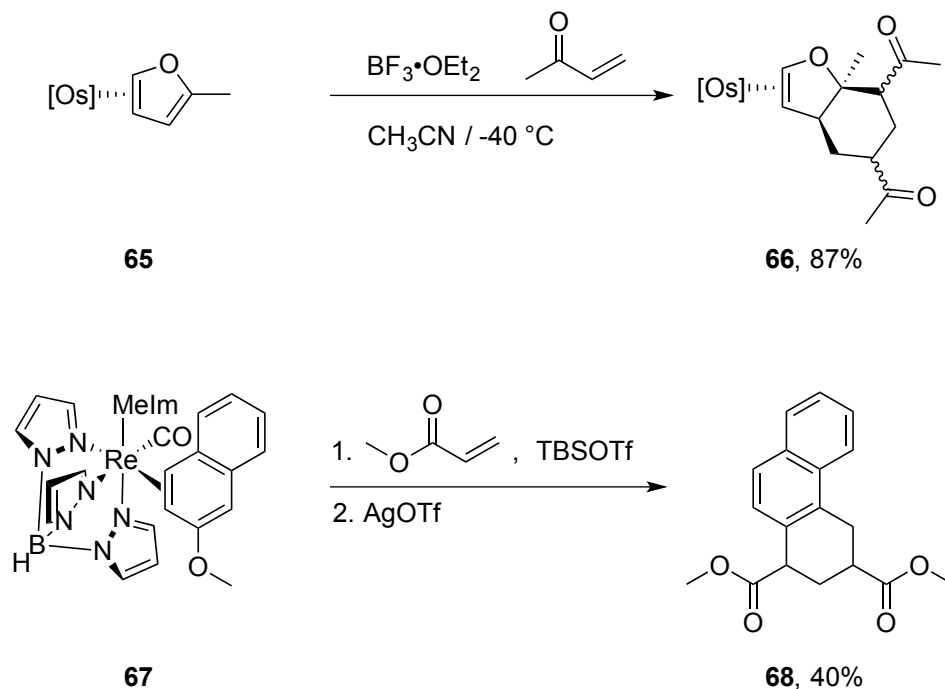
Methods that form C-C bonds with regio- and stereocontrol make up the backbone of organic synthesis. Classical examples of carbon-carbon bond formation include the Claisen condensation, Mannich and Wittig reactions, Friedel-Crafts acylation and alkylation, the use of Grignard reagents, cross coupling reactions and many more.¹ Among these well-known syntheses is the Michael reaction which involves the enolate attack on an α,β -unsaturated carbonyl, yielding a conjugate addition product.²⁻⁴ Furthermore, the enolate formed immediately after nucleophilic attack onto the Michael acceptor can act as a nucleophile itself and attack a second equivalent of Michael acceptor. That resulting enolate can undergo an intramolecular cyclization to form a new ring system. This Michael-Michael-ring closure (MIMIRC) has been thoroughly explored by Gary Posner and others.⁵⁻¹¹ Demonstrating the utility of this reaction, Posner reacted the enol silane of tetralone (**62**) with methyl lithium and subsequently added 2-methyl-2-cyclopentenone yielding **64**, an estrone derivative with a steroidal core (Scheme 4.1).¹¹ Of note, in this MIMIRC example, three new carbon-carbon bonds and three new stereocenters are formed selectively.

Scheme 4.1. Tandem Michael-Michael-ring closure to yield (\pm)-9,11-Dehydroestrone.



To further expand on the work of Posner, the Harman group has demonstrated MIMIRC reactions with the π -systems of aromatic molecules bound to a transition metal in an η^2 fashion. For example, $\{\text{Os}(\text{NH}_3)_5(\eta^2\text{-2-methylfuran})\}^{2+}$ (**65**) is capable of undergoing an electrophilic addition at the beta position of the furan with methyl vinyl keton (MVK) activated by boron trifluoride diethyl etherate ($\text{BF}_3 \cdot \text{OEt}_2$) (Scheme 4.2).¹² The resulting enolate then reacts with a second equivalent of MVK, which then performs an intramolecular nucleophilic attack to yield a benzofuran skeleton (**66**). In an additional example, $\text{TpRe}(\text{CO})(\text{MeIm})(\eta^2\text{-2-methoxynaphthalene})$ (**67**) can undergo an electrophilic addition of methylacrylate, which proceeds through a Michael-Michael-ring closure to yield the final MIMIRC product (**68**) upon oxidative decomplexation.¹³ Encouraging results from the MIMIRC reaction to form **66** demonstrate that the metal center induces stereocontrol of the bridgehead formation through the steric preference of the initial electrophilic addition and the final nucleophilic ring closure both to occur *anti* to the metal. For **68**, the stereocenters set by the metal are lost once the organic is liberated due to an elimination of the methoxy group. It should be noted that Scheme 4.1 shows an example of an [A+B] MIMIRC, wherein the second Michael added is different from the initial. In contrast, Scheme 4.2 represents an [A+A] MIMIRC, wherein the two Michael acceptors being added are the same.

Scheme 4.2. MIMIRC reactions on $\{\text{Os}(\text{NH}_3)_5(\eta^2\text{-2-methylfuran})\}^{2+}$ and $\text{TpRe}(\text{CO})(\text{MeIm})(\eta^2\text{-2-methoxynaphthalene})$.

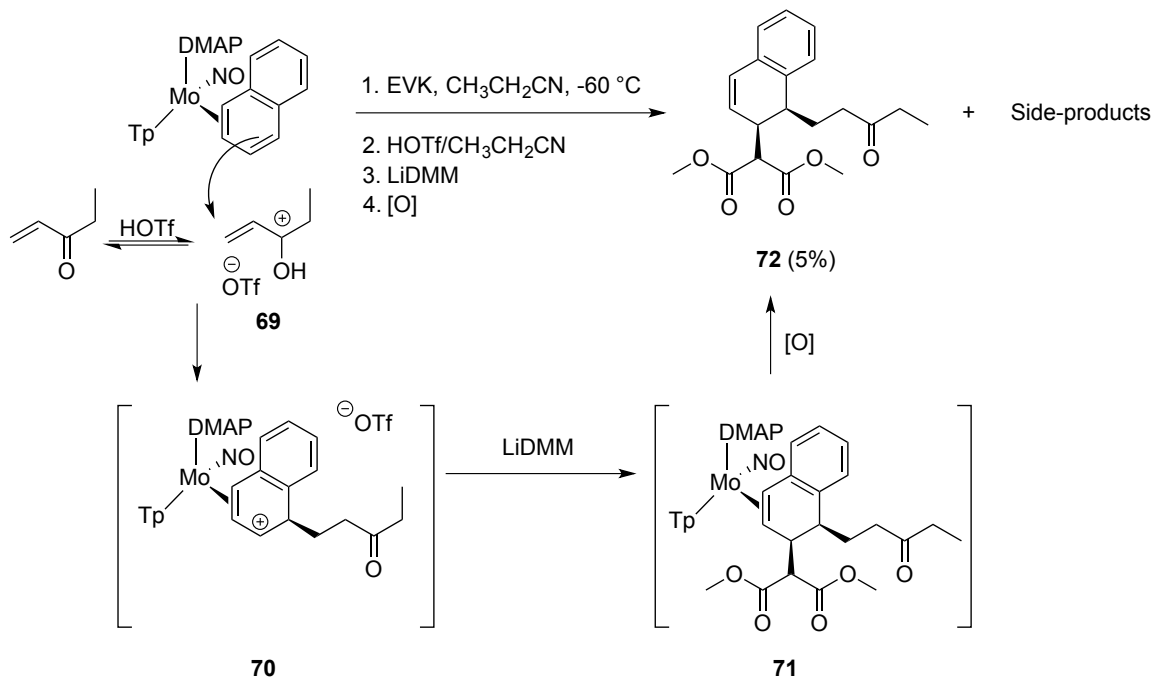


During attempts at carbon-carbon bond formation on $\text{TpMo}(\text{NO})(\text{DMAP})(\eta^2\text{-naphthalene})$ (**24**), the electrophilic addition of ethyl vinyl ketone (EVK) followed by the nucleophilic addition of LiDMM yielded the first example of a MIMIRC reaction of an η^2 -bound aromatic molecule performed using molybdenum; however, this was isolated as a mixture of products (*vide infra*). The following chapter describes the development of a method to perform MIMIRC reactions on **24**, determination of the stereoselectivity of these additions, and exploration of further possible MIMIRC reactions, which can be mediated by the $\{\text{TpMo}(\text{NO})(\text{DMAP})\}$ fragment.

4.2 Results and Discussion

During the initial investigation for electrophilic additions of Michael acceptors onto **24**, triflic acid (HOTf) was used to promote the reaction by the putative formation of the more electrophilic, protonated species, **69**. Under these conditions, **24** is capable of attacking **69** to form an allyl stabilized by the metal center (**70**). With the intention of adding a carbon nucleophile to **70**, LiDMM was added to the reaction mixture and, upon reaction completion, the resulting solution was exposed to air overnight (Scheme 4.3).

Scheme 4.3. Attempted tandem electrophilic-nucleophilic addition of EVK and LiDMM to **24**.



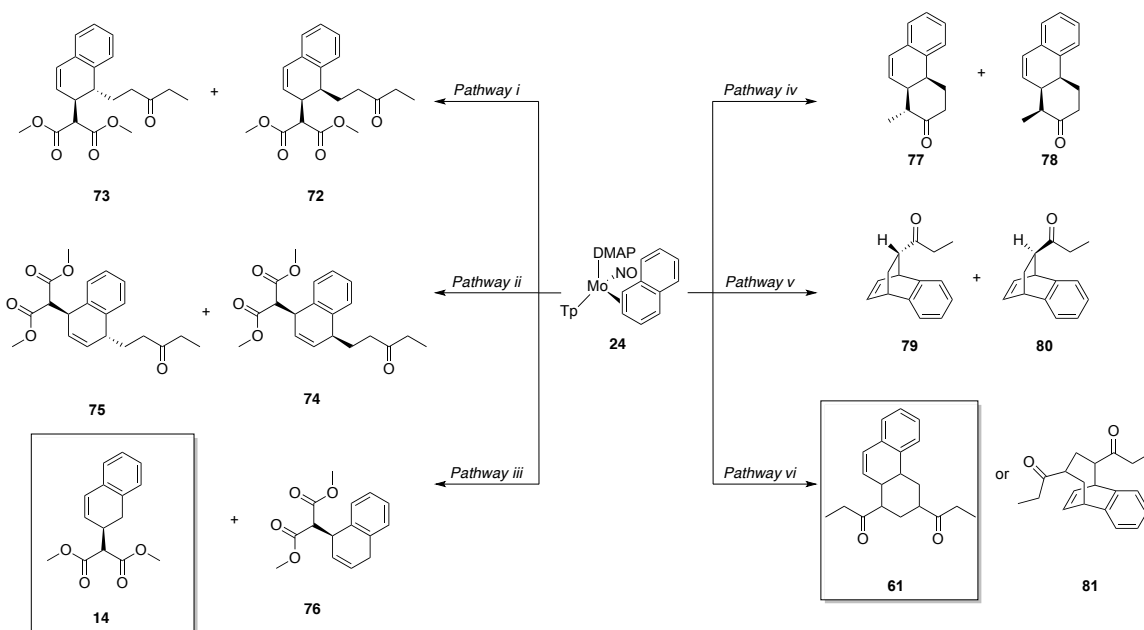
Following oxidative decomplexation to yield **72**, the resulting reaction mixture was chromatographed on a silica gel preparatory plate, which yielded multiple products.

In contrast to the 1,4-additions seen in Chapter 3, one of the products in this mixture was the 1,2-dihydronaphthalene **72**. In the ^1H NMR spectrum of **72**, the isolated alkene resonances are at 6.48 (dd, $J = 10.0$ and 2.7 Hz, H3) and 5.64 (d, $J = 10.0$ Hz, H4) ppm, which are in agreement with typical chemical shifts of a 1,2-addition product. Two singlets at 3.83 and 3.74 ppm, as well as a triplet at 0.98 ppm, each integrate for three protons in comparison to H3 and H4. In the ^{13}C NMR spectrum of **72**, three carbonyl peaks are seen at 218.9, 168.9, and 168.6 ppm representing the ketone and two ester carbonyls, respectively. Lastly, the three CO stretching frequencies at 1755, 1736 and 1712 cm^{-1} are observed in the IR spectrum of **72**. In agreement with the preference for additions to occur *anti* to the metal center, a strong NOE interaction is seen between protons H1 and H2. Therefore, a *cis* geometry is assigned for **72**. Although this evidence indicates that a successful tandem electrophilic-nucleophilic addition to yield **72** occurred, the selective synthesis of this product proved inconsistent and low yielding (< 5%). Furthermore, a 1,2-addition cannot be assumed as the favored regiochemistry due to the plethora of side-products seen when using HOTf as the acid source.

In the investigation of the side-products isolated from the procedure to yield **72**, six main pathways were considered (Scheme 4.4). Considering the synthesis of **72**, Pathway i assumes the possibility that two 1,2-additions occurred wherein the *cis* and *trans* products could be isolated. Similarly, the *cis* and *trans* isomers of a 1,4-addition could have formed (**74** and **75**), as depicted in Pathway ii. As previously seen in Chapter 3 with the isolation of **14** during the synthesis of **43**, the likelihood of one of the side-products being the product of a protonation and subsequent nucleophilic addition is very high, thus Pathway iii considers 1,2- and 1,4-addition products **14** and **76**, respectively.

The initial addition of EVK to naphthalene is believed to form an enol, which can act as a nucleophile. Pathway iv depicts this enol attacking the allylic naphthalene to form a cyclized 1,2-dihydronaphthalene (**77** and **78**). In a similar mechanism, after the allylic ring rearranges on the metal center, the enol can attack, which would yield a cyclized 1,4-dihydronaphthalene (**79** and **80**) as seen in Pathway v. Lastly, the enol formed can attack a second equivalent of Michael acceptor and the subsequent enol can attack the allylic naphthalene yielding either a 1,2- or 1,4-dihydronaphthalene (**61** and **81**) as depicted in Pathway vi.

Scheme 4.4. Analysis of mixture resulting from the attempted tandem electrophilic-nucleophilic addition of EVK and LiDMM to **24**.



One band collected from the preparatory plate was shown by ^1H NMR to have four alkene peaks at 6.52 (dd, $J = 9.6$ and 1.4 Hz), 6.44 (d, $J = 9.7$ Hz), 6.01 (dd, $J = 9.7$

and 6.1 Hz), and 5.95 (dd, $J = 9.6$ and 4.5 Hz) ppm. This was initially thought to be the two epimers of a 1,2-addition or 1,4-addition on naphthalene (Scheme 4.3, Pathway i or Pathway ii). However, comparing this spectrum with that of the cleanly isolated **72** shows this not to be the case. Another key feature in disagreement with Pathway i or ii is the fact that four carbonyl carbons (213.4, 213.2, 168.8, and 168.7 ppm) are present in the ^{13}C NMR spectrum of this mixture, rather than the expected six carbonyls. Furthermore, the chemical shifts and splitting patterns of the alkene resonances do not match those of a 1,4-addition product, thus Pathway i and Pathway ii were determined not to have contributed to this mixture of products.

Through a comparison with previous results it was found that the alkene peaks at 6.52 and 5.95 ppm were in fact due to the presence of the 1,2-dihydronaphthalene **14** (See Chapter 2), the product of a tandem electrophilic-nucleophilic addition of HOTf and LiDMM (e.g., Pathway iii). However, the chemical shifts and splitting patterns of the remaining alkene resonances indicate that a 1,4-addition product was not made. Accounting for the presence of **14**, the remaining peaks were compared to the possible products of Pathways iv, v, and vi.

Key ^1H NMR features for the remaining product include two peaks at 1.09 and 0.98 ppm, both of which are triplets, and each integrating for three protons (relative to the integration of the alkene peaks at 6.44 and 6.01). The triplets at 1.09 and 0.98 ppm couple to two separate methylene groups (identified by HSQC) at 2.55 (2H, m) as well as at 2.27 and 2.42 (1H each, m) ppm, respectively. Using HMBC correlations, these methylene groups were assigned as being adjacent to the carbonyl resonances at 213.4 and 213.2 ppm. Pathways v and vi both yield products with methylene groups adjacent to a

carbonyl and a methyl group; however, compounds **77** and **78** do not, thus disproving Pathway iv.

There is literature precedent supporting the possibility of the 1,4-cyclizations proposed in Pathway v;¹³ however, were Pathway v taken then both products **79** and **80** would need to be in this mixture to support the presence of the two triplets in the ¹H NMR spectrum. As this is not the case (based on the lack of remaining unassigned chemical shifts), Pathway v was ruled out. Following Pathway vi to yield **81** was unlikely as COSY correlation shows only one of the two alkene peaks (6.01 ppm) to correlate with any other protons in this product. This is a common indicator of a product from a 1,2- rather than a 1,4-addition. Thus leading to the investigation of **61** as the unidentified product. This analysis led to the carbon and proton assignments shown in Figure 4.1.

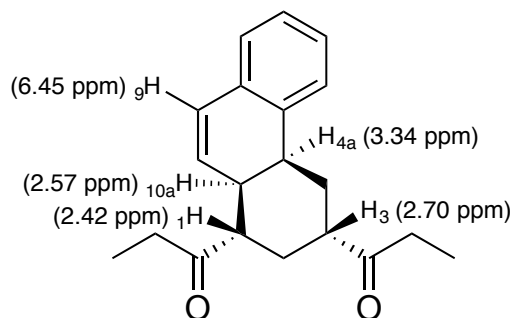
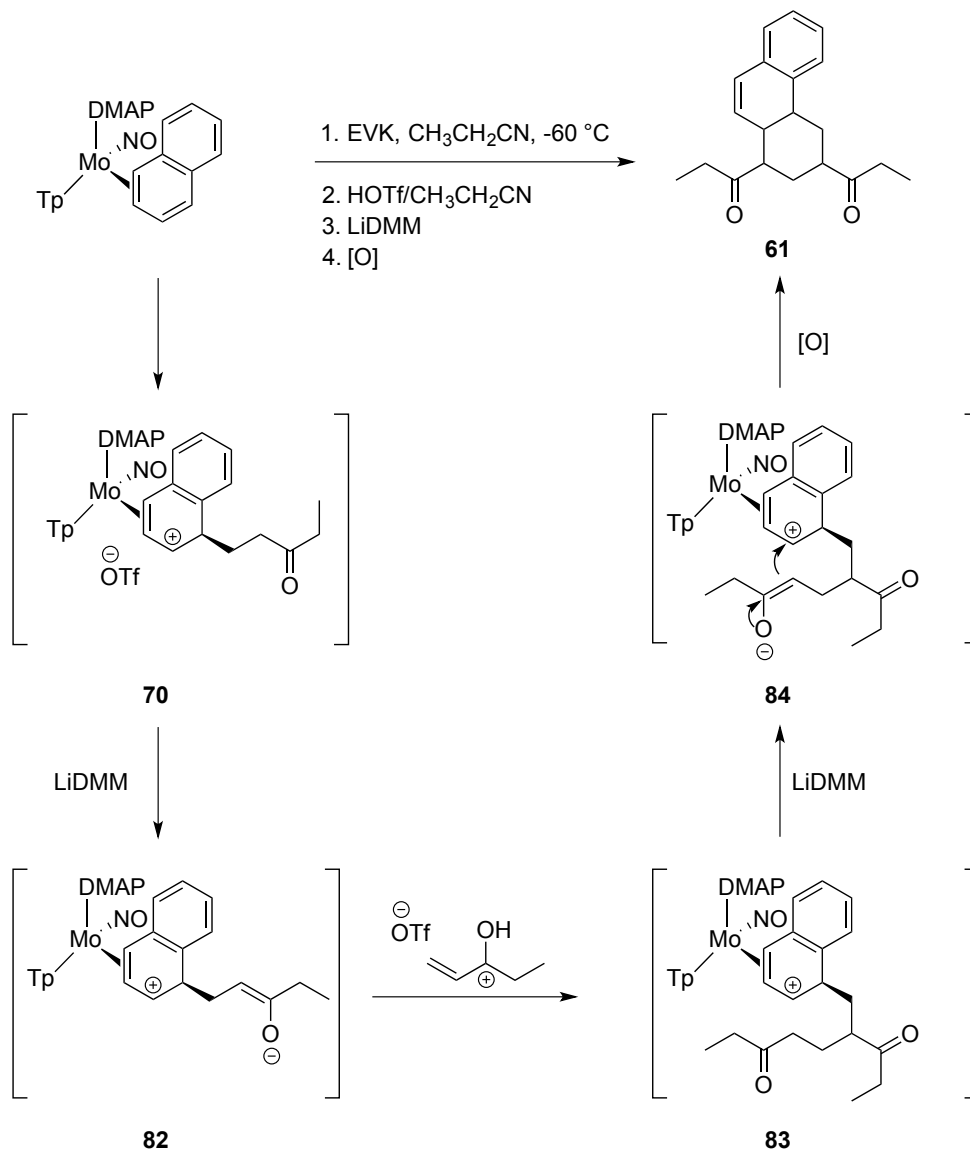


Figure 4.1. Selected proton assignments for **61**.

Under the reaction conditions to form **72**, the following proposed mechanism provides a rationale for the formation of **61**. The initial electrophilic addition of EVK to **24** yields an enol bound allylic species (**70**), which tautomerizes to the keto form. Upon the addition of LiDMM the ketone is deprotonated yielding a nucleophilic enolate (**82**), which can then attack another equivalent of EVK yielding the Michael-Michael addition product (**83**). Subsequently, **83** can be deprotonated and the resulting enolate (**84**) can

attack the electrophilic allyl, yielding the ring-closed product **61** (Scheme 4.5). This proposed mechanism agrees with the observation that formation of **61** requires the presence of a base and does not occur simply with HOTf and EVK.

Scheme 4.5. Proposed mechanism for the synthesis of **61**.

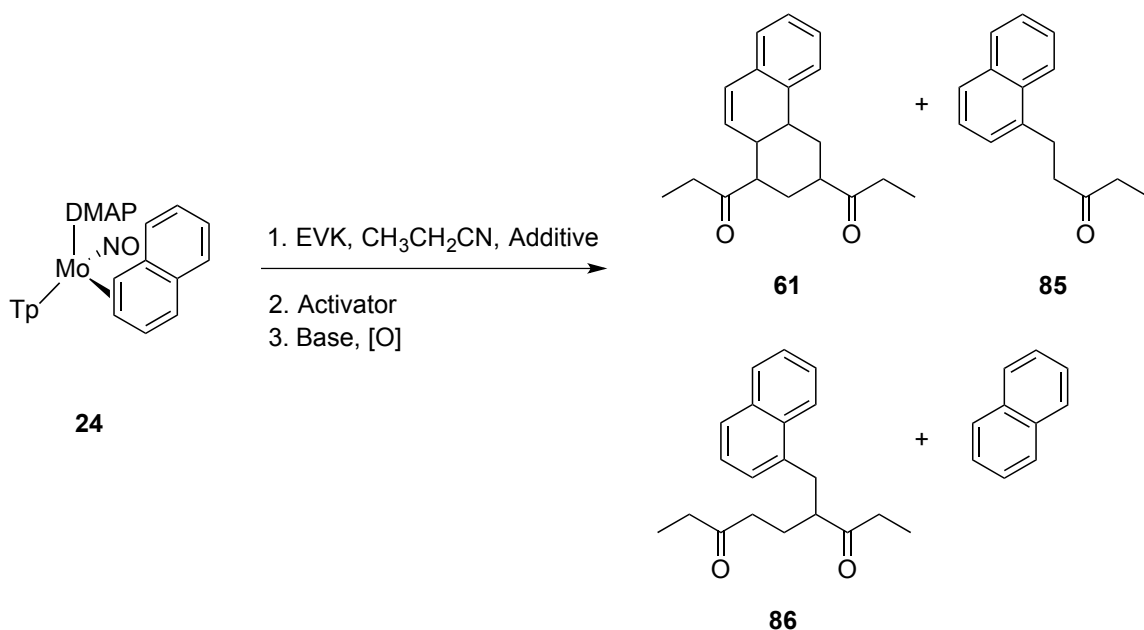


Following determination of the structure of **61**, attempts were made to improve the selectivity, yield, and purity of this MIMIRC reaction product. Optimization of this reaction began by attempting to use LiOMe in place of LiDMM to access **82**, while avoiding the nucleophilic addition of LiDMM. With this replacement, an impure metal complex (broad $E_{p,a} \sim +220$ mV) was isolated and then subjected to iodine oxidation. This procedure yielded a minute amount of desired product (**61**) as well as a substitution product (**85**), which was confirmed by literature reports.¹⁴ This substitution product, **85**, was formed from **70** undergoing deprotonation at the naphthalenium, rather than addition of a second equivalent of EVK. Attempts to reduce these side-products focused on using Lewis acids to activate the Michael acceptor in place of HOTf. The use of LiOTf or $\text{BF}_3 \cdot \text{OEt}_2$ yielded only free naphthalene upon oxidative decomplexation of their reaction mixtures. However, success was found through the use of alkylsilylated triflates.

Trimethylsilyl trifluoromethanesulfonate (TMSOTf) was added to a -60 °C solution of **24** and EVK dissolved in $\text{CH}_3\text{CH}_2\text{CN}$. The resulting solution turned blood red; a change in color consistent with the formation of an allyl. The mixture was left at -60 °C for 18 hours over which time it gradually turned brown. Subsequently, the resulting brown solution was then stirred exposed to air for 24 h. Chromatographing this solution on a silica gel preparatory plate yielded the desired product **61**, the substitution product **85**, as well as another substitution product **86** (Scheme 4.6). Similar to the synthesis of **85**, **86** is the result of the allyl being deprotonated; however, in the synthesis of **86**, the enol has attacked another equivalent of EVK before the deprotonation at the naphthalenium occurs. The pure isolation of **86** has not been accomplished, but key similarities with the ^1H NMR spectrum of **85** allowed for the identification of **86**. For

instance, **86** has 7 aromatic peaks (four doublets and three triplets) as well as two triplets at 1.06 and 0.85 ppm. The formation of **85** and **86** using TMSOTf is believed to occur due to the formation of HOTf when TMSOTf comes into contact with trace amounts of water. This formation of HOTf provides a better electrophile for the enolates **82** and **84** to attack, which hinders the desired annulative process and favors the isolation of substitution products **85** and **86**.

Scheme 4.6. Synthesis of **61** from **24** as well as common side-products (e.g., **85**, **86**, and free naphthalene)



After determining alkylsilylated triflates to be the most efficient activator for these MIMIRC reactions, the reaction was optimized. This optimization was completed using the above description of reaction setup, followed by CV monitoring of the reaction (as these are products of a 1,2-addition, the anodic wave for their eta-2 bound complexes

was suspected to be $\sim +200$ mV; see Chapter 2). After reaction completion was determined, TEA was added and the reaction mixture was stirred while being exposed to air for no less than 18 h. These reaction mixtures were then evaporated *in situ* and the resulting oil was dissolved in DCM. Adding this brown solution to Et₂O (50 mL) induced a precipitation of an undesired inorganic material that was subsequently removed using a 15 mL fritted disc. The filtrate was then evaporated *in vacuo* and the resulting crude organic was isolated as a brown oil, dissolved in CDCl₃, and observed by ¹H NMR.

The success of these reactions was determined through ¹H NMR by identifying the relative concentrations of **61**, **85**, **86**, and free naphthalene. In these crude organic mixtures the following peaks were integrated to compare relative concentrations: product **61**, 6.41 ppm; product **85**, 1.06 ppm; product **86**, 7.96 ppm; and free naphthalene, 7.80 ppm. Using this method of monitoring, the reaction time, temperature, equivalents of TMSOTf, and different alkylsilylated triflates were varied and their results recorded (Table 4.1). Out of the four products described above, free naphthalene was consistently formed in the largest amount. Between **61**, **85**, and **86** it was found that the two major products were **61** and **86**, with minimal observations of **85**. For this reason, Table 4.1 only compares the relative integrations of **61** and **86**. The highest yield of the desired MIMIRC was obtained when di-tert-butylpyridine (DTBP) was present (entry 12), which limits the acid source for protonation of **84** or **82**. This led to a crude organic mixture with only 7% of **86** relative to **61**. After a chromatographic workup of the crude organic described in entry 12, **61** was isolated at 21% from **24**.

Table 4.1. Summary of experiments performed during the optimization of the synthesis of **61**.

Entry	EVK (equiv)	Additive (equiv)	Temperature (°C)	Activator (equiv)	Time (h)	Base	Result
1	5.5	–	-60	HOTf (2.2)	18	TEA	Minute amounts of 61 and 85
2	10	–	-60	LiOTf (2.2)	18	TEA	No Reaction
3	7	–	-60	HOTf (2.2)	0.33	LiOMe	Minute amounts of 61 and 85
4	7	–	-60	TMSOTf (1.6)	18	TEA	1:1:1 amounts of 61 , 85 , and 86
5	7	–	-60	BF ₃ -Etherate (2.2)	18	TEA	No Reaction
6	7	–	-30	TMSOTf (1.6)	18	TEA	Decomposition
7	7	–	-60	TMSOTf (1)	18	TEA	86:61 = 1.0:0.7
8	7	–	-60	TMSOTf (1.6)	1	TEA	86:61 = 0.7:1.0
9	7	–	-60	TMSOTf (1.6)	6	TEA	86:61 = 0.6:1.0
10	7	–	-60	TBDMSOTf (1.6)	18	TEA	86:61 = 1.0:1.0
11	7	–	-60	TIPSOTf (1.6)	18	TEA	86:61 = 1.0:0.6
12	7	DTBP (0.9)	-60	TMSOTf (1.6)	18	TEA	86:61 = 0.07:1.0 (21% isolated yield of 61)
13	7	DBU (0.9)	-60	TMSOTf (1.6)	18	TEA	No Reaction

Following the conditions described in entry 12, with the exception of the oxidative decomplexation, isolation of TpMo(NO)(DMAP)(η^2 -**61**) was accomplished via chromatography and subsequent precipitation in pentane to yield **87** at 45% from **24**. In agreement with an η^2 -bound, 1,2-addition to **24**, the anodic wave of **87** is +160 mV and the stretching frequency for the nitrosyl is 1567 cm⁻¹. Encouragingly, the ¹H NMR of **87** shows there to be one major diastereomer present (dr 8:1), implying stereocontrol not only at the metal center, but also of the newly formed ring. Similar to **61**, the HSQC of **87** was used to identify four methylene groups, two of which are part of the ethyl groups attached to the carbonyl, while the other two represent H4 and H2 (Figure 4.3). Furthermore, the up- (3.31 ppm, 1H, d, H9) and down-bound (2.07 ppm, dd, H10) protons were identified by their upfield chemical shift and coupling constant of 9 Hz, which is typical for adjacent alkene coupling. Through COSY correlation to H10, H10a was identified as a multiplet at 2.77 ppm. Once H10a was identified, the remaining assignments were made in a similar fashion to that described for **61** (*vide supra*).

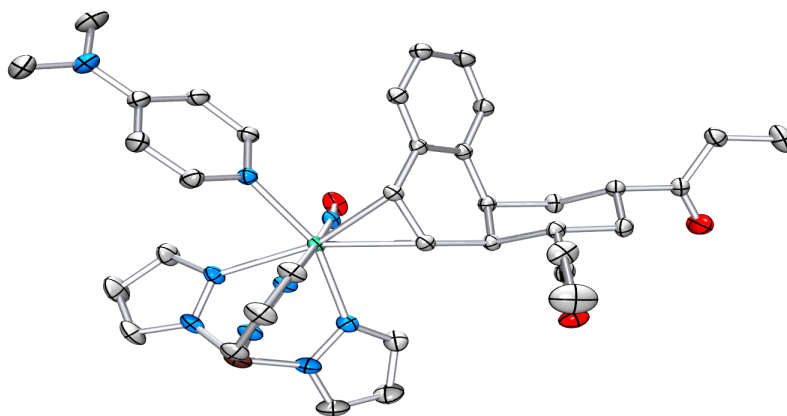


Figure 4.2. Crystal structure of **87**. Bond lengths (Å): Mo—C(9) 2.2348(15); Mo—C(10) 2.2276(15); Mo—N(DMAP) 2.2233(15); Mo—N(NO) 1.7596(14).

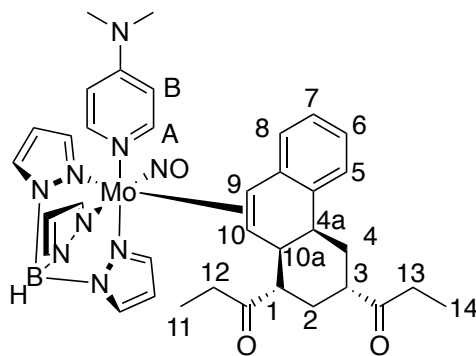


Figure 4.3. Numbering scheme of **87**.

H10a was previously identified, which through COSY correlation led to the assignment of H4a as a multiplet at 3.73 ppm. Furthermore, H10, H4a, and H10a all show strong NOE interaction with Pz3A, which is in agreement with the solid-state depiction of addition occurring *anti* to the metal center. From this analysis it is assumed that the organic isolated from **87** (**61**) would also have a *cis* orientation between H4a and H10a. Dihedral angle analysis to confirm this assumption is not available due the complex splitting pattern of H4a and H10a; however, NOE interaction between these protons is strong, which is in agreement with a *cis* orientation.

The C3 and C1 carbons of **87** are enolizable, which indicates the ability to rearrange until a thermodynamically preferred orientation is achieved. In the case of **87**, as well as **61**, the thermodynamic preference is to place both propanonyl groups in an equatorial position rather than a 1,3-diaxial geometry, which would lead to unfavorable steric interaction (Figure 4.4). This is confirmed by a strong NOE interaction seen between H3 and H1 for complex **87** and the organic **61**. The combination of enolizable carbons and stereochemical control from the metal center allows for improved stereoselectivity during these MIMIRC reactions.

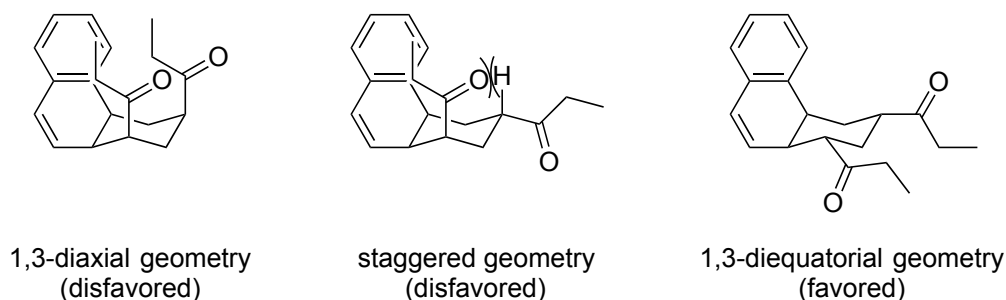


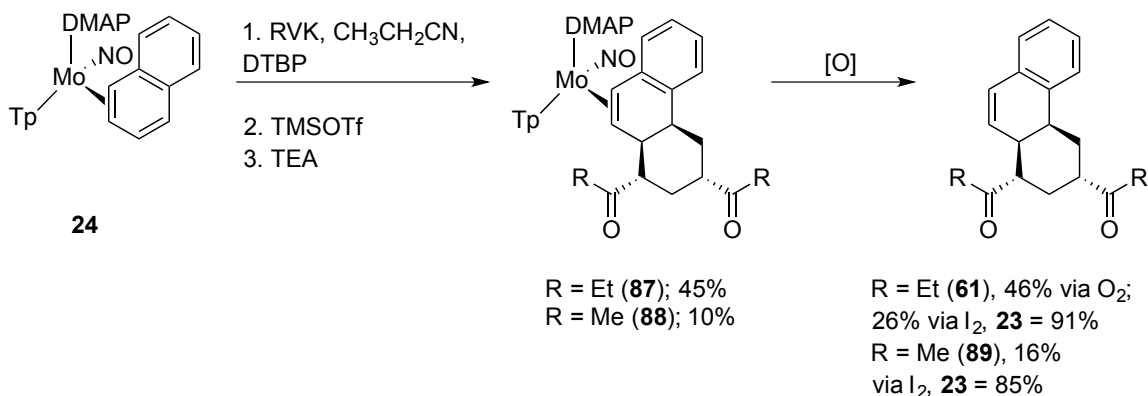
Figure 4.4. Analysis of possible steric interaction among different geometries of **61**.

MVK is also capable of undergoing an [A+A] MIMIRC reaction with **24**; however, the yields for metal complex isolation (**88**) are low (10%). Encouragingly, the spectroscopic assignments made for **87** are identical to **88** with the exception of the methylene protons attributed to the ethyl ketone in **87**. Furthermore, the triplets at 1.00 and 0.68 ppm are no longer present; rather, two singlets at 2.19 and 1.89 ppm are seen in the ^1H NMR of **88**. This implies similar stereocontrol for **88** as that seen for **87**, which is expected.

With the isolation of these complexes, the oxidative decomplexation of their hexahydrophenanthrene organic ligands was pursued. Initial attempts at decomplexation involved a one-pot addition/oxidation sequence directly from the parent naphthalene complex, **24**. A concern during this initial investigation was the presence of a large amount of free naphthalene seen after oxidation. This was believed to be due to a lack of reaction occurring; therefore, upon stirring the reaction mixture open to air, the unreacted complex **24** simply releases free naphthalene. Alternatively, the presence of naphthalene could result from the retro-addition of the organic addition products (**61** and **89**) after the oxidation of complexes **87** and **88**. To discriminate between these two pathways of naphthalene formation, an isolated sample of **87** was dissolved in DCM and stirred open

to air overnight. The resulting mixture was observed by ^1H NMR to reveal **61** as the only diamagnetic product of oxidation, demonstrating that the naphthalene seen in early decomplexation reactions was due to the presence of unreacted **24** in the reaction mixture. Following this, the oxidative decomplexation of the organic products directly from **87** and **88** was accomplished using iodine (Scheme 4.7) yielding **61** and **89** in fair yields with a good recovery of the molybdenum(I) iodo precursor, **23**.

Scheme 4.7. Synthesis of **87** and **88** and their subsequent oxidations to yield **61** and **89**.



To further demonstrate the promise that this method of Michael-Michael ring closure has, [A+B] MIMIRC reactions of **24** were investigated. The goal of this approach is to limit the amount of reactivity once the first Michael acceptor is added to **24** to give a single Michael addition product (e.g., the enolate **82**) and then introduce another Michael acceptor to continue through the ring closure. This was accomplished by limiting the initial Michael acceptor (e.g., EVK) to one molar equivalent so as to prevent a second addition from occurring. For the reactions described in this section the general reaction scheme is as follows: to a $-60\text{ }^\circ\text{C}$ propionitrile solution of **24**, Michael acceptor A (1.0 equivalent), and DTBP, TMSOTf is added; after stirring at $-60\text{ }^\circ\text{C}$ for 1 minute, a

solution of Michael acceptor B (2.5 equivalents) in propionitrile (1 mL) is added to the reaction mixture, which is then left at -60 °C for 18 h.

Using the method described above, success was found when Michael acceptor A was EVK and Michael acceptor B was either MVK or cyclopentenone. The cleanest of these two reactions was the [EVK + MVK] additions, which led to the isolation of the metal complex **90**; however, a pure isolation of **90** is only achieved at a low yield (30%) (Scheme 4.8). This low yield is believed to be due to other side-products from the reaction (*vide infra*). The ¹H NMR of **90** is identical to **87** and **88**; however, it contains a singlet and a triplet in the aliphatic region, rather than two singlets or two triplets. Furthermore, a solid-state structure of **90** was determined through x-ray diffraction as seen in Figure 4.3.

As expected, the solid-state analysis demonstrates a retained 1,3-diequatorial geometry of the alkyl groups. Also seen is a similar *cis* bridgehead with the additions to naphthalene occurring *anti* to the metal center. Although the metal center of **90** can be isolated cleanly at a low yield, more often a higher mass recovery is accomplished with a detriment to purity. For instance, adding iodine to one of these greater mass recovery samples of **90** yields three products, **61**, **89** and the desired [A+B] MIMIRC organic, **91**, in a 1:1:2 ratio. As expected, the ¹H NMR spectrum of **91** shows a great similarity to **61** and **89**, with the exception of the methyl groups' splitting and chemical shifts.

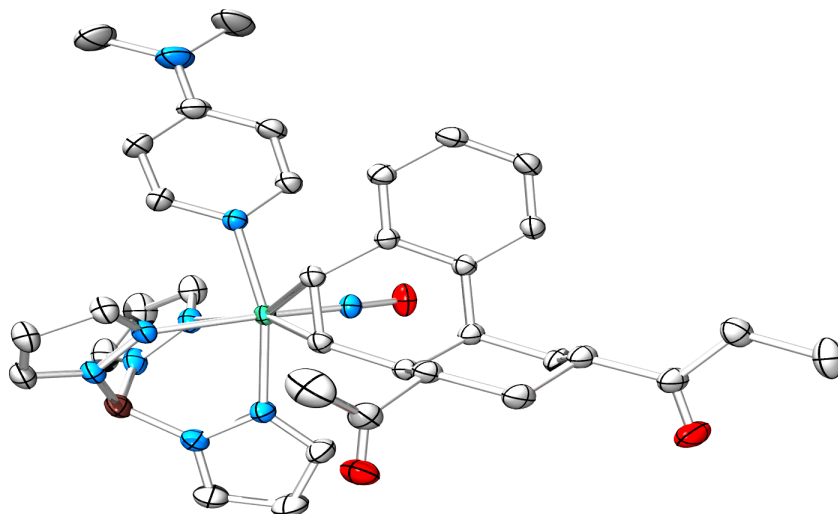
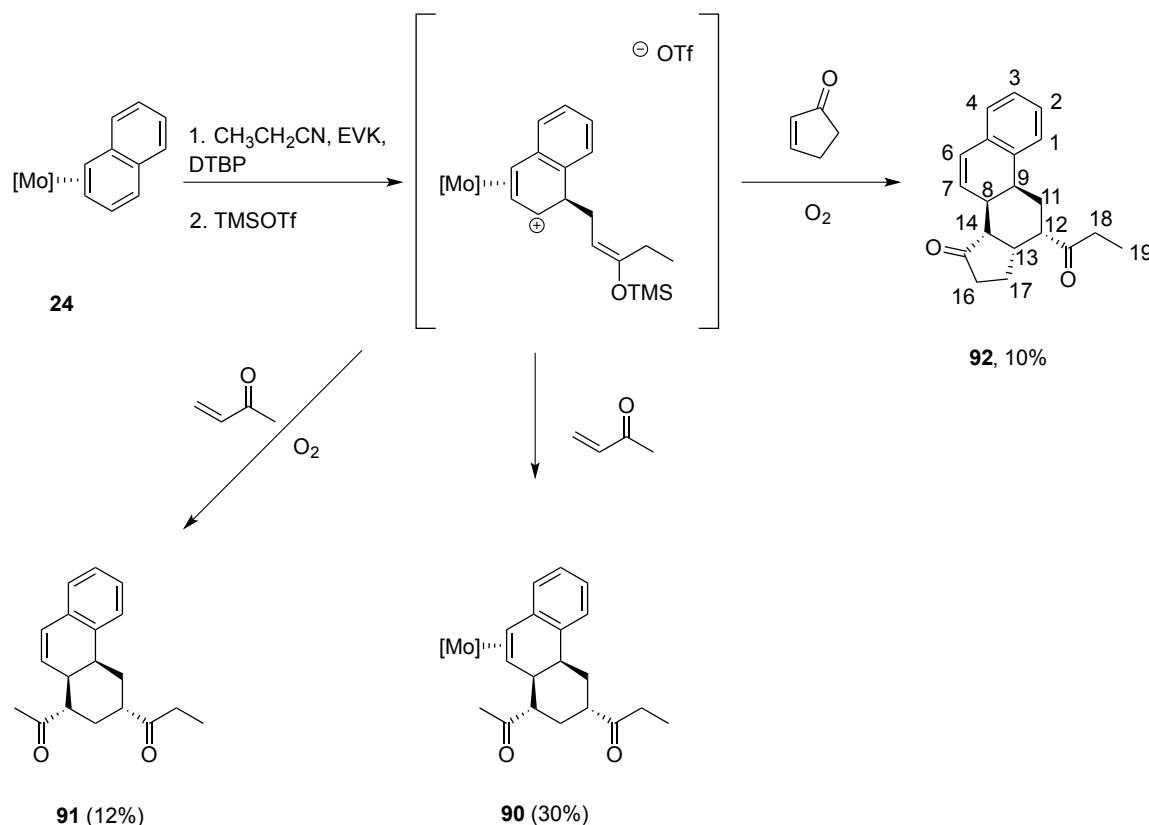


Figure 4.5. Crystal structure of **90**. Bond lengths (Å): Mo—C(9) 2.2291(19); Mo—C(10) 2.226(2); Mo—N(DMAP) 2.2230(18); Mo—N(NO) 1.7549(17).

Further attempts to increase the yield of **90** while retaining purity are underway; however, at this point the only yield confidently reported for **91** is one yielded from an oxidative decomplexation of the reaction mixture, which originates from a pure material, **24**. By stirring the reaction mixture to make **90** exposed to air, **91** can be isolated from **24** in a yield of 12% (Scheme 4.8). In a similar manner, the isolation of **92**, the product of an [EVK + cyclopentenone] MIMIRC addition to **24**, has been achieved at 10% from **24** (Scheme 4.8).

Scheme 4.8. [A+B] MIMIRC additions to **24**.

The ^1H NMR spectrum of **92** contains one major triplet, indicating one [A+B] MIMIRC product, with < 10% impurity determined to be **86**. Although the ^1H NMR spectrum of **92** is convoluted between 2.60 and 1.90 ppm, it is believed that the full characterization of this compound has been carefully completed including the relative stereochemistry of the five newly created stereocenters (Figure 4.6). Correlations observed in the ^1H - ^{13}C HSQC spectrum of **92** show the presence of one primary carbon, four secondary carbons, and five tertiary carbons in the aliphatic region. From a COSY correlation with the alkene peak at 6.15 (dd, H7) ppm, H8 was identified as a multiplet (2.25 ppm). A notably similar peak seen in each of the ^1H NMR spectra of **61**, and **87** -

90 was a multiplet at 3.26 ppm. This peak was determined to represent H9 due to its coupling with H8 as well as with methylene protons at 2.45 and 2.17 ppm. These geminal protons show strong NOE interactions with H2, which confirm their identity as H11. Furthermore, H11 couples to a proton at 3.11 ppm (dt, $J = 13.0$ & 4.4 Hz), which is bound to a tertiary carbon identifying this proton as H12. H12 couples to a proton at 2.57 ppm, which is bound to a tertiary carbon, thus 2.57 ppm was identified as corresponding to H13. H13 couples with geminal protons at 1.97 and 1.69 ppm (H17) as well as with a proton at 2.06 (dd, $J = 12.2$ and 6.7 Hz) ppm that is bound to a tertiary carbon (H14). As confirmation, it was observed in the NMR spectrum that H15 couples to H8.

Of the protons mentioned above, only two splitting patterns were able to be unambiguously identified - H14 and H12. Due to this lack of coupling information, only a few assumptions can be made about the stereochemical assignments of **92**. Assuming a similar stereoselectivity determined by the metal center, protons H8 and H9 will be *cis* to one another, which is in agreement with their strong NOE interaction. Also assumed is that the enolizable carbons adjacent to H14 and H12 will isomerize to a thermodynamically preferred 1,3-diequatorial geometry, which is in agreement with the strong NOE interaction between H12 and H14. Using these assumptions, two models of **92** were built and optimized in Gaussian using a Semi-Empirical method. These two models were based on the two stereoisomers of H13, identified as *cis* or *trans* in relation to H12 and H14 (Figure 4.4). From this, the dihedral angles between H12 to H13 and H12 to H11 (labeled *cis* or *trans* in relation to H12) were identified and subsequently used to predict coupling constants based on the Karplus equation (Tables 4.2 and 4.3).¹⁵

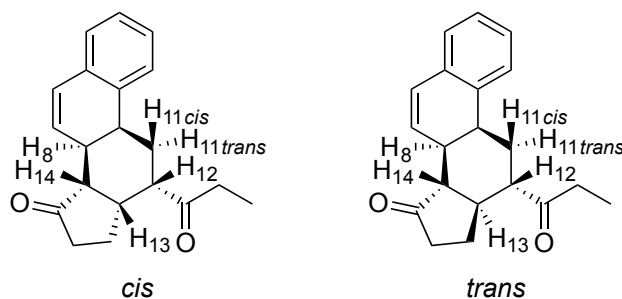


Figure 4.6. *Cis* and *trans* orientations of H13 in **92**.

Table 4.2. Predicted coupling constants where H13 is in a *cis* orientation to H14 and H12.

H13 <i>cis</i> to H14 and H12			
Protons Considered	Dihedral Angle (°)	Dihedral Angle (rad)	Coupling Constant (Hz)
H14 H8	160	2.72	11.66
H14 H13	34	0.578	7.02
H13 H12	46	0.782	5.03
H12 H11 <i>cis</i>	62	1.054	2.44
H12 H11 <i>trans</i>	177	3.009	13.76

Table 4.3. Predicted coupling constants where H13 is in a *trans* orientation to H14 and H12.

H13 <i>trans</i> to H14 and H12			
Protons Considered	Dihedral Angle (°)	Dihedral Angle (rad)	Coupling Constant (Hz)
H14 H8	179	3.043	13.86
H14 H13	171	2.907	13.24
H13 H12	176	2.992	13.69
H12 H11 <i>cis</i>	61	1.037	2.59
H12 H11 <i>trans</i>	176	2.992	13.69

When H13 is *cis* to H12 and H14, the coupling constant between H12 and H13 is predicted to be 5.03 Hz, which is similar to the coupling constant predicted between H12

and H11*cis* (2.44 Hz). The coupling constant between H12 and H11*trans* is predicted to be 13.76 Hz. With coupling between H13 and H11, H12 is expected to resemble a doublet-of-doublet-of-doublets; however, with similar coupling constants between H11*cis* and H13, H12 would most likely be observed as a doublet-of-triplets. In contrast, were H13 in a *trans* orientation to H12, a triplet-of-doublets is predicted due to the similarities in coupling constants from H13 and H11*trans* (13.69 Hz). From this prediction, and the identification of the H12 resonance as a doublet-of-triplets at 3.11 ppm, it was determined that H13 orients *cis* to H12 and H14. To help confirm the accuracy of the predicted values, the only other resolved splitting pattern, H14 (dd, $J = 12.2$ and 6.7 Hz), was also compared. This comparison again shows the *cis* orientation to be in the best agreement with the predicted values. Future attempts will aim to isolate a crystal structure of **92** to confirm these stereochemical determinations.

The isolation of **92** demonstrates future potential for the utility of this method. From naphthalene, a steroidal core containing five new stereocenters and three new carbon-carbon bonds can be isolated (Figure 4.5). Although a majority of naturally occurring steroidal cores have a *trans* bridgehead between rings B and C (Figure 4.5), there have been recent investigations into the effect of inversion of stereochemistry at C8 of steroidal estrogens (**93** and **94**).¹⁶⁻²⁰ These investigations showed **93** and **94** to have an affinity for estrogen receptors while also providing osteoprotective action, a significant benefit for their use in hormone replacement therapy. Although this inversion is not widely studied, the development of a library of B/C *cis* fused ring junctures of steroidal cores could provide more detail into their use. Furthermore, compounds **61**, **89**, and **91** contain the same hexhydrophenanthrene core as substituted tetralins that have been

studied for their efficacy as selective estrogen receptor-beta agonists.²¹ These hexahydrophenanthrenes also share a similar core as aromatic abietane diterpenoids (i.e., carnosic acid, ferruginol, and abietic acid). These abietane diterpenoids have been thoroughly studied for their antimicrobial and antibacterial properties.^{22, 23}

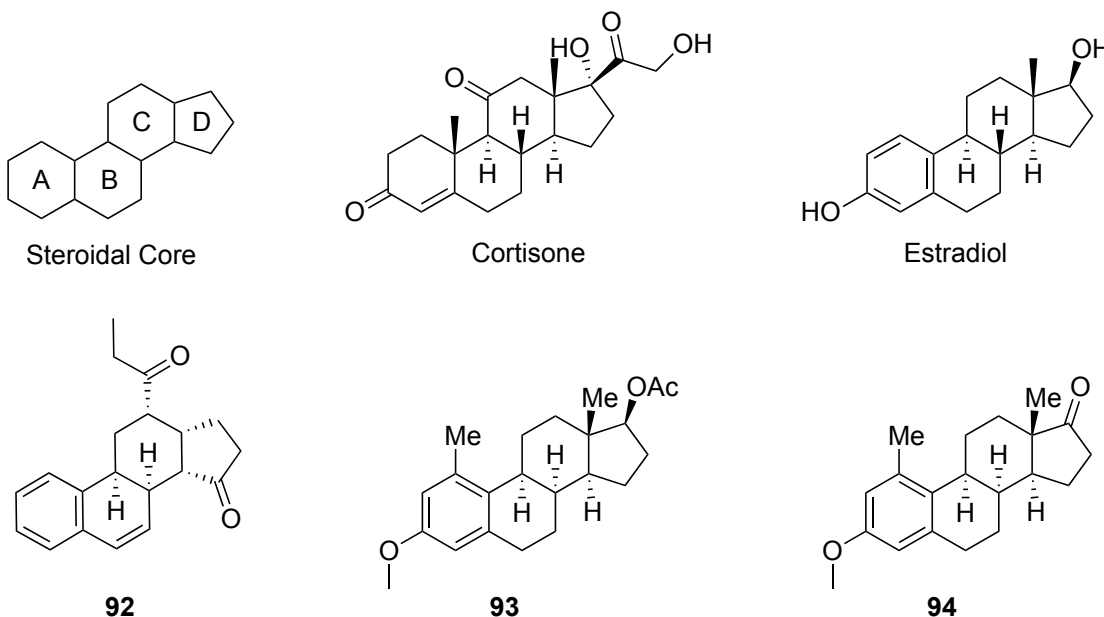
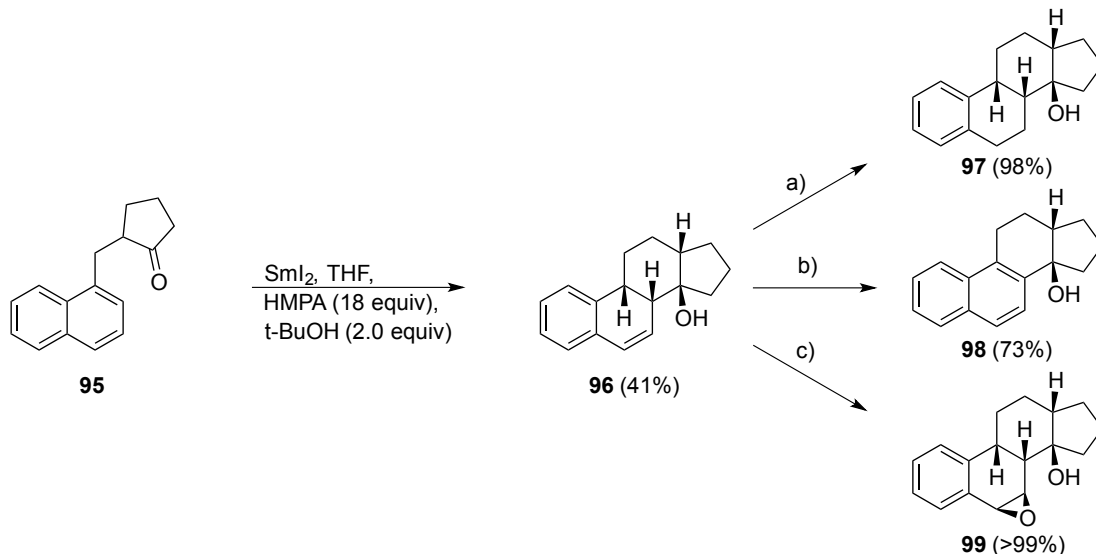


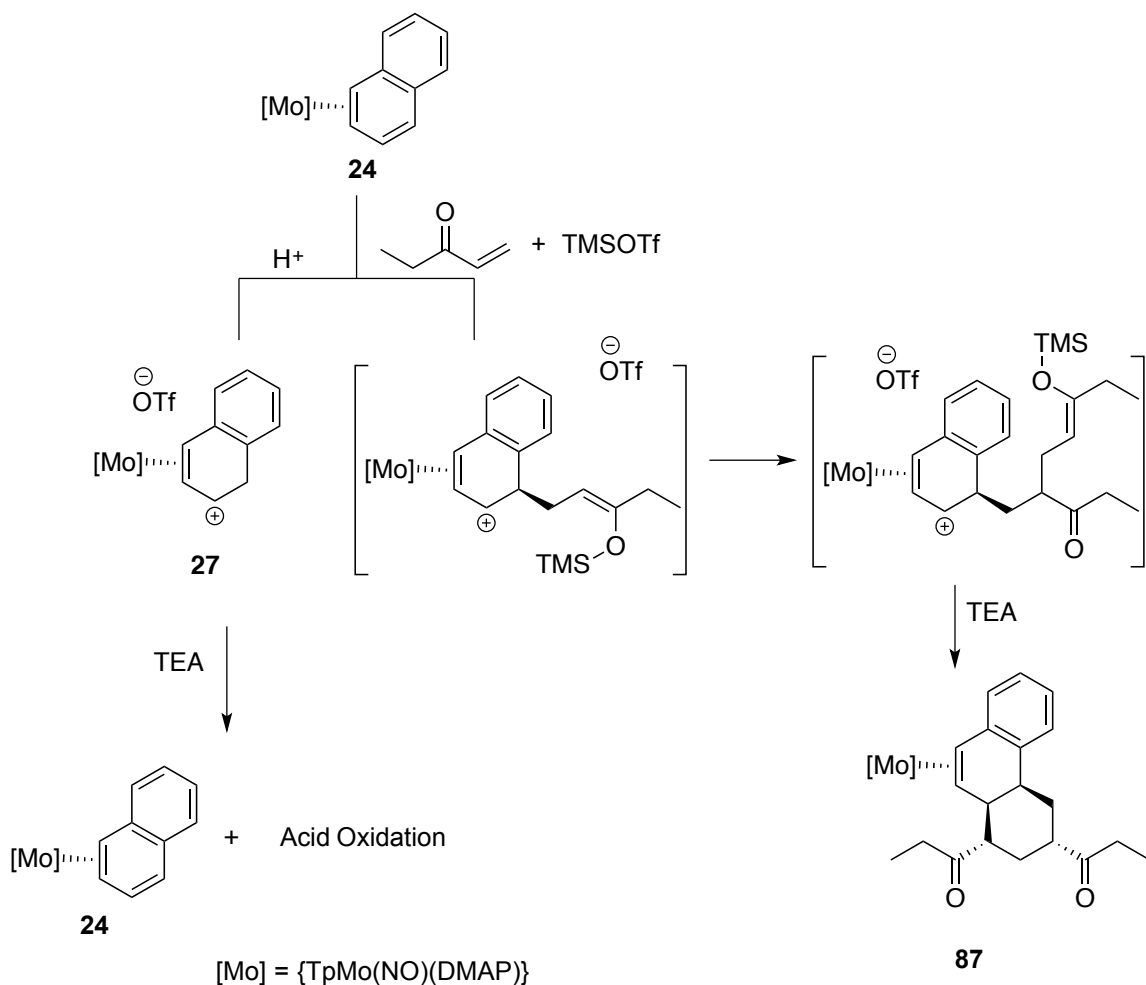
Figure 4.7. Examples of steroidal cores found in the literature.

To our knowledge, only one other example of the synthesis of a steroidal core from naphthalene has been shown: the report by Mathias Berndt *et al.* using samarium diiodide to close a pendant cyclopentanone (Scheme 4.8). Furthermore, Berndt demonstrated the synthetic potential of this methodology by subjecting **96** to additions like catalytic hydrogenation (**97**), oxidation (**98**) with MnO_2 , as well as epoxidation with mCPBA (**99**).^{24, 25} It is presumed that a similar reactivity with **92** would be seen, which would lead to further derivatization.

Scheme 4.8. Samarium diiodide-induced cyclization of naphthyl-substituted ketone (**95**).

Conditions: (a) Pd/C, H_2 , MeOH, rt; (b) MNO_2 , THF, D; (c) *m*-CPBA, MeOH, 0 °C

The optimization of MIMIRC additions to **24** has provided good insight into the reaction conditions needed for their synthesis. As mentioned previously, a significant amount of free naphthalene is obtained during the isolation of **61**, **89**, **91**, and **92** from their respective reaction mixtures. CV monitoring of these reactions often shows a 1:1 ratio of the desired complex ($\sim +200$ mV) and **24** (~ -160 mV). In circumstances where the ratio is in favor of the desired complex in comparison to **24**, an increase in decomposition is seen ($E_{\text{p,c}} \sim -900$ mV). The primary cause of this is believed to be due to a competition between the protonation of **24** and the electrophilic addition of EVK to **24** (Scheme 4.9). Once **24** is protonated, the allyl **27** (see Chapter 3) remains unreactive until TEA is added to stop the reaction, which deprotonates **27** back to **24**.

Scheme 4.9. Competitive pathways encountered during the synthesis of **87**.

The conditions described in entry 12 of Table 4.1 were varied in attempts to increase the reaction progress; however, no further improvements have been made to date. These attempts include increasing the temperature, equivalents of TMSOTf and DTBP , and strength of base present in the reaction mixture. Although these attempts have not improved the reaction progress, a significant increase in decomposition ($E_{\text{p,c}} \sim -900$ mV) is seen. Efforts to purify all reagents through distillation and storage over molecular sieves do not appear to prevent the purported protonation of **24**.

Also desired is a better control during the [A+B] MIMIRC additions. For instance, in the [EVK + MVK] addition to **24**, limiting the equivalents of EVK did not provide full control as **61** and **89** were also obtained in these reactions. While the optimization of this reaction is underway, future attempts to use substituted naphthalenes, vinyl ketones, and cyclopentenones could provide a simple one-pot method for synthesizing various steroidal cores with improved stereocontrol.

4.3 Conclusion

With these examples of MIMIRC additions to **24**, several key features should be noted. First, from a fully aromatic core (naphthalene), organic products with no less than four new stereocenters and three new carbon-carbon bonds have been isolated and characterized. Second, the isolation of complexes from [A+A] MIMIRC reactions has been demonstrated with EVK and MVK, giving promise for optimization of the additional MIMIRC reactions described above. Finally, the regenerative oxidative decomplexation of these complexes with iodine to liberate the functionalized organic ligands, while also recovering a metal precursor complex, has been accomplished.

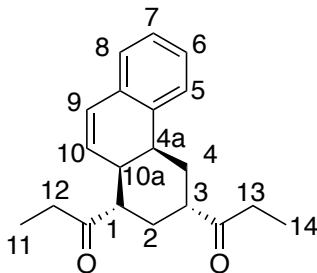
4.4 Experimental

General Methods

NMR spectra were obtained on a 600 or 800 MHz spectrometer. All chemical shifts are reported in ppm, and proton and carbon shifts are referenced to tetramethylsilane (TMS) utilizing residual ^1H or ^{13}C signals of the deuterated solvents as an internal standard. Coupling constants (J) are reported in hertz (Hz). Infrared spectra (IR) were recorded as a glaze on a spectrometer fitted with a horizontal attenuated total reflectance (HATR) accessory or on a diamond anvil ATR assembly. Electrochemical experiments were performed under a dinitrogen atmosphere. Cyclic voltammetry data were taken at ambient temperature ($\sim 25^\circ\text{C}$) at 100 mV/s in a standard three electrode cell with a glassy-carbon working electrode, *N,N*-dimethylacetamide (DMAc) or acetonitrile (CH_3CN) solvent (unless otherwise specified), and tetrabutylammonium hexafluorophosphate (TBAH) electrolyte (approximately 0.5 M). All potentials are reported versus NHE (normal hydrogen electrode) using cobaltocenium hexafluorophosphate ($E_{1/2} = -0.78\text{ V}$), ferrocene ($E_{1/2} = +0.55\text{ V}$), or decamethylferrocene ($E_{1/2} = +0.04\text{ V}$) as an internal standard. The peak-to-peak separation was less than 100 mV for all reversible couples. Unless otherwise noted, all synthetic reactions were performed in a glovebox under a dry nitrogen atmosphere. Deuterated solvents were used as received. Pyrazole (Pz) protons of the hydridotris(pyrazolyl)borate (Tp) ligand were uniquely assigned (e.g., “Pz3B”) using a combination of two-dimensional NMR data and 4-(dimethylamino)pyridine–proton NOE interactions (See Figure 3.4). When unambiguous assignments were not possible, Tp protons were labeled as “Pz3/5 or Pz4”. BH peaks (around 4–5 ppm) are not identified

due to their quadrupole broadening; IR data are used to confirm the presence of a BH group (around 2500 cm^{-1}). All J values for Pz protons are $2 (\pm 0.2)$ Hz.

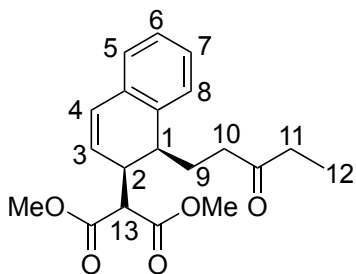
Synthesis of 1,1'-((1*S*,3*S*,4*aS*,10*aS*)-1,2,3,4,4*a*,10*a*-hexahydrophenanthrene-1,3-diyl)bis(propan-1-one) (61).



24 (200 mg, 0.34 mmol), $\text{CH}_3\text{CH}_2\text{CN}$ (6 mL), EVK (0.1 mL, 1.0 mmol), and DTBP (54 mg, 0.3 mmol) were added to a test tube. The reaction mixture was then cooled at $-60\text{ }^\circ\text{C}$ for 15 min. TMSOTf (0.1 mL, 0.5 mmol) was added to the reaction mixture, and the resulting red solution was left stirring at $-60\text{ }^\circ\text{C}$ overnight (~ 18 h). TEA (0.1 mL, 0.74 mmol) was added to the reaction mixture, which was subsequently removed from the glovebox and stirred open to air overnight (~ 18 h). The resulting brown mixture was evaporated *in vacuo*, and the resulting film was dissolved in DCM (1 mL). This solution was then added stirring Et_2O (50 mL), yielding a brown precipitation. The brown precipitate was filtered off on a 15 mL medium porosity fritted disc and washed with Et_2O (3 x 5 mL). The filtrate was then evaporated *in vacuo*. This oil was then dissolved in DCM (3 x 0.3 mL) and the resulting solution was dropwise added onto a 250 μm silica preparatory plate. The product was eluted with 10% EtOAc:hexanes (200 mL), scraped off as a band at R_f : 0.30-0.40 and this silica gel was sonicated in EtOAc (20 mL) for 15

min. The silica was filtered off on a 15 mL fine porosity fritted disc and washed with DCM (3 x 5 mL). The filtrate was evaporated *in vacuo* and desiccated for 15 min to yield the colorless oil **61** (23 mg, 23% yield). IR: $\nu(\text{C-H sp}^2) = 2933 \text{ cm}^{-1}$, $\nu(\text{CO}) = 1702 \text{ cm}^{-1}$. ^1H NMR (CDCl_3 , δ): 7.28 (1H, d, $J = 7.3$, H5), 7.26 (1H, t, $J = 7.0$, H6/7), 7.21 (1H, t, $J = 7.0$, H6/7), 7.10 (1H, d, $J = 7.3$, H8), 6.45 (1H, d, $J = 9.6$, H9), 6.01 (1H, dd, $J = 9.6$ & 6.20, H10), 3.34 (1H, bs, H4a), 2.70 (2H, m, H3 & H4), 2.57 (1H, m, H10a), 2.55 (2H, m, H13), 2.42 (2H, m, H1 & H12), 2.27 (1H, dq, $J = 18.0$ & 7.3, H12), 1.85 (1H, m, H2), 1.80 (1H, m, H4), 1.43 (1H, m, H2), 1.09 (3H, t, $J = 7.4$, H14), 0.98 (3H, t, $J = 7.2$, H11). ^{13}C NMR (CDCl_3 , δ): 213.4 (CO), 213.2 (CO), 135.4 (C8a/4b), 134.2 (C8a/4b), 131.2 (C10), 128.2 (C9), 127.9 (C6/7), 127.1 (C8), 126.7 (C6/7), 124.8 (C4), 49.3 (C1), 44.4 (C3), 37.2 (C10a), 36.5 (C12), 35.9 (C4a), 34.0 (C13), 30.9 (C2), 27.8 (C4), 7.9 (C11/14), 7.6 (C11/14). EA: Calculated for $\text{C}_{20}\text{H}_{24}\text{O}_2 \cdot 0.25 \text{ CH}_2\text{Cl}_2$: C, 76.57; H, 7.77. Found: C, 76.50; H, 7.88.

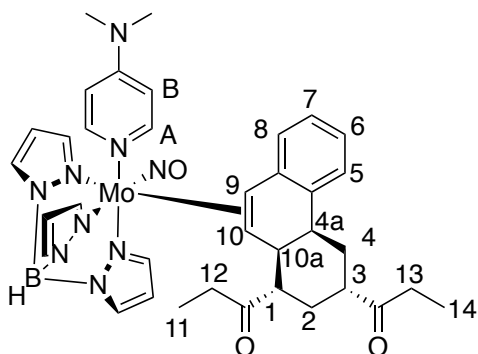
Synthesis of dimethyl 2-((1*S*,2*S*)-1-(3-oxopentyl)-1,2-dihydronaphthalen-2-yl)malonate (72).



24 (100 mg, 0.17 mmol), CH₃CH₂CN (3 mL), and EVK (0.1 mL, 1.0 mmol) were added to a test tube. The reaction mixture was then cooled at -50 °C for 15 min. A -50 °C 1M solution of HOTf in CH₃CH₂CN (0.4 mL, 0.4 mmol) was added to the reaction mixture, and the resulting red solution was left stirring at -50 °C overnight (~18 h). LiDMM (248 mg, 1.8 mmol) was added to the reaction mixture, which was then left at -50 °C for 30 min. The resulting brown solution was evaporated to an oil that was then dissolved in CHCl₃ (10 mL). This solution was then washed with NaHCO₃ (sat. aq., 10 mL), dried with MgSO₄, and filtered through a 15 mL medium porosity fritted disc. The filtrate was evaporated *in vacuo* to an oil that was then dissolved in DCM (1 mL) and added to stirring hexanes (50 mL). The resulting precipitate was collected on a 15 mL fine porosity fritted disc, washed with hexanes (3 x 15 mL), and taken outside of the glovebox. The precipitate was dissolved in DCM (10 mL) and this solution was stirred open to air overnight. The resulting oil was dissolved in DCM (3 x 0.3 mL) and this solution was dropwise added onto a 250 µm silica preparatory plate. The product was eluted with 10% EtOAc:hexanes (200 mL), scraped off as a band at R_f: 0.3-0.4 and this silica gel was sonicated in EtOAc (20 mL) for 15 min. The silica was filtered off on a 15 mL medium porosity fritted disc and washed with DCM (3 x 2 mL). The filtrate was

evaporated *in vacuo* and desiccated to yield the colorless oil **72** (3 mg, 5% yield). IR: $\nu(\text{C-H sp}^2) = 2974 \text{ cm}^{-1}$, $\nu(\text{CO}) = 1755, 1736, \text{ and } 1712 \text{ cm}^{-1}$. $^1\text{H NMR}$ (CDCl_3 , δ): 7.21 (1H, t, $J = 7.7$, H6/7), 7.16 (1H, t, $J = 7.7$, H6/7), 7.07 (1H, d, $J = 7.4$, H5), 6.98 (1H, d, $J = 7.2$, H8), 6.48 (1H, dd, $J = 10.0, 2.7$, H4), 5.64 (1H, d, $J = 8.3$, H3), 3.85 (3H, s, OMe), 3.79 (1H, d, $J = 11.6$, H13), 3.76 (3H, s, OMe), 3.47 (1H, m, H2), 2.72 (1H, m, H1), 2.30 (2H, q, $J = 7.9$, H11), 2.17 (2H, m, H10), 1.75 (2H, m, H9), 0.98 (1H, t, $J = 7.9$, H12). $^{13}\text{C NMR}$ (CDCl_3 , δ): 210.9, 168.9, 168.6, 137.5, 132.9, 128.5, 127.8, 127.2, 126.8, 126.5, 52.8, 52.7, 52.5, 52.3, 39.8, 39.1, 35.9, 20.6, 7.8.

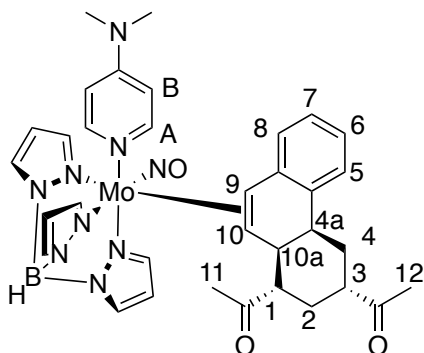
Synthesis of $\text{TpMo}(\text{NO})(\text{DMAP})(\eta^2\text{-}1,1'\text{-(}1S,3S,4aS,10aS\text{)-}1,2,3,4,4a,10a\text{-hexahydrophenanthrene-1,3-diyl})\text{bis}(\text{propan-1-one})$ (87**).**



24 (200 mg, 0.34 mmol), $\text{CH}_3\text{CH}_2\text{CN}$ (6 mL), EVK (84 mg, 1.0 mmol), and DTBP (54 mg, 0.3 mmol) were added to a test tube. The reaction mixture was then cooled at -60°C for 15 min. TMSOTf (0.1 mL, 0.5 mmol) was added to the reaction mixture, and the resulting red solution was left stirring at -60°C overnight (~ 18 h). TEA (0.1 mL, 0.74 mmol) was added to the reaction mixture, which was subsequently warmed to room temperature. This solution was then chromatographed through a 30 mL fine porosity

fritted disc $\frac{3}{4}$ full with silica gel. The product was eluted with 1:1 Et₂O:THF (50 mL) as a yellow band, collected as a yellow solution, and evaporated *in vacuo*. The resulting oil was dissolved in DCM (1 mL) and the product was precipitated in stirring pentane (50 mL). The precipitate was collected on a 15 mL fine porosity fritted disc, washed with pentane (3 x 10 mL), and dried for 15 min yielding the yellow solid **87** (115 mg, 45%). CV (DMAc) $E_{p,a} = +0.16$ V (NHE). IR: $\nu(\text{C-H sp}^2) = 2932\text{ cm}^{-1}$, $\nu(\text{B-H}) = 2480\text{ cm}^{-1}$, $\nu(\text{CO}) = 1703$ and 1620 cm^{-1} , $\nu(\text{NO}) = 1562\text{ cm}^{-1}$. ¹H NMR (d⁶-Acetone, δ): 7.93 (1H, d, Pz5A), 7.87 (1H, d, Pz3A), 7.79 (1H, d, Pz5B), 7.69 (1H, d, Pz3C), 7.41 (2H, bs, DMAP-A), 7.35 (1H, d, $J = 7.9$, H5), 6.98 (1H, d, Pz3B), 6.93 (1H, t, $J = 7.5$, H6), 6.86 (1H, t, $J = 7.5$, H7), 6.51 (2H, m, DMAP-B), 6.37 (1H, t, Pz4A), 6.35 (1H, t, Pz4C), 6.21 (1H, d, $J = 7.2$, H8), 6.09 (1H, t, Pz4B), 3.73 (1H, m, H4a), 3.31 (1H, d, $J = 9.0$, H9), 3.06 (6H, s, NMe), 2.84 (1H, m, H4), 2.77 (1H, m, H10a), 2.65 (3H, m, H3, H1, & H13/12), 2.55 (1H, m, H13/H12), 2.40 (1H, m, H13/H12), 2.30 (1H, m, H13/12), 2.07 (1H, dd, $J = 9.0$ & 2.6 , H10), 1.87 (1H, m, H4), 1.70 (1H, m, H2), 1.52 (1H, q, $J = 12.4$, H2), 1.00 (3H, t, $J = 7.3$, H11/H14), 0.68 (3H, t, $J = 7.2$, H11/14). ¹³C NMR (d⁶-Acetone, δ): 215.1 (CO), 213.8 (CO), 155.1 (DMAP-C), 150.7 (DMAP-A), 144.7 (Pz5), 143.6 (Pz3A), 142.1 (Pz3B), 141.2 (Pz3C), 137.6 (Pz5), 136.9 (Pz5), 135.8, 134.1, 128.1 (C8), 125.6 (C5), 125.1 (C7), 123.9 (C6), 108.3 (2C, DMAP-B), 106.9 (Pz4A/C), 106.8 (Pz4A/C), 106.5 (Pz4B), 70.9 (C10), 68.1 (C9), 55.0, 45.3, 43.1 (C10a), 39.3, 37.5, 35.9 (C4a), 34.3, 32.6 (C2), 31.0 (C4), 8.2 (C11/14), 7.8 (C11/14).

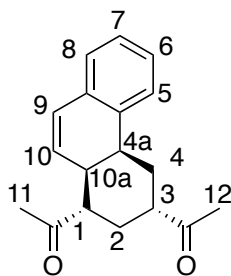
Synthesis of $\text{TpMo(NO)}(\text{DMAP})(\eta^2\text{-1,1'-}((1S,3S,4aS,10aS)\text{-1,2,3,4,4a,10a-hexahydrophenanthrene-1,3-diyl})\text{bis(ethan-1-one)})$ (**88**).



24 (200 mg, 0.34 mmol), $\text{CH}_3\text{CH}_2\text{CN}$ (6 mL), MVK (0.1 mL, 1.0 mmol), and DTBP (54 mg, 0.3 mmol) were added to a test tube. The reaction mixture was then cooled at $-60\text{ }^\circ\text{C}$ for 15 min. TMSOTf (0.1 mL, 0.5 mmol) was added to the reaction mixture, and the resulting red solution was left stirring at $-60\text{ }^\circ\text{C}$ overnight ($\sim 18\text{ h}$). TEA (0.1 mL, 0.74 mmol) was added to the reaction mixture, which was subsequently warmed to room temperature. This solution was then chromatographed through a 30 mL fine porosity fritted disc $\frac{3}{4}$ full with silica gel. The product was eluted with 1:1 $\text{Et}_2\text{O}:\text{THF}$ (50 mL) as a yellow band, collected as a yellow solution, and evaporated *in vacuo*. The resulting oil was dissolved in DCM (1 mL) and the product was precipitated in stirring pentane (50 mL). The precipitate was collected on a 15 mL fine porosity fritted disc, washed with pentane (3 x 10 mL), and dried for 15 min yielding the yellow solid **88** (25 mg, 10%). CV (DMAc) $E_{\text{p,a}} = +0.17\text{ V}$ (NHE). IR: $\nu(\text{C-H sp}^2) = 2920\text{ cm}^{-1}$, $\nu(\text{B-H}) = 2478\text{ cm}^{-1}$, $\nu(\text{CO}) = 1698\text{ and }1619\text{ cm}^{-1}$, $\nu(\text{NO}) = 1562\text{ cm}^{-1}$. $^1\text{H NMR}$ ($\text{d}^6\text{-Acetone}$, δ): 7.94 (1H, d, Pz5A/C), 7.91 (1H, d, Pz3A), 7.88 (1H, d, Pz5A/C), 7.78 (1H, d, Pz5B), 7.72 (1H, d, Pz3C), 7.37 (2H, bs, DMAP-A), 7.34 (1H, d, $J = 7.5$, H5), 6.98 (1H, d, Pz3B), 6.94 (1H, td, $J = 7.5 \text{ \& } 1.5$, H6), 6.86 (1H, t, $J = 7.4$, H7), 6.50 (2H, m, DMAP-B), 6.36 (2H, m,

Pz4A&C), 6.24 (1H, dd, $J = 7.6$ & 1.0 , H8), 6.09 (1H, t, Pz4B), 3.79 (1H, m, H4a), 3.72 (1H, d, $J = 9.5$, H9), 3.05 (6H, s, NMe), 2.87 (1H, m, H4), 2.79 (1H, m, H10a), 2.59 (2H, m, H3 & H1), 2.19 (3H, s, H13), 2.14 (1H, dd, $J = 9.5$ & 2.5 , H10), 1.89 (3H, s, H12), 1.86 (1H, m, H4), 1.77 (1H, m, H2), 1.52 (1H, q, $J = 12.6$, H2). ^{13}C NMR (d^6 -Acetone, δ): 212.5 (CO), 211.0 (CO), 154.9 (DMAP-C), 151.1 (2C, DMAP-A), 144.6 (C4b/9a), 143.5 (Pz3A), 141.9 (Pz3B), 141.3 (Pz3C), 137.5 (Pz5A/C), 136.8 (Pz5A/C), 135.7 (Pz5B), 133.8 (C4b/9a), 128.0 (C8), 125.4 (C5), 124.9 (C7), 123.8 (C6), 108.1 (2C, DMAP-B), 106.9 (Pz4A/C), 106.6 (Pz4A/C), 106.3 (Pz4B), 70.4 (C10), 68.0 (C9), 55.9 (C1/3), 45.9 (C1/3), 42.7 (C10a), 39.1 (2C, DMAP-Me), 35.5 (C4a), 32.2 (C2), 30.7 (C4), 30.2 (C11), 28.1 (C12).

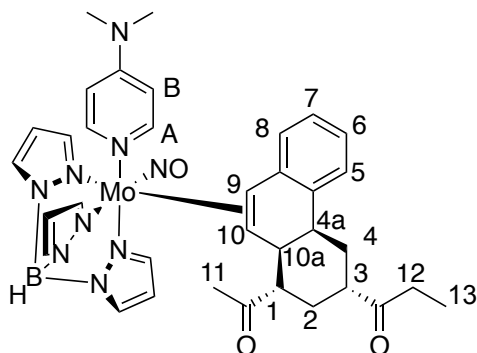
Synthesis of 1,1'-((1*S*,3*S*,4*aS*,10*aS*)-1,2,3,4,4*a*,10*a*-hexahydrophenanthrene-1,3-diyl)bis(ethan-1-one) (89).



To a 50 mL filter flask charged with a stir pea were added **24** (50 mg, 0.07 mmol), DCM (5 mL), and a 0.06 M solution of $\text{I}_2/\text{Et}_2\text{O}$ (0.6 mL, 0.035 mmol), resulting in a green solution. This solution was stirred at RT for 5 min and evaporated *in vacuo*. The resulting green oil was dissolved in DCM (1 mL) forming a green solution. This solution was added to stirring hexanes (50 mL) giving a green precipitation. The green precipitate was collected on a 15 mL fine porosity fritted disc, washed with hexanes (3 x 10 mL), and

desiccated to yield **3** (35 mg, 85%). The filtrate was removed from the glovebox and evaporated *in vacuo* to an oil. The oil was dissolved in DCM (3 x 0.3 mL) and the resulting solution was dropwise added onto a 250 μ m silica preparatory plate. The product was eluted with 10% EtOAc:hexanes (200 mL), scraped off as a band at R_f : 0.27-0.4 and this silica gel was sonicated in EtOAc (20 mL) for 15 min. The silica was filtered off on a 15 mL medium porosity fritted disc and washed with DCM (3 x 2 mL). The filtrate was evaporated *in vacuo* and desiccated to yield the colorless oil **89** (3 mg, 16% yield). IR: $\nu(\text{C-H sp}^2) = 2921 \text{ cm}^{-1}$ $\nu(\text{CO}) = 1701 \text{ cm}^{-1}$. ^1H NMR (CDCl_3 , δ): 7.28 (1H, d, $J = 7.3$, H5), 7.27 (1H, m, H6/7), 7.22 (1H, m, H6/7), 7.10 (1H, d, $J = 7.3$, H8), 6.46 (1H, d, $J = 9.6$, H9), 1H, dd, $J = 9.6$ & 6.08, H10), 3.35 (1H, m, H4a), 2.73 (1H, m, H4), 2.70 (1H, m, H3), 2.54 (1H, m, H10a), 2.45 (1H, td, $J = 12.2$ & 3.5, H1), 2.23 (3H, s, H13), 2.07 (3H, s, H12), 1.95 (1H, m, H2), 1.77 (1H, m, H4), 1.42 (1H, q, $J = 12.3$, H2). ^{13}C NMR (CDCl_3 , δ): 210.8 (CO), 210.6 (CO), 135.3 (C9a/4b), 134.2 (C9a/4b), 131.2 (C10), 128.2 (C9), 128.0 (C6/7), 127.1 (C8), 126.8 (C6/7), 124.8 (C5), 50.2 (C1), 45.3 (C3), 37.0 (C10a), 35.9 (C4a), 30.5 (C2), 30.2 (C11), 28.2 (C12), 27.7 (C4).

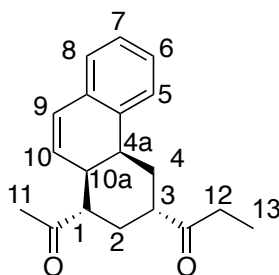
Synthesis of $\text{TpMo}(\text{NO})(\text{DMAP})(\eta^2\text{-1-}(((1S,3S,4aS,10aS)\text{-1-acetyl-1,2,3,4,4a,10a-hexahydrophenanthren-3-yl})\text{propan-1-one}))$ (90**).**



$\text{TpMo}(\text{NO})(\text{DMAP})(\text{naphthalene})$ (200 mg, 0.34 mmol), $\text{CH}_3\text{CH}_2\text{CN}$ (6 mL), EVK (33 mg, 0.4 mmol), and DTBP (54 mg, 0.3 mmol) were added to a test tube. The reaction mixture was then cooled at $-60\text{ }^\circ\text{C}$ for 15 min. TMSOTf (0.1 mL, 0.5 mmol) was added to the reaction mixture, and the resulting red solution was left stirring at $-60\text{ }^\circ\text{C}$ 1 min. Next, MVK (50 mg, 0.7 mmol) was added to the reaction mixture, which was then left stirring at $-60\text{ }^\circ\text{C}$ overnight ($\sim 18\text{ h}$). TEA (0.1 mL, 0.74 mmol) was added to the reaction mixture, which was subsequently warmed to room temperature. This solution was then chromatographed through a 60 mL medium porosity fritted disc $\frac{3}{4}$ full with silica gel. The product was eluted with Et_2O (50 mL) as a yellow band, collected as a yellow solution, and evaporated *in vacuo*. The resulting oil was dissolved in DCM (1 mL) and the product was precipitated in stirring pentane (50 mL). The precipitate was collected on a 15 mL fine porosity fritted disc, washed with pentane (3 x 10 mL), and dried for 15 min yielding the yellow solid **26** (77 mg, 30%). CV (DMAc) $E_{\text{p,a}} = +0.16\text{ V}$ (NHE). IR: $\nu(\text{B-H sp}^2) = 2474\text{ cm}^{-1}$, $\nu(\text{CO}) = 1702 \text{ \& } 1618\text{ cm}^{-1}$, $\nu(\text{NO}) = 1561\text{ cm}^{-1}$. ^1H NMR (d^6 -Acetone, δ): 7.94 (1H, d, Pz5A/C), 7.91 (1H, d, Pz3A), 7.88 (1H, d, Pz5A/C), 7.78 (1H, d, Pz5B), 7.72 (1H, d, Pz3C), 7.37 (2H, bs, DMAP-A), 7.35 (1H, d, $J = 7.4$, H5), 7.00

(1H, d, Pz3B), 6.94 (1H, t, $J = 7.4$, H6), 6.86 (1H, t, $J = 7.5$, H7), 6.51 (2H, m, DMAP-B), 6.37 (1H, t, Pz4A/C), 6.36 (1H, t, Pz4A/C), 6.21 (1H, d, $J = 7.5$, H8), 6.09 (1H, t, Pz4B), 3.78 (1H, m, H4a), 3.31 (1H, d, $J = 9.5$, H9), 3.05 (6H, s, N-Me), 2.83 (1H, m, H4), 2.79 (1H, ddd, $J = 10.6, 5.1, 2.4$, H10a), 2.63 (2H, m, H3 & H12), 2.56 (2H, m, H1 & H12), 2.14 (1H, dd, $J = 9.5, 2.5$, H10), 1.88 (3H, s, H11), 1.74 (1H, d, $J = 12.7$, H2), 1.55 (1H, q, $J = 12.7$, H2), 1.01 (3H, t, $J = 7.3$, H13). ^{13}C NMR (d^6 -Acetone, δ): 213.7 (CO), 212.5 (CO), 155.11 (DMAP-C), 150.7 (2C, DMAP-A), 144.7 (C4b/9a), 143.6 (Pz3A), 142.1 (Pz3B), 141.4 (Pz3C), 137.6 (Pz5A/C), 137.0 (Pz5A/C), 135.8 (Pz5B), 133.9 (C4b/9a), 128.2 (C8), 125.6 (C5), 125.1 (C7), 123.9 (C6), 108.3 (2C, DMAP-B), 107.0 (Pz4A/C), 106.7 (Pz4A/C), 106.5 (Pz4B), 70.6 (C10), 68.2 (C9), 56.2 (C1), 45.2 (C3), 42.9 (C10a), 39.3 (2C, DMAP-Me), 35.7 (C4a), 34.4 (C12), 32.4 (C2), 31.0 (C4), 8.24 (C13).

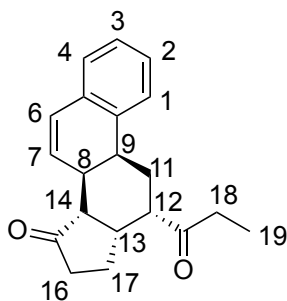
Synthesis of 1-((1*S*,3*S*,4*aS*,10*aS*)-1-acetyl-1,2,3,4,4*a*,10*a*-hexahydrophenanthren-3-yl)propan-1-one (91).



24 (200 mg, 0.34 mmol), $\text{CH}_3\text{CH}_2\text{CN}$ (6 mL), EVK (33 mg, 0.4 mmol), and DTBP (54 mg, 0.3 mmol) were added to a test tube. The reaction mixture was then cooled at $-60\text{ }^\circ\text{C}$ for 15 min. TMSOTf (0.1 mL, 0.5 mmol) was added to the reaction mixture, and the resulting red solution was left stirring at $-60\text{ }^\circ\text{C}$ 1 min. Next, MVK (50 mg, 0.7 mmol)

was added to the reaction mixture, which was then left stirring at -60 °C overnight (~18 h). TEA (0.1 mL, 0.74 mmol) was added to the reaction mixture, which was subsequently removed from the glovebox and stirred open to air overnight (~18 h). The resulting brown mixture was evaporated *in vacuo*, and the resulting film was dissolved in DCM (1 mL). This solution was then added stirring Et₂O (50 mL), yielding a brown precipitation. The brown precipitate was filtered off on a 15 mL medium porosity fritted disc and washed with Et₂O (3 x 5 mL). The filtrate was then evaporated *in vacuo*. This oil was then dissolved in DCM (3 x 0.3 mL) and the resulting solution was dropwise added onto a 250 µm silica preparatory plate. The product was eluted with 10% EtOAc:hexanes (200 mL), scraped off as a band at R_f: 0.32-0.41 and this silica gel was sonicated in EtOAc (20 mL) for 15 min. The silica was filtered off on a 15 mL fine porosity fritted disc and washed with DCM (3 x 5 mL). The filtrate was evaporated *in vacuo* and desiccated for 15 min to yield the colorless oil **27** (11 mg, 12% yield). ¹H NMR (CDCl₃, δ): 7.28 (1H, d, *J* = 7.3, H5), 7.26 (1H, t, *J* = 7.3, H6), 7.21 (1H, t, *J* = 7.1, H7), 7.09 (1H, d, *J* = 7.2, H8), 6.44 (1H, d, *J* = 9.6, H10), 6.08 (1H, dd, *J* = 9.6 & 5.9, H9), 3.34 (1H, bs, H4a), 2.70 (2H, m, H3 & H4), 2.58 (1H, m, H10a), 2.53 (2H, q, H12), 2.42 (1H, m, H1), 2.06 (3H, s, H11), 1.92 (1H, m, H2), 1.78 (1H, m, H4), 1.43 (1H, m, H2), 1.09 (3H, t, *J* = 7.3, H13). ¹³C NMR (CDCl₃, δ): 213.2 (CO), 210.8 (CO), 135.4 (C4b/9a), 134.2 (C4b/9a), 131.2 (C9), 128.1 (C10), 127.9 (C6/7), 127.1 (C8), 126.1 (C6/7), 124.8 (C5), 50.3 (C1), 44.4 (C3), 36.9 (C10a), 35.9 (C4a), 34.1 (C12), 30.6 (C2), 30.1 (C11), 27.9 (C4), 7.9 (C13).

Synthesis of (8*S*,9*S*,12*S*,13*S*,14*S*)-12-propionyl-8,9,11,12,13,14,16,17-octahydro-15*H*-cyclopenta[*a*]phenanthren-15-one (91).



24 (200 mg, 0.34 mmol), CH₃CH₂CN (6 mL), EVK (33 mg, 0.4 mmol), and DTBP (54 mg, 0.3 mmol) were added to a test tube. The reaction mixture was then cooled at -60 °C for 15 min. TMSOTf (0.1 mL, 0.5 mmol) was added to the reaction mixture, and the resulting red solution was left stirring at -60 °C 1 min. Next, cyclopentenone (57 mg, 0.7 mmol) was added to the reaction mixture, which was then left stirring at -60 °C overnight (~18 h). TEA (0.1 mL, 0.74 mmol) was added to the reaction mixture, which was subsequently removed from the glovebox and stirred open to air overnight (~18 h). The resulting brown mixture was evaporated *in vacuo*, and the resulting film was dissolved in DCM (1 mL). This solution was then added stirring Et₂O (50 mL), yielding a brown precipitation. The brown precipitate was filtered off on a 15 mL medium porosity fritted disc and washed with Et₂O (3 x 5 mL). The filtrate was then evaporated *in vacuo*. This oil was then dissolved in DCM (3 x 0.3 mL) and the resulting solution was dropwise added onto a 250 μm silica preparatory plate. The product was eluted with 10% EtOAc:hexanes (200 mL), scraped off as a band at R_f: 0.42-0.50 and this silica gel was sonicated in EtOAc (20 mL) for 15 min. The silica was filtered off on a 15 mL fine porosity fritted disc and washed with DCM (3 x 5 mL). The filtrate was evaporated *in vacuo* and desiccated for 15 min to yield the colorless oil **28** (10 mg, 10% yield). IR: ν(C-H sp²) =

2932 cm^{-1} , $\nu(\text{CO}) = 1731$ and 1703 cm^{-1} . ^1H NMR (CDCl_3 , δ): 7.22 (3H, m, H1, H2, & H3), 7.11 (1H, d, $J = 7.3$, H4), 6.58 (1H, d, $J = 9.6$, H6), 6.15 (1H, dd, $J = 9.6$ & 6.2 , H7), 3.27 (1H, m, H9), 3.11 (1H, dt, $J = 13.0$ & 4.4 , H12), 2.58 (2H, m, H13 & H18), 2.47 (3H, m, H11, H16, H18), 2.25 (1H, m, H8), 2.17 (2H, m, H11 & H16), 2.06 (1H, dd, $J = 12.2$ & 6.7 , H14), 1.97 (1H, m, H17), 1.69 (1H, m, H17), 1.10 (3H, t, $J = 7.2$, H19). ^{13}C NMR (CDCl_3 , δ): 218.5 (CO), 212.5 (CO), 134.6 (C5/10), 134.3 (C5/10), 130.6 (C7), 128.7 (C6), 127.9 (C2/3), 127.2 (C4), 126.8 (C2/3), 124.9 (C1), 51.1 (C14), 43.8 (C12), 37.9 (C13), 37.1 (C16), 35.2 (C9), 34.5 (C18), 30.8 (C8), 21.2 (C11), 21.0 (C17), 7.9 (C19).

4.5 References

1. Bruice, P. Y., *Organic Chemistry*. 5th ed.; Pearson/Prentice Hall: Upper Saddle River, NJ, 2007.
2. Boehm, M.; Lorthiois, E.; Meyyappan, M.; Vasella, A. *Helvetica Chimica Acta* **2003**, 86, (11), 3787.
3. Cheng, W.; Wu, D.; Liu, Y. *Biomacromolecules* **2016**, 17, (10), 3115.
4. Zhang, Y.; Wang, W. *Catalysis Science & Technology* **2012**, 2, (1), 42.
5. Genna, D. T.; Maio, W. A. *Tetrahedron* **2016**, 72, (40), 5956.
6. Posner, G. H. *Chem. Rev.* **1986**, 86, 831.
7. Posner, G. H.; Asirvatham, E. *Tetrahedron Letters* **1986**, 27, (6), 663.
8. Posner, G. H.; Lu, S.-B.; Asirvatham, E. *Tetrahedron Letters* **1986**, 27, (6), 659.
9. Posner, G. H.; Lu, S. B.; Asirvatham, E.; Silversmith, E. F.; Shulman, E. M. *J. Am. Chem. Soc.* **1986**, 108, (3), 511.
10. Posner, G. H.; Mallamo, J. P.; Black, A. Y. *Tetrahedron* **1981**, 37, (23), 3921.
11. Posner, G. H.; Switzer, C. *J. Am. Chem. Soc.* **1986**, 108, (6), 1239.
12. Chen, H.; Liu, R.; Myers, W. H.; Harman, W. D. *J. Am. Chem. Soc.* **1998**, 120, 509.
13. Ding, F.; Valahovic, M. T.; Keane, J. M.; Anstey, M. R.; Sabat, M.; Trindle, C. O.; Harman, W. D. *J. Org. Chem.* **2004**, 69, (7), 2257.
14. Zhang, L.; Xie, X.; Fu, L.; Zhang, Z. *J. Org. Chem.* **2013**, 78, (7), 3434.
15. Karplus, M. *J. Chem. Phys.* **1959**, 30, 11.
16. Belov, V. N.; Dudkin, V. Y.; Urusova, E. A.; Starova, G. L.; Selivanov, S. I.; Nikolaev, S. V.; Eshchenko, N. D.; Morozkina, S. N.; Shavva, A. G. *Russian Journal of Bioorganic Chemistry* **2007**, 33, (3), 293.
17. Dauben, W. G.; Fullerton, D. S. *J. Org. Chem.* **1971**, 36, (22), 3277.
18. Egorov, M. S.; Grinenko, E. V.; Zorina, A. D.; Balykina, L. V.; Selivanov, S. I.; Shavva, A. G. *Russ. J. Org. Chem.* **2001**, 37, (6), 802.
19. Morozkina, S. N.; Abusalimov, S. N.; Selivanov, S. I.; Shavva, A. G. *Russ. J. Org. Chem.* **2013**, 49, (4), 603.

20. Morozkina, S. N.; Abusalimov, S. N.; Starova, G. L.; Selivanov, S. I.; Shavva, A. *G. Russ. J. Org. Chem.* **2010**, 80, (7), 1324.
21. Dodge, J. A.; Krishnan, V. G.; Lugar, C. W.; Neubauer, B. L.; Norman, B. H.; Pfeifer, L. A.; Richardson, T. I., Substituted benzopyrans as selective estrogen receptor-beta agonists. Google Patents: 2003.
22. Gonzalez, M. A. *Nat. Prod. Rep.* **2015**, 32, (5), 684.
23. González, M. A. *Euro. J. Med. Chem.* **2014**, 87, 834.
24. Aulenta, F.; Berndt, M.; Bruedgam, I.; Hartl, H.; Soergel, S.; Reissig, H.-U. *Chem. - Eur. J.* **2007**, 13, (21), 6047.
25. Berndt, M.; Hlobilová, I.; Reissig, H.-U. *Org. Lett.* **2004**, 6, (6), 957.

Chapter 5

Binding and Activation of α,α,α -Trifluorotoluene with {TpMo(NO)(DMAP)}

5.1 Introduction

Although the $\{\text{TpMo}(\text{NO})(\text{L})\}$ fragment has been shown to bind a wide variety of aromatics in an $\eta\text{-}2$ fashion,¹⁻³ one limitation that has discouraged the use of this system has been its inability to form a stable and isolable $\eta\text{-}2$ bound benzene complex. This inability can be rationalized by the comparison of free energy of activation (ΔG^\ddagger) for the dissociative substitution of ligands $\eta\text{-}2$ bound to $\{\text{Os}(\text{NH}_3)_5\}^{2+}$,^{4, 5} $\{\text{TpRe}(\text{CO})(\text{MeIm})\}$,⁶ $\{\text{TpW}(\text{NO})(\text{PMe}_3)\}$,⁷ and $\{\text{TpMo}(\text{NO})(\text{DMAP})\}$ ⁸ with acetone (Table 5.1). According to published reports, the entropy of activation for benzene displacement is typically small and positive, usually 2-5 eu.⁹⁻¹² From this assumption, and the previously reported energies of activation in Table 5.1, the enthalpy of activation (ΔH^\ddagger) for these complexes can be estimated. The ΔH^\ddagger provides a more accurate representation of the bond strength between these metals and their $\eta\text{-}2$ bound ligands. Taking the average of the data available (3 eu) we calculated an approximate value for ΔH^\ddagger of 27.0 kcal/mol for $\text{TpMo}(\text{NO})(\text{DMAP})(\eta^2\text{-naphthalene})$ (**24**), which is an upper limit for the approximate bond dissociation energy (i.e., metal-arene bond strength) for a heterolytic cleavage.

From the differences in enthalpies of activation between the metal-benzene and metal-naphthalene complexes reported in Table 5.1 (between 6-8 kcal/mol), an enthalpy of activation close to 20 kcal/mol is predicted for the purported $\text{TpMo}(\text{NO})(\text{DMAP})(\eta^2\text{-benzene})$ complex; as determined by comparison with the enthalpy of activation for the $\text{TpMo}(\text{NO})(\text{DMAP})(\eta^2\text{-naphthalene})$ (**24**) complex (27.0 kcal/mol). This substantially lower predicted bond strength for $\text{TpMo}(\text{NO})(\text{DMAP})(\eta^2\text{-benzene})$ would account for the inability of its isolation at ambient temperature. From the data in Table 5.1 it can also

be seen that there would be a predicted gain of three kcal/mol of stability achieved by the introduction of a single CF₃ group on benzene (entries 3 and 8). This three kcal/mol increase would give a predicted enthalpy of activation of 23 kcal/mol for the purported TpMo(NO)(DMAP)(η^2 - α,α,α -trifluorotoluene (TFT)) (**100**) complex, which could provide enough stability for its isolation. Thus the synthesis of an η^2 bound TFT complex was pursued in the hopes that its stability would allow for isolation and characterization.

Table 5.1. Comparison of energies for the exchange of various ligands bound to Os, Re, W, and Mo with acetone.

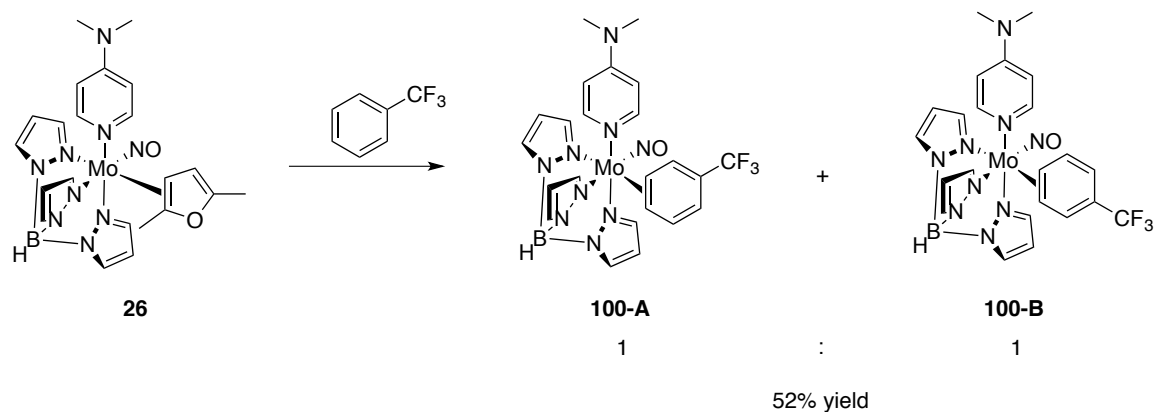
Entry	Compound	T (K)	ΔG^\ddagger (kcal/mol)	ΔS^\ddagger (eu)	ΔH^\ddagger (kcal/mol)	Reference
1	[Os(NH ₃) ₅ (η^2 -naphthalene)] ²⁺	373	29.4	~3	30.5	5
2	[Os(NH ₃) ₅ (η^2 -benzene)] ²⁺	298	23.9	~3	24.8	4
3	[Os(NH ₃) ₅ (η^2 -CF ₃ Ph)] ²⁺	298	25.6	~3	26.5	4
4	TpRe(CO)(MeIm)(η^2 -naphthalene)	373	28.5	~3	29.7	6
5	TpRe(CO)(MeIm)(η^2 -benzene)	295	22.6	~3	23.4	6
6	TpW(NO)(PMe ₃)(η^2 -naphthalene)	351	30.4	~3	31.4	7
7	TpW(NO)(PMe ₃)(η^2 -benzene)	295	22.3	~3	23.2	7
8	TpW(NO)(PMe ₃)(η^2 -CF ₃ Ph)	295	25.4	~3	26.2	7
9	TpMo(NO)(DMAP)(η^2 -naphthalene)	298	25.4	~3	27.0	8

5.2 Results

As discussed in Chapter 3, the TpMo(NO)(DMAP)(η^2 -2,5-dimethylfuran) complex (**26**) has a half-life ($t_{1/2}$) of 130 min in d⁶-acetone (25 °C),⁸ which would allow for a substitution of furan for another ligand within a reasonable timeframe. Following this information, **26** was stirred in an excess of neat TFT and observed over time. The reaction mixture changed from a yellow to a red mixture after 8 h and a shift in the anodic wave from -350 mV to -280 mV (100 mV/s, NHE) was seen. The red precipitate

from this exchange was then collected, and weighed to determine a yield of 52%. This represents the first substituted benzene η^2 bound to the $\{\text{TpMo}(\text{NO})(\text{L})\}$ fragment (**100**) (Scheme 5.1).

Scheme 5.1. Exchange of **26** with TFT to yield **100**.



NMR analysis shows that the TFT ligand is fluxional on the NMR timescale (600 MHz) with severely broadened peaks. However, reducing the temperature of a d^6 -acetone solution of **100** to $-30\text{ }^{\circ}\text{C}$ allows for full characterization of the complex (Figure 5.1).

Various isomers of **100** were modeled using the Gaussian 03 program suite. Relative energies were determined using a hybrid density functional B3LYP expressed in a hybrid basis. The basis incorporates the Los Alamos pseudopotential LANL2DZ and the associated basis functions for molybdenum and Pople's 6-31G(d) basis for all other atoms. This combination has proved reliable for Os, Mo, Re, and W systems for relative (binding) energies, charge transfer, and preferred structures, especially in similar systems.¹³ These results showed that the two thermodynamically preferred orientations of $\text{TpMo}(\text{NO})(\text{DMAP})(\eta^2\text{-TFT})$ are those which place the CF_3 group in quadrants a and d (**100-A** and **100-B**, Figure 5.2).

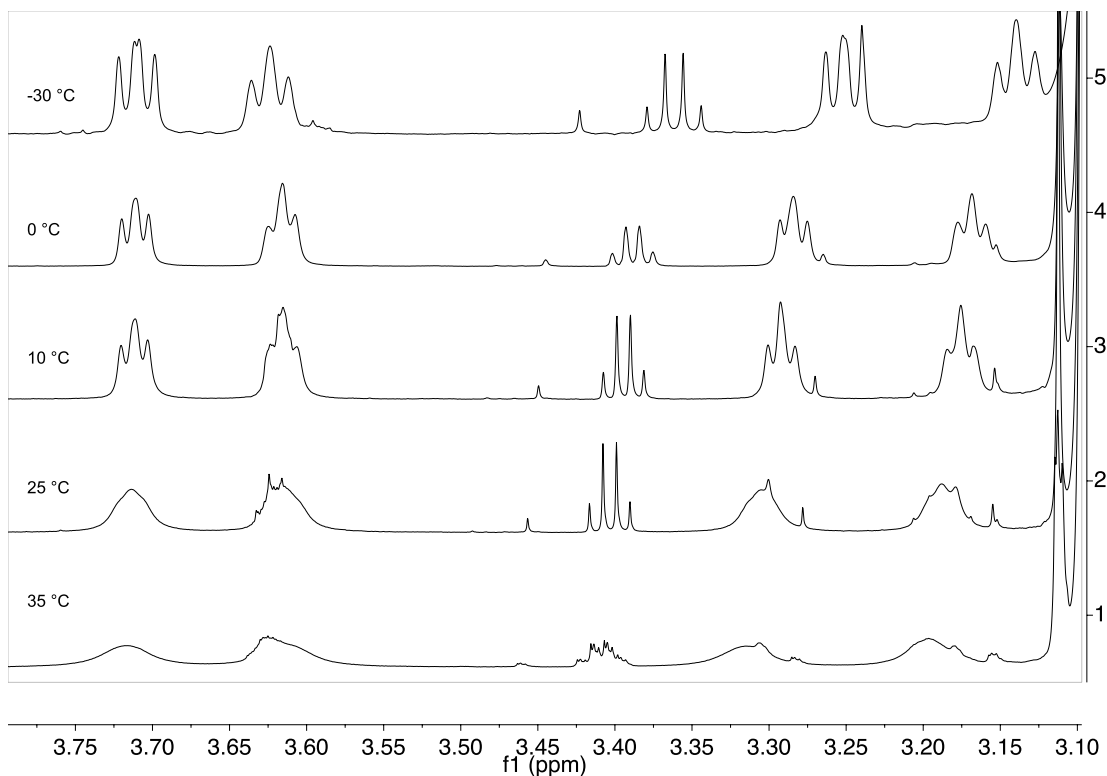


Figure 5.1. ^1H NMR spectra of $\text{TpMo}(\text{NO})(\text{DMAP})(\eta^2\text{-TFT})$ (**100**) in $\text{d}^6\text{-Acetone}$ at various temperatures.

Energies for each isomer are expressed relative to that of isomer **100-A**, which was determined to be the lowest energy orientation. **100-A** and **100-B** are related to one another through either an intrafacial or interfacial isomerization with very little difference in their free energies (0.12 kcal/mol). Spin-saturation experiments have revealed intrafacial isomerization as the dominant dynamic process (*vide infra*). Through intrafacial isomerization of **100-A** or **100-B**, orientations in which the CF_3 group is proximal (**100-C**) or distal (**100-D**) to the DMAP ligand can be obtained with slightly higher free energies relative to **100-A** (0.59 – 1.79 kcal/mol). With a small decrease in thermodynamic stability relative to **100-A**, constitutional isomers **100-C** and **100-D** could be observed; however, no empirical evidence of this has been found. Lastly, through an

intrafacial isomerization of **100-C** or **100-D**, orientations in which the CF₃ group is placed in a sterically disfavored quadrant can be obtained (**100-E** and **100-F**). However, such steric hindrance yields a significant 5 kcal/mol decrease in the thermodynamic stability of orientations **100-E** and **100-F**, relative to **100-A**.

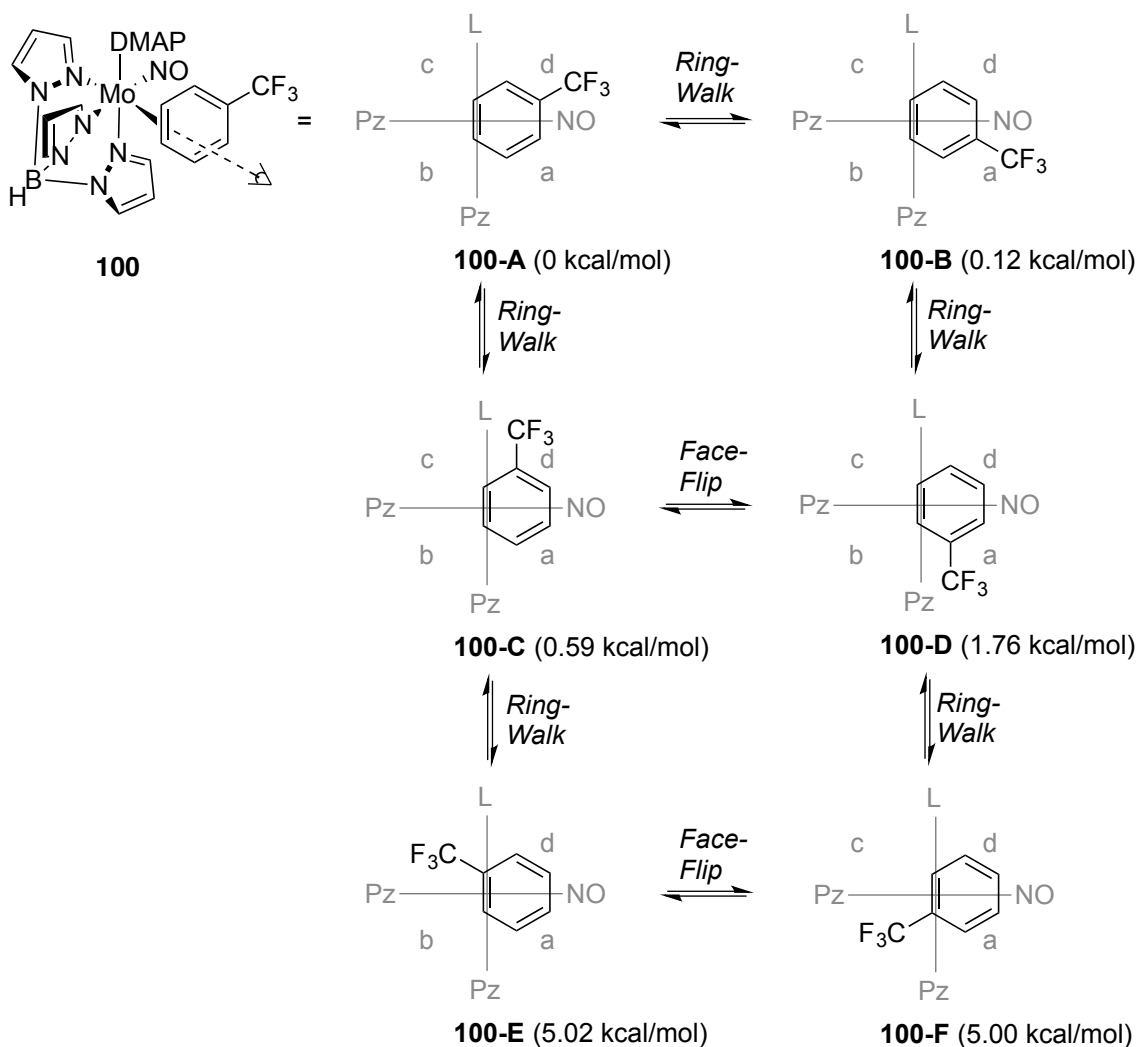


Figure 5.2. Coordination diastereomers of **100** and their relative free energies as predicted from DFT calculations.

Analysis of NOESY data of **100** (via spin-saturation exchange) reveal that the dominant dynamic process is an intrafacial (ring-walk) isomerization occurring on the

seconds time-scale at a temperature of 25 °C (Figure 5.3). Through COSY analysis, peaks at 3.61, 3.30, and 7.10 ppm were identified as belonging to the same spin-system. Likewise peaks at 3.18, 3.71, and 6.70 ppm were also identified as belonging to the same spin-system. The resonance for the upbound proton of **100-A** (H3, 3.61 ppm) exchanges with a peak at 6.70 ppm, identified as H5 of **100-B** (Figure 5.3). Upon intrafacial isomerization, the downbound proton of **100-A** (H4, 3.30 ppm) would be expected to still have significant shielding from the metal center, which agrees with the observed exchange between the resonance for H4 of **100-A** and the peak at 3.71 ppm (H4 of **100-B**). Furthermore, the resonance for H5 of **100-A** (7.11 ppm), identified through COSY as being adjacent to H4 of **100-A**, would be expected to shift significantly upfield from the aromatic region. This is in agreement with the observed exchange between H5 of **100-A** and the peak at 3.18 ppm (H3 of **100-B**).

A ^1H NMR experiment of a d^6 -acetone solution of **100** at 0 °C revealed the coupling constant between H4 and H5 of **100B** to be 6.2 Hz. The difference in chemical shift between H4 of **100A** and H4 of **100B** is 341 Hz at 0 °C. The approximate coalescence temperature (50 °C) between **100A** and **100B** was obtained by VT-NMR in d^6 -acetone (0 – 50 °C). The ^1H NMR spectrum of **100** obtained at 50 °C shows the complex to be very near coalescence and so an upper limit (60 °C) and a lower limit (40 °C) were used to approximate a window of error (± 0.5 kcal/mol). From this information, the approximate rate of isomerization was determined ($k = 750 \text{ s}^{-1}$) and with it the free energy of activation of isomerization was approximated to be 14.7 ± 0.5 kcal/mol at 50 °C.¹⁴ This value is similar to that observed for $[\text{Os}(\text{NH}_3)_5(\eta^2\text{-benzene})]^{2+}$ ($\Delta G^\ddagger = 12.5$ kcal/mol at 10 °C).

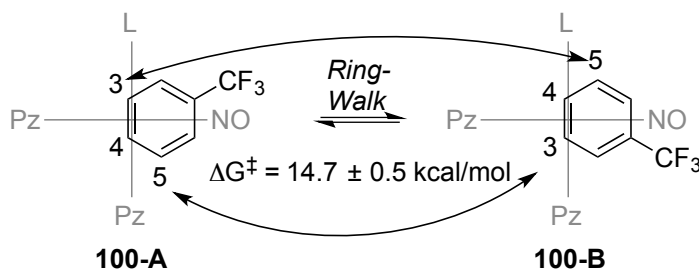


Figure 5.3. Intrafacial isomerization between **100-A** and **100-B**.

In contrast to that observed in the synthesis of the TFT complex, attempts to replace the furan for benzene have not been successful; however, the additional π -acidity provided by the presence of a CF_3 group causes a stronger π -backbond donation, thereby stabilizing the η -2 bond with TFT. The TFT complex (**100**) is stable at ambient temperature and slowly undergoes substitution in neat acetone with a half-life ($t_{1/2} = 39$ minutes) that corresponds to a $\Delta G^\ddagger = 22.3 \pm 0.08$ kcal/mol at 25 °C.

Exchange of the furan ligand of **26** with TFT provided a sufficient method for the isolation of **100** (52% yield); however, an alternate pathway to this complex was investigated. Although the synthesis of **26** can be done with good yields, a direct synthesis of **100** from $\text{TpMo}(\text{NO})(\text{DMAP})(\text{I})$ (**23**) was desired. Removing the furan complex intermediate would also eliminate the presence of **26**, commonly seen as an impurity ($\sim 10\%$) in the isolation of **100** through the ligand exchange reaction. Initial reduction attempts to yield **100** from **23** were performed using THF as a cosolvent, with TFT and sodium dispersion in paraffin wax, but an unexplained decomposition was seen. This was believed to be due to the formation of an overly reduced metal complex reacting with the THF co-solvent (*vide infra*). Success was found by removing the co-solvent. In a similar method for the synthesis of $\text{TpW}(\text{NO})(\text{PMe}_3)(\eta^2\text{-benzene})$ complex, the reduction

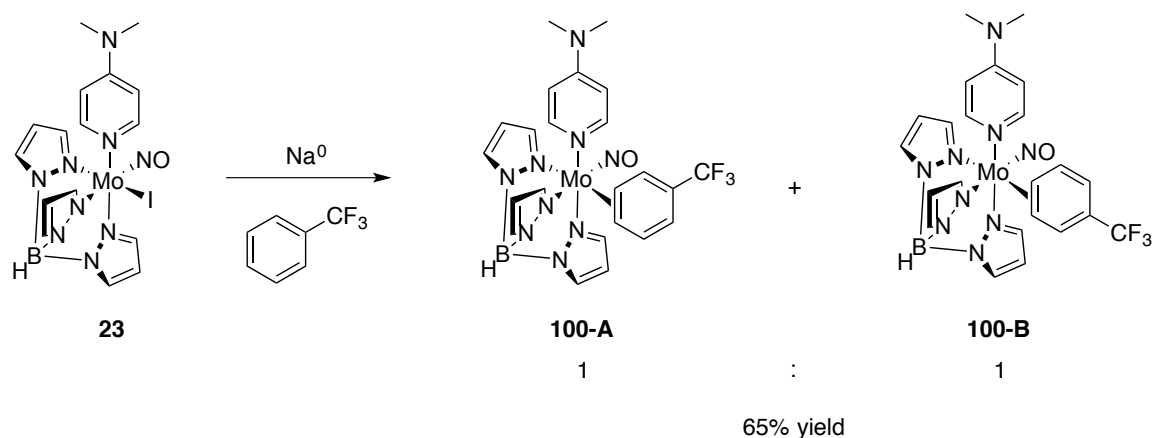
of **23** with elemental sodium in TFT (neat) yielded **100**. However, difficulties in achieving consistent reaction outcomes required an investigation into the isolation of various sizes of elemental sodium.

It was found that after washing sodium dispersion in paraffin wax with hexanes, different sizes of elemental sodium could be obtained. For every gram of sodium dispersion in paraffin wax, approximately 30 mL of hexanes was used for washing. For the reduction of **23** (3 g) to **100**, 1.5 g of sodium dispersion was added to a 50 mL round bottom flask charged with a ½ inch stir egg. To this flask was added hexanes (50 mL) and the resulting grey mixture was stirred overnight (18 h). It was observed that the size of the resulting elemental sodium was a function of the rate of stirring used during the solvation of the wax. For example, in one set of experiments stirring at 1150 rpm resulted in elemental sodium described herein as “flecks” (~1/4 cm in diameter), at ~ 700 rpm yields sodium “flakes” (~1/2 – 1 cm in diameter), and at ~ 350 rpm yields sodium “sheets” (~1 – 2 cm in diameter).

After decanting the hexanes away from this elemental sodium, α,α,α -trifluorotoluene was added, followed by **23**. The resulting green mixture was then stirred at room temperature and the reaction was monitored by cyclic voltammetry (CV). As this reaction is heterogeneous, due to the insolubility of **23** and sodium in TFT, the surface area of the sodium has a significant impact on the rate of the reaction (e.g., the greater the surface area, the greater the rate of the reaction). The most important factors in controlling this surface area include rate of stirring during the washing process, as described above, as well as during the reaction itself. For example, in reactions with otherwise identical conditions, the reaction time for the reduction of **23** to **100** increases

from 6 h with sodium flecks, to 24 h with sodium flakes (Scheme 5.2). Furthermore, with otherwise identical conditions, the reaction time increases from 6 h with the reaction mixture stirring at 1150 rpm, to 3 days with the reaction mixture stirring at 500 rpm. Attempts to solubilize **23** with a co-solvent (i.e., THF, DME or benzene) result in significant decomposition (assumed based on the black color of the reaction mixture and absence of any reducible species in the CV).

Scheme 5.2. Reduction of **23** to **100**.

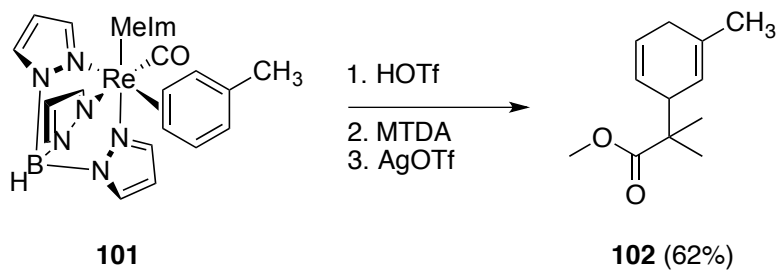


Following optimization of the reduction of **23** to **100**, the isolation of **100** proved difficult. As **100** is insoluble in TFT, it can be isolated from the reaction mixture through filtration; however, the resulting precipitate also contains elemental sodium. After filtering the reaction mixture, THF was added in an attempt to dissolve **100**. The addition of THF to this red solid resulted in a violent, effervescent reaction, which yielded a black solution. For the same reason, attempts to chromatograph **100** away from the sodium proved ineffective. In a similar workup to that of the TpMo(NO)(DMAP)(η^2 -2,5-dimethylfuran) complex, the reaction mixture resulting from the reduction of **23** in TFT can be added slowly to stirring MeOH (CAUTION: hydrogen evolution!), which yields a

red precipitate and the elemental sodium is consumed. The resulting precipitate can then be isolated through filtration and purified with trituration in Et₂O. Utilizing a fast stir rate, sodium flecks, and MeOH precipitation, the scale for the reduction of **23** to **100** was increased to 17 g with a decent yield (65 %) without chromatography.

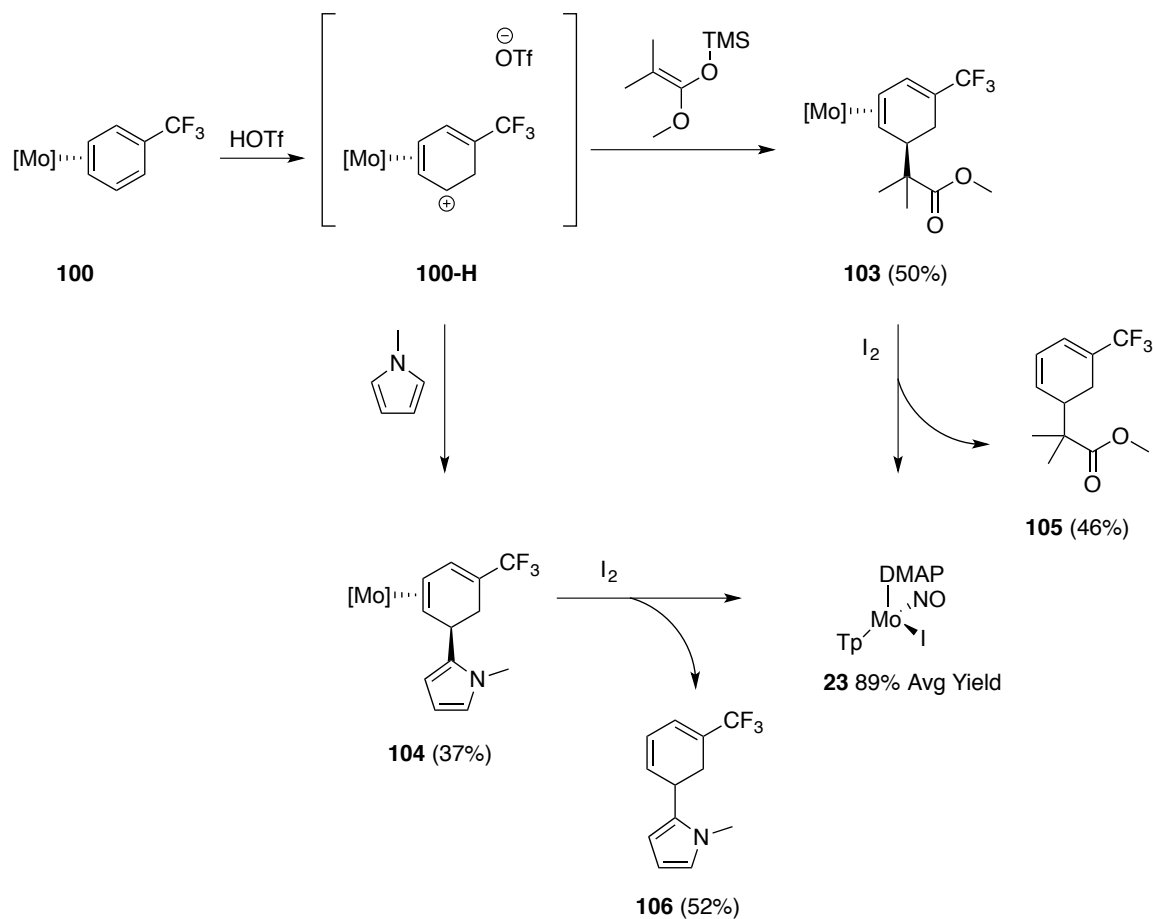
Having developed a reliable synthesis of the complex, the potential synthetic utility of **100** was then evaluated. Previous studies of third-row metal benzene complexes document a broad range of electrophile-nucleophile tandem addition reactions to the benzene ligand resulting in 1,4-hexadienes such as **102** in Scheme 5.3.¹⁵

Scheme 5.3. Tandem addition reaction sequence with TpRe(CO)(MeIm)(η^2 -toluene) (**101**).



The two nucleophiles chosen to test the viability of **100** for this type of reaction, *N*-methylpyrrole and 1-methoxy-2-methyl-1-(trimethylsilyloxy)-1-propene (MTDA), were chosen as representatives of two important classes of carbon-carbon bond forming reactions: Friedel-Crafts alkylation of aromatic heterocycles and addition of protected enolates.

Scheme 5.4. Tandem electrophilic-nucleophilic additions to $\text{TpMo}(\text{NO})(\text{DMAP})(\eta^2\text{-TFT})$ (**100**) complex.



Attempts to characterize the purported allyl intermediate (**100-H**) from the protonation of **100** with HOTf have been unsuccessful. However, when a solution of the trifluorotoluene complex **100** is protonated followed by the addition of MTDA at -60°C , a new complex is formed, **103** (47% yield). A similar reaction sequence can be successfully carried out with *N*-methylpyrrole in place of MTDA, to yield **104** (37%) (Scheme 5.4).

^1H NMR, COSY, NOESY, IR and electrochemical data are consistent with **103** and **104** being 1,3-cyclohexadiene complexes; contrast to that observed for electrophilic-nucleophilic additions to the benzene or toluene third-row metal complexes described

above, which yield non-conjugated dienes. In the ^{13}C NMR spectrum of **103** and **104**, large fluorine coupling with the carbon nuclei is seen for the CF_3 carbon (q, $^1J_{\text{F,C}} \sim 260$ Hz), the carbon adjacent to the CF_3 group (C4, q, $^2J_{\text{F,C}} \sim 39$ Hz), as well as the allylic carbon (C3, q, $^3J_{\text{F,C}} \sim 7$ Hz). The anodic wave for **103** and **104** is significantly positive of the anodic wave of **100** (+0.30 V vs -0.30 V); however, a better representation of electron density at the metal center can be seen in the nitrosyl stretch frequencies for **100** in comparison to **103** (e.g., 1586 vs 1571 cm^{-1}). As the resulting ligand of a 1,2-addition to **100** has a decreased amount of conjugation relative to its aromatic precursor, the metal center is more electron-rich in the case of **103** and **104**, resulting in a lower stretch frequency.

Both protonation and nucleophilic addition were found to be regioselective, and the addition of the nucleophile proved to be stereoselective, with addition occurring *anti* to the metal. Also, in contrast to the complexes described in Chapters 2 and 3, **103** and **104** are isolated as single coordination diastereomers, even though the aromatic precursor **100** showed virtually no diastereoselectivity. Apparently, the electron-withdrawing nature of the CF_3 group directs protonation to the ortho carbon such that the resulting positive charge build-up in the “ η^2 -allyl” complex intermediate (**100-H**) is farther from the CF_3 group and distal to the DMAP ligand. Nucleophilic addition to the allyl group occurs to the meta carbon adjacent to protonation, resulting in 1,3-diene complexes. After isolation, complexes **103** and **104** can be subjected to oxidative decomplexation with iodine to recover **23** at an average 80% yield and the organics **105** and **106** at an average 50% yield.

5.3 Discussion

Selective fluorination has been a significant focus for the development of biologically active small molecules.¹⁶⁻²⁰ The presence of fluorine substituents yields greater lipophilicity and bioavailability, thus improving the pharmacokinetic profile for small molecules containing fluorine. Common fluorine containing pharmaceuticals include fluoxetine, bicalutamide, and fipronil (Figure 5.4). Furthermore, fluorine-containing compounds have demonstrated desirable uses as refrigerants, polymers, dyes, and agrochemicals.²¹⁻²⁴ The important benefits from the inclusion of fluorine have made the selective synthesis of fluorine containing molecules a well-studied area. Classic synthetic methods for fluorination include using electrophilic (i.e., elemental fluorine, organofluoroxo reagents, and perchloryl fluoride) and nucleophilic (i.e., Olah's reagent, SF₄, and BrF₃) sources of fluorine.¹⁸ Also of great focus is the transition metal mediated trifluoromethylation of aromatics.²⁵

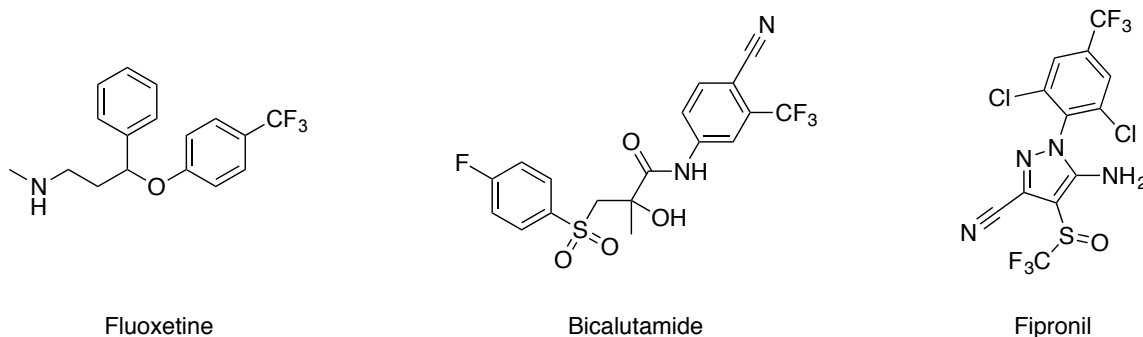
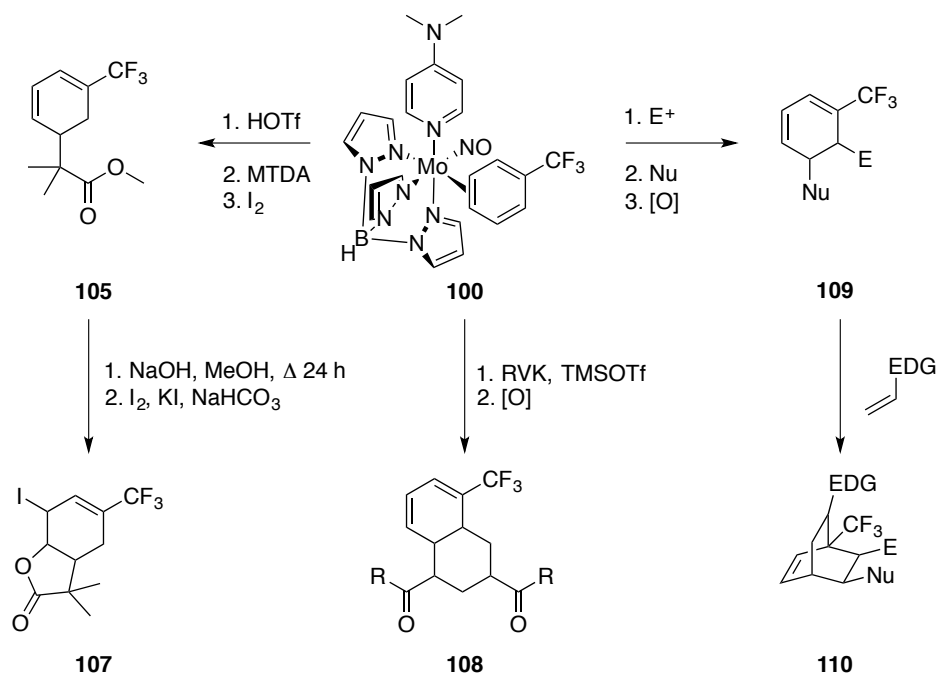


Figure 5.4. Pharmaceuticals containing CF₃ groups.

As a complement to these methods, our approach for the synthesis of small molecules containing fluorine utilizes a stable, commercially available starting material (TFT). After binding this aromatic, the {TpMo(NO)(DMAP)} fragment can control the tandem electrophilic-nucleophilic additions to yield 1,3-dienes, **105** and **106**, with great

regio- and stereocontrol. The formation of these two 1,3-dienes represents a simple method for the synthesis of a variety of new organic molecules bearing a CF₃ group. Of interest is the potential to perform an iodolactonization on **105** to potentially yield the benzofuranone **107** (Scheme 5.5). Furthermore, the recent advances in Michael-Michael ring closing (MIMIRC) reactions could yield multicyclic organics (**108**) with CF₃ groups (Scheme 5.5).

Scheme 5.5. Future reactivity for chemical elaboration from **100**.

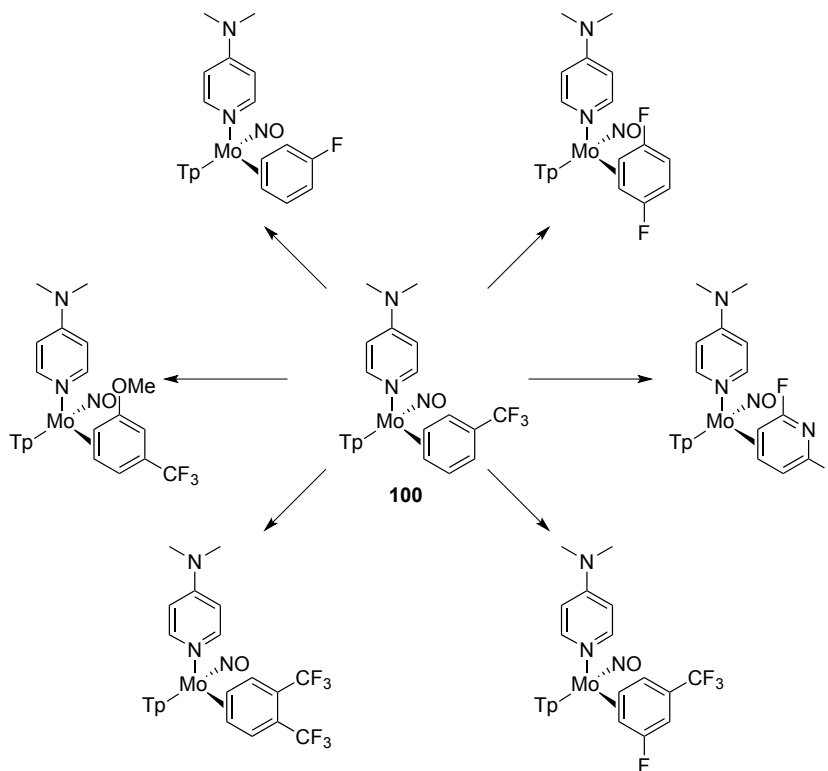


With the compatibility of **100** and HOTf, similar methods for chemical elaboration mentioned in Chapters 2-4 are expected to be applicable to the synthesis of various novel organics from **100**. Future exploration of this chemistry will focus on the use of additional electrophiles (i.e., acetals, Michael acceptors, etc.) and nucleophiles (i.e., pyrazole, LiDMM, nitromethane, etc.) for tandem addition reactions to make **109**.

Reactivity of these 1,3-dienes (**105** and **106**) is virtually unknown due to a lack of practical methods for their synthesis. As such, they represent potential candidates for inverse-electron-demand dienes that could be utilized in Diels-Alder reactions (IEDD) (Scheme 5.5).²¹

With the success demonstrated in the isolation of **100**, the isolation of other eta-2 bound fluorinated aromatic complexes of {TpMo(NO)(DMAP)} is being pursued. Utilizing the significantly lower $t_{1/2}$ for exchange of **100**, in comparison to TpMo(NO)(DMAP)(η^2 -dimethylfuran) complex, the ability to exchange the TFT ligand of **100** with other π -ligands has shown to be an invaluable tool in binding previously inaccessible ligands. Another benefit in using TpMo(NO)(DMAP)(η^2 -TFT) in these exchanges is that the {TpMo(NO)(DMAP)} fragment is a weaker π -base than its third-row congeners. Although this is classically referred to as a disadvantage of the {TpMo(NO)(L)} fragment, having a decreased π -basicity decreases the potential for C-F oxidative addition, which has shown to be the dominant pathway for the attempted exchange reactions of TpW(NO)(PMe₃)(η^2 -benzene) with many fluorinated aromatics. As such, great progress has been achieved as a separate project aimed at binding a variety of fluorinated aromatics without inserting into the C-F bond (Figure 5.5).²⁶ As a future project, these newly discovered complexes will be investigated for their ability to undergo chemical transformation with the hopes of achieving novel, fluorinated organics. Furthermore, the high off-rate of the TFT ligand has been utilized to achieve the binding of free benzene, to yield TpMo(NO)(DMAP)(η^2 -benzene) (**111**).

Figure 5.5. Newly bound fluorinated aromatic complexes of $\{\text{TpMo}(\text{NO})(\text{DMAP})\}$.²⁶



By stirring **100** in a large excess of benzene, **111** can be isolated and characterized by CV and ^1H NMR (Scheme 5.6).²⁷ Considering the TFT complex has a $\Delta G^\ddagger = 22.3 \pm 0.08$ kcal/mol, along with the approximated three kcal/mol additional stability gained from having a CF_3 group on the benzene ring, one would expect this newly reported complex (**111**) to have a $\Delta G^\ddagger \approx 19$ kcal/mol. Monitoring the rate of the exchange of the benzene ligand of **111** for d^6 -acetone, we determined through the Eyring equation that $\text{TpMo}(\text{NO})(\text{DMAP})(\eta^2\text{-benzene})$ has a $\Delta G^\ddagger = 19.4$ kcal/mol, which is in agreement with the predicted value. This breakthrough in second-row dearomatization is currently being investigated as a separate project with the expectation that the expansive chemical

libraries developed with the $\{\text{TpW}(\text{NO})(\text{PMe}_3)\}$ fragment will soon be within reach of the $\{\text{TpMo}(\text{NO})(\text{DMAP})\}$ fragment.

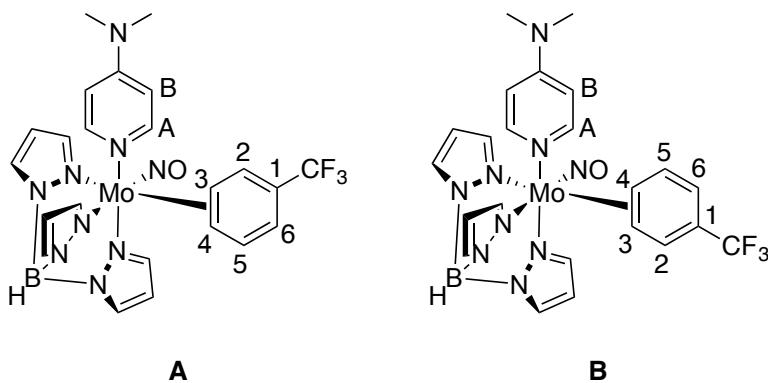
5.4 Conclusion

To our knowledge, complex **100** is the first example of an η^2 bound substituted benzene complex, not derived from a third-row metal, that is thermally stable and capable of undergoing electrophilic-nucleophilic additions on the arene. The synthesis of **100** can be done on a 50 g scale, with fair yields (65%), and its air-stable precursor (**23**) has been produced on a 170 g scale in 66% overall yield from $\text{Mo}(\text{CO})_6$. Although Os, Re, and W have demonstrated similar reactivity, the low cost, superior yields, ease of handling, and recyclability offered with Mo make **100** a potentially valuable new tool for organic synthesis.

5.5 Experimental

General Methods. NMR spectra were obtained on a 600 or 800 MHz spectrometer. All chemical shifts are reported in ppm, and proton and carbon shifts are referenced to tetramethylsilane (TMS) utilizing residual ^1H or ^{13}C signals of the deuterated solvents as an internal standard. Fluorine chemical shifts are referenced to a solution of hexafluorobenzene in d^6 -Acetone (-164.9 ppm relative to CFCl_3) contained in a capillary tube. Coupling constants (J) are reported in hertz (Hz). Infrared spectra (IR) were recorded as a glaze on a spectrometer fitted with a horizontal attenuated total reflectance (HATR) accessory or on a diamond anvil ATR assembly. Electrochemical experiments were performed under a dinitrogen atmosphere. Cyclic voltammetry data were taken at ambient temperature ($\sim 25^\circ\text{C}$) at 100 mV/s in a standard three-electrode cell with a glassy carbon working electrode, *N,N*-dimethylacetamide (DMA) or acetonitrile (CH_3CN) solvent (unless otherwise specified), and tetrabutylammonium hexafluorophosphate (TBAH) electrolyte (approximately 0.5 M). All potentials are reported versus NHE (normal hydrogen electrode) using cobaltocenium hexafluorophosphate ($E_{1/2} = -0.78\text{ V}$), ferrocene ($E_{1/2} = +0.55\text{ V}$), or decamethylferrocene ($E_{1/2} = +0.04\text{ V}$) as an internal standard. The peak-to-peak separation was less than 100 mV for all reversible couples. Unless otherwise noted, all synthetic reactions were performed in a glovebox under a dry nitrogen atmosphere. Deuterated solvents were used as received. Pyrazole (Pz) protons of the (trispyrazolyl) borate (Tp) ligand were uniquely assigned (e.g., “Pz3B”) using a combination of two-dimensional NMR data and (dimethylamino)pyridine–proton NOE interactions (see Figure 3.4). When unambiguous assignments were not possible, Tp protons were labeled as “Pz3/5 or Pz4”. All J values for Pz protons are 2 (± 0.2) Hz.

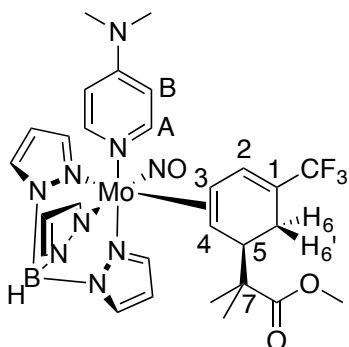
Synthesis of $\text{TpMo}(\text{NO})(\text{DMAP})(3,4\text{-}\eta^2\text{-}\alpha,\alpha,\alpha\text{-trifluorotoluenene})$ (**100**)



To a 250 mL round bottom flask charged with a stir egg were added sodium dispersion (30-35% by weight, 12 g dispersion, 0.183 mol) and hexanes (200 mL). The grey mixture formed was stirred at 1150 RPM for 18 h at which point the hexanes was decanted off. Then, TFT (75 mL, 0.431 mol), Et₂O (25 mL) and **23** (24 g, 0.0408 mol) were added to the remaining solid. The resulting green reaction mixture was stirred at 1150 RPM for 24 h. This dark red mixture was then transferred to a 500 mL Erlenmeyer flask containing Et₂O (200 mL) and the resulting mixture was stirred vigorously. While purging the box with nitrogen, half of this mixture was then slowly added to stirring MeOH (150 mL), yielding a red precipitate. This precipitate was then collected on a 350 mL fine porosity fritted disc. The second half of the reaction mixture was then slowly added to a separate stirring solution of MeOH (150 mL), yielding a red precipitate. This precipitate was then collected on the same 350 mL fine porosity fritted disc and was washed with Et₂O (4 x 50 mL). The resulting red precipitate was transferred to a 250 mL Erlenmeyer flask containing Et₂O (100 mL) and this mixture was stirred for 1 h. This precipitate was then collected on a 350 mL fine porosity fritted disc, washed with Et₂O (3 x 50 mL), and

dessicated for 2 h to yield the solid **100** (13.10 g, 65%). CV (DMAc) $E_{p,a} = -0.28$ V (NHE). IR: $\nu(\text{BH}) = 2481 \text{ cm}^{-1}$, $\nu(\text{NO}) = 1586 \text{ cm}^{-1}$. Two coordination diastereomers **A:B** = 1:1 ^1H NMR (d^6 -Acetone, δ , -30°C): 8.17 (4H, buried broad s, DMAP-A for **A** and **B**), 8.11 (2H, overlapping doubletsy , Tp3,5), 8.02 (1H, d, Tp3,5), 8.01 (1H, d, Tp3,5), 7.95 (3H, m, Tp3,5), 7.84 (1H, d, Tp3,5), 7.58 (1H, d, Tp3,5), 7.57 (1H, d, Tp3,5), 7.46 (1H, d, $J = 6.3$, H2**B**), 7.12 (1H, dd, $J = 9.1$ & 6.2 , H5**A**), 7.08 (1H, d, $J = 5.8$, H2**A**), 6.90 (1H, d, Tp3,5), 6.88 (1H, d, Tp3,5), 6.74 (4H, buried broad s, DMAP-B for **A** and **B**), 6.70 (1H, dd, $J = 9.1$ & 6.2 , H5**B**), 6.41 (3H, m, Tp4), 6.37 (1H, t, Tp4), 6.29 (1H, dd, $J = 9.1$ & 1.5 , H6**A**), 6.25 (1H, dd, $J = 9.1$ & 1.5 , H6**B**), 6.15 (2H, m, Tp4), 3.71 (1H, dd, $J = 8.5$ & 6.2 , H4**B**), 3.60 (1H, t, $J = 7.3$, H3**A**), 3.30 (1H, dd, $J = 8.5$ & 6.3 , H4**A**), 3.14 (1H, t, $J = 7.2$, H3**B**), 3.09 (12H, s, NMe). ^{13}C NMR (d^6 -Acetone, δ , -30°C): 154.7 (DMAP-C), 150.2 (DMAP-C), 142.4 (Tp3,5), 142.3 (Tp3,5), 142.0 (Tp3,5), 141.5 (2C, Tp3,5), 137.5 (2C, Tp3,5), 136.9 (Tp3,5), 136.8 (Tp3,5), 135.9 (4C, C6**A** & C2**B**, Tp3,5), 135.8 (2C, C1**B** & C1**A**), 135.2 (2C, C2**A** & C5**B**), 127.3 (q, $J = 261.0$, CF_3), 125.5 (q, $J = 261.0$, CF_3), 111.7 (C5**A**), 111.4 (C6**B**), 108.0 (4C, DMAP-B), 106.9 (3C, Tp4), 106.4 (3C, Tp4), 78.7 (C4**B**), 76.2 (C4**A**), 75.4 (C3**A**), 72.9 (C3**B**), 30.07 (NMe). ^{19}F NMR (d^6 -Acetone, δ): -62.41.

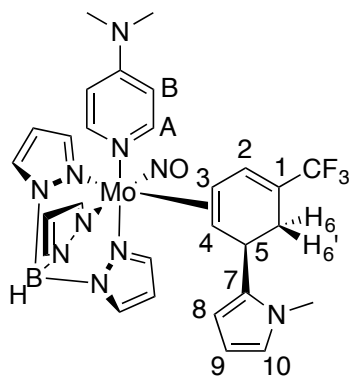
Synthesis of TpMo(NO)(DMAP)(η^2 -methyl 2-methyl-2-(5-(trifluoromethyl)cyclohexa-2,4-dien-1-yl)propanoate) (103**).**



100 (500 mg, 0.80 mmol), CH₃CH₂CN (5 mL) and a stir pea, were added to a test tube and this orange mixture was cooled for 15 min at -60 °C. A -60 °C, 1M solution of HOTf in CH₃CH₂CN (2.0 mL, 2.0 mmol) was added to the reaction mixture and the resulting red solution was left standing at -60 °C. After 15 min, MTDA (1.0 mL, 4.9 mmol) was added to the reaction mixture and the resulting red solution was left stirring at -60 °C. After 18 h, a -60 °C solution of triethylamine (1.0 mL, 7.17 mmol) was added to the reaction mixture and the resulting brown solution was chromatographed through a 60 mL medium porosity fritted disc ³/₄ full with silica gel. The product was eluted with 1:1 Et₂O:benzene (100 mL) as a yellow band, collected as a yellow solution, and evaporated *in vacuo*. The resulting yellow oil was then dissolved in DCM (1 mL) and the product was precipitated in stirring pentane (20 mL). The precipitate was collected on a 15 mL fine porosity fritted disc, washed with pentane (3 x 50 mL), and desiccated for 15 min yielding the light yellow solid **103** (299 mg, 50%). CV (DMAc) $E_{p,a}$ = +0.32 V (NHE). IR: ν (BH) = 2480 cm⁻¹, ν (CO) = 1721 cm⁻¹, ν (NO) = 1571 cm⁻¹. H NMR (d⁶-Acetone, δ): 7.96 (2H, d, Pz5C and Pz3A), 7.92 (1H, d, Pz5A), 7.79 (1H, d, Pz5B), 7.78 (2H, bs, DMAP-A), 7.66 (1H, d, Pz3C), 7.09 (1H, d, Pz3B), 6.62 (3H, m, DMAP-B & H₂), 6.38

(1H, t, Pz4A), 6.37 (1H, t, Pz4C), 6.13 (1H, t, Pz4B), 3.29 (1H, d, $J = 9.8$, H5), 3.24 (3H, s, OMe), 3.08 (6H, s, N-Me), 2.93 (1H, m, H6), 2.86 (1H, t, $J = 7.9$, H3), 2.11 (1H, d, $J = 18.6$, H6'), 1.89 (1H, dt, $J = 9.8$ & 1.8, H4), 1.23 (3H, s, Me), 1.04 (3H, s, Me). ^{13}C NMR (d^6 -Acetone, d): 178.2 (CO), 155.3 (DMAP-C), 151.1 (DMAP-A), 142.6 (Pz3A), 142.1 (Pz3B), 141.6 (Pz3C), 137.5 (q, $J = 6.9$, C2), 137.4 (Pz5C), 137.2 (Pz5A), 135.8 (Pz3B), 126.8 (q, $J = 264.0$, CF_3), 115.5 (1C, q, $J = 29.0$, C1), 108.2 (DMAP-B), 106.9 (Pz4), 106.4 (Pz4), 106.3 (Pz4), 65.3 (C4), 60.8 (C3), 51.2 (OMe), 51.1 (C7), 42.6 (C5), 39.2 (NMe), 22.9 (Me), 22.4 (C6), 22.3 (Me). ^{19}F NMR (d^6 -Acetone, δ): -65.38. EA: Calculated for $\text{C}_{28}\text{H}_{35}\text{BF}_3\text{MoN}_9\text{O}_3$: C, 47.41; H, 4.97; N, 17.77. Found: C, 47.68; H, 5.22; N, 17.65.

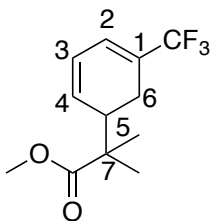
Synthesis of $\text{TpMo}(\text{NO})(\text{DMAP})(\eta^2\text{-1-methyl-2-(5-(trifluoromethyl)cyclohexa-2,4-dien-1-yl)-1H-pyrrole})$ (104).



100 (500 mg, 0.80 mmol), $\text{CH}_3\text{CH}_2\text{CN}$ (5 mL) and a stir pea, were added to a test tube and this orange mixture was cooled for 15 min at -60°C . A -60°C , 1M solution of HOTf in $\text{CH}_3\text{CH}_2\text{CN}$ (2.0 mL, 2.0 mmol) was added to the reaction mixture and the resulting red solution was left standing at -60°C . After 15 min, N-methylpyrrole (1.0 mL, 11.0 mmol) was added to the reaction mixture and the resulting red solution was left stirring at

-60 °C. After 18 h, a -60 °C solution of triethylamine (1.0 mL, 7.17 mmol) was added to the reaction mixture and the resulting brown solution was chromatographed through a 60 mL medium porosity fritted disc $\frac{3}{4}$ full with silica gel. The product was eluted with Et₂O (100 mL) as a yellow band, collected as a yellow solution, and evaporated *in vacuo*. The resulting yellow oil was then dissolved in DCM (2 mL) and the product was precipitated in stirring pentane (75 mL). The precipitate was collected on a 15 mL fine porosity fritted disc, washed with pentane (3 x 10 mL), and desiccated for 15 min yielding the light yellow solid **104** (205 mg, 37%). CV (DMAc) $E_{p,a} = +0.35$ V (NHE). IR: $\nu(\text{BH}) = 2479$ cm⁻¹, $\nu(\text{NO}) = 1574$ cm⁻¹. ¹H NMR (d⁶-Acetone, δ): 8.12 (1H, d, Pz3A), 7.94 (1H, d, Pz3B), 7.93 (1H, d, pz5A), 7.83 (2H, m, DMAP-A), 7.80 (1H, d, Pz5B), 7.61 (1H, d, Pz3C), 7.12 (1H, d, Pz3B), 6.81 (1H, m, H2), 6.63 (2H, m, DMAP-B), 6.40 (1H, t, Pz4A), 6.35 (1H, t, $J = 2.0$, H10), 6.33 (1H, t, Pz4C), 6.14 (1H, t, Pz4B), 6.00 (1H, m, H8), 5.77 (1H, t, $J = 3.0$, H9), 4.03 (1H, d, $J = 8.2$, H5), 3.34 (3H, s, NMe), 3.16 (1H, m, H6), 3.08 (6H, s, NMe), 2.85 (1H, t, $J = 9.1$, H3), 2.33 (1H, t, $J = 9.1$, H6'), 2.24 (1H, dt, $J = 9.1$ & 1.7, H4). ¹³C NMR (d⁶-Acetone, δ): 155.3 (DMAP-C), 151.1 (DMAP-A), 142.8 (Pz3A), 142.2 (Pz3C), 141.6 (Pz3B), 141.3 (C7), 137.5 (q, $J = 6.1$, C2), 137.4 (Pz5C and Pz5A), 135.8 (Pz5B), 126.8 (q, $J = 268.0$, CF3), 120.7 (C10), 114.4 (q, $J = 30.0$, C1), 108.2 (DMAP-B), 106.9 (Pz4C), 106.8 (C9), 106.6 (Pz4A), 106.4 (Pz4B), 105.7 (C8), 71.8 (C4), 58.8 (C3), 39.2 (DMAP Mes), 33.4 (NMe), 32.9 (C5), 27.3 (C6). ¹⁹F NMR (d⁶-Acetone, δ): -65.40.

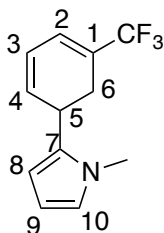
Synthesis of methyl 2-methyl-2-(5-(trifluoromethyl)cyclohexa-2,4-dien-1-yl)propanoate (**105**).



To a 50 mL filter flask charged with a stir pea were added **103** (100 mg, 0.145 mmol), DCM (5 mL), and a 0.06 M solution of I_2/Et_2O (1.2 mL, 0.073 mmol) resulting in a green solution. The solution was stirred at room temperature for 5 min and then evaporated *in vacuo* to an oil. The oil was dissolved in DCM (1 mL), giving a solution that was then added to stirring pentane (25 mL), creating a green precipitation. The precipitate was collected on a 15 mL fine porosity fritted disc, washed with pentane (3 x 10 mL), and desiccated to yield **23** (73 mg, 89%). The filtrate was removed from the glovebox and evaporated *in vacuo* to a brown oil. The oil was dissolved in DCM (3 x 0.3 mL) and the resulting solution was dropwise added onto a 250 μm silica preparatory plate. The product was eluted with 10% EtOAc:hexanes (200 mL), scraped off as a band at R_f : 0.41-0.62 and this silica gel was sonicated in EtOAc (20 mL) for 15 min. The silica was filtered off on a 15 mL medium porosity fritted disc and washed with DCM (3 x 2 mL). The colorless filtrate was then evaporated *in vacuo* and desiccated to yield the colorless oil **105** (16 mg, 46% yield). IR: $\nu(C-H\ sp^2) = 22925\ cm^{-1}$, $\nu(CO) = 1731\ cm^{-1}$. 1H NMR (d^6 -Acetone, δ): 6.36 (1H, m, H2), 6.04 (1H, m, H3), 5.83 (1H, dd, $J = 9.6$ & 3.9 , H4), 3.69 (3H, s, OMe), 2.86 (1H, m, H6), 2.32 (1H, m, H5), 2.21 (1H, m, H6), 1.19 (3H, s, Me), 1.18 (3H, s, Me). ^{13}C NMR (d^6 -Acetone, δ): 177.4 (CO), 131.4 (C4), 125.6 (q, $J = 30.9$, C1), 124.8 (q, $J = 6.5$, C2), 124.0 (q, $J = 270.0$, CF_3), 123.5 (C3), 52.2 (OMe), 45.7

(C7), 40.6 (C5), 22.4 (Me), 22.2 (Me), 21.2 (C6). ^{19}F NMR (d^6 -Acetone, δ): -68.98. EA: Calculated for $\text{C}_{12}\text{H}_{15}\text{F}_3\text{O}_2$: C, 58.06; H, 6.09. Found: C, 58.61; H, 6.22.

Synthesis of 1-methyl-2-(5-(trifluoromethyl)cyclohexa-2,4-dien-1-yl)-1*H*-pyrrole (106).



To a 50 mL filter flask charged with a stir pea were added **104** (100 mg, 0.145 mmol), DCM (5 mL), and a 0.06 M solution of $\text{I}_2/\text{Et}_2\text{O}$ (1.2 mL, 0.073 mmol) resulting in a green solution. The solution was stirred at room temperature for 5 min and then evaporated *in vacuo* to an oil. The oil was dissolved in DCM (1 mL), giving a solution that was then added to stirring hexanes (25 mL), creating a green precipitation. The precipitate was collected on a 15 mL fine porosity fritted disc, washed with hexanes (3 x 10 mL), and desiccated to yield **23** (76 mg, 89%). The filtrate was removed from the glovebox and evaporated *in vacuo* to a brown oil. The oil was dissolved in DCM (3 x 0.3 mL) and the resulting solution was dropwise added onto a 250 μm silica preparatory plate. The product was eluted with 10% EtOAc:hexanes (200 mL), scraped off as a band at R_f : 0.50-0.71 and this silica gel was sonicated in EtOAc (20 mL) for 15 min. The silica was filtered off on a 15 mL medium porosity fritted disc and washed with DCM (3 x 2 mL). The colorless filtrate was then evaporated *in vacuo* and desiccated to yield the colorless oil **106** (17 mg, 52% yield). ^1H NMR (d^6 -Acetone, δ): 6.59 (1H, t, J = 2.3, H10), 6.49 (1H, m, H2), 6.10 (1H, m, H4), 6.08 (1H, t, J = 3.1, H8), 6.07 (1H, m, H3), 6.00 (1H, m,

H9), 3.78 (1H, m, H5), 3.68 (3H, s, NMe), 2.62 (1H, dd, $J = 17.2, 8.9$, H5), 2.49 (1H, m, H6). ^{13}C NMR (d^6 -Acetone, δ): 133.6 (C7), 133.4 (C4), 125.0 (q, $J = 30.5$, C1), 124.9 (q, $J = 6.8$, C2), 124.0 (q, $J = 272.0$, CF_3), 122.6 (C10), 122.4 (C3), 107.1 (C8), 106.2 (C9), 33.9 (NMe), 31.5 (C5), 26.7 (C6). ^{19}F NMR (d^6 -Acetone, δ): -68.81. EA: Calculated for $\text{C}_{12}\text{H}_{12}\text{F}_3\text{N}$: C, 63.43; H, 5.32; N, 6.16. Found: C, 63.22; H, 5.36; N, 6.13.

5.6 References

1. Ha, Y.; Dilsky, S.; Graham, P. M.; Liu, W.; Reichart, T.; Sabat, M.; Kenae, J. M.; Harman, W. D. *Organometallics* **2006**, 25, 5184.
2. Meiere, S. H.; Keane, J. M.; Gunnoe, T. B.; Sabat, M.; Harman, W. D. *J. Am. Chem. Soc.* **2003**, 125, (8), 2024.
3. Mocella, C. J.; Delafuente, D. A.; Keane, J. M.; Warner, G. R.; Friedman, L. A.; Sabat, M.; Harman, W. D. *Organometallics* **2004**, 23, (16), 3772.
4. Harman, W. D.; Sekine, M.; Taube, H. *J. Am. Chem. Soc.* **1988**, 110, 5725.
5. Harman, W. D. *Chem. Rev.* **1997**, 97, 1953.
6. Brooks, B. C.; Meiere, S. H.; Friedman, L. A.; Gunnoe, T. B.; Harman, W. D. *J. Am. Chem. Soc.* **2001**, 123, 3541.
7. Welch, K. D.; Harrison, D. P.; Lis, E. C.; Liu, W.; Salomon, R. J.; Harman, W. D.; Myers, W. H. *Organometallics* **2007**, 26, (10), 2791.
8. Myers, J. T.; Dakermanji, S. J.; Chastanet, T. R.; Shivokevich, P. J.; Strausberg, L. J.; Sabat, M.; Myers, W. H.; Harman, W. D. *Organometallics* **2016**.
9. Bengali, A. A. *Organometallics* **2000**, 19, (19), 4000.
10. Bengali, A. A.; Charlton, S. B. *Journal of Chemical Education* **2000**, 77, (10), 1348.
11. Bengali, A. A.; Grunbeck, A. R. *Organometallics* **2005**, 24, (24), 5919.
12. Bengali, A. A.; Leicht, A. *Organometallics* **2001**, 20, (7), 1345.
13. Rassolov, V. A.; Ratner, M. A.; Pople, J. A.; Redfern, P. C.; Curtiss, L. A. *J. Comput. Chem* **2001**, 22, (9), 976.
14. Mann, B. E. *Ann. Rep. on NMR Spec.* **1982**, 12, 263.
15. Ding, F.; Harman, W. D. *J. Am. Chem. Soc.* **2004**, 126, (42), 13752.
16. Bégué, J.-P.; Bonnet-Delpon, D. *J. Fluorine Chem.* **2006**, 127, (8), 992.
17. Isanbor, C.; O'Hagan, D. *J. Fluorine Chem.* **2006**, 127, (3), 303.
18. Kirk, K. L. *J. Fluorine Chem.* **2006**, 127, (8), 1013.
19. Wang, J.; Sánchez-Roselló, M.; Aceña, J. L.; del Pozo, C.; Sorochinsky, A. E.; Fustero, S.; Soloshonok, V. A.; Liu, H. *Chem. Rev.* **2014**, 114, (4), 2432.

20. Yerien, D. E.; Bonesi, S.; Postigo, A. *Organic & Biomolecular Chemistry* **2016**, 14, (36), 8398.
21. Nagai, T.; Nasu, Y.; Shimada, T.; Shoda, H.; Koyama, M.; Ando, A.; Miki, T.; Kumadaki, I. *J. Fluorine Chem.* **1992**, 57, (1-3), 245.
22. Braden, R. P. J.; Klauke, E. *Pesticide Science* **1986**, 17, (4), 418.
23. Ameduri, B. *Chemical Reviews* **2009**, 109, (12), 6632.
24. Engel, A., Fluorine-Containing Dyes. In *Organofluorine Chemistry: Principles and Commercial Applications*, Banks, R. E.; Smart, B. E.; Tatlow, J. C., Eds. Springer US: Boston, MA, 1994; pp 315.
25. Tomashenko, O. A.; Grushin, V. V. *Chemical Reviews* **2011**, 111, (8), 4475.
26. Full credit is given to Jacob Smith for discovery and isolation of these fluorinated aromatics.
27. Full credit is given to Jacob Smith for discovery and characterization of $\text{TpMo}(\text{NO})(\text{DMAP})(\eta^2\text{-benzene})$.

Chapter 6

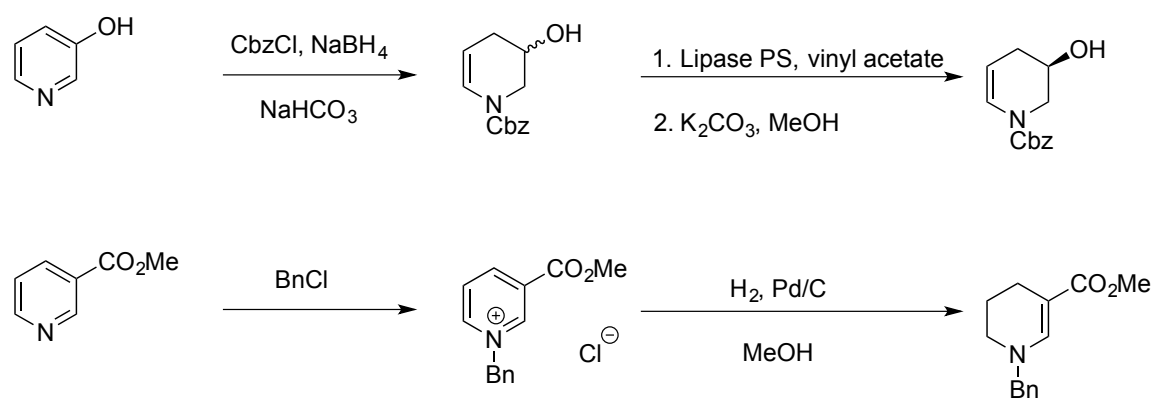
Activation of Pyridines Using



6.1 Introduction

Pyridines are ubiquitous in nature, commercially available, and stable, making them an attractive starting material for the synthesis of alkaloids. Furthermore, dihydropyridines are often used as building blocks for the syntheses of piperidines¹ (a fully saturated pyridine), which can be found in many pharmaceuticals,² agrochemicals,³ and petrochemicals.⁴ The functionalization of pyridine through aromatic substitution (either with electrophiles or nucleophiles) is challenging due to poor chemoselectivity.⁵ Furthermore, in comparison to benzene, pyridine has a lower energy π -system and thus is less reactive with electrophiles. This decrease in reactivity requires harsher reagents for the functionalization of pyridines. For this reason, the synthesis of dihydro-, tetrahydro-, and perhydropyridines from pyridine is most effective when the nitrogen is functionalized first.⁶ This method has been widely utilized in the syntheses of pyridines and 1,2-dihydropyridines, often with good regio- and stereocontrol (Scheme 6.1).

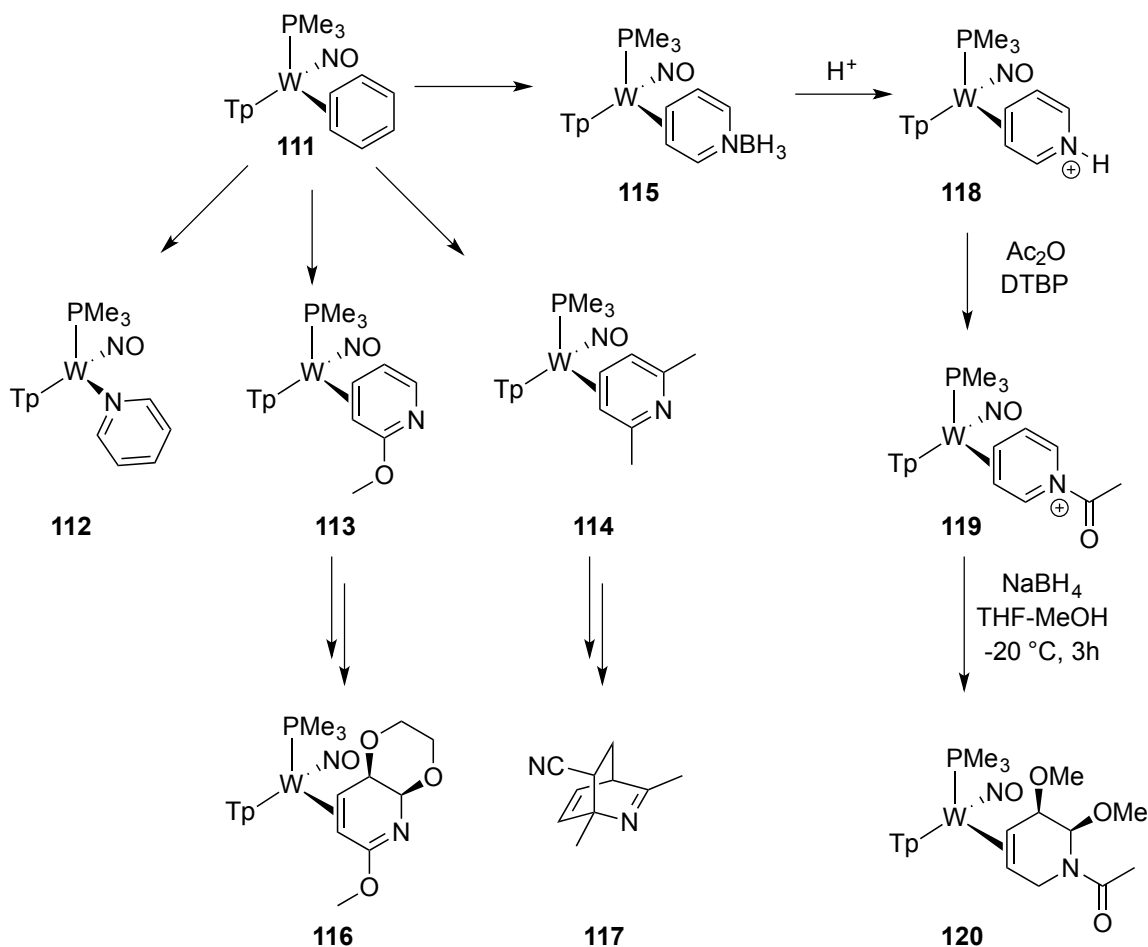
Scheme 6.1. Traditional synthetic methods for the reduction of pyridines.



Although previous reports have shown the ability for metals to bind pyridines in an η^2 fashion,⁷⁻¹³ the {TpW(NO)(PMe₃)₃} fragment is the first dearomatization agent reported that can promote electrophilic additions and subsequent derivatization to yield

dihydropyridines.¹⁴⁻²¹ Initial investigations into the coordination of pyridines by the dearomatization agent $\{\text{TpW}(\text{NO})(\text{PMe}_3)\}$ found that pyridine preferentially binds to the metal center through the nitrogen in a κ^1 -fashion (**112**, Scheme 6.2).

Scheme 6.2. Coordination and reactivity of pyridines dearomatized through coordination to $\{\text{TpW}(\text{NO})(\text{PMe}_3)\}$.



However, by taking advantage of either steric or electronic effects, the isolation of primarily η^2 -bound complexes can be accomplished (**113** and **114**).²² Furthermore, using *N*-protected pyridines, the isolation of η^2 -pyridine complexes without substituents on the ring carbons can also be achieved, such as the pyridine-borane complex (**115**).²³ From

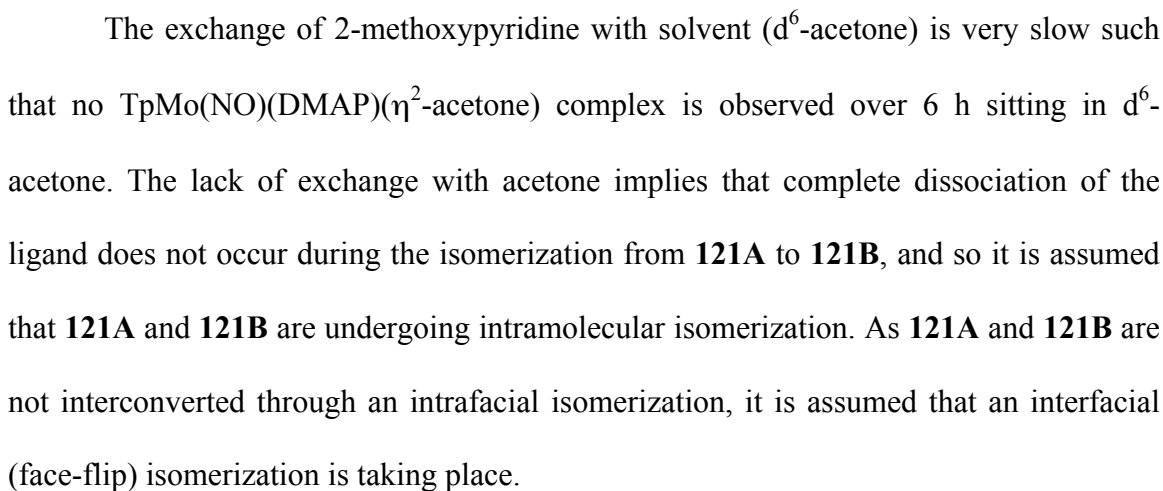
these η^2 -bound pyridine complexes a variety of alkaloid cores have been synthesized with great regio- and stereocontrol by taking advantage of the increased reactivity imparted by coordination to the electron-rich metal (Scheme 6.2). With a goal of replicating the reactivity demonstrated by the dearomatization of pyridines by $\{\text{TpW}(\text{NO})(\text{PMe}_3)\}$, the coordination of pyridines to the more economically viable $\{\text{TpMo}(\text{NO})(\text{DMAP})\}$ fragment was investigated.

6.2 Results and Discussion

As discussed in Chapter 3, the $\text{TpMo}(\text{NO})(\text{DMAP})(\eta^2\text{-2,5-dimethylfuran})$ (**26**) complex can undergo substitution of the furan ligand in the presence of an excess of another viable backbond acceptor. Initial attempts to obtain an η^2 -bound pyridine complex with $\{\text{TpMo}(\text{NO})(\text{DMAP})\}$ focused on ligand exchange reactions with unsubstituted pyridine. These exchanges show similar reactivity to that reported for $\text{TpW}(\text{NO})(\text{PMe}_3)(\eta^2\text{-benzene})$: when **26** was stirred in neat pyridine, a turquoise reaction mixture was obtained. As with $\{\text{TpW}(\text{NO})(\text{PMe}_3)\}$, this turquoise color results from a metal-to-ligand charge transfer and indicates coordination through the nitrogen.²⁴ Due to the inherent stability of the κ^1 -pyridine ligands in these systems, isolation of this complex was not pursued with $\{\text{TpMo}(\text{NO})(\text{DMAP})\}$. Next, we focused on ligand exchanges with nitrogen-protected pyridinium triflates; however, these reactions resulted in oxidative decomposition of the metal center. We then attempted to bind pyridine-borane by stirring **26** in neat pyridine-borane; however, as a dark turquoise reaction mixture was observed, an impurity of free pyridine is believed to have led to the formation of κ^1 -pyridine complex.

Successful isolation of a $\{\text{TpMo}(\text{NO})(\text{DMAP})\}$ complex with an η^2 -bound substituted pyridine was achieved by stirring **26** in neat 2-methoxypyridine. The initial yellow mixture of **26** changes to a slightly darker orange heterogeneous mixture after 24 h. The success of the ligand exchange was determined by the observation of a shift in the first anodic wave over the course of the reaction from -350 mV to -220 mV as seen by CV (100 mV/s, NHE). The orange precipitate was isolated and triturated in Et_2O to give the $\text{TpMo}(\text{NO})(\text{DMAP})(\eta^2\text{-2-methoxypyridine})$ complex (**120**) in yields of 73% on a 5 g scale. Similarly, the successful isolation of $\text{TpMo}(\text{NO})(\text{DMAP})(\eta^2\text{-2,6-dimethoxypyridine})$ (**121**) can be accomplished by stirring **26** in neat 2,6-dimethoxypyridine and filtering the resulting orange mixture to give a yellow precipitate on a 500 mg scale with a yield of 54% (Scheme 6.3).

From the ^1H NMR spectrum of **121** the resonances for H3 and H4 for both coordination diastereomers were assigned. For **121A** the resonance for H4 is seen as a doublet-of-doublets at 3.65 ppm and the resonance for H3 is a doublet at 2.96 ppm. For **121B** the resonance for H3 is seen as a doublet at 3.28 ppm and the resonance for H4 is a doublet-of-doublets at 3.23 ppm. Using COSY analysis, the H5 assignments for both diastereomers were determined (6.24 ppm for **121A** and 5.85 ppm for **121B**) and through NOE interaction with DMAP protons or Pz3A the coordination diastereomers were assigned. In contrast to $\text{TpW}(\text{NO})(\text{PMe}_3)(\eta^2\text{-2-methoxypyridine})$, **121** shows only a slight preference to orient the methoxy towards the ancillary ligand, and so **121A** and **121B** are isolated in a 1:1.4 ratio (Scheme 6.3).



Similar to $\text{TpW}(\text{NO})(\text{PMe}_3)(\eta^2\text{-2,6-dimethoxypyridine})$, **122** is isolated as a 1:1 mixture of coordination diastereomers (**122A** and **122B**). The ^1H NMR spectrum of **122** has significant line-broadening due to isomerization occurring on the NMR time-scale. From spin-saturation exchange experiments it was found that the broadened peaks identified as the resonances for H3 and H4 of **122A** and **122B** exchange with peaks in the aromatic region, which led to the conclusion that the primary method of isomerization is

intrafacial. A ^1H NMR experiment of a CDCl_3 solution of **122** at $0\text{ }^\circ\text{C}$ revealed the coupling constant between H4 and H5 of **122A** to be 5.9 Hz. The difference in chemical shift between H4 of **122A** and H4 of **122B** is 189 Hz at $0\text{ }^\circ\text{C}$. The approximate coalescence temperature ($55\text{ }^\circ\text{C}$) between **122A** and **122B** was obtained by VT-NMR in CDCl_3 ($0 - 55\text{ }^\circ\text{C}$). The low solubility of **122** limited the available deuterated solvents to CDCl_3 , which also limited the temperature range available for these experiments. However, the ^1H NMR spectrum of **122** obtained at $55\text{ }^\circ\text{C}$ shows the complex to be very near coalescence and so an upper limit ($65\text{ }^\circ\text{C}$) and a lower limit ($45\text{ }^\circ\text{C}$) were used to approximate a window of error ($\pm 0.5\text{ kcal/mol}$). From this information, the approximate rate of isomerization was determined ($k = 420\text{ s}^{-1}$) and with it the free energy of activation of isomerization was approximated to be $15.5 \pm 0.5\text{ kcal/mol}$ at $55\text{ }^\circ\text{C}$.²⁵ Further analysis is needed for the full characterization of **122**; however, the conjugate acid of **122** (**127**) has a significantly higher barrier of isomerization for the pyridinium ligand, making its full characterization possible (*vide infra*).

The observed coordination of these methoxypyridines to the $\{\text{TpMo}(\text{NO})(\text{DMAP})\}$ fragment mirrors that seen with $\{\text{TpW}(\text{NO})(\text{PMe}_3)\}$. For the latter, an investigation of binding for a wide range of substituted pyridines determined that the steric presence of a bulky group at the 2 position of pyridine is not sufficient to prevent binding through the nitrogen in the tungsten system, as seen by the κ^1 coordination of both 2-picoline and 2-ethylpyridine. Rather, a combination of sterics and electronic stabilization is needed to favor η^2 coordination, as seen with 2-methoxypyridine. The increased π -donation from the placement of a methoxy group at

the ortho position provides delocalization of electron density over the uncoordinated portion of the ring (Figure 6.1).

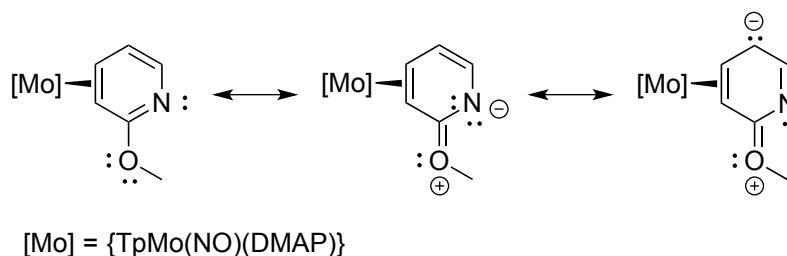
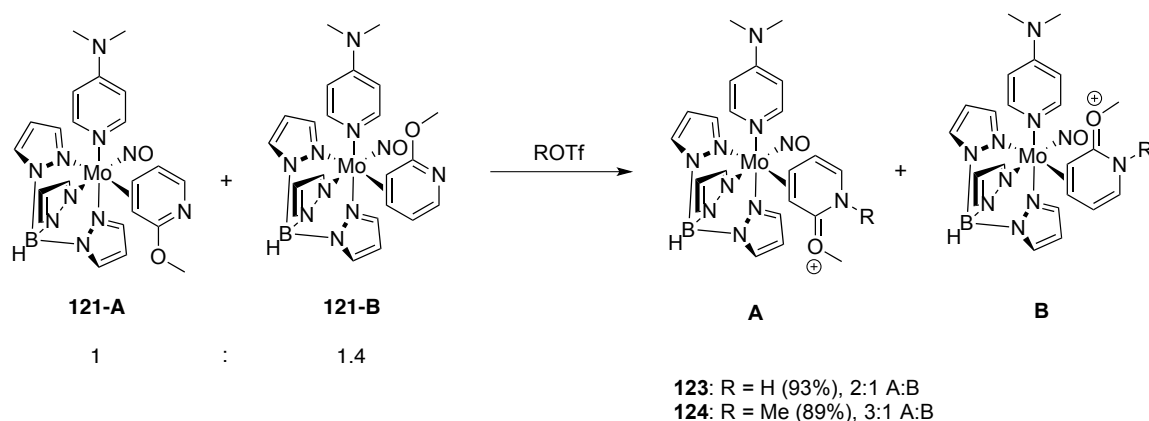


Figure 6.1. Resonance structures showing the delocalization of electron density on 2-methoxypyridine via coordinating at the C3-C4 double bond.

Furthermore, this stabilization provides an energetic preference for coordination diastereomers that retain linear conjugation in the uncoordinated portion of the pyridine ligand (e.g., binding across the C3-C4 bond) and disfavors those with cross conjugation (e.g., binding across the C4-C5 bond). With $\text{TpW}(\text{NO})(\text{PMe}_3)(\eta^2\text{-2-methoxypyridine})$ the methoxy group orients proximal to the PMe_3 ligand in the major isomer,²² whereas the minor isomer has the methoxy group distal ($\text{cdr} = 2:1$).

The investigation of reactivity of these preliminary pyridine complexes has focused on the organic modification of 2-methoxypyridine. Similar to organic reactions of uncoordinated pyridines, initial electrophilic additions to **121** were found to occur at the nitrogen. For instance, the addition of triflic acid (HOTf) or methyl triflate (MeOTf) to **121** yields the pyridinium complexes **123** and **124**, respectively (Scheme 6.4).

Scheme 6.4. Electrophilic addition to **121**.

In the ^1H NMR spectrum of **123**, the methoxy groups shift downfield to 3.83 and 3.80 ppm from 3.79 and 3.62 ppm, the values seen for **121**. Furthermore, the anodic waves (which approximate the formal reduction potentials) shifts from -0.22 V to $\sim +0.80$ V upon electrophilic addition in these reactions, representing a significant decrease in electron density at the metal center. This greater electron withdrawing ability of the cationic ligands is also observed in the nitrosyl stretch frequencies, where **123** and **124** have significantly higher frequencies (1599 and 1596 cm^{-1} , respectively) than **121** (1575 cm^{-1}).

The coordination diastereomer ratio (cdr) for pyridinium complexes **123** (2:1 A:B) and **124** (3:1 A:B) is higher than **121** (1:1.4 A:B). Similar to $\text{TpW}(\text{NO})(\text{PMe}_3)(\eta^2\text{-2-methoxypyridine})$,²² the oxonium species **123** and **124** favor the **A** isomer wherein the methoxy group is distal to ancillary ligand. To access the thermodynamic ratio of **123**, a CD_3CN solution of **123** was added to a CD_3CN solution of di-tert-butylpyridine (DTBP) and observed by ^1H NMR over 2 h. After 5 min, an ^1H NMR spectrum of this solution revealed it to contain **123** at a 4:1 ratio of **A**:**B**. Observing this solution after 2 hours

yielded no further change in the ratio of **A:B**, leading to the conclusion that the thermodynamic ratio of **123** is 4:1.

For the methylation of **121**, the resulting product, **124**, is isolated as a 3:1 ratio of **A:B**. This observed increase in cdr could be due to the selective precipitation of one diastereomer over the other. Considering the reported 89% yield, were the remaining theoretical yield (137 mg) assumed to be **124B** that was not collected during the precipitation, then the overall ratio would be 2:1 **A:B**, which is still higher than the original ratio (1:1.4). This analysis implies that the rate of methylation is slower than the rate of isomerization for **121**. Interestingly, stirring a solution of **123** in CH₃CN overnight yields an orange precipitate. A ¹H NMR spectrum of this solid reveals it to contain a 25:1 ratio of **124A:124B**, with 34% of the mass recovered. However, the filtrate from the isolation of this solid contains **124A** and **124B** at a 2:1 ratio, which indicates this single diastereomer to be isolated by a selective precipitation, not a thermodynamic equilibration. In addition to 2D-NMR, solid-state analysis of **124** through x-ray diffraction shows an orientation in which the methoxy group is distal to DMAP (Figure 6.2). Furthermore, the C-O bond length (1.33 Å) indicates partial double bond character in comparison to an alcohol C-O (1.41 Å) bond and a ketone C-O (1.21 Å) bond.²⁶ This double bond character is in agreement with the resonance structures of **124** wherein the positive charge is distributed between an oxonium and an iminium structure.

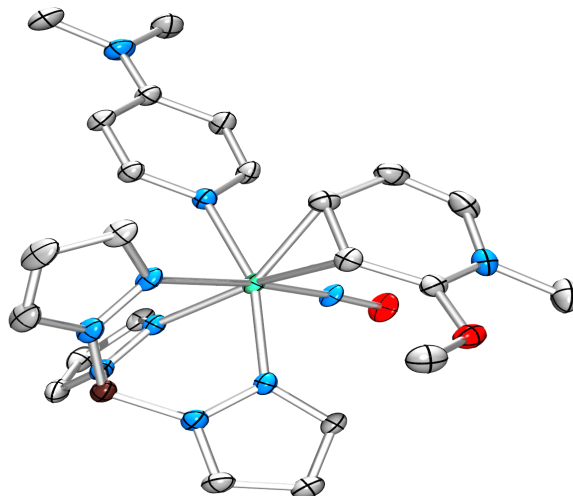
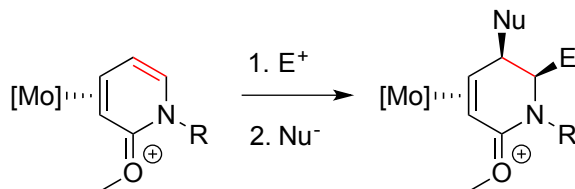
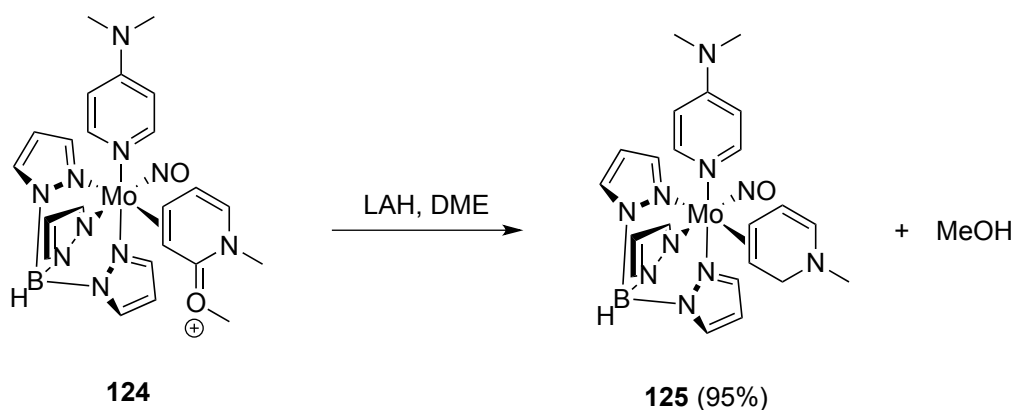


Figure 6.2. Crystal structure of **124A**. The triflate anion is omitted for clarity. Bond lengths (Å): Mo—C(4) 2.231(4); Mo—C(3) 2.291(4); Mo—N(DMAP) 2.228(3); Mo—N(NO) 1.763(3); C(2)—N(NMe) 1.335(6); C(2)—O(OMe) 1.331(5).

After the initial electrophilic additions to form **123** and **124**, tandem electrophilic-nucleophilic additions were attempted (Scheme 6.5). Adding a -30 °C solution of HOTf in CH₃CN to **123** or **124**, followed by a nucleophile (e.g., MTDA, *N*-methylpyrrole, LiDMM, imidazole, or propylamine) results in the isolation of starting material. Attempts to use other electrophiles result in either oxidation of the metal complex, as is the case for halogen electrophiles (e.g., Selectfluor, NBS, and NCS), or no reactivity, as is the case for carbon-based electrophiles (e.g., acetals and Michael acceptors). The lack of electrophilic addition to **123** or **124** is believed to be due to the significant electron-density withdrawal from the metal center, which reduces the nucleophilicity of the uncoordinated π -bond (highlighted in red).

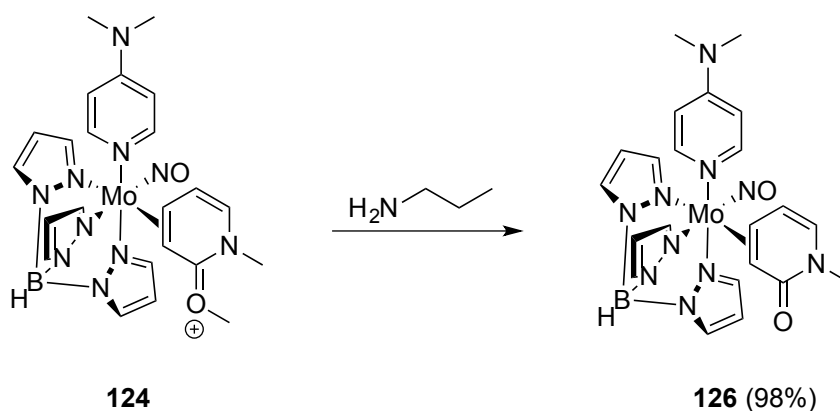
Scheme 6.5. Attempted electrophilic-nucleophilic additions to **123** and **124**.

We then endeavored to reduce the oxonium in an attempt to access a neutral dihydropyridine complex. It was found that $NaBH_4$ and $NaCNBH_3$ were too weak to reduce the oxonium. However, adding lithium aluminum hydride (LAH) to a solution of **124** revealed a new reduced species with an $E_{p,a}$ at -0.2 V, which indicates the presence of a more electron-rich ligand than before the reaction. NMR analysis of this new product showed a lack of any methoxy groups; rather, geminal protons at 3.81 and 3.61 ppm were identified using HSQC. This new species was identified as the product of an over-reduction of **124** to yield the *N*-methylated dihydropyridine complex, **125** (Scheme 6.6).

Scheme 6.6. Reduction of **124** to yield **125**.

With the intention of adding propylamine as a nucleophile to the oxonium carbon, a solution of propylamine in DCM was added to **124** at room temperature and this mixture was stirred for 18 h. The resulting green solution was then washed with NaHCO₃ (aq. sat.), dried with MgSO₄, and added to stirring pentane. The resulting precipitate was isolated, washed with pentane, and desiccated to yield a light green solid. The ¹H NMR spectrum of this solid lacks the presence of a methoxy resonance, similar to that observed for **125**; however, no geminal proton signals are observed, indicating a lack of propylamine addition. Furthermore, resonances for the alkene peaks (H5 and H6) are still seen at 5.33 and 6.07 ppm, respectively, but this upfield shift in their resonance (from 6.43 and 6.34 ppm) would imply a loss of the oxonium. Interestingly, the ¹³C NMR of this solid still has a carbonyl resonance at 173.6 ppm; however, this is more upfield from the carbonyl observed in **124** (175.7 ppm). With this information this new species was identified as the product of a demethylation of the oxonium, yielding **126** (Scheme 6.7).

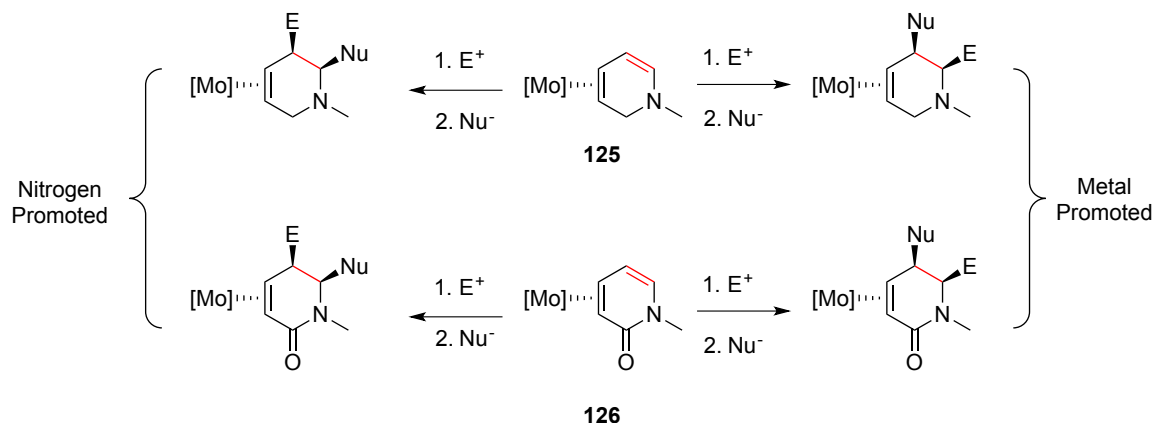
Scheme 6.7. Oxonium demethylation of **124**.



In agreement with this assessment is the negative shift in anodic wave (from +0.80 V to +0.08 V) and a weaker nitrosyl stretch frequency than for **124** (1579 vs 1596 cm^{-1}). Furthermore, a carbonyl stretch at 1615 cm^{-1} is in agreement with **126** containing an amide.

Attempts to perform tandem electrophilic-nucleophilic additions (Scheme 6.8) to **125** and **126** have been unsuccessful. Of interest is whether the metal or the nitrogen will control the reactivity. Interestingly, although not unexpected, subjecting a single coordination diastereomer of **124** (isolated by the selective precipitation described above) to the over-reduction conditions to form **125**, or the demethylation conditions to yield **126**, yields retention of the cdr in the final product.

Scheme 6.8. Attempted tandem electrophilic-nucleophilic additions to **123** and **124**.



An interesting observation was made in the ^1H NMR of **123** and **124**. The protons bound to the DMAP ancillary ligand experience a significant broadening. Typically the DMAP-B protons have a splitting pattern resembling a doublet-of-doublets while the

DMAP-A protons are observed as a broad singlet. A good example of this splitting pattern is seen in the ^1H NMR of **125** (Figure 6.3).

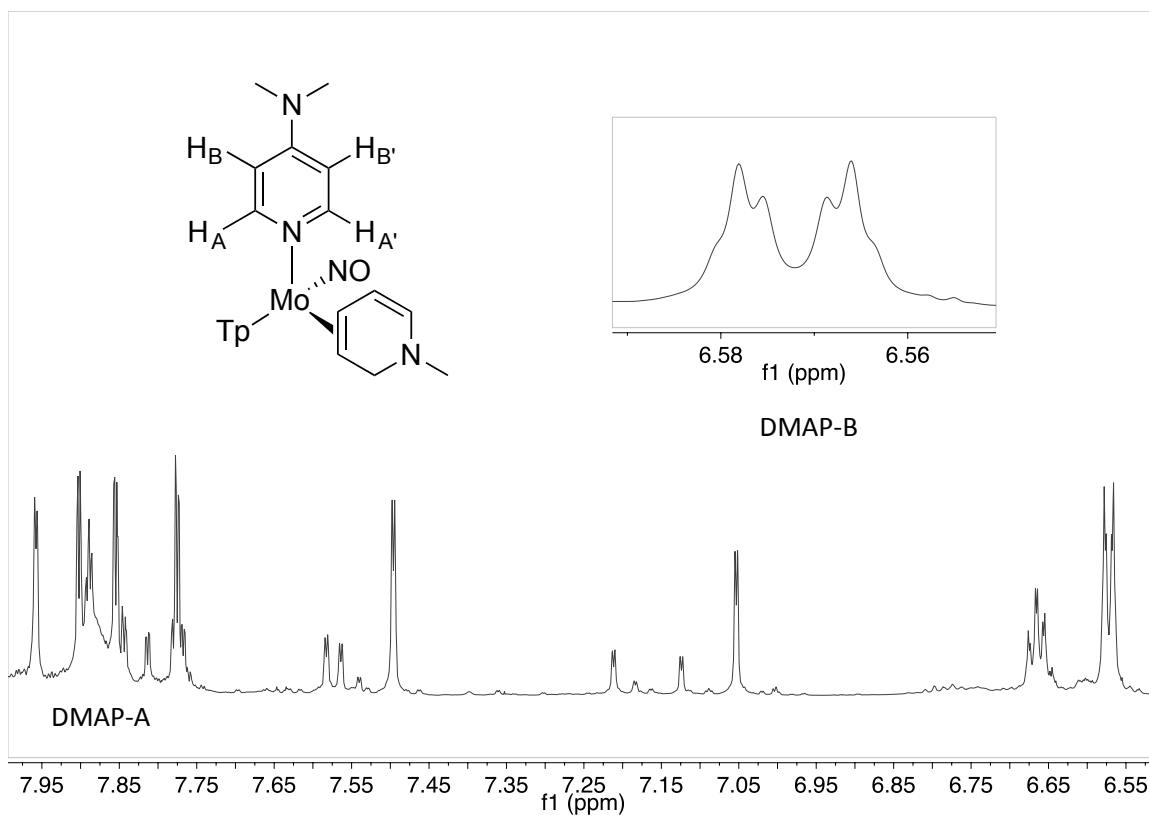


Figure 6.3. ^1H NMR of **125** (d^6 -Acetone, 25 °C).

The averaging of these signals is due to the rotation at the DMAP-Mo bond. The DMAP-B protons experience little difference in magnetic environment upon rotation and so their signal averaging will occur at a lower temperature than the DMAP-A protons. The DMAP-A protons, being close to the metal center, experience significantly different magnetic environments upon rotation at the DMAP-Mo bond. For this reason, DMAP-A protons are observed as a broad singlet because the rotational barrier at the DMAP-Mo bond is great enough to slow signal averaging.

As discussed in Chapter 3, the p-orbitals at the nitrogen within the ring of DMAP are expected to donate into the $d\pi$ symmetric orbitals of molybdenum to stabilize electron

withdrawal from the metal center. As the eta-2 bound ligand's π -acidity increases, so will the donation from DMAP, subsequently increasing the barrier of rotation at the DMAP-Mo bond. This effect can be seen in the ^1H NMR of **124** at room temperature (Figure 6.4). Contrast to the typical doublet-of-doublets seen for the DMAP-B protons, in **124** the DMAP-B protons are observed as a broad singlet while the DMAP-A protons are very near to coalescence. A ^1H NMR experiment of a CD_3CN solution of **124** at 10 °C revealed the coupling constant between DMAP-A of **124B** and DMAP-B of **124B** to be 6.8 Hz. The difference in chemical shift between DMAP-A of **124B** and DMAP-A' of **124B** was determined to be 605 Hz at 10 °C. The approximate coalescence temperature (50 °C) between DMAP-A and DMAP-A' of **124B** was obtained by VT-NMR in CD_3CN (0 – 75 °C). From this information, the approximate rate of isomerization was determined ($k = 1343 \text{ s}^{-1}$) and with it the free energy of activation of isomerization was approximated to be $14.3 \pm 0.5 \text{ kcal/mol}$ at 50 °C. As expected a similar increase in rotational barrier is seen for the $[\text{TpMo}(\text{NO})(\text{DMAP})(2,3,4\text{-}\eta^2\text{-naphthalenium})]^+$ complex **27** (Chapter 3, Figure 3.3). Measuring the rotational barrier of the DMAP-Mo bond gives insight into the electron density at the metal center. However, considering the need for lower temperature ^1H NMR experiments (e.g., $< 0 \text{ }^\circ\text{C}$), other methods for determining relative electron density at the metal center (e.g., CV and IR) remain more advantageous.

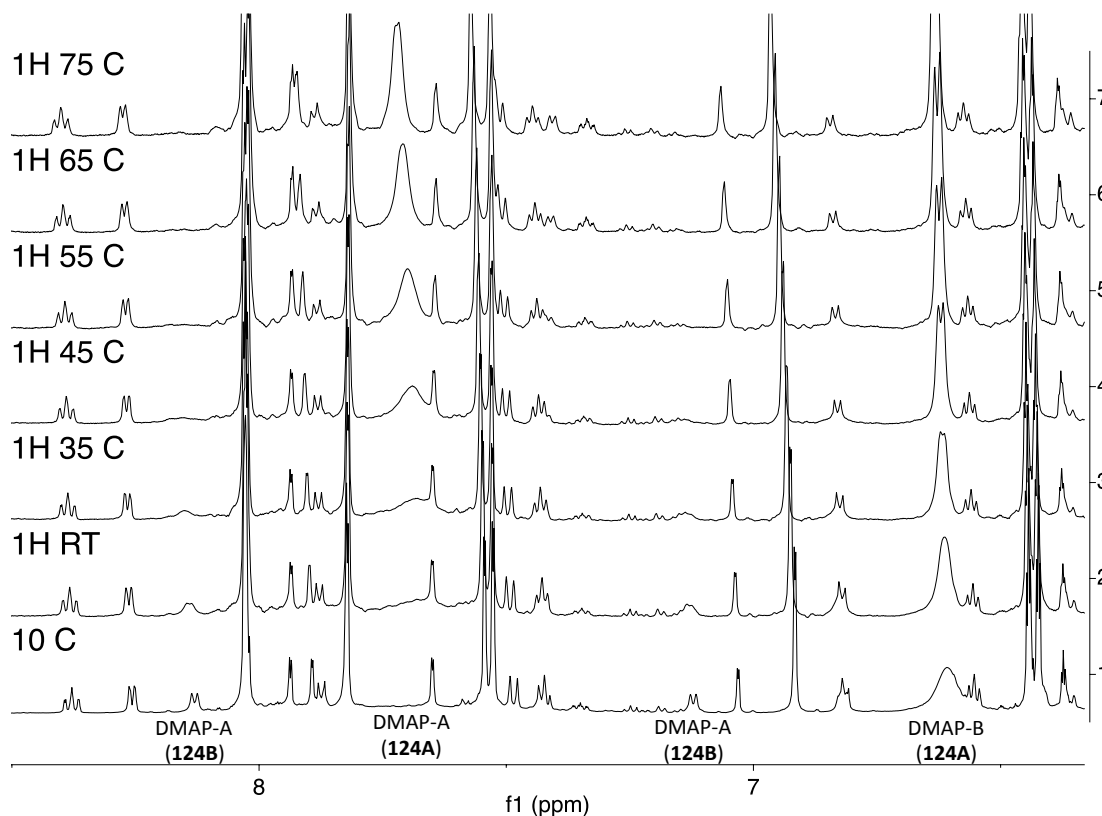
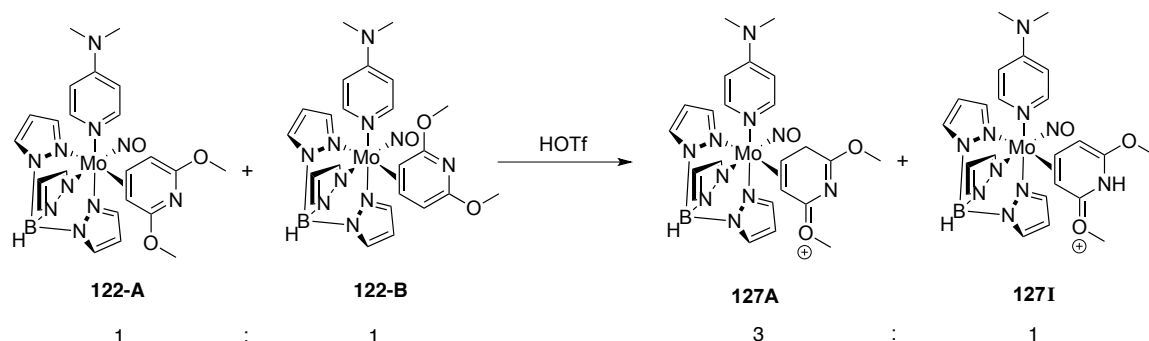


Figure 6.4. ^1H NMR spectra of **124** at various temperatures in CD_3CN .

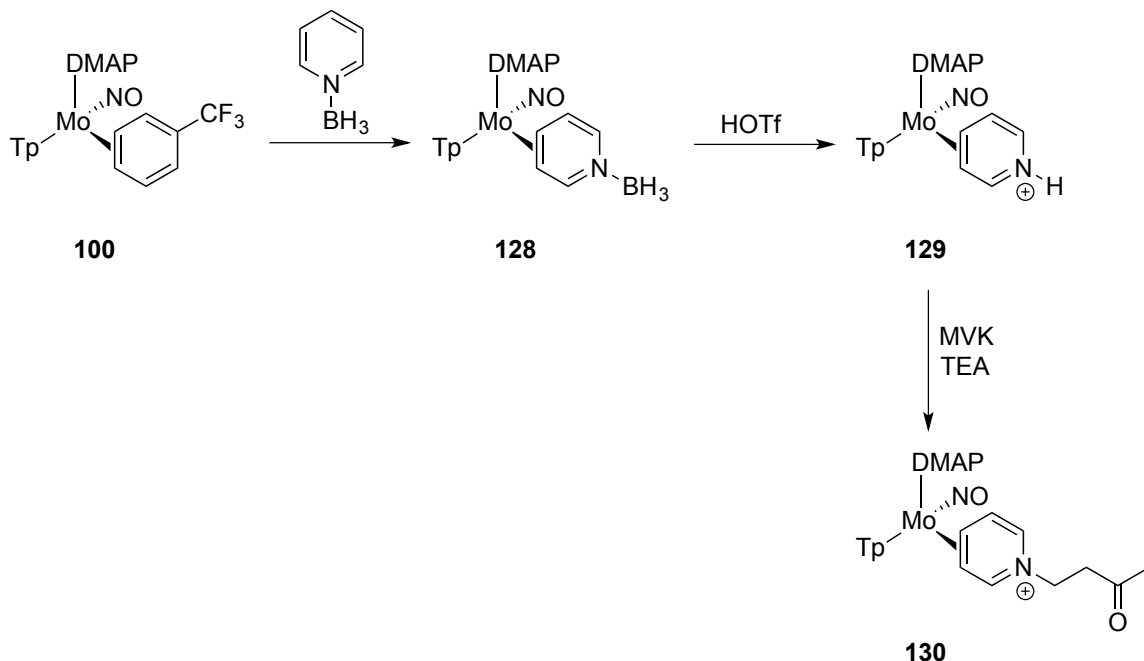
Similar to the protonation of **121**, complex **122** can be protonated by $\text{HOTf}/\text{CH}_3\text{CN}$ at $-30\text{ }^\circ\text{C}$ and isolated as a precipitate upon addition to Et_2O (32 % yield) (Scheme 6.9). A ^1H NMR of this precipitate shows it to contain two main isomers. The expected protonation of the nitrogen to form **127I** is identified by a unique set of Tp signals and a doublet at 5.35 ppm. This doublet represents H5, which, through COSY, was used to identify H4 as a triplet at 4.11 ppm and H3 as a doublet at 2.81 ppm. These chemical shifts are in agreement with the oxonium orienting distal to the DMAP ancillary ligand. However, **127I** is not the major isomer isolated from the protonation of **122**. Although the initial protonation of **122** is believed to occur at the nitrogen, **127I** undergoes a tautomerization to yield **127A**, the product of protonating **122A** at C5. A mixture of **127A** and **127I** is isolated as a 3:1 ratio after precipitation. A key feature used

to identify **127A** is the geminal proton signals at 4.04 and 3.43 ppm, which have a large coupling constant of 22.5 Hz. One of the protons, H5, has a strong NOE interaction with the DMAP-A protons at 7.70 ppm, and this observation identifies the major isomer to be where the oxonium is distal to the DMAP.

Scheme 6.9. Protonation of **122**.



Further investigation into the dearomatization of pyridines is currently being pursued as a separate project. We have demonstrated the potential to use $\text{TpMo}(\text{NO})(\text{DMAP})(3,4\text{-}\eta^2\text{-}\alpha,\alpha,\alpha\text{-trifluorotoluene})$ as an exchange reagent, as such it is currently being used to investigate the binding and activation of pyridines. Encouragingly, the binding of pyridine-borane has shown to be possible, granted the pyridine-borane is stringently purified before use (Scheme 6.10).³⁶ Preliminary results show that this pyridine-borane can be protonated to yield **129**, which can subsequently be deprotonated in the presence of methyl vinyl ketone (MVK) to yield **130**. The ability to bind pyridine-borane represents a significant breakthrough in the dearomatization of pyridines. The tungsten analogue of the pyridine-borane complex was heavily utilized in the synthesis of a large variety of substituted piperidines.

Scheme 6.10. Exchange of TFT ligand for pyridine-borane and subsequent reactivity.

It is our belief that similar reactivity patterns will be found using $\{\text{TpMo}(\text{NO})(\text{DMAP})\}$, which will offer a more economically viable alternative for the dearomatization of pyridines than the $\{\text{TpW}(\text{NO})(\text{PMe}_3)\}$ fragment.

In the Harman Lab, we have demonstrated an ability to selectively bind pyridines to transition metals in an η^2 fashion. While not the first reported η^2 complexes of pyridines, the $\text{TpW}(\text{NO})(\text{PMe}_3)(\eta^2\text{-2,6-lutidine})$ and $\text{TpW}(\text{NO})(\text{PMe}_3)(\eta^2\text{-2-dimethylaminopyridine})$ complexes were the first to demonstrate metal-promoted reactivity of the coordinated pyridine. These addition reactions subsequently yielded a wide variety of substituted dihydro and tetrahydropyridines. Pyridines themselves belong to a broader class of compounds that are referred to as aromatic, nitrogen-containing heterocycles (ANHs). Examples of ANHs include azacycles (i.e., pyrroles and pyridines),

diazacycles (i.e., pyrimidines pyrazoles, and imidazoles), and triazacycles (i.e., triazines and triazoles). Similar to their aromatic, hydrocarbon analogues, ANHs often yield substituted aromatics during attempted addition reactions. While there are synthetic methods to dearomatize ANHs through hydrogenation,²⁷ a lack of selectivity and functional group compatibility often hinders this approach.

To complement current methods for the synthesis of dearomatized azacycles from their aromatic precursors, the Harman Lab has thoroughly explored the binding and subsequent organic transformations of ANHs with $\{\text{Os}(\text{NH}_3)_5\}^{2+}$, $\{\text{TpRe}(\text{CO})(\text{MeIm})\}$, and $\{\text{TpW}(\text{NO})(\text{PMe}_3)\}$.²⁸⁻³³ From the synthesis of epibatidine derivatives from pyrroles,^{30, 34} to the synthesis of azabicyclo[2.2.2]octadienes from pyridines,³⁵ the dearomatization of ANHs has been a prime example of the powerful synthetic ability of these dearomatization agents. In one example, the product of a [4+2] cycloaddition between acrylonitrile and an enantioenriched lutidinium complex yielded an azabicyclic compound with an enantiomeric ratio (er) of 9:1 (ee = 80%).³⁵ The impressive chemistry developed with these dearomatization agents provides a great incentive for investigating ANH dearomatization with $\{\text{TpMo}(\text{NO})(\text{L})\}$.

The eta-2 pyridine complexes described above represent the first examples of binding and activating ANHs with $\{\text{TpMo}(\text{NO})(\text{L})\}$. Molybdenum is far from the expansive chemistry demonstrated with its third-row congeners. However, the initial binding and reactivity described in this chapter gives insight into the electronic and steric conditions required to isolate $\text{TpMo}(\text{NO})(\text{L})(\eta^2\text{-ANH})$ complexes. With a broad horizon ahead, exploring the dearomatization of ANHs with $\{\text{TpMo}(\text{NO})(\text{L})\}$ is sure to further

the fundamental understanding of the synthesis of alkaloid cores from aromatic precursors.

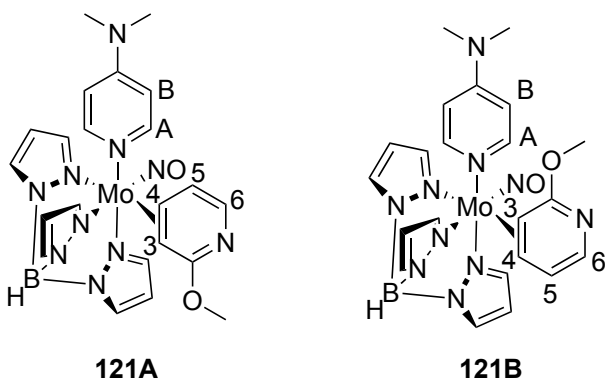
6.3 Conclusion

The binding of 2-methoxy- and 2,6-dimethoxypyridine to {TpMo(NO)(DMAP)} represents the first thermally stable η^2 bound pyridine complexes of molybdenum. Similar to that seen with the TpW(NO)(PMe₃)(η^2 -2-methoxypyridine) complex, initial electrophilic additions to **121** occur at the nitrogen. Subsequently, the syntheses of protonated and methylated pyridinium complexes (e.g., **123** and **124**) were accomplished. Attempts to add electrophiles on the remaining π -bond of **123** and **124** were unsuccessful; however, reduction of the oxonium of **124** was accomplished with LAH to yield **125**. Furthermore, the demethylation of the oxonium methyl of **124** was accomplished to yield the pyridone complex **126**. Future investigations will focus on the organic transformations of the newly isolated TpMo(NO)(DMAP)(η^2 -pyridine-borane) complex.

6.4 Experimental

General Methods. NMR spectra were obtained on a 600 or 800 MHz spectrometer. All chemical shifts are reported in ppm, and proton and carbon shifts are referenced to tetramethylsilane (TMS) utilizing residual ^1H or ^{13}C signals of the deuterated solvents as an internal standard. Coupling constants (J) are reported in hertz (Hz). Infrared spectra (IR) were recorded as a glaze on a spectrometer fitted with a horizontal attenuated total reflectance (HATR) accessory or on a diamond anvil ATR assembly. Electrochemical experiments were performed under a dinitrogen atmosphere. Cyclic voltammetry data were taken at ambient temperature ($\sim 25^\circ\text{C}$) at 100 mV/s in a standard three-electrode cell with a glassy carbon working electrode, *N,N*-dimethylacetamide (DMA) or acetonitrile (CH_3CN) solvent (unless otherwise specified), and tetrabutylammonium hexafluorophosphate (TBAH) electrolyte (approximately 0.5 M). All potentials are reported versus NHE (normal hydrogen electrode) using cobaltocenium hexafluorophosphate ($E_{1/2} = -0.78\text{ V}$), ferrocene ($E_{1/2} = +0.55\text{ V}$), or decamethylferrocene ($E_{1/2} = +0.04\text{ V}$) as an internal standard. The peak-to-peak separation was less than 100 mV for all reversible couples. Unless otherwise noted, all synthetic reactions were performed in a glovebox under a dry nitrogen atmosphere. Deuterated solvents were used as received. Pyrazole (Pz) protons of the (trispyrazolyl) borate (Tp) ligand were uniquely assigned (e.g., “Pz3B”) using a combination of two-dimensional NMR data and (dimethylamino)pyridine–proton NOE interactions (see Figure 3.4). When unambiguous assignments were not possible, Tp protons were labeled as “Pz3/5 or Pz4”. All J values for Pz protons are 2 (± 0.2) Hz.

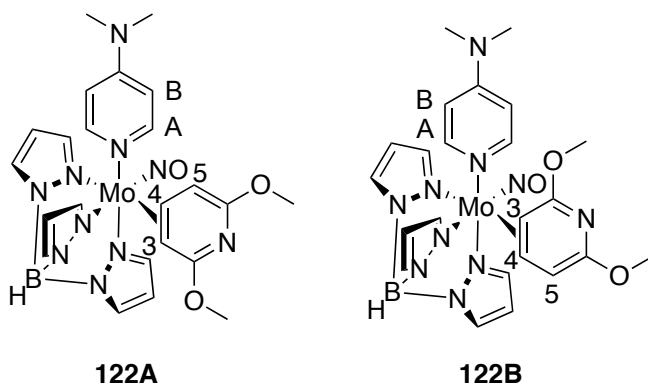
Synthesis of TpMo(NO)(DMAP)(3,4- η^2 -2-methoxypyridine) (121**).**



To a 50 mL round bottom flask charged with a stir pea was added **26** (6 g, 10.77 mmol) and 2-methoxypyridine (20 mL). This yellow mixture was left stirring at room temperature overnight (42 h). The resulting orange precipitate was isolated on a 60 mL fine porosity fritted disc, washed with pentane (5 x 60 mL), and desiccated 1 h to yield **121** (4.48 g, 73% yield). CV (DMAc) $E_{p,a} = -0.22$ V (NHE). IR: $\nu(\text{C-H } sp^2) = 2934 \text{ cm}^{-1}$, $\nu(\text{B-H}) = 2475 \text{ cm}^{-1}$, $\nu(\text{NO}) = 1575 \text{ cm}^{-1}$. 1:1.4 **A**:**B** ratio. ^1H NMR (d^6 -Acetone, 600 MHz): δ 8.03 (1H, d, Pz3/5), 8.00 (1H, d, Pz3/5), 7.92 (1H, d, Pz3/5), 7.87 (1H, d, Pz3/5), 7.85 (3H, m, Pz3/5), 7.75 (4H, buried bs, DMAP-A **121A** and **121B**), 7.51 (1H, d, Pz3/5), 7.50 (1H, d, Pz3/5), 6.97 (1H, d, Pz3/5), 6.95 (1H, d, Pz3/5), 6.67 (2H, bd, DMAP-B **121A/121B**), 6.61 (2H, bd, DMAP-B **121A/121B**), 6.58 (1H, d, $J = 6.4$, 1H, H6 **121B**), 6.56 (1H, d, $J = 6.4$, H6 **121A**), 6.37 (2H, m, Pz4), 6.33 (1H, t, Pz4), 6.26 (1H, t, Pz4), 6.24 (1H, m, H5 **121B**), 6.13 (1H, t, Pz4), 6.12 (1H, t, Pz4), 5.85 (1H, m, H5 **121A**), 3.79 (3H, s, OMe **121A**), 3.65 (1H, dd, $J = 8.8, 5.5$, H3 **121A**), 3.62 (3H, s, OMe **121B**), 3.28 (1H, d, $J = 8.8$, H3 **121B**), 3.23 (1H, dd, $J = 8.8, 5.5$, H4 **121B**), 3.08 (6H, s, NMe **121A**), 3.07 (6H, s, NMe **121B**), 2.96 (1H, d, $J = 8.8$, H4 **121A**). Note: CDCl_3 used for carbon experiment due to solubility issues in d^6 -Acetone making ^{13}C NMR

experiments too low in concentration. ^{13}C NMR (CDCl_3 , 200 MHz): δ 171.4, 170.7, 153.9, 153.8, 146.9, 144.0, 142.2, 142.1, 141.9, 140.2, 139.9, 138.7, 136.4, 136.3, 136.0, 135.9, 134.7, 134.7, 128.4, 128.0, 118.2, 117.3, 116.8, 111.0, 107.4, 105.9, 105.8, 105.6, 105.5, 105.4, 105.2, 78.1, 77.2, 75.4, 65.0, 62.4, 52.4, 52.1, 39.3. HRMS: $\text{C}_{22}\text{H}_{27}\text{N}_{10}\text{O}_2\text{BMo}+\text{H}^+$ obsd (%), calcd (%), ppm: 567.1613 (45), 567.1556 (54), 10.0; 569.1550 (66), 569.1553 (49), -0.5; 570.1533 (88), 570.1552 (81), -3.4; 571.1549 (100), 571.1547 (86), 0.4; 572.1552 (87), 572.1560 (74), -1.3; 573.1544 (92), 573.1546 (100), -0.4; 574.1537 (40), 574.1575 (34), -6.6; 575.1546 (30), 575.1566 (39), -3.4.

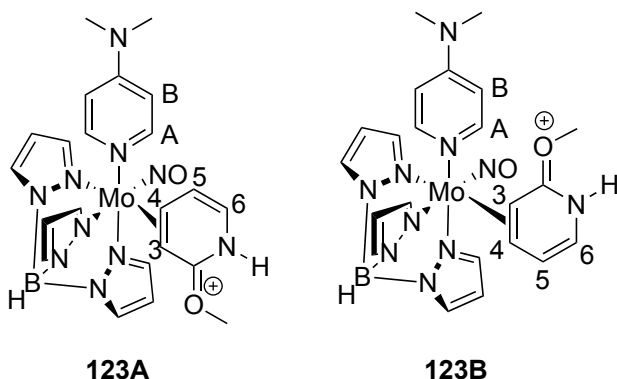
Synthesis of $\text{TpMo}(\text{NO})(\text{DMAP})(3,4\text{-}\eta^2\text{-}2,6\text{-dimethoxypyridine})$ (122**).**



To a 25 mL round bottom flask charged with a stir pea was added **26** (1.0 g, 1.79 mmol) and 2,6-dimethoxypyridine (3 mL). This mixture was stirred at room temperature for 20 h. The resulting orange precipitate was then collected on a 15 mL medium porosity fritted disc, washed with pentane (3 x 15 mL), and dried in vacuo to yield **122** (580 mg, 54% yield). CV (DMAc) $E_{\text{p,a}} = -0.37$ V (NHE). IR: $\nu(\text{C-H sp}^2) = 2935$ cm^{-1} , $\nu(\text{B-H}) = 2471$ cm^{-1} , $\nu(\text{NO}) = 1600$ cm^{-1} . ^1H NMR (CDCl_3 , 600 MHz, @ 0 $^\circ\text{C}$): δ 5.51 (1H, d, $J = 5.0$, H5 **122B**), 5.12 (1H, d, $J = 5.0$, H5 **122A**), 3.71 (1H, dd, $J = 8.6, 5.0$, H4 **122A**), 3.50

(1H, dd, $J = 8.6, 5.0$, H4 **122B**), 3.18 (1H, d, $J = 8.6$, H3 **122B**), 3.06 (1H, buried under OMe, H3 **122A**). ^{13}C NMR (201 MHz, CDCl_3 , @ 0 °C): δ 172.4, 171.6, 163.1, 154.3, 153.9, 153.8, 153.7, 150.7, 144.0, 142.1, 142.0, 141.1, 140.9, 140.3, 140.0, 136.3, 136.2, 135.9, 135.9, 134.7, 134.7, 107.4, 105.9, 105.8, 105.6, 105.4, 105.3, 105.2, 100.8, 88.4, 87.8, 80.5, 61.6, 59.2, 55.0, 54.8, 52.9, 52.5, 39.3, 39.3.

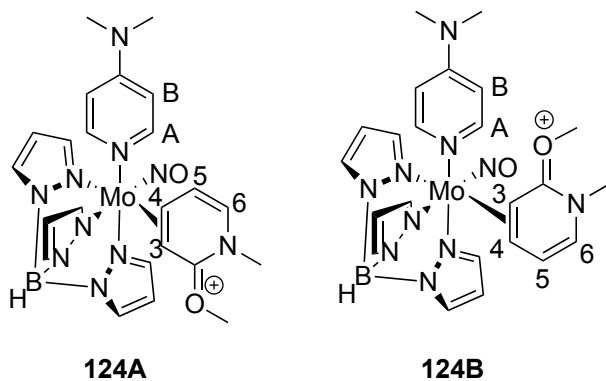
Synthesis of $[\text{TpMo}(\text{NO})(\text{DMAP})(3,4\text{-}\eta^2\text{-2-methoxypyridinium})]^+$ (OTf) (123**).**



To a 4-dram vial was added **121** (1 g, 1.7 mmol) and CH_3CN (10 mL). This mixture was cooled at -30 °C for 15 min. Next, a -30 °C 1M solution of HOTf/ CH_3CN (3.6 mL, 3.6 mmol) was added to the reaction mixture and the resulting yellow solution was left at -30 °C. After 15 min, this solution was then added slowly to stirring Et_2O (400 mL), which yielded a yellow precipitate. This precipitate was collected on a 30 mL fine porosity fritted disc, washed with Et_2O (3 x 30 mL), and desiccated to yield **123** (1.14 g, 93% yield). CV (DMAc) $E_{\text{p,a}} = +0.87$ V (NHE). IR: $\nu(\text{C-H sp}^2) = 3103\text{ cm}^{-1}$, $\nu(\text{B-H}) = 2503\text{ cm}^{-1}$, $\nu(\text{NO}) = 1599\text{ cm}^{-1}$. Product isolated as a 2:1 **A**:**B** ratio. ^1H NMR ($\text{d}^6\text{-Acetone}$, 600 MHz): δ 11.10 (2H, bs, NH **123A** & **123B**), 8.15 (1H, d, Pz5C **123A**), 8.14 (1H, d, Pz5C **123B**), 8.10 (1H, d, Pz5A **123A**), 8.03 (1H, d, Pz5A **123B**), 7.94 (2H, d, Pz5B, **123A** and **123B**), 8.10 (1H, d, Pz5A **123A**), 8.03 (1H, d, Pz5A **123B**), 7.94 (2H, d, Pz5B, **123A** and

123B), 7.92 (1H, d, Pz3A/Pz3C, **123B**), 7.88 (1H, d, Pz3A/Pz3C **123B**), 7.80 (4H, bs, DMAP-A **123A** and **123B**), 7.77 (1H, d, Pz3C **123A**), 7.62 (1H, d, Pz3A **123A**), 7.15 (1H, d, Pz3B **123B**), 7.03 (1H, d, Pz3B **123A**), 6.75 (2H, bs, DMAP-B **123A**), 6.64 (1H, t, $J = 5.9$, H5 **123B**), 6.50 (1H, t, Pz4C **123A**), 6.48 (1H, t, Pz4C **123B**), 6.45 (2H, m, Pz4A **123A** and H6 **123B**), 6.42 (1H, m, H6 **123A**), 6.40 (1H, t, Pz4A **123B**), 6.31 (1H, t, $J = 5.9$, H5 **123A**), 6.19 (1H, t, Pz4B **123B**), 6.18 (1H, t, Pz4B **123A**), 4.17 (1H, dd, $J = 8.5, 5.4$, H4 **123A**), 3.83 (3H, s, OMe **123B**), 3.80 (3H, s, OMe **123A**), 3.54 (1H, d, $J = 8.5$, H2 **123B**), 3.47 (1H, dd, $J = 8.5, 5.4$, H4 **123B**), 3.14 (6H, s NMe **123A**), 3.12 (6H, s NMe **123B**), 2.92 (1H, d, $J = 8.5$, H2 **123A**). ^{13}C NMR (d^6 -Acetone, 200 MHz): δ 175.9 (CO), 155.6 (DMAP-C), 150.4 (2C, DMAP-A), 143.8 (Pz3A), 143.2 (Pz3B), 142.0 (Pz3C), 138.5 (2C, Pz5A & Pz5C), 136.8 (Pz5B), 120.8 (C6), 114.2 (C5), 108.9 (2C, DMAP-B), 107.8 (Pz4A/C), 107.5 (Pz4A/C), 106.9 (Pz4B), 78.2 (C4), 57.9 (OMe), 56.1 (C3), 39.2 (2C, DMAP-Me). HRMS: $\text{C}_{22}\text{H}_{28}\text{N}_{10}\text{O}_2\text{BMo}^+$ obsd (%), calcd (%), ppm: 567.1544 (40), 567.1556 (54), -2.2; 569.1545 (64), 569.1553 (49), -1.4; 570.1541 (96), 570.1552 (81), -2.0; 571.1561 (89), 571.1547 (86), 2.5; 572.1544 (100), 572.1560 (74), -2.7; 573.1549 (77), 573.1546 (100), 0.5; 574.1586 (40), 574.1575 (34), 2.0; 575.1566 (31), 575.1566 (39), 0.0.

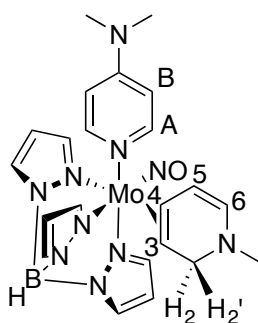
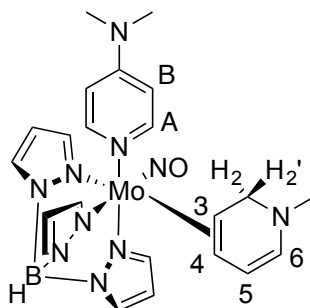
Synthesis of $[\text{TpMo}(\text{NO})(\text{DMAP})(3,4\text{-}\eta^2\text{-2-methoxy-N-methylpyridinium})]^+ (\text{OTf})$ (**124**).



To a 4-dram vial was added **121** (1 g, 1.7 mmol), CH_3CN (5 mL), and MeOTf (400 mg, 2.44 mmol). This orange mixture was left sitting at room temperature for 10 min, yielding a dark red solution. This solution was added to stirring Et_2O (100 mL) to yield a red precipitate, which was then isolated on a 30 mL fine porosity fritted disc, washed with Et_2O (3x30 mL), and desiccated to yield the dark orange product **124** (1.72 g, 89% yield). CV (DMAc) $E_{\text{p,a}} = +0.79$ V (NHE). IR: $\nu(\text{C-H sp}^2) = 3105$ cm^{-1} , $\nu(\text{B-H}) = 2484$ cm^{-1} , $\nu(\text{NO}) = 1596$ cm^{-1} . Product isolated as a 3:1 **A**:**B** ratio. ^1H NMR ($\text{d}^6\text{-Acetone}$, 600 MHz): 8.27 (1H, d, $J = 7.3$, DMAP-A **124B**), 8.16 (1H, d, Pz5C **124A**), 8.15 (1H, d, Pz5A **124A**), 8.13 (1H, d, Pz3/5 **124B**), 8.20 (1H, d, Pz3/5 **124B**), 7.96 (1H, d, Pz3/5 **124B**), 7.94 (1H, d, Pz3/5 **124B**), 7.93 (1H, d, Pz5B **124A**), 7.79 (2H, bs, DMAP-B **124A**), 7.74 (1H, d, Pz3C **124A**), 7.65 (1H, d, Pz3A **124A**), 7.28 (1H, d, $J = 7.3$, DMAP-A **124B**), 7.09 (1H, d, Pz3B **124B**), 7.02 (1H, bs, DMAP-B **124B**), 7.00 (1H, d, Pz3B **124A**), 6.75 (2H, bs, DMAP-B **124A**), 6.61 (1H, bs, DMAP-B **124B**), 6.51 (1H, t, Pz4C **124A**), 6.49 (1H, t, Pz4A **124A**), 6.48 (1H, t, Pz4 **124B**), 6.43 (1H, d, $J = 7.2$, H6 **124A**), 6.34 (1H, t, $J = 6.3$, H5 **124A**), 6.39 (1H, t, Pz4 **124B**), 6.18 (1H, t, Pz4 **124B**), 6.17 (1H,

t, Pz4B **124A**), 4.21 (1H, dd, $J = 8.6, 6.3$, H4 **124A**), 3.75 (3H, s, NMe **124A**), 3.69 (1H, d, $J = 8.6$, H3 **124B**), 3.54 (1H, dd, $J = 8.6, 5.8$, H4 **124B**), 3.50 (3H, s, OMe **124A**), 3.12 (6H, s, NMe **124A**), 3.00 (1H, d, $J = 8.6$, H3 **124A**). ^{13}C NMR (d^6 -Acetone, 200 MHz): δ **124A**: 175.7 (OMe), 155.89 (DMAP-C), 150.5 (2C, DMAP-A), 143.9 (Pz3A), 143.2 (Pz3B), 142.1 (Pz3C), 138.9 (Pz5A/5C), 138.6 (Pz5A/5C), 136.9 (Pz5B), 120.9 (C5/C6), 120.8 (C5/C6), 109.1 (2C, DMAP-B), 108.1 (Pz4A/4C), 107.9 (Pz4A/4C), 106.9 (Pz4B), 78.1 (C4), 58.5 (OMe), 55.9 (C3), 39.3 (DMAP-Me), 37.3 (NMe). **124B** (signals are too small for unambiguous assignment): 175.6, 155.9, 150.2, 143.0, 142.5, 138.5, 137.8, 136.5, 121.5, 121.2, 108.9, 107.7, 107.0, 106.9, 76.7, 66.1, 58.3, 56.4, 39.3, 29.8, 15.6. HRMS: $\text{C}_{23}\text{H}_{30}\text{N}_{10}\text{O}_2\text{BMo}^+$ obsd (%), calcd (%), ppm: 581.1728 (49), 581.1713 (54), 2.6; 583.1713 (48), 583.1710 (49), 0.6; 584.1723 (75), 584.1709 (81), 2.4; 585.1716 (85), 585.1704 (86), 2.1; 586.1716 (73), 586.1716 (74), -0.1; 587.1721 (100), 587.1703 (100), 3.0; 588.1724 (32), 588.1731 (34), -1.3; 589.1738 (39), 589.1723 (39), 2.6.

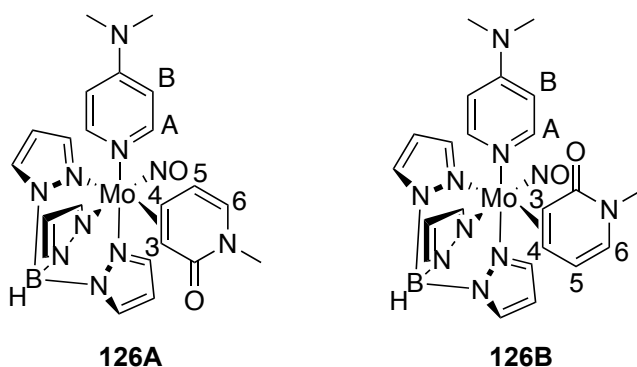
Synthesis of $\text{TpMo}(\text{NO})(\text{DMAP})(3,4\text{-}\eta^2\text{-N-methyldihydropyridine})$ (**125**).

**125A****125B**

To a solution of **124** (500 mg, 0.679 mmol) and dimethoxyethane (5 mL) was added lithium aluminum hydride (LAH) (75 mg, 1.97 mmol). The resulting dark red solution was then stirred at room temperature for 5 min. This solution was then added to stirring H₂O (30 mL) in a 50 mL round bottom flask, yielding a green precipitate. This mixture was let stirring at room temperature for 20 h. The resulting yellow precipitate was isolated on a 30 mL medium porosity fritted disc, washed with H₂O (3 x 20 mL) and hexanes (3 x 20 mL) (Note: do not stir the precipitate with washing solvent, just wash through), and dried *in vacuo* 1 h. This precipitate was then triturated in stirring hexanes (20 mL) for 20 h and the resulting precipitate was isolated on a 15 mL fine porosity fritted disc, washed with hexanes (3 x 10 mL), and desiccated to yield **125** (360 mg, 95% yield). CV (DMAc) $E_{p,a} = -0.23$ V (NHE). IR: $\nu(\text{C-H } sp^2) = 2922 \text{ cm}^{-1}$, $\nu(\text{B-H}) = 2468 \text{ cm}^{-1}$, $\nu(\text{NO}) = 1566 \text{ cm}^{-1}$. Product isolated as a 4:1 **A**:**B** ratio. Confirmed **A** isomer by isolating **125** after selective precipitation of **124**, therefore the only peaks assigned to **B** are based on clean separation from **A** isomer. ¹H NMR (d⁶-Acetone, 600 MHz): δ 7.95 (1H, d, Pz3A **125A**), 7.90 (1H, d, Pz5A/C **125A**), 7.88 (2H, buried bs, DMAP-A **125A**), 7.85 (1H, d, Pz5A/C **125A**), 7.77 (1H, d, Pz5B **125A**), 7.49 (1H, d, Pz3C **125A**), 7.04 (1H, d, Pz3B **125A**), 6.66 (2H, m, DMAP-B **125B**), 6.58 (2H, m, DMAP-B **125A**), 6.30 (2H, t, Pz4A & C **125A**), 6.28 (1H, t, Pz4 **125B**), 6.24 (1H, t, Pz4 **125B**), 6.12 (1H, t, Pz4 **125B**), 6.11 (1H, t, Pz4B **125A**), 5.50 (1H, d, $J = 7.4$, H6 **125A**), 5.44 (1H, d, $J = 7.4$, H6 **125B**), 5.06 (1H, ddd, $J = 7.4, 4.6, \& 0.9$, H5 **125B**), 4.75 (1H, ddd, $J = 7.4, 4.6, \& 0.9$, H5 **125A**), 3.81 (1H dd, $J = 10.9 \& 2.8$, H2 **125A**), 3.61 (1H, dd, $J = 10.9 \& 5.0$, H2' **125A**), 3.05 (6H, s, N-Me **125A**), 2.62 (3H, s, N-Me **125A**), 2.59 (1H, m, H4 **125A**), 2.03 (1H, m, H3 **125A**). ¹³C NMR of **125A** only. ¹³C NMR (d⁶-Acetone, 200 MHz): δ 155.0

(DMAP-C), 151.1 (2C, DMAP-A), 143.5 (Pz3A), 142.0 (Pz3B), 141.3 (Pz3C), 137.1 (Pz5A/C), 136.7 (Pz5A/C), 135.5 (Pz5B), 131.6 (C6), 107.9 (DMAP-B), 106.5 (Pz4A/C), 106.2 (Pz4A/C), 106.1 (Pz4B), 103.6 (C5), 63.5 (C4), 61.7 (C3), 53.9 (C2), 43.2 (NMe), 39.1 (DMAP-Me). HRMS: $C_{22}H_{29}N_{10}OBMo+H^+$ obsd (%), calcd (%), ppm: 553.1769 (36), 553.1764 (54), 1.0; 555.1762 (65), 555.1760 (49), 0.3; 556.1734 (77), 556.1760 (82), -4.6; 557.1730 (92), 557.1754 (86), -4.3; 558.1783 (80), 558.1767 (74), 2.9; 559.1740 (100), 559.1754 (100), -2.4; 560.1814 (46), 560.1782 (34), 5.7; 561.1866 (44), 561.1773 (39), 16.6.

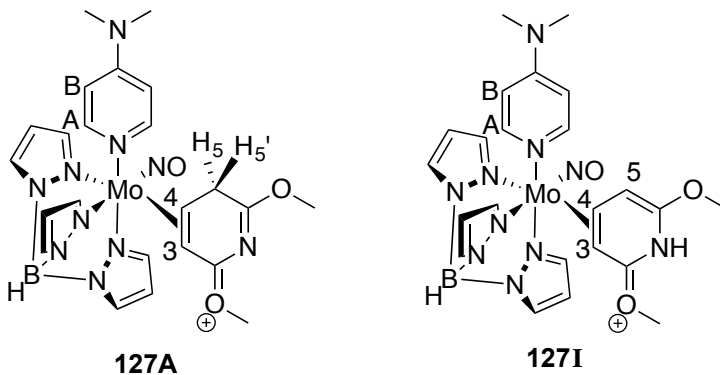
Synthesis of $TpMo(NO)(DMAP)(3,4-\eta^2-N$ -methylpyridin-2(1*H*)-one) (126).



To a 4-dram vial was added **124** (1.0 g, 0.0013 mol), DCM (5 mL), and propylamine (1.2 g, 0.020 mol). This solution was stirred overnight at room temp (20 h). The resulting green solution was washed with $NaHCO_3$ (sat. aq., 10 mL) and the aqueous layer was back-extracted with DCM (3 x 5 mL). The organic layers were combined and subsequently dried with $MgSO_4$. The $MgSO_4$ was removed on a 15 mL medium porosity fritted disc, washed with DCM (3 x 5 mL), and the resulting filtrate was evaporated *in vacuo* to an oil. This oil was then dissolved in DCM (15 mL) and the resulting solution was added to stirring pentane (200 mL), yielding a green precipitate. This precipitate was

isolated on a 30 mL fine porosity fritted disc, washed with pentane (3x10 mL) and desiccated to yield **126** (728 mg, 98% yield). CV (DMAc) $E_{p,a} = +0.08$ V (NHE). IR: $\nu(\text{C-H } sp^2) = 2927 \text{ cm}^{-1}$, $\nu(\text{B-H}) = 2481 \text{ cm}^{-1}$, $\nu(\text{CO}) = 1615 \text{ cm}^{-1}$, $\nu(\text{NO}) = 1579 \text{ cm}^{-1}$. ^1H NMR (d^6 -Acetone, 600 MHz): δ 8.44 (1H, d, Pz5A **126A**), 8.01 (1H, d, Pz3/5 **126B**), 7.99 (1H, d, Pz3/5 **126B**), 7.98 (1H, d, Pz5C **126A**), 7.91 (1H, d, Pz3/5 **126B**), 7.84 (1H, d, Pz5B **126A**), 7.83 (1H, d, Pz3A **126A**), 7.78 (2H, bs, DMAP-A **126A**), 7.71 (3H, d, Pz3/5 & DMAP-A **126B**), 7.60 (1H, d, Pz3C **126A**), 7.51 (1H, d, Pz3/5 **126B**), 7.03 (1H, d, Pz3B **126A**), 7.00 (1H, d, Pz3/5 **126B**), 6.63 (2H, bd, DMAP-B **126A**), 6.51 (2H, bd, DMAP-B **126B**), 6.37 (1H, t, Pz4 **126B**), 6.35 (1H, t, Pz4C **126A**), 6.30 (1H, t, Pz4 **126B**), 6.21 (1H, t, Pz4A **126A**), 6.12 (1H, t, Pz4B **126A**), 6.11 (1H, t, Pz4 **126B**), 6.08 (1H, d, $J = 7.5$, H6 **126B**), 6.07 (1H, d, $J = 7.5$, H6 **126A**), 5.73 (1H, t, $J = 7.4$, H5 **126B**), 5.33 (1H, dd, $J = 7.5$, 5.4, H5 **126A**), 3.48 (1H, dd, $J = 8.6$, 5.4, H4 **126A**), 3.29 (3H, s, NMe **126A**), 3.28 (3H, s, NMe **126B**), 3.07 (6H, s, NMe **126A**), 3.05 (6H, s, NMe **126A**), 3.00 (1H, m, H3 **126B**), 2.69 (1H, d, $J = 8.6$, H3 **126A**), 1.69 (1H, m, H4 **126B**). ^{13}C NMR (d^6 -Acetone, 200 MHz): δ 173.6 (CO), 155.2 (DMAP-C), 150.5 (DMAP-A), 146.7 (Pz5A), 142.5 (Pz3B), 141.6 (Pz3C), 137.7 (Pz5C), 136.7 (Pz3A/5B), 135.8 (Pz3A/5B), 123.4 (C6), 109.8 (C5), 108.3 (DMAP-B), 106.9 (Pz4C), 106.4 (Pz4B), 105.7 (Pz4A), 75.3 (C4), 62.8 (C3), 39.1 (DMAP-Me), 34.6 (NMe).

Synthesis of [TpMo(NO)(DMAP)(3,4- η^2 -2,6-dimethoxypyridinium)]⁺ (OTf) (127**).**



To a -30 °C solution of **122** (100 mg, 0.17 mmol) and CH₃CN (2 mL) was added a -30 °C, 1M solution of HOTf/CH₃CN (0.7 mL, 0.7 mmol). The resulting orange solution was left at -30 °C for 15 min and was subsequently added to stirring Et₂O (50 mL), yielding a bright orange precipitate. This precipitate was isolated on a 15 mL fine porosity fritted disc, washed with Et₂O (3 x 15 mL), and dried *in vacuo* to yield **127** (40 mg, 32% yield). CV (DMAc) $E_{p,a} = +0.98$ V (NHE). IR: $\nu(\text{C-H } sp^2) = 2954 \text{ cm}^{-1}$, $\nu(\text{B-H}) = 2511 \text{ cm}^{-1}$, $\nu(\text{NO}) = 1615 \text{ cm}^{-1}$. ¹H NMR (d⁶-Acetone, 600 MHz): δ 9.93 (1H, bs, N-H **127I**), 8.01 (1H, d, Pz3/5 **127I**), 7.99 (1H, d, Pz3/5 **127I**), 7.98 (1H, d, Pz5A **127A**), 7.93 (1H, d, Pz5C **127A**), 7.82 (1H, d, Pz5B **127A**), 7.74 (1H, d, Pz3C **127A**), 7.73 (2H, buried bs, DMAP-A **127A** and **127I**), 7.58 (1H, d, Pz3/5 **127I**), 7.57 (1H, d, Pz3/5 **127I**), 7.35 (1H, d, Pz3A **127A**), 7.15 (1H, d, Pz3B **127A**), 6.98 (1H, d, Pz3/5 **127I**), 6.83 (2H, m, DMAP-B **127I**), 6.66 (2H, bs, DMAP-B **127A**), 6.44 (1H, t, Pz4C **127A**), 6.41 (1H, t, Pz4A **127A**), 6.17 (1H, t, Pz4B **127A**), 6.13 (1H, t, Pz4 **127I**), 5.34 (1H, d, $J = 5.8$, H5 **127I**), 4.22 (3H, s, OMe **127A**), 4.20 (3H, s, OMe **127A**), 4.11 (1H, t, $J = 6.8$, H4 **127I**), 4.04 (1H, dd, $J = 22.5, 8.4$, H5' **127A**), 3.84 (3H, s, OMe **127I**), 3.73 (1H t, $J = 7.9$, H4 **127A**), 3.49 (3H, s, OMe **127I**), 3.47 (1H, dt, $J = 22.5, 1.3$, H5 **127A**), 3.03 (6H, s, NMe **127I**), 3.02 (6H, s, NMe **127A**), 2.94 (1H, dd, $J = 7.9, 1.3$, H3 **127A**) 2.81 (1H, d, $J = 8.3$,

H3 **127I**). ^{13}C NMR (d^6 -Acetone, 200 MHz): 191.9 (CO), 186.7 (CO), 155.6 (DMAP-C), 149.9 (2C, DMAP-A), 144.8 (Pz3A), 143.1 (Pz3B), 141.9 (Pz3C), 138.7 (Pz5A/5C), 138.3 (Pz5A/5C), 137.4 (Pz5B), 109.5 (2C, DMAP-B), 107.9 (Pz4A/4C), 107.6 (Pz4A/4C), 107.3 (Pz4B), 71.3 (C4), 58.8 (OMe), 58.4 (OMe), 57.0 (C3), 39.4 (DMAP-Me), 33.4 (C5). HRMS: $\text{C}_{23}\text{H}_{30}\text{N}_{10}\text{O}_3\text{BMo}^+$ obsd (%), calcd (%), ppm: 597.1692 (50), 597.1662 (54), 5.0; 599.1664 (55), 599.1659 (49), 0.8; 600.1662 (88), 600.1658 (81), 0.6; 601.1654 (93), 601.1653 (86), 0.2; 602.1664 (87), 602.1666 (75), -0.3; 603.1664 (100), 603.1652 (100), 1.9; 604.1700 (41), 604.1681 (35), 3.2; 605.1690 (41), 605.1672 (39), 3.0.

6.5 References

1. Bates, R. W.; Sa-Ei, K. *Tetrahedron* **2002**, 58, (30), 5957.
2. Baumann, M.; Baxendale, I. R. *Beilstein J. Org. Chem.* **2013**, 9, 2265.
3. Katritzky Ar Fau - Katritzky, A. R.; Wang Z Fau - Wang, Z.; Slavov S Fau - Slavov, S.; Tsikolia M Fau - Tsikolia, M.; Dobchev D Fau - Dobchev, D.; Akhmedov Ng Fau - Akhmedov, N. G.; Hall Cd Fau - Hall, C. D.; Bernier Ur Fau - Bernier, U. R.; Clark Gg Fau - Clark, G. G.; Linthicum Kj Fau - Linthicum, K. J., (0027-8424 (Print)).
4. Metkar, P. S.; Scialdone, M. A.; Moloy, K. G. *Green Chem.* **2014**, 16, (10), 4575.
5. Bull, J. A.; Mousseau, J. J.; Pelletier, G.; Charette, A. B. *Chemical Rev.* **2012**, 112, (5), 2642.
6. Buffat, M. G. P. *Tetrahedron* **2004**, 60, (8), 1701.
7. Cordone, R.; Harman, W. D.; Taube, H. *J. Am. Chem. Soc.* **1989**, 111, 2896.
8. Cordone, R.; Taube, H. *J. Am. Chem. Soc.* **1987**, 109, (26), 8101.
9. Meiere, S. H.; Brooks, B. C.; Gunnoe, T. B.; Sabat, M.; Harman, W. D. *Organometallics* **2001**, 20, 1038.
10. Bonanno, J. B.; Veige, A. S.; Wolczanski, P. T.; Lobkovsky, E. B. *Inorg. Chim. Act.* **2003**, 345, 173.
11. Kleckley, T. S.; Bennett, J. L.; Wolczanski, P. T.; Lobkovsky, E. B. *J. Am. Chem. Soc.* **1997**, 119, 247.
12. Neithamer, D. R.; Parkanyi, L.; Mitchell, J. F.; Wolczanski, P. T. *J. Am. Chem. Soc.* **1988**, 110, 4421.
13. Covert, K. J.; Neithamer, D. R.; Zonneville, M. C.; LaPointe, R. E.; Schaller, C. P.; Wolczanski, P. T. *Inorg. Chem.* **1991**, 30, (11), 2494.
14. Harrison, D. P.; Harman, W. D. *Aldrichimica Acta* **2012**, 45, 45.
15. Harrison, D. P.; Iovan, D. A.; Myers, W. H.; Sabat, M.; Wang, S.; Zottig, V. E.; Harman, W. D. *J. Am. Chem. Soc.* **2011**, 133, (45), 18378.
16. Harrison, D. P.; Kosturko, G. W.; Ramdeen, V. M.; Nichols-Nieler, A. C.; Payne, S. J.; Sabat, M.; Myers, W. H.; Harman, W. D. *Organometallics* **2010**, 29, (8), 1909.
17. Harrison, D. P.; Sabat, M.; Myers, W. H.; Harman, W. D. *J. Am. Chem. Soc.* **2010**, 132, (48), 17282.

18. Harrison, D. P.; Zottig, V. E.; Kosturko, G. W.; Welch, K. D.; Sabat, M.; Myers, W. H.; Harman, W. D. *Organometallics* **2009**, 28, (19), 5682.
19. Kosturko, G. W.; Harrison, D. P.; Sabat, M.; Myers, W. H.; Harman, W. D. *Organometallics* **2009**, 28, (2), 387.
20. Lankenau, A. W.; Iovan, D. A.; Pienkos, J. A.; Salomon, R. J.; Wang, S.; Harrison, D. P.; Myers, W. H.; Harman, W. D. *J. Am. Chem. Soc.* **2015**, 137, (10), 3649.
21. Pienkos, J. A.; Zottig, V. E.; Iovan, D. A.; Li, M.; Harrison, D. P.; Sabat, M.; Salomon, R. J.; Strausberg, L.; Teran, V. A.; Myers, W. H.; Harman, W. D. *Organometallics* **2013**, 32, (2), 691.
22. Delafuente, D. A.; Kosturko, G. W.; Graham, P. M.; Harman, W. H.; Myers, W. H.; Surendranath, Y.; Klet, R. C.; Welch, K. D.; Trindle, C. O.; Sabat, M.; Harman, W. D. *J. Am. Chem. Soc.* **2006**, 129, (2), 406.
23. Harrison, D. P.; Welch, K. D.; Nichols-Nieler, A. C.; Sabat, M.; Myers, W. H.; Harman, W. D. *J. Am. Chem. Soc.* **2008**, 130, (50), 16844.
24. Trindle, C.; Harman, W. D. *J. Comput. Chem.* **2005**, 26, 194.
25. Mann, B. E. *Ann. Rep. on NMR Spec.* **1982**, 12, 263.
26. Allen, F. H.; Kennard, O.; Watson, D. G.; Brammer, L.; Orpen, A. G.; Taylor, R. *J. Chem. Soc., Perkin Trans. 2* **1987**, (12), S1.
27. Glorius, F. *Organic & Biomolecular Chemistry* **2005**, 3, (23), 4171.
28. Welch, K. D.; Smith, P. L.; Keller, A. P.; Myers, W. H.; Sabat, M.; Harman, W. D. *Organometallics* **2006**, 25, (21), 5067.
29. Welch, K. D.; Harrison, D. P.; Sabat, M.; Hejazi, E. Z.; Parr, B. T.; Fanelli, M. G.; Gianfrancesco, N. A.; Nagra, D. S.; Myers, W. H.; Harman, W. D. *Organometallics* **2009**, 28, (20), 5960.
30. Shen, T. Y.; Harman, W. D.; Huang, D. F.; Gonzalez, J. Preparation of 7-azabicyclo[2.2.1]heptane and -heptene derivatives as cholinergic receptor ligands. US5817679A, 1998.
31. Myers, W. H.; Welch, K. D.; Graham, P. M.; Keller, A.; Sabat, M.; Trindle, C. O.; Harman, W. D. *Organometallics* **2005**, 24, (22), 5267.
32. Myers, W. H.; Sabat, M.; Harman, W. D. *J. Am. Chem. Soc.* **1991**, 113, 6682.
33. Myers, W. H.; Koontz, J. I.; Harman, W. D. *J. Am. Chem. Soc.* **1992**, 114, 5684.
34. Badio, B.; Garraffo, M.; Plummer, C. V.; Padgett, W. L.; Daly, J. W. *Euro. J. Pharm.* **1997**, 321, 189.

35. Graham, P. M.; Delafuente, D. A.; Liu, W.; Myers, W. H.; Sabat, M.; Harman, W. D. *J. Am. Chem. Soc.* **2005**, 127, (30), 10568.

36. Full credit is given to Justin Wilde for the discovery and isolation of the complexes in Scheme 6.10.
side

Concluding Remarks

The goal of this research on molybdenum dearomatization agents has been to develop a new system that incorporated the following characteristics: recyclability, scalability, and adjustability in the ligand set. In this vein, we have demonstrated the ability to bind a variety of aromatics by a reduction of TpMo(NO)(L)(I) (where $\text{L} = N$ -methylimidazole (MeIm) or N,N -dimethylaminopyridine (DMAP)) in the presence of the desired coordinating ligand ($\text{L}\pi$). This air-stable iodo complex can be synthesized on a large scale (> 150 g) without chromatography. Coordination complexes of certain aromatic molecules can be isolated from the reduction of this iodo precursor in the presence of the desired ligand on scales up to 13 g. Once bound, the dearomatized ligands are activated toward organic transformations, which, after oxidative decomplexation, yield novel small molecules.

Oxidative decomplexation of the modified organic ligand can be accomplished with a mild oxidant (e.g., air) or with iodine to recover the TpMo(NO)(L)(I) complex. Initial investigations demonstrated the ability to recycle the molybdenum complex and to carry out said process on **6** at a 4 g scale to yield 800 mg of **12** using the $\{\text{TpMo(NO)(MeIm)}\}$ fragment. Variability in the ligand set was explored by exchanging the MeIm ligand with DMAP. This seemingly more robust $\{\text{TpMo(NO)(DMAP)}\}$ fragment has been the focus of our attention over the past four years.

From novel organic reactivity of known arene complexes (Chapters 3 and 4) to newly found aromatics capable of being bound (Chapters 5 and 6), we have demonstrated the true potential for future dearomatization with molybdenum using $\{\text{TpMo(NO)(L)}\}$. The novel organics isolated during the research for this dissertation have been submitted for screening through Eli-Lilly's Open Innovation Drug Discovery Program. Although no

pharmacological uses have yet been found for the submitted compounds, the larger the chemical library we are able to develop, the better understanding we can obtain of the chemistry of these seemingly simple, yet novel molecules.

Furthermore, this work demonstrates that the conditions developed for the organic transformations of one metal-coordinated aromatic (i.e., naphthalene), assist in the understanding of organic transformations of other aromatics (i.e., TFT and substituted pyridines) in these systems. We have demonstrated with the naphtha- and anthrafurane cores **20** and **21** that after oxidative decomplexation, the final products after organic transformations are more reactive than their aromatic precursor. Specifically, the double bond that was protected by coordination with the metal can undergo further chemical transformations without the use of transition metals. The formation of two new carbon-carbon bonds (**41** and **42**) to the π -system of an aromatic while still bound to molybdenum, demonstrates the stereocontrol of not only the nucleophilic addition (as seen in Chapter 2), but also of the initial electrophilic addition. In both additions the incoming electrophile or nucleophile adds *anti* to the metal center. Similarly, novel hexahydrophenanthrenes **61**, **89**, **91**, and **92**, can be synthesized by [A+A] or [A+B] MIMIRC additions to **24**.

In work to widen the scope of the chemistry of these molybdenum systems, the TFT complex (**100**) has proven to be a more effective exchange reagent than the dimethylfuran complex (**26**) and its use in accessing a broader array of aromatic complexes (i.e., 1-fluorobenzene, 1-fluoro-3-trifluoromethylbenzene, 1,2-difluorobenzene, etc.) has been shown. Additionally, the organic transformations demonstrated with **100** suggest that similar reactivity may be possible with the newly

isolated fluorinated aromatics, which were incompatible with previous dearomatization systems. In addition to fluorinated arenes, the advent of the pyridine complexes **120** and **121** has laid the groundwork for an unexplored realm of chemistry, dearomatization of ANHs with molybdenum. The recent binding of pyridine-borane to $\{\text{TpMo}(\text{NO})(\text{DMAP})\}$ is a significant advance in this chemistry and will continue to be explored.

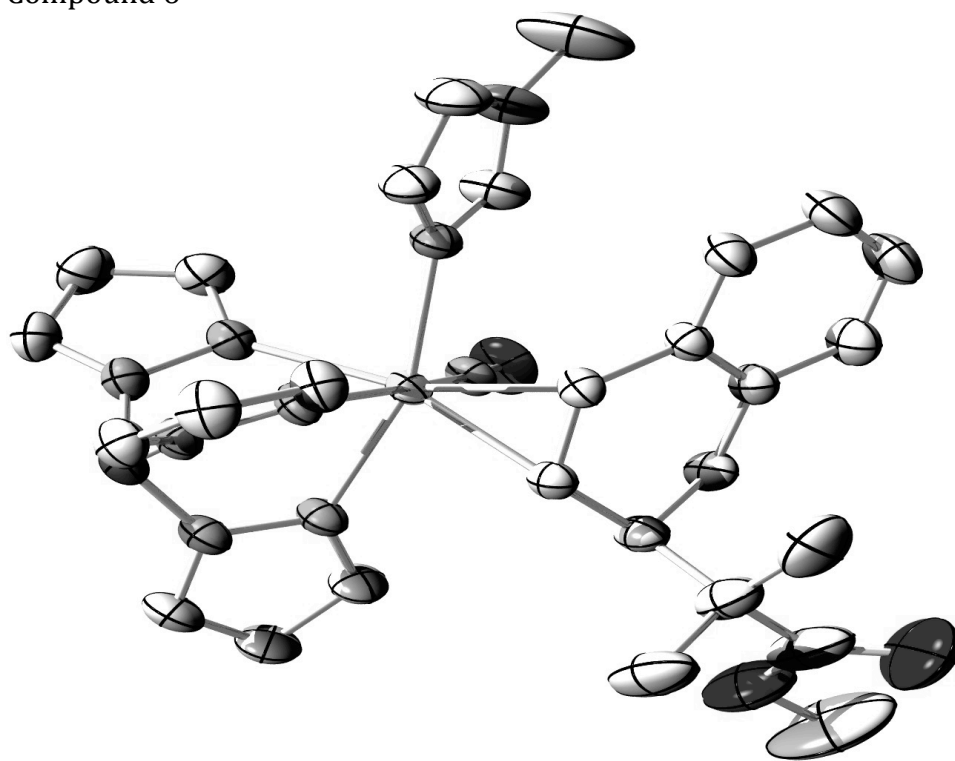
A significant challenge for the synthetic utility of the molybdenum systems is the current lack of a process for enantioenrichment of the metal center. Without an ability to resolve the enantiomers of the aromatic complexes, the use of this molybdenum system for the enantioselective synthesis of organics is limited to the use of chiral auxiliaries on the organic molecule or chiral reagents. However, consider the 13 years of in-depth investigation of dearomatization using the $\{\text{TpW}(\text{NO})(\text{PMe}_3)\}$ fragment before a broadly applicable method for its enantioenrichment was discovered. The lesson from this previous work is that the more we investigate the surprising chemistry of the molybdenum system, the better equipped we will be to solve this problem.

The broader applicability of this research can be divided into two main points. For the organic community, the synthesis of novel small molecules mentioned in this dissertation represents a proof-of-concept for the versatility of this molybdenum scaffold. Although nowhere near an exhaustive search of all electrophiles, nucleophiles, reaction conditions, etc., this dissertation provides a few examples of the wide range of products potentially available through the use of $\{\text{TpMo}(\text{NO})(\text{L})\}$. For the inorganic community, the broader applicability of this dissertation can be seen in the similarities between this second-row dearomatization agent and its third-row congeners. The Harman lab has

previously demonstrated that by fine-tuning the electronics of the metal center, we can invoke similar reactivity between the third-row metals osmium, rhenium and tungsten. This dissertation shows an ability to continue this impressive control of metal electronics while moving up a row on the periodic table. This approach not only affords a decreased toxicity and cost per mole, but also provides insight into the fundamental nature of the chemistry of transition metals.

Appendix

Compound 6



Compound 6

Table 1. Crystal Data for $C_{32}H_{42}BN_9O_4Mo$.

Empirical formula	C ₃₂ H ₄₂ B Mo N ₉ O ₄
Formula weight	651.39
Temperature	233(2) K
Wavelength	0.71073 Å
Crystal system	Orthorhombic
Space group	Pbca
Unit cell dimensions	a = 13.4488(9) Å b = 21.3636(15) Å c = 24.1495(16) Å
Volume	6938.5(8) Å ³
Z	8
Density (calculated)	1.247 Mg/m ³
Absorption coefficient	0.418 mm ⁻¹
F(000)	2688
Crystal size	0.390 x 0.270 x 0.08 mm ³
Theta range for data collection	3.286 to 30.168°.
Index ranges	-19 ≤ h ≤ 19, -30 ≤ k ≤ 30, -34 ≤ l ≤ 34
Reflections collected	125378
Independent reflections	10233 [R(int) = 0.0359]
Completeness to theta = 25.242°	99.8 %
Absorption correction	Empirical
Refinement method	Full-matrix least-squares on F ²
Data / restraints / parameters	10233 / 0 / 461
Goodness-of-fit on F ²	1.054
Final R indices [I > 2σ(I)]	R ₁ = 0.0379, wR ₂ = 0.0959
R indices (all data)	R ₁ = 0.0534, wR ₂ = 0.1072
Largest diff. peak and hole	0.697 and -0.450 e.Å ⁻³

Compound 6

Table 2. Fractional coordinates($\times 10^4$) and equivalent isotropic displacement parameters ($\text{\AA}^2 \times 10^3$) for $\text{C}_{32}\text{H}_{42}\text{BN}_9\text{O}_4\text{Mo}$. $U(\text{eq})$ is defined as one third of the trace of the orthogonalized U^{ij} tensor.

	x	y	z	U(eq)
Mo	3822(1)	7221(1)	6012(1)	31(1)
O(1)	1276(2)	4671(2)	7004(2)	133(1)
O(2)	762(2)	5218(1)	6286(1)	97(1)
O(3)	2071(2)	7830(1)	6534(1)	67(1)
O(4)	4352(6)	5427(8)	3983(6)	320(6)
N(1)	3022(1)	6985(1)	5240(1)	39(1)
N(2)	3423(1)	7107(1)	4735(1)	41(1)
N(3)	4126(1)	8080(1)	5517(1)	38(1)
N(4)	4384(1)	8060(1)	4974(1)	40(1)
N(5)	5168(1)	6872(1)	5517(1)	36(1)
N(6)	5235(1)	7023(1)	4969(1)	37(1)
N(7)	4806(1)	7699(1)	6611(1)	40(1)
N(8)	5220(2)	8213(1)	7362(1)	70(1)
N(9)	2778(1)	7554(1)	6333(1)	39(1)
C(1)	2481(2)	5961(1)	6383(1)	42(1)
C(2)	3493(2)	6216(1)	6209(1)	36(1)
C(3)	4150(1)	6457(1)	6616(1)	34(1)
C(4)	3829(1)	6535(1)	7193(1)	35(1)
C(5)	4513(2)	6680(1)	7610(1)	47(1)
C(6)	4223(2)	6734(2)	8160(1)	60(1)
C(7)	3246(2)	6635(2)	8299(1)	64(1)
C(8)	2565(2)	6485(1)	7895(1)	52(1)
C(9)	2832(2)	6437(1)	7340(1)	40(1)
C(10)	2080(2)	6302(1)	6899(1)	42(1)
C(11)	2493(2)	5233(1)	6457(1)	59(1)
C(12)	1463(3)	5009(2)	6620(2)	86(1)
C(13)	3215(3)	5013(2)	6906(2)	82(1)
C(14)	2750(3)	4910(2)	5905(2)	84(1)
C(15)	-236(3)	5011(3)	6487(3)	165(3)
C(16)	2749(2)	6977(1)	4339(1)	51(1)

C(17)	1900(2)	6770(1)	4581(1)	55(1)
C(18)	2096(2)	6784(1)	5146(1)	47(1)
C(19)	4525(2)	8643(1)	4783(1)	51(1)
C(20)	4358(2)	9054(1)	5206(1)	58(1)
C(21)	4112(2)	8682(1)	5658(1)	48(1)
C(22)	6078(2)	6784(1)	4754(1)	46(1)
C(23)	6576(2)	6471(1)	5163(1)	53(1)
C(24)	5981(2)	6535(1)	5629(1)	45(1)
C(25)	4474(2)	8017(1)	7041(1)	55(1)
C(26)	6079(2)	8015(2)	7127(1)	66(1)
C(27)	5809(2)	7693(1)	6663(1)	51(1)
C(28)	5081(4)	8541(3)	7892(2)	126(2)
C(29B)	3894(14)	5066(10)	3541(7)	139(5)
C(29A)	3730(20)	5699(13)	3586(11)	208(10)
C(30)	2940(20)	5256(10)	3579(7)	284(11)
C(31)	2751(7)	5115(5)	4142(7)	205(5)
C(32)	3667(11)	5304(4)	4442(4)	185(4)
B(1)	4445(2)	7422(1)	4679(1)	40(1)

Compound 6

Table 3. Bond Lengths (Å) and Angles (deg) for C₃₂H₄₂BN₉O₄Mo.

Mo-N(9)	1.7544(17)
Mo-N(1)	2.2103(17)
Mo-N(7)	2.2107(18)
Mo-N(3)	2.2291(18)
Mo-C(3)	2.232(2)
Mo-C(2)	2.242(2)
Mo-N(5)	2.2937(16)
O(1)-C(12)	1.201(5)
O(2)-C(12)	1.319(5)
O(2)-C(15)	1.495(5)
O(3)-N(9)	1.220(2)
O(4)-C(29A)	1.40(3)
O(4)-C(29B)	1.45(2)
O(4)-C(32)	1.466(11)
N(1)-C(18)	1.337(3)
N(1)-N(2)	1.360(2)
N(2)-C(16)	1.346(3)
N(2)-B(1)	1.537(3)
N(3)-C(21)	1.331(3)
N(3)-N(4)	1.358(2)
N(4)-C(19)	1.340(3)
N(4)-B(1)	1.541(3)
N(5)-C(24)	1.336(3)
N(5)-N(6)	1.366(2)
N(6)-C(22)	1.347(3)
N(6)-B(1)	1.532(3)
N(7)-C(25)	1.319(3)
N(7)-C(27)	1.355(3)
N(8)-C(25)	1.336(3)
N(8)-C(26)	1.355(4)
N(8)-C(28)	1.471(4)
C(1)-C(2)	1.525(3)
C(1)-C(10)	1.542(3)

C(1)-C(11)	1.566(4)
C(2)-C(3)	1.419(3)
C(3)-C(4)	1.468(3)
C(4)-C(5)	1.399(3)
C(4)-C(9)	1.403(3)
C(5)-C(6)	1.387(3)
C(6)-C(7)	1.373(4)
C(7)-C(8)	1.376(4)
C(8)-C(9)	1.391(3)
C(9)-C(10)	1.497(3)
C(11)-C(12)	1.517(4)
C(11)-C(13)	1.530(5)
C(11)-C(14)	1.541(4)
C(16)-C(17)	1.358(4)
C(17)-C(18)	1.391(3)
C(19)-C(20)	1.365(4)
C(20)-C(21)	1.390(4)
C(22)-C(23)	1.368(4)
C(23)-C(24)	1.388(3)
C(26)-C(27)	1.363(4)
C(29B)-C(30)	1.34(3)
C(29A)-C(30)	1.42(3)
C(30)-C(31)	1.416(18)
C(31)-C(32)	1.484(11)

N(9)-Mo-N(1)	94.30(7)
N(9)-Mo-N(7)	90.19(8)
N(1)-Mo-N(7)	161.48(7)
N(9)-Mo-N(3)	92.83(8)
N(1)-Mo-N(3)	79.88(7)
N(7)-Mo-N(3)	81.96(7)
N(9)-Mo-C(3)	99.58(8)
N(1)-Mo-C(3)	118.72(7)
N(7)-Mo-C(3)	78.03(7)
N(3)-Mo-C(3)	156.40(7)
N(9)-Mo-C(2)	97.87(8)

N(1)-Mo-C(2)	82.20(7)
N(7)-Mo-C(2)	115.00(7)
N(3)-Mo-C(2)	159.74(7)
C(3)-Mo-C(2)	36.98(7)
N(9)-Mo-N(5)	173.43(8)
N(1)-Mo-N(5)	82.57(6)
N(7)-Mo-N(5)	91.04(7)
N(3)-Mo-N(5)	80.95(6)
C(3)-Mo-N(5)	86.99(7)
C(2)-Mo-N(5)	87.45(7)
C(12)-O(2)-C(15)	110.1(4)
C(29A)-O(4)-C(29B)	57.6(11)
C(29A)-O(4)-C(32)	102.3(12)
C(29B)-O(4)-C(32)	101.1(11)
C(18)-N(1)-N(2)	106.14(17)
C(18)-N(1)-Mo	132.07(16)
N(2)-N(1)-Mo	121.38(13)
C(16)-N(2)-N(1)	109.35(19)
C(16)-N(2)-B(1)	129.04(19)
N(1)-N(2)-B(1)	121.18(16)
C(21)-N(3)-N(4)	106.35(19)
C(21)-N(3)-Mo	130.98(16)
N(4)-N(3)-Mo	122.67(14)
C(19)-N(4)-N(3)	109.80(19)
C(19)-N(4)-B(1)	131.00(19)
N(3)-N(4)-B(1)	119.18(18)
C(24)-N(5)-N(6)	105.61(16)
C(24)-N(5)-Mo	135.64(14)
N(6)-N(5)-Mo	118.76(12)
C(22)-N(6)-N(5)	109.90(18)
C(22)-N(6)-B(1)	128.16(18)
N(5)-N(6)-B(1)	121.92(16)
C(25)-N(7)-C(27)	105.6(2)
C(25)-N(7)-Mo	123.39(16)
C(27)-N(7)-Mo	130.73(16)
C(25)-N(8)-C(26)	107.3(2)

C(25)-N(8)-C(28)	124.0(3)
C(26)-N(8)-C(28)	128.5(3)
O(3)-N(9)-Mo	174.72(19)
C(2)-C(1)-C(10)	111.49(17)
C(2)-C(1)-C(11)	112.21(19)
C(10)-C(1)-C(11)	112.3(2)
C(3)-C(2)-C(1)	119.65(18)
C(3)-C(2)-Mo	71.11(12)
C(1)-C(2)-Mo	125.22(15)
C(2)-C(3)-C(4)	121.06(17)
C(2)-C(3)-Mo	71.91(12)
C(4)-C(3)-Mo	118.67(14)
C(5)-C(4)-C(9)	118.59(19)
C(5)-C(4)-C(3)	121.06(18)
C(9)-C(4)-C(3)	120.30(18)
C(6)-C(5)-C(4)	121.5(2)
C(7)-C(6)-C(5)	119.4(2)
C(6)-C(7)-C(8)	119.9(2)
C(7)-C(8)-C(9)	121.9(2)
C(8)-C(9)-C(4)	118.7(2)
C(8)-C(9)-C(10)	121.7(2)
C(4)-C(9)-C(10)	119.63(18)
C(9)-C(10)-C(1)	115.46(18)
C(12)-C(11)-C(13)	107.4(3)
C(12)-C(11)-C(14)	106.8(2)
C(13)-C(11)-C(14)	109.5(3)
C(12)-C(11)-C(1)	109.5(2)
C(13)-C(11)-C(1)	113.1(2)
C(14)-C(11)-C(1)	110.3(3)
O(1)-C(12)-O(2)	121.8(4)
O(1)-C(12)-C(11)	125.5(5)
O(2)-C(12)-C(11)	112.7(4)
N(2)-C(16)-C(17)	109.2(2)
C(16)-C(17)-C(18)	104.8(2)
N(1)-C(18)-C(17)	110.6(2)
N(4)-C(19)-C(20)	108.5(2)

C(19)-C(20)-C(21)	105.0(2)
N(3)-C(21)-C(20)	110.3(2)
N(6)-C(22)-C(23)	108.5(2)
C(22)-C(23)-C(24)	104.8(2)
N(5)-C(24)-C(23)	111.1(2)
N(7)-C(25)-N(8)	111.4(2)
N(8)-C(26)-C(27)	106.0(2)
N(7)-C(27)-C(26)	109.6(2)
C(30)-C(29B)-O(4)	101.1(14)
O(4)-C(29A)-C(30)	100(2)
C(31)-C(30)-C(29A)	105.5(17)
C(31)-C(30)-C(29B)	100.0(16)
C(29A)-C(30)-C(29B)	59.7(19)
C(30)-C(31)-C(32)	105.0(11)
O(4)-C(32)-C(31)	101.7(8)
N(6)-B(1)-N(2)	109.65(19)
N(6)-B(1)-N(4)	108.56(17)
N(2)-B(1)-N(4)	107.43(18)

Compound 6

Table 4. Anisotropic Thermal Displacement Parameters ($\text{\AA}^2 \times 10^3$) for $\text{C}_{32}\text{H}_{42}\text{BN}_9\text{O}_4\text{Mo}$. The anisotropic displacement factor exponent takes the form: $-2\pi^2 [h^2 a^{*2} U^{11} + \dots + 2 h k a^* b^* U^{12}]$

	U^{11}	U^{22}	U^{33}	U^{23}	U^{13}	U^{12}
Mo	25(1)	42(1)	26(1)	-3(1)	-1(1)	2(1)
O(1)	119(3)	153(3)	128(3)	15(2)	43(2)	-67(2)
O(2)	58(1)	91(2)	142(2)	-26(2)	19(2)	-29(1)
O(3)	51(1)	85(1)	63(1)	-7(1)	14(1)	31(1)
O(4)	159(7)	510(20)	290(13)	1(13)	-7(7)	-6(9)
N(1)	32(1)	52(1)	32(1)	-2(1)	-3(1)	2(1)
N(2)	37(1)	54(1)	31(1)	-4(1)	-5(1)	4(1)
N(3)	38(1)	42(1)	35(1)	1(1)	0(1)	6(1)
N(4)	40(1)	46(1)	35(1)	5(1)	1(1)	5(1)
N(5)	31(1)	46(1)	30(1)	1(1)	3(1)	5(1)
N(6)	34(1)	45(1)	31(1)	-2(1)	6(1)	2(1)
N(7)	36(1)	48(1)	35(1)	-2(1)	-5(1)	-3(1)
N(8)	71(2)	79(2)	58(1)	-26(1)	-18(1)	0(1)
N(9)	32(1)	51(1)	33(1)	-5(1)	0(1)	6(1)
C(1)	34(1)	52(1)	40(1)	-8(1)	2(1)	-6(1)
C(2)	33(1)	43(1)	33(1)	-5(1)	4(1)	-1(1)
C(3)	25(1)	45(1)	32(1)	1(1)	3(1)	2(1)
C(4)	33(1)	41(1)	32(1)	-2(1)	2(1)	2(1)
C(5)	42(1)	63(1)	35(1)	5(1)	-4(1)	0(1)
C(6)	67(2)	77(2)	35(1)	-1(1)	-9(1)	0(1)
C(7)	74(2)	87(2)	31(1)	-4(1)	9(1)	4(2)
C(8)	50(1)	65(2)	43(1)	-3(1)	15(1)	0(1)
C(9)	38(1)	44(1)	36(1)	-3(1)	7(1)	1(1)
C(10)	30(1)	52(1)	45(1)	-5(1)	8(1)	-3(1)
C(11)	54(2)	50(1)	72(2)	-15(1)	17(1)	-14(1)
C(12)	74(2)	73(2)	113(3)	-39(2)	33(2)	-32(2)
C(13)	90(2)	49(2)	107(3)	13(2)	9(2)	1(2)
C(14)	77(2)	74(2)	101(3)	-43(2)	32(2)	-24(2)
C(15)	62(2)	130(4)	301(8)	-48(5)	42(4)	-44(3)
C(16)	53(1)	64(2)	36(1)	-8(1)	-13(1)	5(1)

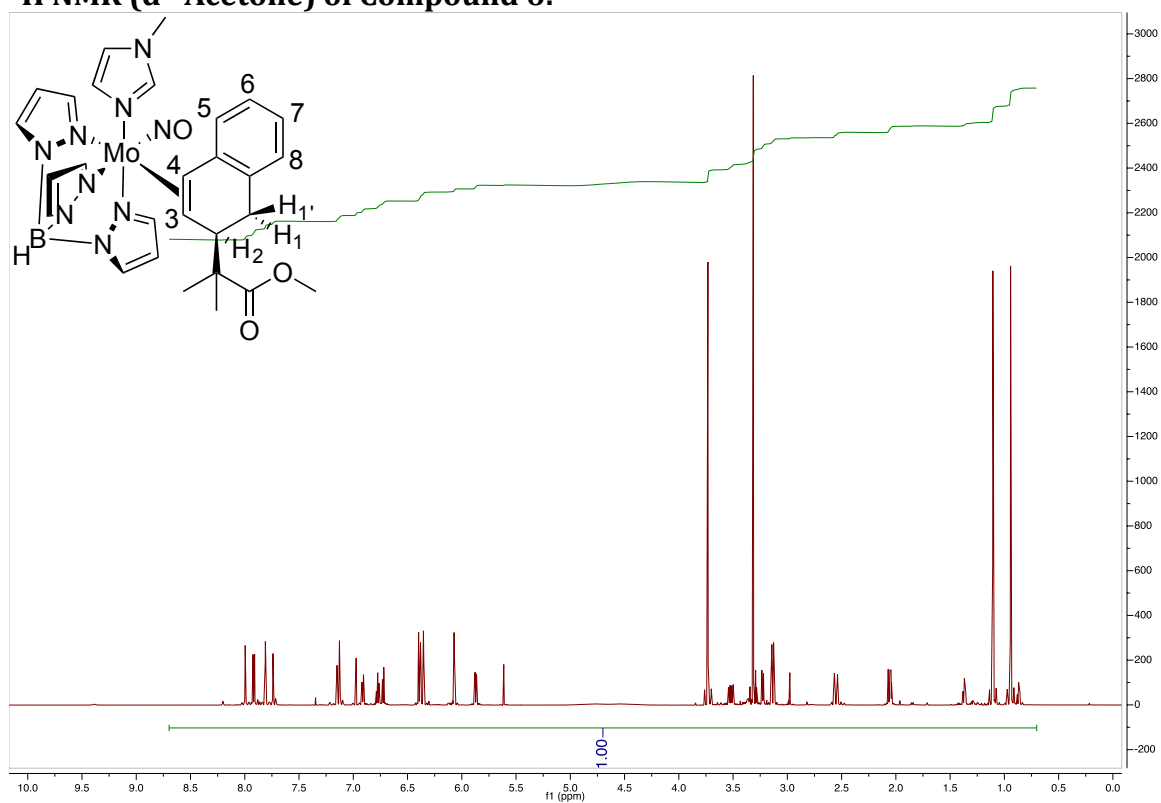
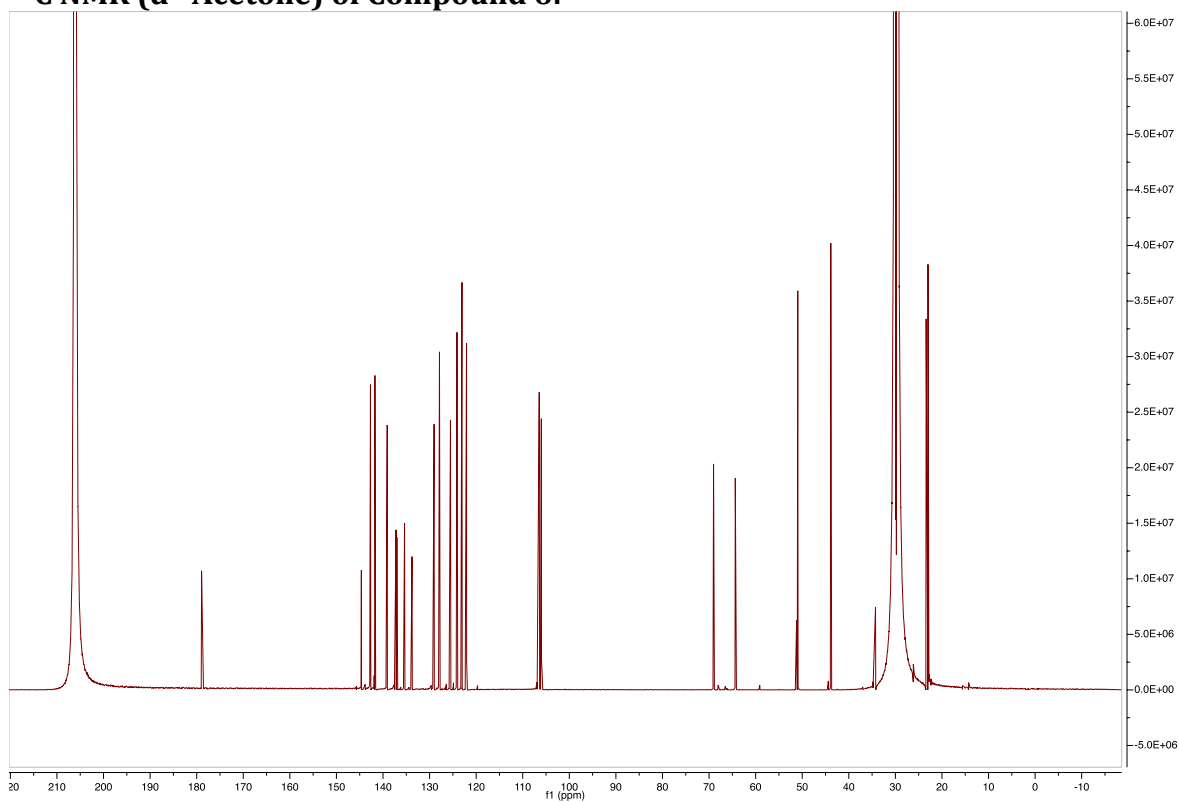
C(17)	45(1)	68(2)	51(1)	-4(1)	-21(1)	-2(1)
C(18)	33(1)	61(1)	47(1)	0(1)	-10(1)	-1(1)
C(19)	51(1)	53(1)	48(1)	12(1)	4(1)	4(1)
C(20)	64(2)	41(1)	67(2)	4(1)	5(1)	3(1)
C(21)	51(1)	43(1)	50(1)	-4(1)	2(1)	8(1)
C(22)	40(1)	56(1)	42(1)	-3(1)	14(1)	4(1)
C(23)	39(1)	62(2)	57(1)	1(1)	11(1)	16(1)
C(24)	37(1)	55(1)	43(1)	5(1)	4(1)	11(1)
C(25)	49(1)	65(2)	51(1)	-18(1)	-7(1)	4(1)
C(26)	48(1)	88(2)	63(2)	-14(2)	-16(1)	-15(1)
C(27)	37(1)	70(2)	45(1)	-4(1)	-2(1)	-11(1)
C(28)	123(4)	150(4)	104(3)	-77(3)	-35(3)	12(3)
C(29B)	147(12)	149(14)	120(11)	-28(9)	27(10)	-3(10)
C(29A)	230(30)	200(20)	190(20)	-5(17)	70(20)	-78(19)
C(30)	390(30)	290(20)	174(13)	73(12)	-85(16)	-110(20)
C(31)	135(7)	135(7)	345(16)	17(10)	13(9)	3(5)
C(32)	270(13)	151(7)	135(6)	12(5)	7(8)	52(7)
B(1)	41(1)	50(1)	28(1)	-1(1)	1(1)	4(1)

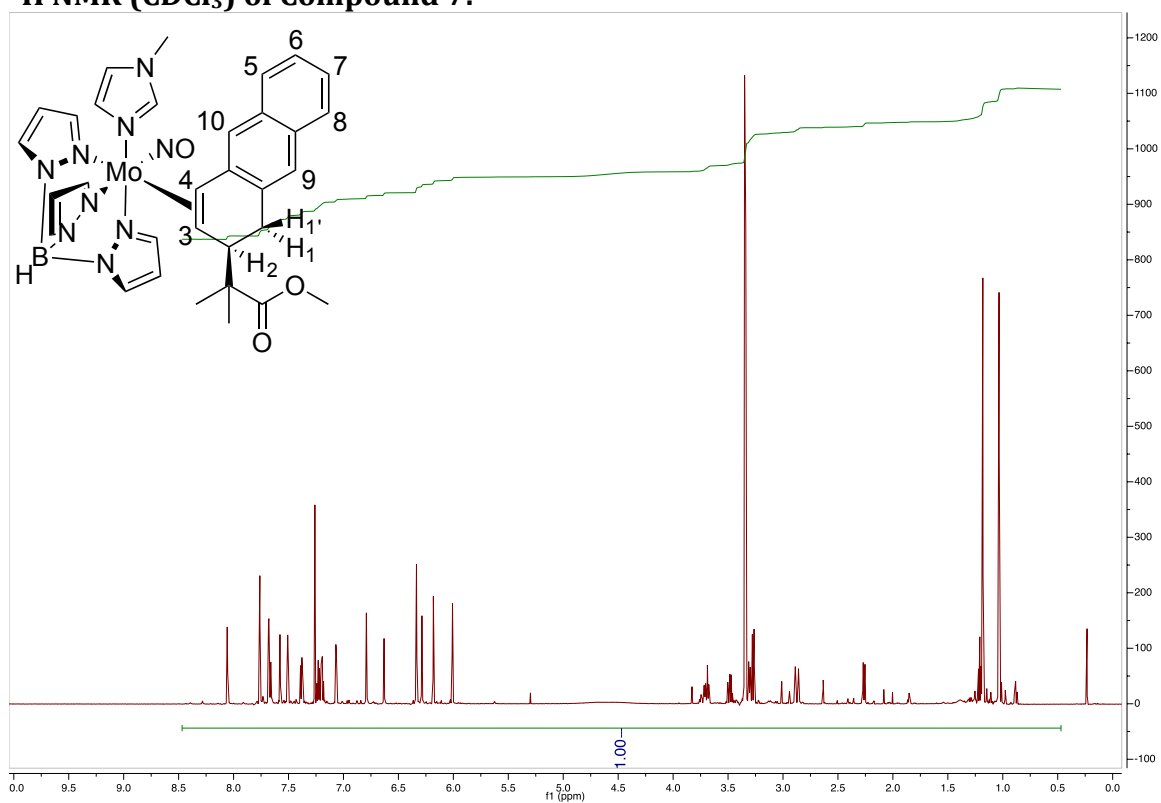
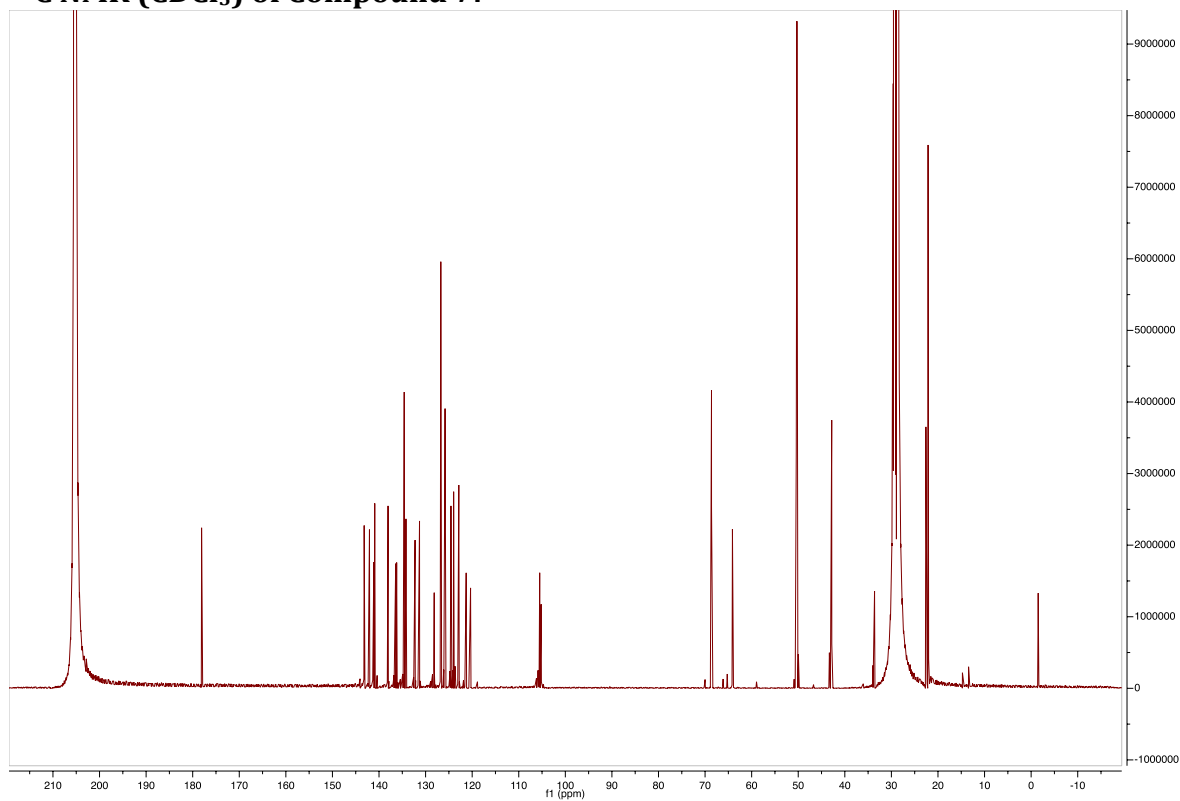
Compound 6

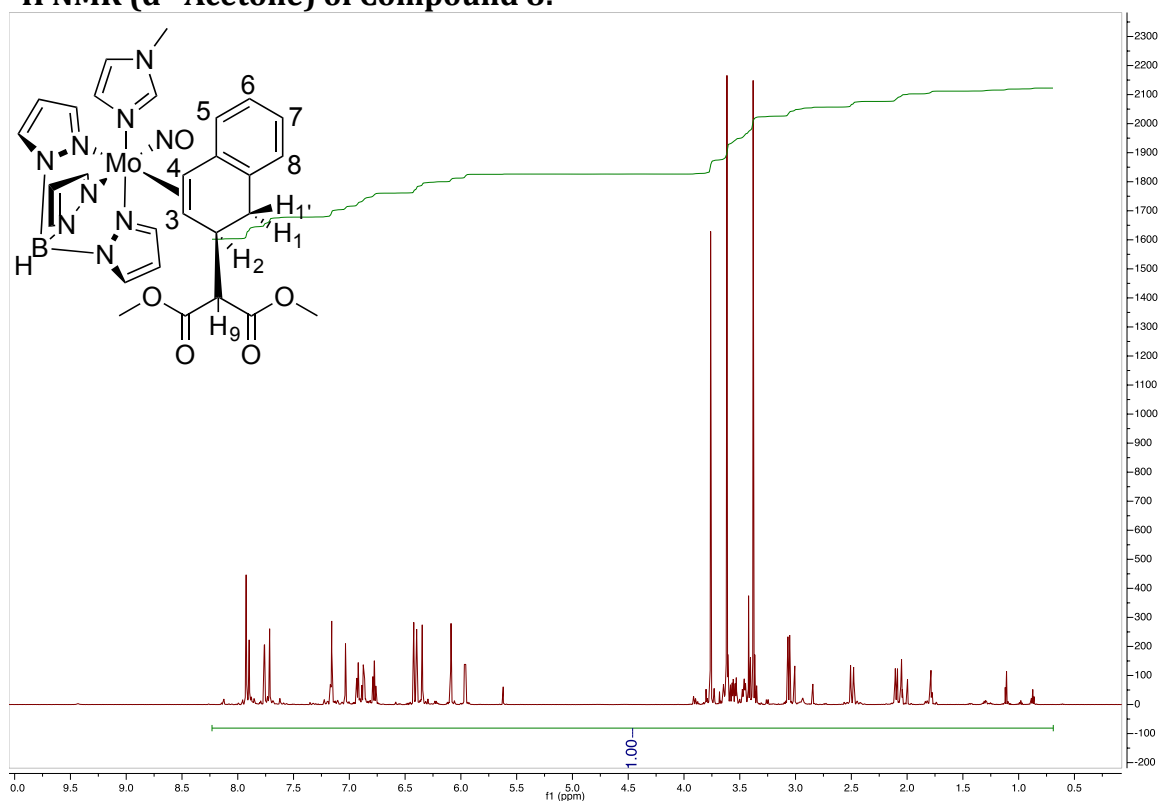
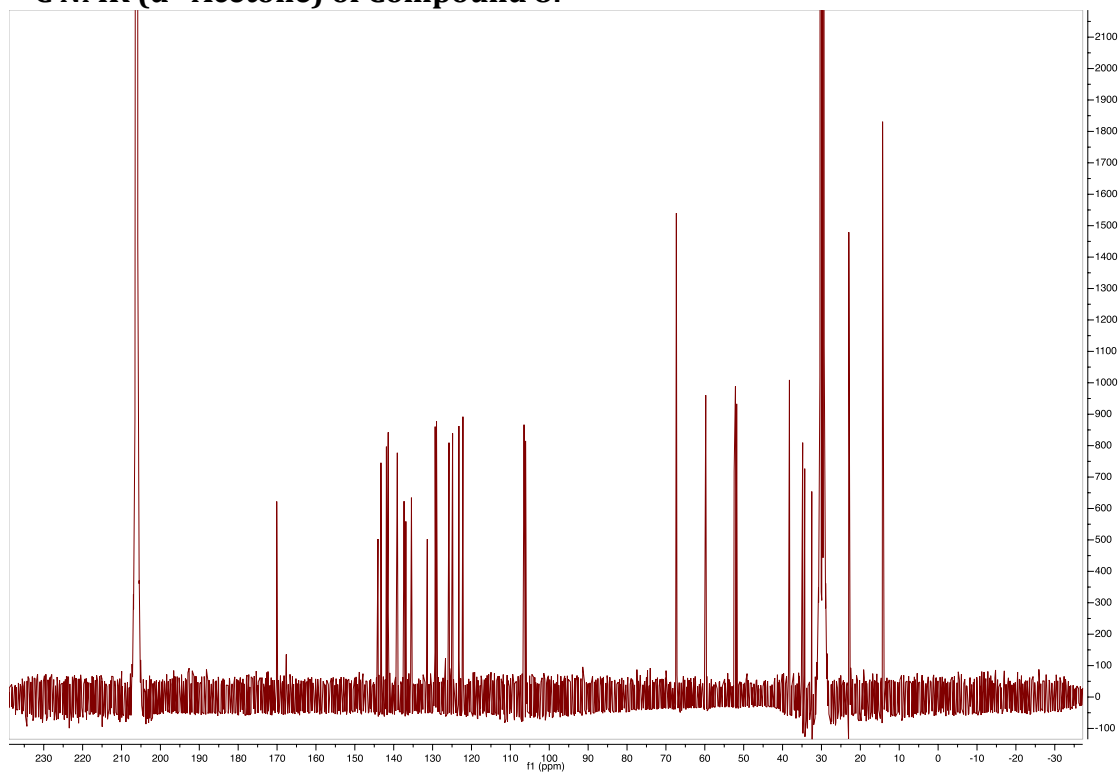
Table 5. Hydrogen Atom Fractional Coordinates and Thermal Displacement Parameters ($\text{\AA}^2 \times 10^{-3}$) for $\text{C}_{32}\text{H}_{42}\text{BN}_9\text{O}_4\text{Mo}$.

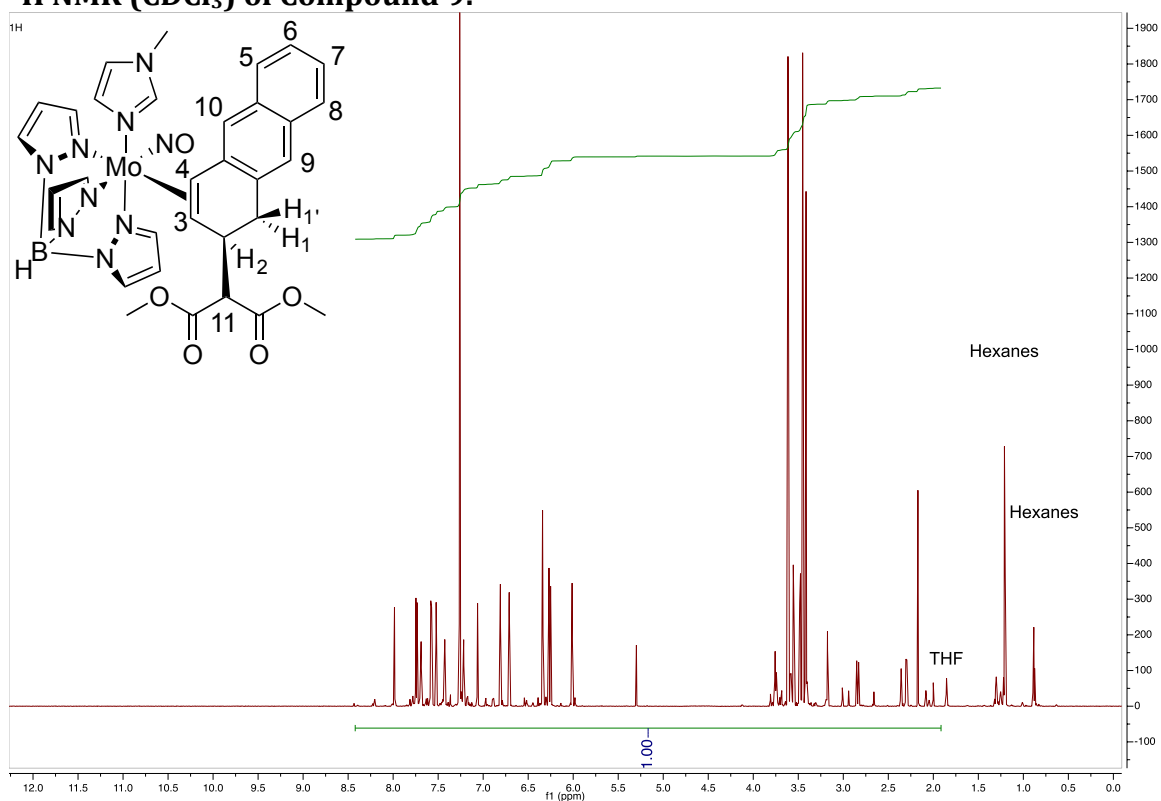
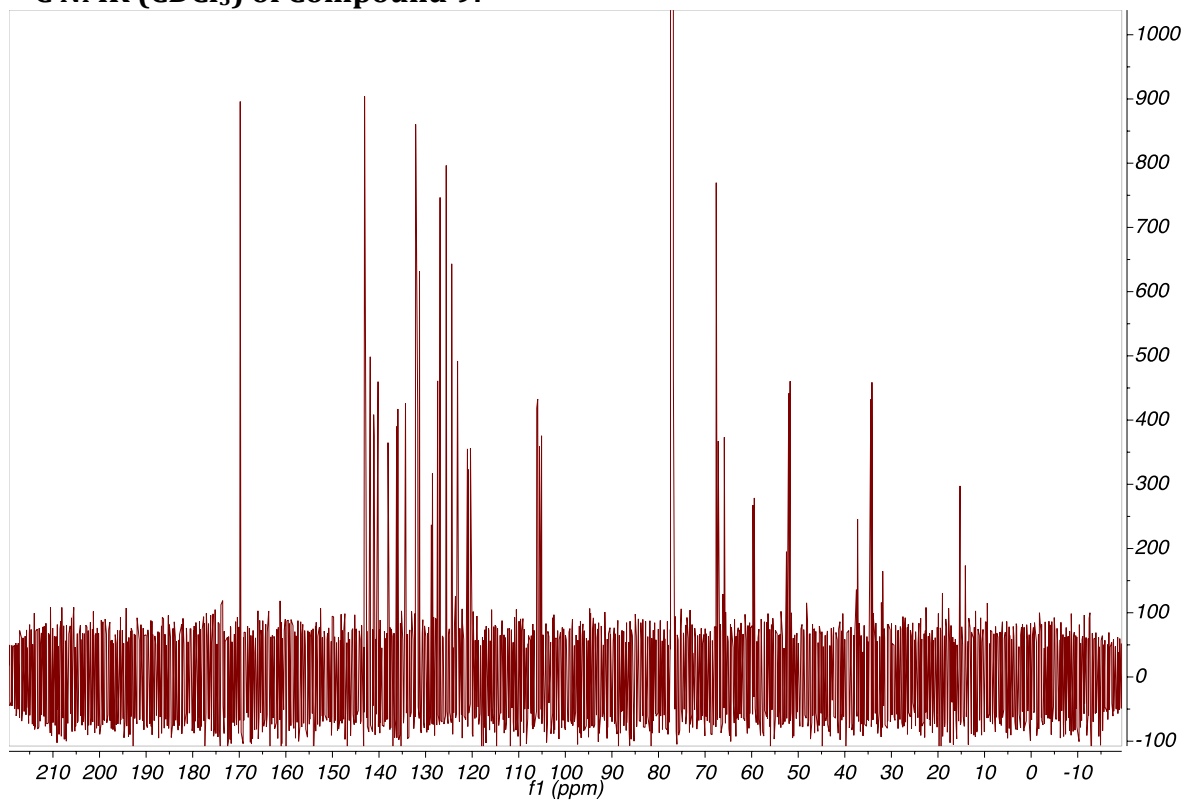
	x	y	z	U(eq)
H(5)	5177	6741	7518	56
H(6)	4686	6837	8431	71
H(7)	3045	6669	8666	77
H(8)	1907	6414	7996	63
H(10A)	1785	6695	6782	51
H(10B)	1554	6049	7060	51
H(13A)	3033	5197	7254	123
H(13B)	3879	5139	6810	123
H(13C)	3188	4566	6936	123
H(14A)	2672	4466	5944	126
H(14B)	3425	5004	5806	126
H(14C)	2312	5060	5620	126
H(15A)	-445	4649	6282	247
H(15B)	-709	5342	6434	247
H(15C)	-197	4908	6873	247
H(16)	2850	7022	3960	61
H(17)	1315	6645	4407	66
H(18)	1645	6670	5421	57
H(19)	4706	8749	4424	61
H(20)	4401	9488	5194	69
H(21)	3959	8833	6009	58
H(22)	6286	6825	4388	55
H(23)	7180	6262	5135	63
H(24)	6128	6365	5974	54
H(25)	3806	8095	7112	66
H(26)	6721	8084	7256	79
H(27)	6247	7499	6419	61
H(28A)	4415	8702	7912	189
H(28B)	5546	8881	7918	189

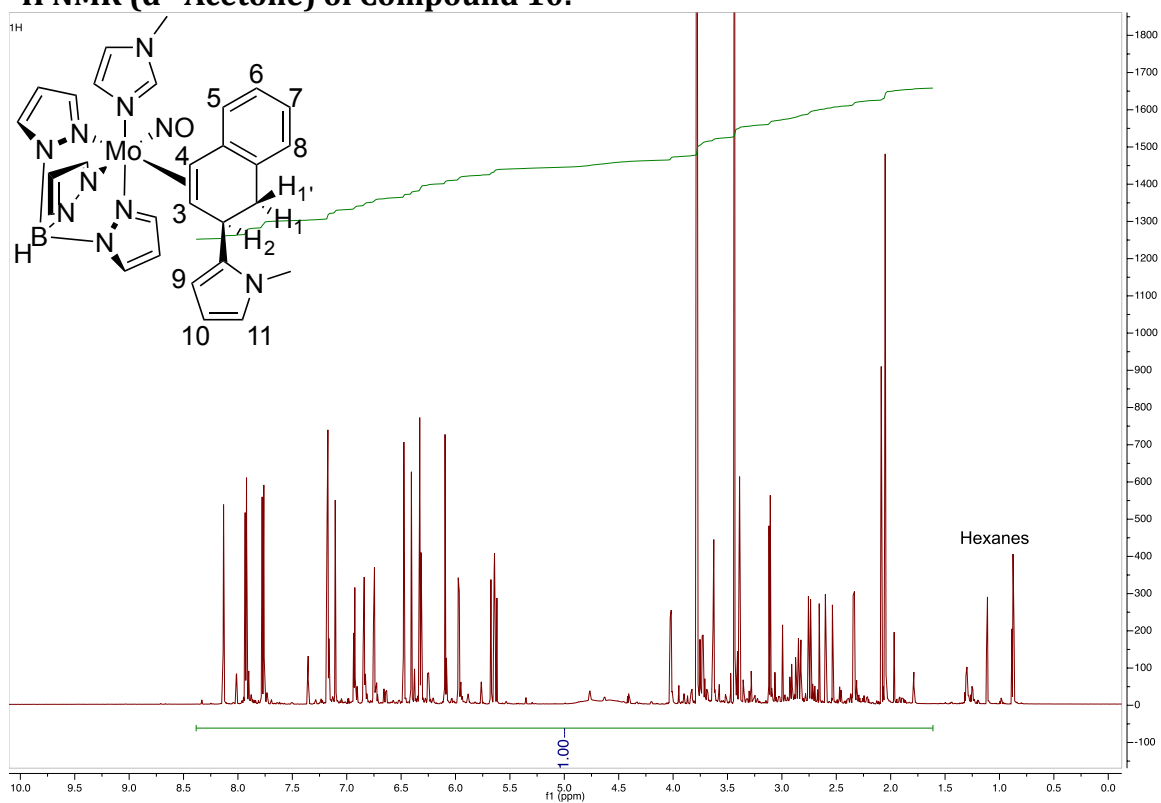
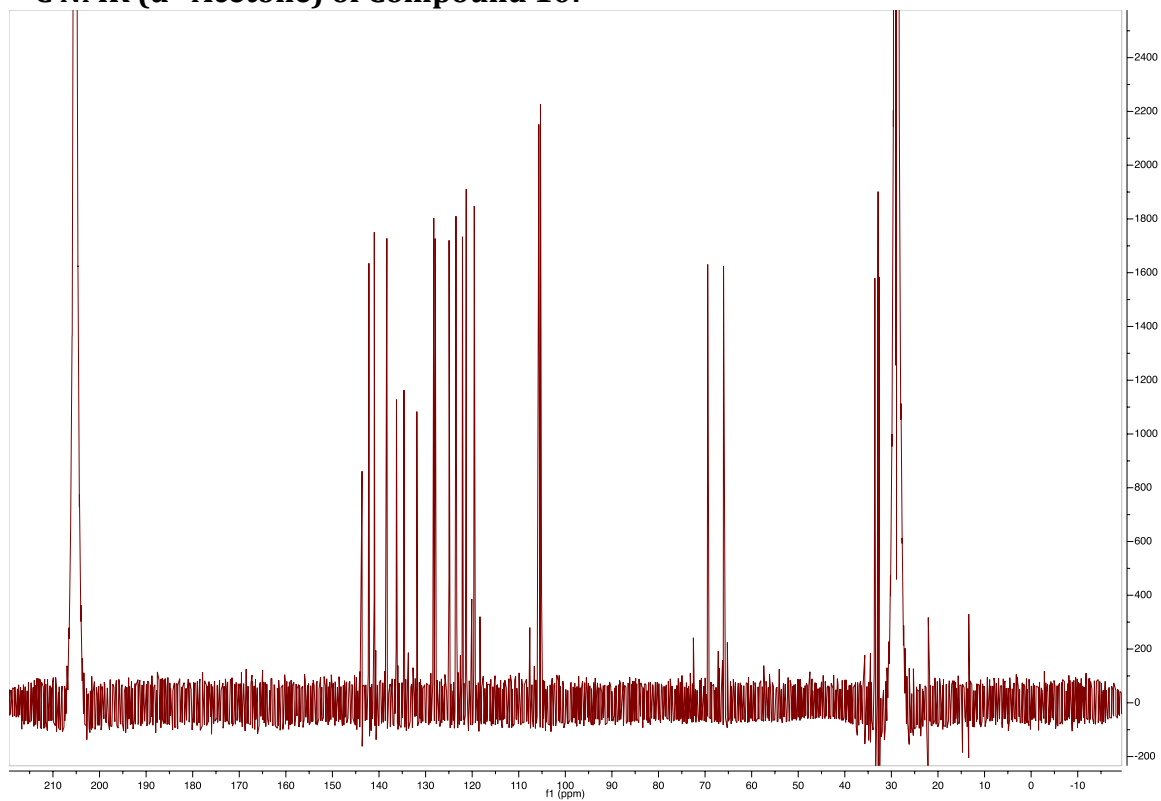
H(28C)	5191	8255	8192	189
H(29A)	4178	5167	3183	166
H(29B)	3954	4619	3606	166
H(29C)	4049	5731	3228	249
H(29D)	3496	6109	3701	249
H(31A)	2624	4672	4190	246
H(31B)	2181	5348	4276	246
H(32A)	3557	5677	4663	222
H(32B)	3909	4970	4678	222
H(1)	2010(20)	6035(13)	6088(10)	48(7)
H(1B)	4674(16)	7489(11)	4252(10)	36(6)
H(2)	3768(18)	6020(13)	5895(11)	46(7)
H(3)	4852(18)	6384(10)	6551(9)	37(6)
H(30A)	2870(90)	5530(60)	3380(40)	30(9)
H(30B)	2980(30)	4821(15)	3795(16)	49(9)

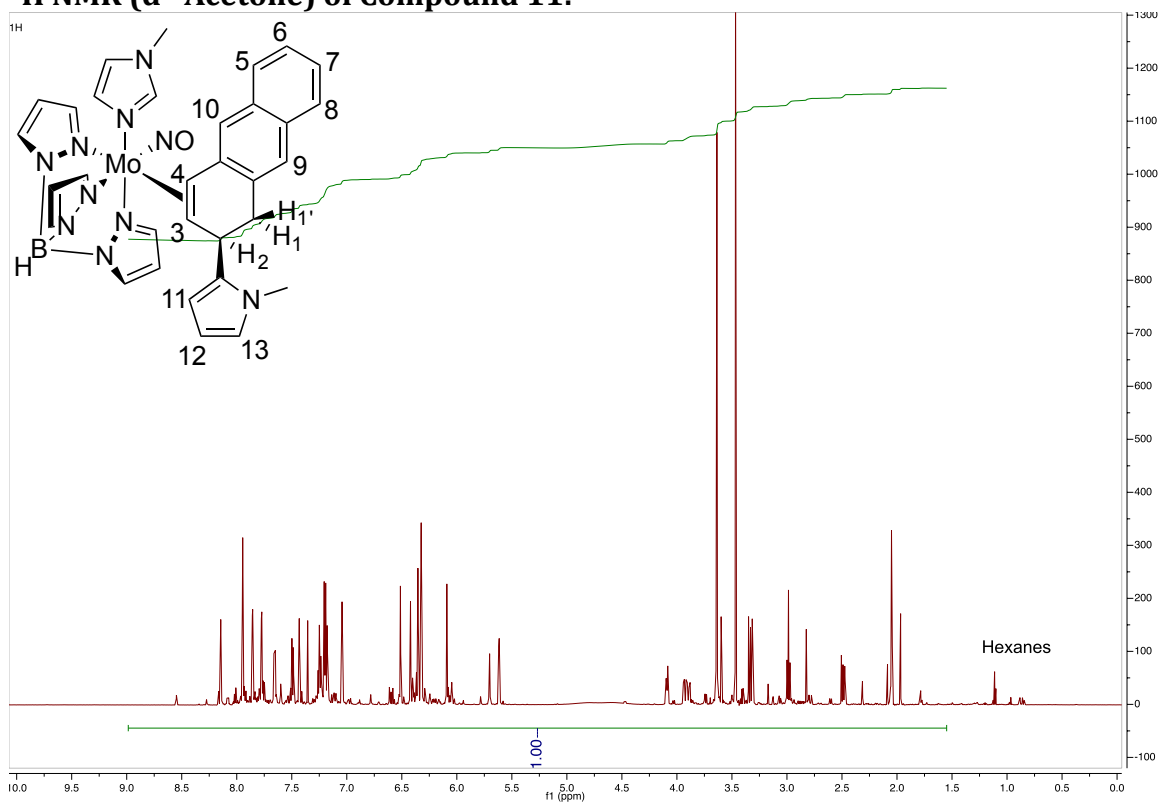
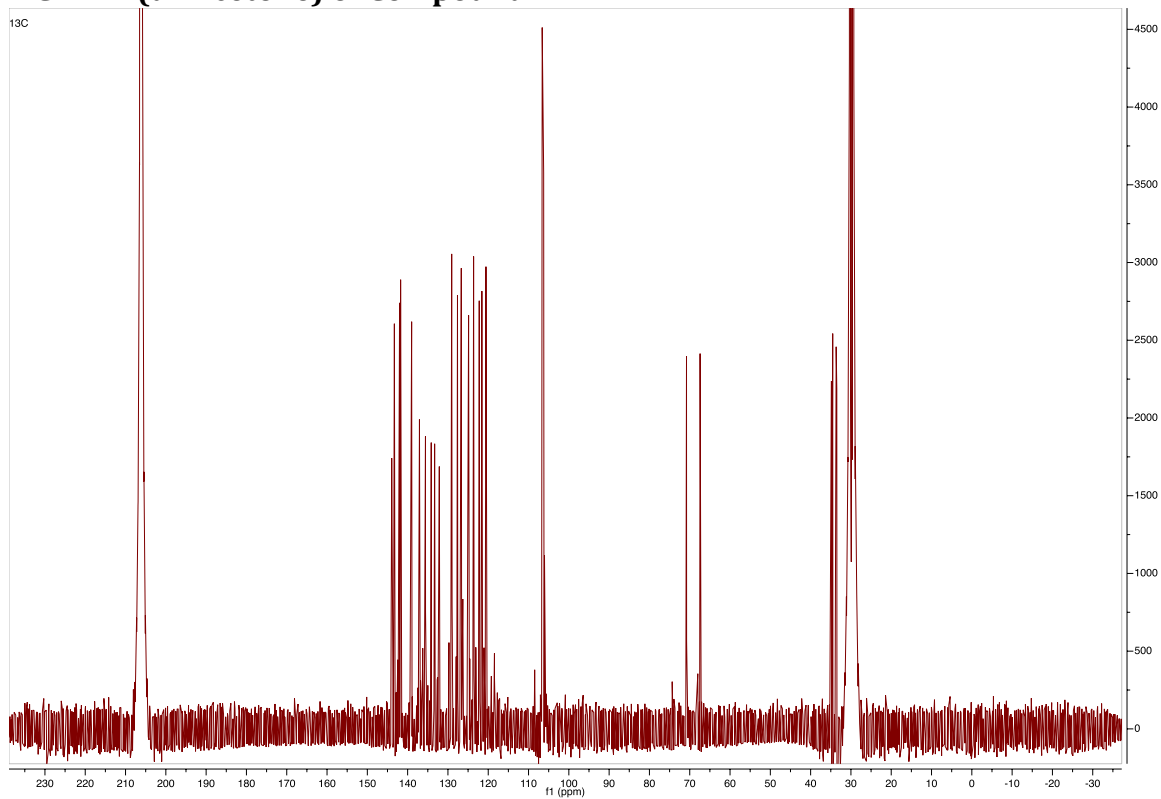
^1H NMR ($\text{d}^6\text{-Acetone}$) of Compound 6: **^{13}C NMR ($\text{d}^6\text{-Acetone}$) of Compound 6:**

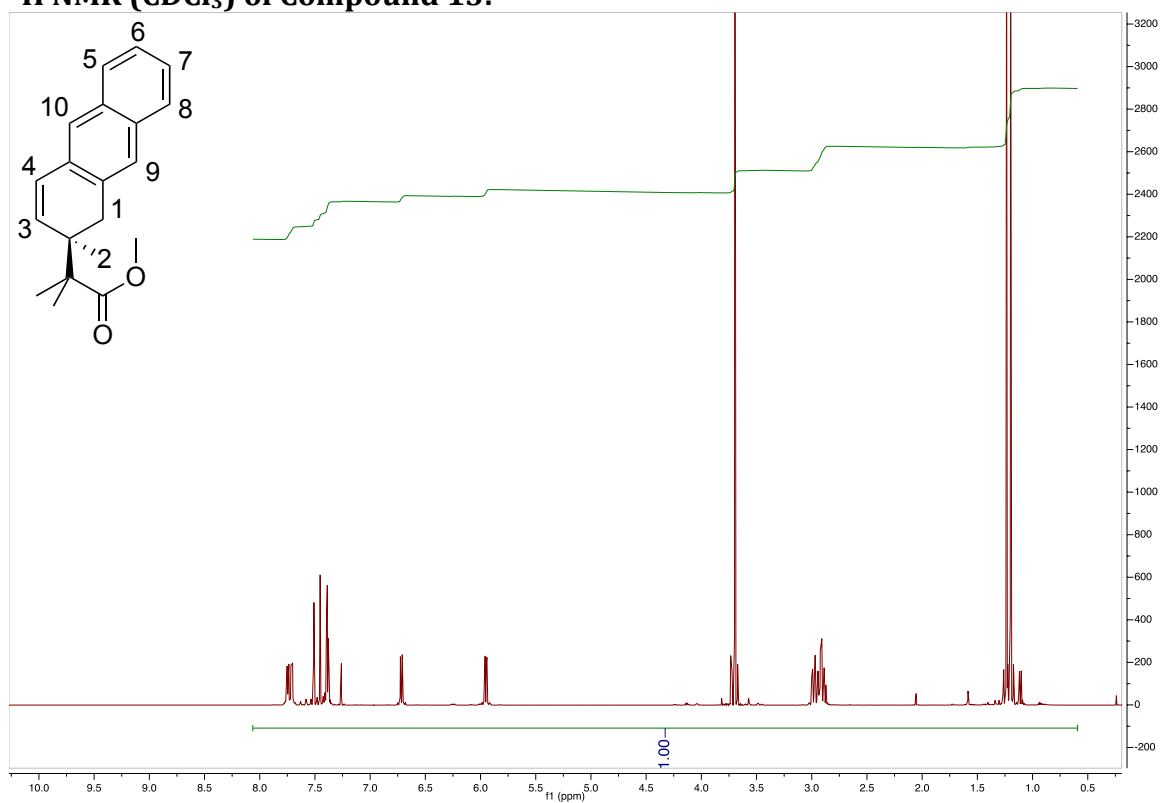
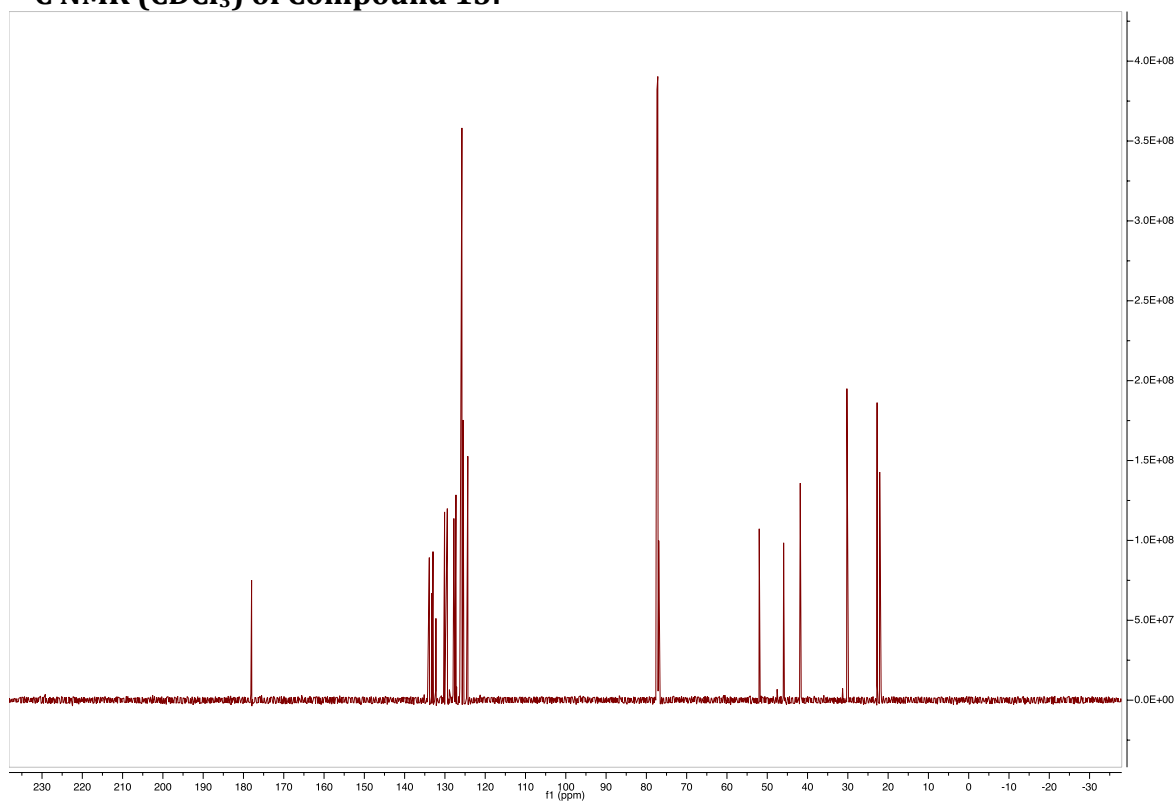
^1H NMR (CDCl_3) of Compound 7: **^{13}C NMR (CDCl_3) of Compound 7:**

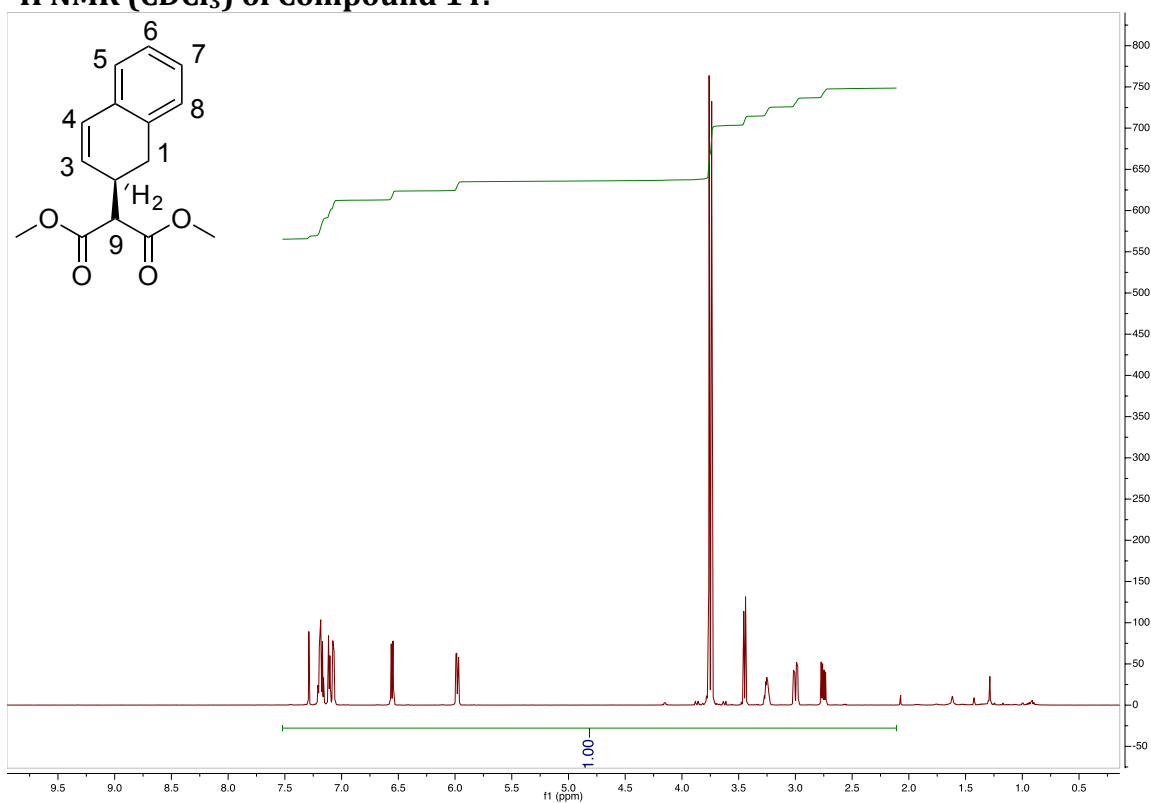
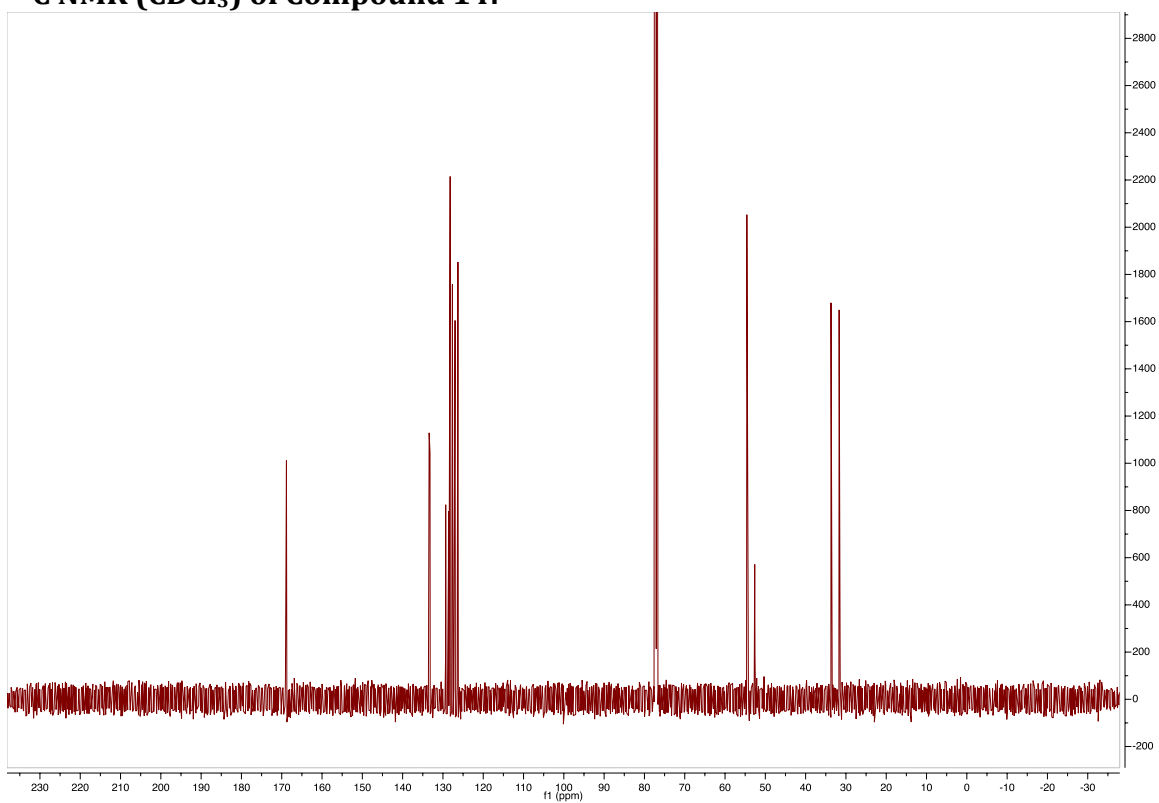
^1H NMR ($\text{d}^6\text{-Acetone}$) of Compound 8: **^{13}C NMR ($\text{d}^6\text{-Acetone}$) of Compound 8:**

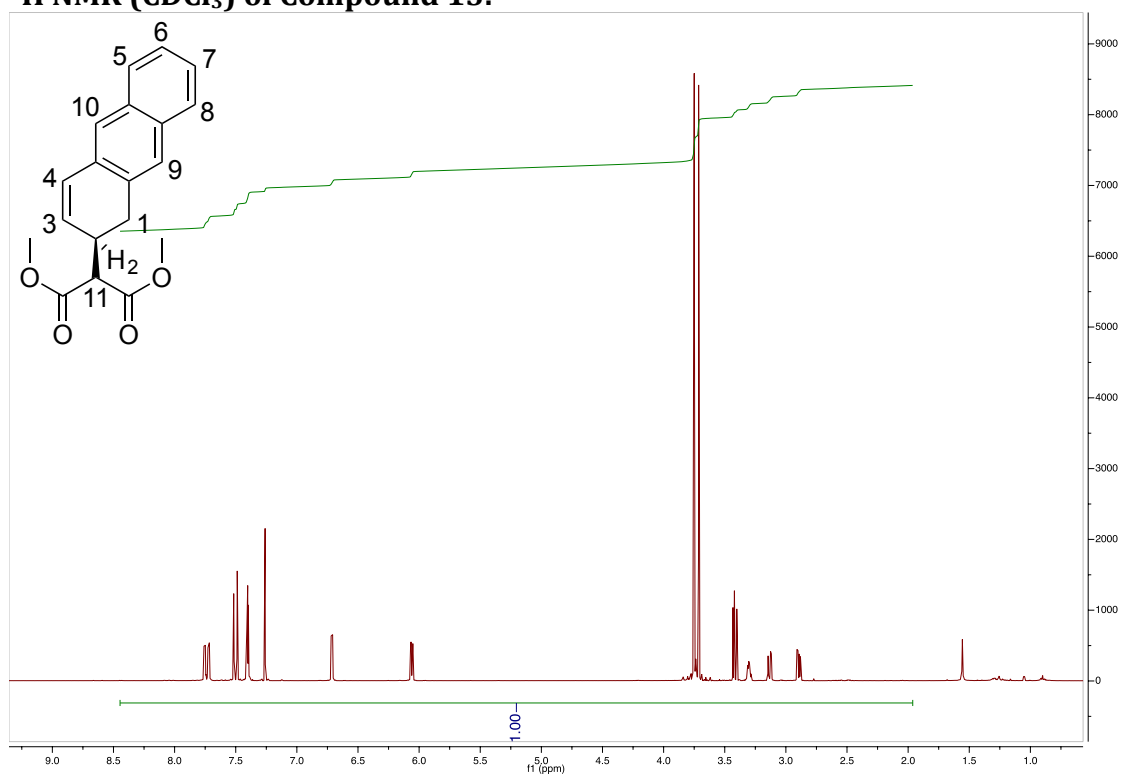
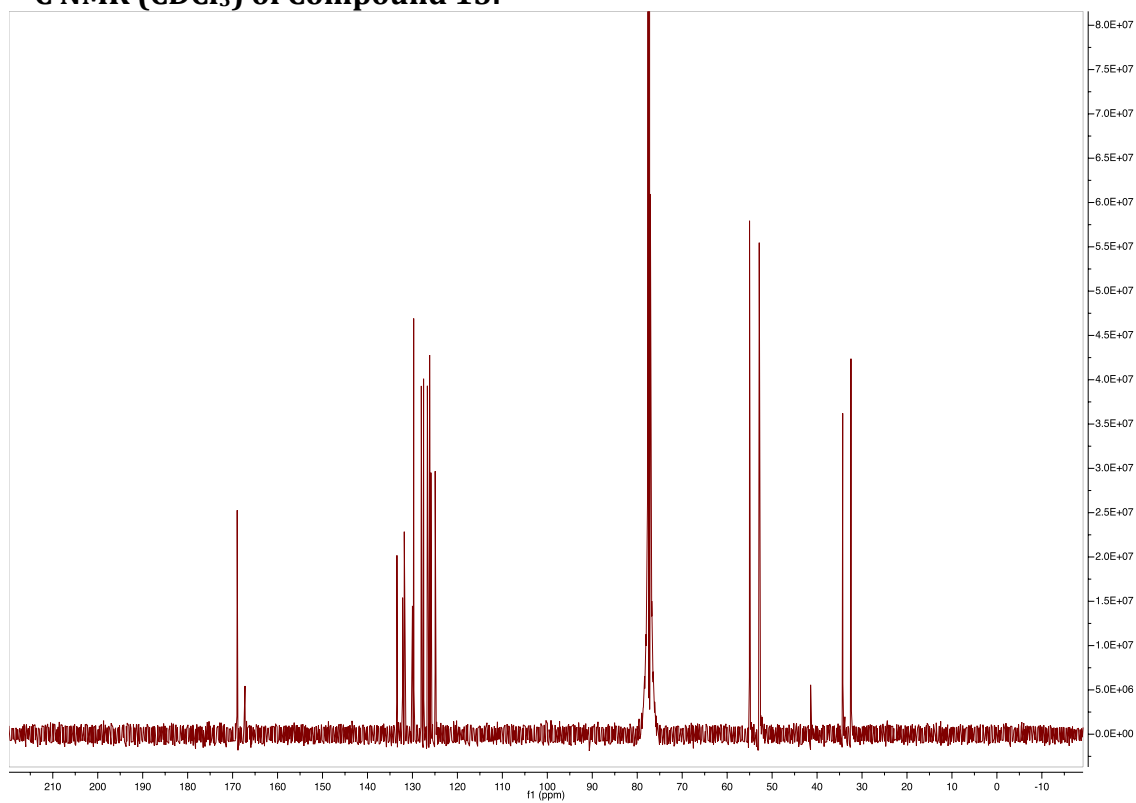
^1H NMR (CDCl_3) of Compound 9: **^{13}C NMR (CDCl_3) of Compound 9:**

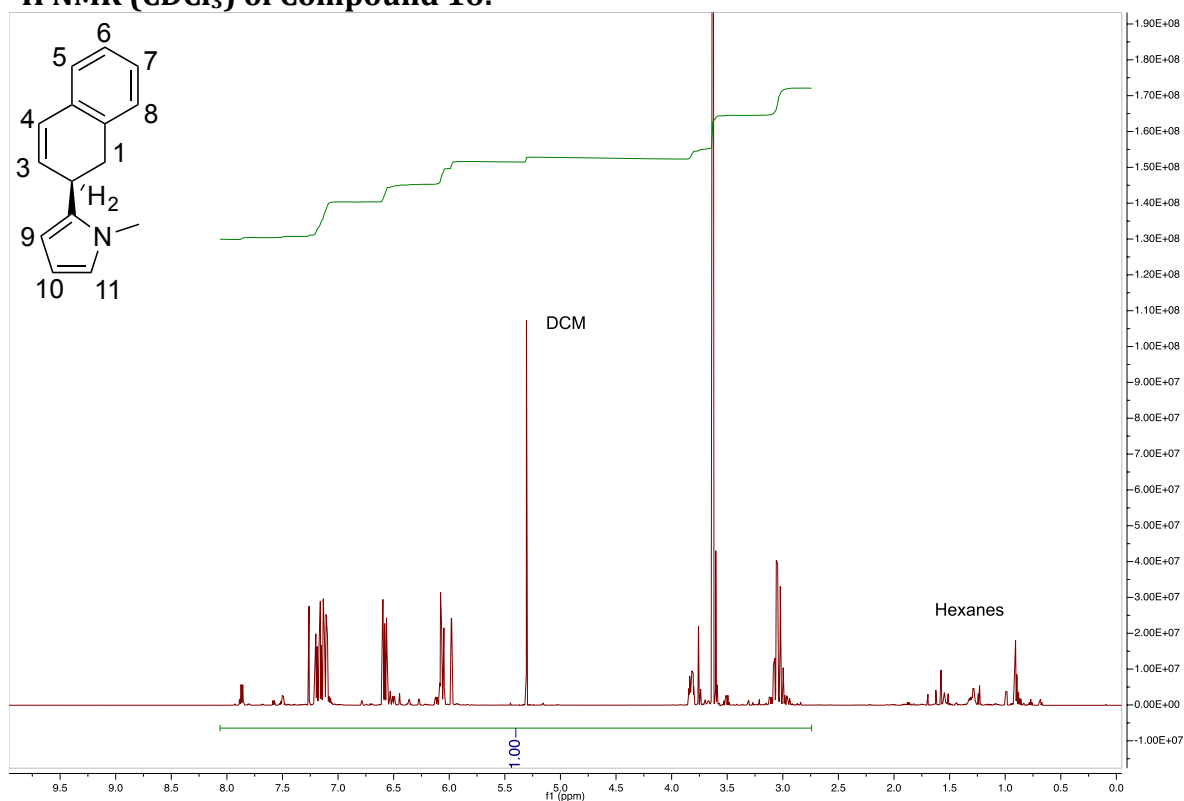
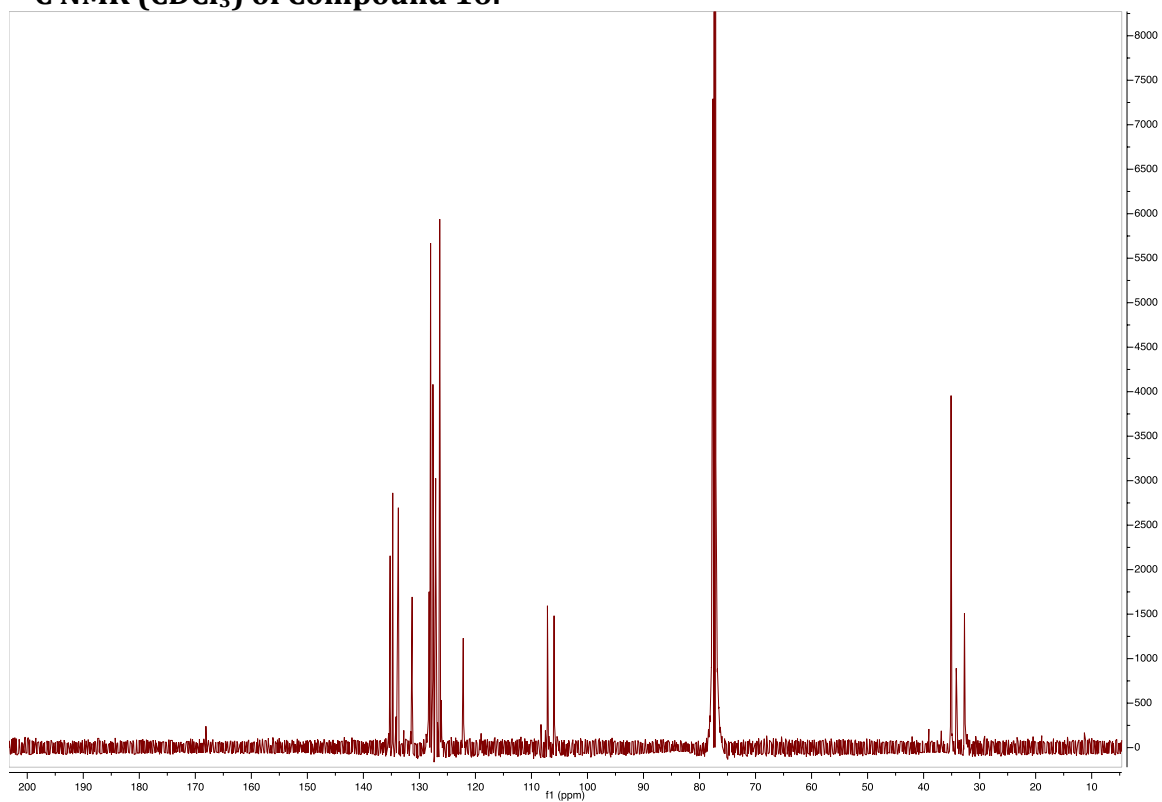
^1H NMR ($\text{d}^6\text{-Acetone}$) of Compound 10: **^{13}C NMR ($\text{d}^6\text{-Acetone}$) of Compound 10:**

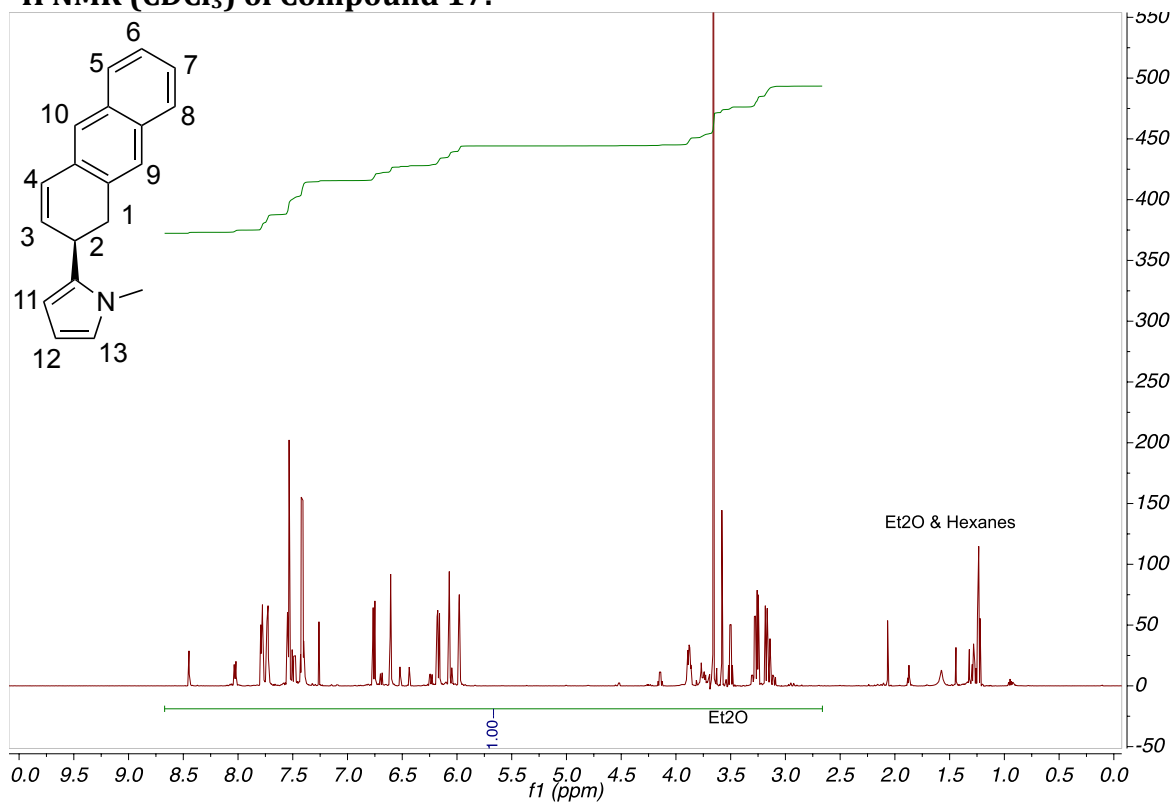
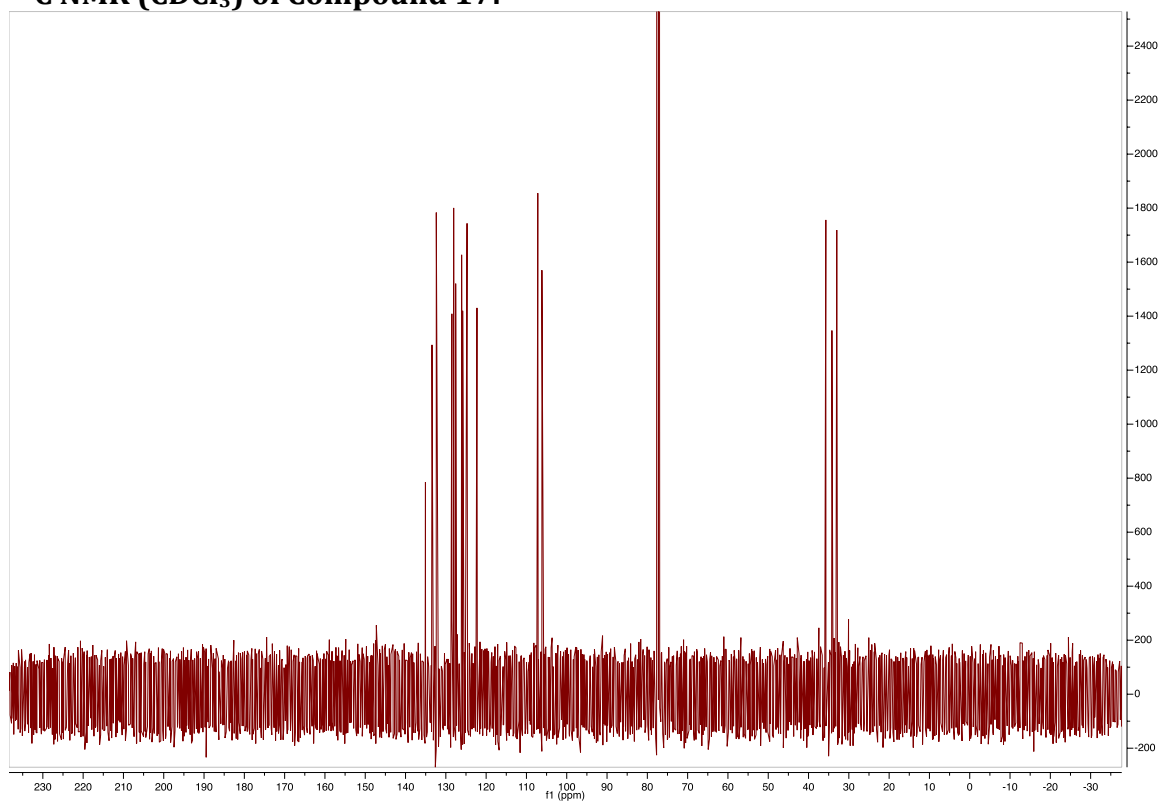
^1H NMR ($\text{d}^6\text{-Acetone}$) of Compound 11: **^{13}C NMR ($\text{d}^6\text{-Acetone}$) of Compound 11:**

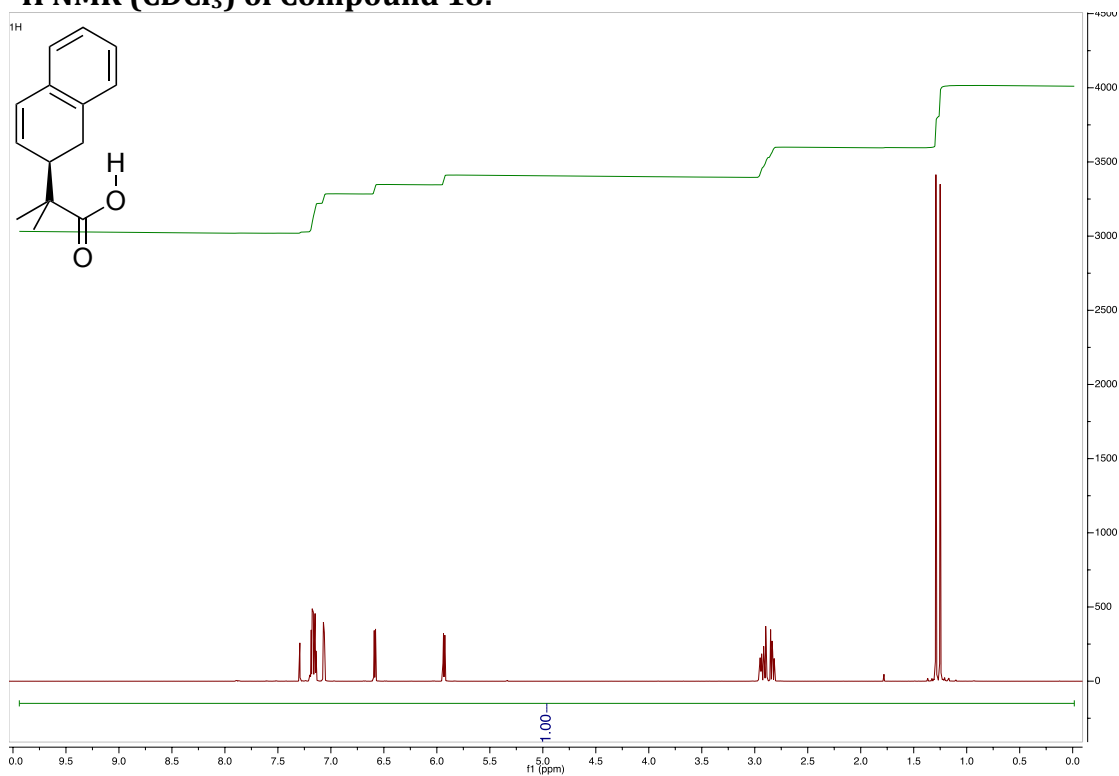
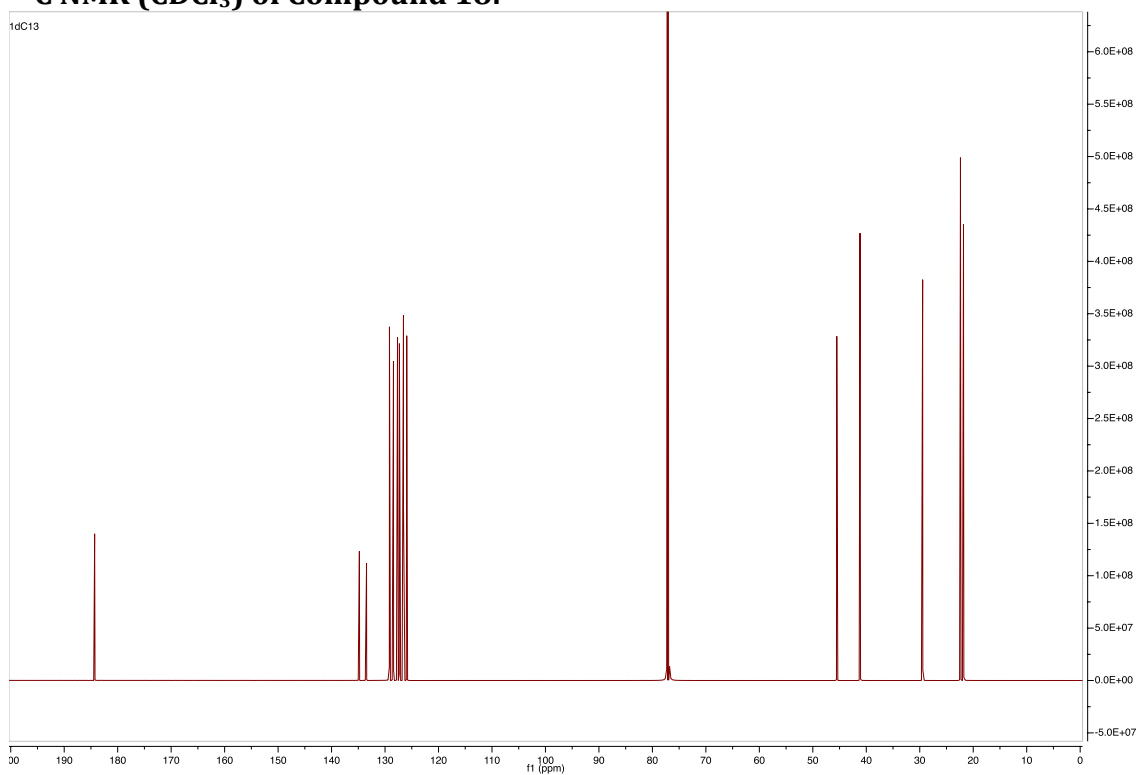
^1H NMR (CDCl_3) of Compound 13: **^{13}C NMR (CDCl_3) of Compound 13:**

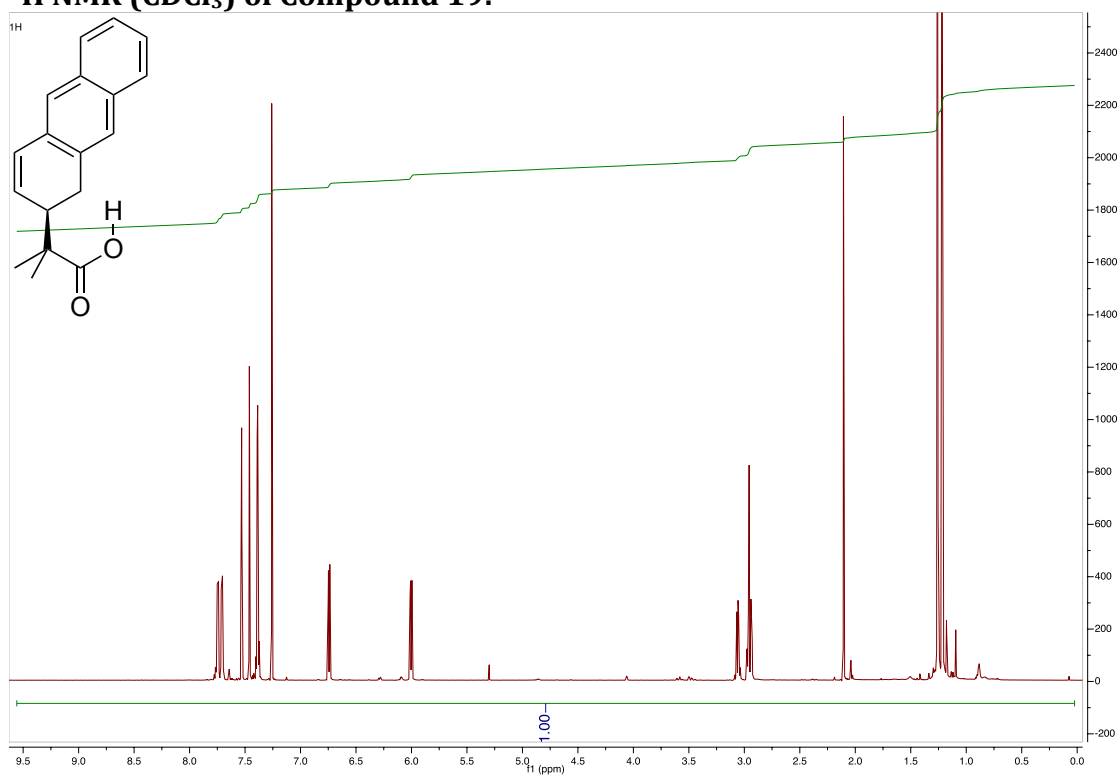
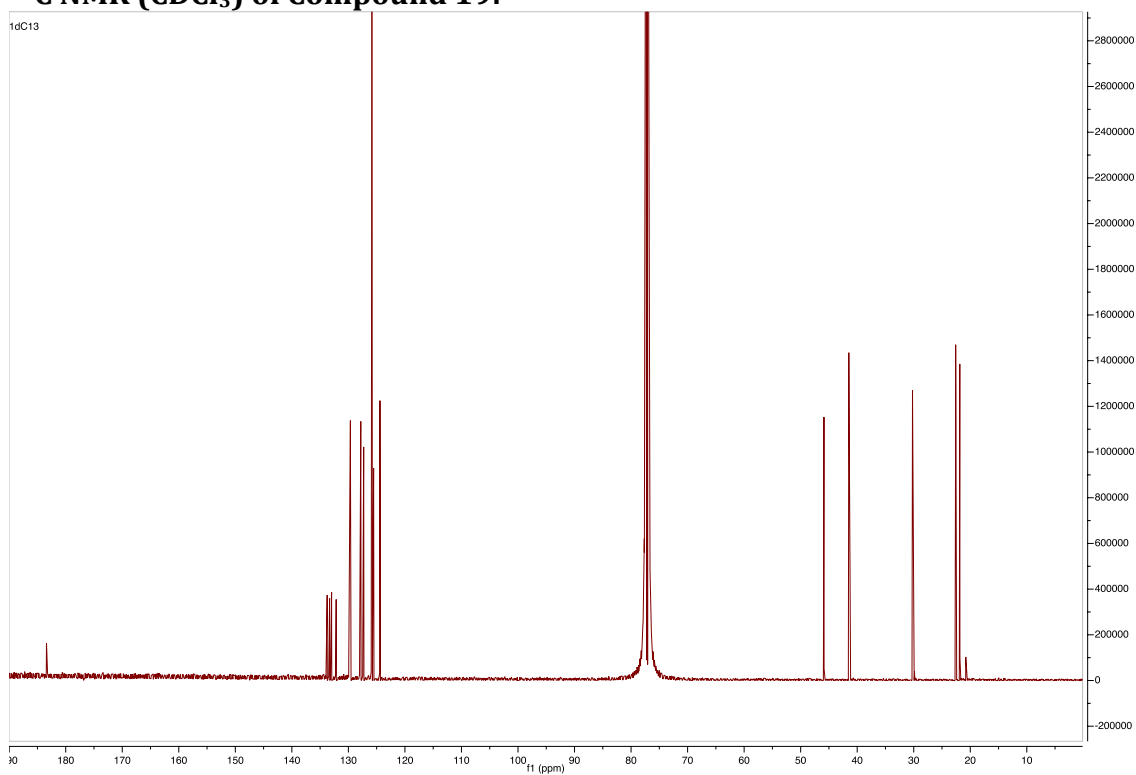
^1H NMR (CDCl_3) of Compound 14: **^{13}C NMR (CDCl_3) of Compound 14:**

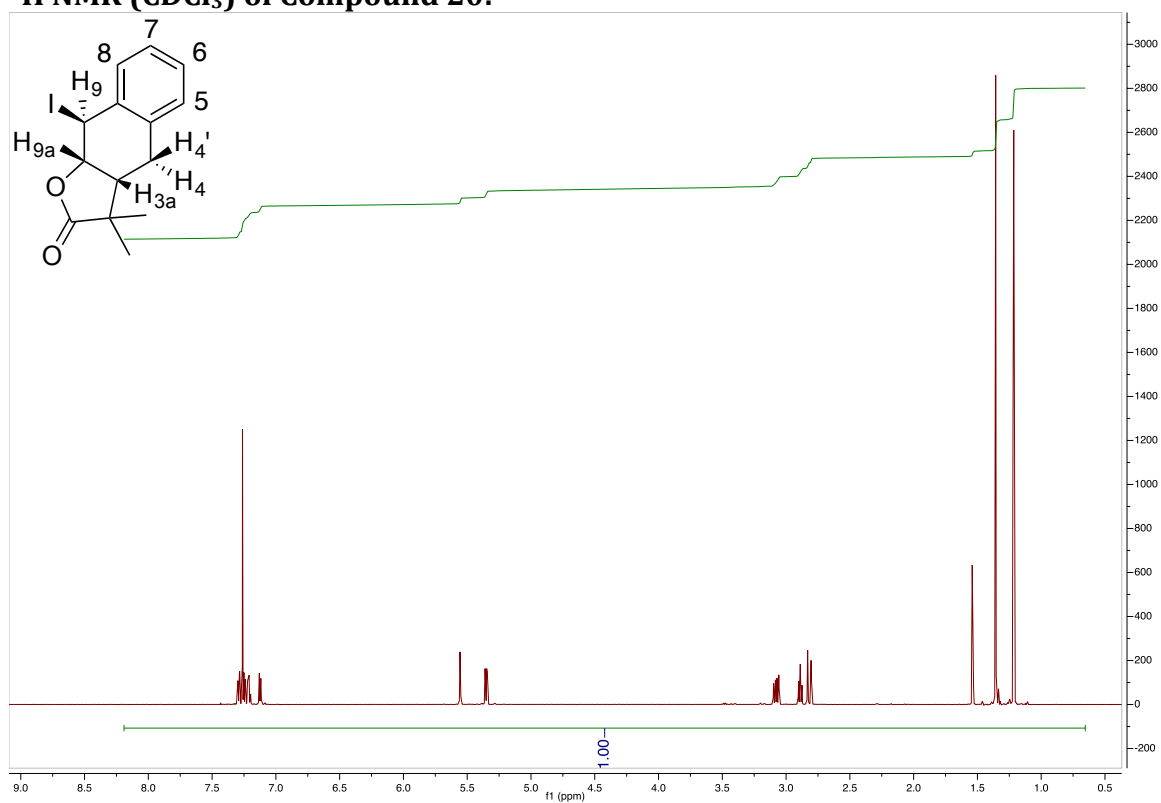
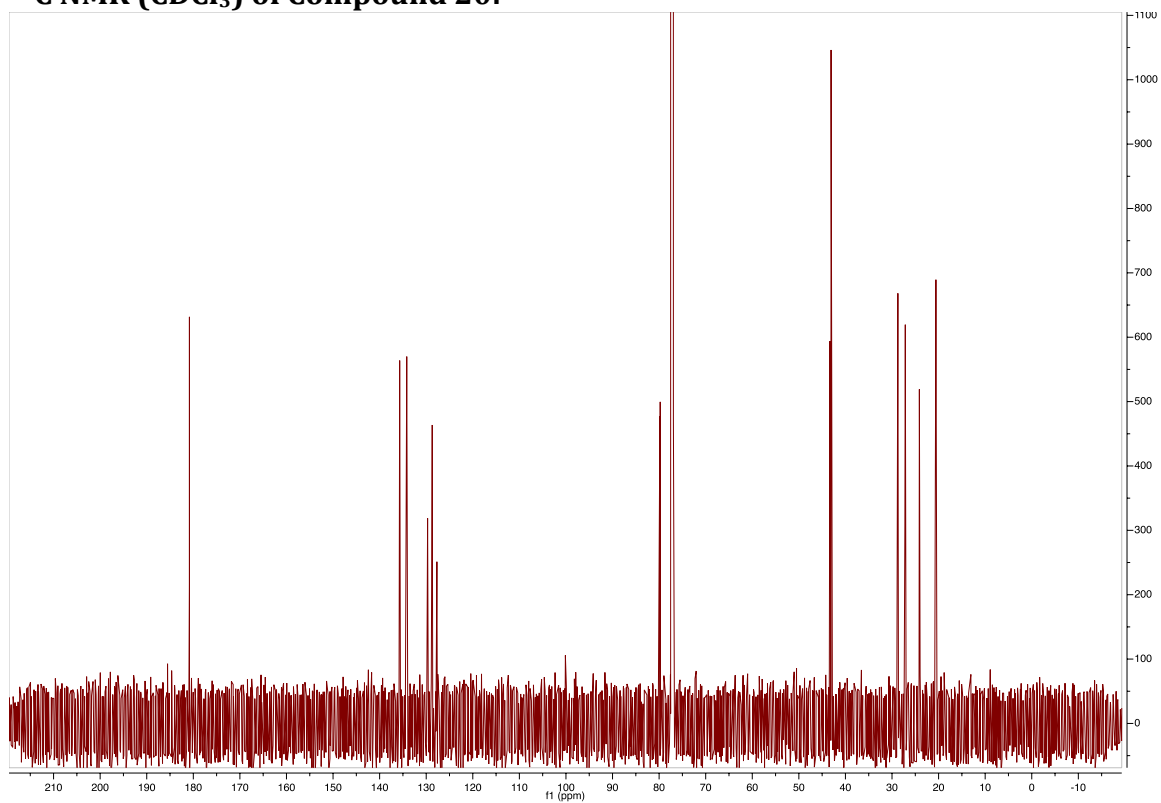
^1H NMR (CDCl_3) of Compound 15: **^{13}C NMR (CDCl_3) of Compound 15:**

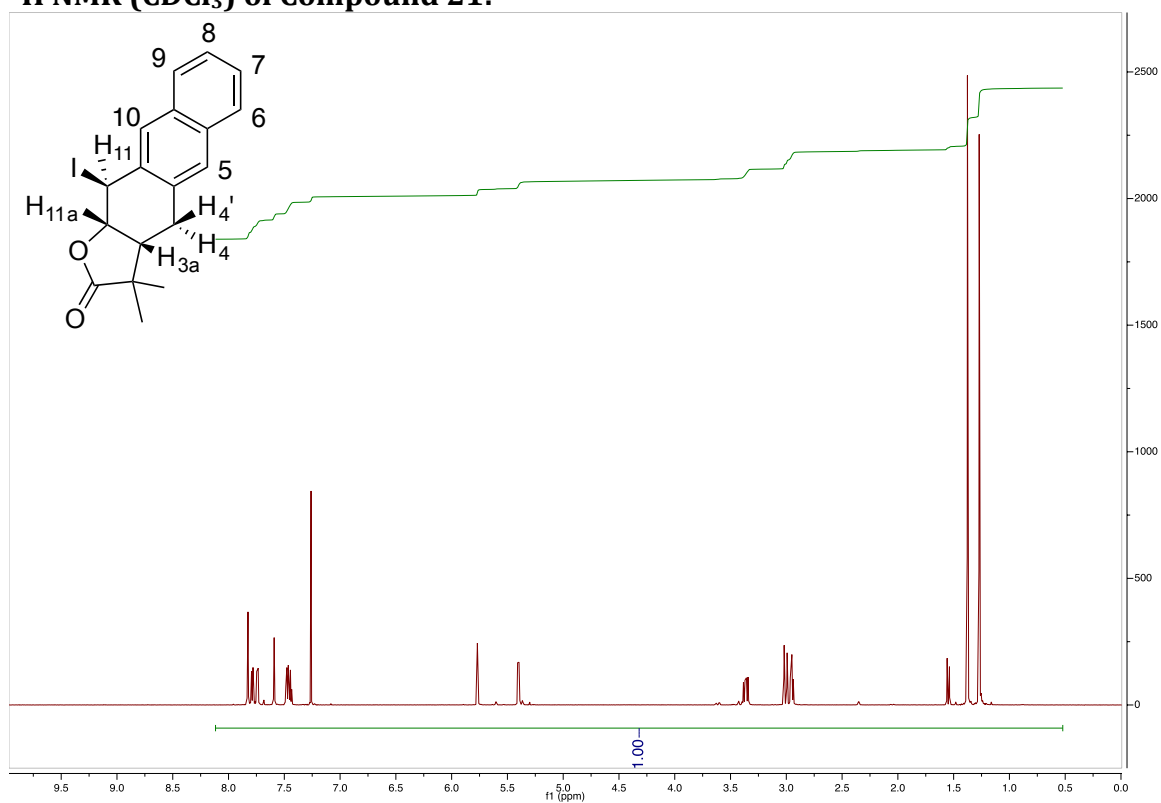
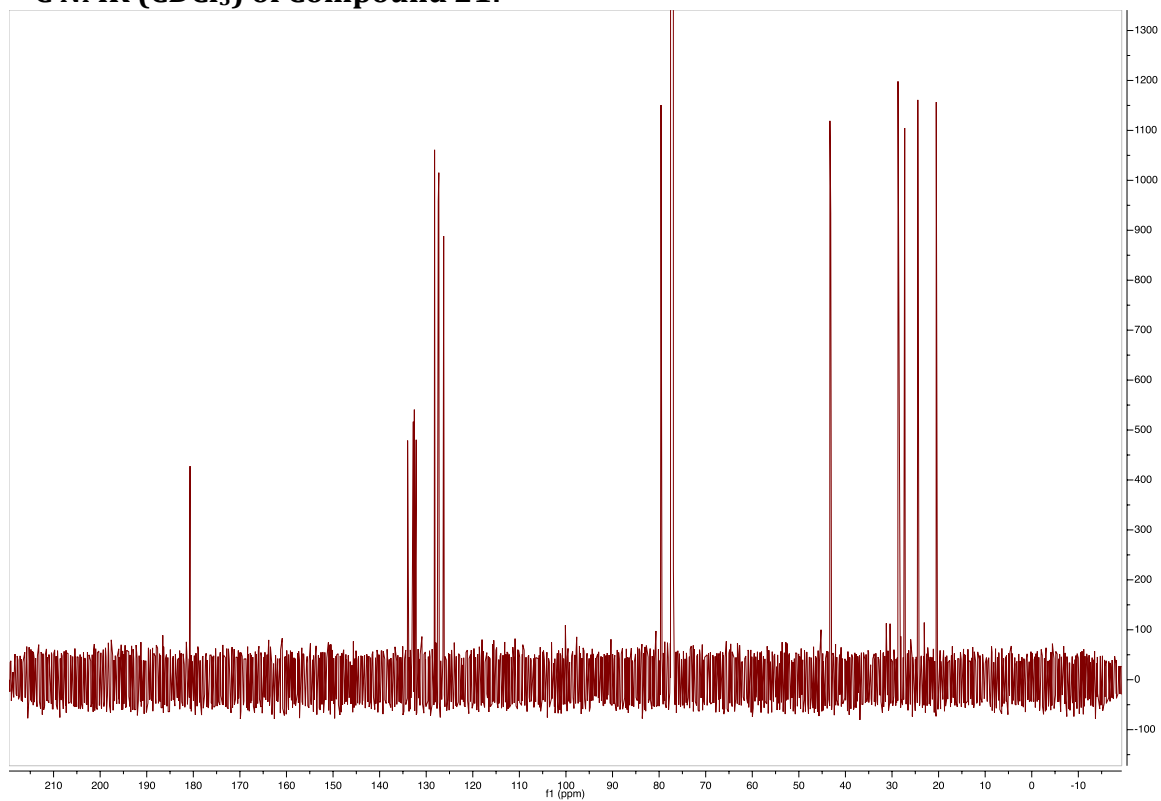
^1H NMR (CDCl_3) of Compound 16: **^{13}C NMR (CDCl_3) of Compound 16:**

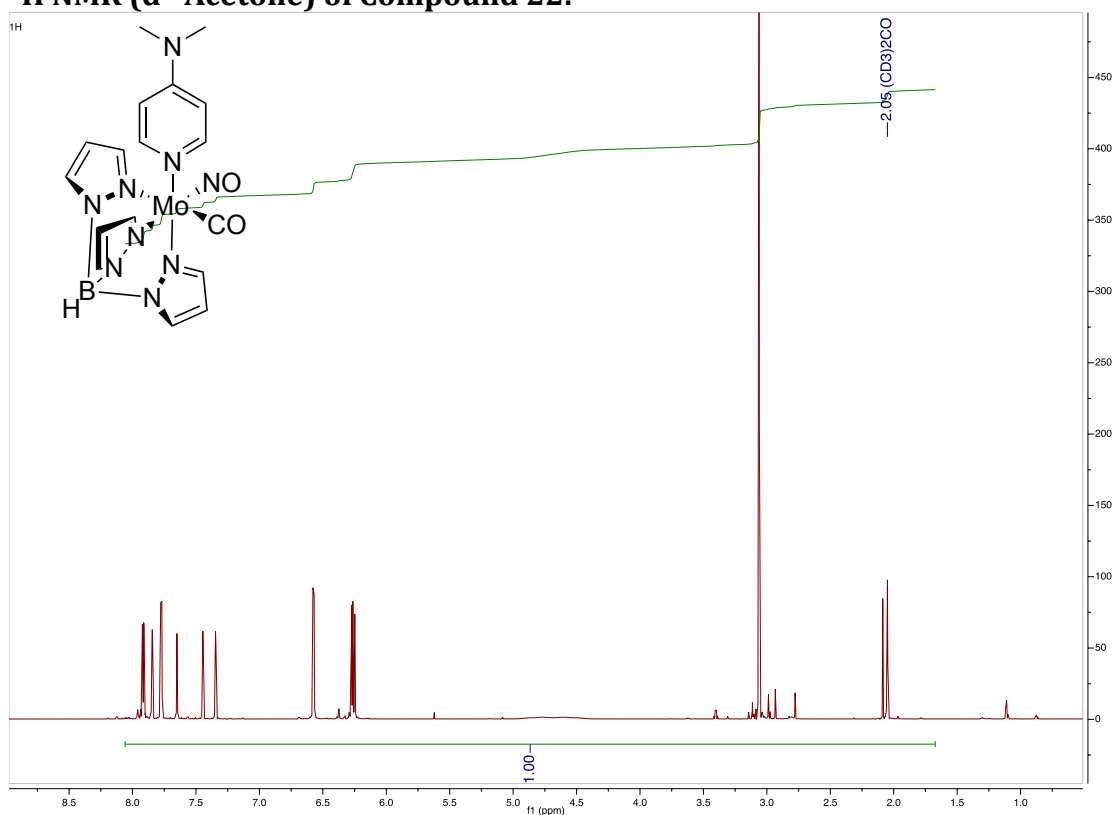
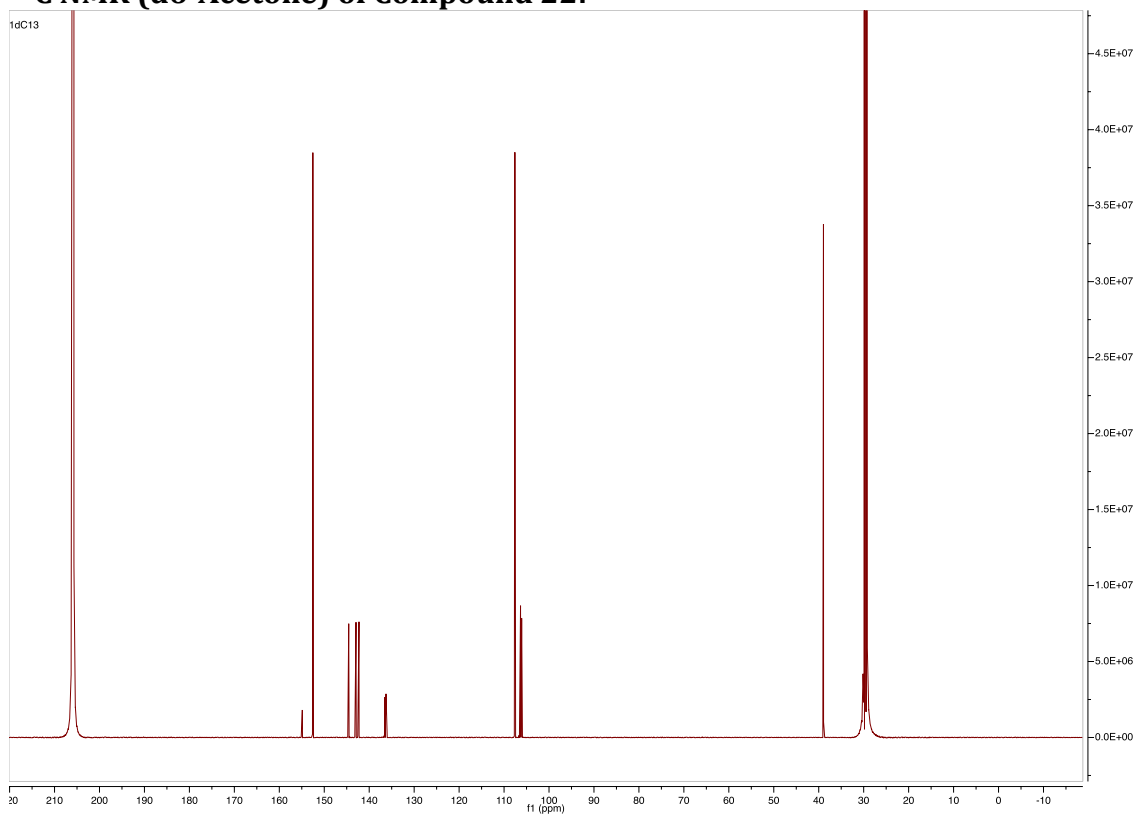
^1H NMR (CDCl_3) of Compound 17: **^{13}C NMR (CDCl_3) of Compound 17:**

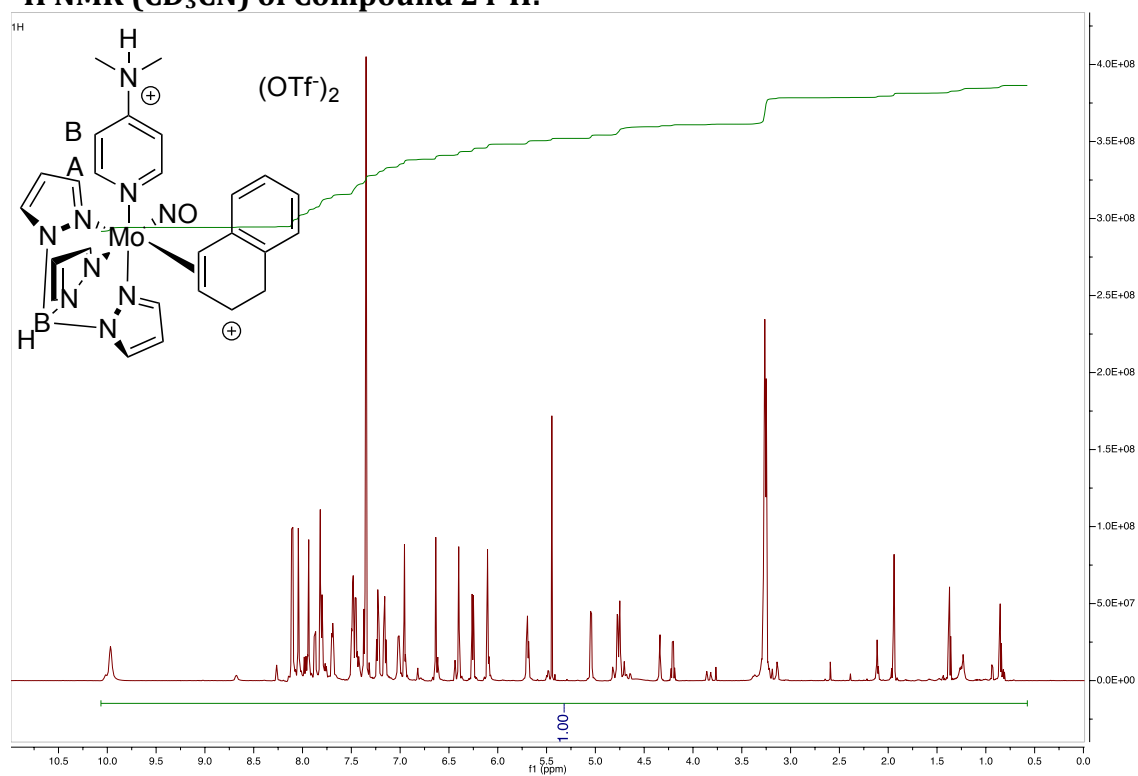
^1H NMR (CDCl_3) of Compound 18: **^{13}C NMR (CDCl_3) of Compound 18:**

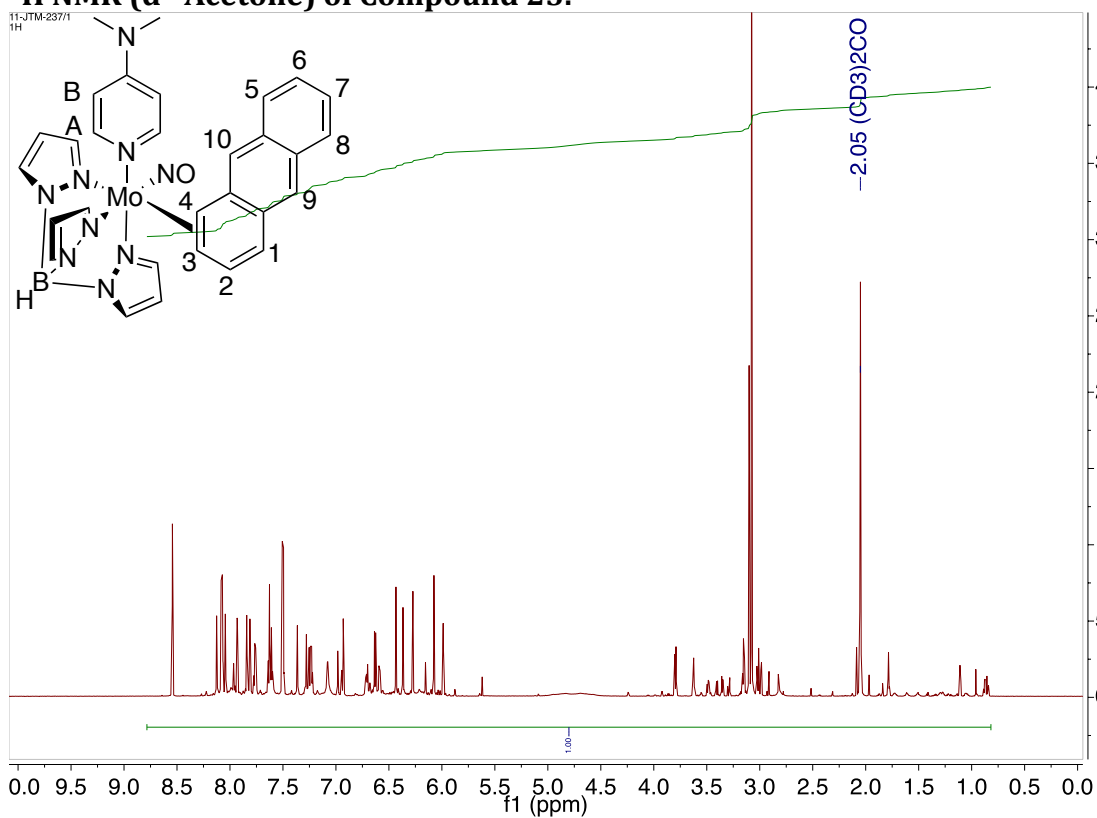
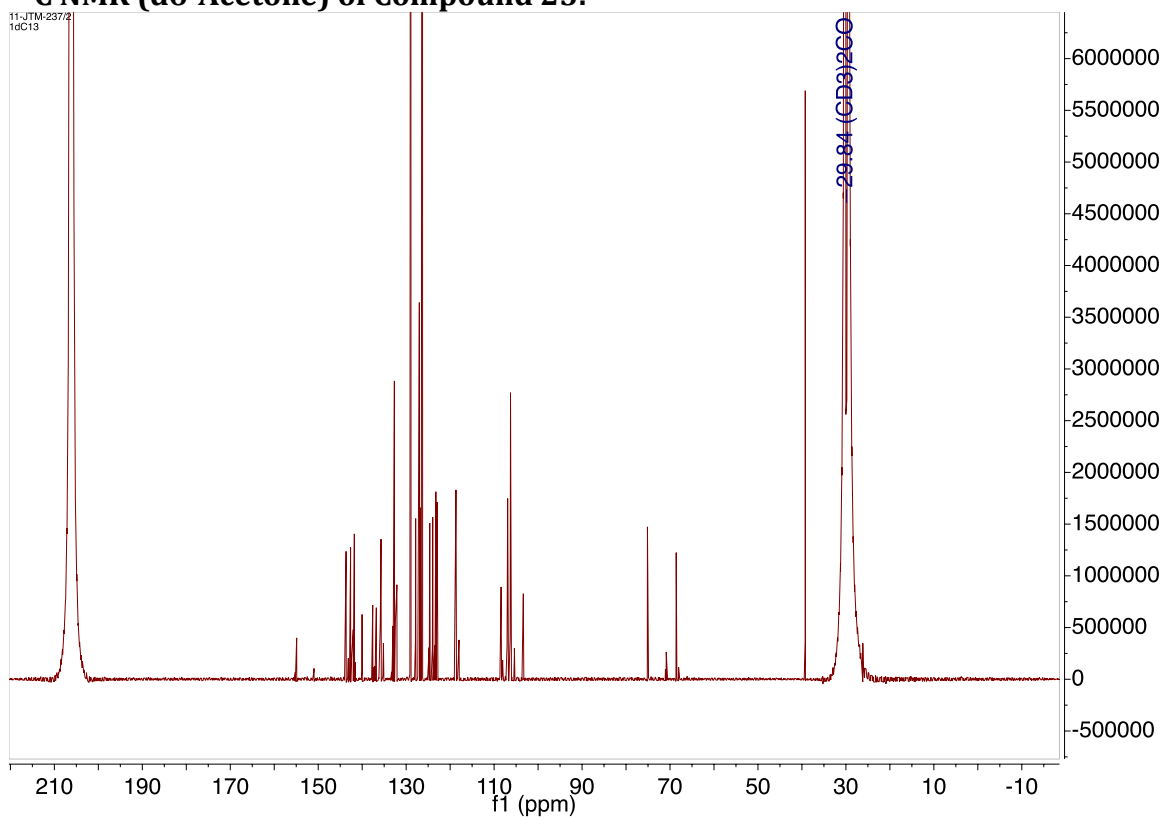
^1H NMR (CDCl_3) of Compound 19: **^{13}C NMR (CDCl_3) of Compound 19:**

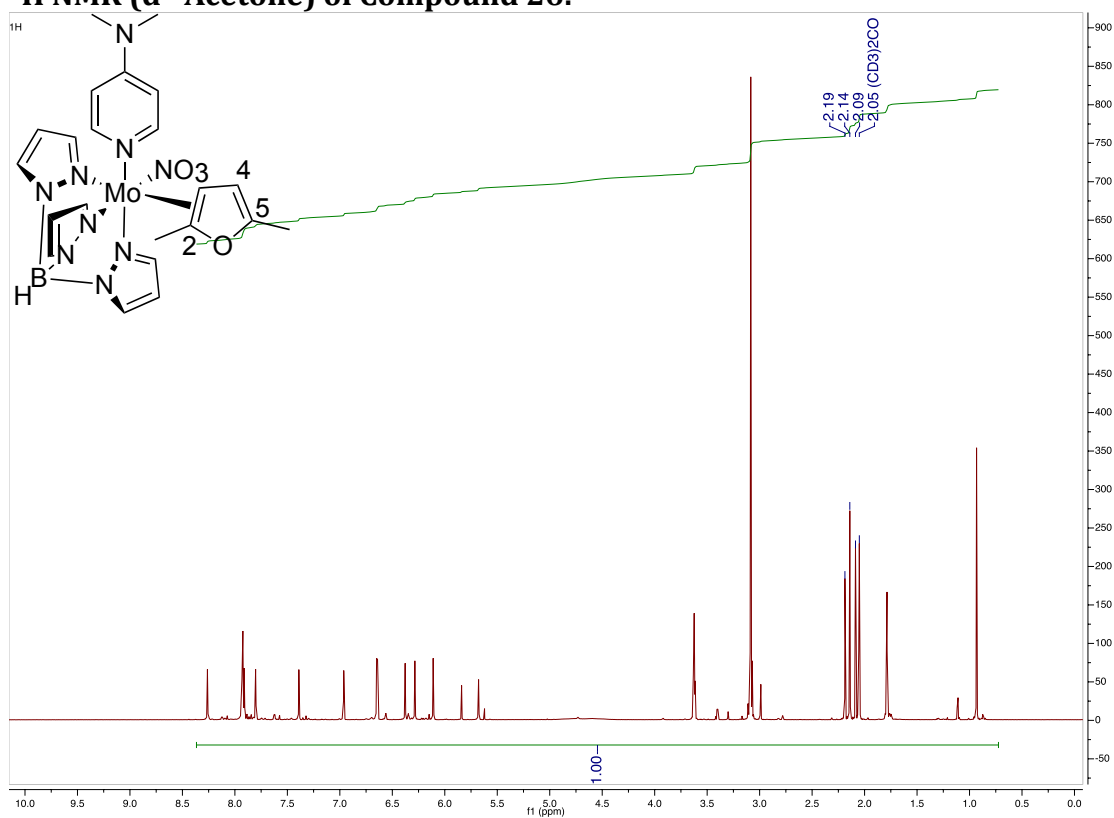
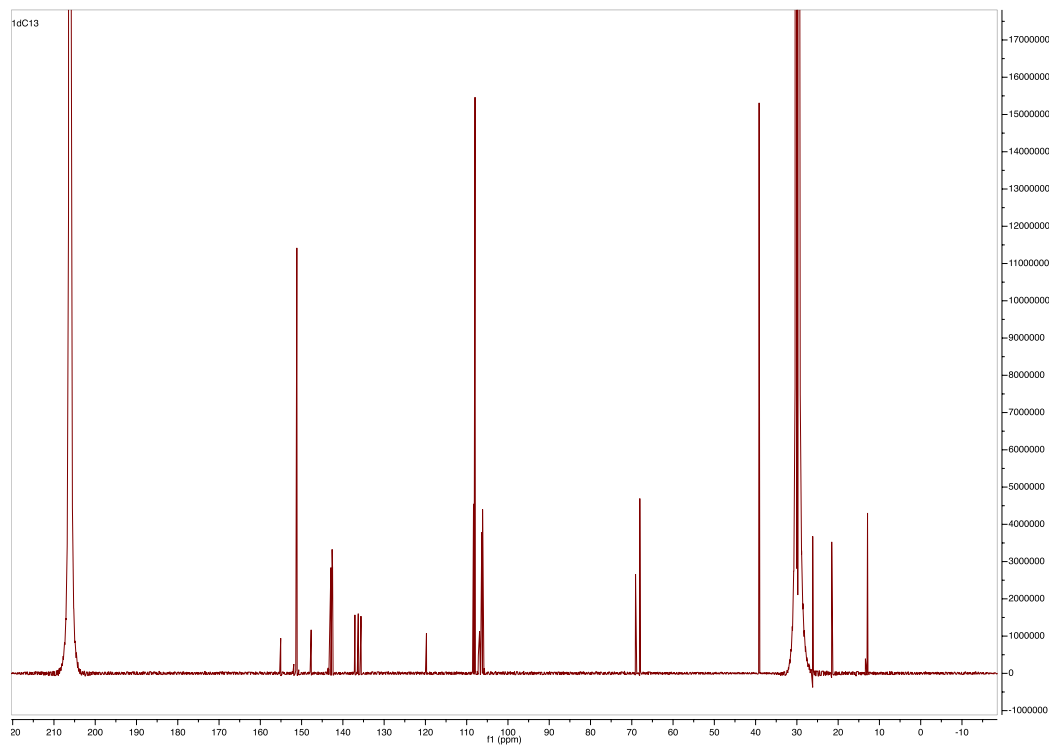
^1H NMR (CDCl_3) of Compound 20: **^{13}C NMR (CDCl_3) of Compound 20:**

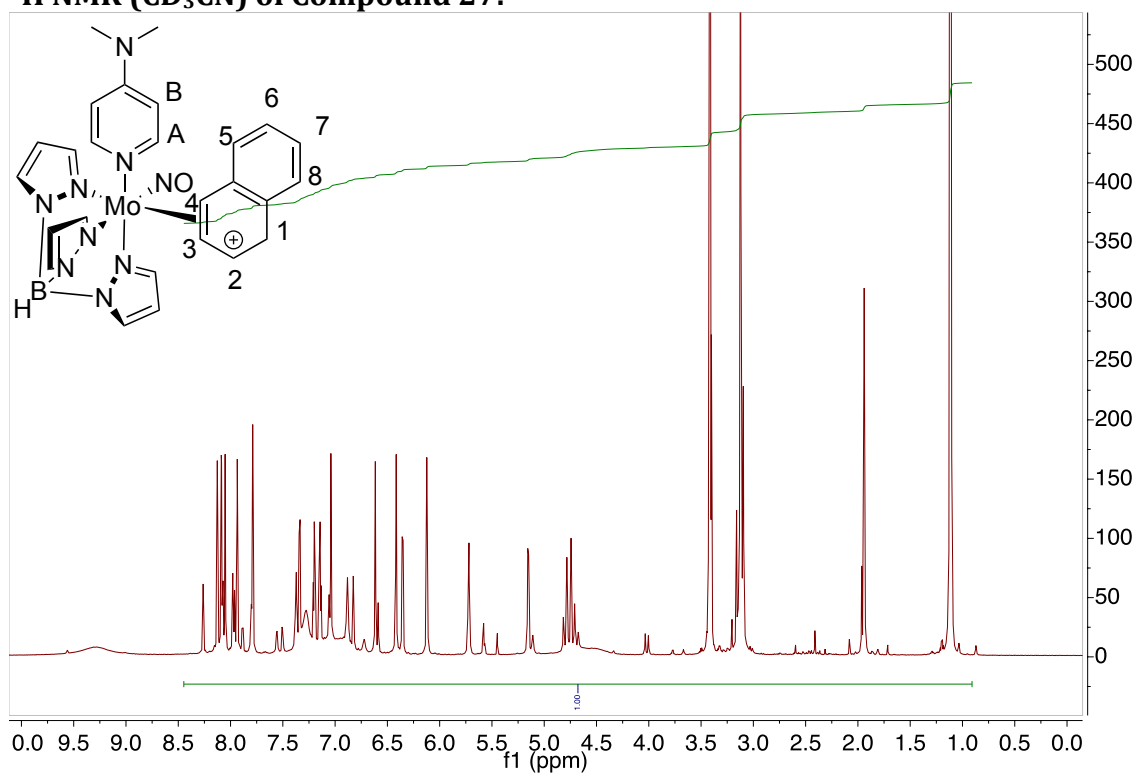
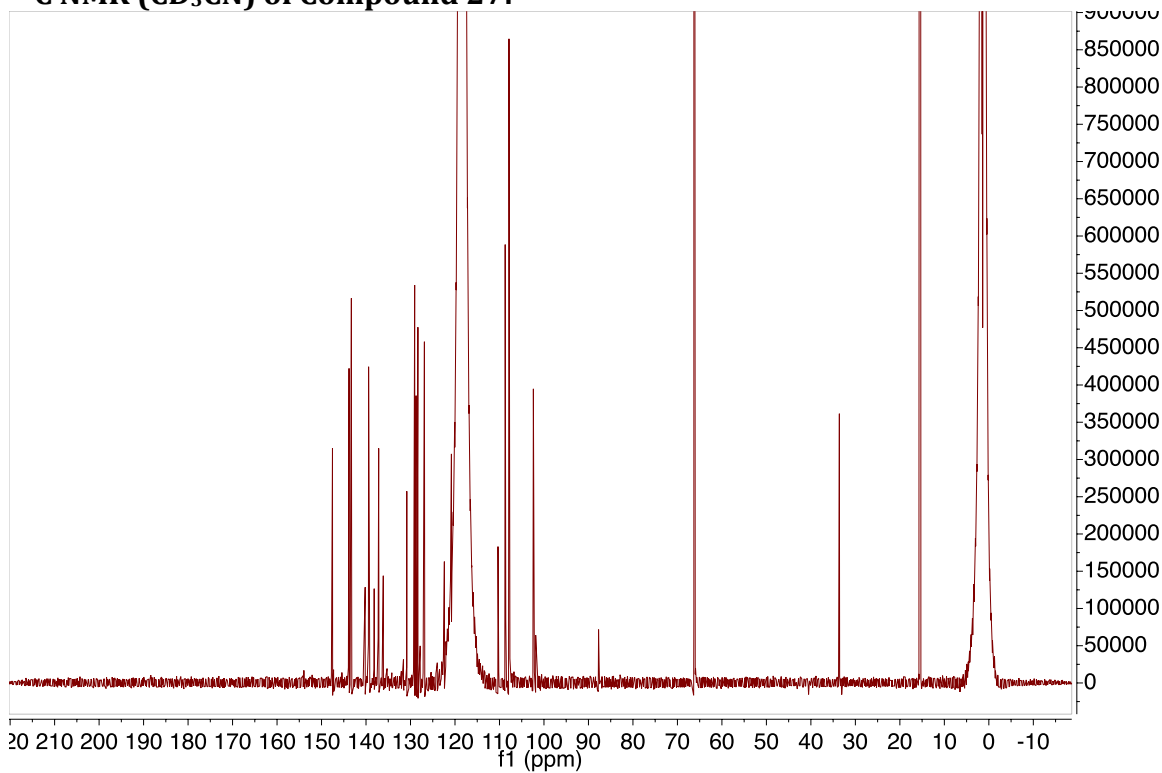
^1H NMR (CDCl_3) of Compound 21: **^{13}C NMR (CDCl_3) of Compound 21:**

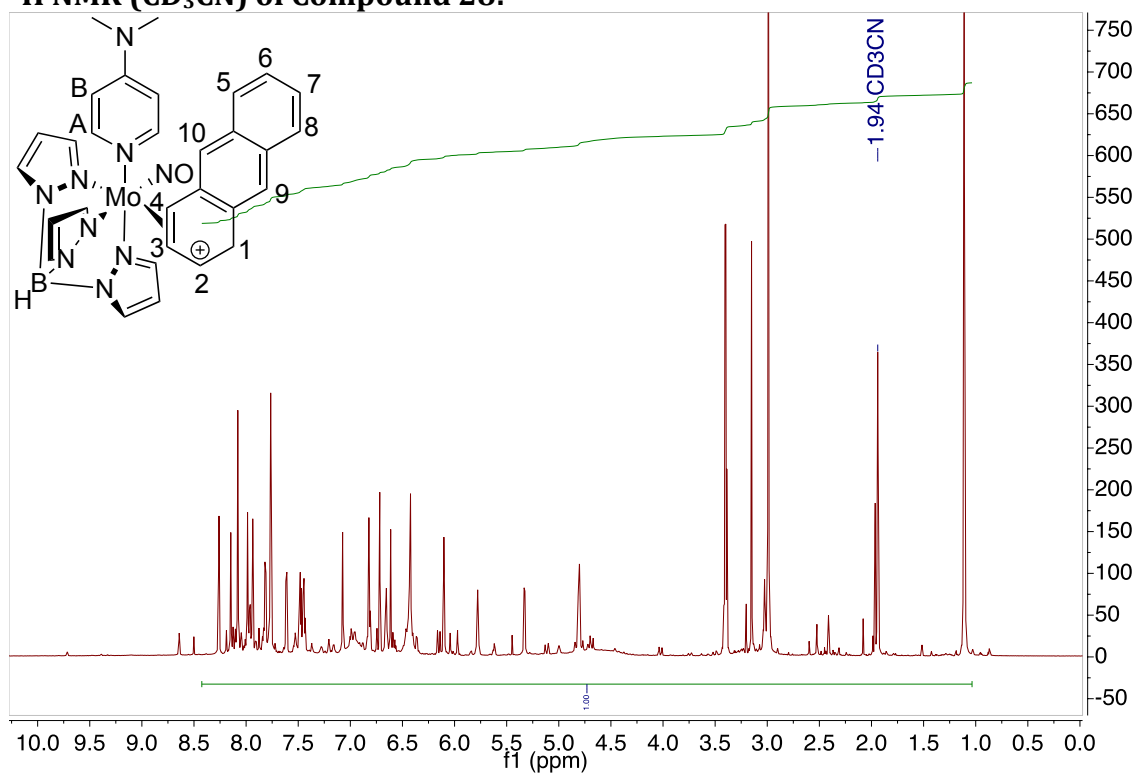
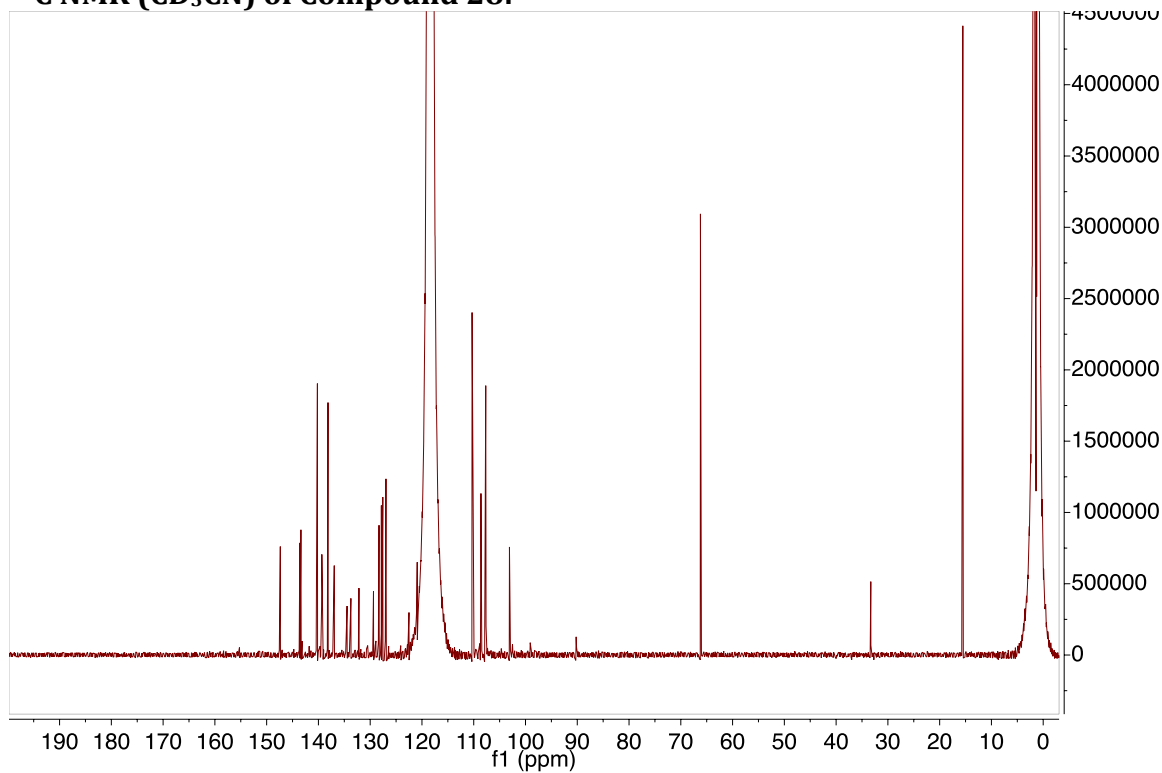
^1H NMR (d_6 -Acetone) of Compound 22: **^{13}C NMR (d_6 -Acetone) of Compound 22:**

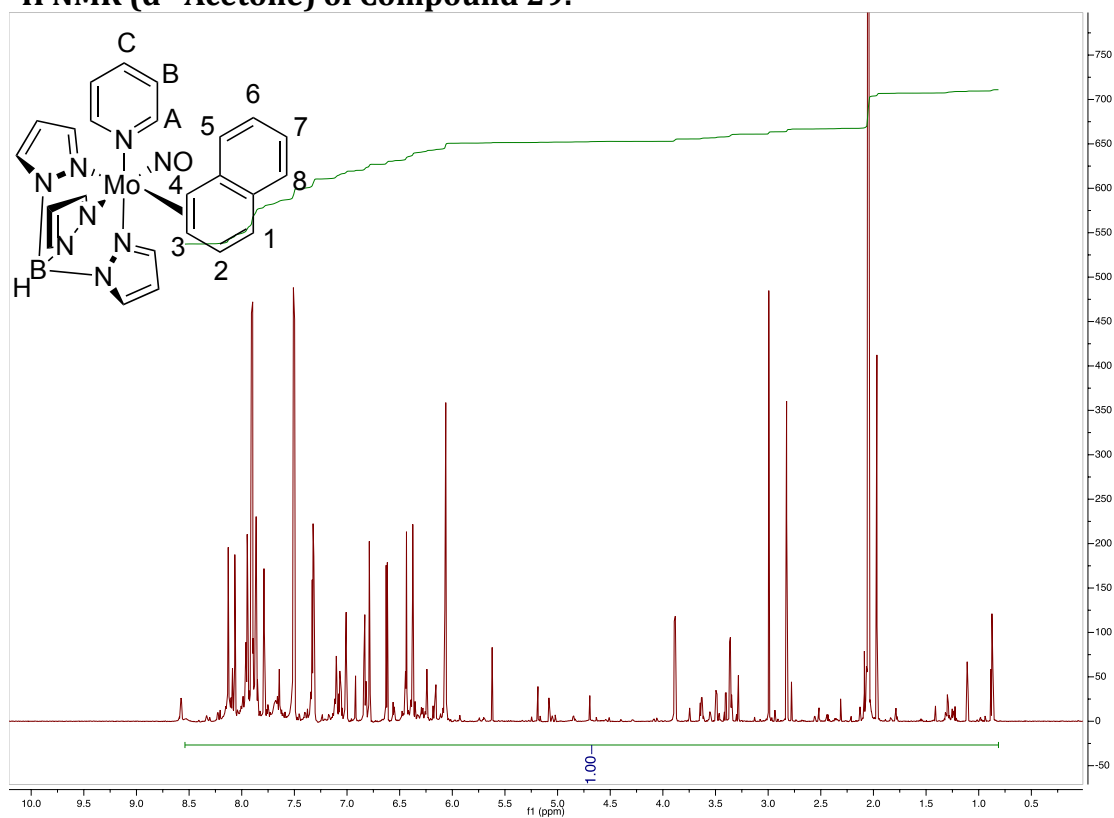
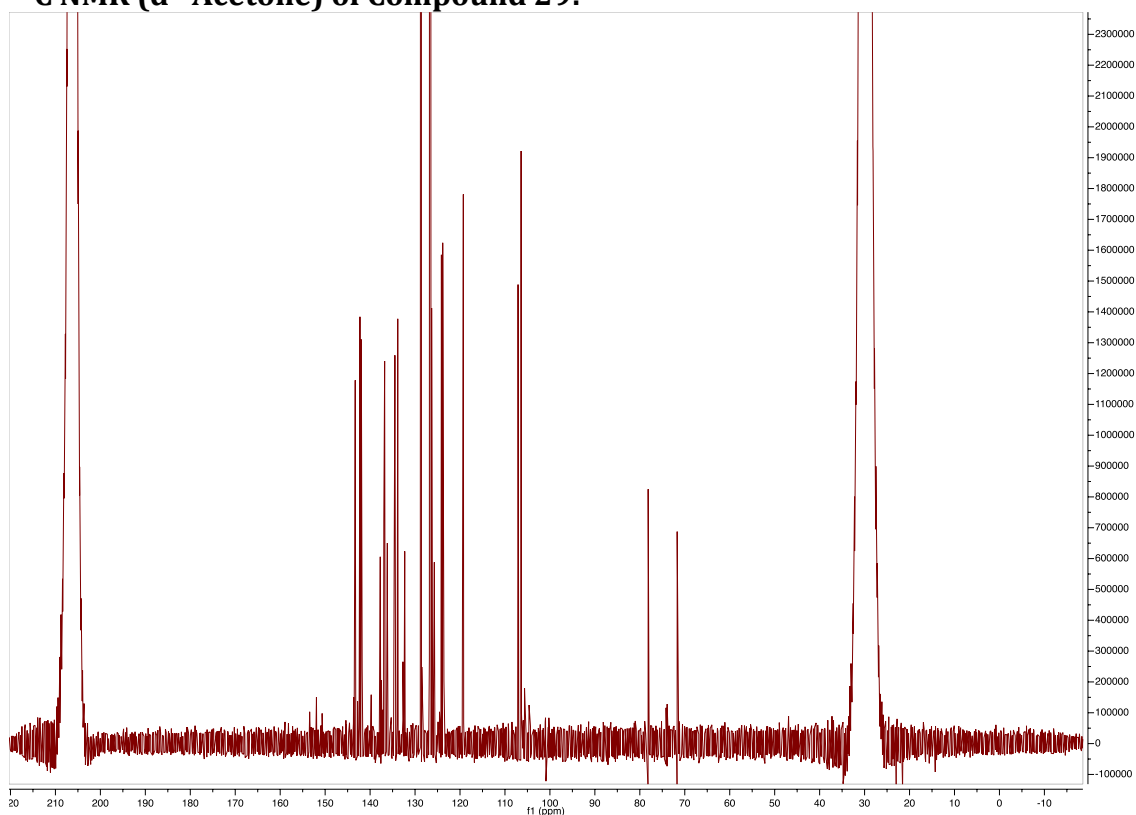
^1H NMR (CD_3CN) of Compound 24-H:

^1H NMR ($\text{d}^6\text{-Acetone}$) of Compound 25: **^{13}C NMR ($\text{d}^6\text{-Acetone}$) of Compound 25:**

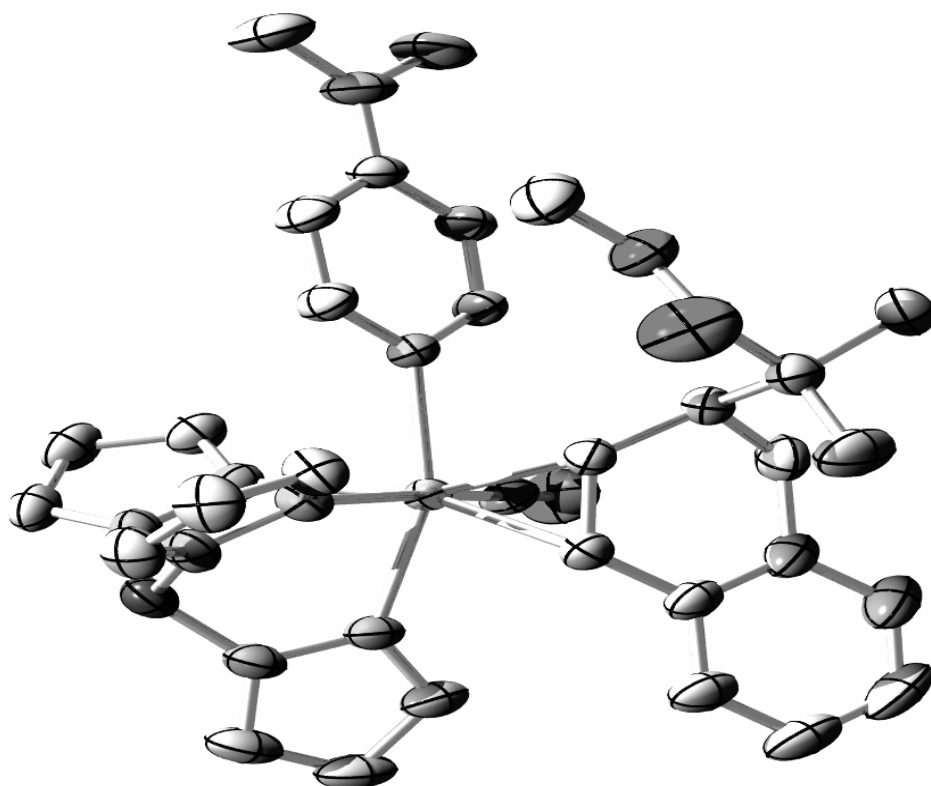
^1H NMR (d_6 -Acetone) of Compound 26: **^{13}C NMR (d_6 -Acetone) of Compound 26:**

^1H NMR (CD_3CN) of Compound 27: **^{13}C NMR (CD_3CN) of Compound 27:**

^1H NMR (CD_3CN) of Compound 28: **^{13}C NMR (CD_3CN) of Compound 28:**

^1H NMR ($\text{d}^6\text{-Acetone}$) of Compound 29: **^{13}C NMR ($\text{d}^6\text{-Acetone}$) of Compound 29:**

Compound 30



Compound 30

Table 1. Crystallographic Data for $C_{31}H_{38}BN_9O_3Mo$.

Empirical formula	$C_{31}H_{38}BN_9O_3$	
Formula weight	691.45	
Temperature	233(2) K	
Wavelength	0.71073 Å	
Crystal system	Monoclinic	
Space group	$P2_1/c$	
Unit cell dimensions	$a = 15.2403(6)$ Å	$\beta = 111.099(1)^\circ$.
	$b = 13.9028(6)$ Å	
	$c = 16.4382(7)$ Å	
Volume	$3249.5(2)$ Å ³	
Z	4	
Density (calculated)	1.413 Mg/m ³	
Absorption coefficient	0.451 mm ⁻¹	
F(000)	1432	
Crystal size	0.390 x 0.380 x 0.140 mm ³	
Theta range for data collection	3.218 to 37.213°.	
Index ranges	$-25 \leq h \leq 25$, $-23 \leq k \leq 22$, $-27 \leq l \leq 26$	
Reflections collected	81168	
Independent reflections	16014 [$R(\text{int}) = 0.0292$]	
Completeness to $\theta = 25.242^\circ$	99.7 %	
Absorption correction	Empirical	
Refinement method	Full-matrix least-squares on F^2	
Data / restraints / parameters	16014 / 0 / 423	
Goodness-of-fit on F^2	1.040	
Final R indices [$I > 2\sigma(I)$]	$R1 = 0.0460$, $wR2 = 0.1197$	
R indices (all data)	$R1 = 0.0774$, $wR2 = 0.1359$	
Largest diff. peak and hole	1.511 and -0.764 e.Å ⁻³	

Compound 30

Table 2. Fractional coordinates ($\times 10^4$) and equivalent isotropic displacement parameters ($\text{\AA}^2 \times 10^3$) for $\text{C}_{31}\text{H}_{38}\text{BN}_9\text{O}_3\text{Mo}$. $U(\text{eq})$ is defined as one third of the trace of the orthogonalized U_{ij} tensor.

	x	y	z	U(eq)
Mo	7344(1)	-716(1)	8006(1)	33(1)
O(1)	7608(2)	3228(2)	8291(2)	92(1)
O(2)	6189(1)	2554(2)	7811(1)	62(1)
O(3)	6270(2)	-1522(2)	6261(1)	79(1)
N(1)	6036(1)	-74(1)	8072(1)	37(1)
N(2)	3417(2)	752(2)	8160(2)	64(1)
N(3)	8523(1)	-1729(1)	8223(1)	43(1)
N(4)	8947(1)	-2164(1)	9008(1)	48(1)
N(5)	6932(1)	-1876(1)	8734(1)	41(1)
N(6)	7567(1)	-2290(1)	9454(1)	43(1)
N(7)	8216(1)	-236(1)	9403(1)	40(1)
N(8)	8675(1)	-920(1)	9996(1)	45(1)
N(9)	6721(1)	-1180(1)	6965(1)	44(1)
C(1)	6853(2)	1306(2)	6843(1)	43(1)
C(2)	7504(2)	791(1)	7643(1)	39(1)
C(3)	8302(1)	270(2)	7625(1)	41(1)
C(4)	8475(2)	155(2)	6815(2)	47(1)
C(5)	9337(2)	-199(2)	6817(2)	56(1)
C(6)	9514(2)	-301(2)	6058(2)	70(1)
C(7)	8842(3)	-3(2)	5277(2)	78(1)
C(8)	8001(2)	374(2)	5267(2)	66(1)
C(9)	7803(2)	447(2)	6028(2)	51(1)
C(10)	6857(2)	812(2)	5999(2)	55(1)
C(11)	7079(2)	2413(2)	6892(2)	53(1)
C(12)	8060(2)	2629(2)	6897(3)	80(1)
C(13)	6341(3)	2965(2)	6147(2)	74(1)
C(14)	7010(2)	2783(2)	7740(2)	55(1)
C(15)	6080(3)	2803(2)	8613(2)	75(1)
C(16)	5243(2)	-39(2)	7357(1)	44(1)

C(17)	4384(2)	235(2)	7357(2)	48(1)
C(18)	4266(2)	501(2)	8134(2)	45(1)
C(19)	5091(2)	482(2)	8876(2)	53(1)
C(20)	5931(2)	195(2)	8816(1)	48(1)
C(21)	2592(2)	768(3)	7369(3)	83(1)
C(22)	3309(3)	1075(3)	8943(3)	89(1)
C(23)	9581(2)	-2809(2)	8944(2)	62(1)
C(24)	9574(2)	-2796(2)	8117(2)	64(1)
C(25)	8897(2)	-2116(2)	7679(2)	52(1)
C(26)	7132(2)	-2950(2)	9779(2)	53(1)
C(27)	6202(2)	-2967(2)	9266(2)	59(1)
C(28)	6108(2)	-2290(2)	8623(2)	50(1)
C(29)	9193(2)	-499(2)	10749(2)	56(1)
C(30)	9090(2)	473(2)	10660(2)	61(1)
C(31)	8472(2)	609(2)	9815(2)	50(1)
B(1)	8603(2)	-1996(2)	9767(2)	48(1)

Compound 30

Table 3. Bond lengths and angles for $C_{31}H_{38}BN_9O_3Mo$.

Mo-N(9)	1.7549(17)
Mo-N(3)	2.2079(17)
Mo-C(2)	2.2157(19)
Mo-N(1)	2.2228(16)
Mo-N(5)	2.2287(17)
Mo-C(3)	2.2492(19)
Mo-N(7)	2.2992(17)
O(1)-C(14)	1.199(4)
O(2)-C(14)	1.337(3)
O(2)-C(15)	1.428(3)
O(3)-N(9)	1.210(2)
N(1)-C(20)	1.343(3)
N(1)-C(16)	1.350(3)
N(2)-C(18)	1.355(3)
N(2)-C(22)	1.428(4)
N(2)-C(21)	1.447(4)
N(3)-C(25)	1.336(3)
N(3)-N(4)	1.359(3)
N(4)-C(23)	1.349(3)
N(4)-B(1)	1.536(3)
N(5)-C(28)	1.333(3)
N(5)-N(6)	1.358(2)
N(6)-C(26)	1.350(3)
N(6)-B(1)	1.529(3)
N(7)-C(31)	1.341(3)
N(7)-N(8)	1.361(2)
N(8)-C(29)	1.341(3)
N(8)-B(1)	1.538(3)
C(1)-C(2)	1.512(3)
C(1)-C(10)	1.550(3)
C(1)-C(11)	1.572(3)
C(2)-C(3)	1.425(3)
C(3)-C(4)	1.456(3)

C(4)-C(9)	1.391(4)
C(4)-C(5)	1.403(3)
C(5)-C(6)	1.375(4)
C(6)-C(7)	1.387(5)
C(7)-C(8)	1.379(5)
C(8)-C(9)	1.392(3)
C(9)-C(10)	1.513(4)
C(11)-C(12)	1.523(4)
C(11)-C(13)	1.537(4)
C(11)-C(14)	1.525(4)
C(16)-C(17)	1.363(3)
C(17)-C(18)	1.403(3)
C(18)-C(19)	1.402(4)
C(19)-C(20)	1.377(3)
C(23)-C(24)	1.356(4)
C(24)-C(25)	1.394(4)
C(26)-C(27)	1.363(4)
C(27)-C(28)	1.384(4)
C(29)-C(30)	1.362(4)
C(30)-C(31)	1.383(3)

N(9)-Mo-N(3)	92.65(8)
N(9)-Mo-C(2)	99.09(8)
N(3)-Mo-C(2)	119.01(7)
N(9)-Mo-N(1)	90.86(7)
N(3)-Mo-N(1)	160.08(6)
C(2)-Mo-N(1)	79.67(7)
N(9)-Mo-N(5)	95.71(8)
N(3)-Mo-N(5)	79.74(6)
C(2)-Mo-N(5)	155.27(7)
N(1)-Mo-N(5)	80.41(6)
N(9)-Mo-C(3)	97.48(8)
N(3)-Mo-C(3)	82.08(7)
C(2)-Mo-C(3)	37.21(7)
N(1)-Mo-C(3)	116.88(7)
N(5)-Mo-C(3)	157.96(7)

N(9)-Mo-N(7)	175.13(8)
N(3)-Mo-N(7)	83.11(7)
C(2)-Mo-N(7)	85.10(7)
N(1)-Mo-N(7)	92.33(6)
N(5)-Mo-N(7)	81.22(6)
C(3)-Mo-N(7)	84.34(7)
C(14)-O(2)-C(15)	116.4(2)
C(20)-N(1)-C(16)	114.86(17)
C(20)-N(1)-Mo	124.02(14)
C(16)-N(1)-Mo	120.64(13)
C(18)-N(2)-C(22)	122.0(3)
C(18)-N(2)-C(21)	120.4(3)
C(22)-N(2)-C(21)	117.5(3)
C(25)-N(3)-N(4)	106.53(18)
C(25)-N(3)-Mo	131.88(17)
N(4)-N(3)-Mo	121.25(13)
C(23)-N(4)-N(3)	109.3(2)
C(23)-N(4)-B(1)	128.9(2)
N(3)-N(4)-B(1)	121.22(17)
C(28)-N(5)-N(6)	106.06(17)
C(28)-N(5)-Mo	132.28(16)
N(6)-N(5)-Mo	121.64(12)
C(26)-N(6)-N(5)	109.61(18)
C(26)-N(6)-B(1)	130.0(2)
N(5)-N(6)-B(1)	120.36(16)
C(31)-N(7)-N(8)	105.63(17)
C(31)-N(7)-Mo	135.79(15)
N(8)-N(7)-Mo	118.36(13)
C(29)-N(8)-N(7)	109.65(19)
C(29)-N(8)-B(1)	128.1(2)
N(7)-N(8)-B(1)	122.16(18)
O(3)-N(9)-Mo	177.4(2)
C(2)-C(1)-C(10)	110.81(18)
C(2)-C(1)-C(11)	110.86(19)
C(10)-C(1)-C(11)	114.09(18)
C(3)-C(2)-C(1)	121.41(18)

C(3)-C(2)-Mo	72.67(11)
C(1)-C(2)-Mo	125.53(15)
C(2)-C(3)-C(4)	120.73(19)
C(2)-C(3)-Mo	70.12(11)
C(4)-C(3)-Mo	122.49(15)
C(9)-C(4)-C(5)	118.6(2)
C(9)-C(4)-C(3)	120.3(2)
C(5)-C(4)-C(3)	121.0(2)
C(6)-C(5)-C(4)	121.6(3)
C(7)-C(6)-C(5)	119.3(3)
C(6)-C(7)-C(8)	119.8(3)
C(7)-C(8)-C(9)	121.2(3)
C(4)-C(9)-C(8)	119.3(3)
C(4)-C(9)-C(10)	120.08(19)
C(8)-C(9)-C(10)	120.6(3)
C(9)-C(10)-C(1)	115.5(2)
C(12)-C(11)-C(13)	110.0(2)
C(12)-C(11)-C(14)	108.6(3)
C(13)-C(11)-C(14)	106.8(2)
C(12)-C(11)-C(1)	113.0(2)
C(13)-C(11)-C(1)	111.3(2)
C(14)-C(11)-C(1)	106.93(18)
O(1)-C(14)-O(2)	122.5(3)
O(1)-C(14)-C(11)	125.5(3)
O(2)-C(14)-C(11)	111.9(2)
C(17)-C(16)-N(1)	124.62(19)
C(16)-C(17)-C(18)	120.9(2)
N(2)-C(18)-C(17)	122.2(2)
N(2)-C(18)-C(19)	123.1(2)
C(17)-C(18)-C(19)	114.67(19)
C(20)-C(19)-C(18)	120.6(2)
N(1)-C(20)-C(19)	124.4(2)
C(24)-C(23)-N(4)	108.8(2)
C(23)-C(24)-C(25)	105.3(2)
N(3)-C(25)-C(24)	110.0(2)
N(6)-C(26)-C(27)	108.4(2)

C(26)-C(27)-C(28)	105.0(2)
N(5)-C(28)-C(27)	110.9(2)
N(8)-C(29)-C(30)	109.1(2)
C(29)-C(30)-C(31)	104.7(2)
N(7)-C(31)-C(30)	110.9(2)
N(6)-B(1)-N(4)	107.46(19)
N(6)-B(1)-N(8)	108.43(18)
N(4)-B(1)-N(8)	109.33(19)

Compound 30

Table 4. Anisotropic thermal displacement parameters ($\text{\AA}^2 \times 10^3$) for $\text{C}_{31}\text{H}_{38}\text{BN}_9\text{O}_3\text{Mo}$.

The anisotropic displacement factor exponent takes the form: $-2\pi^2 [h^2 a^{*2} U^{11} + \dots + 2 h k a^* b^* U^{12}]$

	U^{11}	U^{22}	U^{33}	U^{23}	U^{13}	U^{12}
Mo	33(1)	35(1)	35(1)	0(1)	16(1)	2(1)
O(1)	86(2)	94(2)	99(2)	-34(2)	35(1)	-26(1)
O(2)	66(1)	70(1)	60(1)	-4(1)	33(1)	1(1)
O(3)	91(2)	90(2)	52(1)	-33(1)	20(1)	-8(1)
N(1)	37(1)	41(1)	38(1)	1(1)	18(1)	4(1)
N(2)	52(1)	64(1)	87(2)	-3(1)	39(1)	15(1)
N(3)	39(1)	37(1)	59(1)	1(1)	25(1)	3(1)
N(4)	40(1)	40(1)	66(1)	7(1)	20(1)	8(1)
N(5)	41(1)	41(1)	46(1)	2(1)	20(1)	-2(1)
N(6)	47(1)	38(1)	46(1)	4(1)	20(1)	-1(1)
N(7)	40(1)	38(1)	40(1)	1(1)	11(1)	1(1)
N(8)	40(1)	47(1)	42(1)	4(1)	7(1)	-1(1)
N(9)	47(1)	48(1)	41(1)	-9(1)	22(1)	1(1)
C(1)	45(1)	42(1)	46(1)	7(1)	22(1)	5(1)
C(2)	44(1)	37(1)	39(1)	2(1)	18(1)	1(1)
C(3)	38(1)	42(1)	46(1)	5(1)	19(1)	0(1)
C(4)	52(1)	40(1)	61(1)	0(1)	35(1)	-6(1)
C(5)	54(1)	47(1)	82(2)	-3(1)	41(1)	-7(1)
C(6)	73(2)	64(2)	98(2)	-14(2)	62(2)	-17(1)
C(7)	114(3)	68(2)	88(2)	-17(2)	79(2)	-22(2)
C(8)	95(2)	61(2)	58(1)	-1(1)	45(2)	-7(2)
C(9)	67(1)	45(1)	51(1)	-2(1)	34(1)	-3(1)
C(10)	63(1)	60(1)	40(1)	6(1)	18(1)	3(1)
C(11)	61(1)	43(1)	66(1)	10(1)	35(1)	6(1)
C(12)	82(2)	53(2)	131(3)	5(2)	71(2)	-7(1)
C(13)	99(2)	63(2)	71(2)	26(1)	45(2)	28(2)
C(14)	62(1)	43(1)	64(1)	2(1)	26(1)	4(1)
C(15)	100(2)	72(2)	68(2)	-1(1)	48(2)	9(2)
C(16)	42(1)	54(1)	39(1)	1(1)	17(1)	7(1)

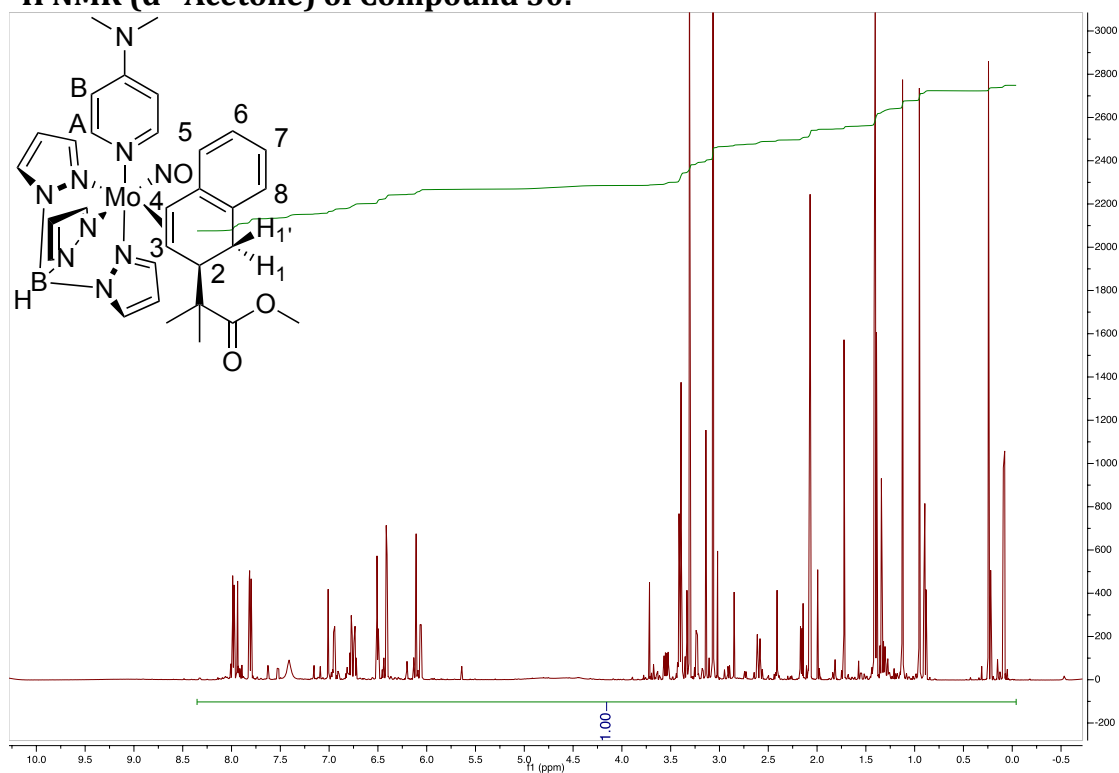
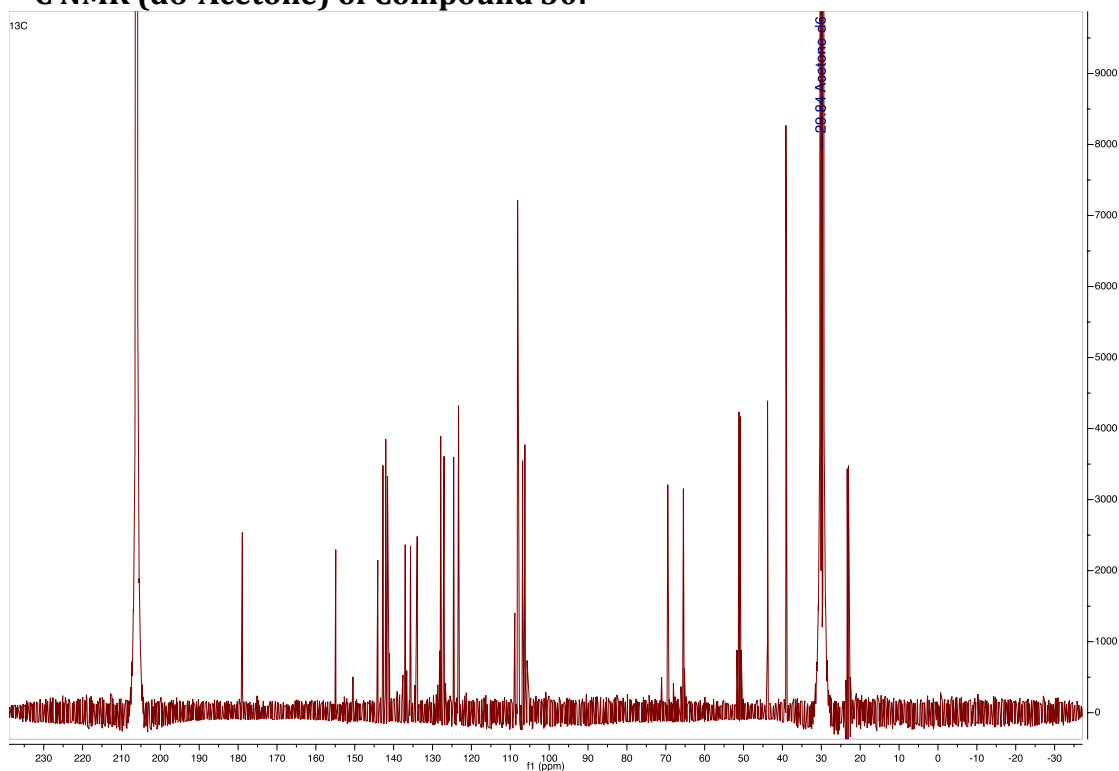
C(17)	40(1)	55(1)	49(1)	2(1)	16(1)	9(1)
C(18)	44(1)	37(1)	64(1)	2(1)	30(1)	7(1)
C(19)	55(1)	62(1)	50(1)	-8(1)	29(1)	5(1)
C(20)	46(1)	60(1)	41(1)	-5(1)	19(1)	3(1)
C(21)	49(2)	92(2)	108(3)	10(2)	30(2)	27(2)
C(22)	85(2)	100(3)	107(3)	-4(2)	67(2)	23(2)
C(23)	44(1)	40(1)	99(2)	6(1)	24(1)	10(1)
C(24)	52(1)	42(1)	111(2)	-6(1)	46(2)	5(1)
C(25)	51(1)	40(1)	78(2)	-6(1)	40(1)	-3(1)
C(26)	72(2)	40(1)	56(1)	6(1)	33(1)	-5(1)
C(27)	67(2)	53(1)	68(2)	0(1)	37(1)	-16(1)
C(28)	46(1)	51(1)	58(1)	-2(1)	23(1)	-10(1)
C(29)	49(1)	63(1)	44(1)	3(1)	3(1)	-7(1)
C(30)	65(2)	62(1)	46(1)	-10(1)	8(1)	-13(1)
C(31)	56(1)	42(1)	45(1)	-5(1)	11(1)	-2(1)
B(1)	44(1)	42(1)	52(1)	9(1)	12(1)	5(1)

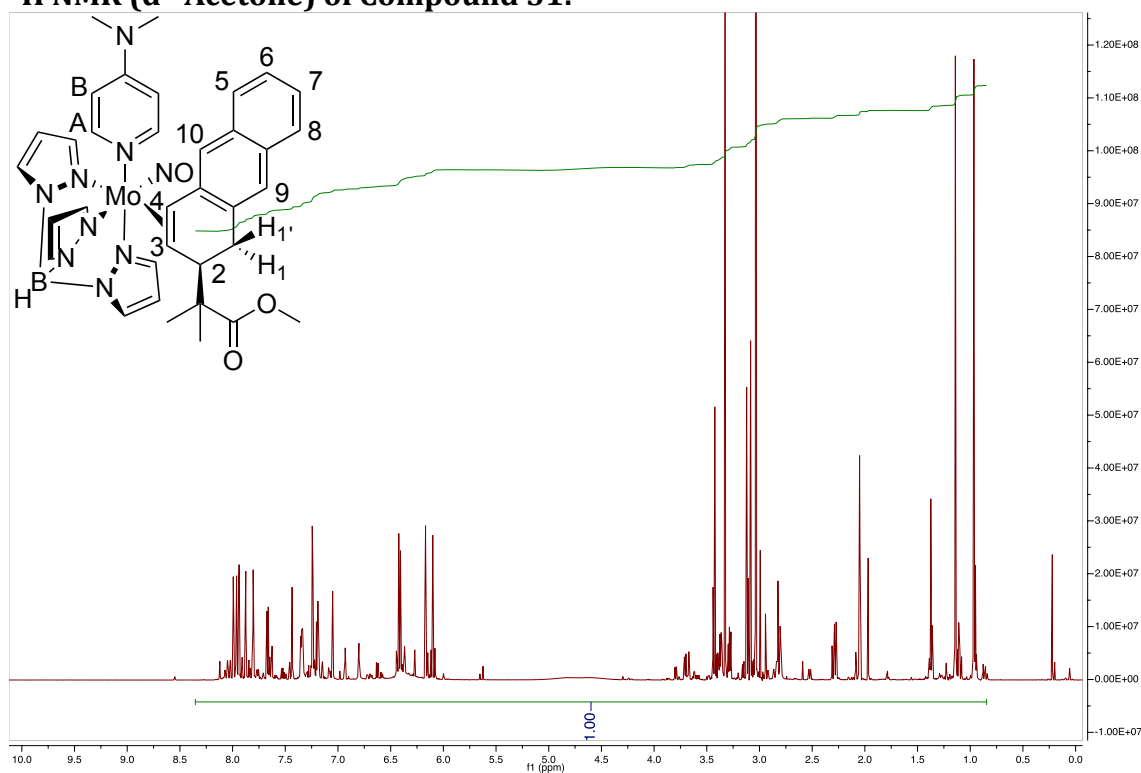
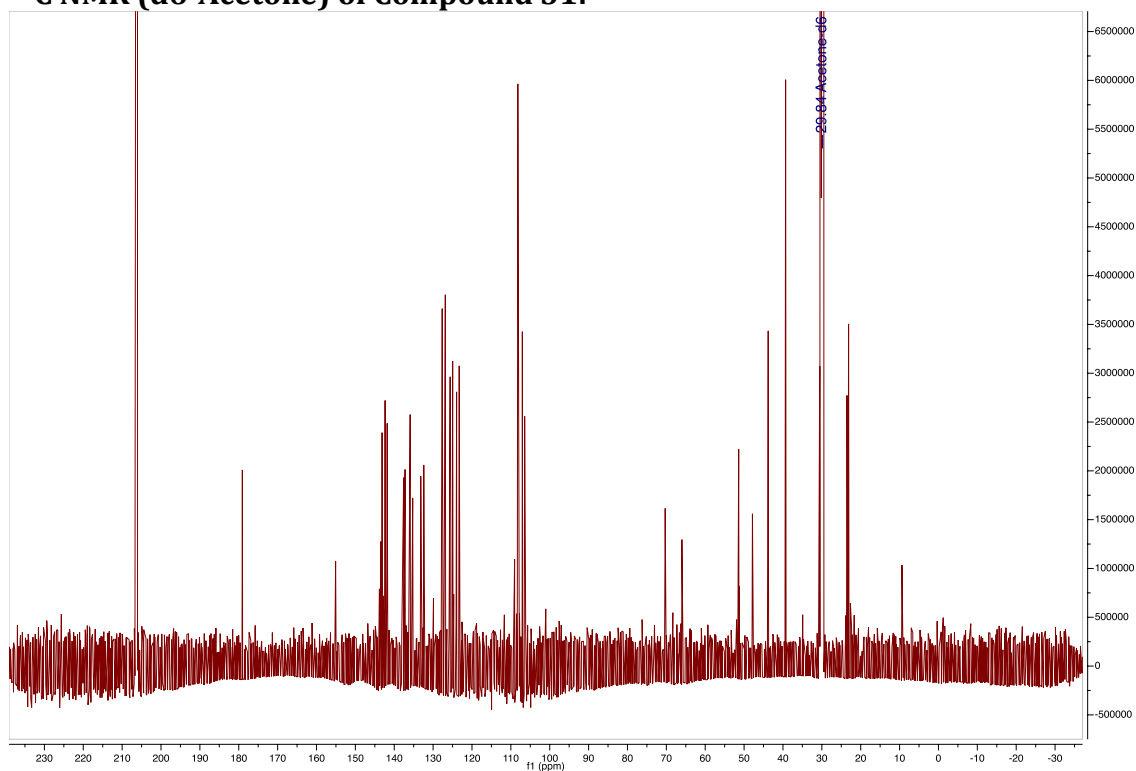
Compound 30

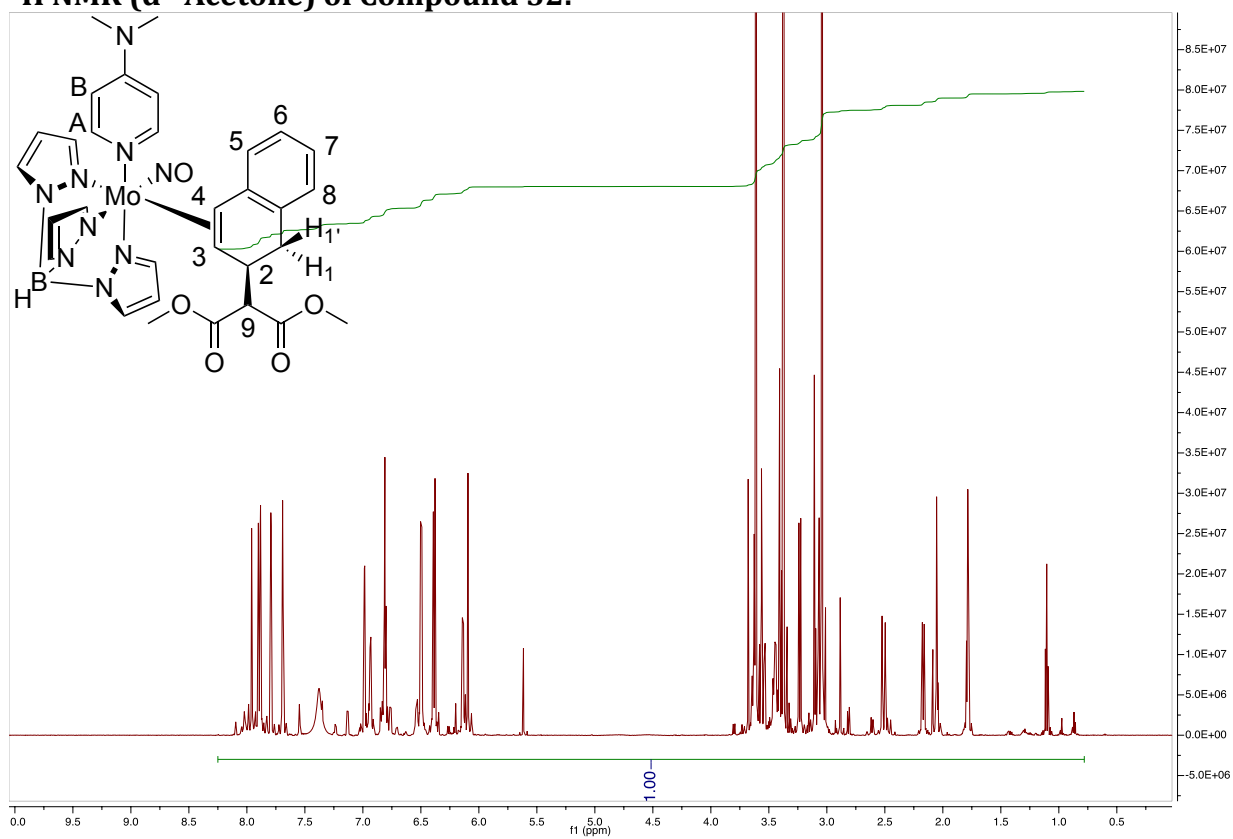
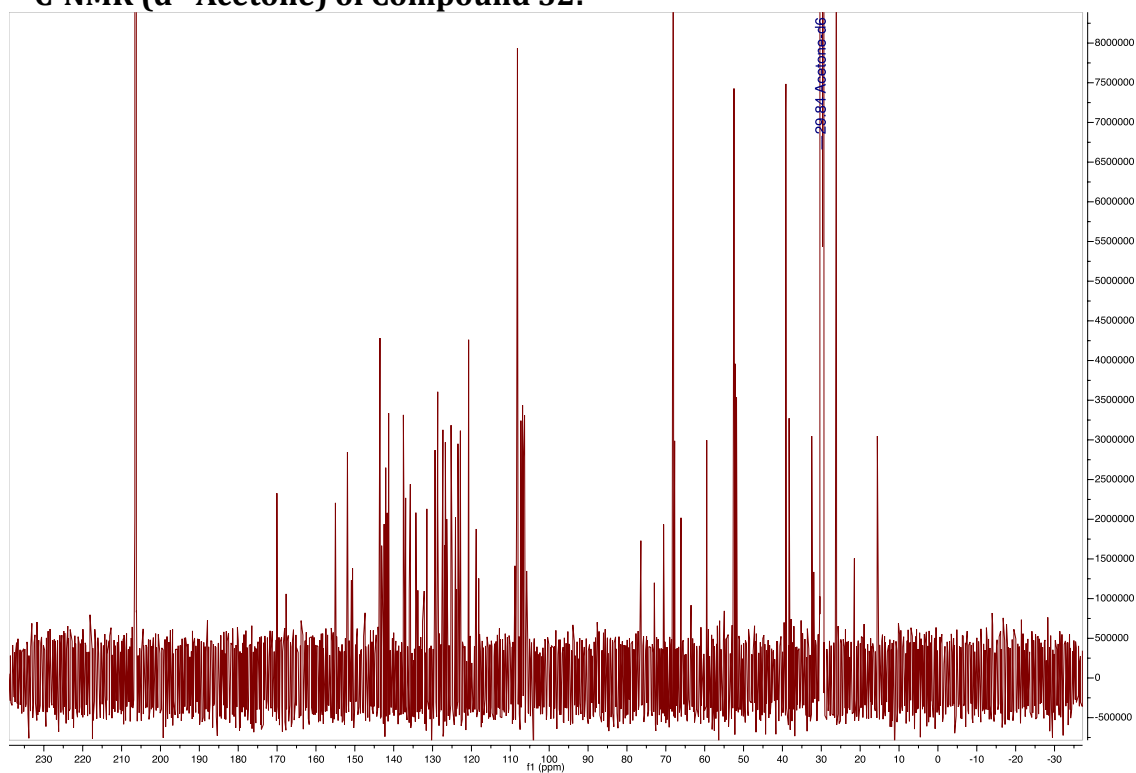
Table 5. Fractional coordinates ($\times 10^4$) and isotropic thermal displacement parameters ($\text{\AA}^2 \times 10^3$) for hydrogen atoms of $\text{C}_{31}\text{H}_{38}\text{BN}_9\text{O}_3\text{Mo}$.

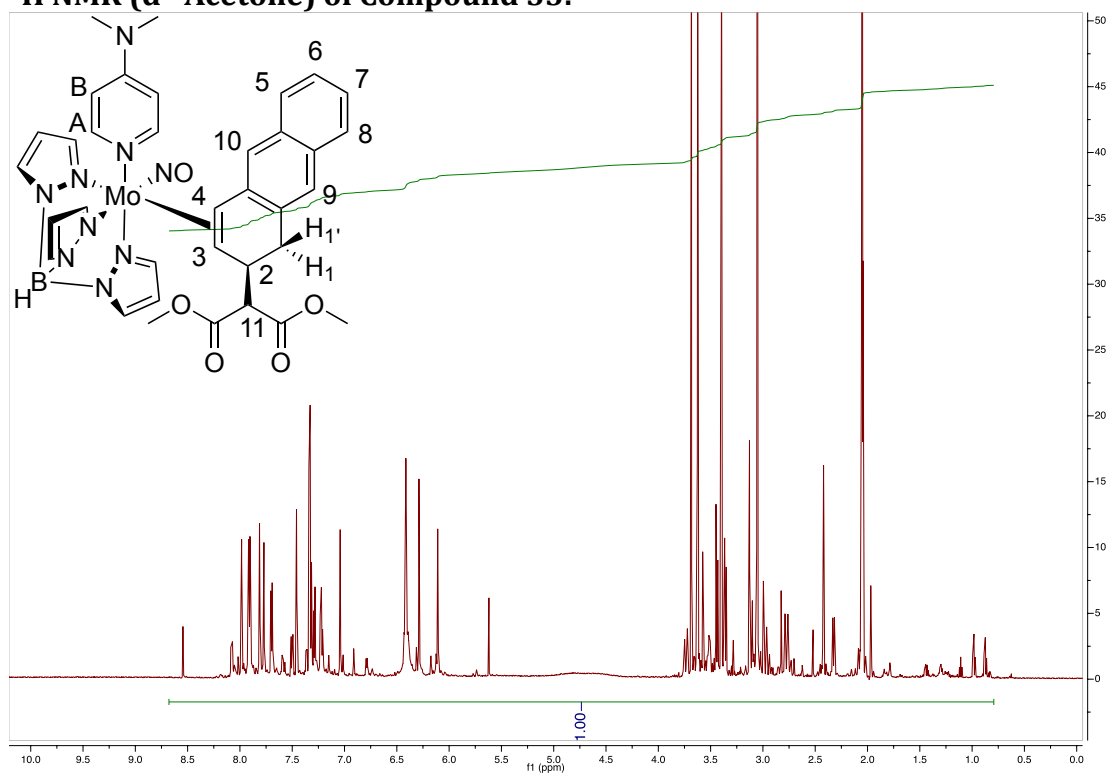
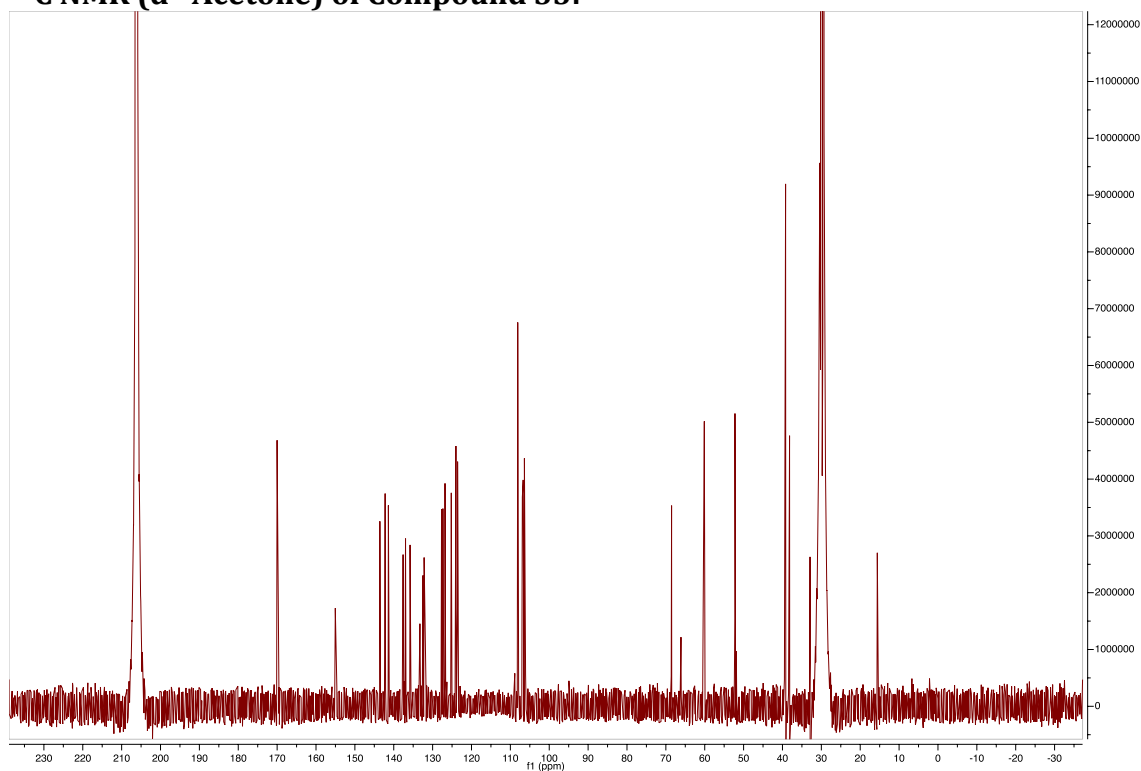
	x	y	z	U(eq)
H(1)	6208	1240	6848	52
H(5)	9806	-370	7349	68
H(6)	10084	-570	6069	84
H(7)	8959	-58	4755	94
H(8)	7554	586	4737	80
H(10A)	6418	269	5868	66
H(10B)	6618	1271	5517	66
H(12A)	8158	3319	6917	120
H(12B)	8123	2370	6373	120
H(12C)	8525	2334	7405	120
H(13A)	6431	3651	6252	111
H(13B)	5716	2786	6119	111
H(13C)	6412	2807	5599	111
H(15A)	6513	2426	9084	113
H(15B)	5440	2671	8569	113
H(15C)	6215	3482	8730	113
H(16)	5286	-216	6820	53
H(17)	3865	245	6830	58
H(19)	5071	666	9419	63
H(20)	6466	187	9331	57
H(21A)	2664	1263	6981	124
H(21B)	2040	904	7512	124
H(21C)	2519	147	7082	124
H(22A)	3366	532	9329	133
H(22B)	2695	1369	8803	133
H(22C)	3794	1543	9229	133
H(23)	9964	-3203	9398	74
H(24)	9947	-3167	7888	76
H(25)	8729	-1954	7087	62

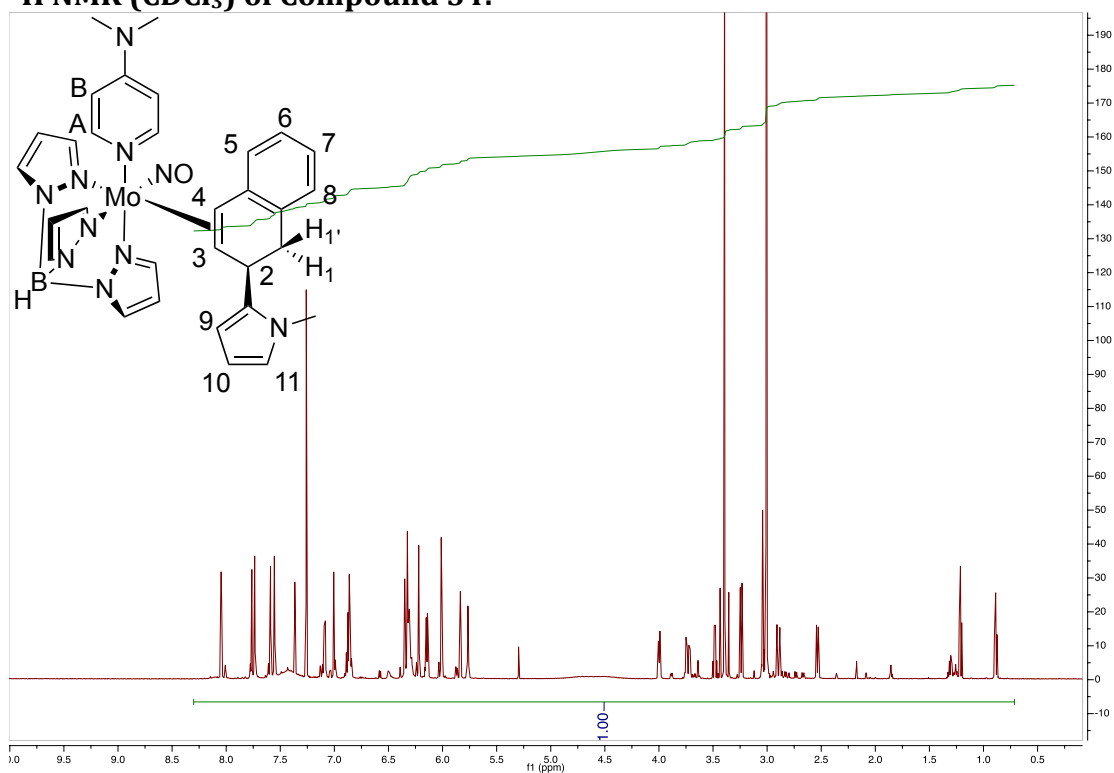
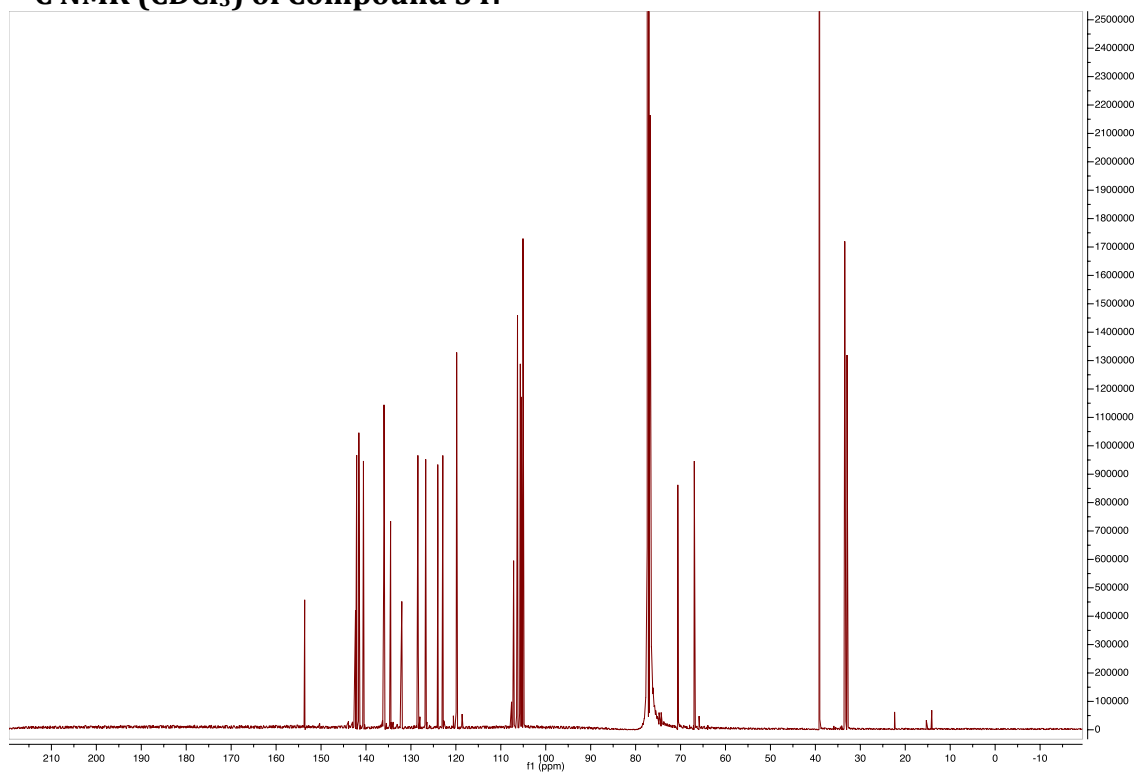
H(26)	7421	-3333	10275	64
H(27)	5728	-3354	9335	71
H(28)	5540	-2143	8169	60
H(29)	9568	-822	11258	67
H(30)	9375	947	11080	73
H(31)	8260	1213	9562	59
H(2)	7669(18)	1193(19)	8185(16)	43(6)
H(3)	8870(20)	270(20)	8150(20)	65(8)
H(1B)	9021(17)	-2417(18)	10331(16)	42(6)

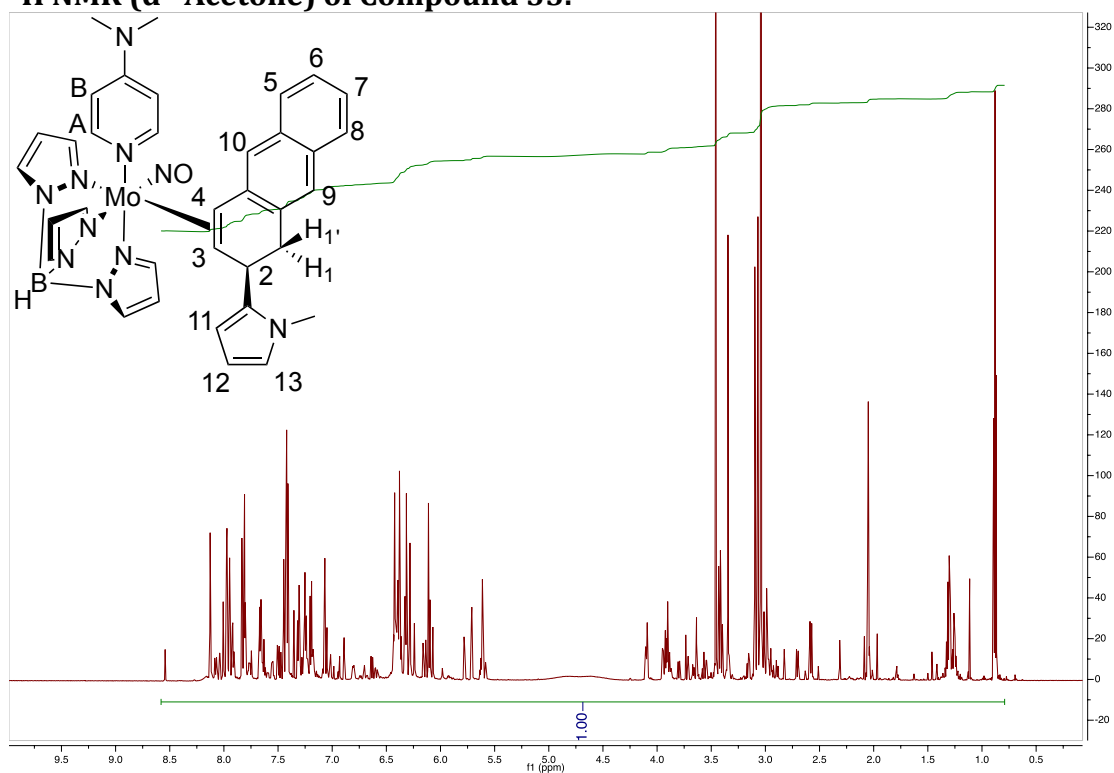
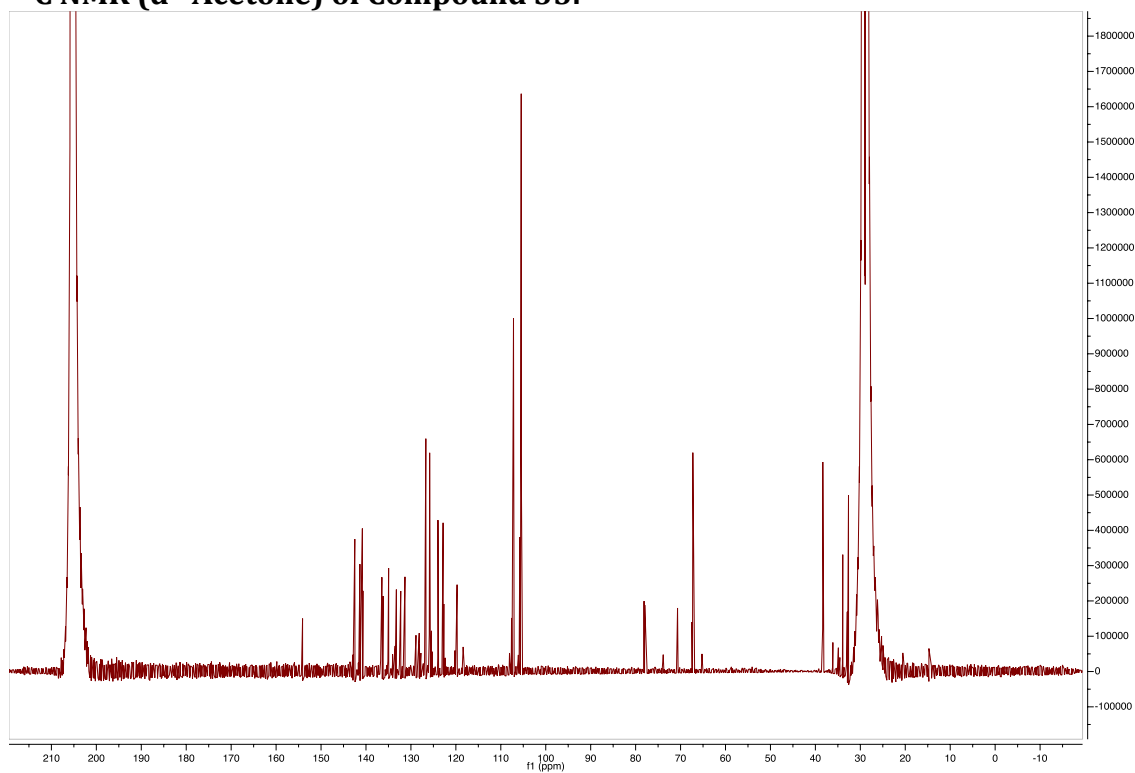
^1H NMR ($\text{d}^6\text{-Acetone}$) of Compound 30: **^{13}C NMR ($\text{d}^6\text{-Acetone}$) of Compound 30:**

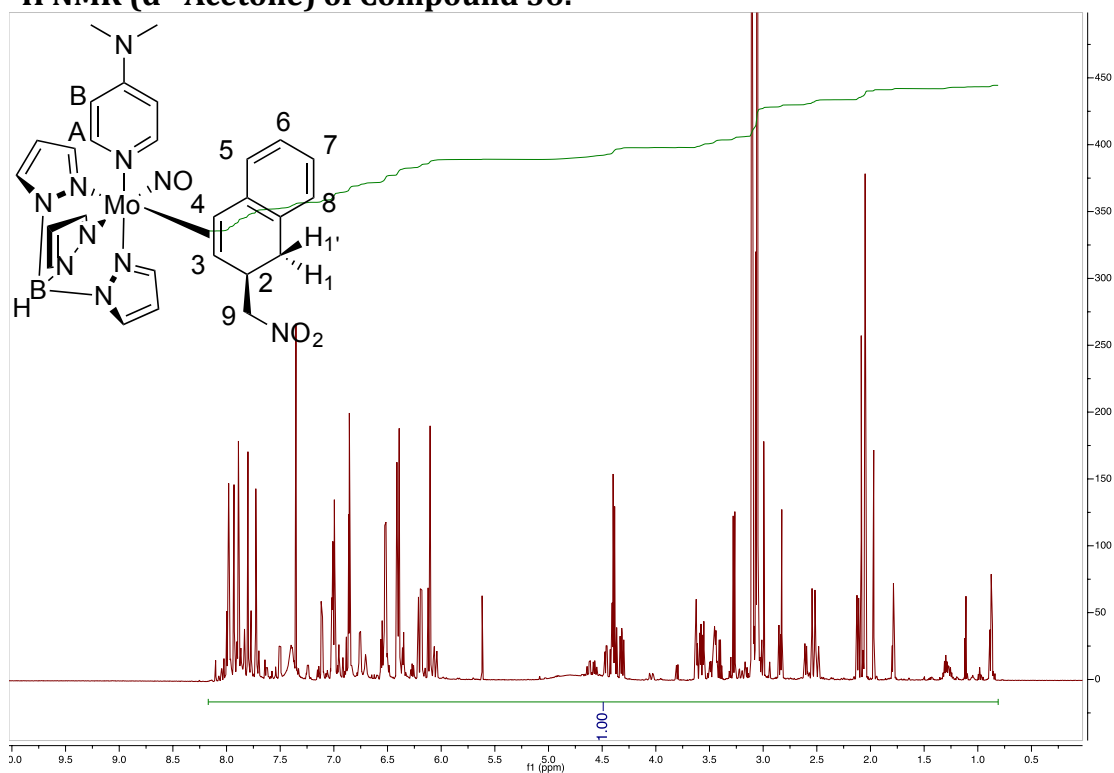
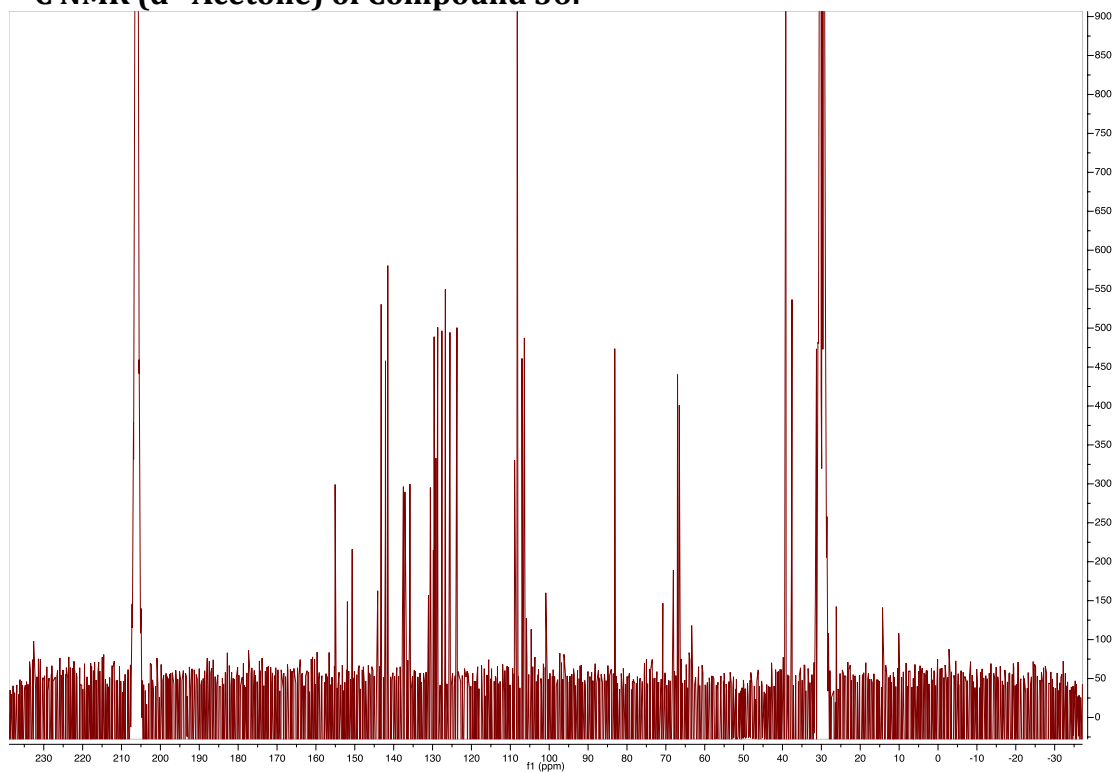
^1H NMR (d_6 -Acetone) of Compound 31: **^{13}C NMR (d_6 -Acetone) of Compound 31:**

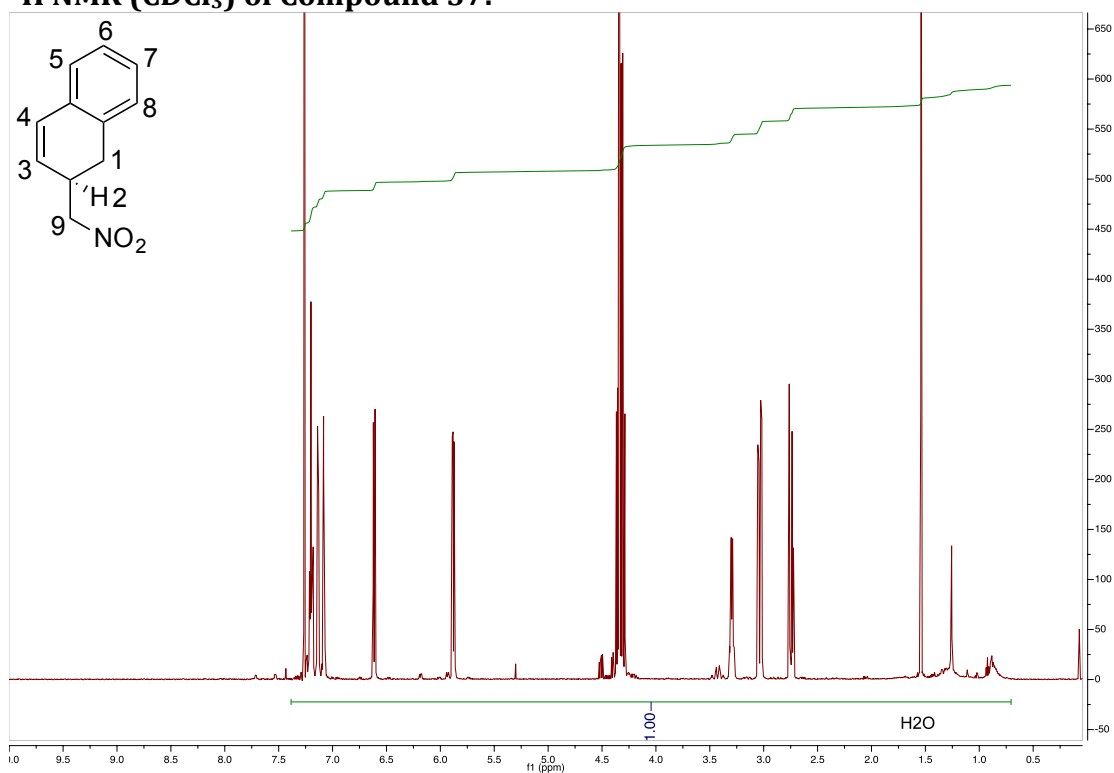
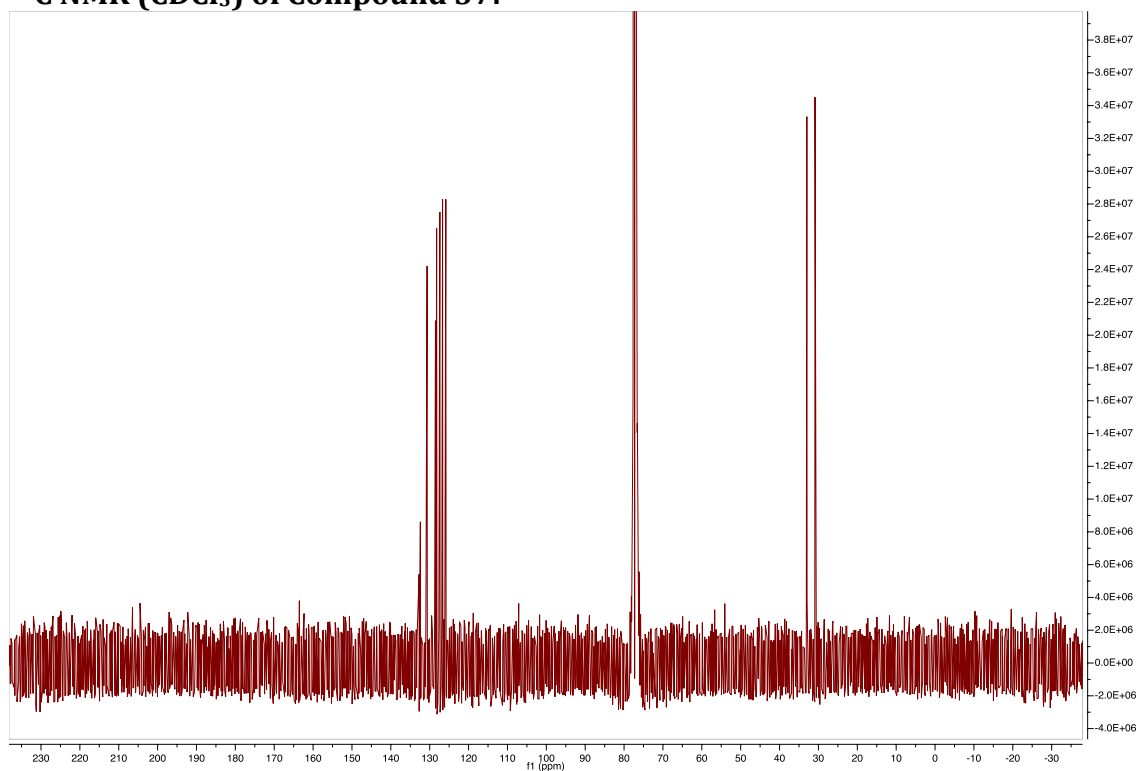
^1H NMR (d^6 -Acetone) of Compound 32: **^{13}C -NMR (d^6 -Acetone) of Compound 32:**

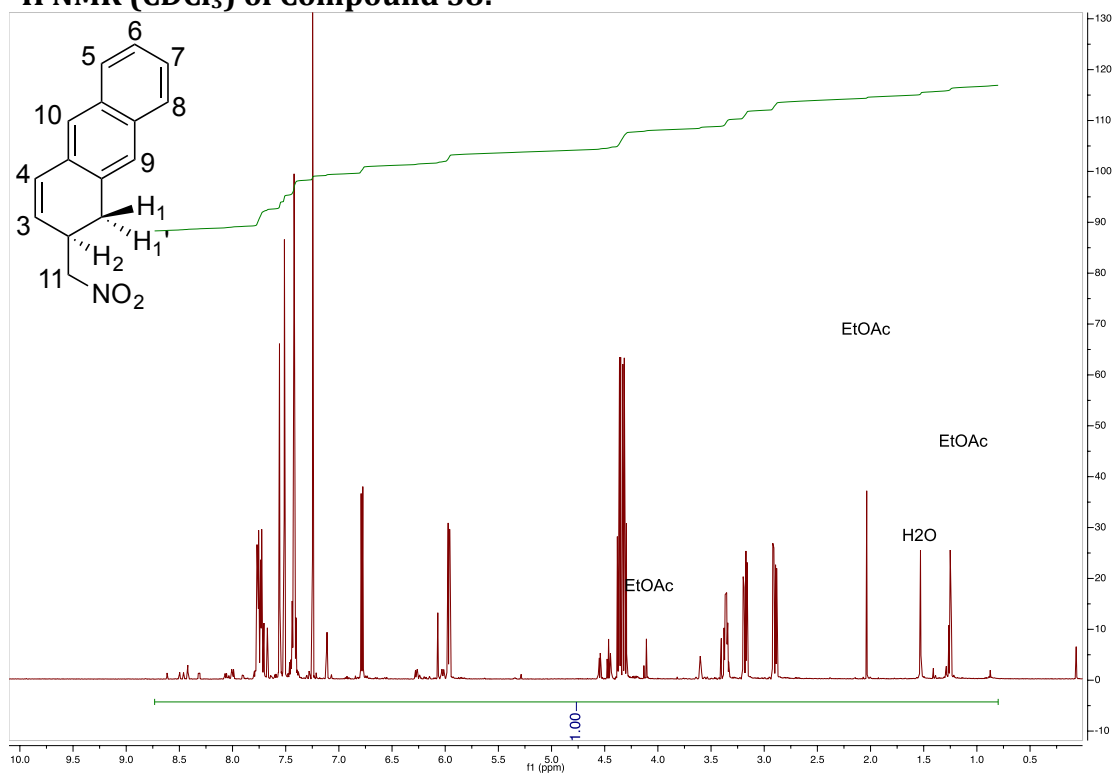
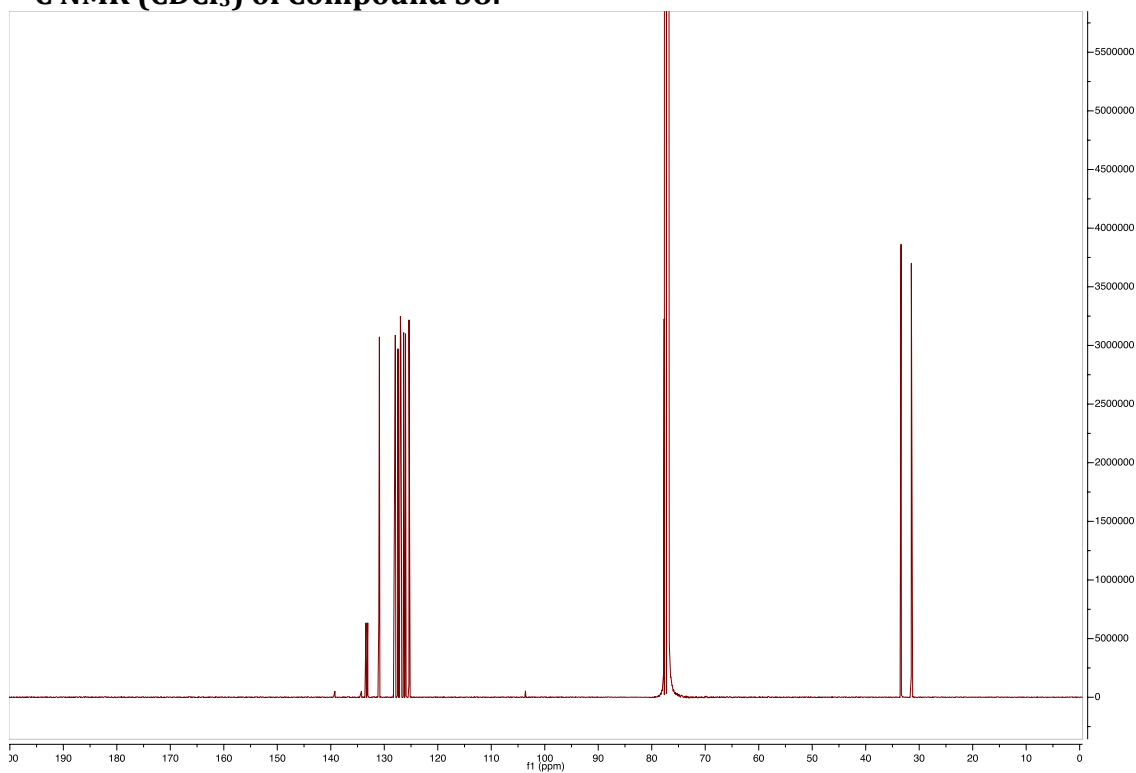
^1H NMR ($\text{d}^6\text{-Acetone}$) of Compound 33: **^{13}C NMR ($\text{d}^6\text{-Acetone}$) of Compound 33:**

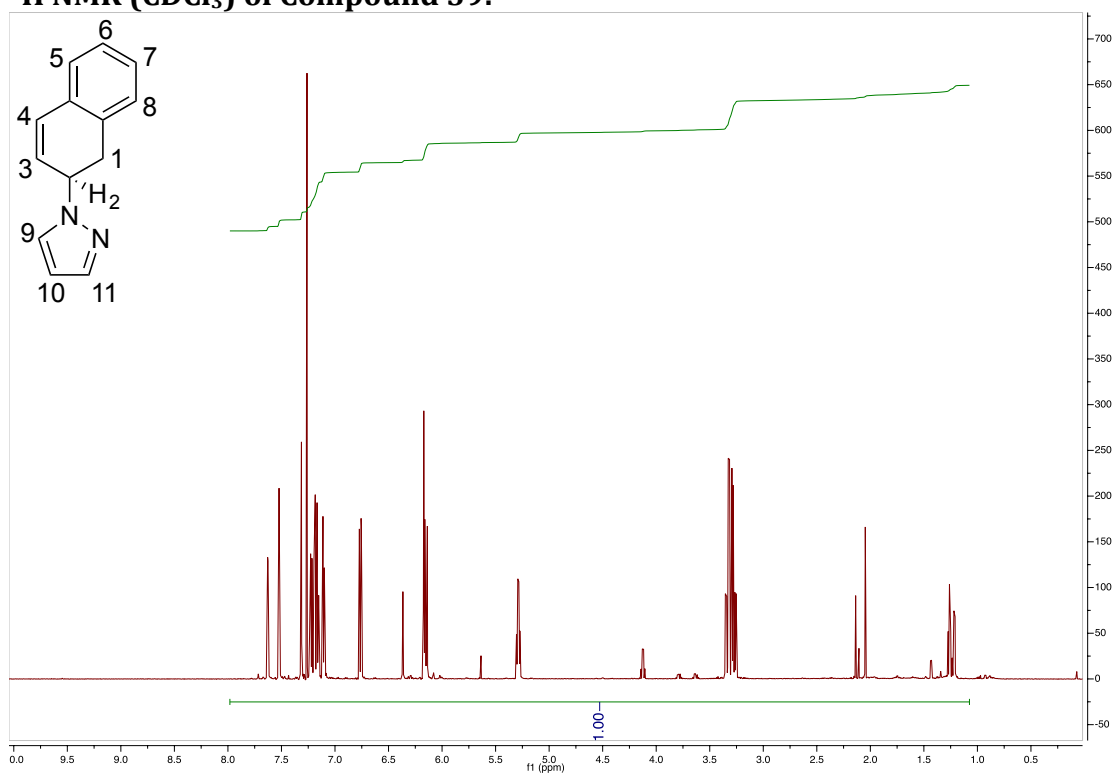
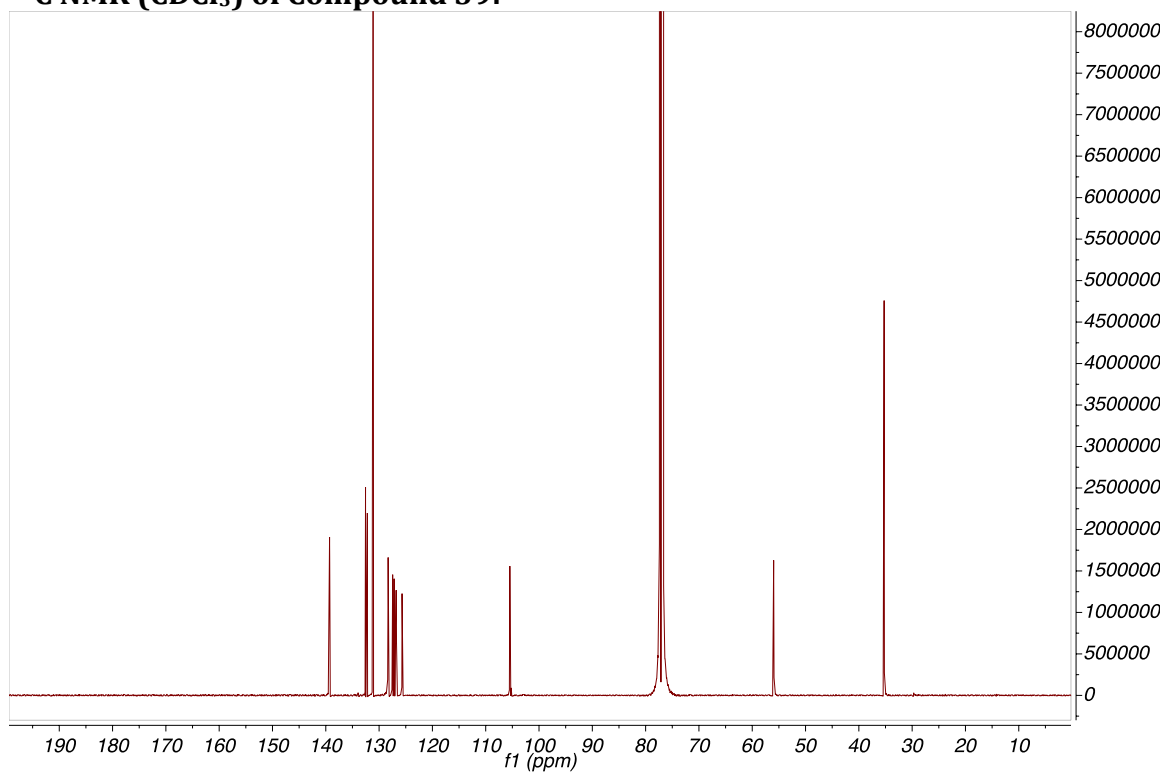
^1H NMR (CDCl_3) of Compound 34: **^{13}C NMR (CDCl_3) of Compound 34:**

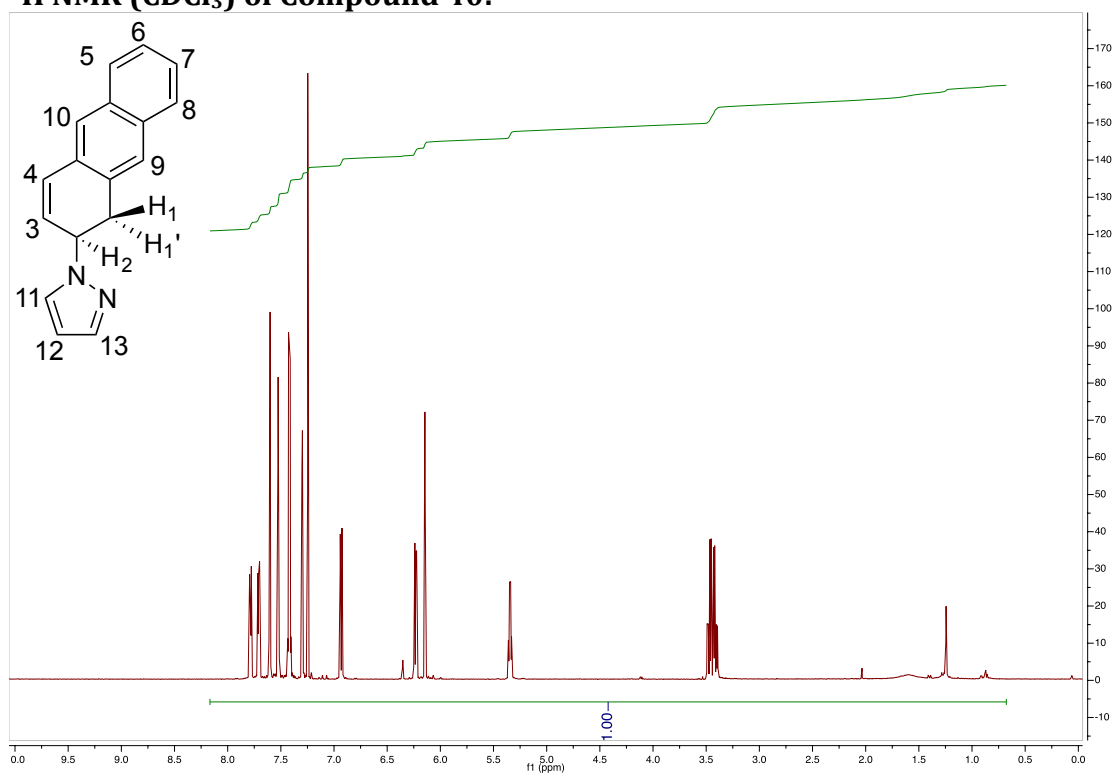
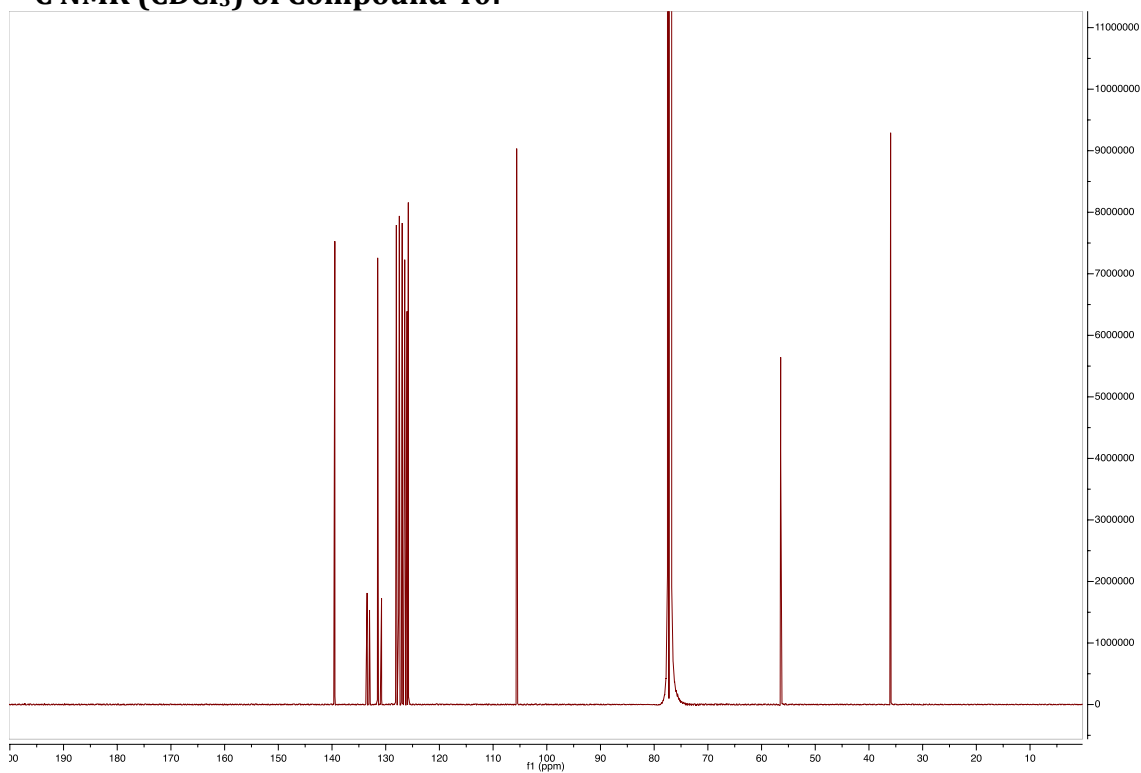
^1H NMR ($\text{d}^6\text{-Acetone}$) of Compound 35: **^{13}C NMR ($\text{d}^6\text{-Acetone}$) of Compound 35:**

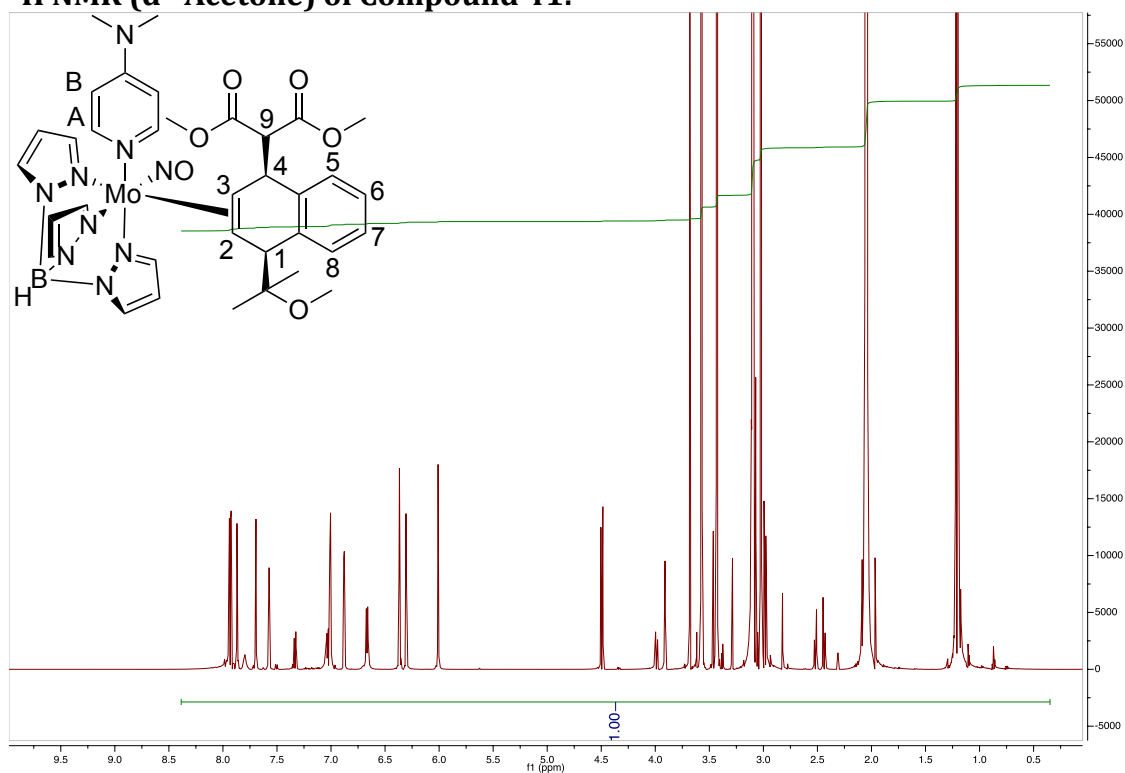
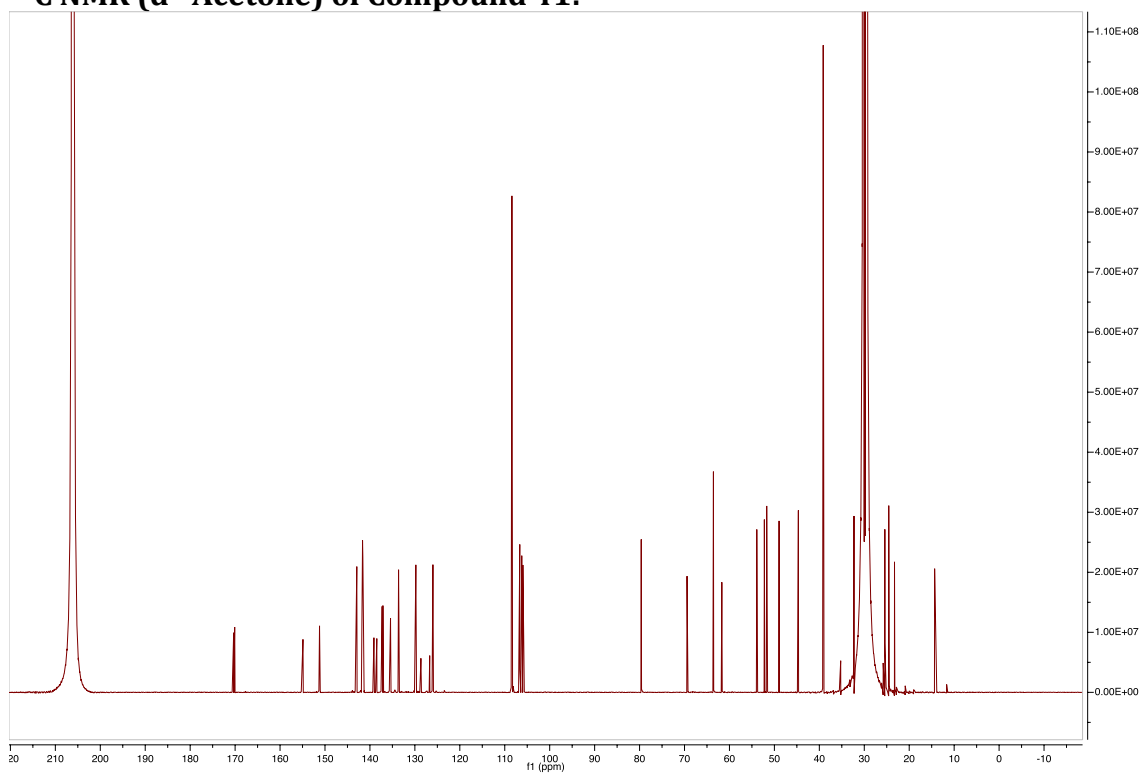
^1H NMR ($\text{d}^6\text{-Acetone}$) of Compound 36: **^{13}C NMR ($\text{d}^6\text{-Acetone}$) of Compound 36:**

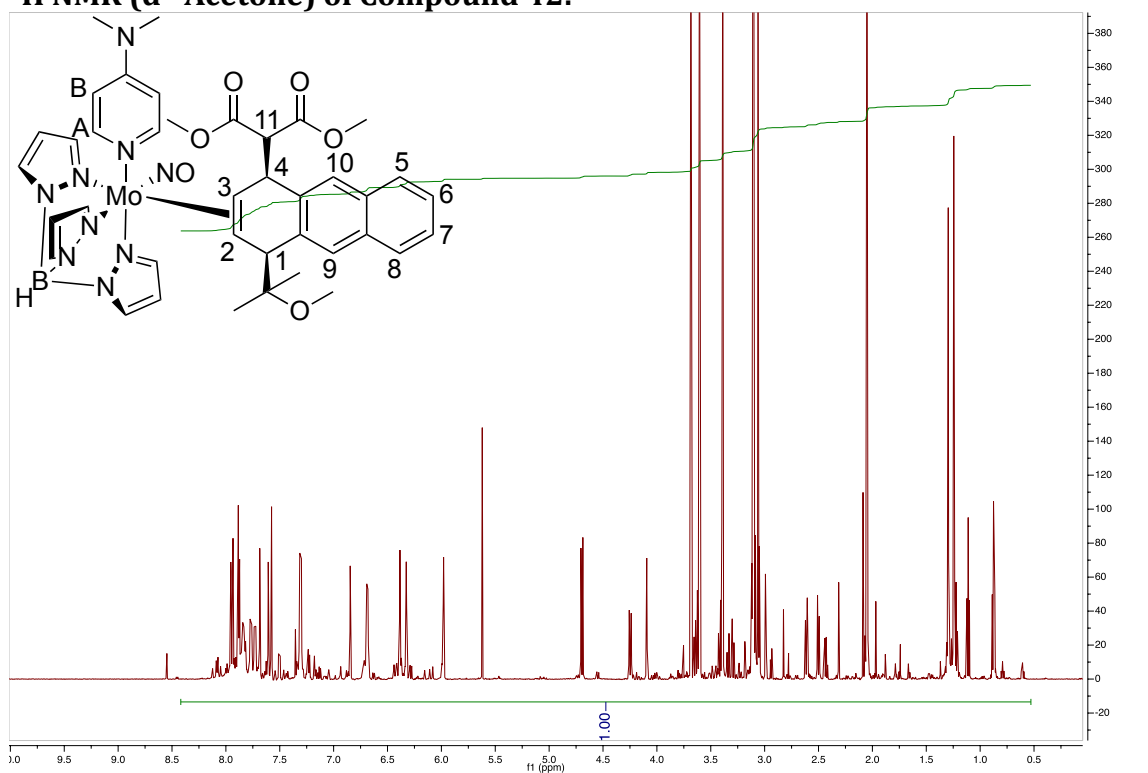
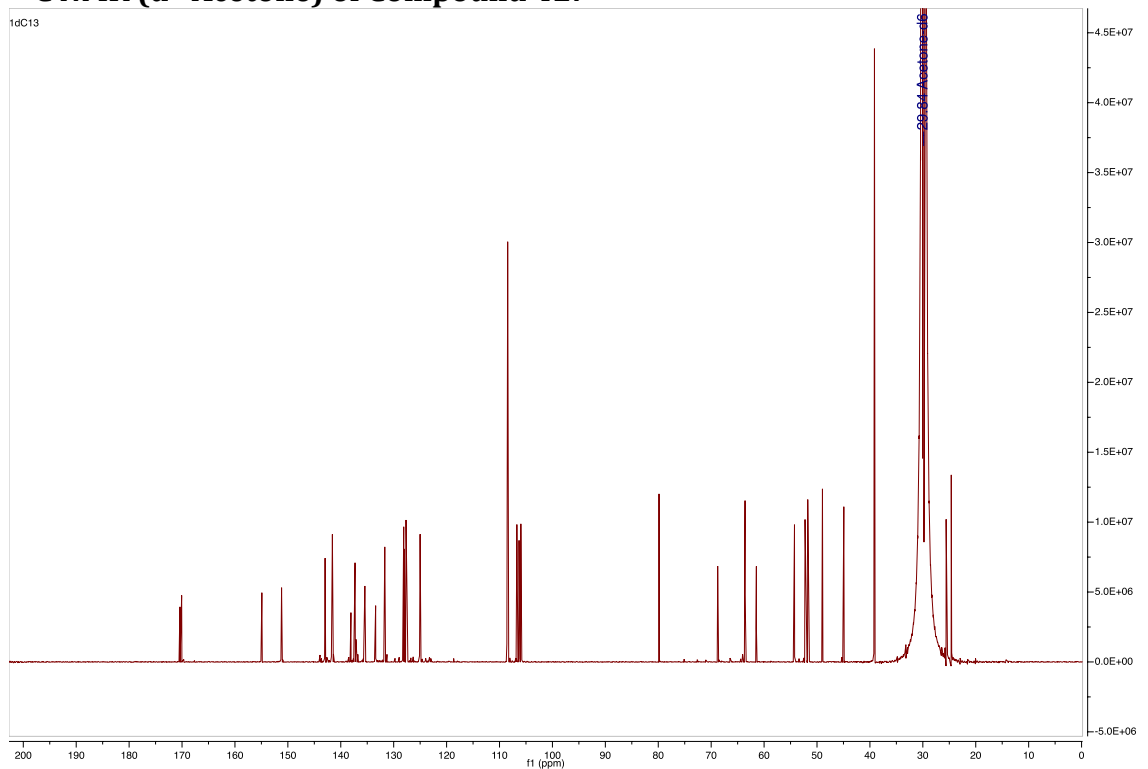
^1H NMR (CDCl_3) of Compound 37: **^{13}C NMR (CDCl_3) of Compound 37:**

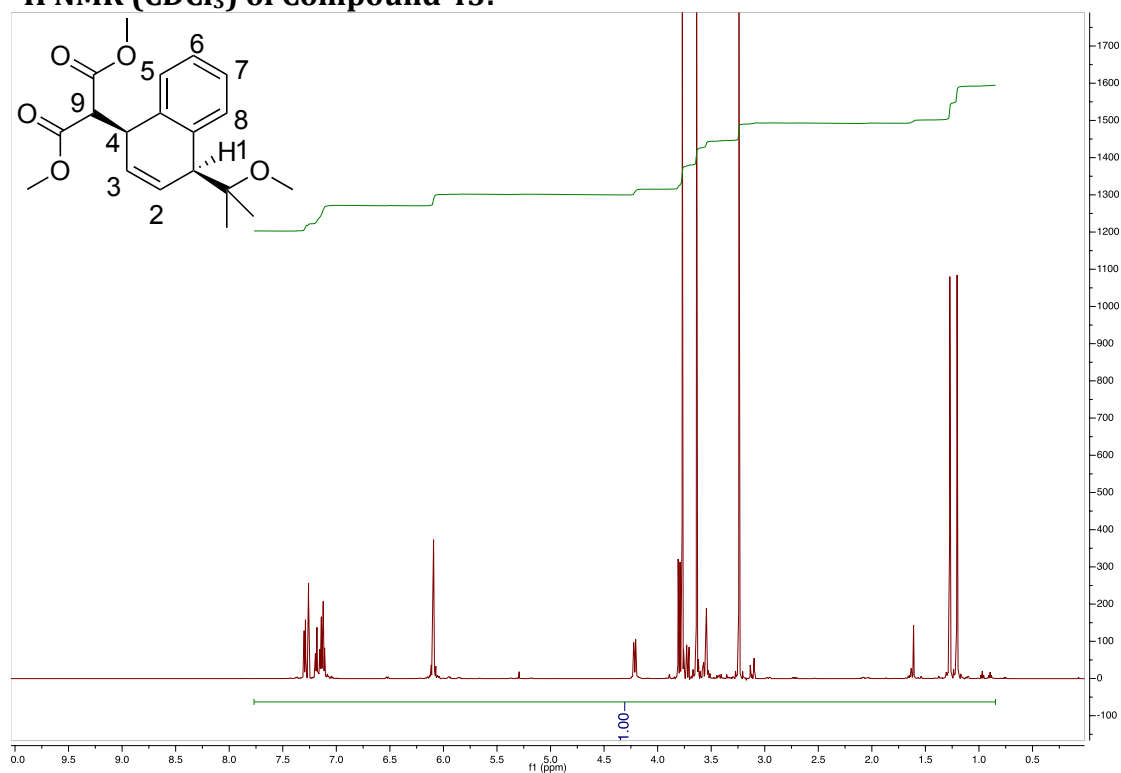
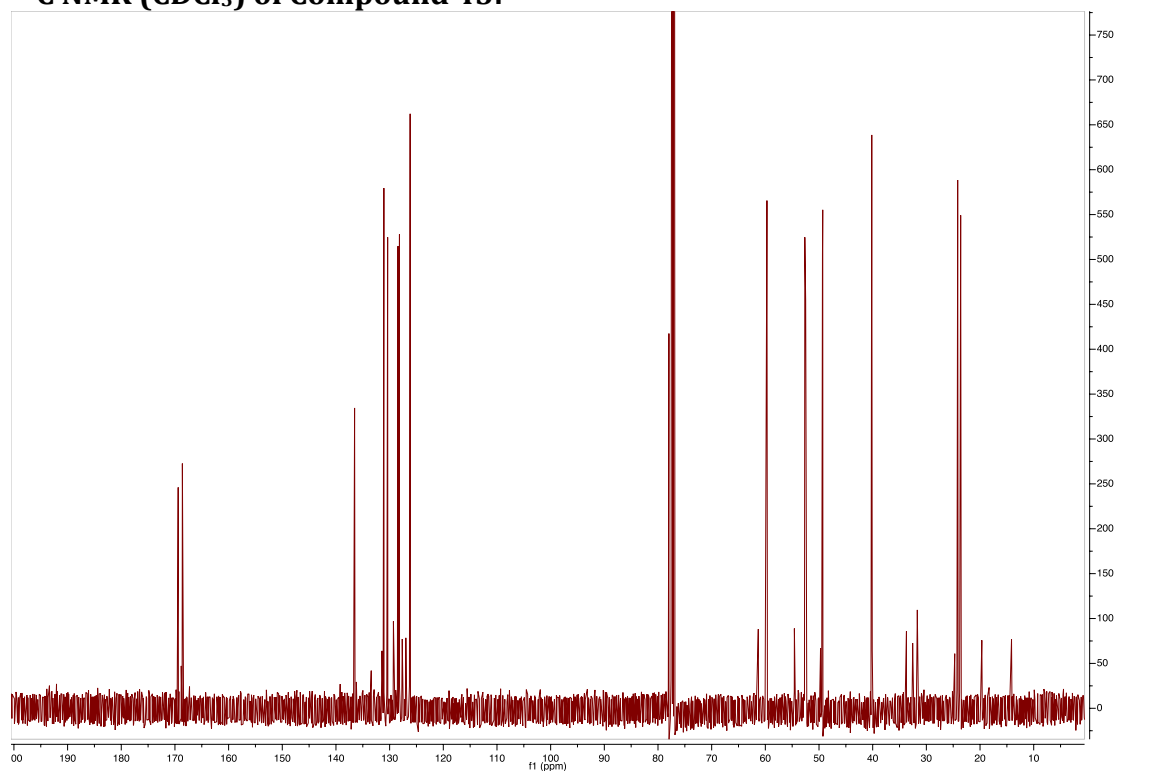
^1H NMR (CDCl_3) of Compound 38: **^{13}C NMR (CDCl_3) of Compound 38:**

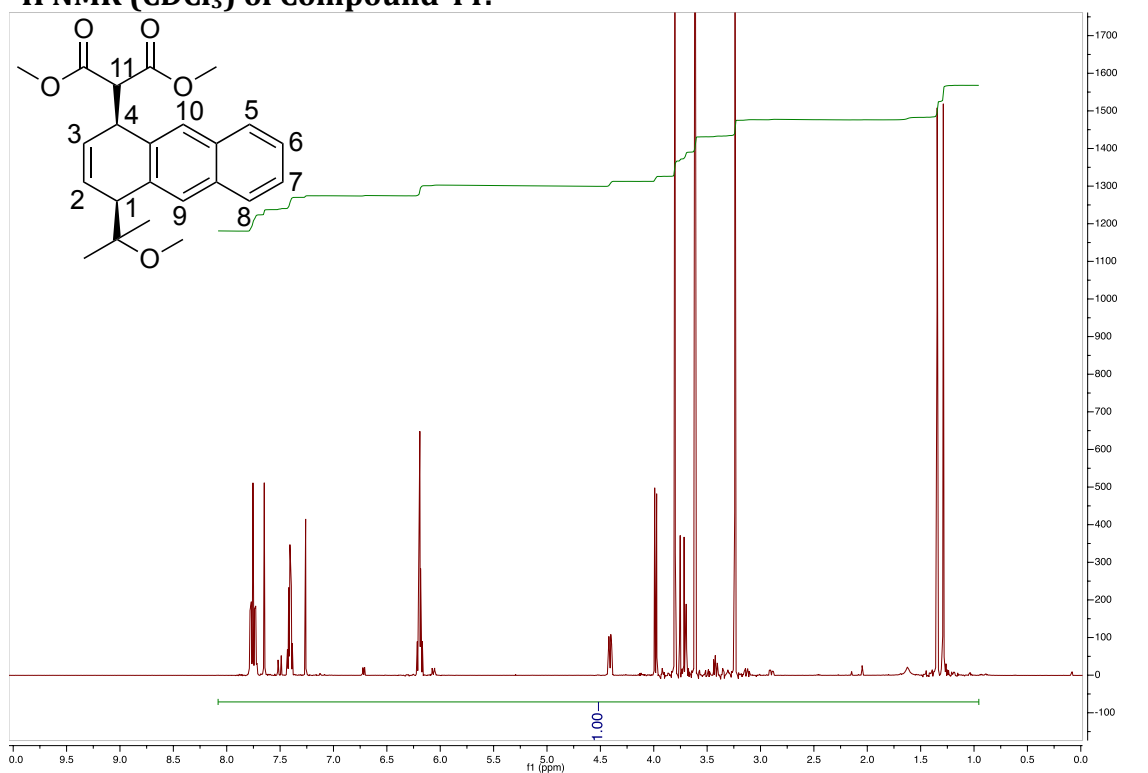
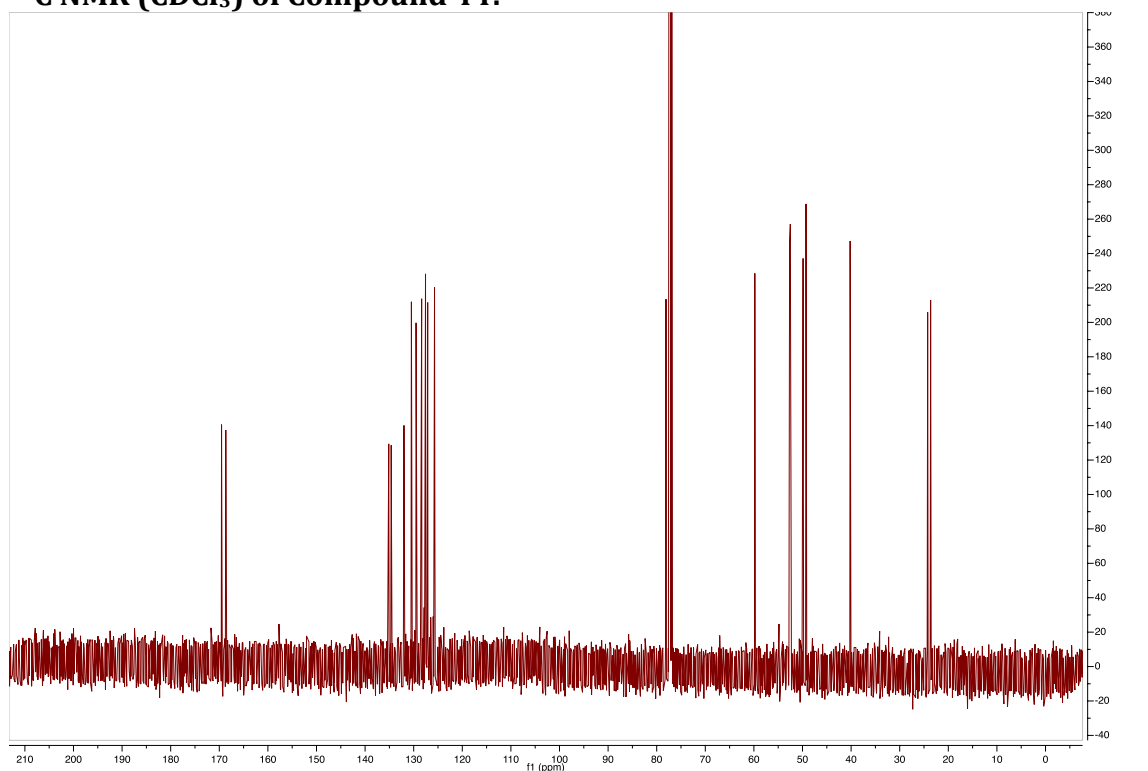
^1H NMR (CDCl_3) of Compound 39: **^{13}C NMR (CDCl_3) of Compound 39:**

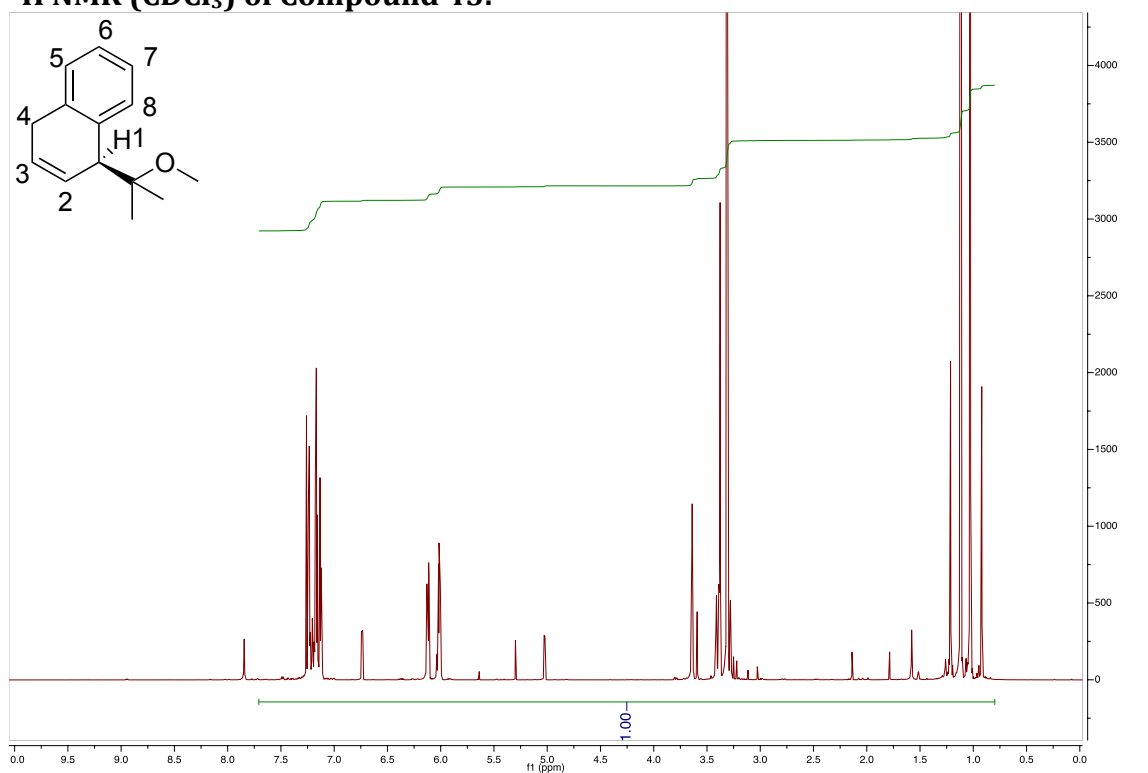
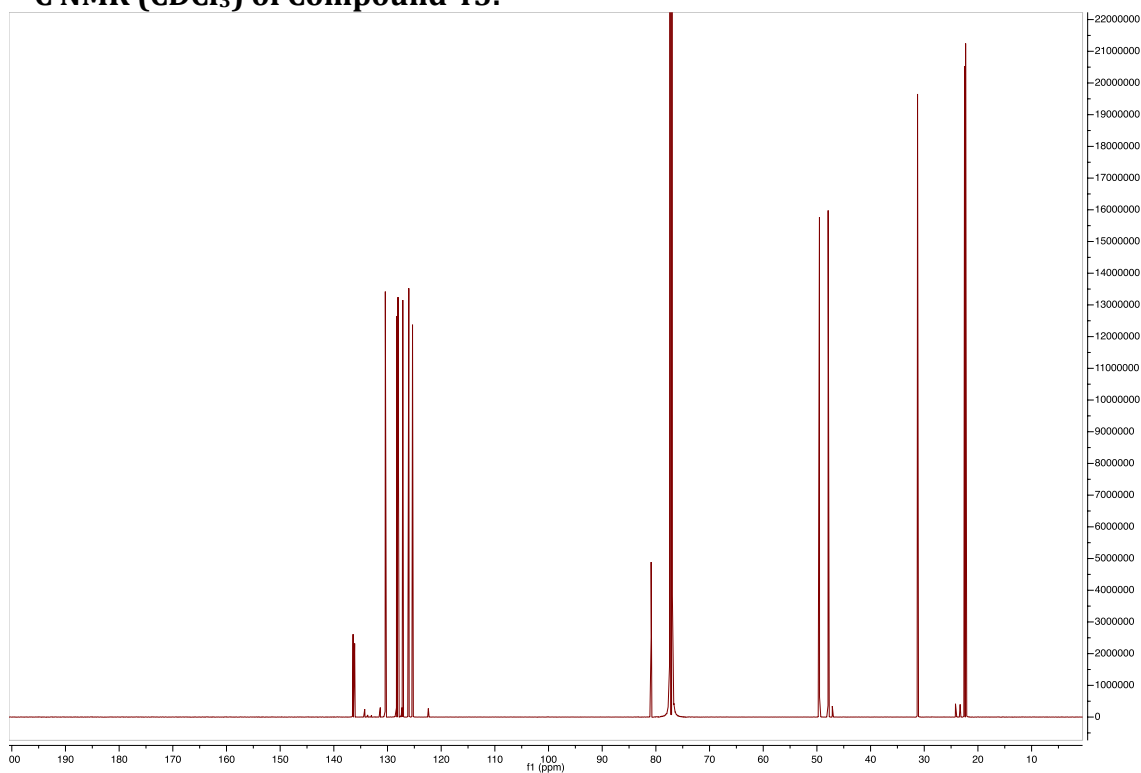
^1H NMR (CDCl_3) of Compound 40: **^{13}C NMR (CDCl_3) of Compound 40:**

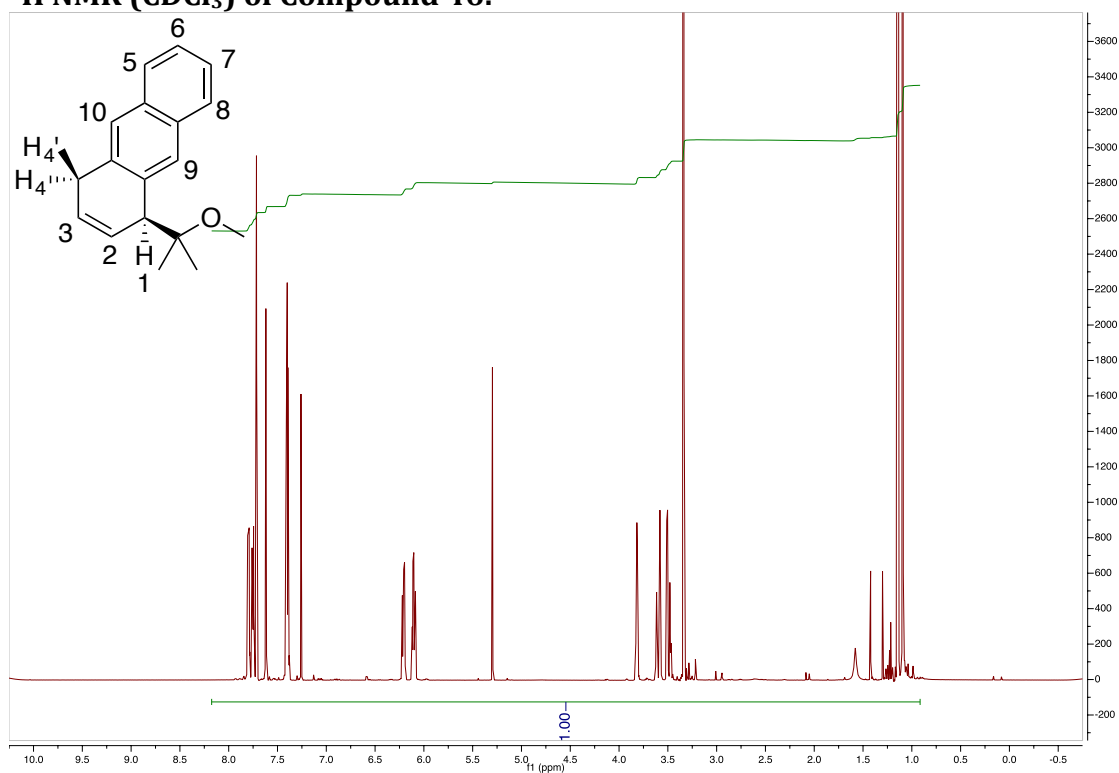
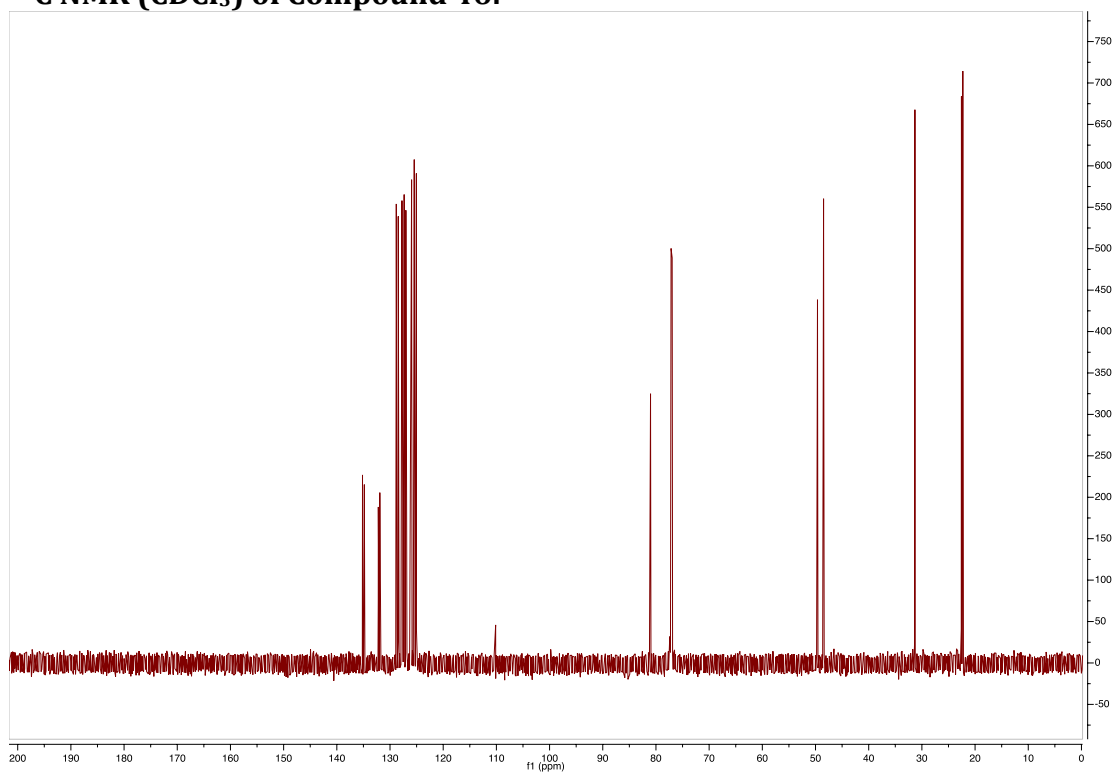
^1H NMR ($\text{d}^6\text{-Acetone}$) of Compound 41: **^{13}C NMR ($\text{d}^6\text{-Acetone}$) of Compound 41:**

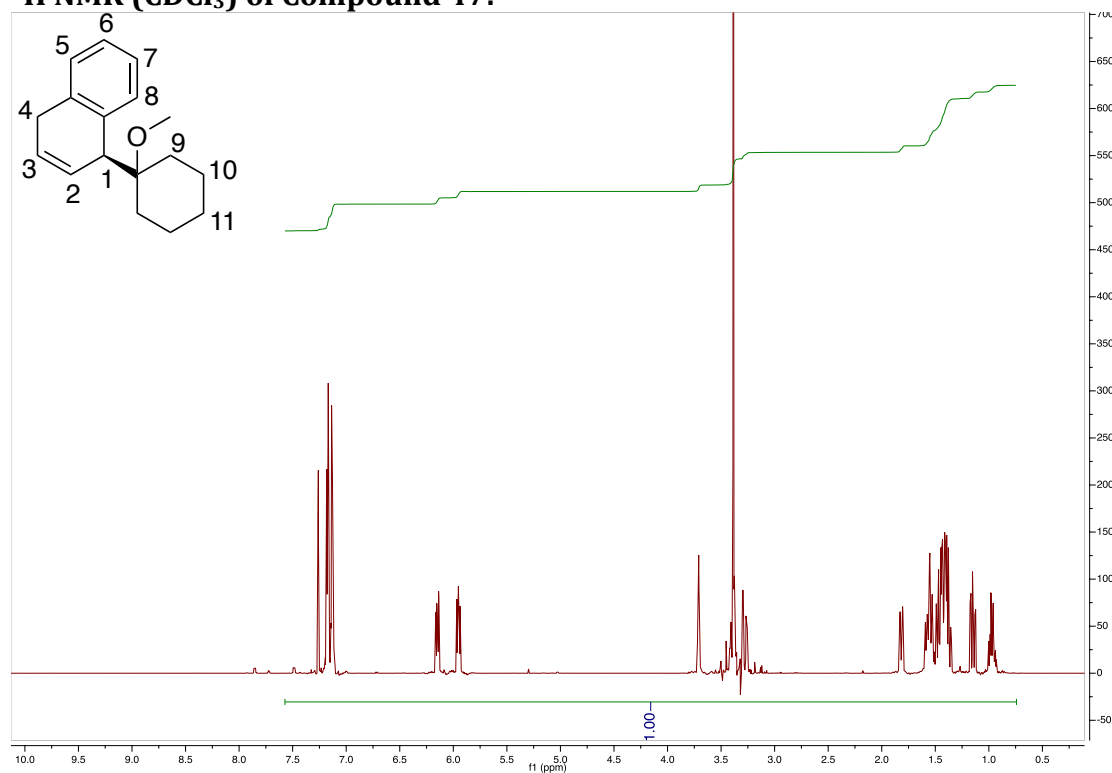
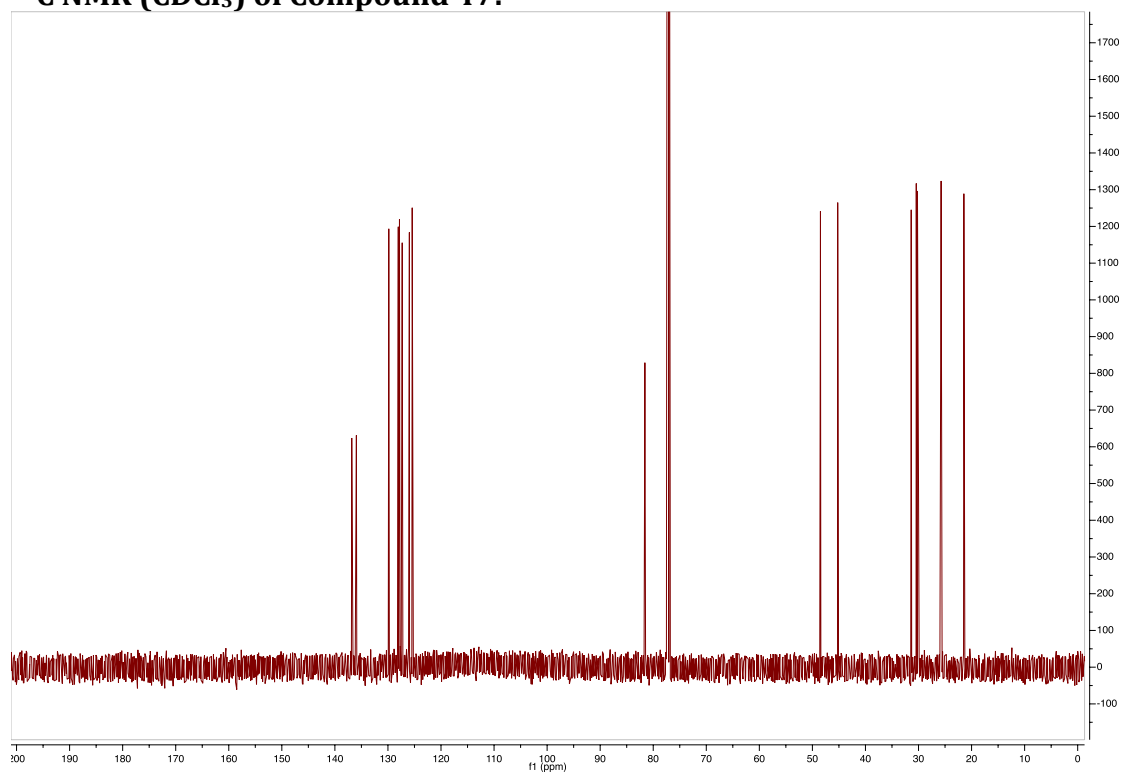
¹H NMR (d⁶-Acetone) of Compound 42:**¹³C NMR (d⁶-Acetone) of Compound 42:**

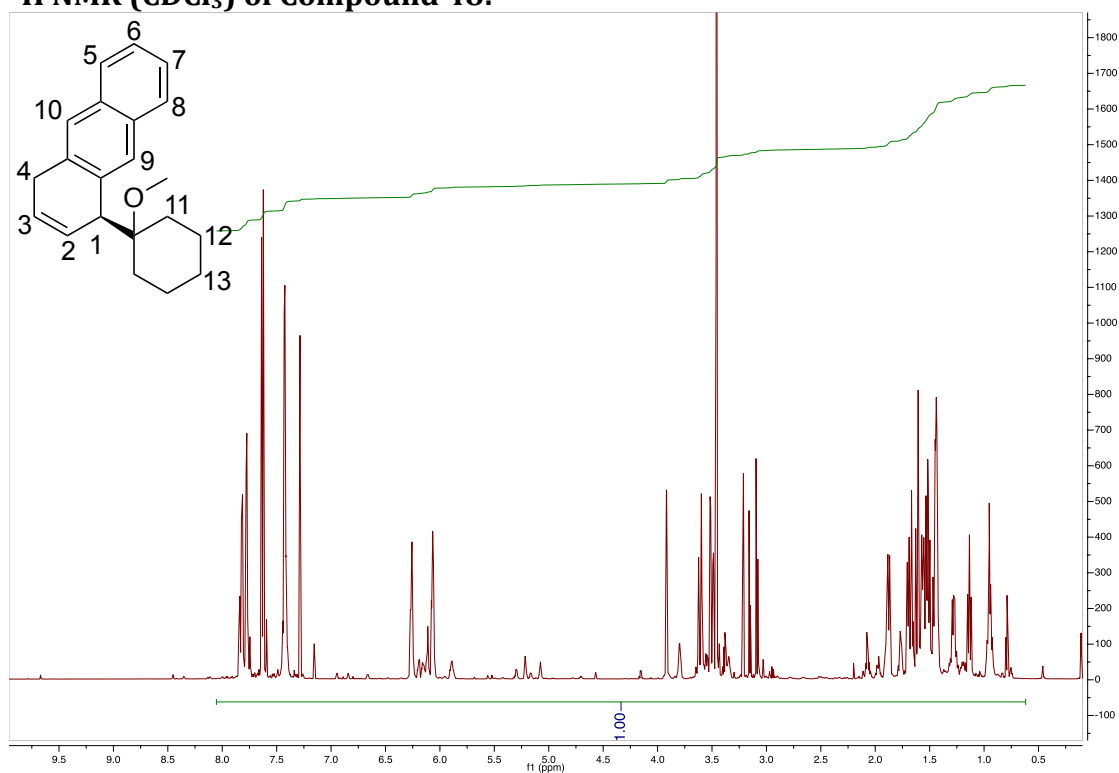
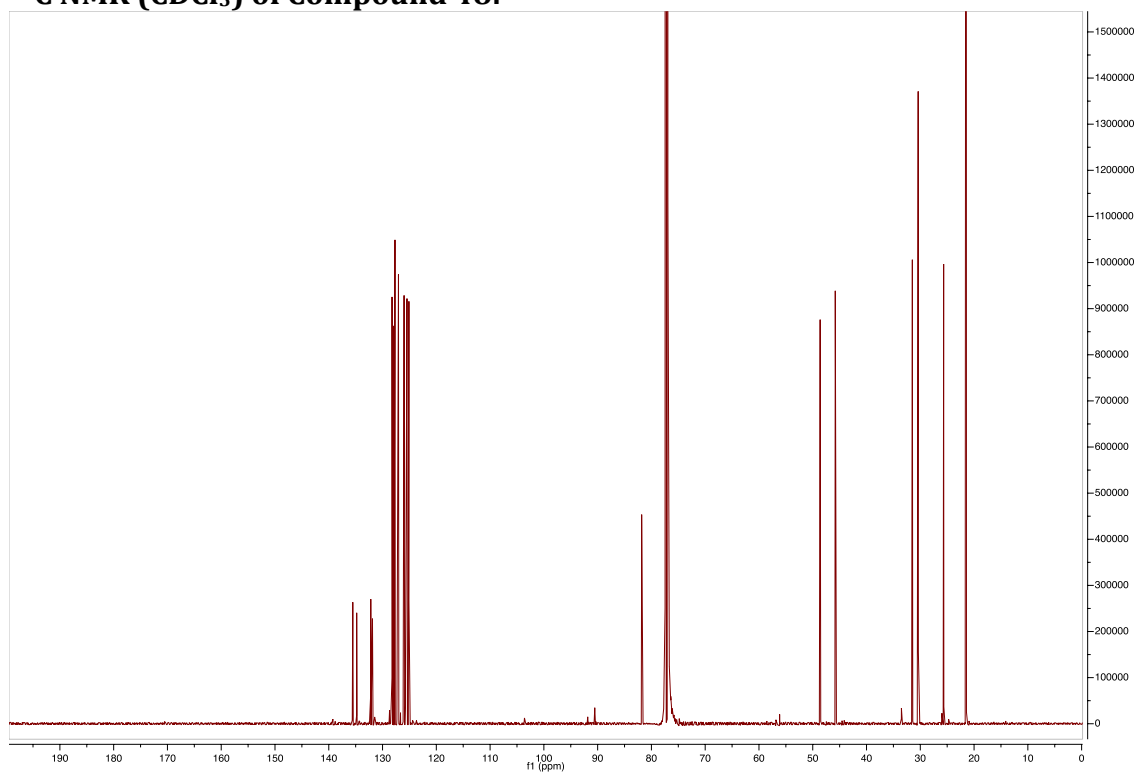
^1H NMR (CDCl_3) of Compound 43: **^{13}C NMR (CDCl_3) of Compound 43:**

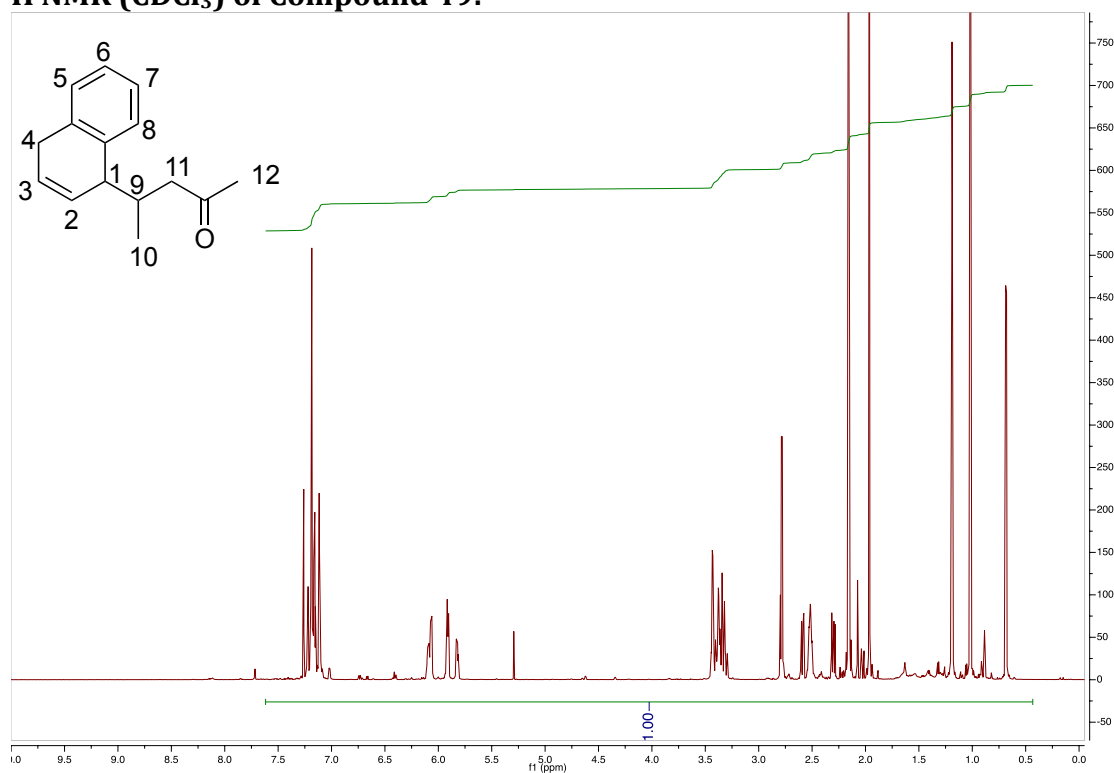
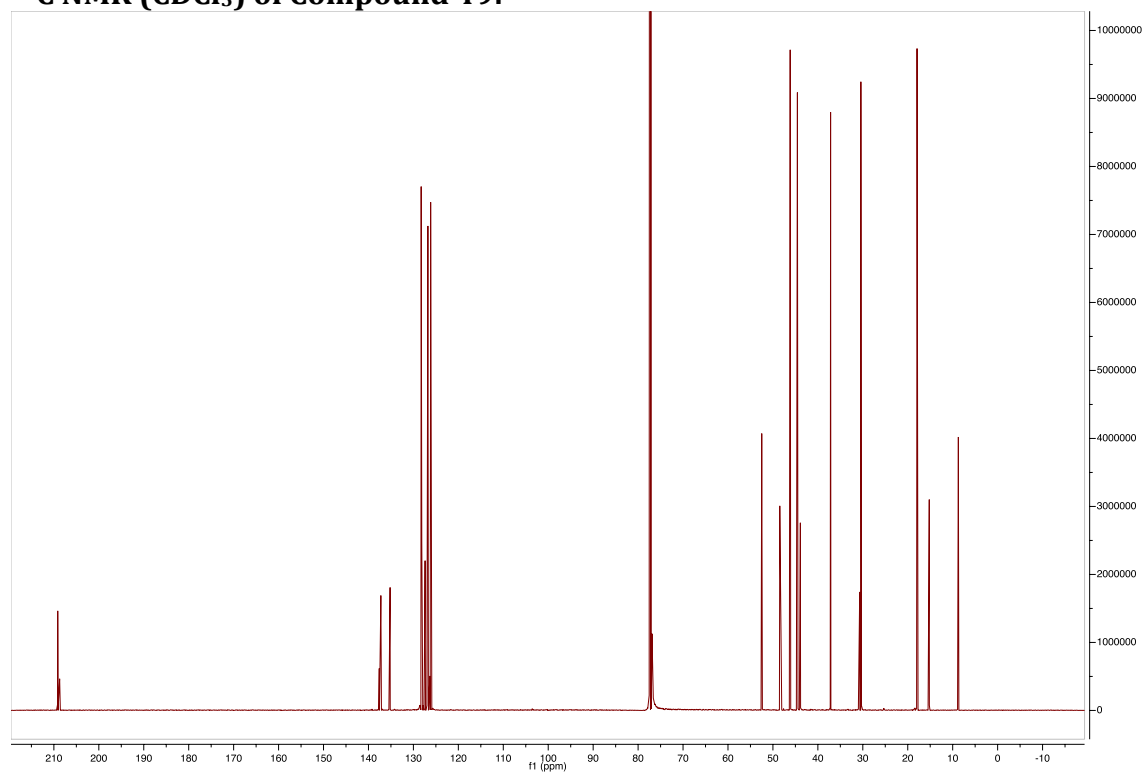
^1H NMR (CDCl_3) of Compound 44: **^{13}C NMR (CDCl_3) of Compound 44:**

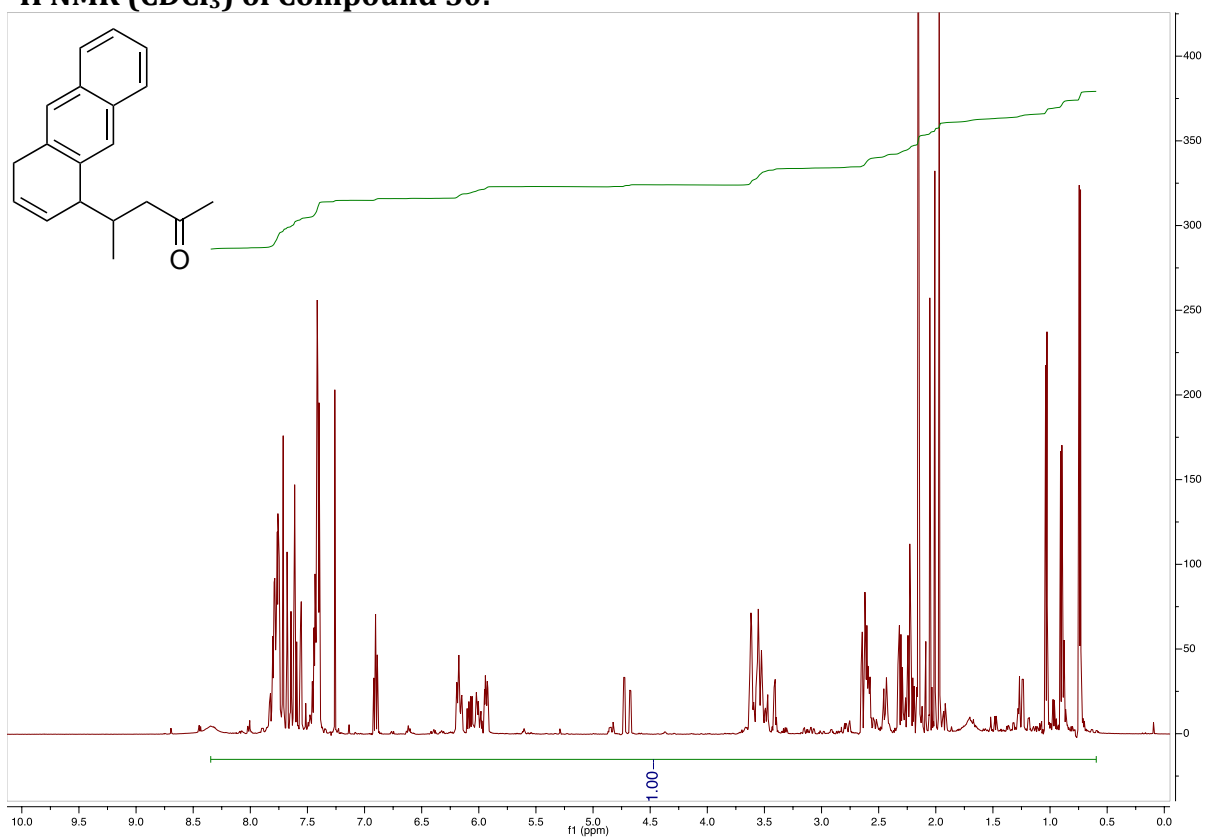
^1H NMR (CDCl_3) of Compound 45: **^{13}C NMR (CDCl_3) of Compound 45:**

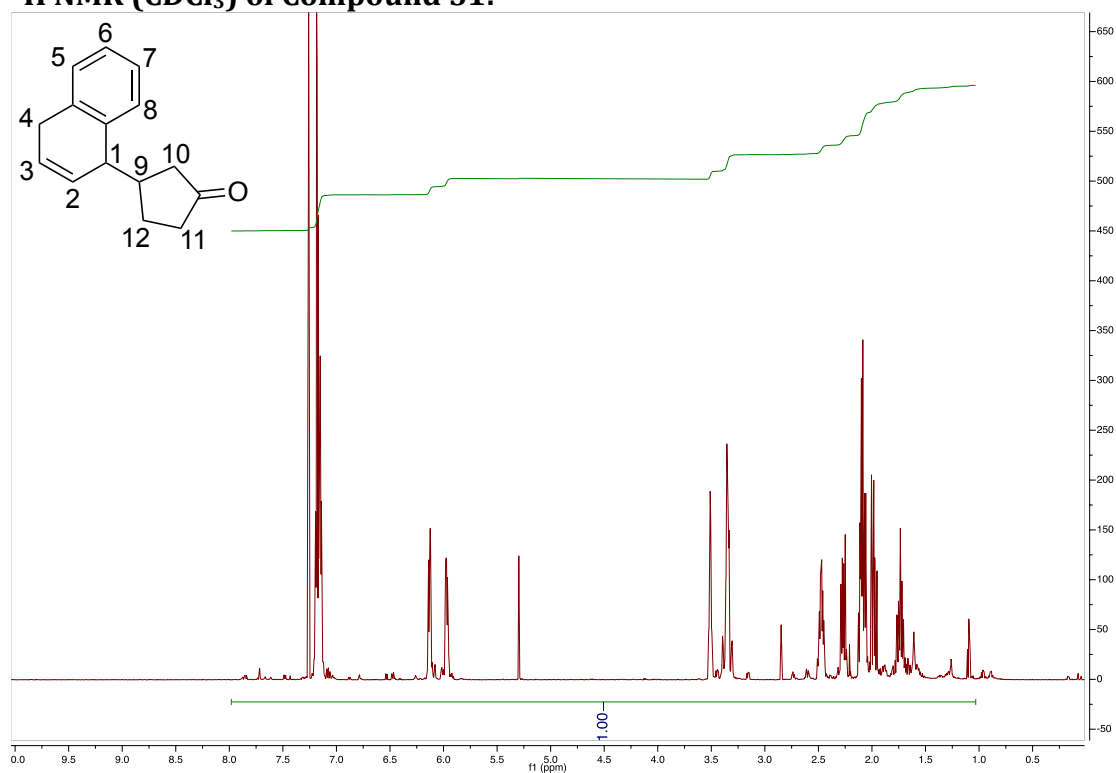
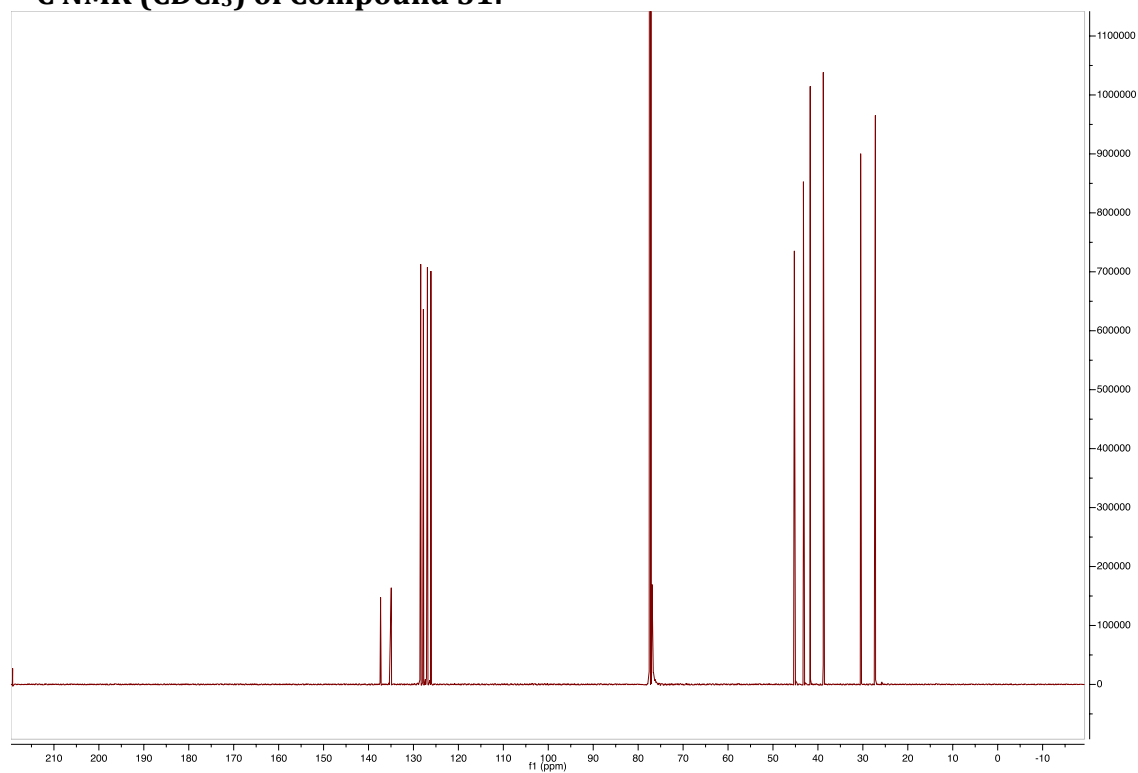
^1H NMR (CDCl_3) of Compound 46: **^{13}C NMR (CDCl_3) of Compound 46:**

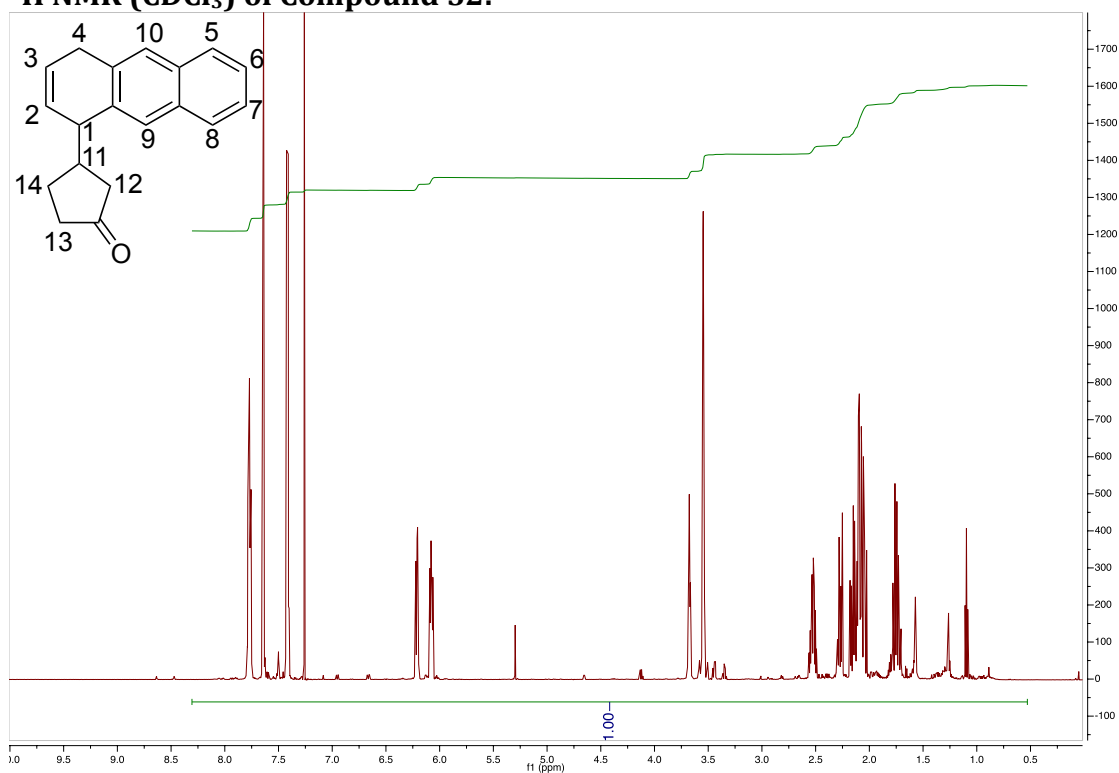
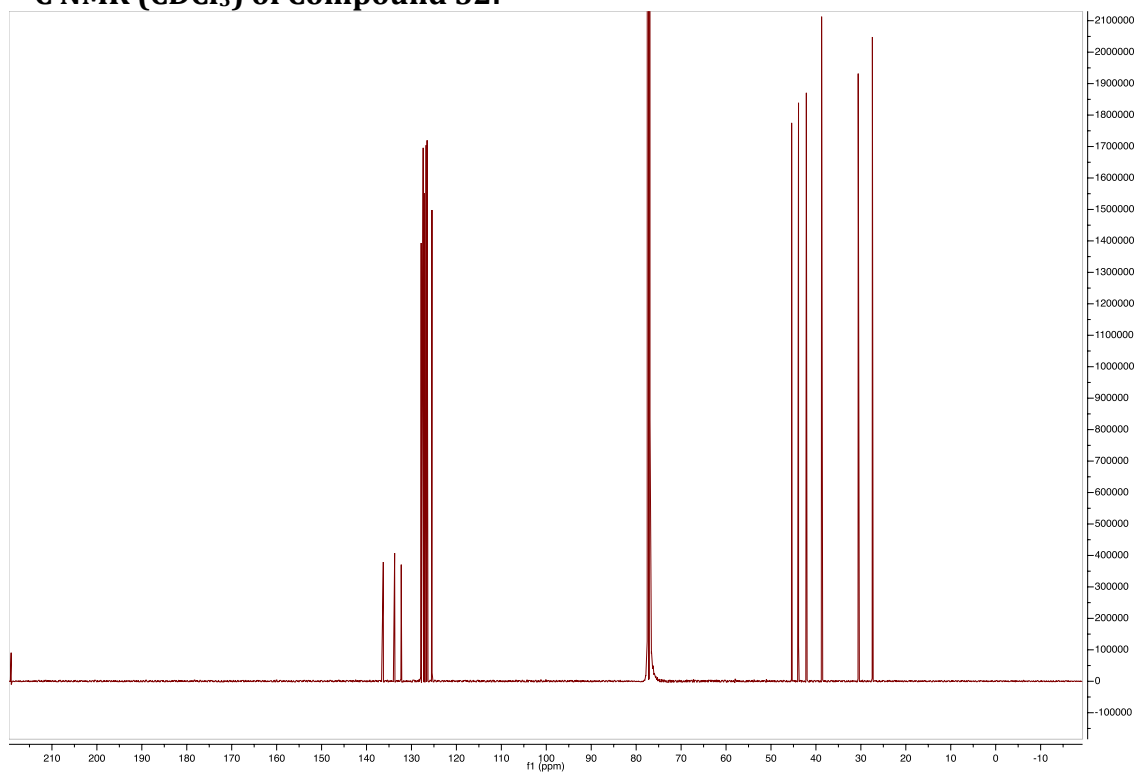
^1H NMR (CDCl_3) of Compound 47: **^{13}C NMR (CDCl_3) of Compound 47:**

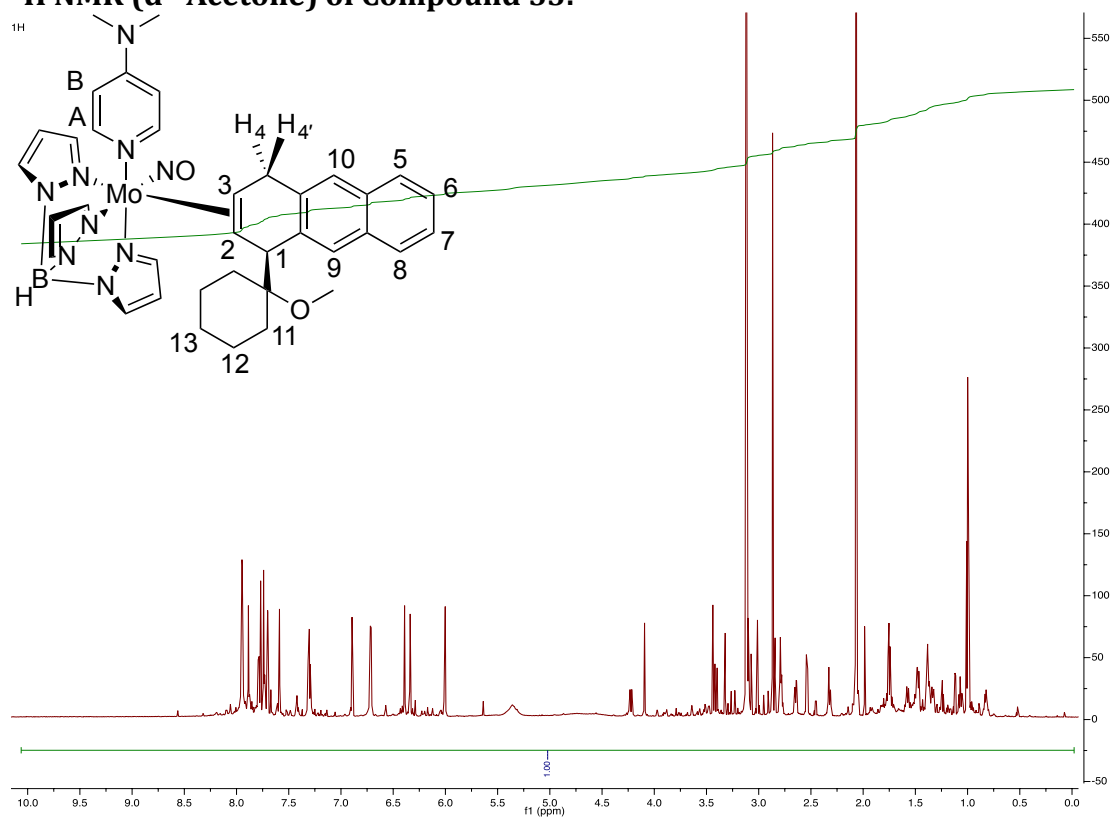
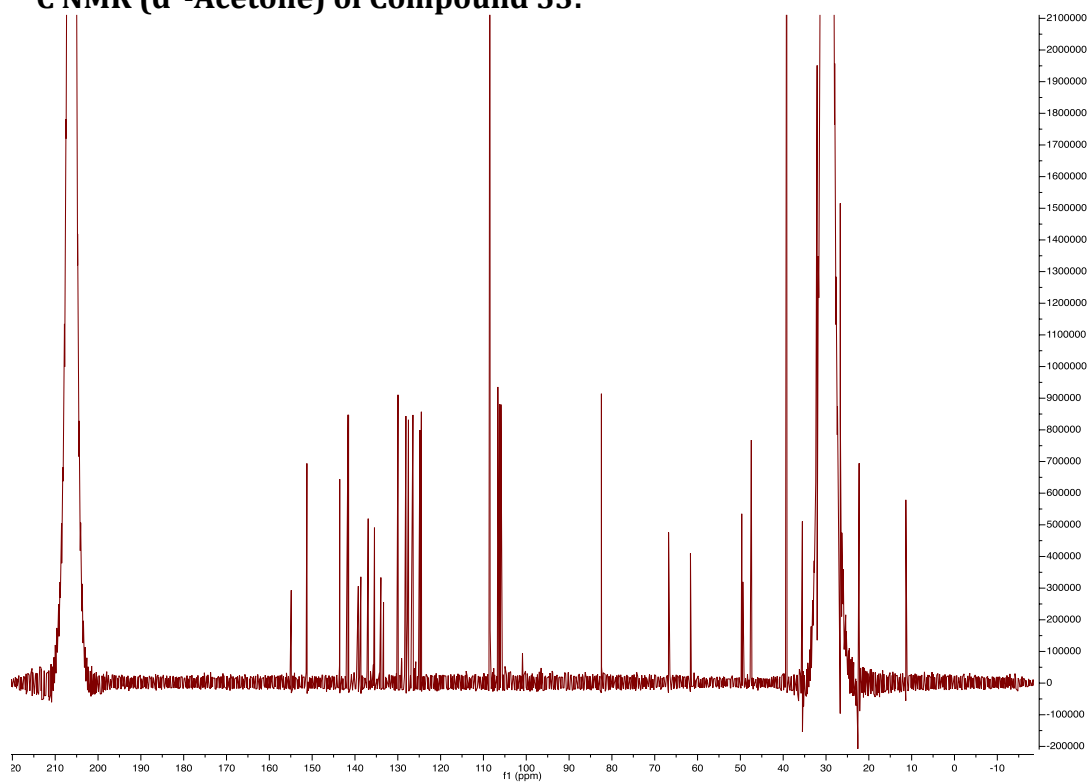
^1H NMR (CDCl_3) of Compound 48: **^{13}C NMR (CDCl_3) of Compound 48:**

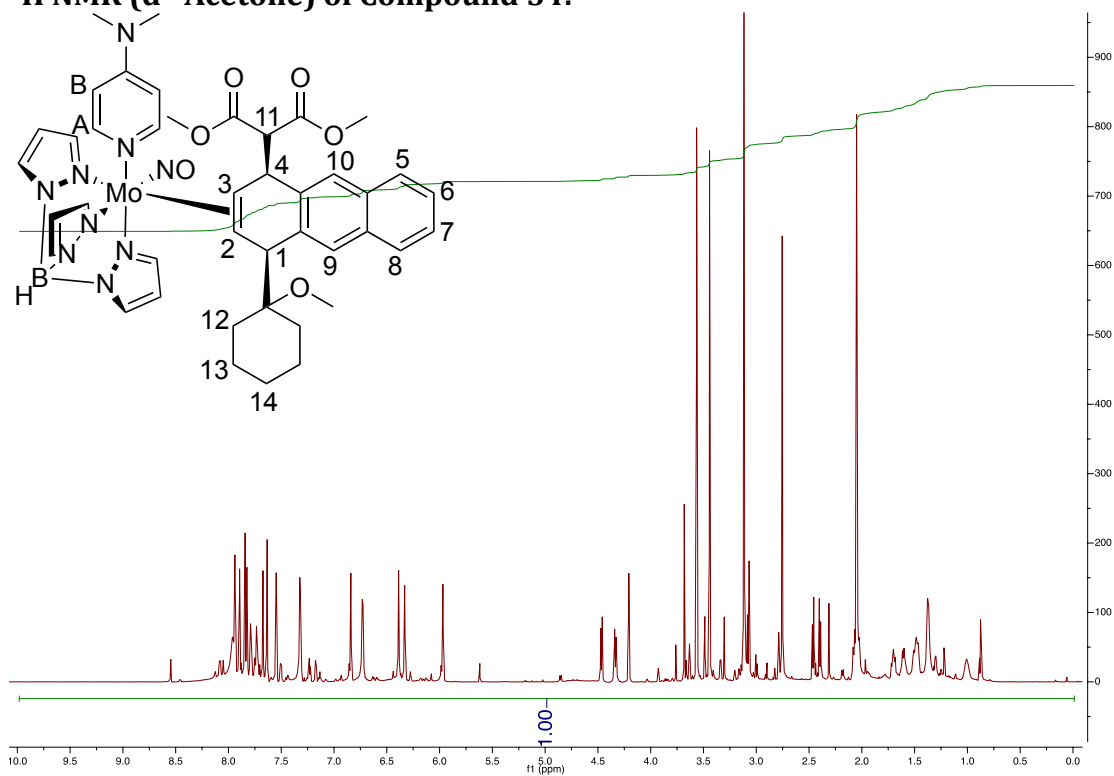
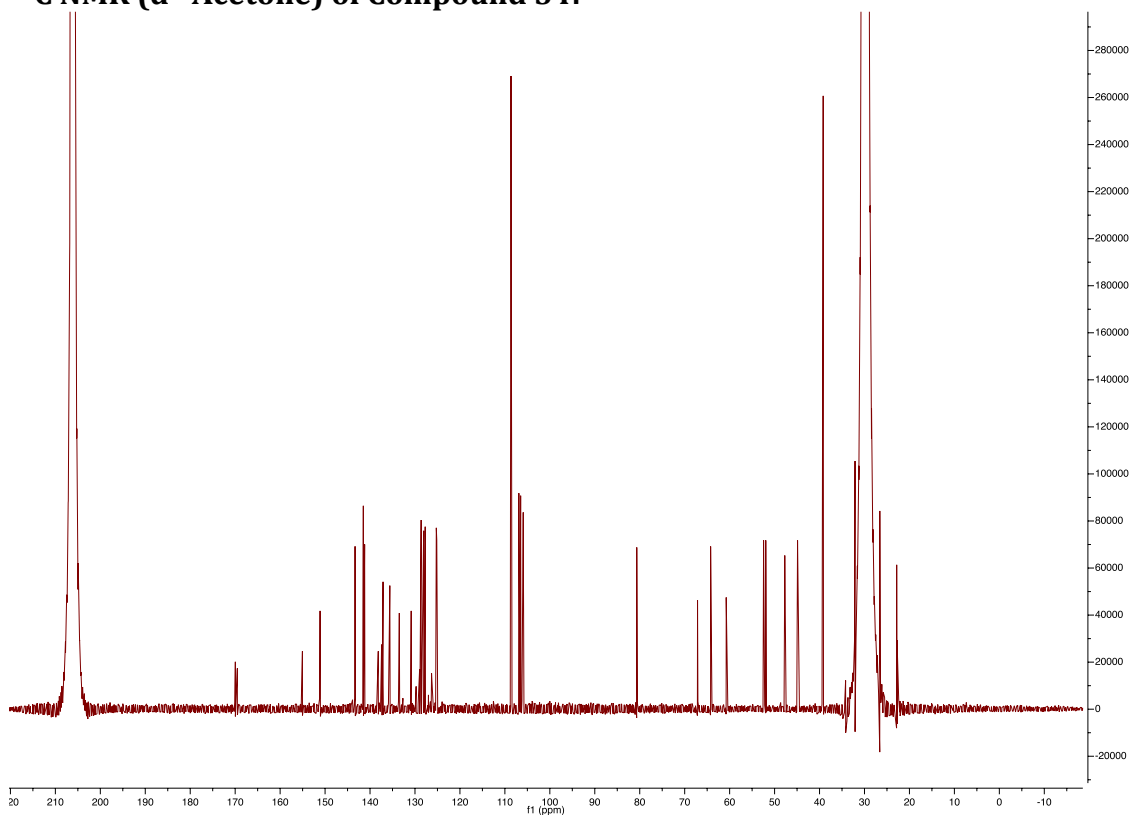
¹H NMR (CDCl₃) of Compound 49:**¹³C NMR (CDCl₃) of Compound 49:**

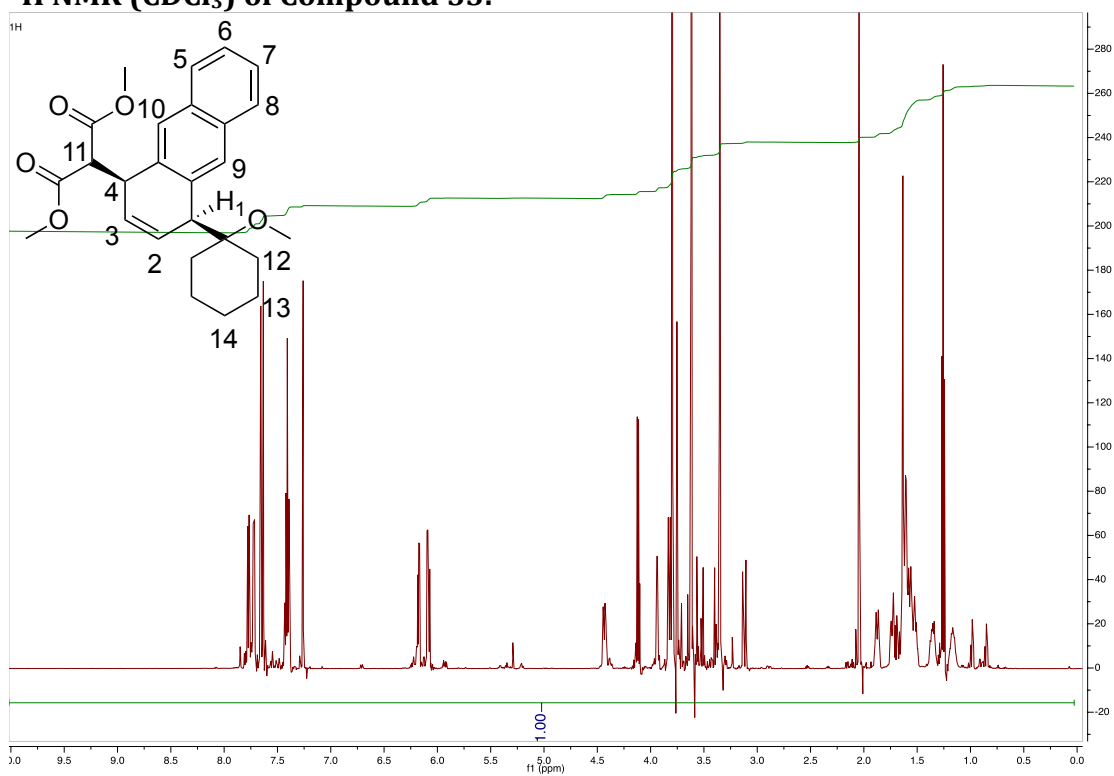
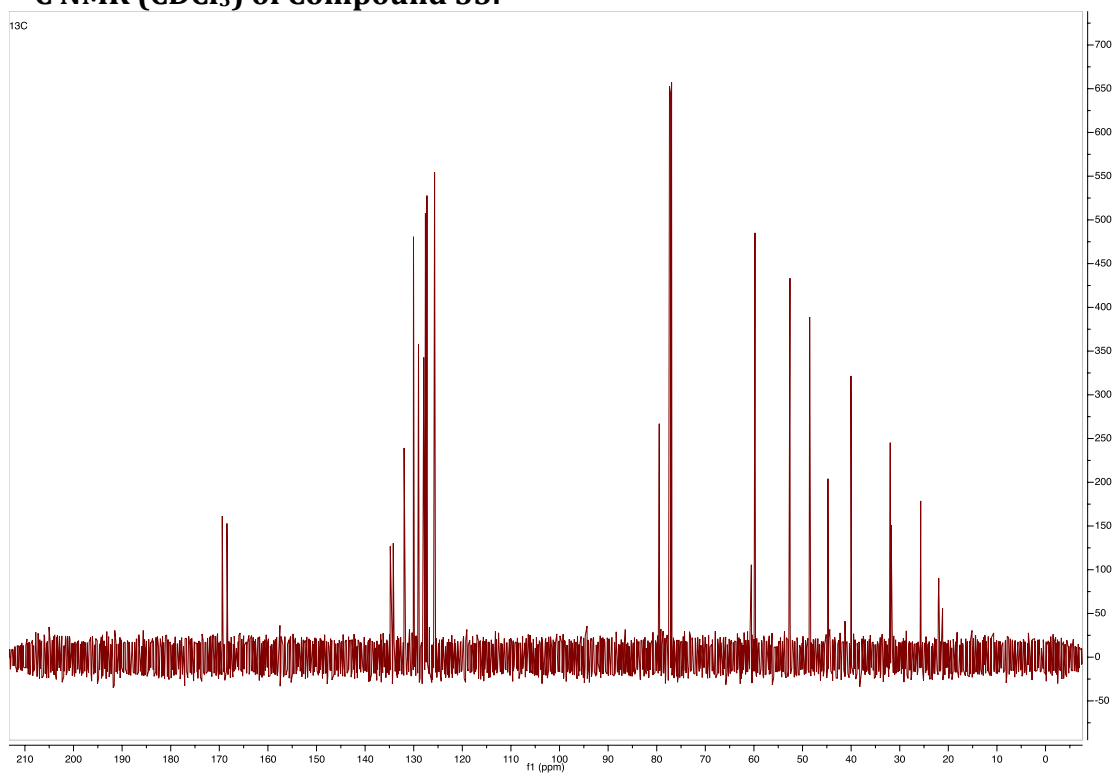
^1H NMR (CDCl_3) of Compound 50:

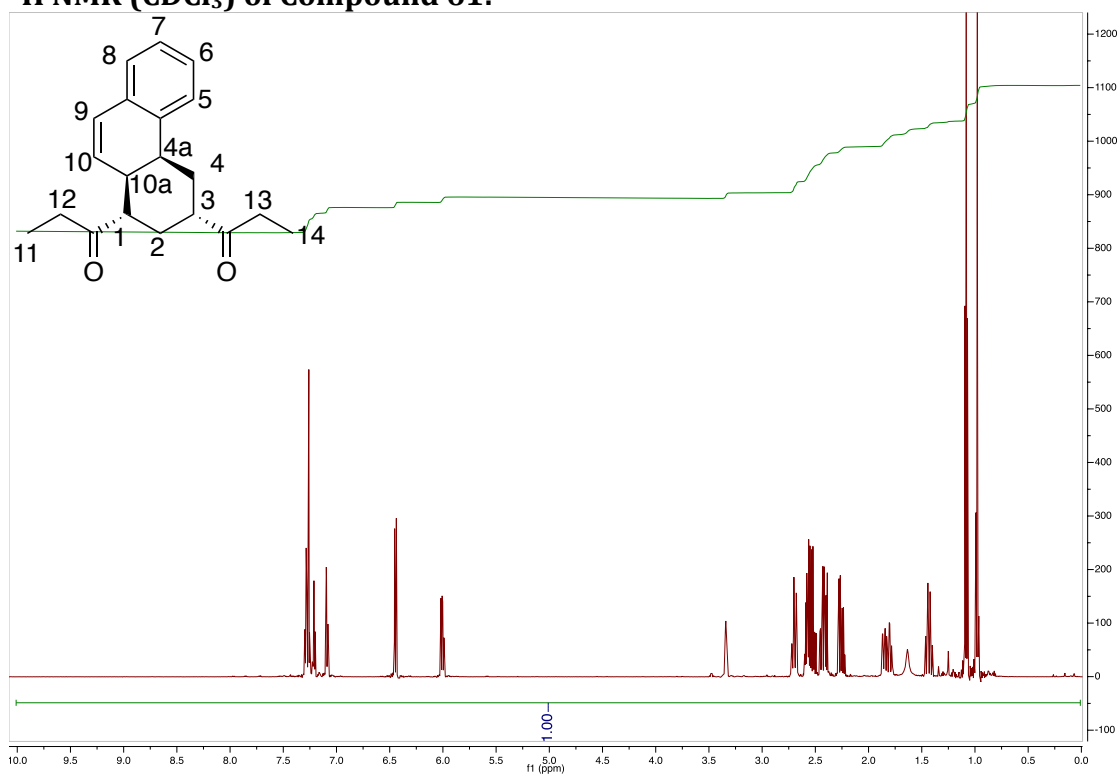
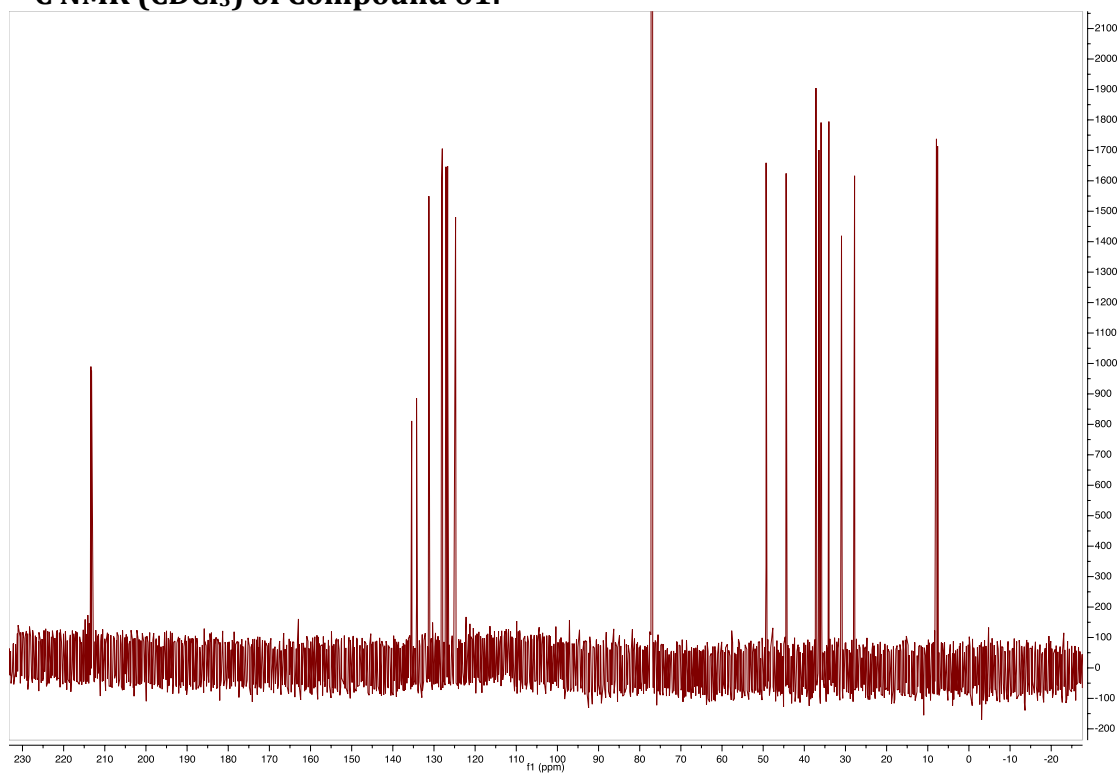
^1H NMR (CDCl_3) of Compound 51: **^{13}C NMR (CDCl_3) of Compound 51:**

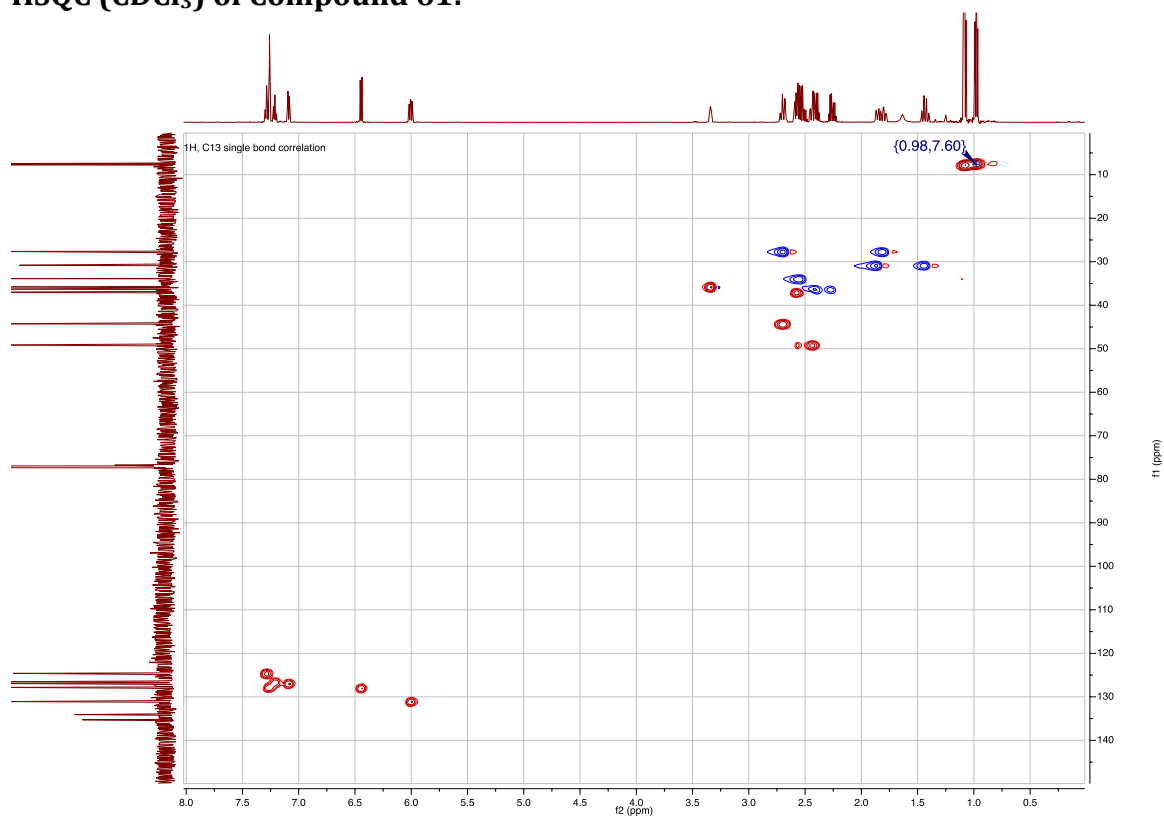
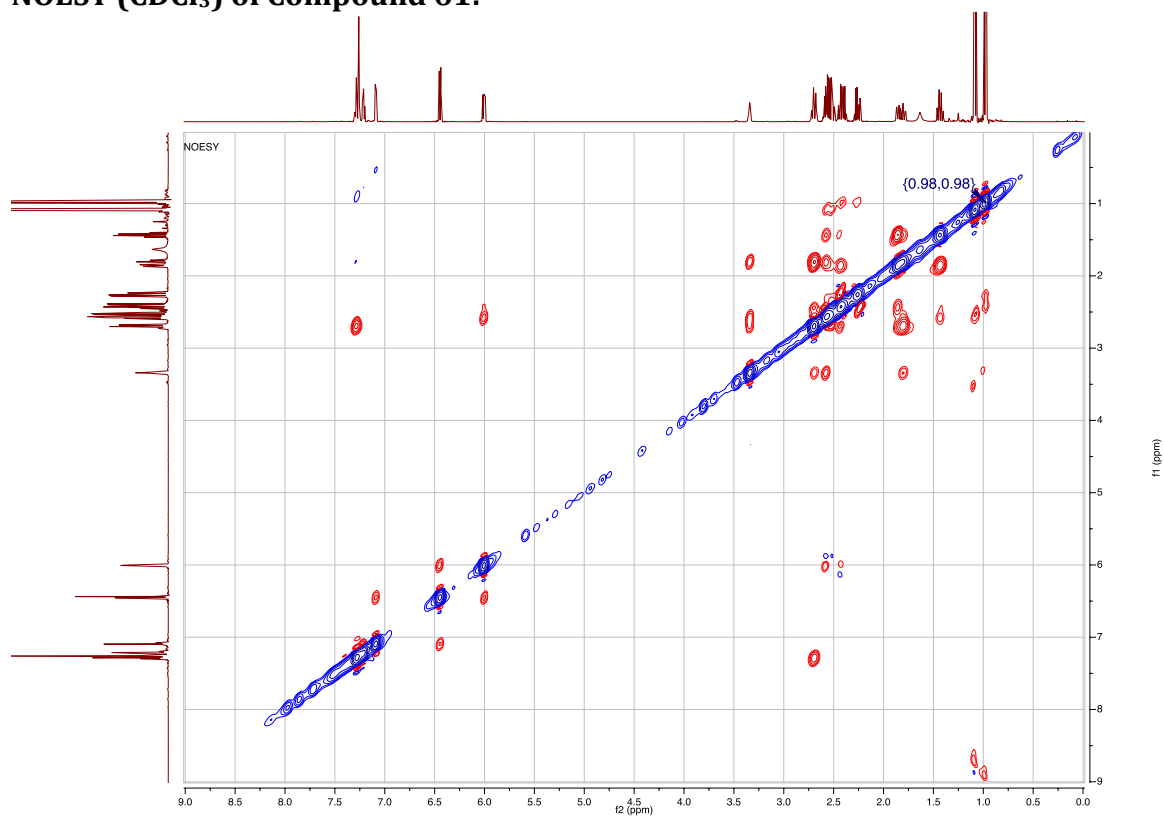
^1H NMR (CDCl_3) of Compound 52: **^{13}C NMR (CDCl_3) of Compound 52:**

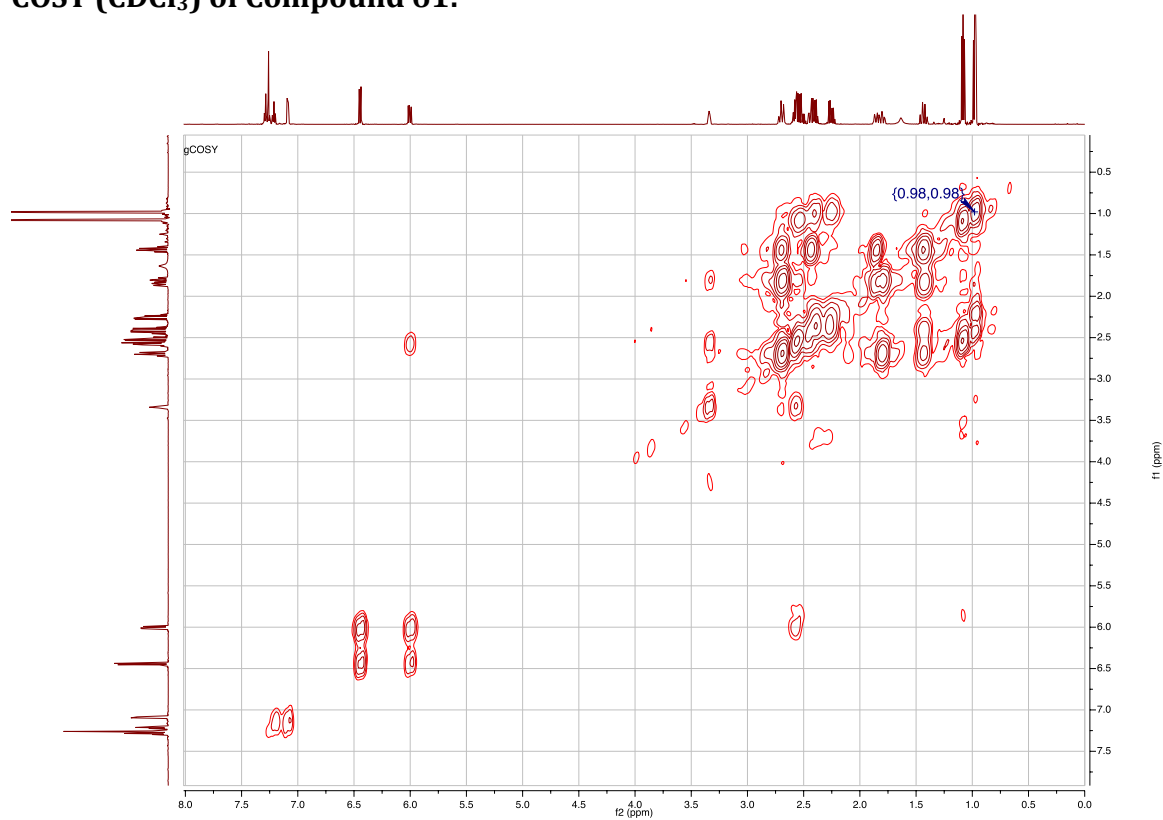
^1H NMR ($\text{d}^6\text{-Acetone}$) of Compound 53: **^{13}C NMR ($\text{d}^6\text{-Acetone}$) of Compound 53:**

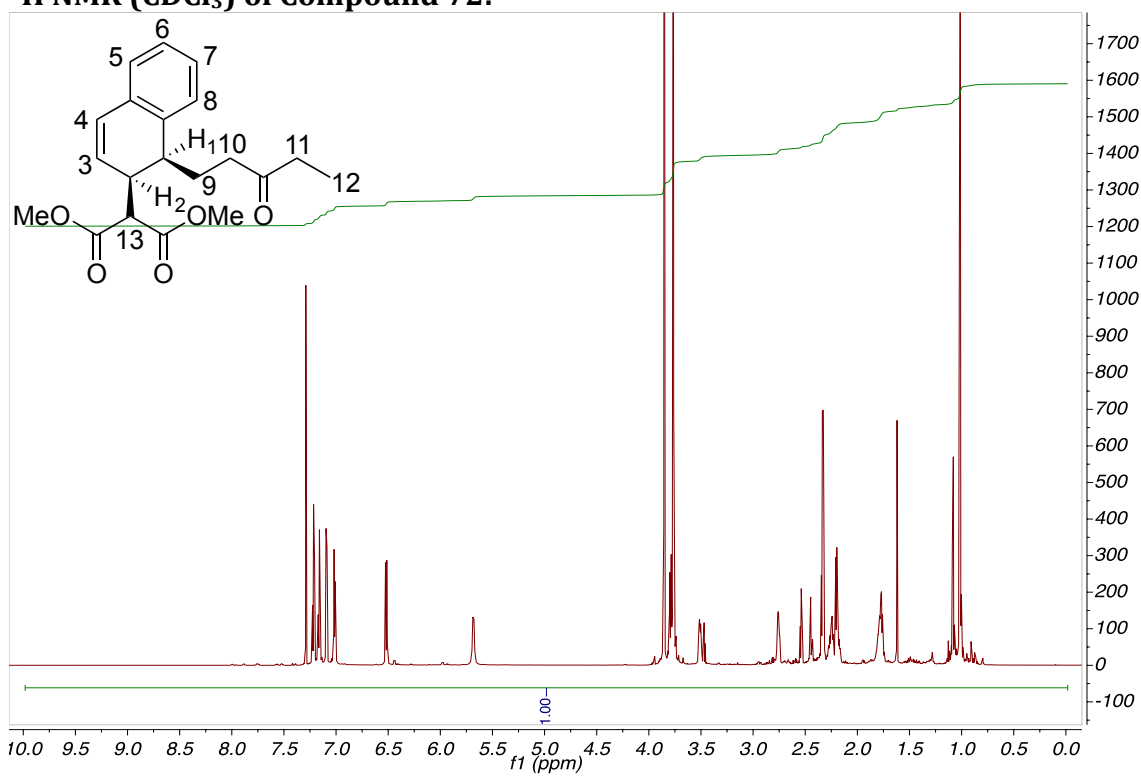
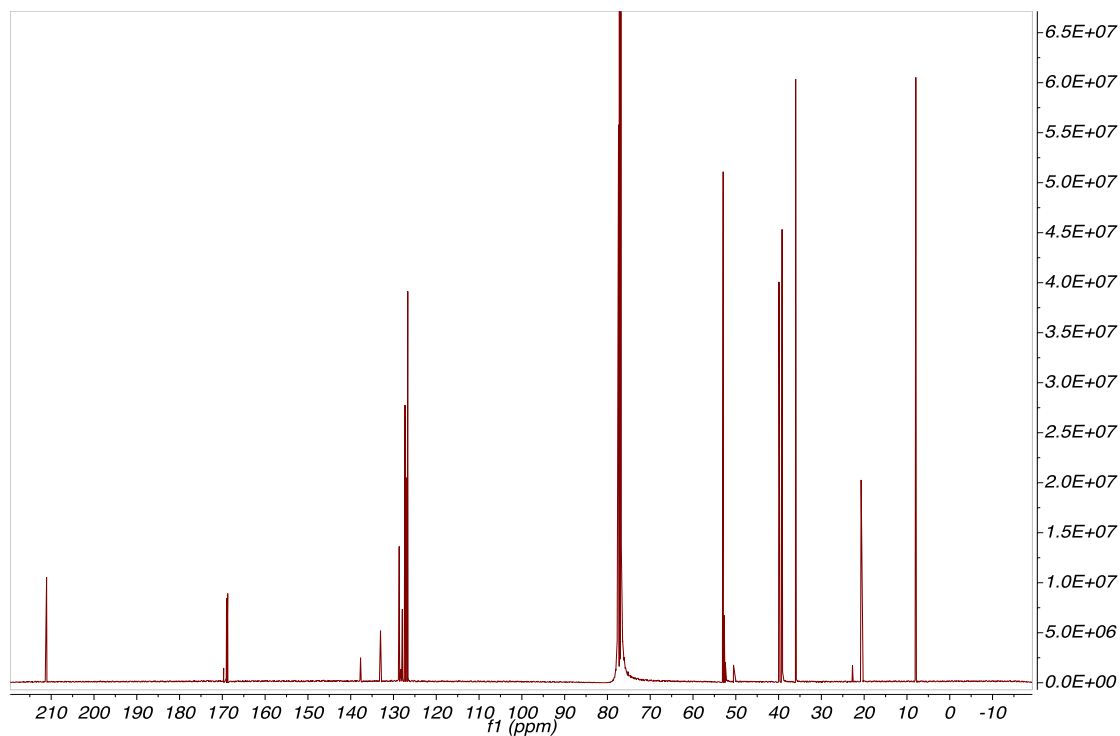
¹H NMR (d⁶-Acetone) of Compound 54:**¹³C NMR (d⁶-Acetone) of Compound 54:**

^1H NMR (CDCl_3) of Compound 55: **^{13}C NMR (CDCl_3) of Compound 55:**

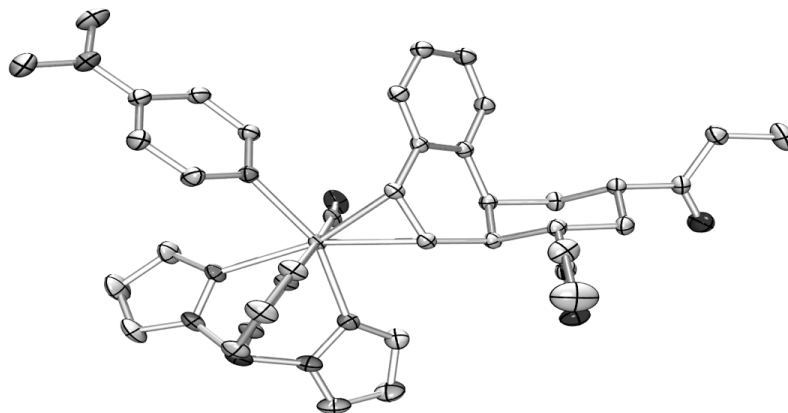
^1H NMR (CDCl_3) of Compound 61: **^{13}C NMR (CDCl_3) of Compound 61:**

HSQC (CDCl₃) of Compound 61:**NOESY (CDCl₃) of Compound 61:**



^1H NMR (CDCl_3) of Compound 72: **^{13}C NMR (CDCl_3) of Compound 72:**

Compound 87



Compound 87

Table 1. Crystal data and structure refinement for $C_{42}H_{56}BMoN_9O_{4.50}$

Crystal data	
Chemical formula	$C_{42}H_{56}BMoN_9O_{4.50}$
M_r	865.70
Crystal system, space group	Monoclinic, $P2_1/n$
Temperature (K)	153
a, b, c (Å)	10.0104 (11), 19.628 (2), 23.526 (3)
β (°)	101.949 (2)
V (Å ³)	4522.2 (9)
Z	4
Radiation type	Mo $K\alpha$
μ (mm ⁻¹)	0.34
Crystal size (mm)	$0.44 \times 0.38 \times 0.36$
Data collection	
Diffractometer	Bruker <i>APEX</i> -II CCD
Absorption correction	Empirical (using intensity measurements) Bruker <i>SADABS</i>
T_{\min}, T_{\max}	0.678, 0.747
No. of measured, independent and observed [$I > 2\sigma(I)$] reflections	111328, 21907, 19447
R_{int}	0.026
$(\sin \theta/\lambda)_{\text{max}}$ (Å ⁻¹)	0.851
Refinement	
$R[F^2 > 2\sigma(F^2)], wR(F^2), S$	0.051, 0.143, 1.04
No. of reflections	21907
No. of parameters	549
H-atom treatment	H atoms treated by a mixture of independent and constrained refinement
$\Delta\rho_{\text{max}}, \Delta\rho_{\text{min}}$ (e Å ⁻³)	1.04, -1.98
Compound 87	

Table 2. Fractional atomic coordinates and isotropic or equivalent isotropic displacement parameters (\AA^2) for $\text{C}_{42}\text{H}_{56}\text{BMoN}_9\text{O}_{4.5}$

	<i>x</i>	<i>y</i>	<i>z</i>	$U_{\text{iso}}^*/U_{\text{eq}}$
Mo	0.84250 (2)	0.65147 (2)	0.32291 (2)	0.01664 (4)
O1	0.7640 (3)	0.62989 (10)	0.65262 (8)	0.0474 (5)
O2	0.51219 (16)	0.76134 (8)	0.45716 (7)	0.0317 (3)
O3	1.08043 (14)	0.58696 (9)	0.40100 (7)	0.0316 (3)
O4	0.2012 (4)	0.88504 (17)	0.53952 (14)	0.0889 (10)
O5	0.1355 (12)	0.0534 (10)	0.3473 (4)	0.216 (9)
N1	0.83314 (15)	0.56303 (8)	0.26317 (6)	0.0212 (2)
N2	0.9071 (3)	0.41238 (11)	0.14647 (10)	0.0419 (5)
N3	0.98066 (15)	0.68633 (8)	0.26574 (7)	0.0233 (3)
N4	0.97560 (16)	0.75017 (9)	0.24344 (7)	0.0265 (3)
N5	0.88812 (15)	0.75500 (8)	0.35838 (7)	0.0227 (2)
N6	0.89011 (18)	0.80927 (8)	0.32225 (8)	0.0268 (3)
N7	0.68590 (14)	0.70855 (7)	0.25596 (7)	0.0210 (2)
N8	0.72334 (16)	0.76805 (8)	0.23349 (7)	0.0231 (3)
N9	0.97943 (14)	0.61333 (8)	0.37146 (6)	0.0197 (2)
C1	0.67464 (15)	0.59264 (8)	0.34973 (7)	0.0182 (2)
H1	0.5898	0.5889	0.3188	0.022*
C2	0.68963 (15)	0.65663 (8)	0.37943 (7)	0.0184 (2)
H2	0.6132	0.6884	0.3631	0.022*
C3	0.71699 (15)	0.65534 (8)	0.44561 (7)	0.0184 (2)
H3	0.7552	0.7006	0.4603	0.022*
C4	0.57961 (16)	0.64485 (9)	0.46529 (8)	0.0208 (3)
H4	0.5378	0.6012	0.4484	0.025*
C5	0.59909 (19)	0.64112 (10)	0.53190 (8)	0.0250 (3)
H5A	0.6331	0.6855	0.5491	0.030*
H5B	0.5102	0.6318	0.5425	0.030*
C6	0.70110 (19)	0.58478 (9)	0.55639 (7)	0.0231 (3)
H6	0.6639	0.5401	0.5398	0.028*
C7	0.83756 (18)	0.59807 (10)	0.53816 (7)	0.0229 (3)
H7A	0.9033	0.5618	0.5542	0.027*
H7B	0.8755	0.6421	0.5546	0.027*
C8	0.82003 (16)	0.59989 (8)	0.47157 (7)	0.0191 (2)
H8	0.9102	0.6134	0.4630	0.023*
C9	0.78180 (16)	0.53177 (8)	0.44195 (7)	0.0188 (2)
C10	0.81479 (19)	0.47026 (9)	0.47148 (8)	0.0238 (3)

H10	0.8644	0.4712	0.5105	0.029*
C11	0.7773 (2)	0.40791 (10)	0.44542 (9)	0.0279 (3)
H11	0.8008	0.3669	0.4665	0.033*
C12	0.7049 (2)	0.40571 (9)	0.38805 (9)	0.0266 (3)
H12	0.6767	0.3633	0.3701	0.032*
C13	0.67442 (18)	0.46618 (9)	0.35732 (8)	0.0222 (3)
H13	0.6275	0.4644	0.3179	0.027*
C14	0.71126 (15)	0.52967 (8)	0.38317 (7)	0.0179 (2)
C15	0.7202 (2)	0.58162 (10)	0.62227 (8)	0.0258 (3)
C16	0.6814 (2)	0.51600 (11)	0.64723 (9)	0.0294 (3)
H16A	0.7419	0.4795	0.6381	0.035*
H16B	0.5868	0.5043	0.6277	0.035*
C17	0.6899 (3)	0.51693 (16)	0.71239 (10)	0.0413 (5)
H17A	0.7846	0.5249	0.7324	0.062*
H17B	0.6587	0.4731	0.7247	0.062*
H17C	0.6318	0.5535	0.7221	0.062*
C18	0.48229 (17)	0.70278 (10)	0.44298 (8)	0.0235 (3)
C19	0.3486 (2)	0.68405 (13)	0.40388 (11)	0.0350 (4)
H19A	0.3004	0.6515	0.4248	0.042*
H19B	0.3678	0.6603	0.3693	0.042*
C20	0.2542 (3)	0.74337 (18)	0.38356 (17)	0.0572 (8)
H20A	0.2406	0.7698	0.4173	0.086*
H20B	0.1660	0.7262	0.3623	0.086*
H20C	0.2948	0.7726	0.3579	0.086*
C21	0.89953 (19)	0.50447 (9)	0.28137 (8)	0.0243 (3)
H21	0.9305	0.4979	0.3220	0.029*
C22	0.9249 (2)	0.45375 (10)	0.24462 (9)	0.0287 (3)
H22	0.9726	0.4139	0.2602	0.034*
C23	0.8805 (2)	0.46073 (10)	0.18393 (9)	0.0300 (4)
C24	0.8075 (3)	0.52061 (11)	0.16505 (9)	0.0328 (4)
H24	0.7719	0.5278	0.1248	0.039*
C25	0.7880 (2)	0.56877 (10)	0.20513 (8)	0.0282 (3)
H25	0.7393	0.6089	0.1909	0.034*
C26	0.9782 (4)	0.35031 (14)	0.16825 (16)	0.0562 (8)
H26A	1.0657	0.3618	0.1937	0.084*
H26B	0.9944	0.3229	0.1355	0.084*
H26C	0.9224	0.3243	0.1902	0.084*
C27	0.8654 (4)	0.42189 (16)	0.08404 (12)	0.0522 (7)
H27A	0.7664	0.4287	0.0737	0.078*

H27B	0.8902	0.3815	0.0640	0.078*
H27C	0.9117	0.4619	0.0723	0.078*
C28	1.0785 (2)	0.75867 (14)	0.21485 (11)	0.0382 (5)
H28	1.0972	0.7990	0.1956	0.046*
C29	1.1515 (3)	0.69892 (16)	0.21834 (13)	0.0447 (6)
H29	1.2292	0.6897	0.2023	0.054*
C30	1.0867 (2)	0.65482 (12)	0.25052 (11)	0.0333 (4)
H30	1.1138	0.6092	0.2602	0.040*
C31	0.9353 (2)	0.86481 (11)	0.35385 (11)	0.0362 (4)
H31	0.9458	0.9089	0.3387	0.043*
C32	0.9640 (3)	0.84749 (13)	0.41174 (11)	0.0391 (5)
H32	0.9976	0.8762	0.4440	0.047*
C33	0.9328 (2)	0.77820 (11)	0.41236 (9)	0.0295 (4)
H33	0.9420	0.7512	0.4465	0.035*
C34	0.6168 (2)	0.79340 (10)	0.19456 (9)	0.0284 (3)
H34	0.6174	0.8344	0.1731	0.034*
C35	0.5071 (2)	0.75019 (12)	0.19094 (10)	0.0323 (4)
H35	0.4186	0.7549	0.1671	0.039*
C36	0.55511 (19)	0.69800 (10)	0.23004 (9)	0.0272 (3)
H36	0.5022	0.6600	0.2373	0.033*
C37	0.1838 (9)	0.8166 (4)	0.5613 (2)	0.138 (3)
H37A	0.1292	0.7880	0.5303	0.166*
H37B	0.1369	0.8185	0.5944	0.166*
C38	0.3268 (8)	0.7879 (3)	0.5805 (3)	0.110 (2)
H38A	0.3446	0.7761	0.6223	0.132*
H38B	0.3376	0.7463	0.5581	0.132*
C39	0.4194 (8)	0.8397 (3)	0.5700 (3)	0.113 (2)
H39A	0.4961	0.8201	0.5547	0.136*
H39B	0.4564	0.8660	0.6057	0.136*
C40	0.3327 (8)	0.8817 (3)	0.5267 (2)	0.0982 (18)
H40A	0.3717	0.9281	0.5270	0.118*
H40B	0.3270	0.8619	0.4876	0.118*
C42	0.2807 (16)	0.0292 (10)	0.4234 (5)	0.147 (7)
H42A	0.3577	0.0618	0.4304	0.176*
H42B	0.3057	-0.0113	0.4485	0.176*
C43	0.1550 (17)	0.0611 (14)	0.4339 (5)	0.216 (13)
H43A	0.1005	0.0288	0.4521	0.259*
H43B	0.1752	0.1022	0.4586	0.259*
C41	0.2501 (15)	0.0132 (10)	0.3727 (5)	0.150 (7)

H41A	0.2267	-0.0359	0.3689	0.180*
H41B	0.3271	0.0219	0.3532	0.180*
C44	0.097 (2)	0.0757 (12)	0.3840 (7)	0.220 (13)
H44A	-0.0003	0.0624	0.3793	0.264*
H44B	0.0991	0.1259	0.3801	0.264*
B1	0.8662 (2)	0.79986 (11)	0.25592 (10)	0.0269 (4)
H1B	0.880 (3)	0.8484 (14)	0.2359 (12)	0.027 (7)*

Compound 87

Table 3. Atomic displacement parameters (\AA^2) for $\text{C}_{42}\text{H}_{56}\text{BMoN}_9\text{O}_{4.5}$

	U^{11}	U^{22}	U^{33}	U^{12}	U^{13}	U^{23}
Mo	0.01410 (5)	0.01836 (6)	0.01768 (6)	0.00136 (4)	0.00384 (4)	0.00340 (4)
O1	0.0788 (15)	0.0388 (9)	0.0266 (7)	-0.0176 (9)	0.0158 (8)	-0.0092 (6)
O2	0.0281 (7)	0.0267 (6)	0.0390 (8)	0.0040 (5)	0.0039 (6)	-0.0035 (6)
O3	0.0170 (5)	0.0467 (8)	0.0309 (7)	0.0097 (5)	0.0040 (5)	0.0157 (6)
O4	0.118 (3)	0.074 (2)	0.0615 (17)	0.0042 (19)	-0.0121 (18)	-0.0102 (15)
O5	0.157 (9)	0.42 (2)	0.064 (5)	0.186 (13)	-0.002 (5)	-0.004 (9)
N1	0.0217 (6)	0.0215 (6)	0.0215 (6)	0.0022 (5)	0.0069 (5)	0.0021 (5)
N2	0.0600 (14)	0.0300 (9)	0.0410 (10)	-0.0009 (9)	0.0227 (10)	-0.0099 (8)
N3	0.0189 (6)	0.0265 (6)	0.0258 (6)	0.0002 (5)	0.0078 (5)	0.0054 (5)
N4	0.0226 (6)	0.0303 (7)	0.0266 (7)	-0.0045 (5)	0.0055 (5)	0.0091 (6)
N5	0.0190 (6)	0.0248 (6)	0.0241 (6)	-0.0026 (5)	0.0037 (5)	0.0007 (5)
N6	0.0267 (7)	0.0217 (6)	0.0303 (7)	-0.0035 (5)	0.0019 (6)	0.0020 (5)
N7	0.0171 (5)	0.0211 (6)	0.0240 (6)	0.0003 (4)	0.0021 (4)	0.0046 (5)
N8	0.0220 (6)	0.0204 (6)	0.0257 (6)	0.0011 (5)	0.0024 (5)	0.0068 (5)
N9	0.0137 (5)	0.0258 (6)	0.0203 (6)	0.0024 (4)	0.0051 (4)	0.0057 (5)
C1	0.0142 (5)	0.0203 (6)	0.0200 (6)	0.0001 (4)	0.0030 (5)	0.0026 (5)
C2	0.0148 (5)	0.0199 (6)	0.0210 (6)	0.0023 (4)	0.0048 (5)	0.0024 (5)
C3	0.0153 (5)	0.0208 (6)	0.0199 (6)	0.0004 (5)	0.0058 (5)	0.0004 (5)
C4	0.0158 (6)	0.0238 (7)	0.0242 (7)	-0.0004 (5)	0.0077 (5)	-0.0018 (5)
C5	0.0233 (7)	0.0294 (8)	0.0252 (7)	0.0006 (6)	0.0118 (6)	-0.0012 (6)
C6	0.0258 (7)	0.0242 (7)	0.0211 (7)	-0.0022 (6)	0.0092 (6)	-0.0018 (5)
C7	0.0211 (7)	0.0292 (7)	0.0186 (6)	-0.0001 (6)	0.0049 (5)	0.0000 (5)
C8	0.0160 (6)	0.0233 (6)	0.0186 (6)	0.0015 (5)	0.0048 (5)	0.0006 (5)
C9	0.0165 (6)	0.0216 (6)	0.0193 (6)	0.0029 (5)	0.0056 (5)	0.0019 (5)
C10	0.0252 (7)	0.0250 (7)	0.0214 (7)	0.0065 (6)	0.0059 (6)	0.0054 (5)
C11	0.0322 (9)	0.0231 (7)	0.0304 (8)	0.0059 (6)	0.0112 (7)	0.0062 (6)
C12	0.0288 (8)	0.0215 (7)	0.0317 (8)	0.0005 (6)	0.0116 (7)	0.0004 (6)
C13	0.0209 (7)	0.0227 (7)	0.0237 (7)	-0.0017 (5)	0.0062 (5)	-0.0002 (5)
C14	0.0140 (5)	0.0209 (6)	0.0194 (6)	-0.0001 (4)	0.0049 (4)	0.0023 (5)
C15	0.0295 (8)	0.0283 (8)	0.0219 (7)	-0.0011 (6)	0.0104 (6)	-0.0003 (6)
C16	0.0267 (8)	0.0315 (9)	0.0323 (9)	0.0008 (7)	0.0114 (7)	0.0056 (7)
C17	0.0322 (10)	0.0614 (15)	0.0321 (10)	0.0004 (10)	0.0107 (8)	0.0158 (10)
C18	0.0164 (6)	0.0288 (7)	0.0266 (7)	0.0020 (5)	0.0077 (5)	-0.0021 (6)
C19	0.0175 (7)	0.0421 (11)	0.0437 (11)	0.0002 (7)	0.0020 (7)	-0.0052 (9)

C20	0.0219 (10)	0.0576 (17)	0.083 (2)	0.0055 (10)	-0.0091 (12)	0.0039 (16)
C21	0.0257 (7)	0.0216 (7)	0.0272 (8)	0.0020 (6)	0.0094 (6)	0.0027 (6)
C22	0.0329 (9)	0.0204 (7)	0.0350 (9)	0.0016 (6)	0.0124 (7)	0.0002 (6)
C23	0.0364 (10)	0.0241 (7)	0.0333 (9)	-0.0052 (7)	0.0160 (8)	-0.0052 (7)
C24	0.0430 (11)	0.0311 (9)	0.0250 (8)	-0.0011 (8)	0.0090 (8)	-0.0027 (7)
C25	0.0337 (9)	0.0270 (8)	0.0231 (7)	0.0041 (7)	0.0039 (6)	-0.0003 (6)
C26	0.079 (2)	0.0353 (12)	0.0596 (18)	0.0094 (13)	0.0275 (17)	-0.0137 (12)
C27	0.079 (2)	0.0437 (14)	0.0398 (13)	-0.0067 (14)	0.0259 (14)	-0.0135 (11)
C28	0.0301 (9)	0.0484 (12)	0.0392 (11)	-0.0081 (9)	0.0145 (8)	0.0143 (9)
C29	0.0301 (10)	0.0586 (15)	0.0524 (14)	-0.0003 (10)	0.0252 (10)	0.0121 (12)
C30	0.0248 (8)	0.0394 (10)	0.0405 (11)	0.0047 (7)	0.0175 (8)	0.0077 (8)
C31	0.0362 (10)	0.0235 (8)	0.0460 (12)	-0.0061 (7)	0.0016 (9)	-0.0039 (8)
C32	0.0410 (12)	0.0364 (11)	0.0381 (11)	-0.0104 (9)	0.0039 (9)	-0.0117 (9)
C33	0.0256 (8)	0.0365 (9)	0.0255 (8)	-0.0078 (7)	0.0031 (6)	-0.0040 (7)
C34	0.0276 (8)	0.0262 (8)	0.0297 (8)	0.0050 (6)	0.0016 (6)	0.0091 (6)
C35	0.0213 (7)	0.0368 (10)	0.0350 (9)	0.0021 (7)	-0.0030 (7)	0.0130 (8)
C36	0.0194 (7)	0.0295 (8)	0.0304 (8)	-0.0008 (6)	-0.0003 (6)	0.0083 (7)
C37	0.167 (7)	0.172 (7)	0.059 (3)	-0.090 (6)	-0.019 (3)	0.014 (4)
C38	0.147 (6)	0.077 (3)	0.098 (4)	0.003 (4)	0.008 (4)	0.019 (3)
C39	0.152 (6)	0.101 (4)	0.088 (4)	0.032 (4)	0.028 (4)	-0.027 (3)
C40	0.159 (6)	0.062 (3)	0.080 (3)	0.004 (3)	0.038 (4)	-0.011 (2)
C42	0.126 (11)	0.236 (19)	0.075 (7)	0.087 (12)	0.016 (7)	0.032 (10)
C43	0.142 (13)	0.43 (4)	0.063 (7)	0.163 (19)	0.001 (7)	-0.033 (13)
C41	0.123 (10)	0.242 (19)	0.069 (6)	0.093 (12)	-0.013 (6)	-0.049 (9)
C44	0.25 (2)	0.30 (3)	0.084 (9)	0.22 (2)	-0.026 (12)	-0.022 (13)
B1	0.0263 (9)	0.0226 (8)	0.0296 (9)	-0.0053 (7)	0.0009 (7)	0.0076 (7)

Compound 87

Table 4. Geometric parameters (Å, °) for C₄₂H₅₆BMoN₉O_{4.5}.

Mo—N9	1.7596 (14)	C16—H16A	0.9900
Mo—N5	2.2082 (16)	C16—H16B	0.9900
Mo—N1	2.2233 (15)	C17—H17A	0.9800
Mo—N3	2.2271 (15)	C17—H17B	0.9800
Mo—C2	2.2276 (15)	C17—H17C	0.9800
Mo—C1	2.2348 (15)	C18—C19	1.504 (3)
Mo—N7	2.2740 (14)	C19—C20	1.513 (4)
O1—C15	1.212 (3)	C19—H19A	0.9900
O2—C18	1.217 (2)	C19—H19B	0.9900
O3—N9	1.2174 (18)	C20—H20A	0.9800
O4—C40	1.411 (7)	C20—H20B	0.9800
O4—C37	1.460 (8)	C20—H20C	0.9800
O5—C44	1.107 (16)	C21—C22	1.376 (3)
O5—C41	1.419 (15)	C21—H21	0.9500
N1—C25	1.351 (2)	C22—C23	1.412 (3)
N1—C21	1.352 (2)	C22—H22	0.9500
N2—C23	1.359 (3)	C23—C24	1.406 (3)
N2—C26	1.450 (4)	C24—C25	1.377 (3)
N2—C27	1.453 (4)	C24—H24	0.9500
N3—C30	1.340 (2)	C25—H25	0.9500
N3—N4	1.355 (2)	C26—H26A	0.9800
N4—C28	1.352 (3)	C26—H26B	0.9800
N4—B1	1.540 (3)	C26—H26C	0.9800
N5—C33	1.336 (2)	C27—H27A	0.9800
N5—N6	1.366 (2)	C27—H27B	0.9800
N6—C31	1.344 (3)	C27—H27C	0.9800
N6—B1	1.540 (3)	C28—C29	1.375 (4)
N7—C36	1.341 (2)	C28—H28	0.9500
N7—N8	1.366 (2)	C29—C30	1.395 (3)
N8—C34	1.349 (2)	C29—H29	0.9500
N8—B1	1.550 (3)	C30—H30	0.9500
C1—C2	1.430 (2)	C31—C32	1.375 (4)
C1—C14	1.470 (2)	C31—H31	0.9500
C1—H1	1.0000	C32—C33	1.396 (3)
C2—C3	1.524 (2)	C32—H32	0.9500

C2—H2	1.0000	C33—H33	0.9500
C3—C8	1.536 (2)	C34—C35	1.376 (3)
C3—C4	1.553 (2)	C34—H34	0.9500
C3—H3	1.0000	C35—C36	1.394 (3)
C4—C18	1.518 (2)	C35—H35	0.9500
C4—C5	1.540 (3)	C36—H36	0.9500
C4—H4	1.0000	C37—C38	1.517 (11)
C5—C6	1.534 (3)	C37—H37A	0.9900
C5—H5A	0.9900	C37—H37B	0.9900
C5—H5B	0.9900	C38—C39	1.432 (9)
C6—C15	1.523 (2)	C38—H38A	0.9900
C6—C7	1.536 (2)	C38—H38B	0.9900
C6—H6	1.0000	C39—C40	1.450 (9)
C7—C8	1.540 (2)	C39—H39A	0.9900
C7—H7A	0.9900	C39—H39B	0.9900
C7—H7B	0.9900	C40—H40A	0.9900
C8—C9	1.520 (2)	C40—H40B	0.9900
C8—H8	1.0000	C42—C41	1.211 (16)
C9—C10	1.398 (2)	C42—C43	1.471 (18)
C9—C14	1.417 (2)	C42—H42A	0.9900
C10—C11	1.385 (3)	C42—H42B	0.9900
C10—H10	0.9500	C43—C44	1.232 (17)
C11—C12	1.394 (3)	C43—H43A	0.9900
C11—H11	0.9500	C43—H43B	0.9900
C12—C13	1.390 (3)	C41—H41A	0.9900
C12—H12	0.9500	C41—H41B	0.9900
C13—C14	1.402 (2)	C44—H44A	0.9900
C13—H13	0.9500	C44—H44B	0.9900
C15—C16	1.500 (3)	B1—H1B	1.08 (3)
C16—C17	1.518 (3)		
N9—Mo—N5	94.24 (6)	C16—C17—H17C	109.5
N9—Mo—N1	90.19 (6)	H17A—C17—H17C	109.5
N5—Mo—N1	159.35 (6)	H17B—C17—H17C	109.5
N9—Mo—N3	91.43 (6)	O2—C18—C19	122.39 (18)
N5—Mo—N3	80.78 (6)	O2—C18—C4	120.58 (16)
N1—Mo—N3	78.94 (6)	C19—C18—C4	117.03 (17)
N9—Mo—C2	99.84 (6)	C18—C19—C20	115.1 (2)
N5—Mo—C2	81.17 (6)	C18—C19—H19A	108.5

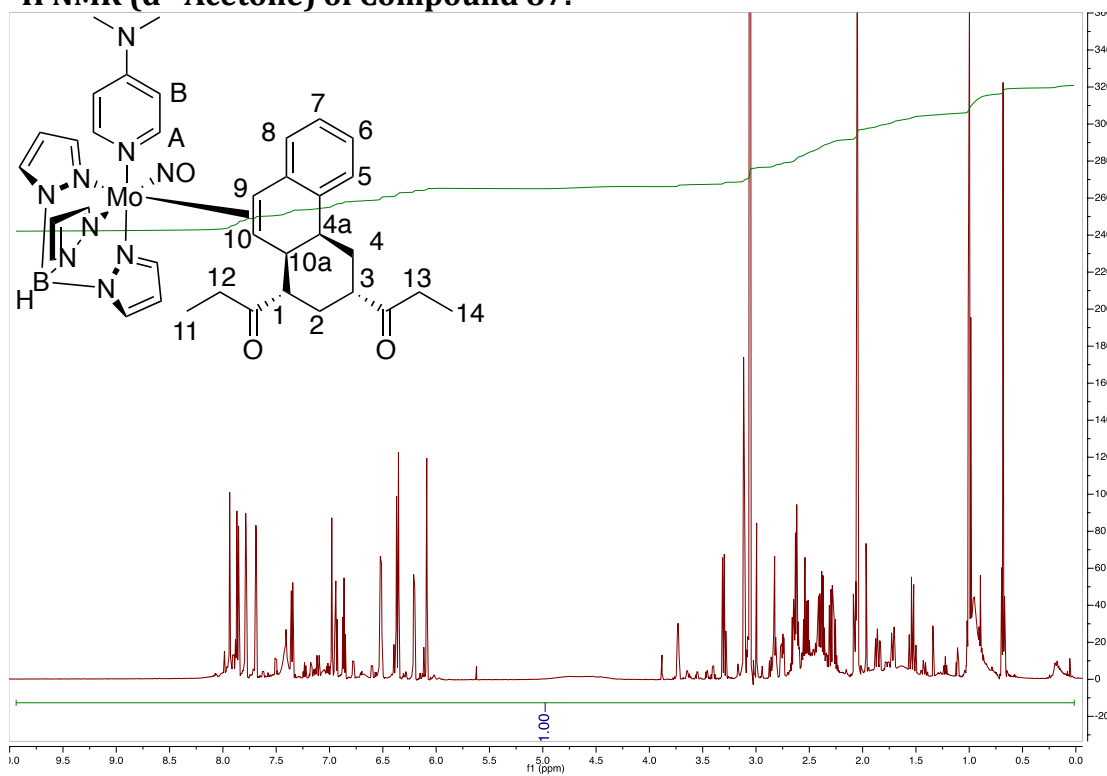
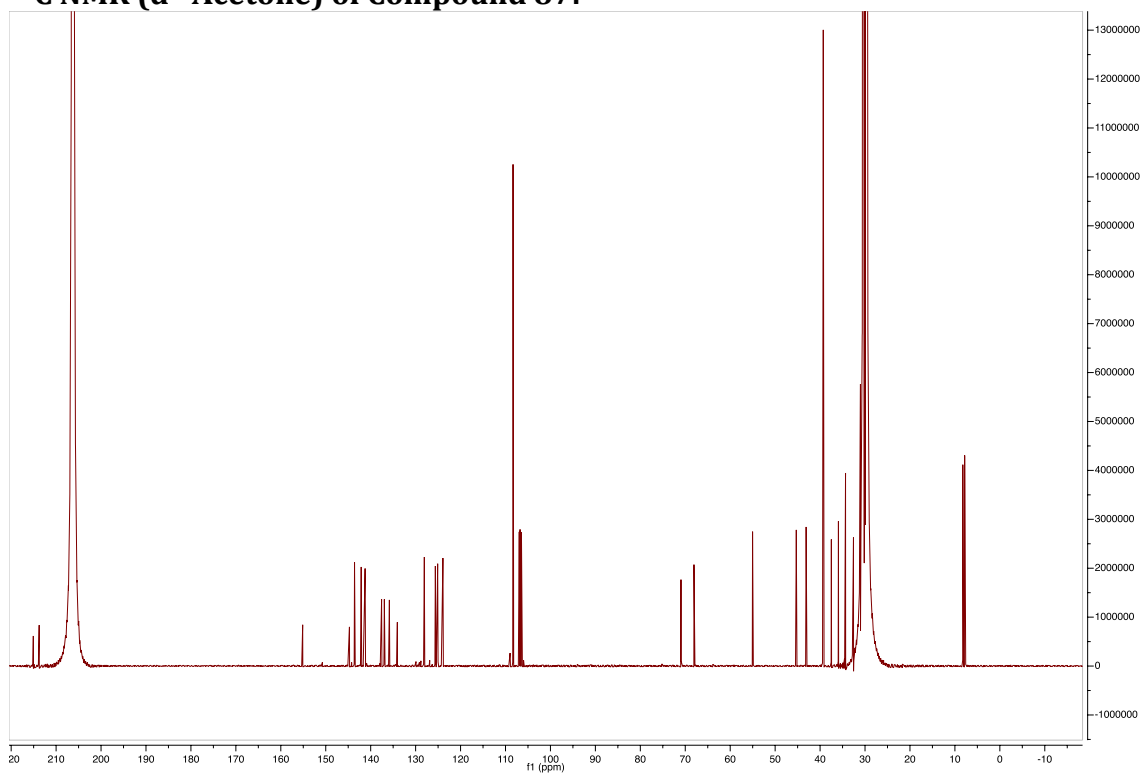
N1—Mo—C2	117.94 (6)	C20—C19—H19A	108.5
N3—Mo—C2	159.35 (6)	C18—C19—H19B	108.5
N9—Mo—C1	97.30 (6)	C20—C19—H19B	108.5
N5—Mo—C1	118.53 (6)	H19A—C19—H19B	107.5
N1—Mo—C1	80.75 (6)	C19—C20—H20A	109.5
N3—Mo—C1	157.89 (6)	C19—C20—H20B	109.5
C2—Mo—C1	37.38 (6)	H20A—C20—H20B	109.5
N9—Mo—N7	172.74 (6)	C19—C20—H20C	109.5
N5—Mo—N7	82.38 (6)	H20A—C20—H20C	109.5
N1—Mo—N7	90.80 (6)	H20B—C20—H20C	109.5
N3—Mo—N7	81.70 (5)	N1—C21—C22	123.95 (18)
C2—Mo—N7	86.03 (6)	N1—C21—H21	118.0
C1—Mo—N7	89.96 (5)	C22—C21—H21	118.0
C40—O4—C37	102.5 (5)	C21—C22—C23	120.31 (18)
C44—O5—C41	105.9 (11)	C21—C22—H22	119.8
C25—N1—C21	115.51 (16)	C23—C22—H22	119.8
C25—N1—Mo	122.36 (12)	N2—C23—C24	122.5 (2)
C21—N1—Mo	120.65 (12)	N2—C23—C22	121.7 (2)
C23—N2—C26	120.4 (2)	C24—C23—C22	115.78 (18)
C23—N2—C27	120.8 (2)	C25—C24—C23	119.70 (19)
C26—N2—C27	118.8 (2)	C25—C24—H24	120.2
C30—N3—N4	106.94 (15)	C23—C24—H24	120.2
C30—N3—Mo	130.17 (13)	N1—C25—C24	124.70 (19)
N4—N3—Mo	122.66 (12)	N1—C25—H25	117.6
C28—N4—N3	109.60 (18)	C24—C25—H25	117.6
C28—N4—B1	131.45 (18)	N2—C26—H26A	109.5
N3—N4—B1	118.88 (14)	N2—C26—H26B	109.5
C33—N5—N6	106.30 (16)	H26A—C26—H26B	109.5
C33—N5—Mo	132.47 (14)	N2—C26—H26C	109.5
N6—N5—Mo	120.73 (12)	H26A—C26—H26C	109.5
C31—N6—N5	109.57 (18)	H26B—C26—H26C	109.5
C31—N6—B1	128.43 (18)	N2—C27—H27A	109.5
N5—N6—B1	121.20 (15)	N2—C27—H27B	109.5
C36—N7—N8	106.04 (14)	H27A—C27—H27B	109.5
C36—N7—Mo	134.99 (12)	N2—C27—H27C	109.5
N8—N7—Mo	118.96 (11)	H27A—C27—H27C	109.5
C34—N8—N7	109.66 (15)	H27B—C27—H27C	109.5
C34—N8—B1	128.82 (15)	N4—C28—C29	108.36 (19)
N7—N8—B1	121.38 (14)	N4—C28—H28	125.8

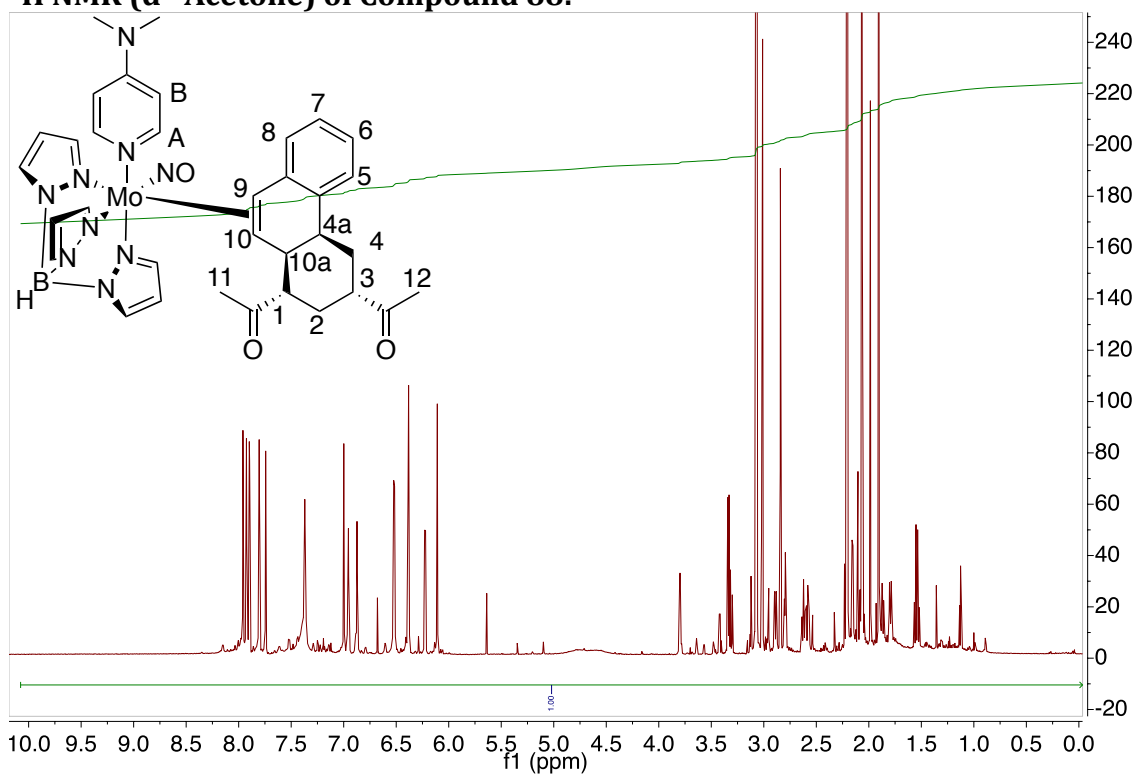
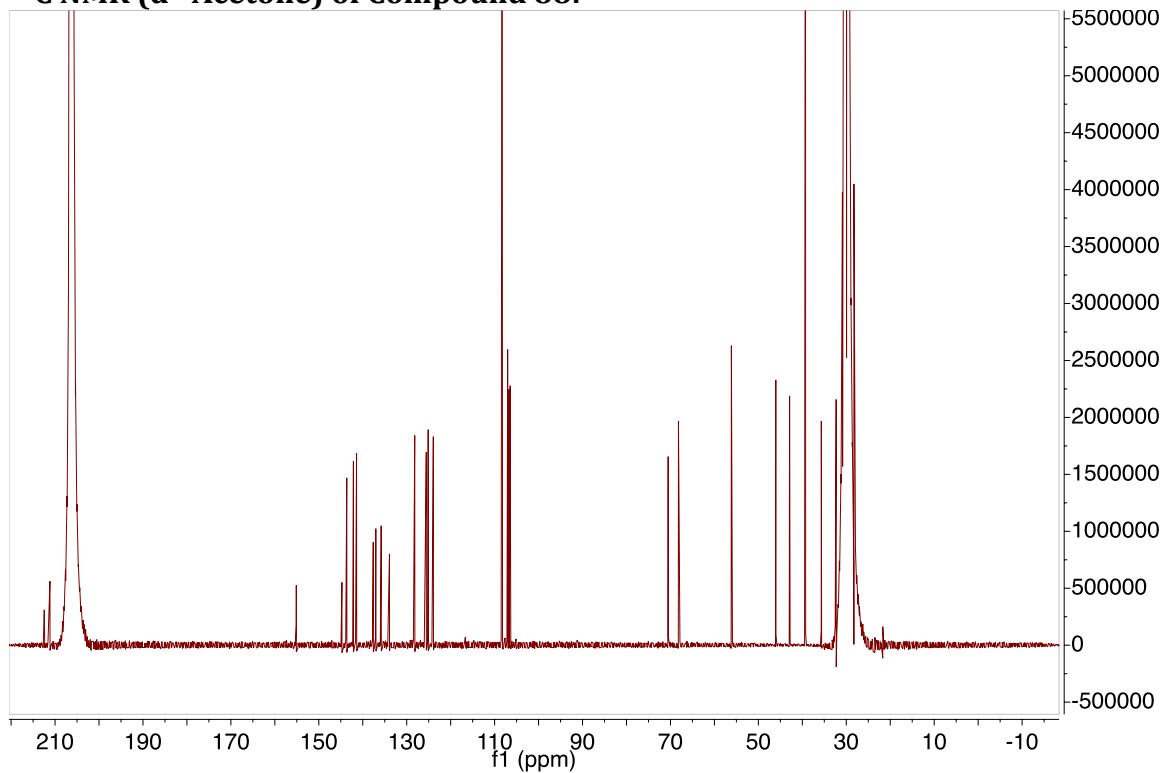
O3—N9—Mo	174.14 (13)	C29—C28—H28	125.8
C2—C1—C14	119.18 (14)	C28—C29—C30	105.13 (19)
C2—C1—Mo	71.04 (9)	C28—C29—H29	127.4
C14—C1—Mo	117.82 (10)	C30—C29—H29	127.4
C2—C1—H1	114.1	N3—C30—C29	110.0 (2)
C14—C1—H1	114.1	N3—C30—H30	125.0
Mo—C1—H1	114.1	C29—C30—H30	125.0
C1—C2—C3	117.58 (13)	N6—C31—C32	108.9 (2)
C1—C2—Mo	71.58 (9)	N6—C31—H31	125.5
C3—C2—Mo	127.49 (10)	C32—C31—H31	125.5
C1—C2—H2	111.4	C31—C32—C33	104.47 (19)
C3—C2—H2	111.4	C31—C32—H32	127.8
Mo—C2—H2	111.4	C33—C32—H32	127.8
C2—C3—C8	112.43 (13)	N5—C33—C32	110.7 (2)
C2—C3—C4	108.90 (13)	N5—C33—H33	124.6
C8—C3—C4	110.52 (13)	C32—C33—H33	124.6
C2—C3—H3	108.3	N8—C34—C35	108.85 (16)
C8—C3—H3	108.3	N8—C34—H34	125.6
C4—C3—H3	108.3	C35—C34—H34	125.6
C18—C4—C5	108.92 (14)	C34—C35—C36	104.52 (16)
C18—C4—C3	110.00 (14)	C34—C35—H35	127.7
C5—C4—C3	112.10 (14)	C36—C35—H35	127.7
C18—C4—H4	108.6	N7—C36—C35	110.93 (17)
C5—C4—H4	108.6	N7—C36—H36	124.5
C3—C4—H4	108.6	C35—C36—H36	124.5
C6—C5—C4	110.52 (14)	O4—C37—C38	105.8 (5)
C6—C5—H5A	109.5	O4—C37—H37A	110.6
C4—C5—H5A	109.5	C38—C37—H37A	110.6
C6—C5—H5B	109.5	O4—C37—H37B	110.6
C4—C5—H5B	109.5	C38—C37—H37B	110.6
H5A—C5—H5B	108.1	H37A—C37—H37B	108.7
C15—C6—C5	110.18 (14)	C39—C38—C37	106.9 (5)
C15—C6—C7	111.07 (15)	C39—C38—H38A	110.3
C5—C6—C7	109.50 (14)	C37—C38—H38A	110.4
C15—C6—H6	108.7	C39—C38—H38B	110.3
C5—C6—H6	108.7	C37—C38—H38B	110.3
C7—C6—H6	108.7	H38A—C38—H38B	108.6
C6—C7—C8	111.55 (14)	C38—C39—C40	102.1 (6)
C6—C7—H7A	109.3	C38—C39—H39A	111.4

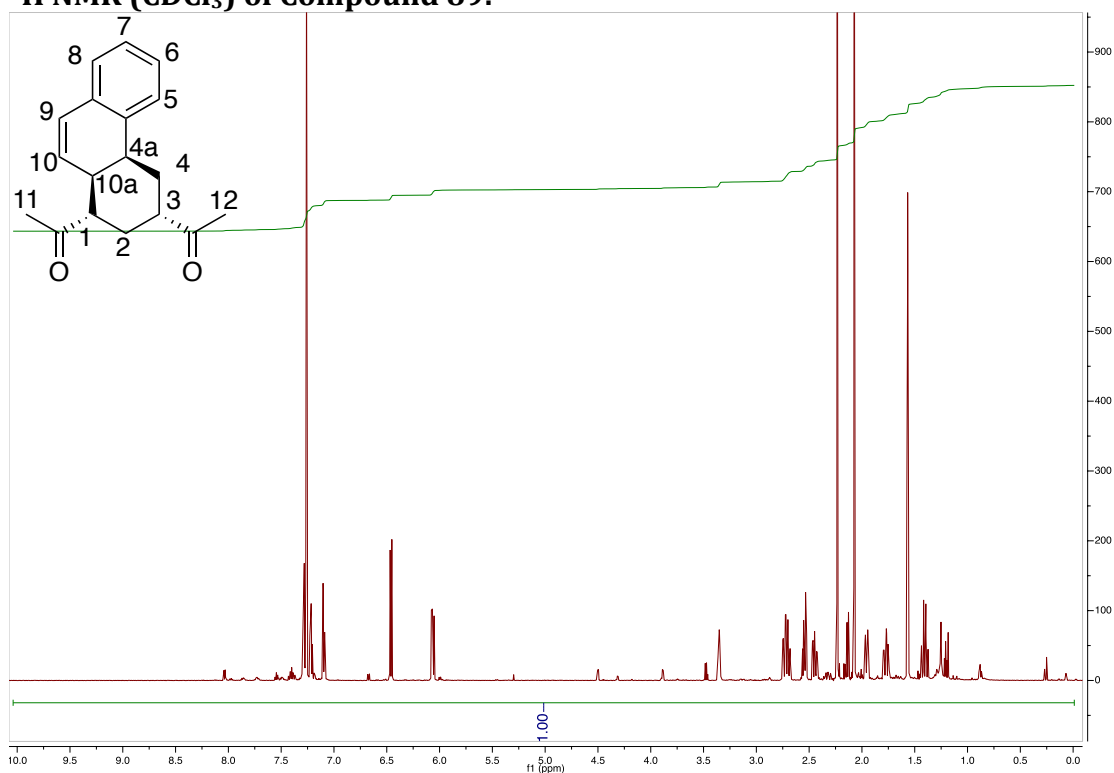
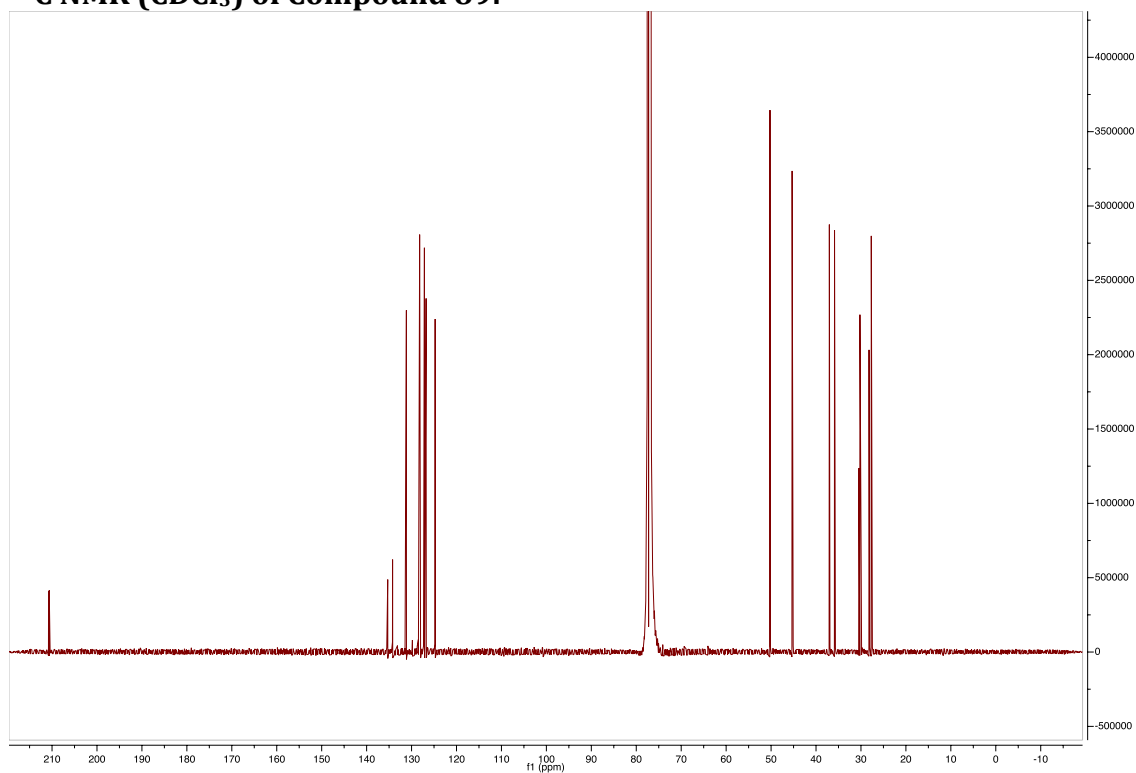
C8—C7—H7A	109.3	C40—C39—H39A	111.4
C6—C7—H7B	109.3	C38—C39—H39B	111.3
C8—C7—H7B	109.3	C40—C39—H39B	111.3
H7A—C7—H7B	108.0	H39A—C39—H39B	109.2
C9—C8—C3	110.88 (13)	O4—C40—C39	109.1 (5)
C9—C8—C7	114.26 (14)	O4—C40—H40A	109.9
C3—C8—C7	110.27 (13)	C39—C40—H40A	109.9
C9—C8—H8	107.0	O4—C40—H40B	109.9
C3—C8—H8	107.0	C39—C40—H40B	109.9
C7—C8—H8	107.0	H40A—C40—H40B	108.3
C10—C9—C14	118.59 (15)	C41—C42—C43	103.0 (12)
C10—C9—C8	121.39 (15)	C41—C42—H42A	111.2
C14—C9—C8	120.02 (14)	C43—C42—H42A	111.1
C11—C10—C9	121.91 (17)	C41—C42—H42B	111.1
C11—C10—H10	119.0	C43—C42—H42B	111.3
C9—C10—H10	119.0	H42A—C42—H42B	109.1
C10—C11—C12	119.64 (17)	C44—C43—C42	101.0 (13)
C10—C11—H11	120.2	C44—C43—H43A	111.9
C12—C11—H11	120.2	C42—C43—H43A	111.4
C13—C12—C11	119.42 (17)	C44—C43—H43B	111.5
C13—C12—H12	120.3	C42—C43—H43B	111.5
C11—C12—H12	120.3	H43A—C43—H43B	109.3
C12—C13—C14	121.57 (17)	C42—C41—O5	106.7 (12)
C12—C13—H13	119.2	C42—C41—H41A	110.5
C14—C13—H13	119.2	O5—C41—H41A	110.1
C13—C14—C9	118.83 (15)	C42—C41—H41B	110.4
C13—C14—C1	120.07 (14)	O5—C41—H41B	110.5
C9—C14—C1	121.09 (14)	H41A—C41—H41B	108.6
O1—C15—C16	122.14 (18)	O5—C44—C43	118.6 (14)
O1—C15—C6	121.43 (18)	O5—C44—H44A	107.0
C16—C15—C6	116.43 (17)	C43—C44—H44A	107.3
C15—C16—C17	114.9 (2)	O5—C44—H44B	108.5
C15—C16—H16A	108.6	C43—C44—H44B	107.8
C17—C16—H16A	108.6	H44A—C44—H44B	107.1
C15—C16—H16B	108.6	N6—B1—N4	107.56 (16)
C17—C16—H16B	108.6	N6—B1—N8	109.41 (16)
H16A—C16—H16B	107.5	N4—B1—N8	108.81 (16)
C16—C17—H17A	109.5	N6—B1—H1B	109.1 (15)
C16—C17—H17B	109.5	N4—B1—H1B	108.4 (15)

H17A—C17—H17B 109.5

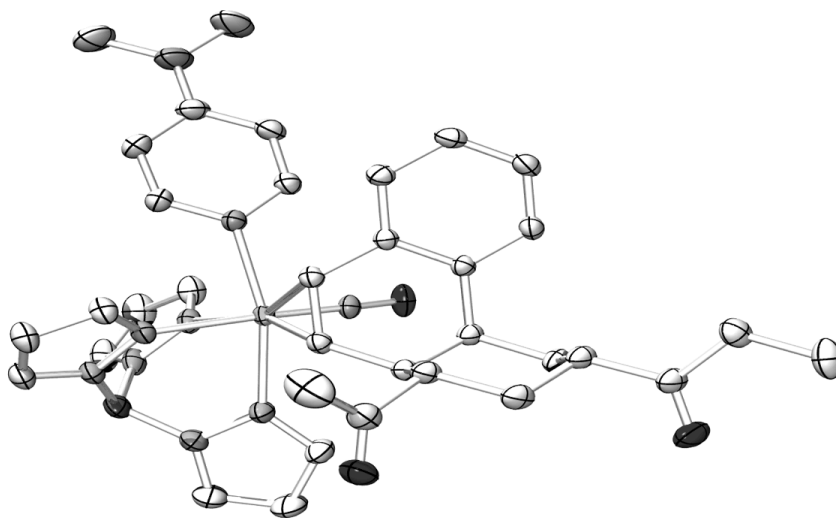
N8—B1—H1B 113.4 (16)

^1H NMR ($\text{d}^6\text{-Acetone}$) of Compound 87: **^{13}C NMR ($\text{d}^6\text{-Acetone}$) of Compound 87:**

^1H NMR ($\text{d}^6\text{-Acetone}$) of Compound 88: **^{13}C NMR ($\text{d}^6\text{-Acetone}$) of Compound 88:**

^1H NMR (CDCl_3) of Compound 89: **^{13}C NMR (CDCl_3) of Compound 89:**

Compound 90



Compound 90

Table 1. Crystal data and structure refinement for C₃₁H₅₄BN₉O_{4.5}Mo.

Empirical formula	C ₄₁ H ₅₄ B Mo N ₉ O _{4.50}	
Formula weight	851.68	
Temperature	153(2) K	
Wavelength	0.71073 Å	
Crystal system	Monoclinic	
Space group	P2 ₁ /c	
Unit cell dimensions	a = 9.7852(18) Å	
	b = 19.692(4) Å	β = 99.408(3)°.
	c = 23.463(4) Å	
Volume	4460.3(14) Å ³	
Z	4	
Density (calculated)	1.268 Mg/m ³	
Absorption coefficient	0.344 mm ⁻¹	
F(000)	1784	
Crystal size	0.350 x 0.230 x 0.220 mm ³	
Theta range for data collection	3.136 to 37.212°.	
Index ranges	-16 ≤ h ≤ 15, -33 ≤ k ≤ 32, -39 ≤ l ≤ 39	
Reflections collected	111241	
Independent reflections	21393 [R(int) = 0.0351]	
Completeness to theta = 25.242°	99.7 %	
Absorption correction	empirical	
Refinement method	Full-matrix least-squares on F ²	
Data / restraints / parameters	21393 / 0 / 540	
Goodness-of-fit on F ²	1.062	
Final R indices [I > 2σ(I)]	R ₁ = 0.0561, wR ₂ = 0.1433	
R indices (all data)	R ₁ = 0.0865, wR ₂ = 0.1728	
Largest diff. peak and hole	2.246 and -0.961 e.Å ⁻³	

Compound 90

Table 2. Atomic coordinates ($\times 10^4$) and equivalent isotropic displacement parameters ($\text{\AA}^2 \times 10^3$) for C₃₁H₅₄BN₉O_{4.5}Mo. U(eq) is defined as one third of the trace of the orthogonalized U^{ij} tensor.

	x	y	z	U(eq)
Mo	4672(1)	6576(1)	3249(1)	23(1)
O(1)	9282(2)	7725(1)	4533(1)	48(1)
O(2)	8932(3)	6293(1)	6460(1)	55(1)
O(3)	3103(2)	5937(1)	4089(1)	40(1)
O(4)	3329(4)	8805(2)	5463(1)	85(1)
O(5)	2010(10)	4359(8)	8424(4)	180(6)
N(1)	4196(2)	5691(1)	2663(1)	27(1)
N(2)	2385(3)	4163(1)	1532(1)	57(1)
N(3)	5595(2)	7148(1)	2560(1)	28(1)
N(4)	5022(2)	7754(1)	2360(1)	30(1)
N(5)	2719(2)	6931(1)	2708(1)	31(1)
N(6)	2569(2)	7571(1)	2491(1)	34(1)
N(7)	4530(2)	7598(1)	3613(1)	32(1)
N(8)	4187(3)	8148(1)	3264(1)	38(1)
N(9)	3801(2)	6194(1)	3763(1)	26(1)
C(1)	6788(2)	6635(1)	3768(1)	25(1)
C(2)	6652(2)	6002(1)	3466(1)	25(1)
C(3)	6646(2)	5367(1)	3795(1)	23(1)
C(4)	6748(2)	4742(1)	3520(1)	27(1)
C(5)	6811(2)	4133(1)	3825(1)	30(1)
C(6)	6717(2)	4142(1)	4409(1)	32(1)
C(7)	6583(2)	4756(1)	4684(1)	28(1)
C(8)	6568(2)	5375(1)	4391(1)	24(1)
C(9)	6458(2)	6046(1)	4699(1)	25(1)
C(10)	6982(2)	6015(1)	5354(1)	30(1)
C(11)	8547(2)	5896(1)	5484(1)	30(1)
C(12)	9286(2)	6484(1)	5231(1)	33(1)
C(13)	8787(2)	6548(1)	4576(1)	28(1)
C(14)	7188(2)	6616(1)	4423(1)	25(1)
C(15)	9496(3)	7159(1)	4362(1)	37(1)

C(16)	10470(4)	7039(2)	3948(2)	63(1)
C(17)	9039(2)	5828(1)	6131(1)	33(1)
C(18)	9667(2)	5158(1)	6334(1)	37(1)
C(19)	10179(3)	5115(2)	6979(1)	50(1)
C(20)	4120(3)	5739(1)	2085(1)	35(1)
C(21)	3568(3)	5248(1)	1696(1)	41(1)
C(22)	3009(3)	4651(1)	1895(1)	40(1)
C(23)	3127(3)	4590(1)	2500(1)	37(1)
C(24)	3709(2)	5105(1)	2854(1)	31(1)
C(25)	2297(5)	4236(2)	908(2)	72(1)
C(26)	1827(6)	3557(2)	1756(2)	82(2)
C(27)	5712(3)	8000(1)	1954(1)	36(1)
C(28)	6759(3)	7561(1)	1883(1)	38(1)
C(29)	6646(2)	7037(1)	2271(1)	33(1)
C(30)	1261(3)	7653(2)	2206(1)	46(1)
C(31)	564(3)	7051(2)	2234(1)	53(1)
C(32)	1509(2)	6611(1)	2552(1)	38(1)
C(33)	4020(4)	8694(1)	3593(1)	52(1)
C(34)	4253(4)	8508(2)	4162(1)	57(1)
C(35)	4555(3)	7812(1)	4154(1)	42(1)
C(36)	1875(7)	8777(3)	5339(2)	88(2)
C(37)	1347(8)	8334(3)	5745(3)	102(2)
C(38)	2426(10)	7824(4)	5824(5)	155(4)
C(39)	3744(9)	8125(5)	5685(3)	136(3)
C(40)	1080(12)	4790(7)	8575(5)	94(3)
C(41)	1466(11)	4904(7)	9163(5)	106(4)
C(42)	2737(15)	4555(8)	9334(4)	116(5)
C(43)	2906(18)	4204(11)	8870(7)	170(9)
B(1)	3798(3)	8066(1)	2607(1)	36(1)

Compound 90

Table 3. Bond lengths [Å] and angles [°] for C₃₁H₅₄BN₉O_{4.5}Mo.

Mo-N(9)	1.7549(17)
Mo-N(7)	2.2003(19)
Mo-N(1)	2.2230(18)
Mo-C(1)	2.226(2)
Mo-N(5)	2.2271(18)
Mo-C(2)	2.2291(19)
Mo-N(3)	2.2756(17)
O(1)-C(15)	1.213(3)
O(2)-C(17)	1.212(3)
O(3)-N(9)	1.217(2)
O(4)-C(36)	1.406(7)
O(4)-C(39)	1.471(8)
O(5)-C(43)	1.287(16)
O(5)-C(40)	1.333(15)
N(1)-C(20)	1.350(3)
N(1)-C(24)	1.351(3)
N(2)-C(22)	1.361(3)
N(2)-C(26)	1.448(5)
N(2)-C(25)	1.459(5)
N(3)-C(29)	1.338(3)
N(3)-N(4)	1.367(2)
N(4)-C(27)	1.345(3)
N(4)-B(1)	1.542(3)
N(5)-C(32)	1.338(3)
N(5)-N(6)	1.359(3)
N(6)-C(30)	1.354(3)
N(6)-B(1)	1.538(4)
N(7)-C(35)	1.333(3)
N(7)-N(8)	1.367(3)
N(8)-C(33)	1.347(3)
N(8)-B(1)	1.535(3)
C(1)-C(2)	1.428(3)
C(1)-C(14)	1.524(3)

C(1)-H(1)	1.0000
C(2)-C(3)	1.471(3)
C(2)-H(2)	1.0000
C(3)-C(4)	1.400(3)
C(3)-C(8)	1.413(3)
C(4)-C(5)	1.394(3)
C(4)-H(4)	0.9500
C(5)-C(6)	1.387(3)
C(5)-H(5)	0.9500
C(6)-C(7)	1.386(3)
C(6)-H(6)	0.9500
C(7)-C(8)	1.398(3)
C(7)-H(7)	0.9500
C(8)-C(9)	1.519(3)
C(9)-C(14)	1.531(3)
C(9)-C(10)	1.540(3)
C(9)-H(9)	1.0000
C(10)-C(11)	1.530(3)
C(10)-H(10A)	0.9900
C(10)-H(10B)	0.9900
C(11)-C(17)	1.522(3)
C(11)-C(12)	1.535(3)
C(11)-H(11)	1.0000
C(12)-C(13)	1.539(3)
C(12)-H(12A)	0.9900
C(12)-H(12B)	0.9900
C(13)-C(15)	1.515(3)
C(13)-C(14)	1.553(3)
C(13)-H(13)	1.0000
C(14)-H(14)	1.0000
C(15)-C(16)	1.488(4)
C(16)-H(16A)	0.9800
C(16)-H(16B)	0.9800
C(16)-H(16C)	0.9800
C(17)-C(18)	1.500(3)
C(18)-C(19)	1.517(4)

C(18)-H(18A)	0.9900
C(18)-H(18B)	0.9900
C(19)-H(19A)	0.9800
C(19)-H(19B)	0.9800
C(19)-H(19C)	0.9800
C(20)-C(21)	1.377(3)
C(20)-H(20)	0.9500
C(21)-C(22)	1.408(4)
C(21)-H(21)	0.9500
C(22)-C(23)	1.410(4)
C(23)-C(24)	1.375(3)
C(23)-H(23)	0.9500
C(24)-H(24)	0.9500
C(25)-H(25A)	0.9800
C(25)-H(25B)	0.9800
C(25)-H(25C)	0.9800
C(26)-H(26A)	0.9800
C(26)-H(26B)	0.9800
C(26)-H(26C)	0.9800
C(27)-C(28)	1.371(4)
C(27)-H(27)	0.9500
C(28)-C(29)	1.394(3)
C(28)-H(28)	0.9500
C(29)-H(29)	0.9500
C(30)-C(31)	1.375(5)
C(30)-H(30)	0.9500
C(31)-C(32)	1.391(4)
C(31)-H(31)	0.9500
C(32)-H(32)	0.9500
C(33)-C(34)	1.368(4)
C(33)-H(33)	0.9500
C(34)-C(35)	1.402(4)
C(34)-H(34)	0.9500
C(35)-H(35)	0.9500
C(36)-C(37)	1.449(8)
C(36)-H(36A)	0.9900

C(36)-H(36B)	0.9900
C(37)-C(38)	1.447(10)
C(37)-H(37A)	0.9900
C(37)-H(37B)	0.9900
C(38)-C(39)	1.503(12)
C(38)-H(38A)	0.9900
C(38)-H(38B)	0.9900
C(39)-H(39A)	0.9900
C(39)-H(39B)	0.9900
C(40)-C(41)	1.387(15)
C(40)-H(40A)	0.9900
C(40)-H(40B)	0.9900
C(41)-C(42)	1.420(16)
C(41)-H(41A)	0.9900
C(41)-H(41B)	0.9900
C(42)-C(43)	1.322(16)
C(42)-H(42A)	0.9900
C(42)-H(42B)	0.9900
C(43)-H(43A)	0.9900
C(43)-H(43B)	0.9900
B(1)-H(1B)	1.09(3)
N(9)-Mo-N(7)	93.28(8)
N(9)-Mo-N(1)	90.70(8)
N(7)-Mo-N(1)	159.72(7)
N(9)-Mo-C(1)	99.18(7)
N(7)-Mo-C(1)	81.52(7)
N(1)-Mo-C(1)	117.45(7)
N(9)-Mo-N(5)	93.34(7)
N(7)-Mo-N(5)	80.33(7)
N(1)-Mo-N(5)	79.59(7)
C(1)-Mo-N(5)	158.46(7)
N(9)-Mo-C(2)	97.35(7)
N(7)-Mo-C(2)	118.90(7)
N(1)-Mo-C(2)	80.19(7)
C(1)-Mo-C(2)	37.40(7)

N(5)-Mo-C(2)	157.20(7)
N(9)-Mo-N(3)	173.67(7)
N(7)-Mo-N(3)	83.13(7)
N(1)-Mo-N(3)	90.92(7)
C(1)-Mo-N(3)	85.48(7)
N(5)-Mo-N(3)	80.94(7)
C(2)-Mo-N(3)	88.95(7)
C(36)-O(4)-C(39)	104.4(5)
C(43)-O(5)-C(40)	109.9(9)
C(20)-N(1)-C(24)	115.38(19)
C(20)-N(1)-Mo	122.57(15)
C(24)-N(1)-Mo	120.90(14)
C(22)-N(2)-C(26)	120.8(3)
C(22)-N(2)-C(25)	120.4(3)
C(26)-N(2)-C(25)	118.8(3)
C(29)-N(3)-N(4)	105.97(17)
C(29)-N(3)-Mo	134.84(14)
N(4)-N(3)-Mo	119.19(13)
C(27)-N(4)-N(3)	109.47(19)
C(27)-N(4)-B(1)	129.25(19)
N(3)-N(4)-B(1)	121.26(17)
C(32)-N(5)-N(6)	107.34(18)
C(32)-N(5)-Mo	130.30(16)
N(6)-N(5)-Mo	122.30(15)
C(30)-N(6)-N(5)	109.3(2)
C(30)-N(6)-B(1)	131.4(2)
N(5)-N(6)-B(1)	119.29(18)
C(35)-N(7)-N(8)	106.57(19)
C(35)-N(7)-Mo	131.75(16)
N(8)-N(7)-Mo	121.15(14)
C(33)-N(8)-N(7)	109.2(2)
C(33)-N(8)-B(1)	128.7(2)
N(7)-N(8)-B(1)	121.01(18)
O(3)-N(9)-Mo	174.95(15)
C(2)-C(1)-C(14)	117.91(16)
C(2)-C(1)-Mo	71.41(11)

C(14)-C(1)-Mo	127.83(14)
C(2)-C(1)-H(1)	111.2
C(14)-C(1)-H(1)	111.2
Mo-C(1)-H(1)	111.2
C(1)-C(2)-C(3)	119.26(16)
C(1)-C(2)-Mo	71.18(11)
C(3)-C(2)-Mo	118.22(13)
C(1)-C(2)-H(2)	113.9
C(3)-C(2)-H(2)	113.9
Mo-C(2)-H(2)	113.9
C(4)-C(3)-C(8)	119.04(17)
C(4)-C(3)-C(2)	119.87(17)
C(8)-C(3)-C(2)	121.08(17)
C(5)-C(4)-C(3)	121.31(19)
C(5)-C(4)-H(4)	119.3
C(3)-C(4)-H(4)	119.3
C(6)-C(5)-C(4)	119.43(19)
C(6)-C(5)-H(5)	120.3
C(4)-C(5)-H(5)	120.3
C(7)-C(6)-C(5)	119.85(19)
C(7)-C(6)-H(6)	120.1
C(5)-C(6)-H(6)	120.1
C(6)-C(7)-C(8)	121.72(19)
C(6)-C(7)-H(7)	119.1
C(8)-C(7)-H(7)	119.1
C(7)-C(8)-C(3)	118.60(17)
C(7)-C(8)-C(9)	121.41(17)
C(3)-C(8)-C(9)	119.99(16)
C(8)-C(9)-C(14)	111.29(16)
C(8)-C(9)-C(10)	113.78(16)
C(14)-C(9)-C(10)	110.38(16)
C(8)-C(9)-H(9)	107.0
C(14)-C(9)-H(9)	107.0
C(10)-C(9)-H(9)	107.0
C(11)-C(10)-C(9)	111.28(17)
C(11)-C(10)-H(10A)	109.4

C(9)-C(10)-H(10A)	109.4
C(11)-C(10)-H(10B)	109.4
C(9)-C(10)-H(10B)	109.4
H(10A)-C(10)-H(10B)	108.0
C(17)-C(11)-C(10)	110.76(19)
C(17)-C(11)-C(12)	111.03(18)
C(10)-C(11)-C(12)	109.06(17)
C(17)-C(11)-H(11)	108.6
C(10)-C(11)-H(11)	108.6
C(12)-C(11)-H(11)	108.6
C(11)-C(12)-C(13)	110.76(17)
C(11)-C(12)-H(12A)	109.5
C(13)-C(12)-H(12A)	109.5
C(11)-C(12)-H(12B)	109.5
C(13)-C(12)-H(12B)	109.5
H(12A)-C(12)-H(12B)	108.1
C(15)-C(13)-C(12)	107.97(17)
C(15)-C(13)-C(14)	110.64(17)
C(12)-C(13)-C(14)	112.40(18)
C(15)-C(13)-H(13)	108.6
C(12)-C(13)-H(13)	108.6
C(14)-C(13)-H(13)	108.6
C(1)-C(14)-C(9)	112.50(15)
C(1)-C(14)-C(13)	108.60(17)
C(9)-C(14)-C(13)	111.16(15)
C(1)-C(14)-H(14)	108.1
C(9)-C(14)-H(14)	108.1
C(13)-C(14)-H(14)	108.1
O(1)-C(15)-C(16)	121.7(3)
O(1)-C(15)-C(13)	120.5(2)
C(16)-C(15)-C(13)	117.8(2)
C(15)-C(16)-H(16A)	109.5
C(15)-C(16)-H(16B)	109.5
H(16A)-C(16)-H(16B)	109.5
C(15)-C(16)-H(16C)	109.5
H(16A)-C(16)-H(16C)	109.5

H(16B)-C(16)-H(16C)	109.5
O(2)-C(17)-C(18)	122.3(2)
O(2)-C(17)-C(11)	121.6(2)
C(18)-C(17)-C(11)	116.11(19)
C(17)-C(18)-C(19)	114.7(2)
C(17)-C(18)-H(18A)	108.6
C(19)-C(18)-H(18A)	108.6
C(17)-C(18)-H(18B)	108.6
C(19)-C(18)-H(18B)	108.6
H(18A)-C(18)-H(18B)	107.6
C(18)-C(19)-H(19A)	109.5
C(18)-C(19)-H(19B)	109.5
H(19A)-C(19)-H(19B)	109.5
C(18)-C(19)-H(19C)	109.5
H(19A)-C(19)-H(19C)	109.5
H(19B)-C(19)-H(19C)	109.5
N(1)-C(20)-C(21)	124.6(2)
N(1)-C(20)-H(20)	117.7
C(21)-C(20)-H(20)	117.7
C(20)-C(21)-C(22)	119.9(2)
C(20)-C(21)-H(21)	120.1
C(22)-C(21)-H(21)	120.1
N(2)-C(22)-C(21)	122.7(3)
N(2)-C(22)-C(23)	121.6(3)
C(21)-C(22)-C(23)	115.7(2)
C(24)-C(23)-C(22)	120.2(2)
C(24)-C(23)-H(23)	119.9
C(22)-C(23)-H(23)	119.9
N(1)-C(24)-C(23)	124.3(2)
N(1)-C(24)-H(24)	117.9
C(23)-C(24)-H(24)	117.9
N(2)-C(25)-H(25A)	109.5
N(2)-C(25)-H(25B)	109.5
H(25A)-C(25)-H(25B)	109.5
N(2)-C(25)-H(25C)	109.5
H(25A)-C(25)-H(25C)	109.5

H(25B)-C(25)-H(25C)	109.5
N(2)-C(26)-H(26A)	109.5
N(2)-C(26)-H(26B)	109.5
H(26A)-C(26)-H(26B)	109.5
N(2)-C(26)-H(26C)	109.5
H(26A)-C(26)-H(26C)	109.5
H(26B)-C(26)-H(26C)	109.5
N(4)-C(27)-C(28)	109.2(2)
N(4)-C(27)-H(27)	125.4
C(28)-C(27)-H(27)	125.4
C(27)-C(28)-C(29)	104.4(2)
C(27)-C(28)-H(28)	127.8
C(29)-C(28)-H(28)	127.8
N(3)-C(29)-C(28)	111.0(2)
N(3)-C(29)-H(29)	124.5
C(28)-C(29)-H(29)	124.5
N(6)-C(30)-C(31)	108.1(2)
N(6)-C(30)-H(30)	126.0
C(31)-C(30)-H(30)	126.0
C(30)-C(31)-C(32)	105.7(2)
C(30)-C(31)-H(31)	127.1
C(32)-C(31)-H(31)	127.1
N(5)-C(32)-C(31)	109.5(2)
N(5)-C(32)-H(32)	125.2
C(31)-C(32)-H(32)	125.2
N(8)-C(33)-C(34)	109.2(2)
N(8)-C(33)-H(33)	125.4
C(34)-C(33)-H(33)	125.4
C(33)-C(34)-C(35)	104.5(2)
C(33)-C(34)-H(34)	127.7
C(35)-C(34)-H(34)	127.7
N(7)-C(35)-C(34)	110.5(2)
N(7)-C(35)-H(35)	124.8
C(34)-C(35)-H(35)	124.8
O(4)-C(36)-C(37)	110.1(5)
O(4)-C(36)-H(36A)	109.6

C(37)-C(36)-H(36A)	109.6
O(4)-C(36)-H(36B)	109.6
C(37)-C(36)-H(36B)	109.6
H(36A)-C(36)-H(36B)	108.2
C(38)-C(37)-C(36)	99.8(6)
C(38)-C(37)-H(37A)	111.8
C(36)-C(37)-H(37A)	111.8
C(38)-C(37)-H(37B)	111.8
C(36)-C(37)-H(37B)	111.8
H(37A)-C(37)-H(37B)	109.5
C(37)-C(38)-C(39)	109.5(6)
C(37)-C(38)-H(38A)	109.8
C(39)-C(38)-H(38A)	109.8
C(37)-C(38)-H(38B)	109.8
C(39)-C(38)-H(38B)	109.8
H(38A)-C(38)-H(38B)	108.2
O(4)-C(39)-C(38)	103.8(5)
O(4)-C(39)-H(39A)	111.0
C(38)-C(39)-H(39A)	111.0
O(4)-C(39)-H(39B)	111.0
C(38)-C(39)-H(39B)	111.0
H(39A)-C(39)-H(39B)	109.0
O(5)-C(40)-C(41)	106.2(9)
O(5)-C(40)-H(40A)	110.5
C(41)-C(40)-H(40A)	110.5
O(5)-C(40)-H(40B)	110.5
C(41)-C(40)-H(40B)	110.5
H(40A)-C(40)-H(40B)	108.7
C(40)-C(41)-C(42)	106.7(9)
C(40)-C(41)-H(41A)	110.4
C(42)-C(41)-H(41A)	110.4
C(40)-C(41)-H(41B)	110.4
C(42)-C(41)-H(41B)	110.4
H(41A)-C(41)-H(41B)	108.6
C(43)-C(42)-C(41)	104.0(10)
C(43)-C(42)-H(42A)	111.0

C(41)-C(42)-H(42A)	111.0
C(43)-C(42)-H(42B)	111.0
C(41)-C(42)-H(42B)	111.0
H(42A)-C(42)-H(42B)	109.0
O(5)-C(43)-C(42)	112.6(11)
O(5)-C(43)-H(43A)	109.1
C(42)-C(43)-H(43A)	109.1
O(5)-C(43)-H(43B)	109.1
C(42)-C(43)-H(43B)	109.1
H(43A)-C(43)-H(43B)	107.8
N(8)-B(1)-N(6)	107.6(2)
N(8)-B(1)-N(4)	109.9(2)
N(6)-B(1)-N(4)	108.3(2)
N(8)-B(1)-H(1B)	107.5(19)
N(6)-B(1)-H(1B)	109.9(19)
N(4)-B(1)-H(1B)	113.6(19)

Symmetry transformations used to generate equivalent atoms:

Compound 90

Table 4. Anisotropic displacement parameters ($\text{\AA}^2 \times 10^3$) for C₃₁H₅₄BN₉O_{4.5}Mo. The anisotropic displacement factor exponent takes the form: $-2\pi^2 [h^2 a^{*2} U^{11} + \dots + 2 h k a^* b^* U^{12}]$

	U ¹¹	U ²²	U ³³	U ²³	U ¹³	U ¹²
Mo	25(1)	24(1)	20(1)	4(1)	1(1)	3(1)
O(1)	60(1)	31(1)	51(1)	1(1)	-1(1)	-8(1)
O(2)	76(2)	47(1)	33(1)	-12(1)	-14(1)	17(1)
O(3)	30(1)	58(1)	32(1)	17(1)	5(1)	-2(1)
O(4)	111(3)	89(2)	59(2)	-18(2)	26(2)	-18(2)
O(5)	103(6)	361(18)	68(5)	-86(8)	-12(4)	98(9)
N(1)	28(1)	27(1)	23(1)	2(1)	0(1)	0(1)
N(2)	82(2)	35(1)	46(1)	-10(1)	-15(1)	-2(1)
N(3)	30(1)	26(1)	27(1)	6(1)	5(1)	2(1)
N(4)	37(1)	26(1)	27(1)	7(1)	5(1)	4(1)
N(5)	30(1)	35(1)	25(1)	7(1)	2(1)	7(1)
N(6)	36(1)	38(1)	28(1)	12(1)	4(1)	14(1)
N(7)	42(1)	29(1)	25(1)	2(1)	2(1)	9(1)
N(8)	54(1)	26(1)	33(1)	3(1)	6(1)	12(1)
N(9)	25(1)	32(1)	22(1)	6(1)	1(1)	3(1)
C(1)	25(1)	25(1)	25(1)	4(1)	1(1)	-1(1)
C(2)	26(1)	25(1)	23(1)	3(1)	3(1)	2(1)
C(3)	21(1)	25(1)	22(1)	2(1)	1(1)	2(1)
C(4)	28(1)	26(1)	27(1)	-1(1)	3(1)	2(1)
C(5)	30(1)	23(1)	36(1)	-2(1)	1(1)	2(1)
C(6)	34(1)	25(1)	34(1)	6(1)	-2(1)	-2(1)
C(7)	32(1)	29(1)	24(1)	6(1)	1(1)	-1(1)
C(8)	23(1)	24(1)	22(1)	2(1)	-1(1)	0(1)
C(9)	24(1)	27(1)	23(1)	0(1)	-1(1)	2(1)
C(10)	30(1)	34(1)	22(1)	-2(1)	-2(1)	4(1)
C(11)	30(1)	30(1)	26(1)	-3(1)	-5(1)	6(1)
C(12)	29(1)	33(1)	34(1)	-2(1)	-8(1)	1(1)
C(13)	26(1)	26(1)	29(1)	-1(1)	-2(1)	1(1)
C(14)	25(1)	24(1)	25(1)	0(1)	-3(1)	3(1)
C(15)	31(1)	37(1)	40(1)	2(1)	-4(1)	-3(1)

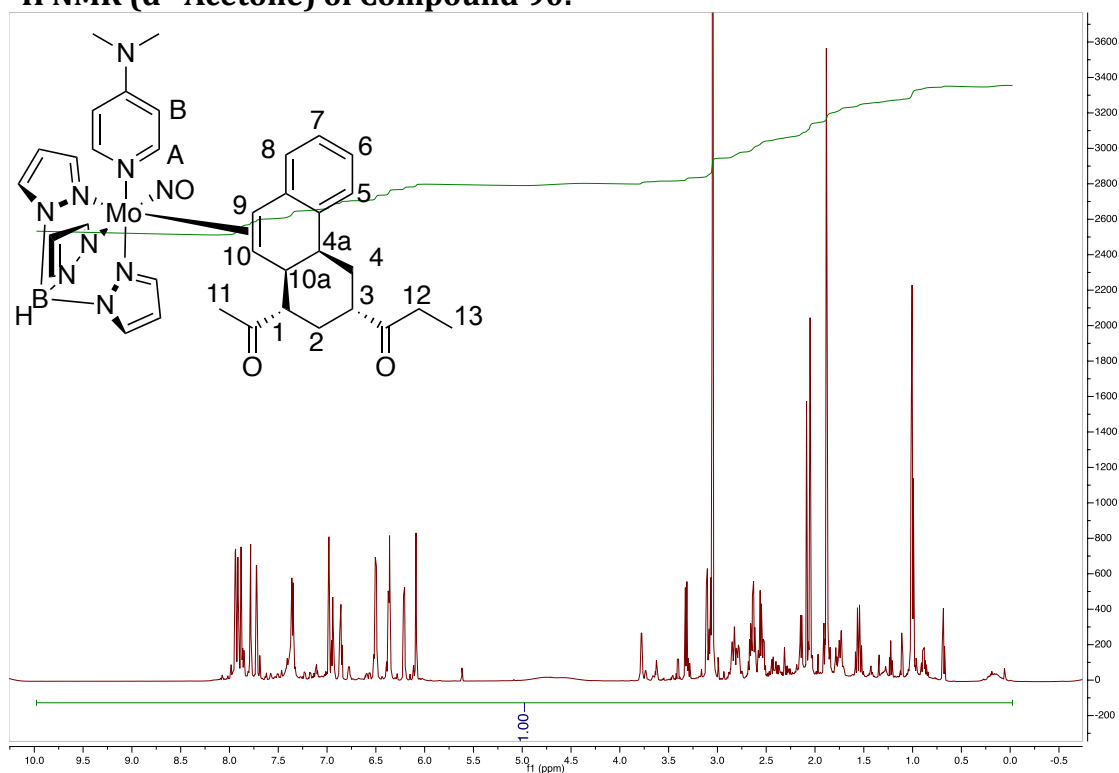
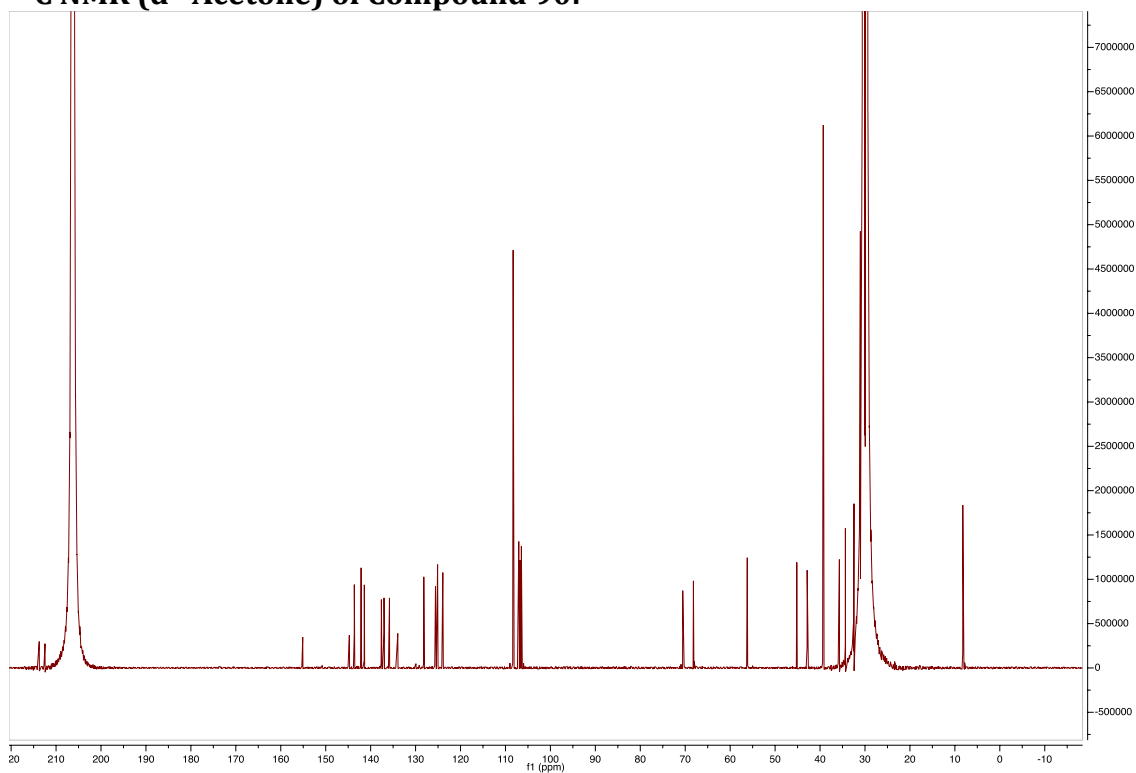
C(16)	49(2)	61(2)	87(3)	9(2)	31(2)	3(2)
C(17)	31(1)	35(1)	29(1)	-2(1)	-7(1)	5(1)
C(18)	29(1)	37(1)	41(1)	7(1)	-5(1)	3(1)
C(19)	35(1)	69(2)	44(1)	23(1)	1(1)	8(1)
C(20)	45(1)	35(1)	25(1)	0(1)	5(1)	-3(1)
C(21)	53(2)	40(1)	27(1)	-4(1)	2(1)	-1(1)
C(22)	48(1)	29(1)	38(1)	-6(1)	-5(1)	4(1)
C(23)	44(1)	25(1)	40(1)	2(1)	-2(1)	1(1)
C(24)	36(1)	28(1)	29(1)	3(1)	0(1)	1(1)
C(25)	105(3)	56(2)	45(2)	-18(1)	-17(2)	1(2)
C(26)	131(4)	35(1)	65(2)	-4(1)	-30(2)	-22(2)
C(27)	42(1)	33(1)	33(1)	11(1)	5(1)	-1(1)
C(28)	37(1)	42(1)	37(1)	14(1)	10(1)	1(1)
C(29)	32(1)	34(1)	34(1)	8(1)	9(1)	4(1)
C(30)	35(1)	62(2)	39(1)	19(1)	2(1)	19(1)
C(31)	28(1)	76(2)	52(2)	17(2)	-4(1)	11(1)
C(32)	26(1)	50(1)	38(1)	11(1)	1(1)	3(1)
C(33)	79(2)	31(1)	46(1)	-2(1)	12(1)	16(1)
C(34)	90(3)	40(1)	40(1)	-10(1)	9(2)	20(2)
C(35)	57(2)	41(1)	27(1)	-2(1)	5(1)	16(1)
C(36)	124(5)	66(3)	68(3)	-2(2)	-2(3)	-9(3)
C(37)	122(5)	95(4)	86(4)	-3(3)	6(3)	-25(4)
C(38)	157(8)	82(4)	239(11)	47(6)	69(7)	16(5)
C(39)	156(7)	181(8)	70(3)	-13(4)	12(4)	88(6)
C(40)	80(6)	117(9)	81(6)	24(6)	-2(5)	-17(6)
C(41)	80(6)	121(9)	124(9)	-80(8)	35(6)	-15(6)
C(42)	123(10)	159(12)	55(5)	-22(6)	-17(6)	33(9)
C(43)	138(13)	260(20)	109(10)	-45(12)	15(9)	122(14)
B(1)	47(1)	28(1)	34(1)	8(1)	7(1)	13(1)

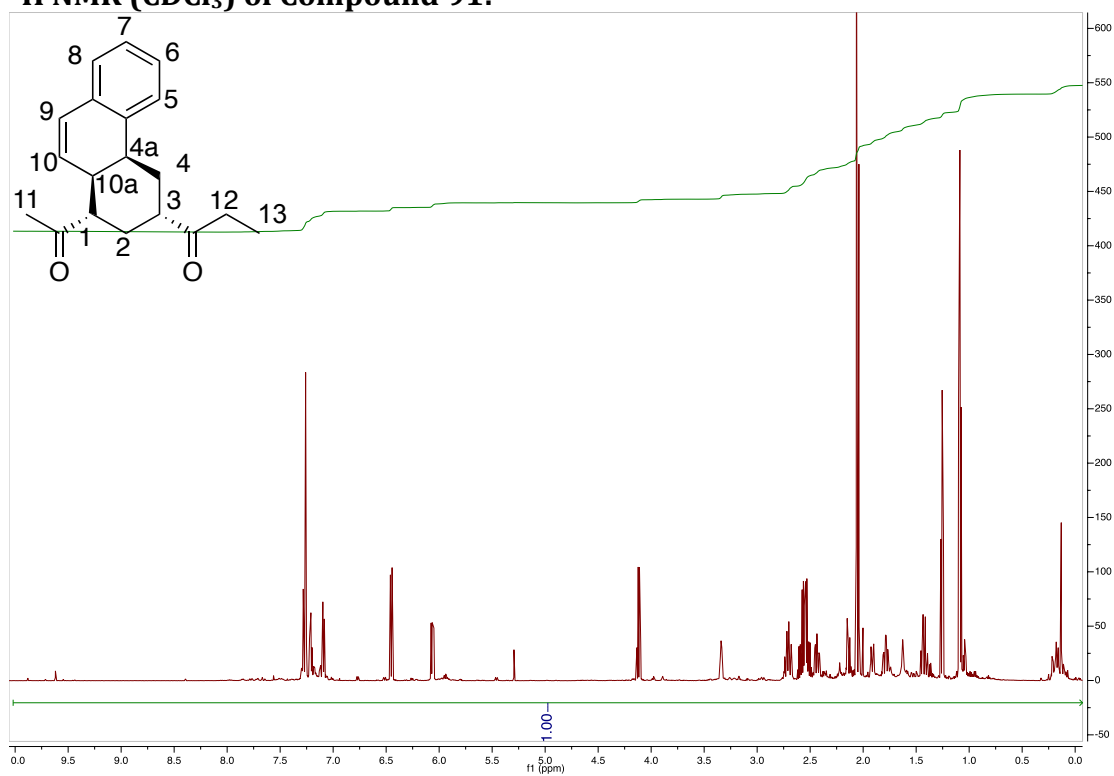
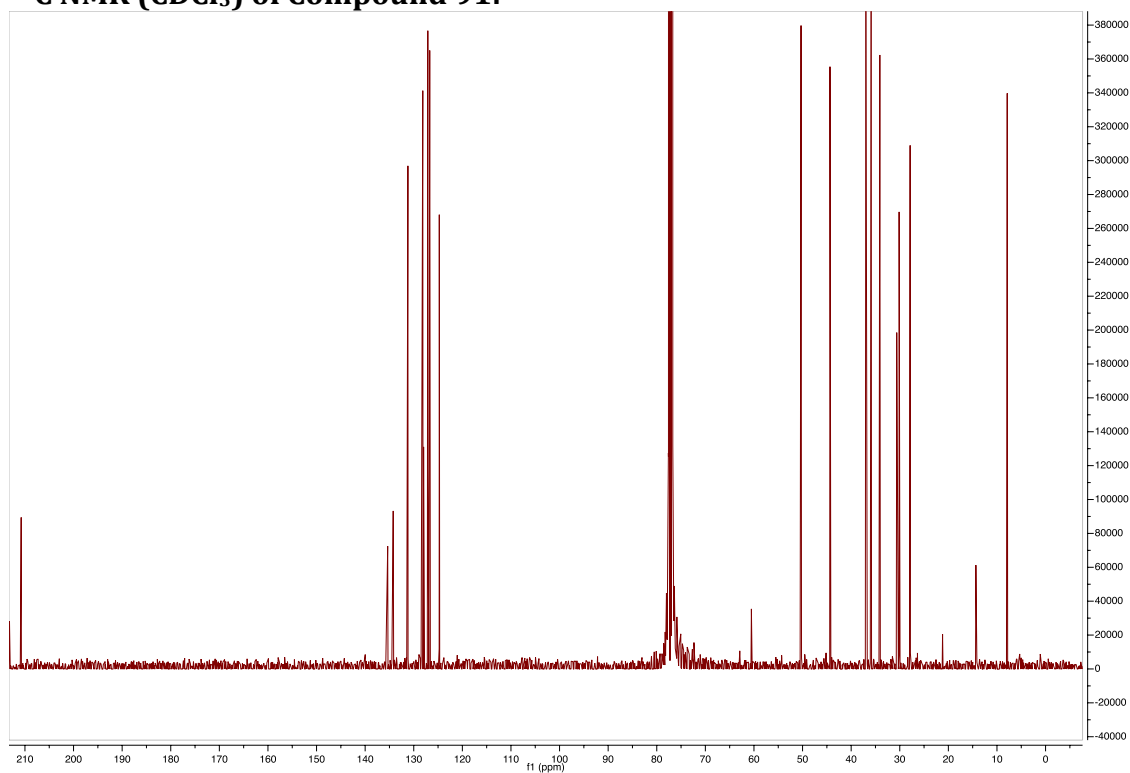
Compound 90

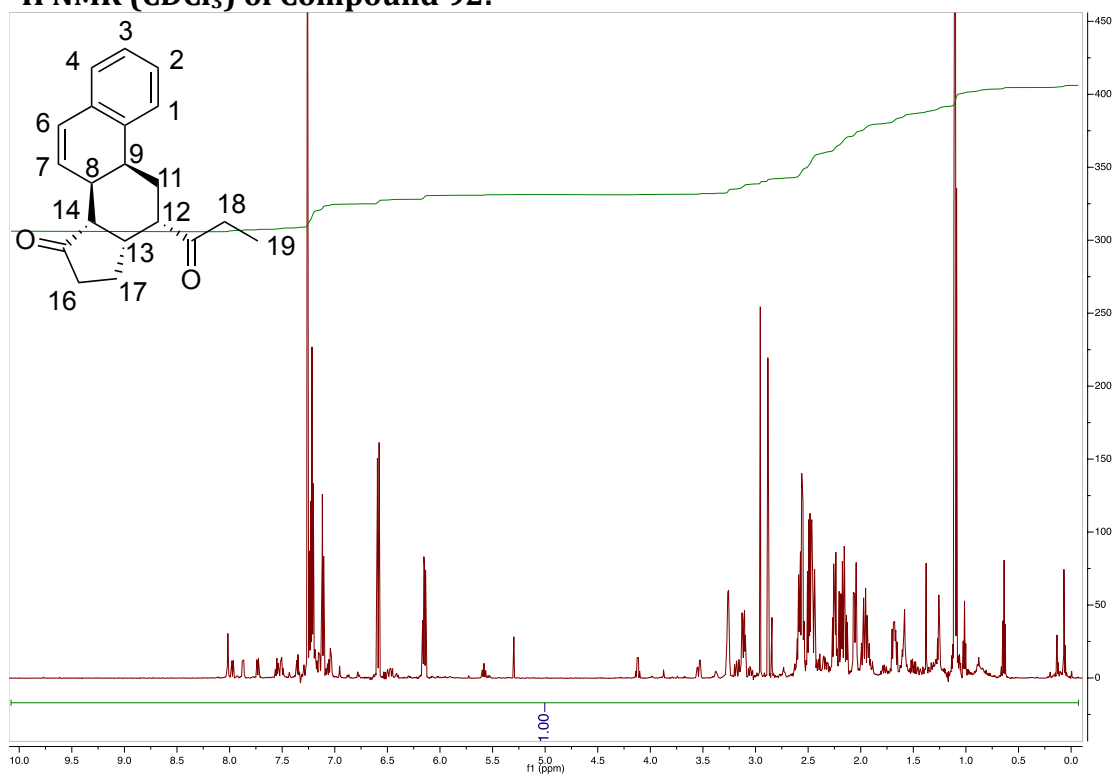
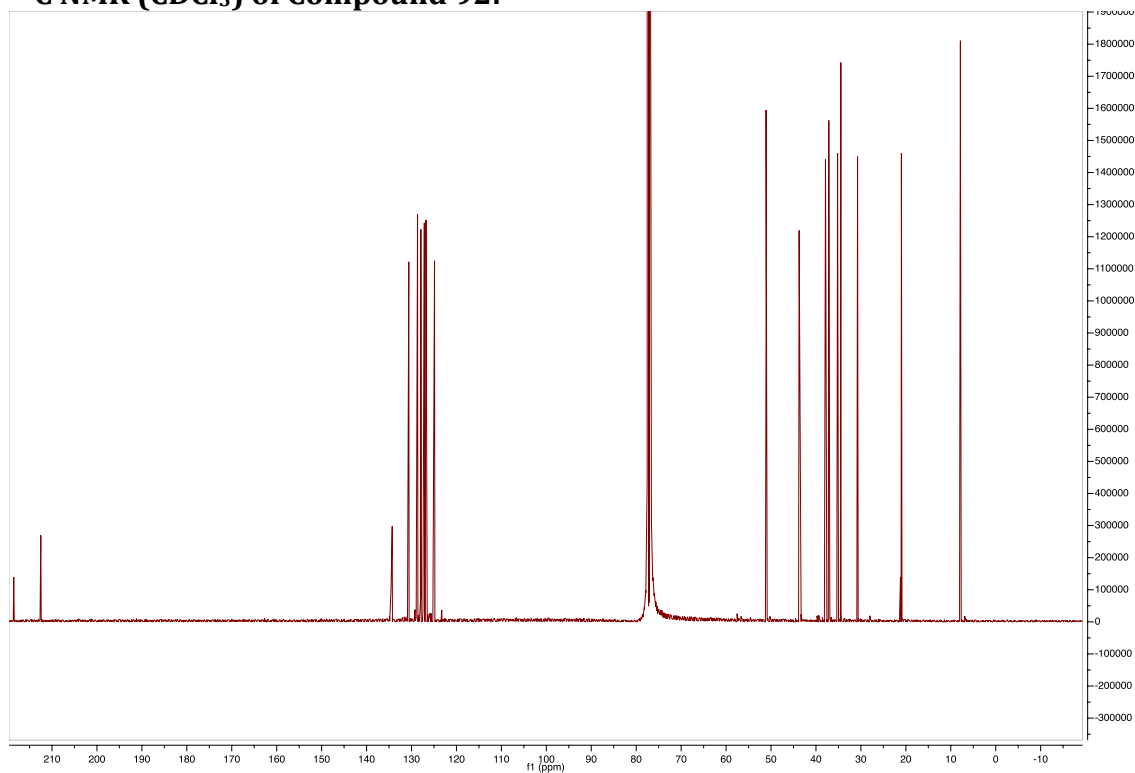
Table 5. Hydrogen coordinates ($\times 10^4$) and isotropic displacement parameters ($\text{\AA}^2 \times 10^{-3}$) for C₃₁H₅₄BN₉O_{4.5}Mo.

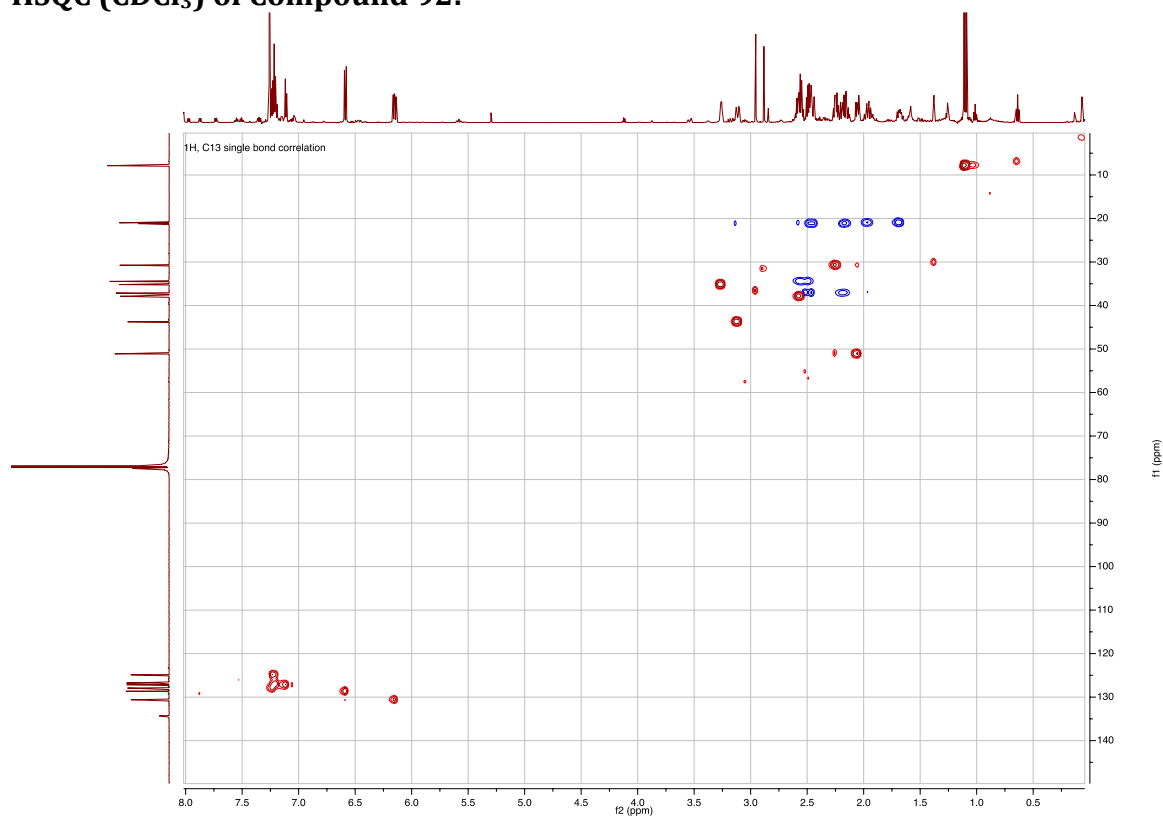
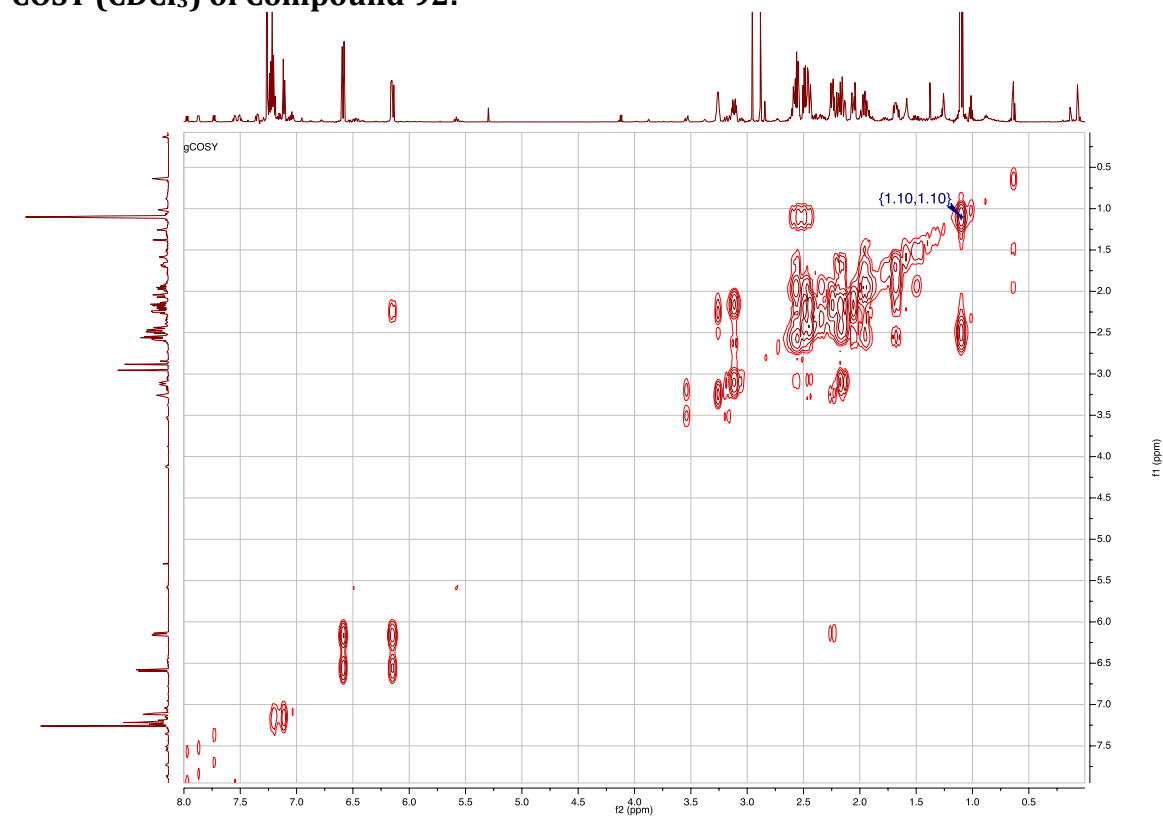
	x	y	z	U(eq)
H(1)	7387	6958	3591	30
H(2)	7198	5976	3141	30
H(4)	6774	4734	3117	33
H(5)	6918	3715	3635	36
H(6)	6745	3729	4619	38
H(7)	6499	4755	5081	34
H(9)	5452	6166	4647	31
H(10A)	6758	6447	5534	35
H(10B)	6502	5644	5526	35
H(11)	8763	5465	5292	36
H(12A)	10298	6405	5306	40
H(12B)	9097	6914	5424	40
H(13)	9080	6133	4383	34
H(14)	6914	7059	4580	30
H(16A)	10926	7466	3876	95
H(16B)	9955	6865	3583	95
H(16C)	11169	6705	4110	95
H(18A)	10454	5065	6129	44
H(18B)	8968	4798	6225	44
H(19A)	10839	5483	7097	75
H(19B)	10636	4677	7071	75
H(19C)	9392	5157	7187	75
H(20)	4471	6139	1935	42
H(21)	3565	5312	1294	49
H(23)	2802	4191	2663	45
H(24)	3774	5046	3259	38
H(25A)	1744	4638	777	108
H(25B)	1857	3831	715	108
H(25C)	3230	4287	813	108

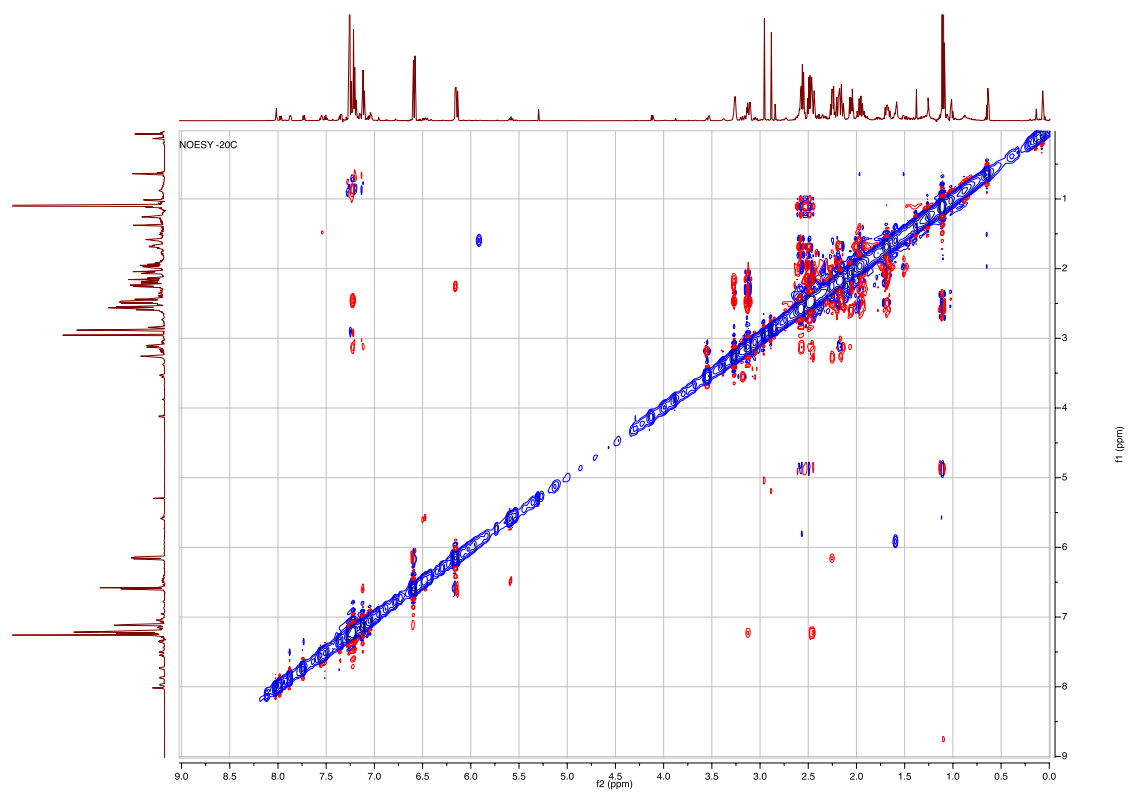
H(26A)	2589	3260	1926	123
H(26B)	1238	3317	1442	123
H(26C)	1276	3683	2053	123
H(27)	5506	8414	1748	43
H(28)	7413	7604	1627	46
H(29)	7236	6651	2324	40
H(30)	890	8055	2018	55
H(31)	-370	6955	2071	64
H(32)	1324	6154	2644	46
H(33)	3779	9137	3451	62
H(34)	4218	8787	4489	69
H(35)	4751	7532	4487	50
H(36A)	1583	8606	4941	106
H(36B)	1488	9239	5362	106
H(37A)	1274	8571	6111	123
H(37B)	436	8139	5580	123
H(38A)	2143	7433	5567	186
H(38B)	2575	7661	6228	186
H(39A)	4460	8153	6035	164
H(39B)	4109	7851	5389	164
H(40A)	139	4591	8493	113
H(40B)	1083	5221	8358	113
H(41A)	749	4728	9377	127
H(41B)	1587	5396	9242	127
H(42A)	3510	4879	9443	139
H(42B)	2682	4250	9665	139
H(43A)	3848	4288	8784	204
H(43B)	2828	3713	8952	204
H(1B)	3490(40)	8562(17)	2428(15)	46(9)

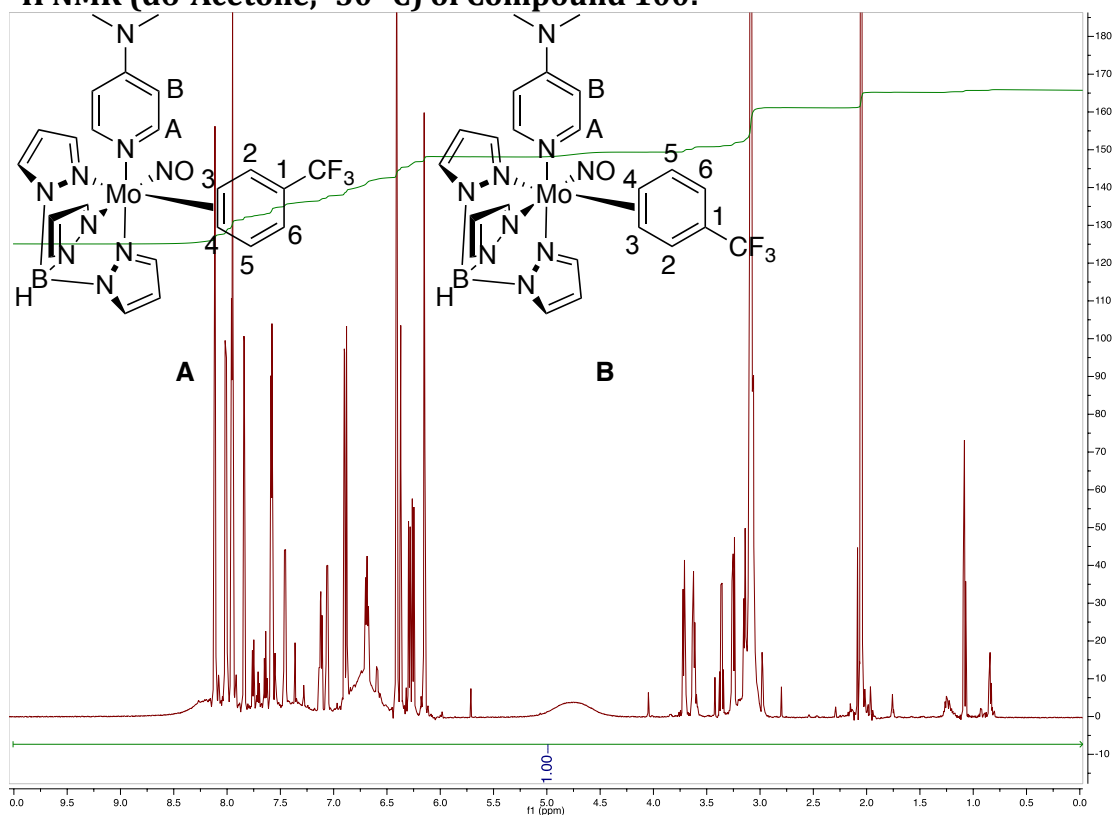
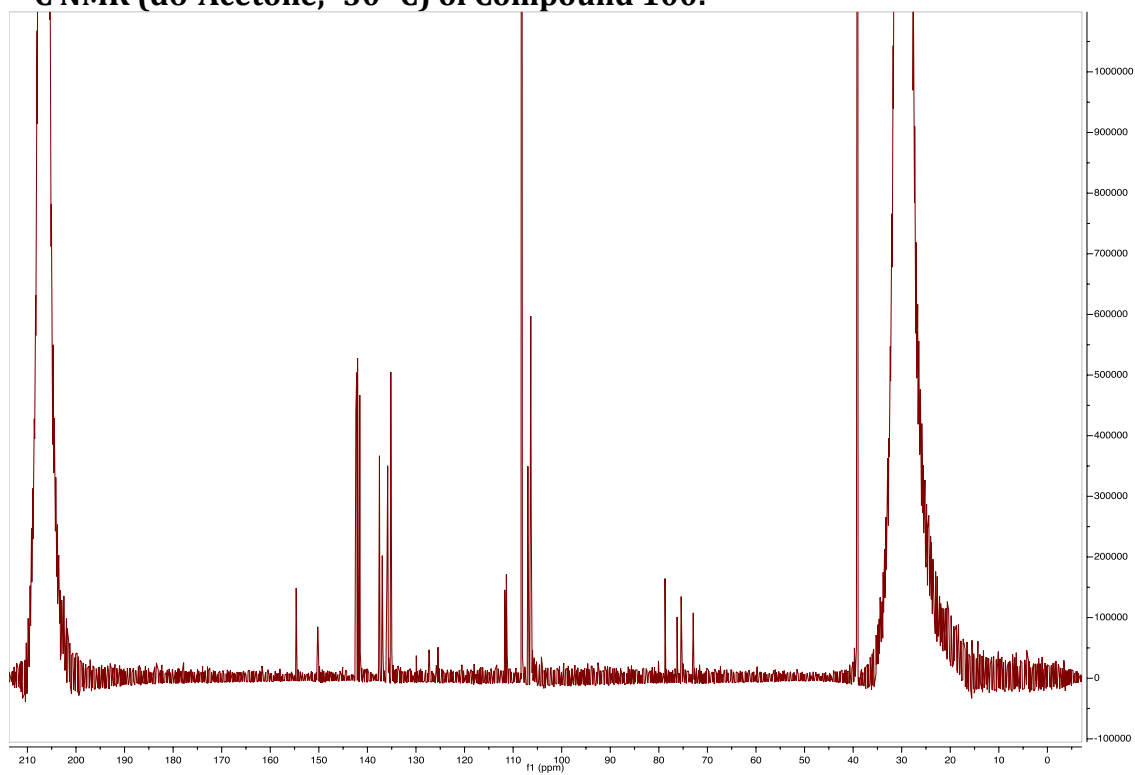
^1H NMR (d^6 -Acetone) of Compound 90: **^{13}C NMR (d^6 -Acetone) of Compound 90:**

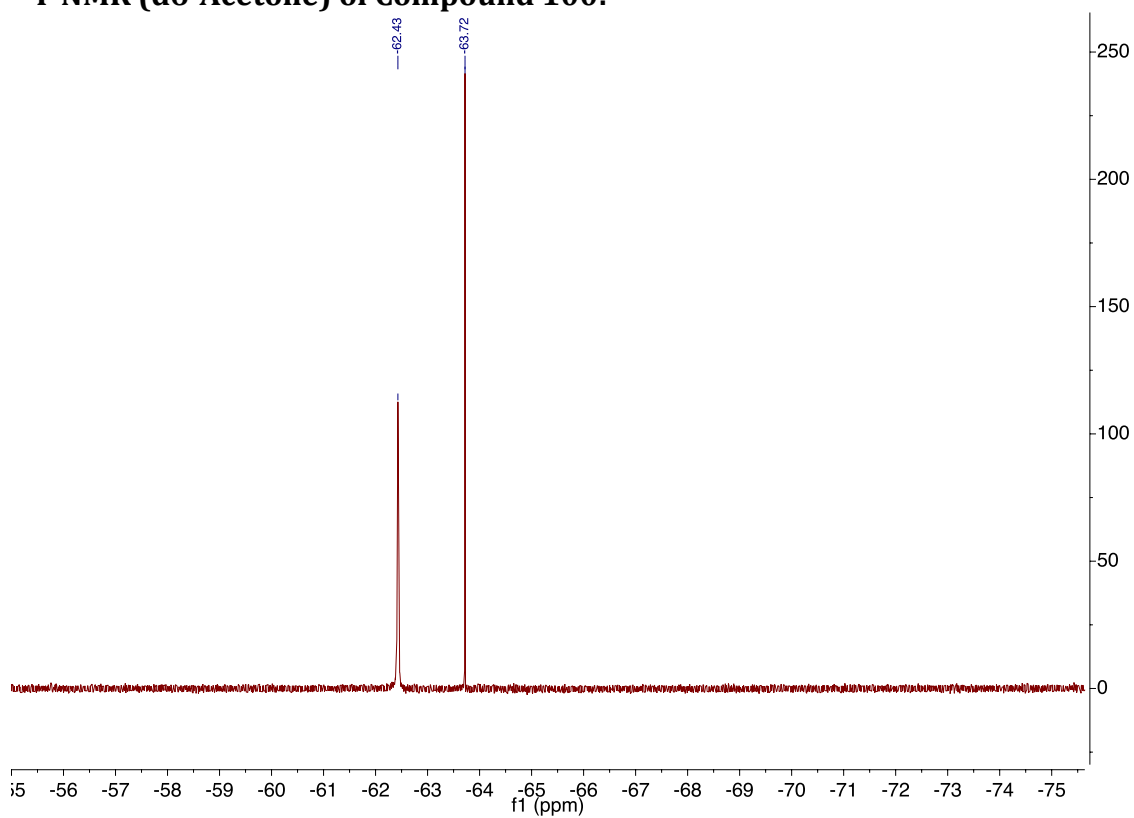
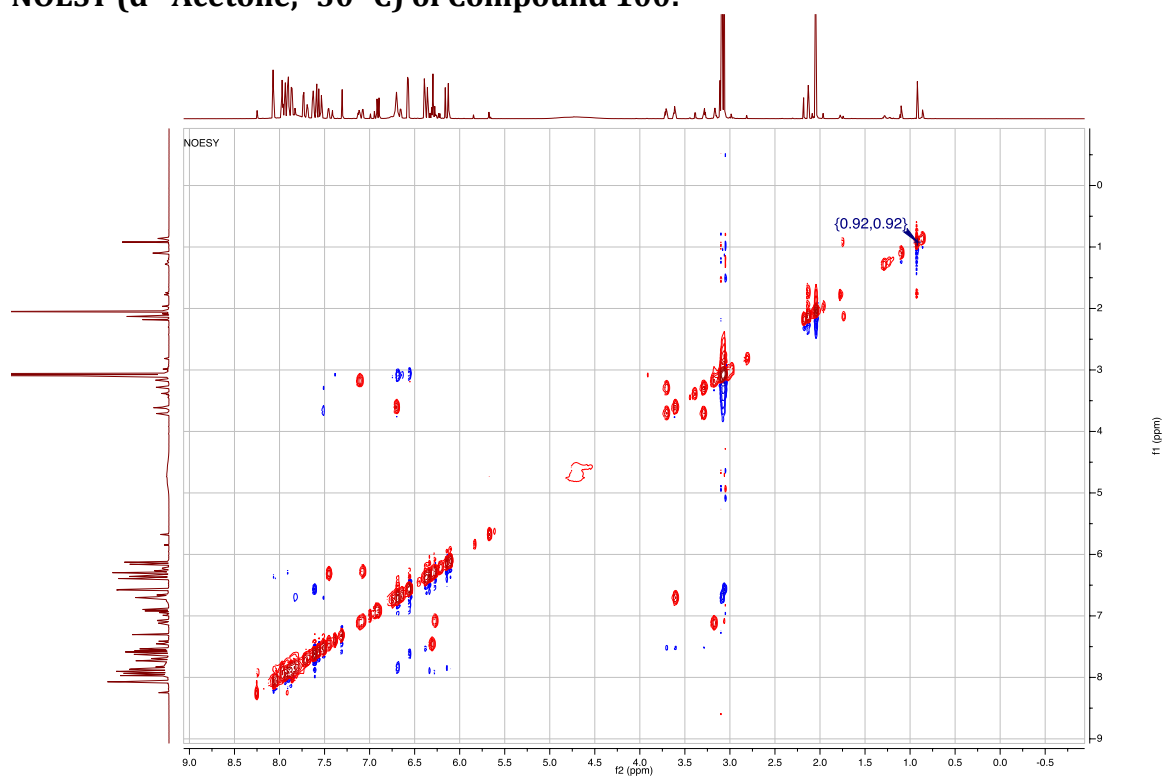
^1H NMR (CDCl_3) of Compound 91: **^{13}C NMR (CDCl_3) of Compound 91:**

^1H NMR (CDCl_3) of Compound 92: **^{13}C NMR (CDCl_3) of Compound 92:**

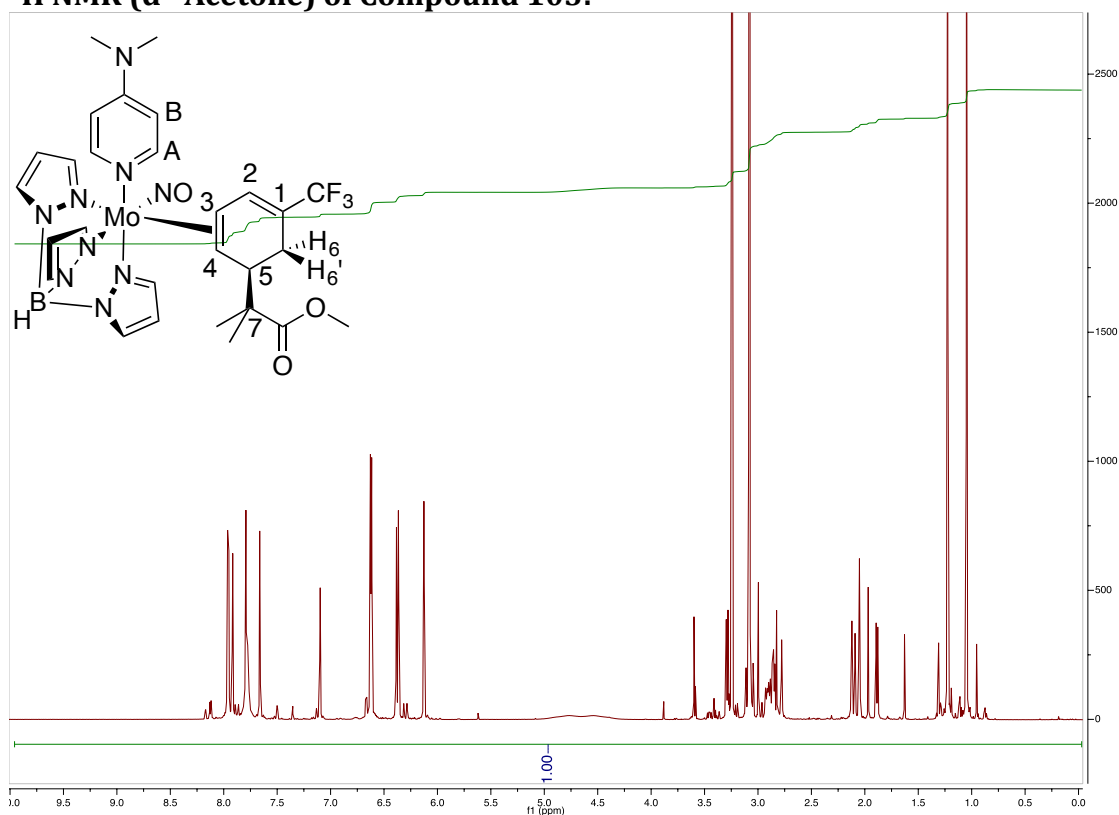
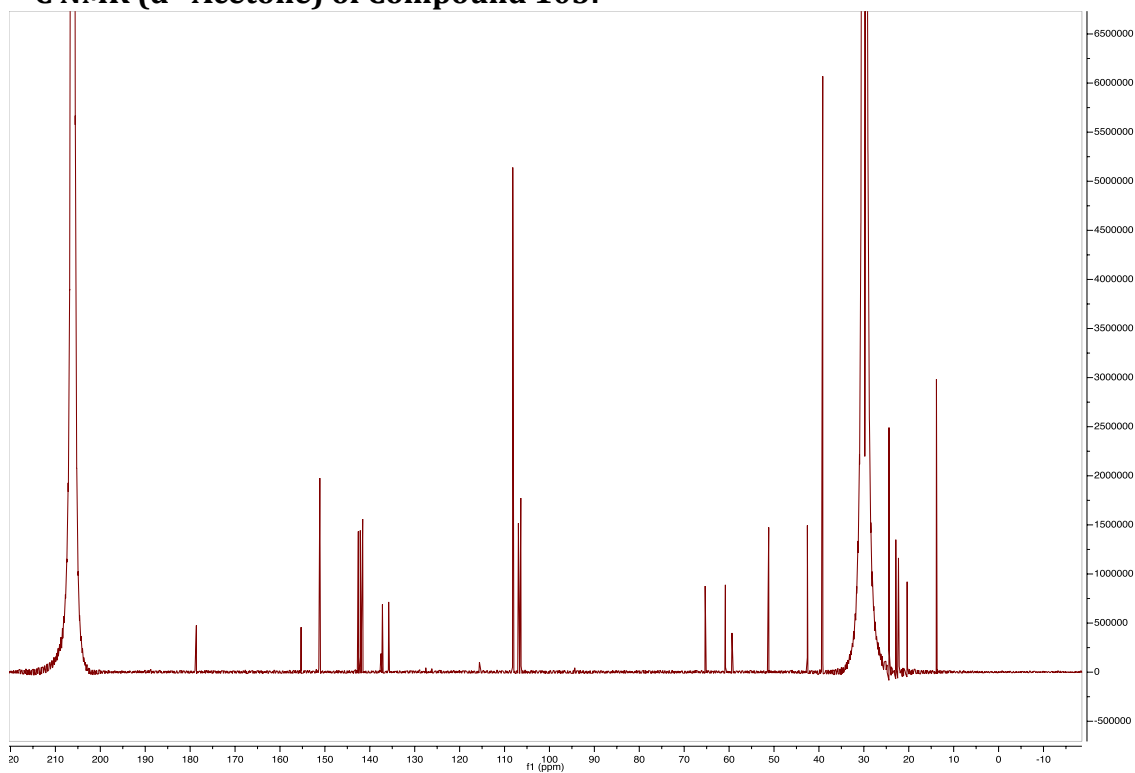
HSQC (CDCl₃) of Compound 92:**COSY (CDCl₃) of Compound 92:**

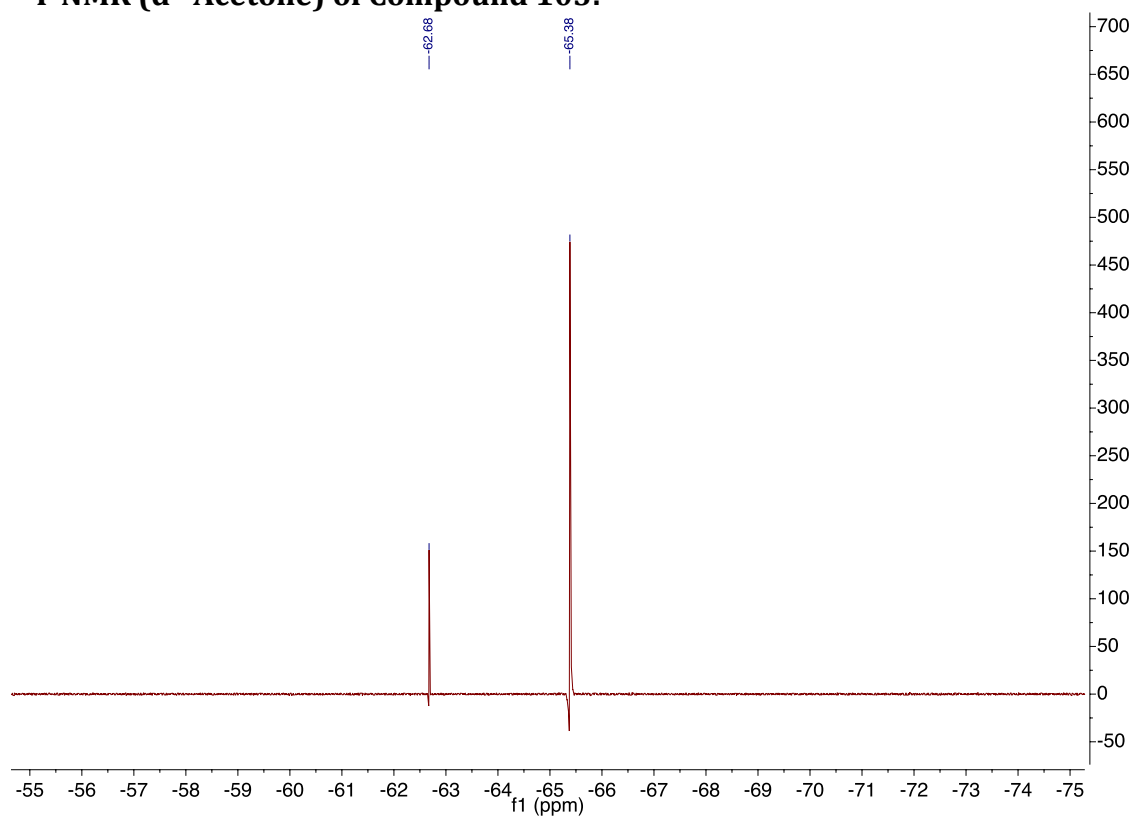
NOESY (CDCl₃) of Compound 92:

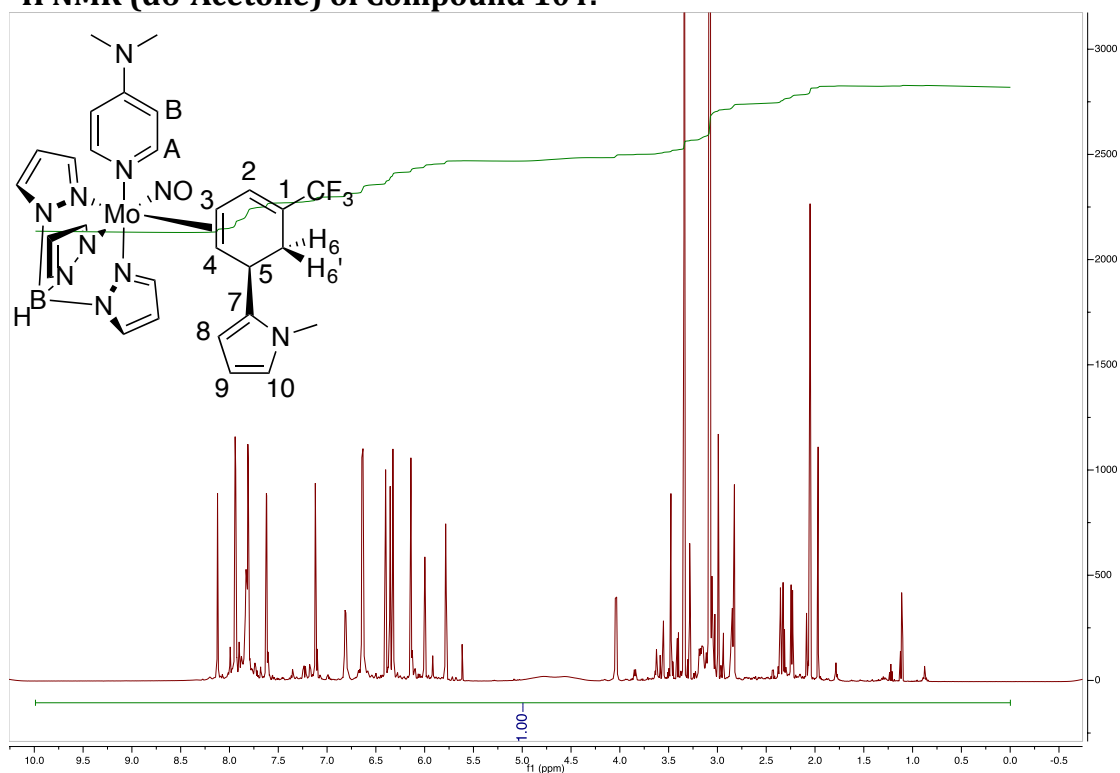
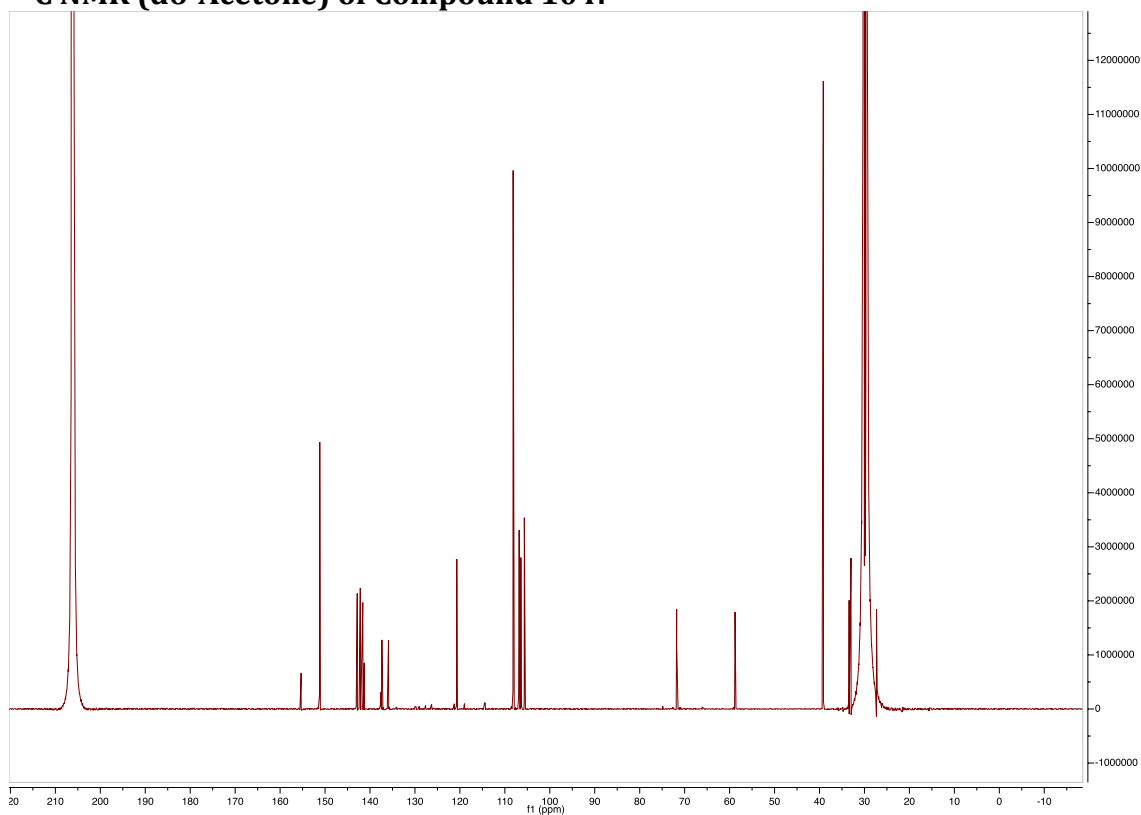
^1H NMR (d6-Acetone, -30 °C) of Compound 100: **^{13}C NMR (d6-Acetone, -30 °C) of Compound 100:**

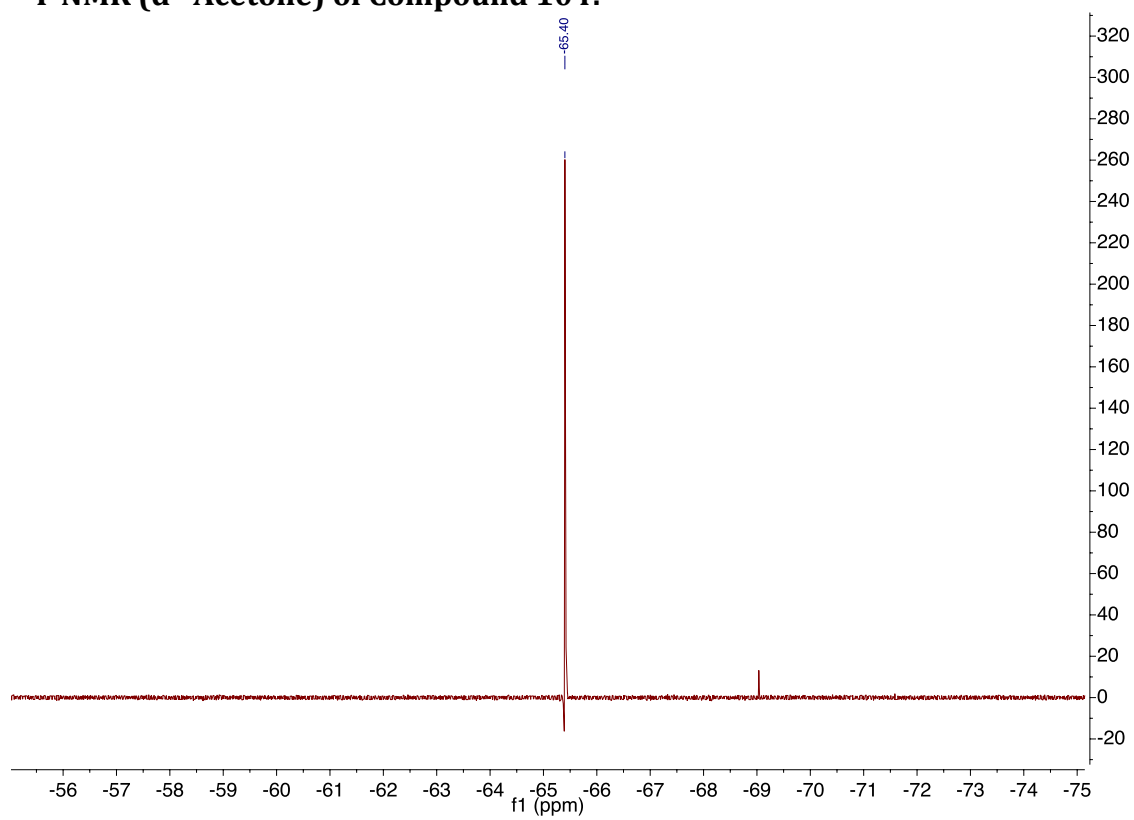
^{19}F NMR (d 6 -Acetone) of Compound 100:**NOESY (d 6 -Acetone, -30 °C) of Compound 100:**

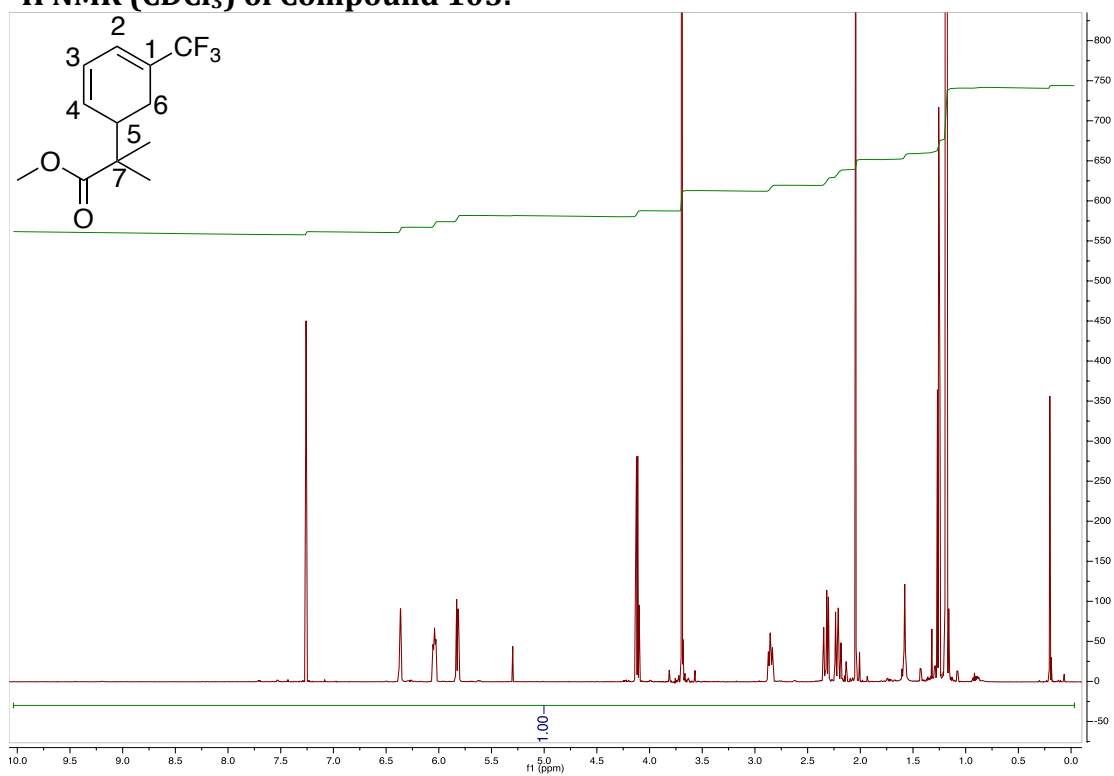
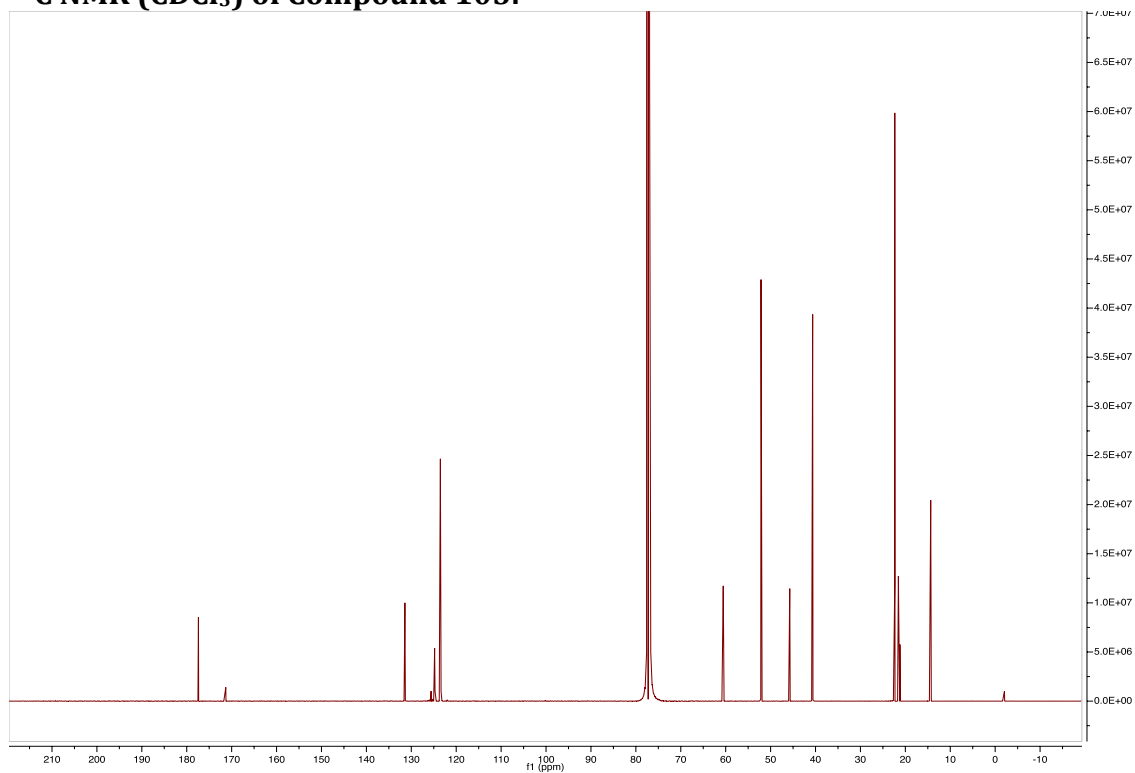
COSY (d⁶-Acetone, -30 °C) of Compound 100:

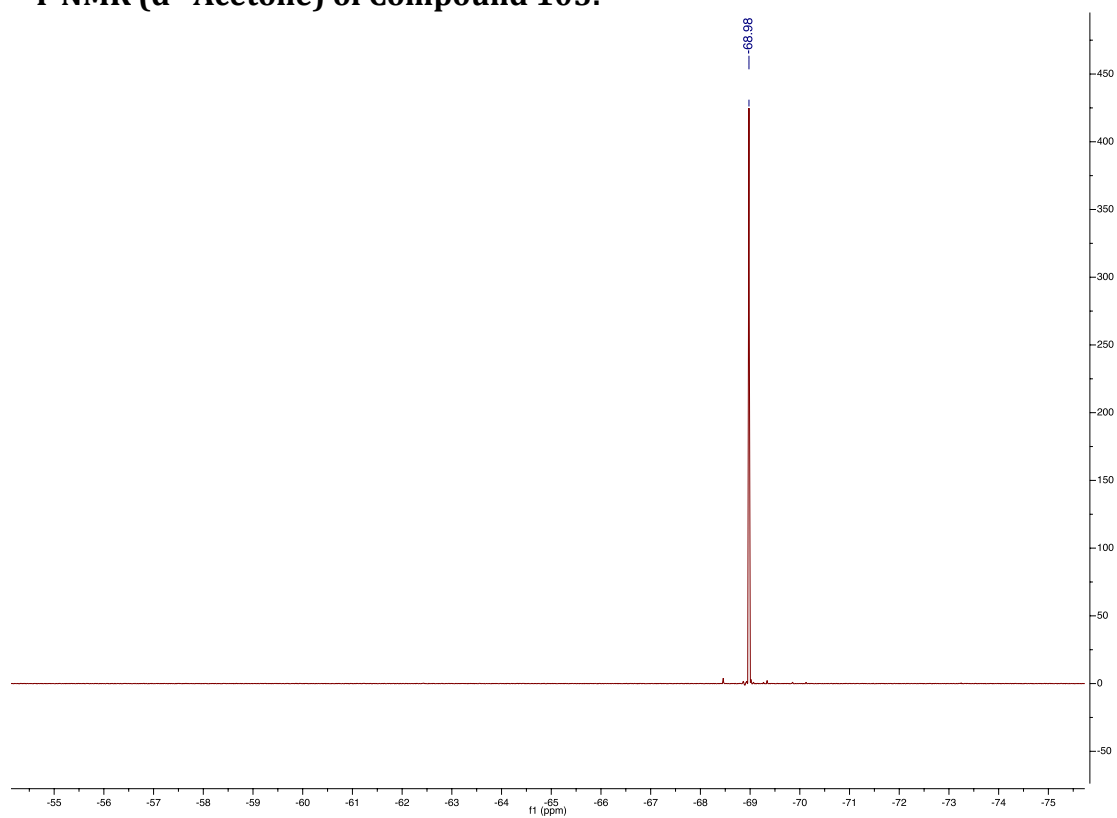
^1H NMR ($\text{d}^6\text{-Acetone}$) of Compound 103: **^{13}C NMR ($\text{d}^6\text{-Acetone}$) of Compound 103:**

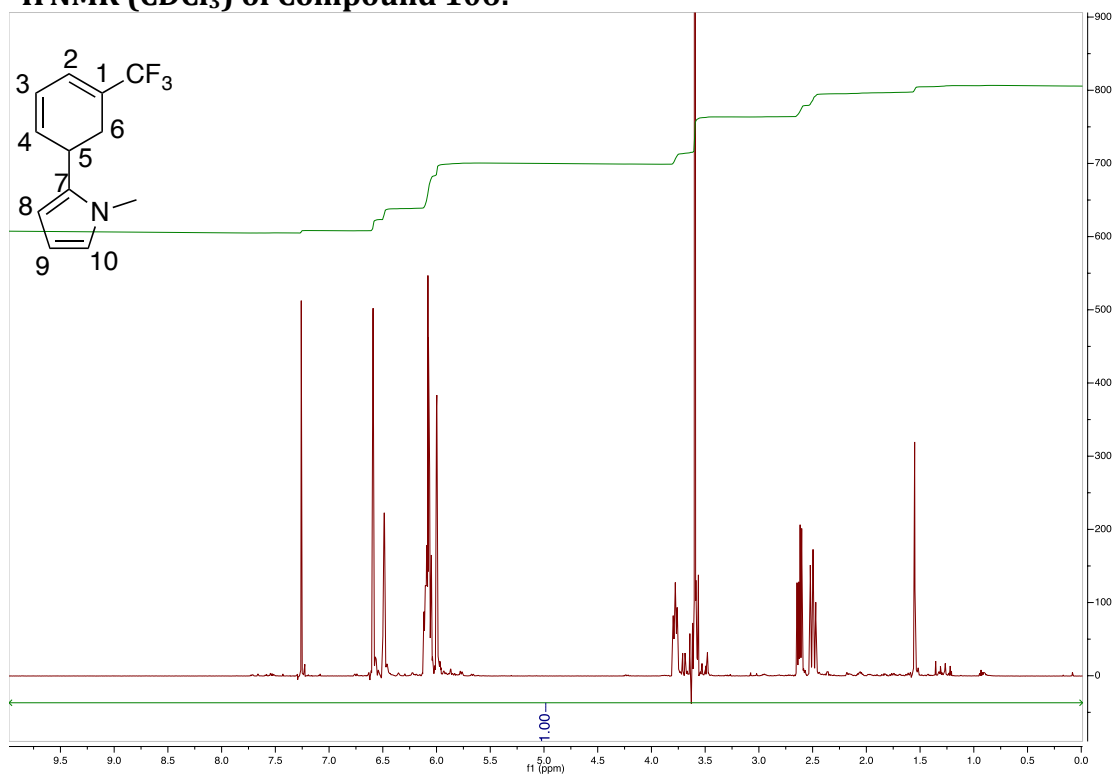
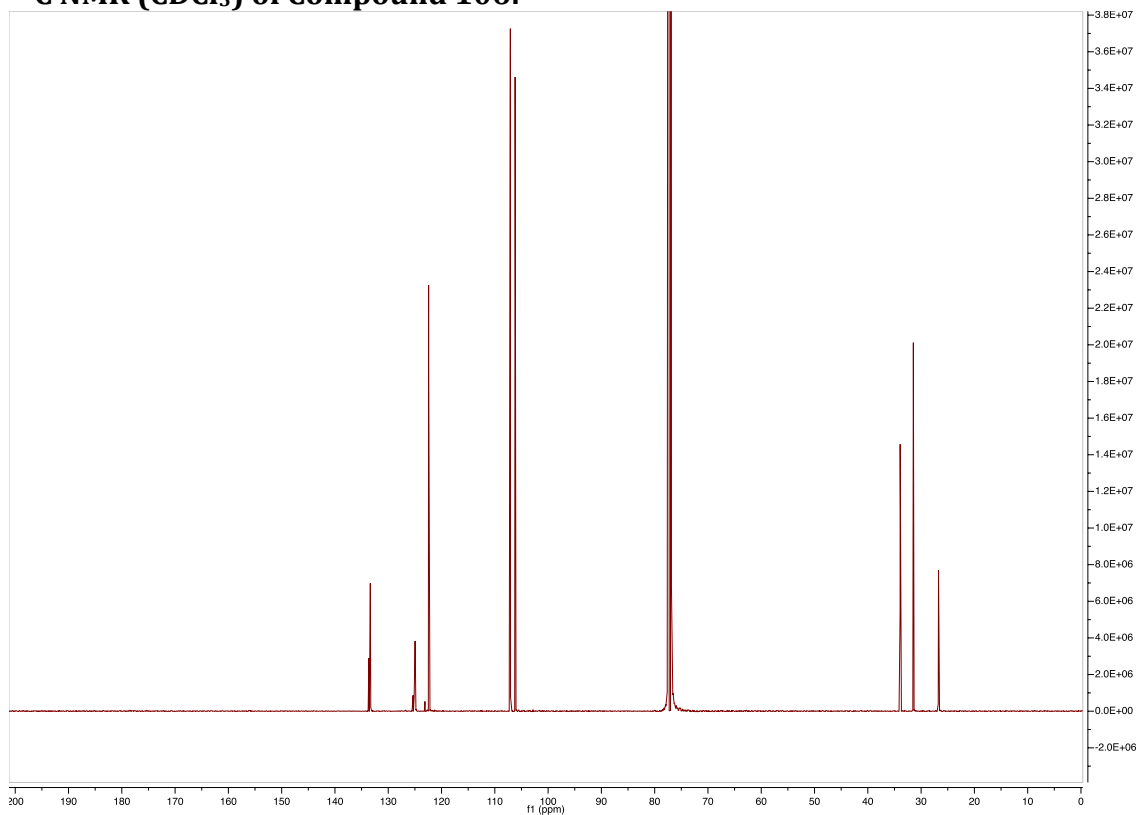
^{19}F NMR (d^6 -Acetone) of Compound 103:

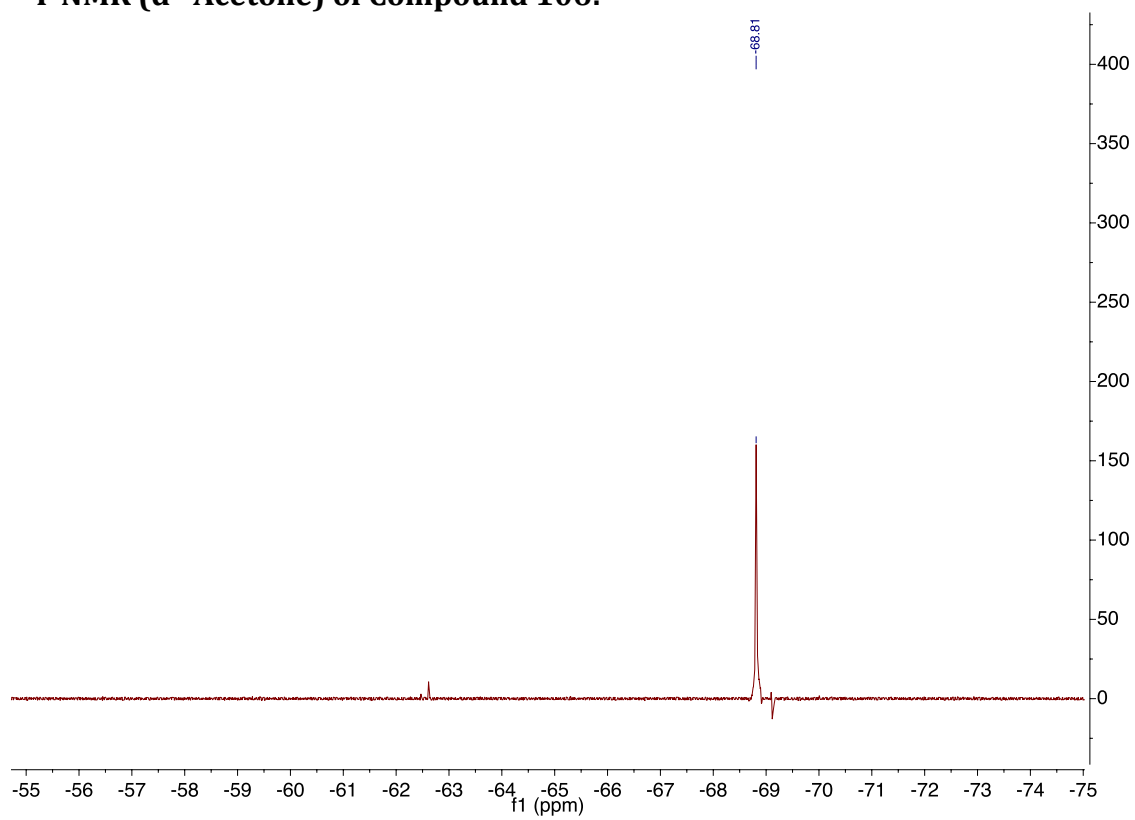
¹H NMR (d6-Acetone) of Compound 104:**¹³C NMR (d6-Acetone) of Compound 104:**

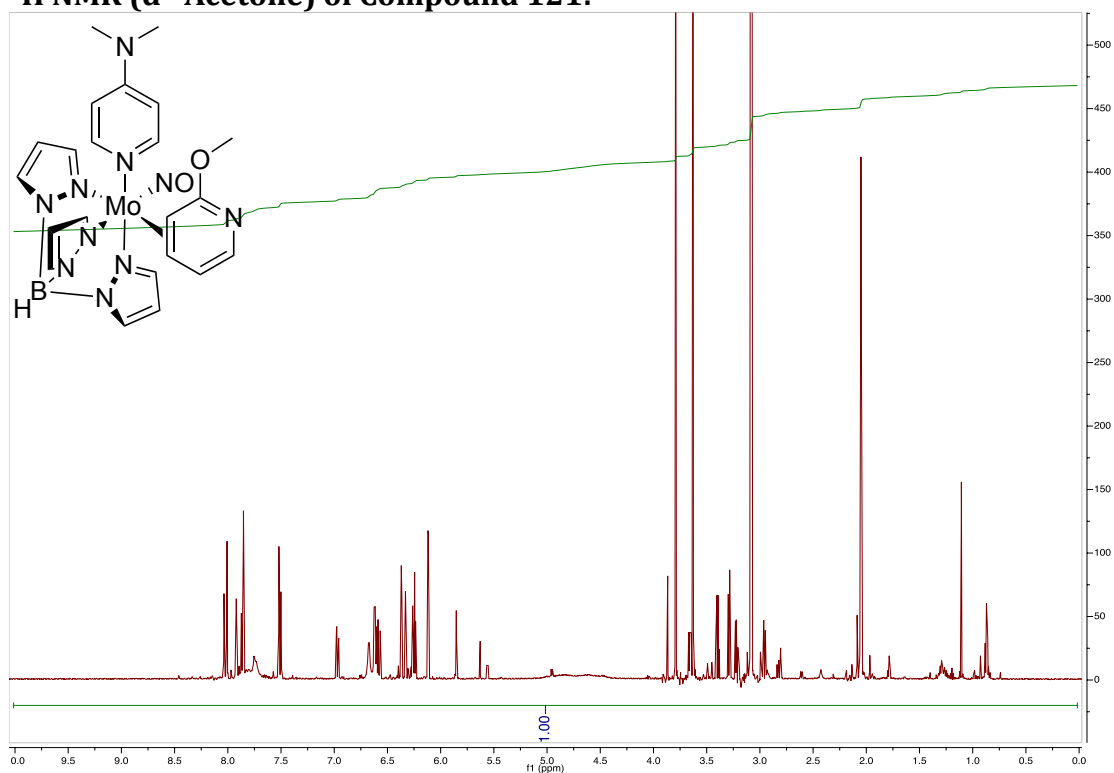
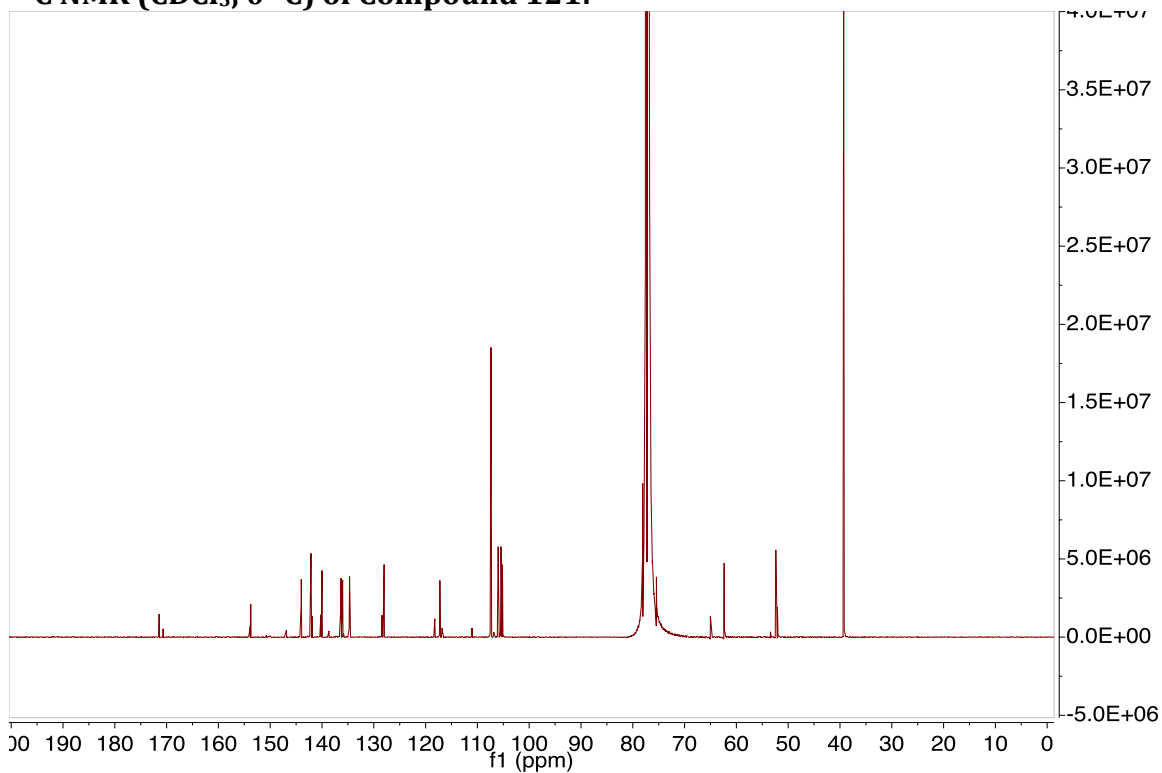
^{19}F NMR (d^6 -Acetone) of Compound 104:

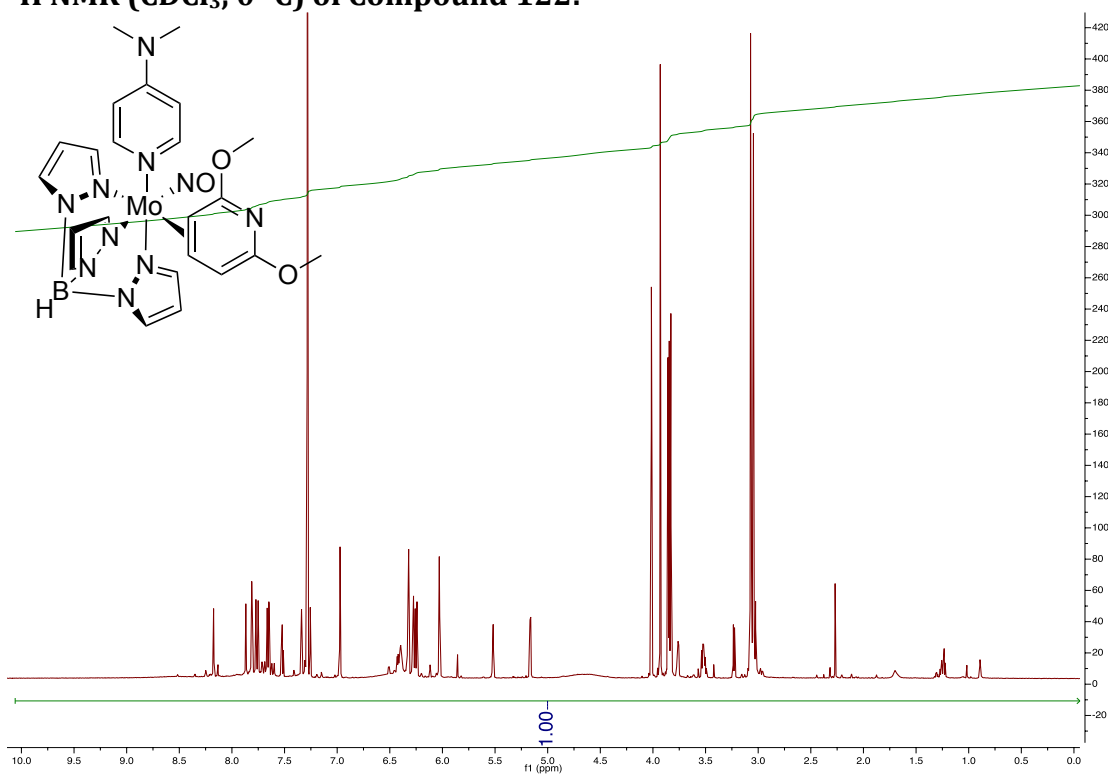
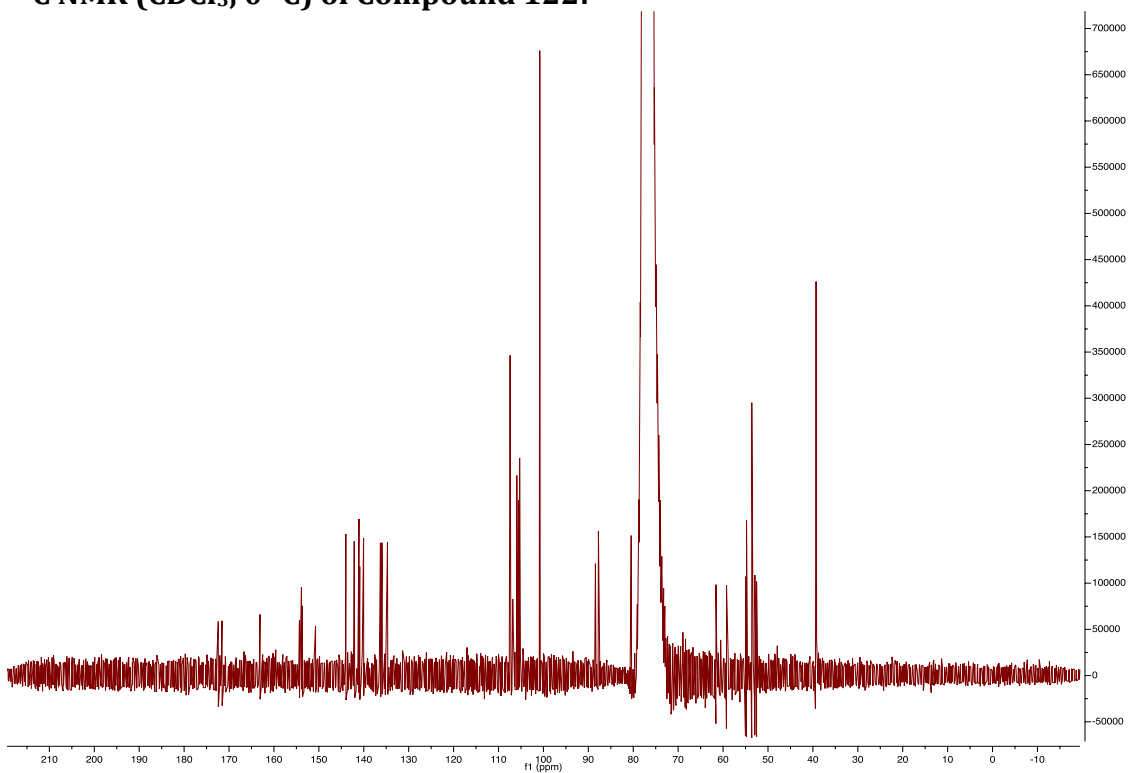
^1H NMR (CDCl_3) of Compound 105: **^{13}C NMR (CDCl_3) of Compound 105:**

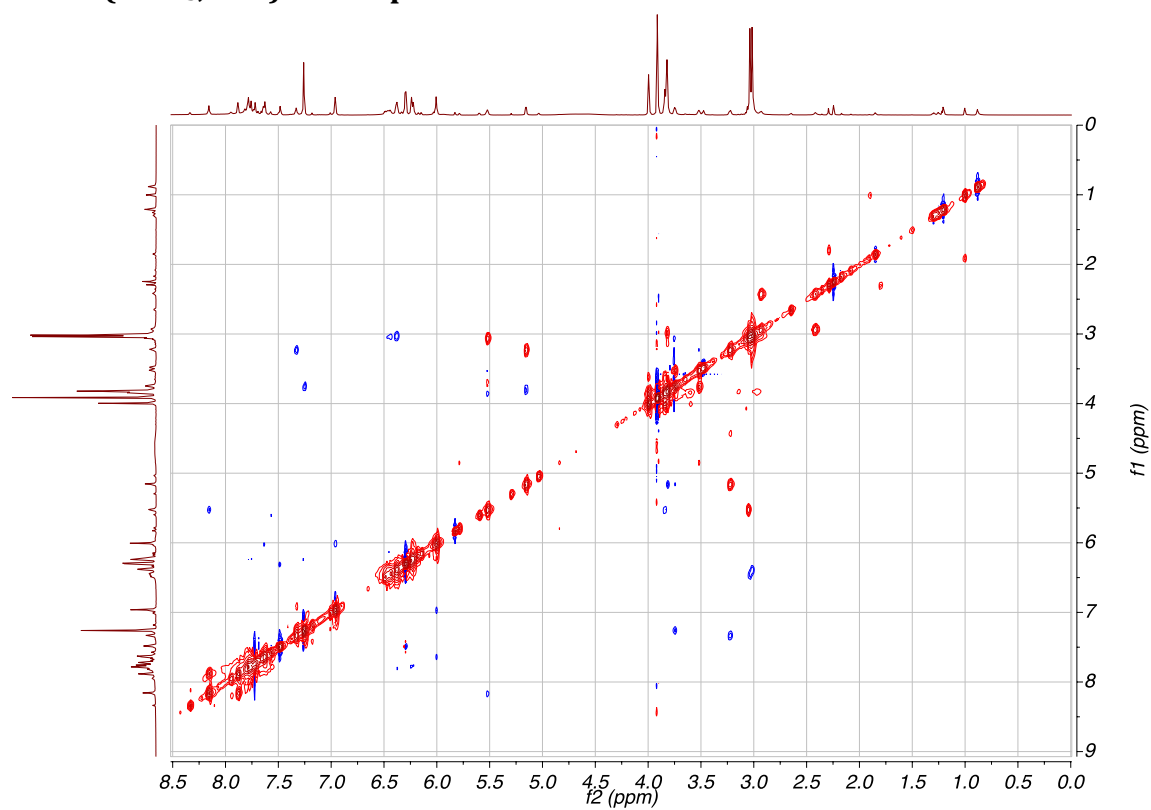
^{19}F NMR (d^6 -Acetone) of Compound 105:

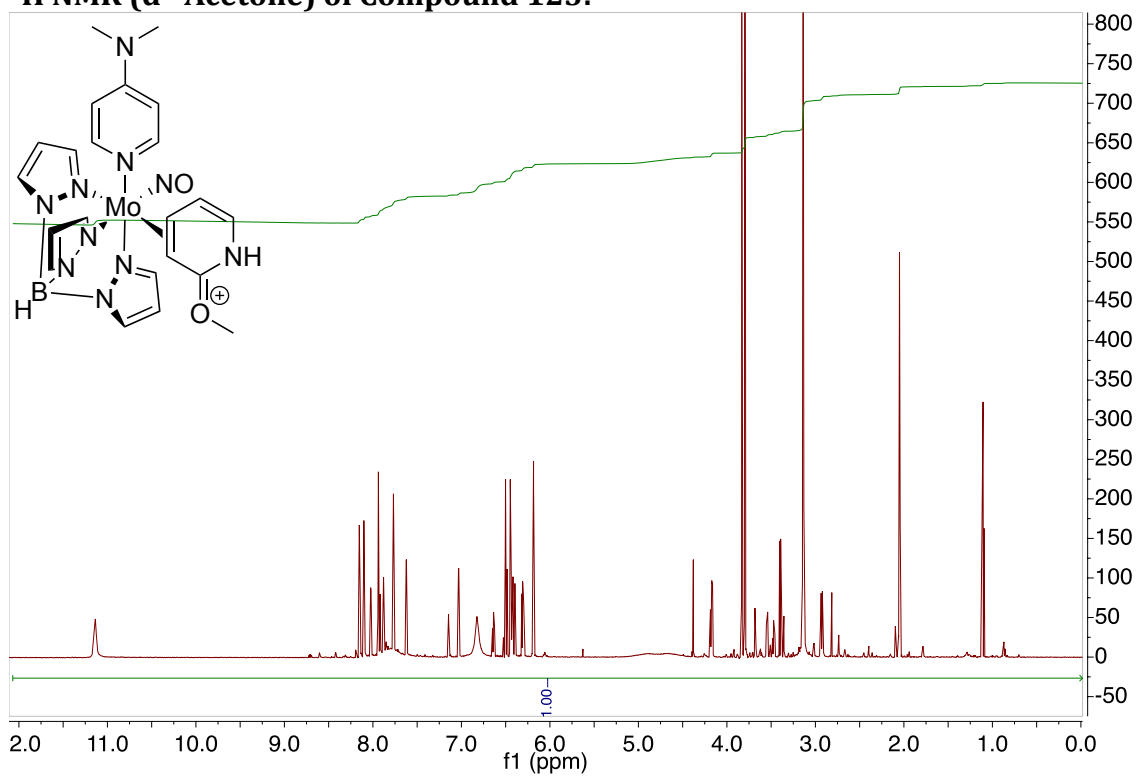
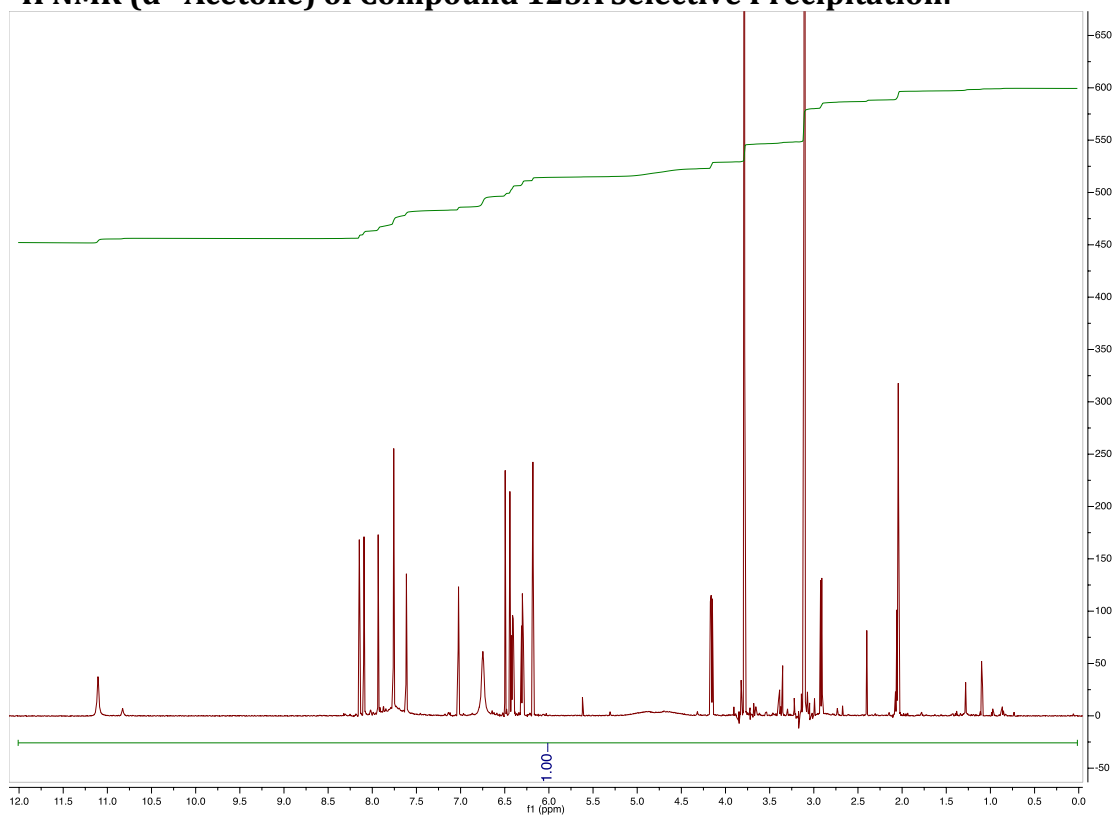
^1H NMR (CDCl_3) of Compound 106: **^{13}C NMR (CDCl_3) of Compound 106:**

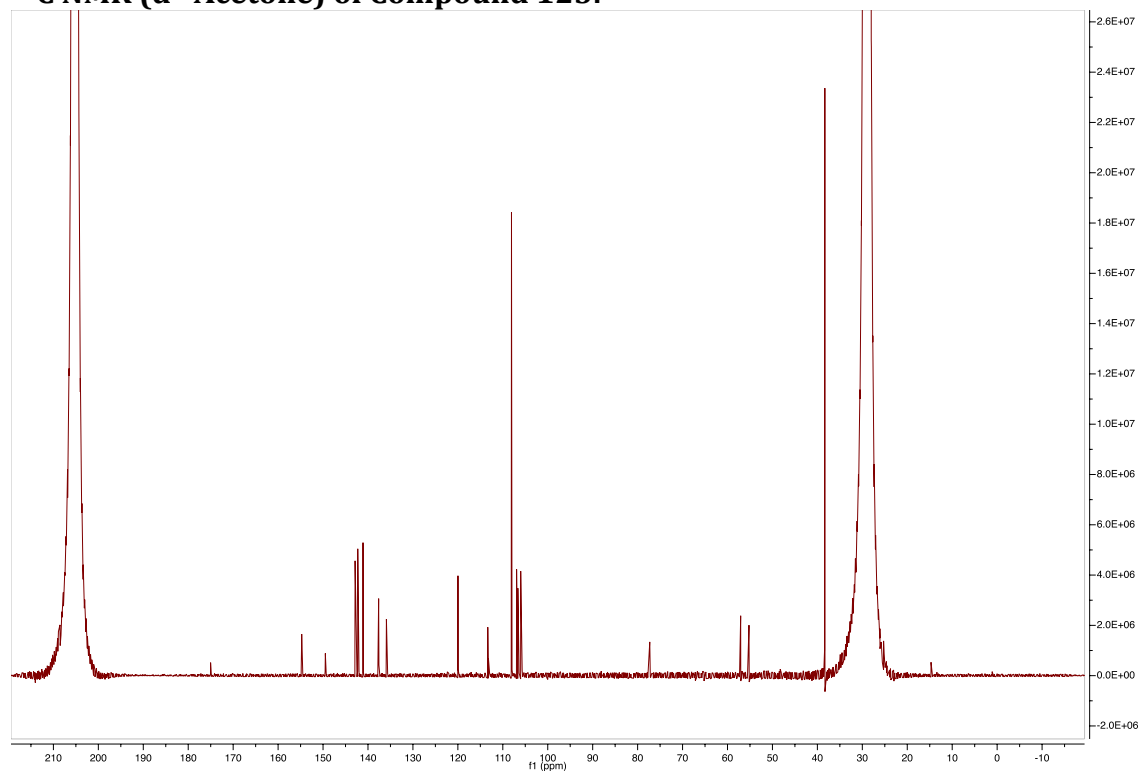
^{19}F NMR (d^6 -Acetone) of Compound 106:

^1H NMR ($\text{d}^6\text{-Acetone}$) of Compound 121: **^{13}C NMR (CDCl_3 , $0\text{ }^\circ\text{C}$) of Compound 121:**

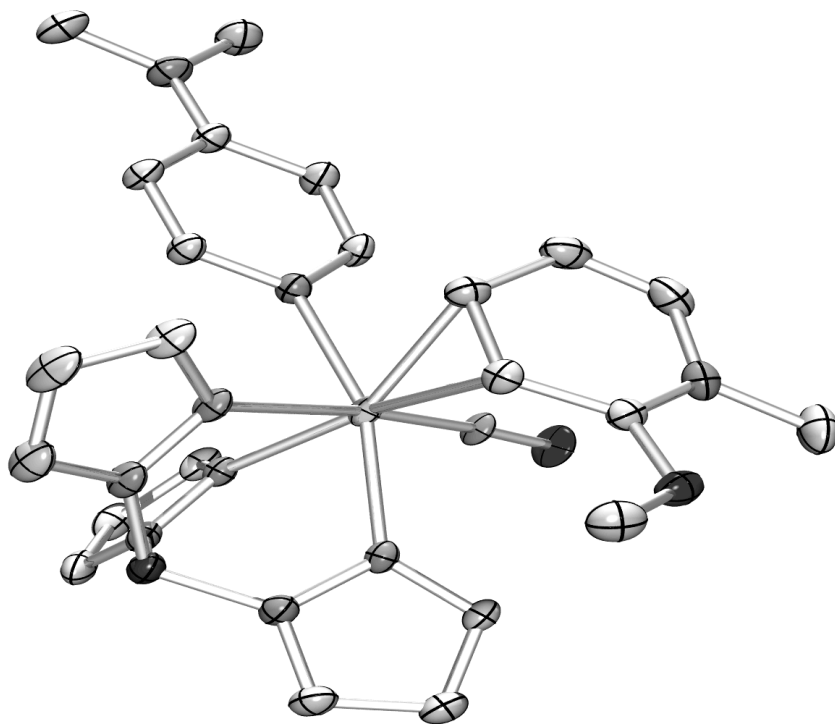
^1H NMR (CDCl_3 , 0 °C) of Compound 122: **^{13}C NMR (CDCl_3 , 0 °C) of Compound 122:**

NOESY (CDCl₃, 0 °C) of Compound 122:

¹H NMR (d⁶-Acetone) of Compound 123:**¹H NMR (d⁶-Acetone) of Compound 123A Selective Precipitation:**

^{13}C NMR ($\text{d}^6\text{-Acetone}$) of Compound 123:

Compound 124



Compound 124

Table 1. Crystal data and structure refinement for $C_{24}H_{30}BF_3MoN_{10}O_5S$.

Empirical formula	C ₂₄ H ₃₀ B F ₃ Mo N ₁₀ O ₅ S	
Formula weight	734.39	
Temperature	153(2) K	
Wavelength	0.71073 Å	
Crystal system	Triclinic	
Space group	P-1	
Unit cell dimensions	a = 9.612(3) Å	α = 78.584(6)°.
	b = 10.704(3) Å	β = 87.543(5)°.
	c = 15.335(4) Å	γ = 77.379(6)°.
Volume	1509.1(8) Å ³	
Z	2	
Density (calculated)	1.616 Mg/m ³	
Absorption coefficient	0.576 mm ⁻¹	
F(000)	748	
Crystal size	0.410 x 0.150 x 0.130 mm ³	
Theta range for data collection	3.474 to 37.245°.	
Index ranges	-15 ≤ h ≤ 16, -15 ≤ k ≤ 18, -25 ≤ l ≤ 25	
Reflections collected	26372	
Independent reflections	12051 [R(int) = 0.0505]	
Completeness to theta = 25.242°	95.4 %	
Absorption correction	Empirical	
Refinement method	Full-matrix least-squares on F ²	
Data / restraints / parameters	12051 / 0 / 414	
Goodness-of-fit on F ²	1.105	
Final R indices [I > 2σ(I)]	R1 = 0.0879, wR2 = 0.2261	
R indices (all data)	R1 = 0.1082, wR2 = 0.2461	
Largest diff. peak and hole	3.728 and -3.495 e.Å ⁻³	

Compound 124

Table 2. Atomic coordinates ($\times 10^4$) and equivalent isotropic displacement parameters ($\text{\AA}^2 \times 10^3$) for $\text{C}_{24}\text{H}_{30}\text{BF}_3\text{MoN}_{10}\text{O}_5\text{S}$. U(eq) is defined as one third of the trace of the orthogonalized U_{ij} tensor.

	x	y	z	U(eq)
Mo	2497(1)	7598(1)	6989(1)	18(1)
S(1)	7003(1)	2858(2)	8477(1)	35(1)
F(1)	8675(5)	1456(5)	7466(3)	64(1)
F(2)	9216(6)	3285(7)	7499(5)	91(2)
F(3)	9707(5)	1685(7)	8611(4)	87(2)
O(1)	6763(3)	7535(4)	6949(2)	30(1)
O(2)	2625(4)	10344(3)	6995(3)	34(1)
O(3)	6125(5)	3356(7)	7704(4)	68(2)
O(4)	6732(7)	1679(6)	9023(4)	65(2)
O(5)	7226(7)	3825(6)	8950(4)	63(2)
N(1)	5451(4)	8563(4)	7936(3)	28(1)
N(2)	744(3)	7508(4)	7983(2)	22(1)
N(3)	-2546(4)	7356(5)	9873(2)	29(1)
N(4)	3628(3)	7739(3)	5706(2)	19(1)
N(5)	3278(3)	7187(4)	5043(2)	23(1)
N(6)	653(3)	8091(3)	6089(2)	19(1)
N(7)	670(3)	7588(4)	5343(2)	24(1)
N(8)	2536(4)	5575(4)	6781(2)	22(1)
N(9)	2217(4)	5402(4)	5957(2)	24(1)
N(10)	2533(3)	9227(3)	7022(2)	20(1)
C(1)	5642(4)	7585(5)	7491(2)	23(1)
C(2)	4717(4)	6709(4)	7593(3)	22(1)
C(3)	3631(4)	6791(5)	8285(3)	26(1)
C(4)	3655(5)	7750(6)	8848(3)	33(1)
C(5)	4480(5)	8605(6)	8647(3)	34(1)
C(6)	35(4)	6529(4)	8139(3)	24(1)
C(7)	-1022(4)	6415(5)	8766(3)	25(1)
C(8)	-1452(4)	7399(5)	9283(3)	25(1)
C(9)	-718(4)	8431(5)	9127(3)	28(1)

C(10)	343(4)	8441(5)	8488(3)	25(1)
C(11)	-3174(5)	6220(6)	10065(3)	35(1)
C(12)	-2958(5)	8362(7)	10415(3)	37(1)
C(13)	4628(4)	8407(4)	5372(2)	21(1)
C(14)	4932(4)	8276(5)	4493(3)	27(1)
C(15)	4060(5)	7485(5)	4315(3)	27(1)
C(16)	-511(5)	8171(6)	4856(3)	31(1)
C(17)	-1347(4)	9084(5)	5297(3)	31(1)
C(18)	-564(4)	9004(5)	6067(3)	24(1)
C(19)	2222(5)	4139(5)	5991(3)	33(1)
C(20)	2534(6)	3453(5)	6842(4)	37(1)
C(21)	2735(5)	4389(4)	7308(3)	29(1)
C(22)	6294(6)	9591(6)	7718(4)	42(1)
C(23)	7255(5)	6359(6)	6585(3)	36(1)
C(24)	8747(6)	2287(8)	7988(5)	48(1)
B(1)	1976(5)	6539(5)	5151(3)	24(1)

Compound 124

Table 3. Bond lengths [\AA] and angles [$^\circ$] for $\text{C}_{24}\text{H}_{30}\text{BF}_3\text{MoN}_{10}\text{O}_5\text{S}$.

Mo-N(10)	1.763(3)
Mo-N(6)	2.200(3)
Mo-N(4)	2.201(3)
Mo-N(2)	2.228(3)
Mo-C(3)	2.231(4)
Mo-N(8)	2.242(4)
Mo-C(2)	2.291(4)
S(1)-O(3)	1.428(5)
S(1)-O(5)	1.432(5)
S(1)-O(4)	1.438(6)
S(1)-C(24)	1.836(6)
F(1)-C(24)	1.322(9)
F(2)-C(24)	1.331(9)
F(3)-C(24)	1.323(8)
O(1)-C(1)	1.331(5)
O(1)-C(23)	1.454(7)
O(2)-N(10)	1.210(5)
N(1)-C(1)	1.335(6)
N(1)-C(5)	1.407(6)
N(1)-C(22)	1.484(7)
N(2)-C(6)	1.348(6)
N(2)-C(10)	1.363(5)
N(3)-C(8)	1.360(5)
N(3)-C(11)	1.447(7)
N(3)-C(12)	1.465(7)
N(4)-C(13)	1.345(5)
N(4)-N(5)	1.361(5)
N(5)-C(15)	1.343(5)
N(5)-B(1)	1.546(6)
N(6)-C(18)	1.348(5)
N(6)-N(7)	1.356(5)
N(7)-C(16)	1.347(5)
N(7)-B(1)	1.551(6)

N(8)-C(21)	1.342(6)
N(8)-N(9)	1.370(5)
N(9)-C(19)	1.342(6)
N(9)-B(1)	1.539(7)
C(1)-C(2)	1.409(6)
C(2)-C(3)	1.458(5)
C(2)-H(2)	1.0000
C(3)-C(4)	1.471(7)
C(3)-H(3)	1.0000
C(4)-C(5)	1.321(8)
C(4)-H(4)	0.9500
C(5)-H(5)	0.9500
C(6)-C(7)	1.378(5)
C(6)-H(6)	0.9500
C(7)-C(8)	1.422(6)
C(7)-H(7)	0.9500
C(8)-C(9)	1.413(7)
C(9)-C(10)	1.384(5)
C(9)-H(9)	0.9500
C(10)-H(10)	0.9500
C(11)-H(11A)	0.9800
C(11)-H(11B)	0.9800
C(11)-H(11C)	0.9800
C(12)-H(12A)	0.9800
C(12)-H(12B)	0.9800
C(12)-H(12C)	0.9800
C(13)-C(14)	1.395(5)
C(13)-H(13)	0.9500
C(14)-C(15)	1.384(7)
C(14)-H(14)	0.9500
C(15)-H(15)	0.9500
C(16)-C(17)	1.389(8)
C(16)-H(16)	0.9500
C(17)-C(18)	1.405(6)
C(17)-H(17)	0.9500
C(18)-H(18)	0.9500

C(19)-C(20)	1.374(8)
C(19)-H(19)	0.9500
C(20)-C(21)	1.389(7)
C(20)-H(20)	0.9500
C(21)-H(21)	0.9500
C(22)-H(22A)	0.9800
C(22)-H(22B)	0.9800
C(22)-H(22C)	0.9800
C(23)-H(23A)	0.9800
C(23)-H(23B)	0.9800
C(23)-H(23C)	0.9800
B(1)-H(1B)	1.04(6)

N(10)-Mo-N(6)	95.32(14)
N(10)-Mo-N(4)	90.89(14)
N(6)-Mo-N(4)	80.80(11)
N(10)-Mo-N(2)	93.91(14)
N(6)-Mo-N(2)	80.05(12)
N(4)-Mo-N(2)	160.60(12)
N(10)-Mo-C(3)	94.05(17)
N(6)-Mo-C(3)	154.85(13)
N(4)-Mo-C(3)	122.36(13)
N(2)-Mo-C(3)	76.06(13)
N(10)-Mo-N(8)	173.26(14)
N(6)-Mo-N(8)	82.36(13)
N(4)-Mo-N(8)	82.50(13)
N(2)-Mo-N(8)	91.92(13)
C(3)-Mo-N(8)	90.63(16)
N(10)-Mo-C(2)	95.93(15)
N(6)-Mo-C(2)	161.81(13)
N(4)-Mo-C(2)	84.77(13)
N(2)-Mo-C(2)	113.33(13)
C(3)-Mo-C(2)	37.59(14)
N(8)-Mo-C(2)	84.84(14)
O(3)-S(1)-O(5)	114.8(4)
O(3)-S(1)-O(4)	115.2(4)

O(5)-S(1)-O(4)	115.4(3)
O(3)-S(1)-C(24)	101.8(3)
O(5)-S(1)-C(24)	104.6(4)
O(4)-S(1)-C(24)	102.4(4)
C(1)-O(1)-C(23)	118.0(4)
C(1)-N(1)-C(5)	120.2(4)
C(1)-N(1)-C(22)	121.1(4)
C(5)-N(1)-C(22)	118.7(5)
C(6)-N(2)-C(10)	115.8(3)
C(6)-N(2)-Mo	122.9(3)
C(10)-N(2)-Mo	121.4(3)
C(8)-N(3)-C(11)	120.0(4)
C(8)-N(3)-C(12)	120.4(4)
C(11)-N(3)-C(12)	118.9(4)
C(13)-N(4)-N(5)	106.5(3)
C(13)-N(4)-Mo	131.5(3)
N(5)-N(4)-Mo	121.7(2)
C(15)-N(5)-N(4)	110.0(3)
C(15)-N(5)-B(1)	129.4(3)
N(4)-N(5)-B(1)	119.8(3)
C(18)-N(6)-N(7)	106.7(3)
C(18)-N(6)-Mo	130.5(3)
N(7)-N(6)-Mo	122.2(2)
C(16)-N(7)-N(6)	110.1(4)
C(16)-N(7)-B(1)	130.4(4)
N(6)-N(7)-B(1)	119.4(3)
C(21)-N(8)-N(9)	105.7(4)
C(21)-N(8)-Mo	135.1(3)
N(9)-N(8)-Mo	119.1(3)
C(19)-N(9)-N(8)	109.4(4)
C(19)-N(9)-B(1)	129.0(4)
N(8)-N(9)-B(1)	121.6(4)
O(2)-N(10)-Mo	175.4(3)
O(1)-C(1)-N(1)	113.7(4)
O(1)-C(1)-C(2)	124.3(4)
N(1)-C(1)-C(2)	122.0(4)

C(1)-C(2)-C(3)	118.1(4)
C(1)-C(2)-Mo	114.4(3)
C(3)-C(2)-Mo	69.0(2)
C(1)-C(2)-H(2)	115.7
C(3)-C(2)-H(2)	115.7
Mo-C(2)-H(2)	115.7
C(2)-C(3)-C(4)	116.1(4)
C(2)-C(3)-Mo	73.4(2)
C(4)-C(3)-Mo	115.1(3)
C(2)-C(3)-H(3)	115.2
C(4)-C(3)-H(3)	115.2
Mo-C(3)-H(3)	115.2
C(5)-C(4)-C(3)	120.8(4)
C(5)-C(4)-H(4)	119.6
C(3)-C(4)-H(4)	119.6
C(4)-C(5)-N(1)	121.5(5)
C(4)-C(5)-H(5)	119.3
N(1)-C(5)-H(5)	119.3
N(2)-C(6)-C(7)	124.7(4)
N(2)-C(6)-H(6)	117.6
C(7)-C(6)-H(6)	117.6
C(6)-C(7)-C(8)	119.4(4)
C(6)-C(7)-H(7)	120.3
C(8)-C(7)-H(7)	120.3
N(3)-C(8)-C(9)	122.5(4)
N(3)-C(8)-C(7)	121.0(4)
C(9)-C(8)-C(7)	116.5(3)
C(10)-C(9)-C(8)	119.4(4)
C(10)-C(9)-H(9)	120.3
C(8)-C(9)-H(9)	120.3
N(2)-C(10)-C(9)	124.2(4)
N(2)-C(10)-H(10)	117.9
C(9)-C(10)-H(10)	117.9
N(3)-C(11)-H(11A)	109.5
N(3)-C(11)-H(11B)	109.5
H(11A)-C(11)-H(11B)	109.5

N(3)-C(11)-H(11C)	109.5
H(11A)-C(11)-H(11C)	109.5
H(11B)-C(11)-H(11C)	109.5
N(3)-C(12)-H(12A)	109.5
N(3)-C(12)-H(12B)	109.5
H(12A)-C(12)-H(12B)	109.5
N(3)-C(12)-H(12C)	109.5
H(12A)-C(12)-H(12C)	109.5
H(12B)-C(12)-H(12C)	109.5
N(4)-C(13)-C(14)	110.2(4)
N(4)-C(13)-H(13)	124.9
C(14)-C(13)-H(13)	124.9
C(15)-C(14)-C(13)	104.8(3)
C(15)-C(14)-H(14)	127.6
C(13)-C(14)-H(14)	127.6
N(5)-C(15)-C(14)	108.5(4)
N(5)-C(15)-H(15)	125.7
C(14)-C(15)-H(15)	125.7
N(7)-C(16)-C(17)	108.7(4)
N(7)-C(16)-H(16)	125.7
C(17)-C(16)-H(16)	125.7
C(16)-C(17)-C(18)	104.3(4)
C(16)-C(17)-H(17)	127.8
C(18)-C(17)-H(17)	127.8
N(6)-C(18)-C(17)	110.2(4)
N(6)-C(18)-H(18)	124.9
C(17)-C(18)-H(18)	124.9
N(9)-C(19)-C(20)	109.5(4)
N(9)-C(19)-H(19)	125.2
C(20)-C(19)-H(19)	125.2
C(19)-C(20)-C(21)	104.1(5)
C(19)-C(20)-H(20)	128.0
C(21)-C(20)-H(20)	128.0
N(8)-C(21)-C(20)	111.3(5)
N(8)-C(21)-H(21)	124.4
C(20)-C(21)-H(21)	124.4

N(1)-C(22)-H(22A)	109.5
N(1)-C(22)-H(22B)	109.5
H(22A)-C(22)-H(22B)	109.5
N(1)-C(22)-H(22C)	109.5
H(22A)-C(22)-H(22C)	109.5
H(22B)-C(22)-H(22C)	109.5
O(1)-C(23)-H(23A)	109.5
O(1)-C(23)-H(23B)	109.5
H(23A)-C(23)-H(23B)	109.5
O(1)-C(23)-H(23C)	109.5
H(23A)-C(23)-H(23C)	109.5
H(23B)-C(23)-H(23C)	109.5
F(1)-C(24)-F(3)	107.5(6)
F(1)-C(24)-F(2)	107.7(6)
F(3)-C(24)-F(2)	108.2(6)
F(1)-C(24)-S(1)	111.4(5)
F(3)-C(24)-S(1)	111.3(5)
F(2)-C(24)-S(1)	110.6(5)
N(9)-B(1)-N(5)	109.2(3)
N(9)-B(1)-N(7)	108.7(3)
N(5)-B(1)-N(7)	106.9(4)
N(9)-B(1)-H(1B)	112(4)
N(5)-B(1)-H(1B)	113(3)
N(7)-B(1)-H(1B)	107(3)

Compound 124

Table 4. Anisotropic displacement parameters ($\text{\AA}^2 \times 10^3$) for $\text{C}_{24}\text{H}_{30}\text{BF}_3\text{MoN}_{10}\text{O}_5\text{S}$.

The anisotropic displacement factor exponent takes the form: $-2\pi^2 [h^2 a^{*2} U^{11} + \dots + 2 h k a^* b^* U^{12}]$

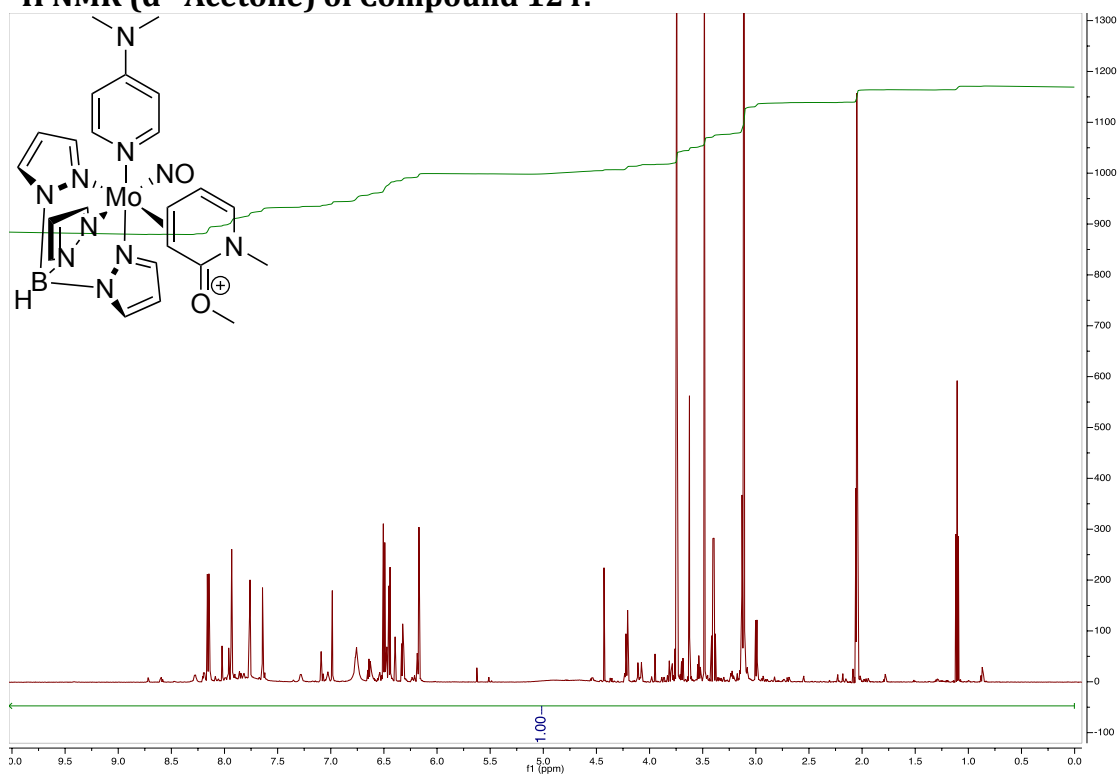
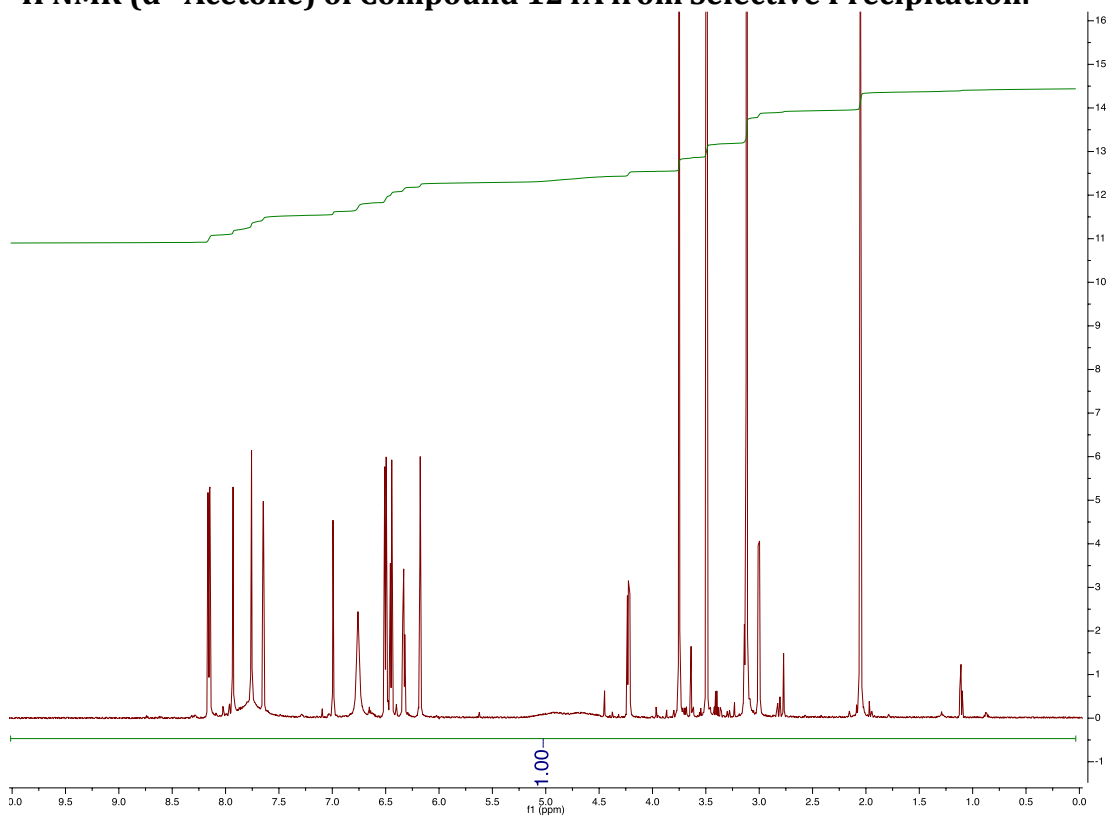
	U ¹¹	U ²²	U ³³	U ²³	U ¹³	U ¹²
Mo	19(1)	11(1)	25(1)	-2(1)	1(1)	-4(1)
S(1)	36(1)	31(1)	41(1)	-16(1)	6(1)	-8(1)
F(1)	70(3)	55(3)	65(2)	-25(2)	16(2)	1(2)
F(2)	63(3)	69(4)	133(5)	3(4)	44(3)	-22(3)
F(3)	51(3)	82(5)	121(5)	-15(4)	-34(3)	7(3)
O(1)	23(1)	34(2)	32(1)	-4(1)	4(1)	-7(1)
O(2)	44(2)	9(1)	50(2)	-5(1)	0(1)	-9(1)
O(3)	46(2)	77(5)	76(3)	-31(3)	-17(2)	15(3)
O(4)	94(4)	53(3)	62(3)	-25(3)	36(3)	-40(3)
O(5)	92(4)	45(3)	67(3)	-31(3)	10(3)	-27(3)
N(1)	26(1)	26(2)	34(2)	-9(2)	-5(1)	-6(1)
N(2)	21(1)	20(2)	25(1)	-7(1)	3(1)	-5(1)
N(3)	27(1)	31(2)	30(2)	-7(1)	9(1)	-6(1)
N(4)	17(1)	14(1)	26(1)	-4(1)	0(1)	-4(1)
N(5)	24(1)	21(2)	25(1)	-7(1)	5(1)	-7(1)
N(6)	17(1)	14(1)	26(1)	-3(1)	2(1)	-3(1)
N(7)	22(1)	22(2)	26(1)	0(1)	0(1)	-10(1)
N(8)	24(1)	11(1)	31(1)	-3(1)	4(1)	-5(1)
N(9)	28(1)	15(2)	33(2)	-9(1)	6(1)	-6(1)
N(10)	22(1)	8(1)	31(1)	-3(1)	3(1)	-5(1)
C(1)	21(1)	24(2)	24(1)	-3(1)	-2(1)	-3(1)
C(2)	24(1)	15(2)	28(2)	-5(1)	1(1)	-2(1)
C(3)	24(2)	28(2)	25(1)	-3(1)	2(1)	-4(2)
C(4)	28(2)	44(3)	25(2)	-8(2)	2(1)	-4(2)
C(5)	33(2)	40(3)	32(2)	-17(2)	-6(2)	-2(2)
C(6)	26(2)	19(2)	27(2)	-7(1)	5(1)	-6(1)
C(7)	25(2)	19(2)	30(2)	-4(1)	7(1)	-7(1)
C(8)	22(1)	26(2)	26(1)	-5(1)	4(1)	-7(1)
C(9)	26(2)	26(2)	33(2)	-12(2)	8(1)	-8(2)

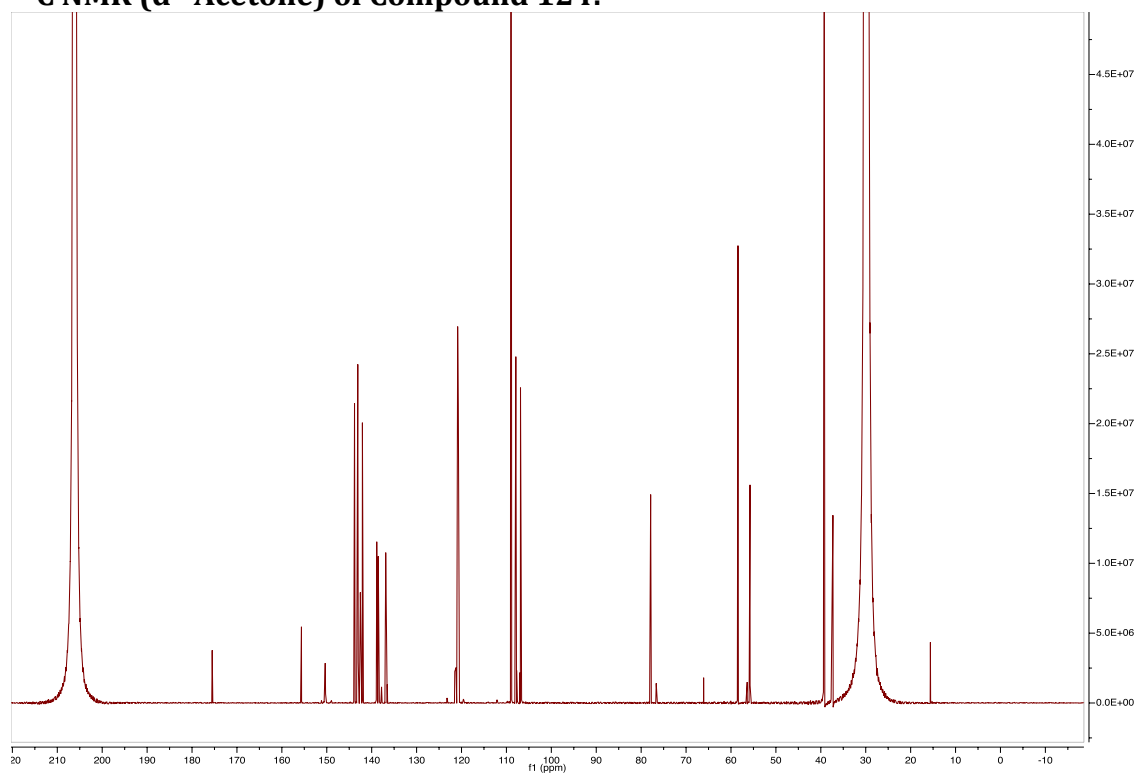
C(10)	23(1)	21(2)	32(2)	-8(2)	4(1)	-8(1)
C(11)	33(2)	32(3)	38(2)	-1(2)	12(2)	-9(2)
C(12)	35(2)	44(3)	38(2)	-16(2)	13(2)	-12(2)
C(13)	18(1)	17(2)	27(1)	-2(1)	2(1)	-5(1)
C(14)	24(2)	27(2)	29(2)	-1(2)	6(1)	-6(2)
C(15)	30(2)	26(2)	25(2)	-6(2)	9(1)	-7(2)
C(16)	27(2)	34(3)	32(2)	2(2)	-7(1)	-16(2)
C(17)	19(1)	28(2)	42(2)	6(2)	-6(1)	-5(2)
C(18)	16(1)	18(2)	35(2)	2(1)	2(1)	-1(1)
C(19)	40(2)	20(2)	44(2)	-16(2)	11(2)	-11(2)
C(20)	46(3)	14(2)	54(3)	-11(2)	17(2)	-10(2)
C(21)	32(2)	11(2)	40(2)	-3(2)	6(2)	-2(2)
C(22)	45(3)	31(3)	56(3)	-7(2)	-14(2)	-17(2)
C(23)	28(2)	36(3)	38(2)	-7(2)	4(2)	2(2)
C(24)	36(2)	41(4)	63(4)	-3(3)	3(2)	-6(2)
B(1)	25(2)	22(2)	27(2)	-7(2)	5(1)	-9(2)

Compound 124

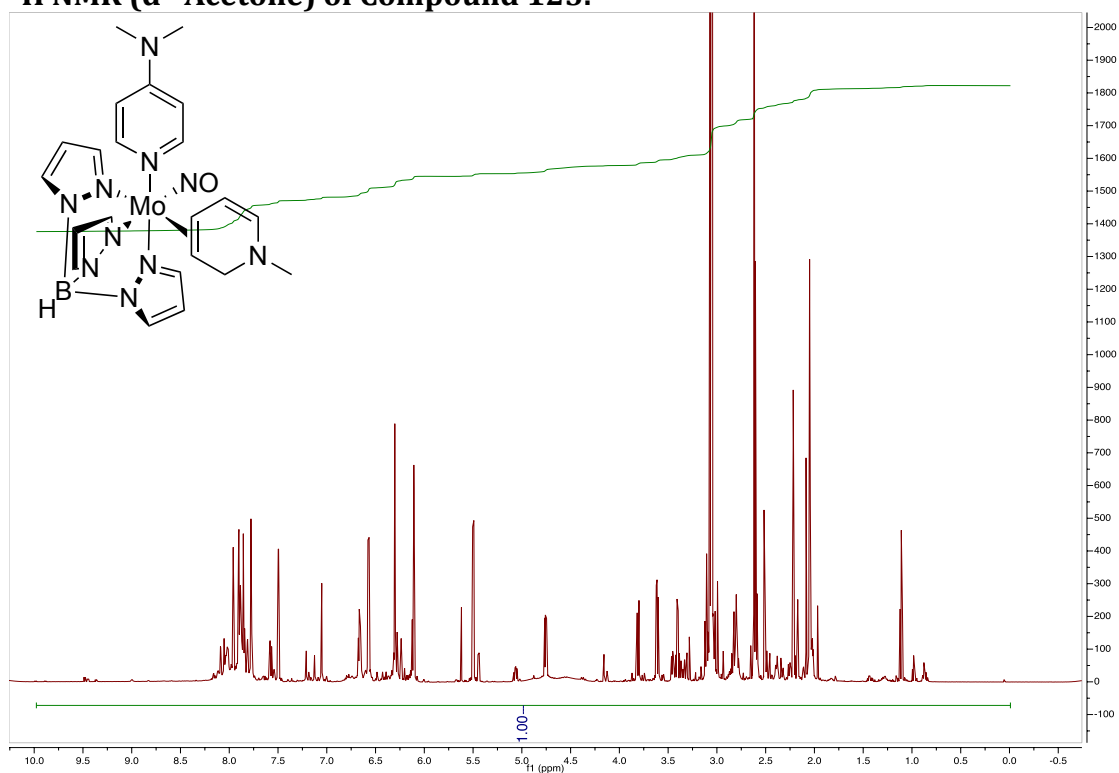
Table 5. Hydrogen coordinates ($\times 10^4$) and isotropic displacement parameters ($\text{\AA}^2 \times 10^3$) for $\text{C}_{24}\text{H}_{30}\text{BF}_3\text{MoN}_{10}\text{O}_5\text{S}$.

	x	y	z	U(eq)
H(2)	5155	5810	7496	27
H(3)	3444	5935	8606	31
H(4)	3069	7755	9363	40
H(5)	4415	9262	8991	41
H(6)	283	5871	7791	28
H(7)	-1460	5685	8852	30
H(9)	-951	9111	9457	33
H(10)	822	9144	8395	30
H(11A)	-3605	6118	9522	53
H(11B)	-3910	6330	10523	53
H(11C)	-2434	5442	10279	53
H(12A)	-2300	8171	10919	56
H(12B)	-3930	8370	10639	56
H(12C)	-2920	9217	10052	56
H(13)	5064	8897	5689	25
H(14)	5593	8647	4103	33
H(15)	4020	7201	3769	33
H(16)	-735	7989	4303	37
H(17)	-2244	9637	5118	38
H(18)	-852	9519	6508	29
H(19)	2038	3774	5503	39
H(20)	2598	2548	7061	45
H(21)	2981	4212	7920	35
H(22A)	7312	9189	7785	64
H(22B)	6028	10207	8123	64
H(22C)	6098	10057	7104	64
H(23A)	7407	5595	7070	53
H(23B)	8154	6403	6265	53
H(23C)	6537	6285	6174	53
H(1B)	1750(60)	6240(70)	4580(40)	23(13)

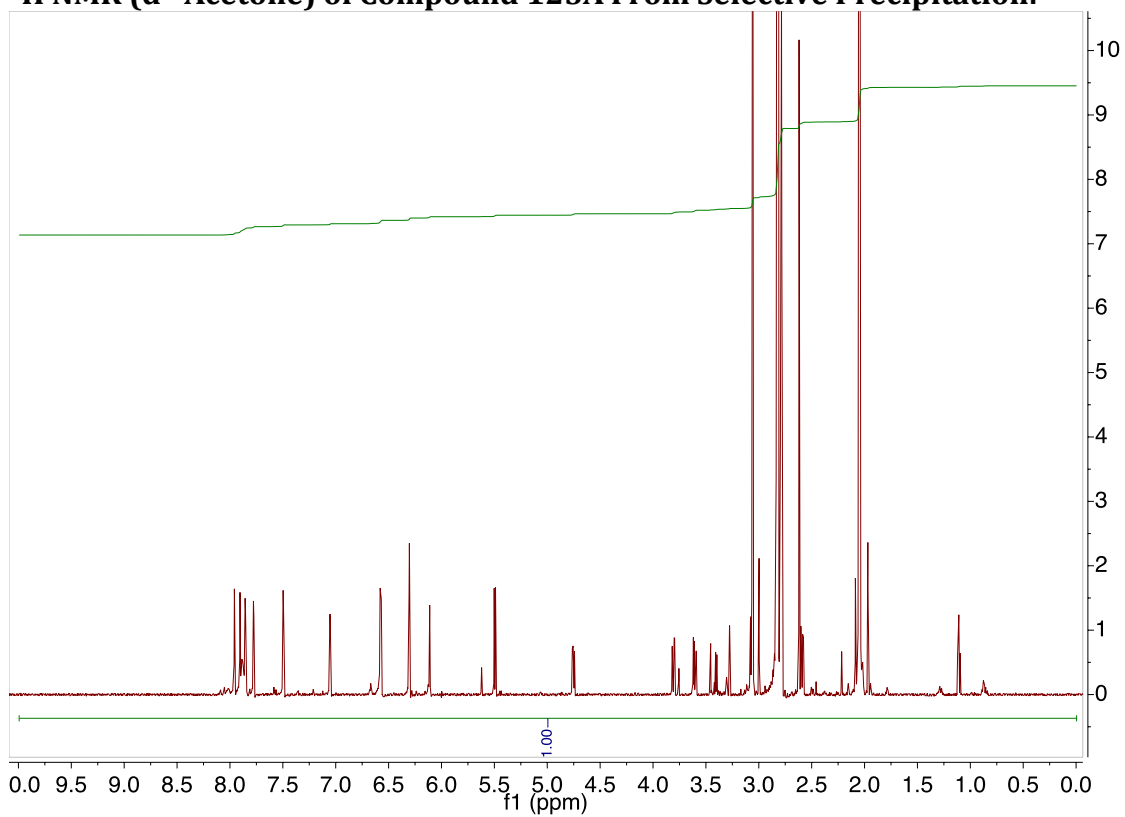
¹H NMR (d⁶-Acetone) of Compound 124:**¹H NMR (d⁶-Acetone) of Compound 124A from Selective Precipitation:**

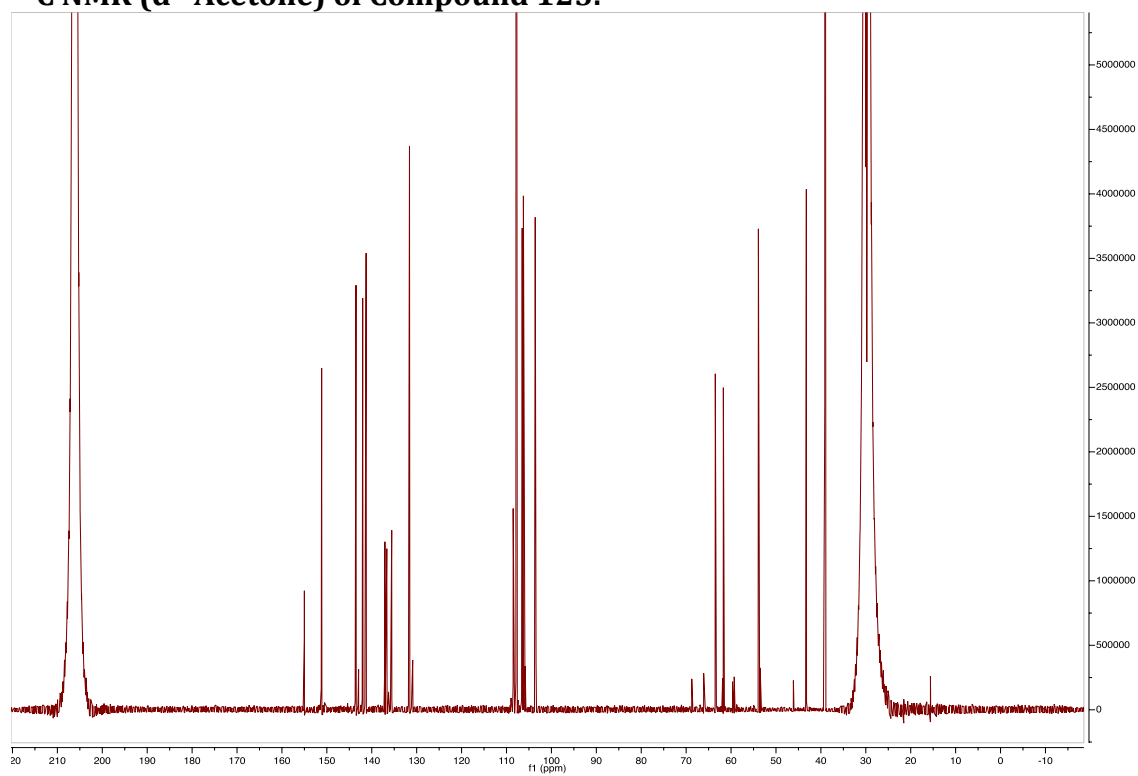
^{13}C NMR (d^6 -Acetone) of Compound 124:

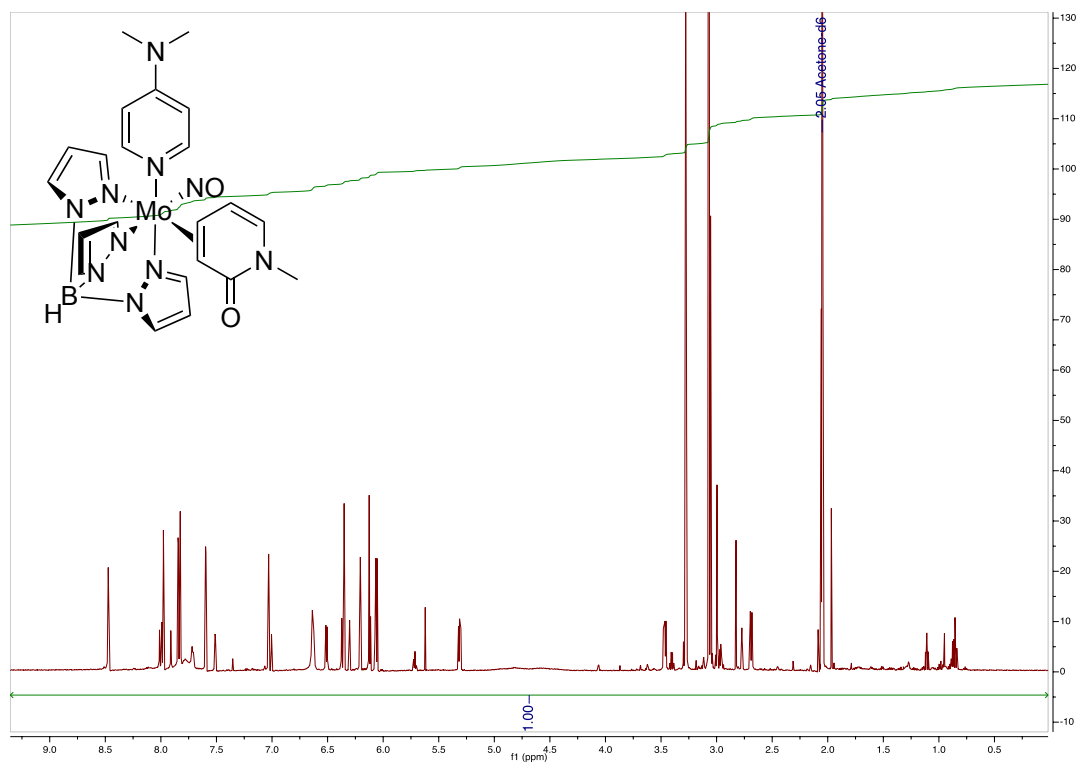
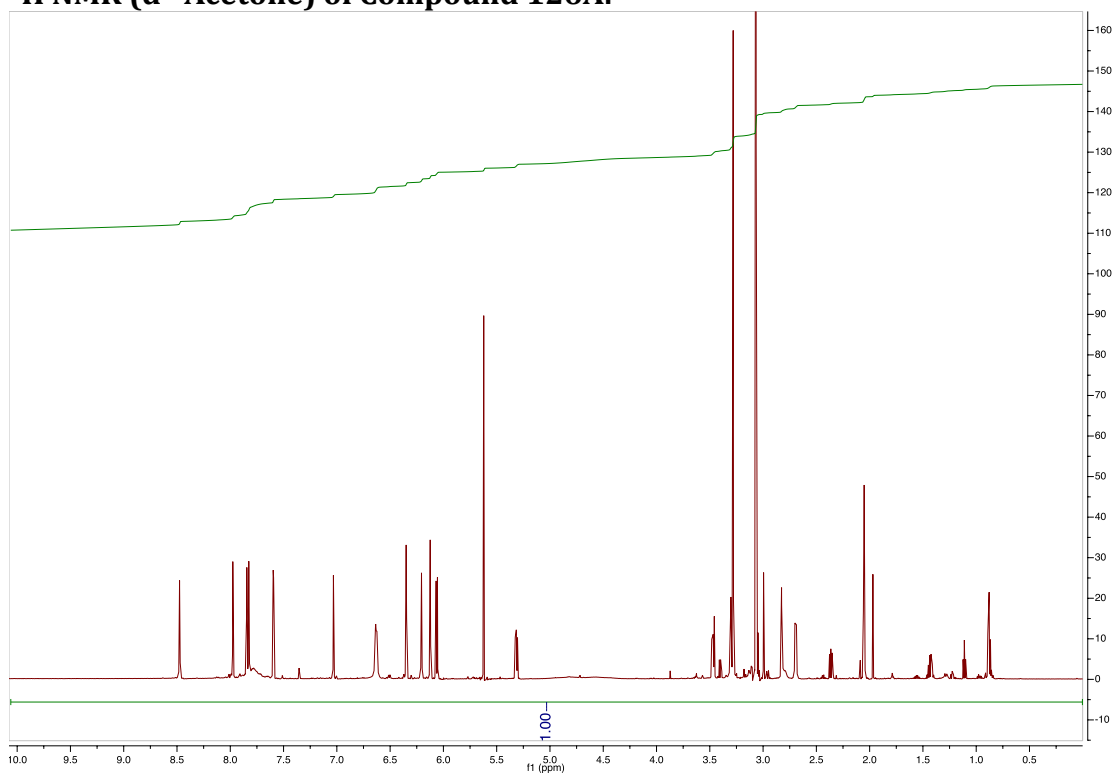
¹H NMR (d⁶-Acetone) of Compound 125:

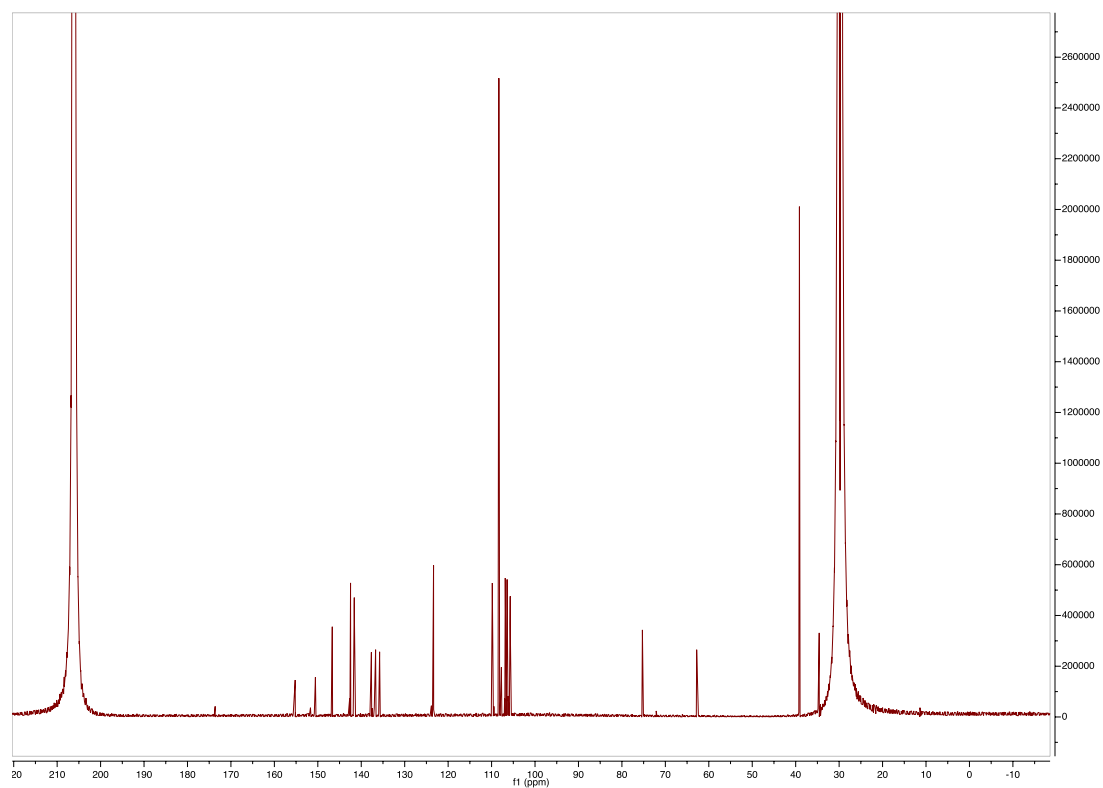


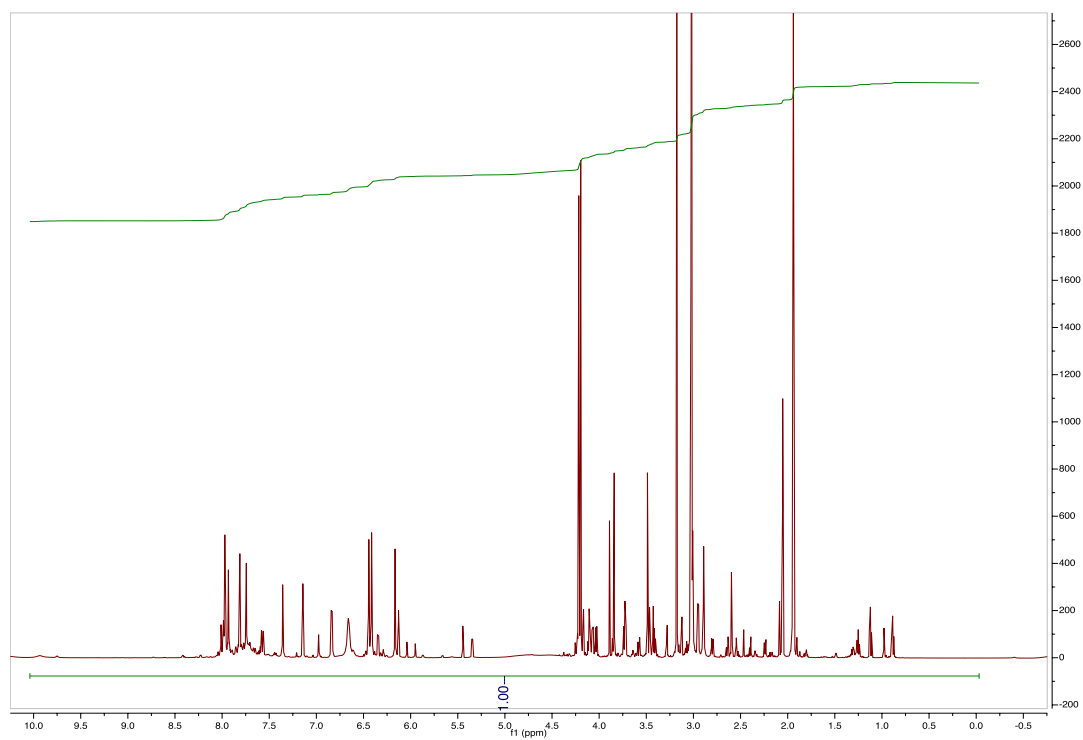
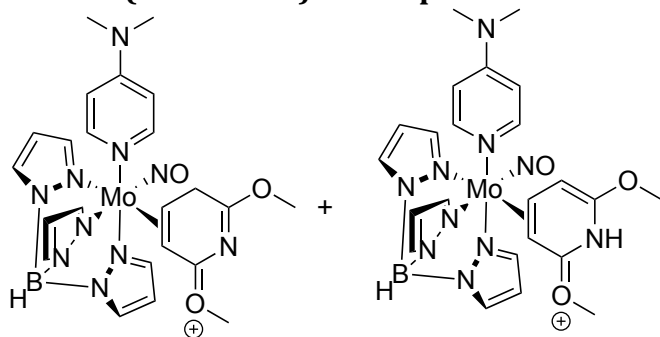
¹H NMR (d⁶-Acetone) of Compound 125A From Selective Precipitation:



^{13}C NMR ($\text{d}^6\text{-Acetone}$) of Compound 125:

^1H NMR (d^6 -Acetone) of Compound 126: **^1H NMR (d^6 -Acetone) of Compound 126A:**

^{13}C NMR (d^6 -Acetone) of Compound 126:

^1H NMR ($\text{d}^6\text{-Acetone}$) of Compound 127:

^{13}C NMR (d^6 -Acetone) of Compound 127: